

The link between metabolic syndrome and chronic kidney disease: Focus on diagnosis and therapeutics, volume II

Edited by

Ningning Hou, Guiting Lin and Weixia Sun

Published in

Frontiers in Endocrinology



FRONTIERS EBOOK COPYRIGHT STATEMENT

The copyright in the text of individual articles in this ebook is the property of their respective authors or their respective institutions or funders. The copyright in graphics and images within each article may be subject to copyright of other parties. In both cases this is subject to a license granted to Frontiers.

The compilation of articles constituting this ebook is the property of Frontiers.

Each article within this ebook, and the ebook itself, are published under the most recent version of the Creative Commons CC-BY licence. The version current at the date of publication of this ebook is CC-BY 4.0. If the CC-BY licence is updated, the licence granted by Frontiers is automatically updated to the new version.

When exercising any right under the CC-BY licence, Frontiers must be attributed as the original publisher of the article or ebook, as applicable.

Authors have the responsibility of ensuring that any graphics or other materials which are the property of others may be included in the CC-BY licence, but this should be checked before relying on the CC-BY licence to reproduce those materials. Any copyright notices relating to those materials must be complied with.

Copyright and source acknowledgement notices may not be removed and must be displayed in any copy, derivative work or partial copy which includes the elements in question.

All copyright, and all rights therein, are protected by national and international copyright laws. The above represents a summary only. For further information please read Frontiers' Conditions for Website Use and Copyright Statement, and the applicable CC-BY licence.

ISSN 1664-8714
ISBN 978-2-8325-5066-3
DOI 10.3389/978-2-8325-5066-3

About Frontiers

Frontiers is more than just an open access publisher of scholarly articles: it is a pioneering approach to the world of academia, radically improving the way scholarly research is managed. The grand vision of Frontiers is a world where all people have an equal opportunity to seek, share and generate knowledge. Frontiers provides immediate and permanent online open access to all its publications, but this alone is not enough to realize our grand goals.

Frontiers journal series

The Frontiers journal series is a multi-tier and interdisciplinary set of open-access, online journals, promising a paradigm shift from the current review, selection and dissemination processes in academic publishing. All Frontiers journals are driven by researchers for researchers; therefore, they constitute a service to the scholarly community. At the same time, the *Frontiers journal series* operates on a revolutionary invention, the tiered publishing system, initially addressing specific communities of scholars, and gradually climbing up to broader public understanding, thus serving the interests of the lay society, too.

Dedication to quality

Each Frontiers article is a landmark of the highest quality, thanks to genuinely collaborative interactions between authors and review editors, who include some of the world's best academicians. Research must be certified by peers before entering a stream of knowledge that may eventually reach the public - and shape society; therefore, Frontiers only applies the most rigorous and unbiased reviews. Frontiers revolutionizes research publishing by freely delivering the most outstanding research, evaluated with no bias from both the academic and social point of view. By applying the most advanced information technologies, Frontiers is catapulting scholarly publishing into a new generation.

What are Frontiers Research Topics?

Frontiers Research Topics are very popular trademarks of the *Frontiers journals series*: they are collections of at least ten articles, all centered on a particular subject. With their unique mix of varied contributions from Original Research to Review Articles, Frontiers Research Topics unify the most influential researchers, the latest key findings and historical advances in a hot research area.

Find out more on how to host your own Frontiers Research Topic or contribute to one as an author by contacting the Frontiers editorial office: frontiersin.org/about/contact

The link between metabolic syndrome and chronic kidney disease: Focus on diagnosis and therapeutics, volume II

Topic editors

Ningning Hou — AFFILIATED HOSPITAL OF SHANDONG SECOND MEDICAL UNIVERSITY, China

Guiting Lin — University of California, San Francisco, United States

Weixia Sun — The First hospital of Jilin University, China

Citation

Hou, N., Lin, G., Sun, W., eds. (2024). *The link between metabolic syndrome and chronic kidney disease: Focus on diagnosis and therapeutics, volume II*.

Lausanne: Frontiers Media SA. doi: 10.3389/978-2-8325-5066-3

Table of contents

- 05 **Editorial: The link between metabolic syndrome and chronic kidney disease: focus on diagnosis and therapeutics - volume II**
Kexin Zhang, Weixia Sun, Guiting Lin and Ningning Hou
- 08 **A high triglyceride glucose index is associated with early renal impairment in the hypertensive patients**
Jiankai Dong, Huijie Yang, Yaping Zhang, Lianglong Chen and Quanzhong Hu
- 19 **Investigate the genetic mechanisms of diabetic kidney disease complicated with inflammatory bowel disease through data mining and bioinformatic analysis**
Xiaoyu Zhang, Huijie Xiao, Shaojie Fu, Jinyu Yu, Yanli Cheng and Yang Jiang
- 31 **Prognostic value of low-density lipoprotein cholesterol in IgA nephropathy and establishment of nomogram model**
Zhang-Yu Tian, Ai-Mei Li, Ling Chu, Jing Hu, Xian Xie and Hao Zhang
- 40 **Cardiovascular-renal protective effect and molecular mechanism of finerenone in type 2 diabetic mellitus**
Ruolin Lv, Lili Xu, Lin Che, Song Liu, Yangang Wang and Bingzi Dong
- 55 **Identification of biomarkers for the diagnosis of chronic kidney disease (CKD) with non-alcoholic fatty liver disease (NAFLD) by bioinformatics analysis and machine learning**
Yang Cao, Yiwei Du, Weili Jia, Jian Ding, Juzheng Yuan, Hong Zhang, Xuan Zhang, Kaishan Tao and Zhaoxu Yang
- 67 **Autophagy and its therapeutic potential in diabetic nephropathy**
Yu-Peng Han, Li-Juan Liu, Jia-Lin Yan, Meng-Yuan Chen, Xiang-Fei Meng, Xin-Ru Zhou and Ling-Bo Qian
- 80 **Could METS-VF provide a clue as to the formation of kidney stones?**
Zhenyu Guo, Guoxiang Li, Yan Chen, Shuai Fan, Shuai Sun, Yunwu Hao and Wei Wang
- 88 **Association between remnant cholesterol and chronic kidney disease in Chinese hypertensive patients**
Ting Yuan, Congcong Ding, Yanyou Xie, Xinlei Zhou, Chong Xie, Tao Wang, Chao Yu, Wei Zhou, Lingjuan Zhu, Huihui Bao and Xiaoshu Cheng
- 96 **New potential biomarkers for early chronic kidney disease diagnosis in patients with different glucose tolerance status**
Velia Cassano, Corrado Pelaia, Giuseppe Armentaro, Sofia Miceli, Valeria Tallarico, Daniele Dallimonti Perini, Vanessa T. Fiorentino, Egidio Imbalzano, Raffaele Maio, Elena Succurro, Marta L. Hribal, Francesco Andreozzi, Giorgio Sesti and Angela Sciacqua

- 104 **mDIXON-Quant for differentiation of renal damage degree in patients with chronic kidney disease**
Yue Wang, Ye Ju, Qi An, Liangjie Lin and Ai Lian Liu
- 115 **Relationship between serum uric acid and estimated glomerular filtration rate in adolescents aged 12-19 years with different body mass indices: a cross-sectional study**
Qiuwei Tian, Caixia He, Zisai Wang, Marady Hun, Yi-Cheng Fu, Mingyi Zhao and Qingnan He
- 125 **The relationship between triglyceride-glucose index and albuminuria in United States adults**
Zhaoxiang Wang, Han Qian, Shao Zhong, Tian Gu, Mengjiao Xu and Qichao Yang
- 136 **Metabolic effects of vasopressin in pathophysiology of diabetic kidney disease**
Svetlana Lebedeva, Arus Margaryan, Elena Smolyarchuk, Andrey Nedorubov, Maria Materenchuk, Alexander Tonevitsky and Kerim Mutig
- 146 **Identification of the key immune-related genes and immune cell infiltration changes in renal interstitial fibrosis**
Zhitao Dong, Fangzhi Chen, Shuang Peng, Xiongfei Liu, Xingyang Liu, Lizhe Guo, E. Wang and Xiang Chen



OPEN ACCESS

EDITED AND REVIEWED BY
Ralf Jockers,
Université Paris Cité, France

*CORRESPONDENCE
Ningning Hou
✉ ningning.hou@sdsu.edu.cn
Guiting Lin
✉ guiting.lin@ucsf.edu

[†]These authors have contributed equally to this work

RECEIVED 03 June 2024
ACCEPTED 05 June 2024
PUBLISHED 13 June 2024

CITATION
Zhang K, Sun W, Lin G and Hou N (2024)
Editorial: The link between metabolic
syndrome and chronic kidney disease: focus
on diagnosis and therapeutics - volume II.
Front. Endocrinol. 15:1442803.
doi: 10.3389/fendo.2024.1442803

COPYRIGHT
© 2024 Zhang, Sun, Lin and Hou. This is an
open-access article distributed under the terms
of the [Creative Commons Attribution License](#)
(CC BY). The use, distribution or reproduction
in other forums is permitted, provided the
original author(s) and the copyright owner(s)
are credited and that the original publication
in this journal is cited, in accordance with
accepted academic practice. No use,
distribution or reproduction is permitted
which does not comply with these terms.

Editorial: The link between metabolic syndrome and chronic kidney disease: focus on diagnosis and therapeutics - volume II

Kexin Zhang^{1†}, Weixia Sun^{2†}, Guiting Lin^{3*} and Ningning Hou^{1*}

¹Department of Endocrinology and Metabolism, Clinical Research Center, Shandong Provincial Key Medical and Health Discipline of Endocrinology, Affiliated Hospital of Shandong Second Medical University, Weifang, China, ²Department of Nephrology, the First Hospital of Jilin University, Jilin, China, ³Knappe Molecular Urology Laboratory, Department of Urology, University of California, San Francisco, San Francisco, CA, United States

KEYWORDS

metabolic syndrome, obesity, chronic kidney disease, diagnosis, therapeutics

Editorial on the Research Topic

The link between metabolic syndrome and chronic kidney disease: focus on diagnosis and therapeutics - volume II

Metabolic syndrome (MS), characterized by obesity, hyperglycemia, hyperuricemia, etc., is intricately associated with the development of chronic kidney disease (CKD) (1–3). Understanding this association has become paramount due to the rising prevalence of MS. However, the diverse pathophysiology of kidney injury stemming from various metabolic risk factors pose challenges for accurate diagnosis and effective therapy. Investigating the interactions between MS-related ailments and CKD is crucial for enhancing diagnostic and therapeutic approaches. This Research Topic provides a comprehensive platform for presenting recent advancements in diagnosing and treating multiple MS-related CKD, comprising a total of 14 articles, including 10 original research articles, 3 review articles, and 1 hypothesis and theory article.

One significant area of interest lies in identifying biomarkers heralding CKD onset or progression in individuals with MS. The Triglyceride-glucose (TyG) index emerges as a calculated measure used in clinical research to assess insulin resistance. Wang et al. underscore the significance of the TyG index as a valuable marker for assessing metabolic dysfunction and its association with albuminuria in the adult population of the United States. They found that elevated TyG index levels were independently linked to albuminuria, demonstrating its superiority over traditional indicators such as insulin resistance in predicting albuminuria. Similarly, Dong et al. highlight the significant association between the TyG index and early renal impairment in hypertensive patients. Elevated TyG index levels correlate with increased serum levels of β 2-microglobulin and cystatin C, suggesting a role in renal dysfunction progression. However, caution is advised in using the TyG index alone as a predictor since it falls short of surpassing traditional markers like triglycerides in predicting early renal impairment. Further research is needed

to clarify its utility and limitations in assessing renal health, highlighting the need for further investigation.

In addition, lipid metabolism emerges as pivotal in CKD progression, with [Tian et al.](#) presenting a nomogram model integrating low-density lipoprotein cholesterol levels for precise prognostication in IgA nephropathy. The association between remnant cholesterol (RC) levels and CKD in hypertensive patients, as elucidated by [Yuan et al.](#), further underscores the importance of lipid management in CKD prevention and treatment. They found a linear positive relationship between RC and CKD risk. Subgroup analysis further indicated a more pronounced association among patients with a BMI ≥ 24 kg/m² and those who were current non-smokers. Their findings provide valuable insights into the modifiable risk factors for CKD in high-risk populations, informing targeted interventions and personalized management strategies.

Identifying new biomarkers for early CKD diagnosis is crucial, especially in newly diagnosed patients with different glycemic statuses. [Cassano et al.](#) discovered that elevated 1-hour post-load glucose levels (≥ 155 mg/dl) are linked to higher CKD risk in these patients. They also observed escalating oxidative stress, platelet activation, and deteriorating metabolic profiles in early CKD. Moreover, the exploration of novel markers such as METS-VF for kidney stone risk assessment, as investigated by [Guo et al.](#), highlights the multifaceted nature of MS-related renal complications. Research utilizing NHANES data investigated METS-VF's correlation with kidney stones in 29,246 participants. Results uncovered a positive correlation between METS-VF and kidney stone prevalence and progression. These findings underscore the potential of METS-VF as a marker for assessing kidney stone risk and emphasize the crucial role of addressing visceral fat in preventive strategies.

Diagnostic innovations also take center stage, with [Cao et al.](#) leveraging bioinformatics analysis and machine learning to identify biomarkers for CKD in patients with non-alcoholic fatty liver disease (NAFLD). The study identifies four diagnostic markers (DUSP1, NR4A1, FOSB, ZFP36) enriched in immune-related pathways and inflammatory responses, showing promising diagnostic utility in CKD patients with NAFLD. Moreover, innovative imaging techniques, such as mDIXON-Quant, offer promise for early CKD diagnosis and assessment of renal damage severity. [Wang et al.](#)'s retrospective study underscores the clinical promise of mDIXON-Quant imaging for early CKD detection and assessing renal damage severity, fostering enhanced patient stratification and management approaches.

Advancements in biomarker diagnosis for CKD are paving the way for personalized early detection and treatment strategies. [Tian et al.](#)'s cross-sectional study underscores serum uric acid (SUA) levels as an independent risk factor for CKD in adolescents, advocating for early monitoring and intervention, especially across diverse BMI populations. They found a negative association between SUA and eGFR, notably among adolescents aged 12–19 years. Higher BMI correlated with elevated SUA, impacting eGFR, particularly in underweight adolescents. Tailored CKD prevention and management strategies in adolescence are warranted based on these findings.

Optimal treatment for CKD remains a significant challenge beyond diagnosis. Emerging therapeutic modalities offer hope for improved outcomes in patients with MS-related CKD. [Lv et al.](#)'s review on finerenone underscores its potential in mitigating cardiovascular and renal complications in type 2 diabetes patients with CKD. As a third-generation mineralocorticoid receptor antagonist, finerenone offers improved safety and efficacy, potentially benefiting not only cardiovascular and renal health but also conditions like diabetic kidney disease (DKD). The heightened selectivity and efficacy of finerenone present a promising avenue for addressing the intricate web of metabolic and renal dysfunction in these patients.

Vasopressin, known as a stress hormone, influences kidney function and metabolism through various receptor types. [Lebedeva et al.](#) explore how elevated plasma vasopressin levels contribute to the pathophysiology of DKD. Excessive activation of renal V2 receptors leads to glomerular hyperfiltration, while stimulation of extra-renal V1a/V1b receptors worsens DKD by promoting catabolic metabolism. Selective vasopressin receptor antagonists show promise in separating renal and extra-renal effects, offering potential for therapeutic development. Understanding these mechanisms is vital for advancing future treatment strategies for DKD.

[Dong et al.](#) identified immune-related genes (IRGs) with potential as therapeutic targets for renal interstitial fibrosis (RIF) in CKD. They pinpointed 17 IRGs associated with immune response, highlighting six key ones: apolipoprotein H, epidermal growth factor, lactotransferrin, lysozyme, phospholipid transfer protein, and secretory leukocyte peptidase inhibitor. Further analysis revealed these IRGs' connections to T cell populations and the NF- κ B signaling pathway, suggesting their promise for RIF treatment in CKD.

[Han et al.](#)'s review highlights autophagy as a promising therapeutic target in DKD. Dysregulated autophagy, influenced by nutrient-sensing and stress pathways such as AMPK, mTOR, and oxidative stress, drives DKD progression by disrupting cellular homeostasis. Targeted interventions aimed at restoring autophagic flux hold promise for mitigating renal dysfunction in DKD, offering hope for improved patient outcomes in addressing this pressing public health concern.

[Zhang et al.](#) conducted a thorough analysis of the genetic landscape of DKD complicated with inflammatory bowel disease IBD. They identified 495 risk genes, with MMP2, HGF, FGF2, IL-18, IL-13, and CCL5 emerging as key players. These genes are involved in inflammatory responses, oxidative stress, and immune dysfunction, suggesting potential targets for personalized treatments.

In summary, this research topic signifies a notable advancement in elucidating the complex interplay between MS and CKD. From novel biomarkers and therapeutic targets to innovative diagnostic modalities, the contributions within this collection pave the way for improved patient outcomes and personalized management strategies in this complex and multifaceted disease paradigm. Collaboration across disciplines and concerted research efforts will be essential in translating these findings into clinical practice and improving patient lives worldwide.

Author contributions

KZ: Conceptualization, Investigation, Writing – review & editing, Formal analysis, Methodology, Writing – original draft. WS: Conceptualization, Investigation, Methodology, Writing – original draft. GL: Conceptualization, Writing – review & editing, Data curation, Project administration, Supervision, Validation. NH: Conceptualization, Investigation, Supervision, Validation, Writing – review & editing.

Acknowledgments

We are grateful to all the authors and reviewers for their excellent contributions and insightful comments to this Research Topic.

References

1. Katsiki N, Anagnostis P, Kotsa K, Goulis DG, Mikhailidis DP. Obesity, metabolic syndrome and the risk of microvascular complications in patients with diabetes mellitus. *Curr Pharm Des.* (2019) 25:2051–9. doi: 10.2174/1381612825666190708192134
2. Li X, Liang Q, Zhong J, Gan L, Zuo L. The effect of metabolic syndrome and its individual components on renal function: A meta-analysis. *J Clin Med.* (2023) 12:1614. doi: 10.3390/jcm12041614
3. Copur S, Demiray A, Kanbay M. Uric acid in metabolic syndrome: Does uric acid have a definitive role. *Eur J Intern Med.* (2022) 103:4–12. doi: 10.1016/j.ejim.2022.04.022

Conflict of interest

The authors declare that the research was conducted in the absence of any commercial or financial relationships that could be construed as a potential conflict of interest.

Publisher's note

All claims expressed in this article are solely those of the authors and do not necessarily represent those of their affiliated organizations, or those of the publisher, the editors and the reviewers. Any product that may be evaluated in this article, or claim that may be made by its manufacturer, is not guaranteed or endorsed by the publisher.



OPEN ACCESS

EDITED BY

Ningning Hou,
Affiliated Hospital of Weifang Medical
University, China

REVIEWED BY

Josef Fritz,
Innsbruck Medical University, Austria
Antonio Junior Lepedda,
University of Sassari, Italy

*CORRESPONDENCE

Lianglong Chen
✉ chen19720000@163.com
Quanzhong Hu
✉ qinghaihospital@126.com

[†]These authors have contributed
equally to this work

SPECIALTY SECTION

This article was submitted to
Renal Endocrinology,
a section of the journal
Frontiers in Endocrinology

RECEIVED 07 September 2022

ACCEPTED 02 December 2022

PUBLISHED 14 December 2022

CITATION

Dong J, Yang H, Zhang Y, Chen L and
Hu Q (2022) A high triglyceride
glucose index is associated with early
renal impairment in the
hypertensive patients.
Front. Endocrinol. 13:1038758.
doi: 10.3389/fendo.2022.1038758

COPYRIGHT

© 2022 Dong, Yang, Zhang, Chen and
Hu. This is an open-access article
distributed under the terms of the
Creative Commons Attribution License
(CC BY). The use, distribution or
reproduction in other forums is
permitted, provided the original
author(s) and the copyright owner(s)
are credited and that the original
publication in this journal is cited, in
accordance with accepted academic
practice. No use, distribution or
reproduction is permitted which does
not comply with these terms.

A high triglyceride glucose index is associated with early renal impairment in the hypertensive patients

Jiankai Dong ^{1†}, Huijie Yang ^{2†}, Yaping Zhang ², Lianglong Chen ^{1*} and Quanzhong Hu ^{2*}

¹Department of Cardiology, Fujian Medical University Union Hospital, Fujian Cardiovascular Medical Center, Fujian Institute of Coronary Heart Disease, Fuzhou, China, ²Department of Cardiology, Qinghai Provincial People's Hospital, Xining, China

Objective: Serum β 2-microglobulin (β 2-MG) and serum cystatin C (CysC) are sensitive and reliable indicators of early renal impairment. Triglyceride glucose index (TyG) is an emerging vital indicator of insulin resistance and is associated with increased risk of hypertension. We aimed to analyze the relationship between TyG and early renal impairment in hypertensive patients.

Methods: A retrospective analysis was performed on 881 hypertensive patients treated in Qinghai Provincial People's Hospital from March 2018 to March 2021, their clinical data and corresponding laboratory index values were recorded, and the TyG index was calculated. According to the TyG index, the patients were divided into a low TyG (L-TyG) group ($\text{TyG} \leq 8.50$, $n=306$), medium TyG (M-TyG) group ($8.51 \leq \text{TyG} \leq 8.94$, $n=281$), and high TyG (H-TyG) group ($\text{TyG} > 8.95$, $n=294$) in sequence by using tertiles. Then, according to serum β 2-MG and CysC levels, they were divided into a normal renal function group (β 2-MG ≤ 2.4 mg/L, $n=700$ and CysC ≤ 1.25 mg/L, $n=721$) and a renal function injury group (β 2-MG > 2.4 mg/L, $n=181$, and CysC > 1.25 mg/L, $n=160$). Multivariate linear regression analysis was used to analyze the influencing factors of serum β 2-microglobulin and cystatin C. Multivariate Logistic regression was used to analyze the relationship between the TyG index and early renal impairment in hypertensive patients. The receiver operating characteristic curve (ROC) was used to determine the value of the TyG index in predicting early renal impairment in patients with hypertension.

Result: As the TyG index level increased, serum β 2-MG and CysC levels also gradually increased. Multivariate linear regression analysis showed that TyG index was the influencing factor of serum β 2-MG ($B=0.060$, $P=0.007$) and serum CysC ($B=0.096$, $P<0.001$). For every 1 standard deviation increase in the TyG index, the serum β 2-MG and CysC increased by 0.06mg/L and 0.096mg/L, respectively. When compared to the normal group, the TyG level (8.91 ± 0.65 vs 8.64 ± 0.60 , $P<0.001$) was higher in the renal impairment group with β 2-MG > 2.4 mg/L. The results of multivariate logistic regression analysis revealed that for every 1 standard deviation increase in the TyG index, the risk of early

renal impairment in hypertensive patients increased 1.53 times (OR=1.53, 95% CI 1.006–2.303). The ROC curves showed that the TyG index was not superior to TG in predicting early renal impairment in hypertensive patients. The AUC values were 0.623 and 0.617, respectively. Then, when CysC > 1.25 mg/L was used as the renal damage group, the level of TyG was still higher than that in the normal group (8.94 ± 0.67 and 8.64 ± 0.60 , $P < 0.001$). Multivariate Logistic regression analysis showed that for every 1 standard deviation increase in the TyG index, the risk of early renal impairment in hypertensive patients increased 2.82 times (OR=2.82, 95%CI 1.863–4.262). The ROC curves showed that the TyG index was not superior to TG in predicting early renal impairment in hypertensive patients. The AUC values were 0.629 and 0.626, respectively.

Conclusion: TyG index is an influential factor in serum $\beta 2$ -MG and CysC levels. The elevated TyG index levels are closely associated with the occurrence and development of early renal impairment in hypertensive patients, but it should be used cautiously in the prediction of early renal impairment.

KEYWORDS

hypertension, triglyceride glucose index, insulin resistance, renal impairment, $\beta 2$ microglobulin, Urine microalbumin, cystatin C

1 Introduction

With an aging population, hypertension has become the most important risk factor for cardiovascular disease morbidity and mortality (1). In addition, hypertension is a long-term progressive chronic disease, and renal injury is its major complication. Currently, serum urea nitrogen, serum creatinine (SCr) and glomerular filtration rate (GFR) are widely used clinically to evaluate renal function. but the diagnostic specificity is low due to the high storage capacity of the kidney and the influence of drugs, age and glomerular filtration rate. Studies have shown that urine microalbumin, serum $\beta 2$ -microglobulin ($\beta 2$ -MG) and serum cystatin C (CysC) are sensitive and reliable indicators of early renal injury, and their sensitivity and specificity are higher than those of serum urea nitrogen and serum creatinine (2, 3).

Insulin resistance (IR) is common in patients with hypertension (4), and IR is strongly associated with the prevalence of chronic renal insufficiency (5). A recent study found that the triglyceride-glucose index (TyG index) derived from the log-transformation of the product of plasma triglyceride (TG) and fasting plasma glucose (FPG) was a potential IR marker (6, 7). It has been shown that an elevated TyG index is associated with the occurrence and development of atherosclerosis (8), coronary artery disease (8), hypertension (9), diabetes (10), Diabetic kidney disease (11), nonalcoholic fatty liver (12), and nephric microvascular damage (13), etc. However, there are few reports on the relationship

between the TyG index and early renal injury in hypertensive patients at home and abroad.

Therefore, this study aimed to investigate the correlation between the TyG index and early renal impairment in hypertensive patients, to provide a reference basis for the early prevention, monitoring, and treatment of chronic kidney disease (CKD).

2 Patients & methods

2.1 Study population

A total of 881 inpatients with primary hypertension from March 2018 to March 2021 in Qinghai Provincial People's Hospital were included as the subjects, including 464 males and 417 females, aged from 40 to 92 years old, with an average age of (60.06 ± 12.23) years old.

Inclusion criteria: ① Age ≥ 40 years old, no sex limitation, and complete clinical data. ② Hypertension was defined as having two independent blood pressure measurements $\geq 140/90$ mmHg or having received antihypertensive drug treatment. ③ eGFR ≥ 60 ml/min/1.73m².

Exclusion criteria: secondary hypertension, coronary atherosclerotic heart disease, heart failure, diabetes; Various acute and chronic infectious diseases, primary glomerular disease, renal artery stenosis; Patients with severe liver and

kidney function impairment; Thyroid disease, malignant tumor, clear familial hyperlipidemia, and lipid-lowering drugs in the past 1 month; Cognitive dysfunction, mental illness. The study protocol was approved by the Ethics Committee of Qinghai Provincial People's Hospital. All participants signed the informed consent.

2.2 Data collection

Clinical data such as sex, age, body weight, smoking history, and duration of hypertension of the subjects were accurately recorded, and body mass index (BMI) was calculated as follows.

$$\text{BMI} = \text{body mass (kg)} / \text{height (m)}^2$$

All subjects fasted for 10–12 hours one day before the experiment, 4–5 mL venous blood were drawn next morning, and the serum was collected after centrifugation at 4 000 r/min. The fasting plasma glucose (FPG) was measured by the glucose oxidase method. Triglyceride (TG), urea nitrogen (BUN), serum creatinine (Scr), total cholesterol (TC), high-density lipoprotein cholesterol (HDL-C), low-density lipoprotein cholesterol (LDL-C), and serum uric acid (SUA) were measured by enzyme method. Serum β 2-microglobulin (0.8–2.4 mg/L) was determined by ELISA, and cystatin C (0.54–1.25 mg/L) was determined by latex nephelometry. The above indexes were performed with a Beckman AU5800 automatic biochemical analyzer. The estimated glomerular filtration rate (eGFR) was calculated using the CKD-EPI formula.

2.3 Groups

TyG index (6) = $\ln[\text{fasting TG (mg/dL)} \times \text{FBG (mg/dL)} / 2]$, where TG (1 mg/dL = 0.011 mmol/L) and FBG (1 mg/dL = 0.056 mmol/L). According to the TyG index, patients were divided into a low TyG (L-TyG) group ($\text{TyG} \leq 8.50$, $n=306$), medium TyG (M-TyG) group ($8.51 \leq \text{TyG} \leq 8.94$, $n=281$) and high TyG (H-TyG) group ($\text{TyG} > 8.95$, $n=294$) in sequence by using tertiles. In addition, 881 hypertensive patients were divided into a normal renal function group (serum β 2-MG ≤ 2.4 mg/L and CysC ≤ 1.25 mg/L) and an impaired renal function group (serum β 2-MG > 2.4 mg/L and CysC > 1.25 mg/L) according to serum β 2-MG and CysC levels.

2.4 Statistical analysis

Statistical analysis was performed using SPSS 26.0 (SPSS Inc.). The single-sample k-s test (two-sided test) was used to test whether the measurement data conformed to a normal distribution. Measurement data of normal distribution are

expressed as the mean \pm standard deviation. Student's t-test was used for comparisons between two groups, a one-way analysis of variance was used for comparisons among three groups, and the LSD test was used for pairwise comparisons between groups. The measurement data with a nonnormal distribution are expressed as M(Q25, Q75). Means of 2 groups were compared using the Mann-Whitney U test. Multiple-group comparisons were made by Kruskal-Wallis tests. Enumeration data were compared using the χ^2 test. Multifactor linear stepwise regression was used to analyze the influencing factors of serum β 2-microglobulin and cystatin C. Logistic regression analysis was used to analyze the influencing factors of early renal impairment in patients with hypertension. The receiver operating characteristic curve (ROC) was used to determine the value of the TyG index in predicting early renal impairment in patients with hypertension. $P < 0.05$ was considered statistically significant.

3 Results

3.1 Comparison of general data and clinical indicators among three groups of TyG index

A total of 881 patients (mean age 60.06 ± 12.23 years, 464 men) with hypertension were included in the study. The baseline clinical characteristics and laboratory measurements of patients within the groups are presented in Table 1. Participants were grouped into tertiles according to their TyG level. There were no significant differences among the three groups in sex, smoking history, BMI, hypertension course, HS-CRP, mALB, BUN and eGFR levels ($P > 0.05$). The levels of TC, HDL-C, LDL-C, Alb, TG, FBG, β 2-MG, CysC and SUA were compared and the differences were statistically different ($P < 0.05$, as shown in Table 1). Besides, the levels of β 2-MG (1.96 ± 0.82) and CysC (1.04 ± 0.27) in the M-TyG group were significantly higher than that in the L-TyG group (1.87 ± 0.65 and 1.03 ± 0.44). The levels in the H-TyG group (2.29 ± 1.04 and 1.18 ± 0.44) were significantly higher than that in the M-TyG group (1.96 ± 0.82 and 1.04 ± 0.27).

3.2 Multivariate linear regression analysis

The relationship between the TyG index and early renal injury indicators was analyzed by Multivariate linear regression with serum β 2-MG and serum cystatin C as dependent variables and age, BMI, TC, hypertension course, LDL-C, Alb, HS-CRP, HDL-C, eGFR, SUA, TyG index, BUN, mALB and Sex as independent variables. The results showed that the TyG index level was an influencing factor of serum β 2-MG ($B=0.060$, 95%

TABLE 1 Comparison of general data and clinical indicators of the L-TyG group, M-TyG group, and H-TyG.

	L-TyG group (n=306)	M-TyG group (n=281)	H-TyG group (n=294)	P value
Male [n,(%)]	175 (57.2%)	135 (48.0%)	155 (52.7%)	0.086
Smoking history [, (%)]	64 (20.9%)	54 (19.2%)	80 (27.2)	0.052
Age (y)	62.00 ± 12.92	60.53 ± 11.85	57.61 ± 11.47 ^{ab}	<0.001
BMI (kg/m ²)	25.09 ± 4.11	25.59 ± 3.79	25.64 ± 3.62	0.153
hypertension course (months)	60.00 (36.00-120.00)	60.00 (24.00-120.00)	54.00 (24.00-120.00)	0.103
TC (mmol/l)	3.97 ± 0.89	4.32 ± 0.83 ^a	4.38 ± 2.22 ^{ab}	<0.001
HDL-C (mmol/L)	1.11 ± 0.29	1.05 ± 0.22 ^a	0.97 ± 0.20 ^{ab}	<0.001
LDL-C (mmol/L)	2.40 ± 0.74	2.68 ± 0.70 ^a	2.72 ± 0.77 ^a	<0.001
Alb (mg/L)	39.05 ± 4.24	40.22 ± 3.86 ^a	40.88 ± 3.93 ^a	<0.001
Scr (μmol/L)	68.48 ± 14.17	69.57 ± 13.64	71.59 ± 14.93 ^a	0.026
eGFR[ml.min ⁻¹ .(1.73m ²)-1]	94.96 ± 16.13	92.68 ± 16.64	92.93 ± 17.76	0.179
HS-CRP (mg/dl)	0.13 (0.06-0.33)	0.14 (0.06-0.29)	0.15 (0.08-0.30)	0.465
BUN (mmol/L)	5.75 ± 1.67	5.49 ± 1.51	5.57 ± 1.42	0.138
SUA (μmol/L)	347.54 ± 109.99	358.45 ± 96.54	385.25 ± 104.74 ^{ab}	<0.001
TG (mmol/L)	0.92 ± 0.29	1.63 ± 0.32 ^a	2.99 ± 0.84 ^{ab}	<0.001
FBG (mmol/L)	4.50 ± 0.61	4.78 ± 0.56 ^a	5.20 ± 0.53 ^{ab}	<0.001
mALB (mg/L)	1.00 (0.59-2.45)	1.06 (0.61-2.16)	1.11 (0.59-2.36)	0.957
β ₂ -MG (mg/L)	1.87 ± 0.65	1.96 ± 0.82	2.29 ± 1.04 ^{ab}	<0.001
CysC (mg/L)	1.03 ± 0.44	1.04 ± 0.27	1.18 ± 0.44 ^{ab}	<0.001

Data are expressed as the mean ± SD, median (25th–75th percentiles), or number (percentage). BMI, body mass index; Fib, fibrinogen; TC, cholesterol; HDL-C, high-density lipoprotein cholesterol level; LDL-C, low-density lipoprotein cholesterol level; Alb, albumin; Scr, serum creatinine; eGFR, estimated glomerular filtration rate; HS-CRP, high-sensitivity C-reactive protein; BUN, Blood Urea Nitrogen; SUA, Serum uric acid; TG, triglyceride; FBG, fasting blood-glucose; mALB, urine microalbumin; β₂-MG, serum β₂ microglobulin; CysC, Serum cystatin C.

^ap < 0.05 compared with the L-TyG group; p < 0.01 compared with the M-TyG group.

CI 0.017–0.103, P=0.007) and CysC (B=0.096, 95%CI 0.055–0.137, P<0.001). For every 1 standard deviation increase in the TyG index, the serum β₂-MG and CysC increased by 0.06mg/L and 0.096mg/L, respectively (Table 2).

3.3 Comparison of general data and clinical index between two groups on β₂-MG level

Patients were divided into a normal renal function group (β₂-MG ≤ 2.4 mg/L) and an impaired renal function group (β₂-MG > 2.4 mg/L) according to β₂-MG level. The age of patients in the renal impairment group (66.54 ± 12.19) was significantly higher than that in the normal renal function group (58.40 ± 11.69, P<0.001), and there was no significant difference in the levels of sex, smoking history, BMI, TC, LDL-C or mALB between the two groups (P>0.05). The levels of hypertension course, Scr, HS-CRP, BUN, SUA, TG and TyG index in the renal function injury group were significantly higher than those in the normal renal function

group. HDL-C, Alb, and eGFR levels were significantly lower than those in the normal renal function group, and the differences were statistically significant (P<0.05, see Table 3).

3.4 Comparison of general data and clinical index between two groups on the level of CysC

Patients were divided into a normal renal function group (CysC ≤ 1.25 mg/L) and an impaired renal function group (CysC > 1.25 mg/L) according to CysC level. There was no significant difference in the levels of sex, BMI, TC, HDL-C, LDL-C or mALB levels between the two groups (P>0.05). The levels of age, hypertension course, Scr, HS-CRP, BUN, SUA, TG, and TyG index in the renal impairment group were significantly higher than those in the normal renal function group. The smoking history, Alb, and eGFR levels were significantly lower than those in the normal renal function group, and the differences were statistically significant (P<0.05, see Table 4).

TABLE 2 Multivariate linear regression analysis.

Dependent variable	Independent variable	B	SE	Beta	t	P value	95% CI
β 2-MG	Age	0.004	0.001	0.113	2.811	0.005	(0.001, 0.006)
	BMI	0.005	0.003	0.047	1.519	0.129	(-0.001, 0.011)
	hypertension course	0.001	0.002	0.01	0.307	0.759	(-0.003, 0.004)
	TC	0.01	0.006	0.057	1.794	0.073	(-0.001, 0.022)
	LDL-C	-0.007	0.018	-0.014	-0.414	0.679	(-0.042, 0.027)
	mALB	0	0.001	0.011	0.348	0.728	(-0.002, 0.003)
	eGFR	-0.006	0.001	-0.262	-6.508	<0.001	(-0.008, -0.004)
	Alb	-0.006	0.003	-0.058	-1.73	0.084	(-0.012, 0.001)
	HS-CRP	0.083	0.017	0.152	4.91	<0.001	(0.05, 0.117)
	SUA	0.001	0	0.136	3.671	<0.001	(0, 0.001)
	BUN	0.007	0.009	0.026	0.793	0.428	(-0.01, 0.024)
	HDL-C	-0.132	0.055	-0.082	-2.399	0.017	(-0.24, -0.024)
	TyG index	0.060	0.022	0.092	2.714	0.007	(0.017, 0.103)
	Sex (Male)	0.071	0.029	0.088	2.408	0.016	(0.013, 0.129)
CysC	Age	0.003	0.001	0.095	2.357	0.019	(0, 0.005)
	BMI	-0.003	0.003	-0.034	-1.102	0.271	(-0.009, 0.003)
	hypertension course	0.001	0.002	0.018	0.542	0.588	(-0.003, 0.004)
	TC	-0.008	0.006	-0.046	-1.422	0.155	(-0.019, 0.003)
	LDL-C	0.012	0.017	0.023	0.71	0.478	(-0.021, 0.045)
	mALB	0.003	0.001	0.075	2.461	0.014	(0.001, 0.005)
	eGFR	-0.006	0.001	-0.256	-6.342	<0.001	(-0.008, -0.004)
	Alb	-0.008	0.003	-0.087	-2.591	0.010	(-0.014, -0.002)
	HS-CRP	0.046	0.016	0.088	2.836	0.005	(0.014, 0.078)
	SUA	0	0	0.131	3.529	<0.001	(0, 0.001)
	BUN	0.019	0.008	0.075	2.252	0.025	(0.002, 0.035)
	HDL-C	0.058	0.053	0.038	1.11	0.267	(-0.045, 0.162)
	TyG index	0.096	0.021	0.155	4.545	<0.001	(0.055, 0.137)
	Sex(Male)	-0.054	0.028	-0.07	-1.913	0.056	(-0.109, 0.001)

Abbreviations as given in Table 1.

3.5 Multi-factor logistic regression analysis of influencing factors of early renal impairment in patients with hypertension

Taking the occurrence of renal impairment (β 2-MG>2.4 mg/L) as the dependent variable, and taking age, BMI, total cholesterol, hypertension course, LDL-C, Alb, HS-CRP, HDL-C, eGFR, SUA, TyG index, BUN, mALB, and Sex as the independent variables, a multivariate Logistic regression analysis was performed. The results showed that age

(OR=1.03, 95%CI 1.011-1.055, P=0.003), TyG index (OR=1.53, 95%CI 1.008-2.319, P=0.046), HS-CRP (OR=1.81, 95%CI 1.349-2.415, P<0.001), SUA (OR=1.01, 95%CI 1.002-1.006, P=0.001), HDL-C (OR=0.29, 95%CI 1.349-2.415, P=0.014), eGFR (OR=0.95, 95%CI 0.932-0.964, P<0.001) and Male (OR=0.62, 95%CI 0.385-0.989, P=0.045), these were the risk factors for early renal impairment in patients with hypertension (P<0.05, see Table 5).

Then, renal impairment (CysC>1.25mg/L) was used as the dependent variable. A multivariate Logistic regression analysis was performed. The results showed that age (OR=1.04, 95%CI

TABLE 3 Comparison of general data and clinical index between two groups on β 2-MG level.

	Normal renal function group (n=700)	Impaired renal function group (n=181)	P value
Male [n,(%)]	380 (54.3%)	85 (47.0%)	0.079
Smoking history [n, (%)]	163 (23.3%)	35 (19.3%)	0.257
Age (y)	58.40 \pm 11.69	66.54 \pm 12.19	<0.001
BMI(kg/m ²)	25.31 \pm 3.71	25.93 \pm 4.36	0.084
hypertension course (months)	48.00 (24.00-120.00)	84.00 (36.00-132.00)	0.001
TC (mmol/l)	4.30 \pm 0.89	4.72 \pm 4.57	0.219
HDL-C (mmol/L)	1.06 \pm 0.24	0.99 \pm 0.29	0.001
LDL-C (mmol/L)	2.59 \pm 0.73	2.62 \pm 0.83	0.640
Alb (mg/L)	40.40 \pm 3.96	38.63 \pm 4.30	<0.001
Scr (μ mol/L)	68.32 \pm 13.63	75.87 \pm 15.31	<0.001
eGFR [ml.min ⁻¹ .(1.73m ²)-1]	96.91 \pm 15.58	80.60 \pm 15.35	<0.001
HS-CRP (mg/dl)	0.12 (0.06-0.26)	0.24 (0.11-0.56)	<0.001
BUN (mmol/L)	5.48 \pm 1.46	6.12 \pm 1.77	<0.001
SUA (μ mol/L)	353.31 \pm 96.08	403.43 \pm 127.48	<0.001
TG (mmol/L)	1.75 \pm 0.96	2.22 \pm 1.18	<0.001
FBG (mmol/L)	4.79 \pm 0.65	4.97 \pm 0.58	0.001
TyG index	8.64 \pm 0.60	8.91 \pm 0.65	<0.001
mALB (mg/dl)	1.01 (0.60-2.07)	1.19 (0.63-3.22)	0.051

Data are expressed as the mean \pm SD, median (25th–75th percentiles), or number (percentage). TyG index, Triglyceride glucose index.

1.015–1.062, $P=0.001$), TyG index (OR=2.98, 95%CI 1.954–4.535, $P<0.001$), HS-CRP (OR=1.40, 95%CI 1.095–1.792, $P=0.007$), SUA (OR=1.01, 95%CI 1.001–1.006, $P=0.002$), Alb (OR=0.93, 95%CI 0.871–0.985, $P=0.015$), eGFR (OR=0.95, 95%CI 0.938–0.970, $P<0.001$) and Male (OR=1.88, 95%CI 1.114–3.038, $P=0.013$), these were the risk factors for early renal impairment in patients with hypertension ($P<0.05$, see Table 6).

3.6 ROC curve of TyG index in predicting early renal impairment in hypertensive patients

The ROC curve of the TyG index predicting early renal impairment in hypertensive patients was further drawn. The renal impairment was defined as β 2-MG > 2.4 mg/L. The results showed that the area under the ROC curve of the TyG index in predicting early renal impairment in hypertensive patients was 0.623 ($P<0.001$; 95%CI 0.574–0.671), when the TyG index is 9.205, the Jouden index is 0.225, the sensitivity is 39.2%, and the specificity is 83.3%. The AUC of the FPG and TG levels for predicting early renal impairment occurs in hypertensive patients was 0.573 (95%CI 0.528–0.618, $P=0.002$) and 0.617 (95%CI 0.569–0.665, $P<0.001$), respectively (Figure 1).

Then with CysC >1.25 mg/L as the occurrence of renal impairment, the ROC curve of the TyG index predicting early renal impairment in hypertensive patients was also drawn, and the area under the curve was 0.629 ($P<0.001$; 95%CI 0.577–0.681), when the TyG index is 9.315, the maximum Jouden index is 0.266, the sensitivity is 38.8%, and the specificity is 87.8%. The AUC of the FPG and TG levels for predicting early renal impairment occurs in hypertensive patients was 0.570 (95%CI 0.522–0.619, $P=0.005$) and 0.626 (95%CI 0.574–0.678, $P<0.001$), respectively (Figure 2).

4 Discussion

This study investigated the relationship between the TyG index and early renal impairment in hypertensive patients. The results of Multivariate linear regression analysis showed that the level of TyG index was an influencing factor of serum β 2-MG and CysC. Logistic regression analysis showed that the relative risk of developing renal impairment was higher in patients with elevated TyG index, suggesting that the TyG index was significantly associated with early renal impairment in hypertensive patients.

CKD is associated with increased mortality, and one of the factors contributing to increased mortality is IR. IR is present in

TABLE 4 Comparison of general data and clinical index between two groups on the CysC level.

	Normal renal function group (n=721)	Impaired renal function group (n=160)	P value
Male [n,(%)]	369 (51.2%)	95 (59.4%)	0.063
Smoking history [n, (%)]	150 (20.8%)	47 (29.4%)	0.019
Age (y)	58.55 ± 11.74	66.94 ± 12.12	<0.001
BMI (kg/m ²)	25.43 ± 3.72	25.47 ± 4.45	0.927
hypertension course(months)	54.00 (24.00-120.00)	72.00 (36.00-153.00)	0.001
TC (mmol/l)	4.39 ± 2.40	4.39 ± 1.07	0.996
HDL-C (mmol/L)	1.06 ± 0.25	1.02 ± 0.26	0.122
LDL-C (mmol/L)	2.59 ± 0.73	2.65 ± 0.83	0.395
Alb (mg/L)	40.38 ± 3.95	38.50 ± 4.38	<0.001
Scr (μmol/L)	67.78 ± 13.83	79.25 ± 12.68	<0.001
eGFR [ml.min ⁻¹ .(1.73m ²) ⁻¹]	96.61 ± 15.85	79.72 ± 14.21	<0.001
HS-CRP (mg/dl)	0.13 (0.06-0.28)	0.22 (0.10-0.52)	<0.001
BUN (mmol/L)	5.44 ± 1.44	6.39 ± 1.75	<0.001
SUA (μmol/L)	352.42 ± 97.91	414.28 ± 121.40	<0.001
TG (mmol/L)	1.74 ± 0.94	2.32 ± 1.26	<0.001
FBG (mmol/L)	4.80 ± 0.63	4.95 ± 0.65	0.008
TyG index	8.64 ± 0.60	8.94 ± 0.67	<0.001
mALB (mg/L)	1.03 (0.60-2.10)	1.18 (0.63-3.52)	0.107

Data are expressed as mean ± SD, median (25th–75th percentiles), or number (percentage). TyG index, Triglyceride glucose index.

TABLE 5 Multivariate Logistic regression analysis of early renal impairment (β2-MG>2.4mg/L) in hypertensive patients.

	β	SE	Wald X ² value	P value	OR value	95%CI
Age	0.032	0.011	8.689	0.003	1.03	(1.011, 1.055)
BMI	0.046	0.026	3.163	0.075	1.05	(0.995, 1.101)
hypertension course	0	0.014	0.001	0.973	1	(0.974, 1.027)
TyG index	0.425	0.212	3.994	0.046	1.53	(1.008, 2.319)
TC	0.486	0.251	3.747	0.053	1.63	(0.994, 2.659)
LDL-C	-0.479	0.284	2.837	0.092	0.62	(0.355, 1.082)
Alb	-0.051	0.030	2.866	0.090	0.95	(0.896, 1.008)
HS-CRP	0.590	0.149	15.800	<0.001	1.81	(1.349, 2.415)
HDL-C	-1.243	0.506	6.037	0.014	0.29	(0.107, 0.778)
eGFR	-0.054	0.008	39.900	<0.001	0.95	(0.932, 0.964)
SUA	0.004	0.001	11.153	0.001	1.01	(1.002, 1.006)
BUN	0.015	0.070	0.045	0.832	1.02	(0.885, 1.163)
mALB	0.001	0.008	0.007	0.932	1.00	(0.986, 1.105)
Sex (Male)	-0.482	0.241	4.019	0.045	0.62	(0.385, 0.989)

Abbreviations as given in Table 1.

TABLE 6 Multivariate Logistic regression analysis of early renal impairment (CysC>1.25mg/L) in hypertensive patients.

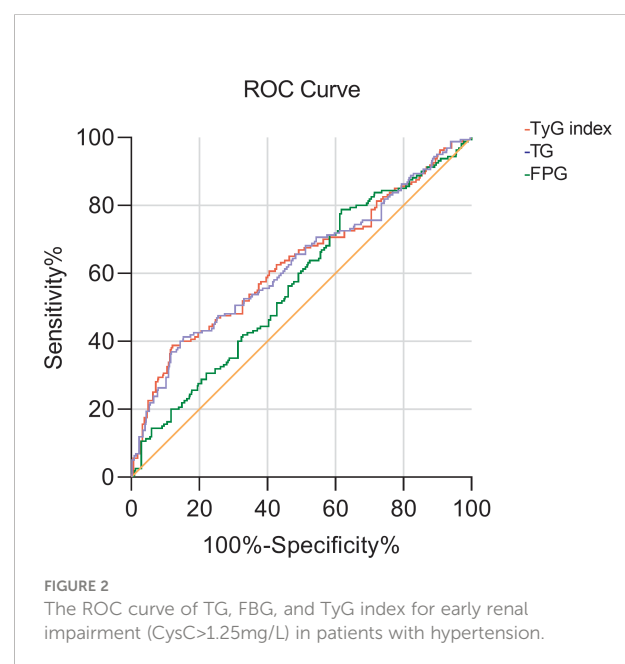
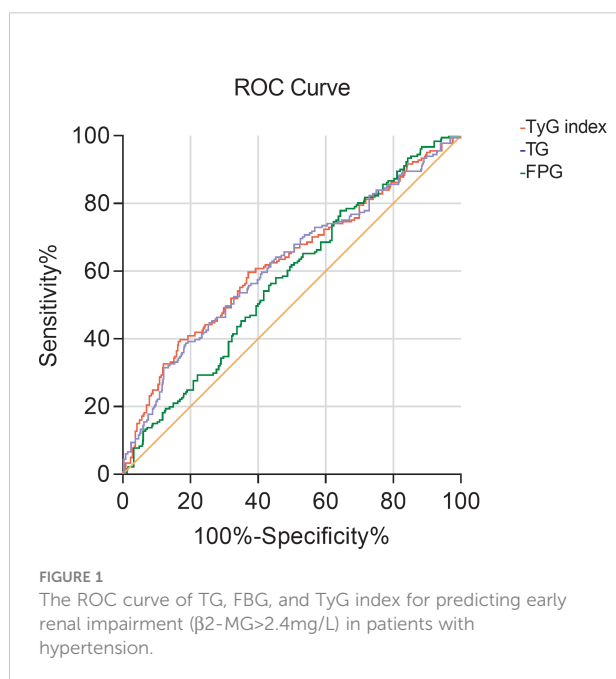
	β	SE	Wald χ^2 value	P value	OR value	95%CI
Age	0.038	0.012	10.387	0.001	1.04	(1.015, 1.062)
BMI	-0.19	0.028	0.462	0.497	0.99	(0.929, 1.036)
hypertension course	0.004	0.014	0.080	0.778	1.01	(0.977, 1.032)
TyG index	1.091	0.215	25.774	<0.001	2.98	(1.954, 4.535)
TC	-0.061	0.094	0.418	0.518	0.94	(0.782, 1.132)
LDL-C	0.080	0.174	0.214	0.644	1.09	(0.771, 1.524)
Alb	-0.076	0.032	5.884	0.015	0.93	(0.871, 0.985)
HS-CRP	0.337	0.126	7.197	0.007	1.40	(1.095, 1.792)
HDL-C	0.683	0.457	2.235	0.135	1.98	(0.809, 4.846)
eGFR	-0.048	0.009	31.172	<0.001	0.95	(0.938, 0.970)
SUA	0.004	0.001	9.987	0.002	1.01	(1.001, 1.006)
BUN	0.127	0.071	3.160	0.075	1.14	(0.987, 1.305)
mALB	0.013	0.009	2.006	0.157	1.013	(0.995, 1.032)
Sex (Male)	0.630	0.253	6.217	0.013	1.878	(1.144, 3.083)

Abbreviations as given in Table 1.

patients with early CKD and progressively worsens as the disease progresses to end-stage renal disease. IR may participate in the occurrence and development of CKD through such mechanisms as a hyperinsulinemic reaction (14), induction of oxidative stress (15), activation of a sympathetic renin-angiotensin-aldosterone system (16), activation of inflammatory factors (17), and inhibition of insulin signaling pathway (18). Cheng HT al

(19). have found that IR plays an important role in the occurrence and development of renal lesions in chronic renal diseases, which is associated with a rapid decline in the prevalence and renal function of CKD.

Microalbuminuria is an early manifestation of hypertensive renal injury and can be used as an early indication of renal injury (20). Urinary microalbumin cannot pass the glomerular



filtration membrane under physiological conditions, and its content is extremely low. When the glomerulus is damaged, the protein filtration barrier will be damaged, with increased permeability and excretion of microalbumin in urine. Hence, microalbuminuria is one of the sensitive indicators of early glomerular injury (21). However, the random urine test has mixed influencing factors, such as urine concentration and exercise, which can affect its test results, resulting in poor applicability of clinical diagnosis. In addition, BUN and SCr are widely used clinically to evaluate renal function. However, due to the strong renal storage capacity, as well as the influence of drugs, age, glomerular filtration rate and other factors, significant abnormalities only appear in severe renal impairment, and its diagnostic specificity is low in the early stage of renal impairment. Therefore, in this study, the correlation between the TyG index and markers of renal disease such as mAlb, eGFR and BUN was small. CysC is a cysteine protease inhibitor, produced by nucleated cells. This molecule is widely present in tissues throughout the body and is produced at a constant rate (22). The kidney is the only organ of CysC clearance and the glomerular filtration rate determines its concentration in the serum. Therefore, CysC is a sensitive indicator reflecting the glomerular filtration rate (23). The previous study has found that the sensitivity and specificity of CysC in the diagnosis of kidney injury were superior to those of creatinine and urea nitrogen, and it had higher sensitivity and stronger specificity, which gradually increased with the aggravation of the disease (24). Meanwhile, Khan et al. (25) studied 300 patients with CKD aged ≥ 65 and found that CysC was not related to body mass index and age of patients, and CysC had better performance than serum creatinine in assessing the renal function of patients, which is consistent with the results of this study. $\beta 2$ -MG is a small molecular protein with low content in the body, but the concentration remains constant. $\beta 2$ -MG is excreted through the glomerular filtration membrane, and decreased glomerular filtration rate can lead to increased $\beta 2$ -MG level, suggesting impairment of renal function. Studies have confirmed that the abnormal rate of $\beta 2$ -MG reaches 42.07% when the serum creatinine is increased by 0.7%, which is a sensitive indicator of early lesions in hypertensive kidney injury (26).

IR is an underlying condition for hypertension onset (27). The current gold standard for IR measurement is the normal blood glucose clamp test. However, due to the time-consuming, expensive, and complex nature of glucose clamp testing, it is difficult to apply in large-population research and clinical settings. Guerrero-Romero et al. (7) investigated a TyG index derived from fasting triglyceride and glucose concentrations as an IR index and validated it against the normoglycemic clamp test in a Mexican population, showing its superiority over HOMA-IR. Studies have confirmed that the TyG index predicts the development of hypertension in Chinese populations (28) and may reflect cardiac remodeling,

dysfunction, and atherosclerosis (29). KHAN et al. (30) found a high positive correlation between the TyG index and urine albumin creatine ratio in a cross-sectional study that included 227 patients with metabolic syndrome. Fritz et al. (31) found that the TyG index appeared to be associated with ESKD risk and mediates nearly half of the total association between BMI and ESKD in the general population. This study was the first to explore the relationship between the TyG index and early renal impairment in hypertensive patients. Because of the special geographical location of our hospital in the northwest plateau, we have a medical center for hypertension, so our study mainly included patients whose blood pressure was unstable at an early stage, and who did not have heart disease, tumors, etc. This is the advantage of our study, which can better assess the relationship between the TyG index and early renal function in hypertensive patients. The results showed that markers of early renal impairment such as serum $\beta 2$ -MG and CysC in the H-TyG index group were significantly higher than those in the M-TyG group and L-TyG group, and the level in the M-TyG group was also higher than that in the L-TyG group. However, the results of this study showed that the TyG index was not related to urinary microalbumin, which could be affected by several confounding factors. In addition, $\beta 2$ -MG > 2.4 mg/L and CysC > 1.25 mg/L in serum were considered as the early stage of renal impairment. All the results have shown that the TyG index level in the renal impairment group was significantly higher than that in the normal renal function group. The results of the ROC curve analysis showed that the TyG index had some value in predicting early renal impairment in hypertensive patients, but was not superior to TG alone. TyG index is the product index of TG and FBG, which is respectively an index of blood glucose and lipid metabolism, reflecting well the fat toxicity and sugar toxicity playing very important roles in Diabetic Kidney Disease.

Study limitations

This study has certain limitations. First, results were obtained from a retrospective study, and selection bias was inevitable. Second, we only measured fasting triglycerides and fasting plasma glucose levels at admission; these parameters were not measured continuously. Third, we can only prove the correlation between the TyG index and early renal impairment in patients with hypertension, but whether they have a causal relationship requires further prospective studies.

Conclusion

TyG index is an influential factor in serum $\beta 2$ -MG and CysC levels. The elevated TyG index levels are closely associated with the occurrence and development of early renal impairment in hypertensive patients, but it should be used cautiously in the

prediction of early renal impairment. Therefore, for hypertensive patients, to protect target organ function, the treatment of IR should be paid attention to delay the occurrence of renal damage while strictly controlling blood pressure to reach the standard.

Data availability statement

The original contributions presented in the study are included in the article/supplementary material. Further inquiries can be directed to the corresponding authors.

Ethics statement

The studies involving human participants were reviewed and approved by Qinghai Provincial People's Hospital. The patients/participants provided their written informed consent to participate in this study.

Author contributions

JD and HY: Data collection, analyses and interpretation, and writing of the final manuscript. JD, HY, YZ, LC, and QH: Study

design, Data interpretation, and revising the manuscript. All authors contributed to the article and approved the submitted version.

Funding

This research was supported by Qinghai Science and Technology Program Fund, with the project number (2019ZJ7051).

Conflict of interest

The authors declare that the research was conducted in the absence of any commercial or financial relationships that could be construed as a potential conflict of interest.

Publisher's note

All claims expressed in this article are solely those of the authors and do not necessarily represent those of their affiliated organizations, or those of the publisher, the editors and the reviewers. Any product that may be evaluated in this article, or claim that may be made by its manufacturer, is not guaranteed or endorsed by the publisher.

References

- Lotfaliany M, Akbarpour S, Mozafari A, Boloukat R, Azizi F, Hadaegh F. Hypertension phenotypes and incident cardiovascular disease and mortality events in a decade follow-up of a middle East cohort. *J Hypertens* (2015) 33(6):1153–61. doi: 10.1097/hjh.0000000000000540
- Meng L, Yang Y, Qi L, Wang X, Xu G, Zhang B. Elevated serum cystatin c is an independent predictor of cardiovascular events in people with relatively normal renal function. *J Nephrol* (2012) 25(3):426–30. doi: 10.5301/jn.5000020
- Bevc S, Hojs N, Knehtl M, Ekart R, Hojs R. Cystatin c as a predictor of mortality in elderly patients with chronic kidney disease. *Aging male: Off J Int Soc Study Aging Male* (2019) 22(1):62–7. doi: 10.1080/13685538.2018.1479386
- Tessari P, Cecchet D, Vettore M, Coracina A, Puricelli L, Kiwanuka E. Decreased homocysteine trans-sulfuration in hypertension with hyperhomocysteinemia: Relationship with insulin resistance. *J Clin Endocrinol Metab* (2018) 103(1):56–63. doi: 10.1210/jc.2017-01076
- Artunc F, Schleicher E, Weigert C, Fritsche A, Stefan N, Häring H. The impact of insulin resistance on the kidney and vasculature. *Nat Rev Nephrol* (2016) 12(12):721–37. doi: 10.1038/nrneph.2016.145
- Guerrero-Romero F, Villalobos-Molina R, Jiménez-Flores J, Simental-Mendía L, Méndez-Cruz R, Murguía-Romero M, et al. Fasting triglycerides and glucose index as a diagnostic test for insulin resistance in young adults. *Arch Med Res* (2016) 47(5):382–7. doi: 10.1016/j.arcmed.2016.08.012
- Guerrero-Romero F, Simental-Mendía L, González-Ortiz M, Martínez-Abundis E, Ramos-Zavala M, Hernández-González S, et al. The product of triglycerides and glucose, a simple measure of insulin sensitivity: comparison with the euglycemic-hyperinsulinemic clamp. *J Clin Endocrinol Metab* (2010) 95(7):3347–51. doi: 10.1210/jc.2010-0288
- Mao Q, Zhou D, Li Y, Wang Y, Xu S-C, Zhao X-H. The triglyceride-glucose index predicts coronary artery disease severity and cardiovascular outcomes in patients with non-ST-Segment elevation acute coronary syndrome. *Dis Markers* (2019) 2019(1–11): 6891537. doi: 10.1155/2019/6891537
- Wang Y, Yang W, Jiang X. Association between triglyceride-glucose index and hypertension: A meta-analysis. *Front Cardiovasc Med* (2021) 8:644035 (644035). doi: 10.3389/fcvm.2021.644035
- Li X, Li G, Cheng T, Liu J, Song G, Ma H. Association between triglyceride-glucose index and risk of incident diabetes: a secondary analysis based on a Chinese cohort study: TyG index and incident diabetes. *Lipids Health Dis* (2020) 19(1):236. doi: 10.1186/s12944-020-01403-7
- Lv L, Zhou Y, Chen X, Gong L, Wu J, Luo W, et al. Relationship between the TyG index and diabetic kidney disease in patients with type-2 diabetes mellitus. *Diabetes Metab syndr obesity: Targets Ther* (2021) 14:3299–06. doi: 10.2147/dmso.S318255
- Zhang S, Du T, Zhang J, Lu H, Lin X, Xie J, et al. The triglyceride and glucose index (TyG) is an effective biomarker to identify nonalcoholic fatty liver disease. *Lipids Health Dis* (2017) 16(1):15. doi: 10.1186/s12944-017-0409-6
- Zhao S, Yu S, Chi C, Fan X, Tang J, Ji H, et al. Association between macro- and microvascular damage and the triglyceride glucose index in community-dwelling elderly individuals: the northern shanghai study. *Cardiovasc Diabetol* (2019) 18(1):95. doi: 10.1186/s12933-019-0898-x
- Lindblad Y, Axelsson J, Bárány P, Celsi G, Lindholm B, Qureshi A, et al. Hyperinsulinemia and insulin resistance, early cardiovascular risk factors in children with chronic kidney disease. *Blood purif* (2008) 26(6):518–25. doi: 10.1159/000167799
- Wang C, Blough E, Arvapalli R, Dai X, Paturi S, Manne N, et al. Metabolic syndrome-induced tubulointerstitial injury: role of oxidative stress and preventive effects of acetaminophen. *Free Radical Biol Med* (2013) 65:1417–26. doi: 10.1016/j.freeradbiomed.2013.10.005
- Thethi T, Kamiyama M, Kobori H. The link between the renin-angiotensin-aldosterone system and renal injury in obesity and the metabolic syndrome. *Curr hypertens Rep* (2012) 14(2):160–9. doi: 10.1007/s11906-012-0245-z

17. Shimobayashi M, Albert V, Woelnerhanssen B, Frei I, Weissenberger D, Meyer-Gerspach A, et al. Insulin resistance causes inflammation in adipose tissue. *J Clin Invest* (2018) 128(4):1538–50. doi: 10.1172/jci96139
18. Manrique C, Lastra G, Gardner M, Sowers J. The renin angiotensin aldosterone system in hypertension: roles of insulin resistance and oxidative stress. *Med Clinics North America* (2009) 93(3):569–82. doi: 10.1016/j.mcna.2009.02.014
19. Cheng H, Huang J, Chiang C, Yen C, Hung K, Wu K. Metabolic syndrome and insulin resistance as risk factors for development of chronic kidney disease and rapid decline in renal function in elderly. *J Clin Endocrinol Metab* (2012) 97(4):1268–76. doi: 10.1210/jc.2011-2658
20. Oz-Sig O, Kara O, Erdogan H. Microalbuminuria and serum cystatin c in prediction of early-renal insufficiency in children with obesity. *Indian J Pediatr* (2020) 87(12):1009–13. doi: 10.1007/s12098-020-03294-z
21. Rosner M, Bolton W. Renal function testing. *Am J Kidney Dis* (2006) 47(1):174–83. doi: 10.1053/j.ajkd.2005.08.038
22. Zhang Y, Sun L. Cystatin c in cerebrovascular disorders. *Curr neurovascular Res* (2017) 14(4):406–14. doi: 10.2174/1567202614666171116102504
23. Onopiuk A, Tokarzewicz A, Gorodkiewicz E. Cystatin C: A kidney function biomarker. *Advances in clinical chemistry* (2015) 68:57–69. doi: 10.1016/bs.acc.2014.11.007
24. Pavkov M, Knowler W, Hanson R, Williams D, Lemley K, Myers B, et al. Comparison of serum cystatin c, serum creatinine, measured GFR, and estimated GFR to assess the risk of kidney failure in American indians with diabetic nephropathy. *Am J Kidney Dis: Off J Natl Kidney Found* (2013) 62(1):33–41. doi: 10.1053/j.ajkd.2012.11.044
25. Khan I, Khan A, Adnan A, Sulaiman S, Hamzah A, Ahmed N, et al. Effect of socio-demographic factors on endogenous biomarkers (cystatin c and creatinine) among elderly chronic kidney disease patients: a cross-sectional study. *Int Urol Nephrol* (2018) 50(6):1113–21. doi: 10.1007/s11255-018-1834-9
26. Shirzai A, Yildiz N, Biyikli N, Ustunsoy S, Benzer M, Alpay H. Is microalbuminuria a risk factor for hypertension in children with solitary kidney? *Pediatr Nephrol (Berlin Germany)* (2014) 29(2):283–8. doi: 10.1007/s00467-013-2641-2
27. da Silva A, do Carmo J, Li X, Wang Z, Mouton A, Hall J. Role of hyperinsulinemia and insulin resistance in hypertension: Metabolic syndrome revisited. *Can J Cardiol* (2020) 36(5):671–82. doi: 10.1016/j.cjca.2020.02.066
28. Yang K, Liu W. Triglyceride and glucose index and sex differences in relation to major adverse cardiovascular events in hypertensive patients without diabetes. *Front Endocrinol (Lausanne)* (2021) 12:761397(761397). doi: 10.3389/fendo.2021.761397
29. Chiu T, Tsai H, Chiou H, Wu P, Huang J, Chen S. A high triglyceride-glucose index is associated with left ventricular dysfunction and atherosclerosis. *Int J Med Sci* (2021) 18(4):1051–7. doi: 10.7150/ijms.53920
30. Khan S, Sobia F, Niazi N, Manzoor S, Fazal N, Ahmad F. Metabolic clustering of risk factors: evaluation of triglyceride-glucose index (TyG index) for evaluation of insulin resistance. *Diabetol Metab syndr* (2018) 10:74. doi: 10.1186/s13098-018-0376-8
31. Fritz J, Brozek W, Concin H, Nagel G, Kerschbaum J, Lhotta K, et al. The triglyceride-glucose index and obesity-related risk of end-stage kidney disease in Austrian adults. *JAMA netw Open* (2021) 4(3):e212612. doi: 10.1001/jamanetworkopen.2021.2612



OPEN ACCESS

EDITED BY

Ningning Hou,
Affiliated Hospital of Weifang Medical
University, China

REVIEWED BY

Chi Zhang,
Third Affiliated Hospital of Wenzhou
Medical University, China
Bo Wang,
Hainan General Hospital, China

*CORRESPONDENCE

Yanli Cheng
✉ chengyanli@jlu.edu.cn
Yang Jiang
✉ jiangyang@jlu.edu.cn

SPECIALTY SECTION

This article was submitted to
Renal Endocrinology,
a section of the journal
Frontiers in Endocrinology

RECEIVED 27 October 2022

ACCEPTED 21 December 2022

PUBLISHED 16 January 2023

CITATION

Zhang X, Xiao H, Fu S, Yu J, Cheng Y
and Jiang Y (2023) Investigate the
genetic mechanisms of diabetic kidney
disease complicated with
inflammatory bowel disease through
data mining and bioinformatic analysis.
Front. Endocrinol. 13:1081747.
doi: 10.3389/fendo.2022.1081747

COPYRIGHT

© 2023 Zhang, Xiao, Fu, Yu, Cheng and
Jiang. This is an open-access article
distributed under the terms of the
Creative Commons Attribution License
(CC BY). The use, distribution or
reproduction in other forums is
permitted, provided the original
author(s) and the copyright owner(s)
are credited and that the original
publication in this journal is cited, in
accordance with accepted academic
practice. No use, distribution or
reproduction is permitted which does
not comply with these terms.

Investigate the genetic mechanisms of diabetic kidney disease complicated with inflammatory bowel disease through data mining and bioinformatic analysis

Xiaoyu Zhang¹, Huijie Xiao¹, Shaojie Fu², Jinyu Yu³,
Yanli Cheng^{2*} and Yang Jiang^{1*}

¹Department of Gastrointestinal and Colorectal Surgery, China-Japan Union Hospital of Jilin University, Changchun, China, ²Department of Nephrology, The First Hospital of Jilin University, Changchun, China, ³Department of Urology, The First Hospital of Jilin University, Changchun, China

Background: Patients with diabetic kidney disease (DKD) often have gastrointestinal dysfunction such as inflammatory bowel disease (IBD). This study aims to investigate the genetic mechanism leading to IBD in DKD patients through data mining and bioinformatics analysis.

Methods: The disease-related genes of DKD and IBD were searched from the five databases of OMIM, GeneCards, PharmGkb, TTD, and DrugBank, and the intersection part of the two diseases were taken to obtain the risk genes of DKD complicated with IBD. A protein–protein interaction (PPI) network analysis was performed on risk genes, and three topological parameters of degree, betweenness, and closeness of nodes in the network were used to identify key risk genes. Finally, Gene Ontology (GO) analysis and Kyoto Encyclopedia of Genes and Genomes (KEGG) analysis were performed on the risk genes to explore the related mechanism of DKD merging IBD.

Results: This study identified 495 risk genes for DKD complicated with IBD. After constructing a protein–protein interaction network and screening for three times, six key risk genes were obtained, including matrix metalloproteinase 2 (MMP2), hepatocyte growth factor (HGF), fibroblast growth factor 2 (FGF2), interleukin (IL)-18, IL-13, and C–C motif chemokine ligand 5 (CCL5). Based on GO enrichment analysis, we found that DKD genes complicated with IBD were associated with 3,646 biological processes such as inflammatory response regulation, 121 cellular components such as cytoplasmic vesicles, and 276 molecular functions such as G-protein-coupled receptor binding. Based on KEGG enrichment analysis, we found that the risk genes of DKD combined with IBD were associated with 181 pathways, such as the PI3K-Akt signaling pathway, advanced glycation end

product–receptor for AGE (AGE-RAGE) signaling pathway and hypoxia-inducible factor (HIF)-1 signaling pathway.

Conclusion: There is a genetic mechanism for the complication of IBD in patients with CKD. Oxidative stress, chronic inflammatory response, and immune dysfunction were possible mechanisms for DKD complicated with IBD.

KEYWORDS

diabetic kidney disease, inflammatory bowel disease, data mining, bioinformatic analysis, signaling pathway

Introduction

Diabetic kidney disease (DKD) is the most common cause of chronic kidney disease and end-stage renal disease worldwide, affecting approximately 30%–40% of people with diabetes (1). In recent years, the incidence of diabetes worldwide has increased in parallel with the prevalence of DKD due to changes in obesity rates, metabolic syndrome, and lifestyle habits (2). At the same time, due to the high medical cost and poor prognosis in the advanced stage of the disease, DKD has brought a heavy burden to the whole society and families (3).

Inflammatory bowel disease (IBD) is a chronic inflammatory disease of the gastrointestinal tract of unknown etiology. IBD has traditionally been viewed as a disease of the Western world. However, data over the past decade have shown that IBD has become a global disease with a dramatic increase in incidence and prevalence in the East (4). Due to the early onset of IBD, complex clinical symptoms (fatigue, diarrhea, and pain), and fluctuating disease course (prolonged disease course, recurrent attacks, and difficult to cure), it has a great impact on the quality of life and psychological state of patients (5). Although the precise cause and pathogenesis of IBD remain unknown and an effective cure is lacking, genetic research is now providing insight into the biological mechanisms behind the disease, which may hold promise for future therapies (6). Recently, extraintestinal symptoms and associated diseases of IBD have attracted increasing attention, most of which are related to autoimmune diseases such as type 1 diabetes mellitus, thyroid disease, and dermatitis herpetiformis (7). DKD and IBD are common and complex chronic diseases that are clinically heterogeneous and progressive. Some studies have shown that DKD and IBD are related disorders that probably share susceptibility genes. Patients with DKD are often associated with gastrointestinal dysfunction and may be more susceptible to IBD (8–10). However, the mechanism of DKD concurrent IBD remains unclear. As DKD and IBD are currently incurable, they represent a major public health challenge worldwide.

Therefore, a clear knowledge of the key risk genes implicated in DKD complicated with IBD could help to identify potential therapeutic targets for the development of new drugs, in addition to the possible discovery of new potential diagnostic biomarkers for the early diagnosis of DKD complicated with IBD, while an understanding of the possible molecular mechanisms implicated in DKD and IBD could help improve the prognostic and therapeutic tools leading to a better quality of life of the patients, delaying the progression of the disease.

In recent years, with the continuous development of molecular biotechnology, bioinformatics has played an increasingly important role in exploring the molecular mechanisms of human diseases through systematic analysis of available biomedical data (11). In this study, we systematically explored the key targets and important pathways of DKD combined with IBD using bioinformatics methods, which enhanced our understanding of the underlying molecular mechanisms of DKD and IBD and provided potential targets for further research.

Methods

Collection of gene targets in DKD and IBD

The human genes associated with DKD and IBD were gathered from Online Mendelian Inheritance in Man (OMIM, <https://omim.org/>) (12), GeneCards (<https://www.genecards.org/>), Pharmacogenomics Knowledge Base (PharmGkb, <https://www.pharmgkb.org/>), Therapeutic Target Database (TTD, <http://db.idrblab.net/ttd/>), and DrugBank (<https://www.drugbank.ca/>). GeneCards is a comprehensive database that provides information on all predicted and annotated human genes, and genes with a correlation coefficient >10 are filtered as relevant genes (13). PharmGKB is a comprehensive resource on how human genetic variation leads to variation in drug response

(14). TTD is a database that provides information on known and explored therapeutic proteins and targeted diseases (15). DrugBank, a comprehensive bioinformatics database, also provides relevant information on disease targets (16). The search terms “diabetic kidney disease” and “inflammatory bowel disease” were used to retrieve data from the above five databases, respectively.

Identification of the risk genes for DKD with IBD

We gathered the DKD- and IBD-related genes. The potential risk genes for DKD and IBD were identified from the above-shared genes.

Protein–protein interaction network

The risk genes of DKD and IBD were imported into the STRING database to obtain their interaction relationship. STRING (<https://string-db.org/>, version 11.0) is a database containing known and predicted PPI, which gathers information using bioinformatics strategies (17). These species are restricted to “*Homo sapiens*,” and a PPI with a confidence score >0.9 was chosen for this study.

Network construction

The PPI network of risk genes for DKD with IBD was built by linking them to their interacting genes. Next, the network visualization software Cytoscape version 3.4.2 (<http://www.cytoscape.org/>) was used to present the network. Lastly, Network Analyzer was used to calculate four topological parameters of each node in the network, including the degree, betweenness centrality, closeness centrality, and clustering coefficient (18). Nodes with values above the median for all four topological parameters were selected to construct a subnetwork, where another selection was finally performed to obtain the core risk genes for DKD and IBD.

GO and KEGG pathway enrichment analysis

To further understand the role of DKD and IBD risk genes in biological process (BP), cellular component (CC), and molecular function (MF), we used the Gene Ontology (GO) database (<http://geneontology.org/>) to clarify the possible biological mechanisms. KEGG (<https://www.kegg.jp/>) is a database for extracting biological information on functional classification, annotation, and enriched pathways of various genes. In this

study, we used an R-package-Bioconductor clusterProfiler for GO and KEGG enrichment analysis. The R-package-Bioconductor clusterProfiler is widely used to automate biological term classification and enrichment analysis of gene clusters (19).

Results

The flowchart of the study based on data mining and bioinformatic analysis is presented in Figure 1.

Collection of gene targets in DKD and IBD

Using “diabetic nephropathy” and “inflammatory bowel disease” as keywords, their related genes were retrieved from OMIM, GeneCards, PharmGkb, TTD, and DrugBank databases, respectively. As shown in Figure 2A, a total of 756 genes related to DKD were collected, and 2,096 genes related to IBD were retrieved, as shown in Figure 2B. For both DKD and IBD, the GeneCards database is the most common source of disease-related genes, suggesting that it has the advantage of being comprehensive in terms of human genetic information.

Identification of the risk genes for DKD with IBD

Since the targeted genes for both DKD and IBD were gathered, using the shared genes described above, 459 possible risk genes for DKD complicated with IBD were obtained, as shown in Figure 2C. A total of 459 disease-associated risk genes are obviously too many, suggesting that further screening for key risk genes among them is necessary.

Risk genes for DKD with IBD’ PPI network

The PPI network of risk genes for DKD with IBD is shown in Figure 3A, including 407 nodes and 2,330 edges. Four topological features of 407 targets were calculated using a network analyzer to identify key nodes in the network. The detailed information of all the risk genes in the PPI network is displayed in Supplementary Table S1. The median values of the degree, node betweenness, closeness, and clustering coefficient were 7, 0.00142208, 0.3137558, and 0.333333, respectively. As shown in Figures 3B, C, nodes with values of all four topological parameters exceeding the median were selected to construct subnetworks. In the subnetwork, another selection was performed to finally obtain the central targets (Figure 3D). Finally, six genes were identified as central risk genes

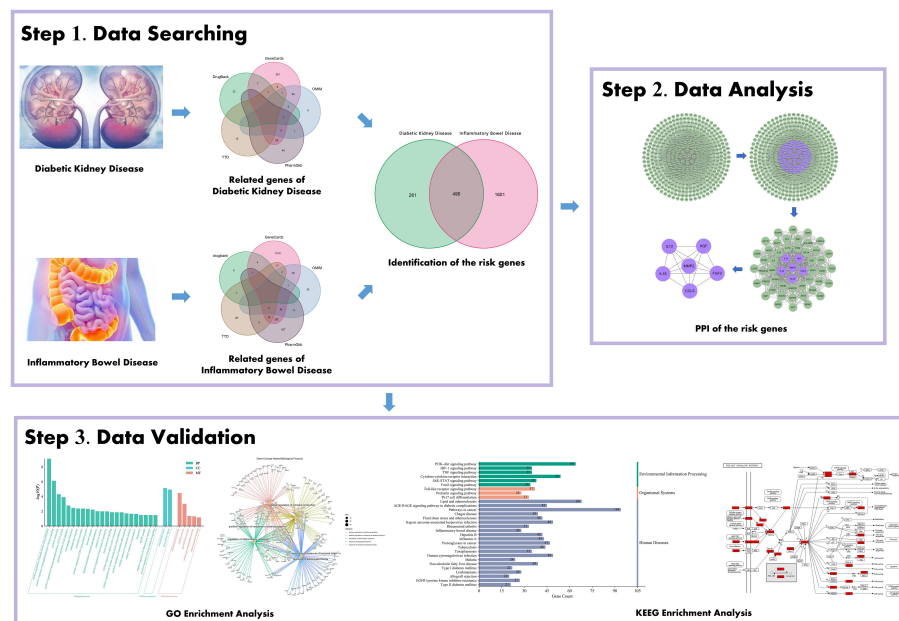


FIGURE 1

Schematic illustration showing the investigative process undertaken in the present study. This investigation is organized into three sections: Step 1, collection of gene targets/identification of the risk genes for diabetic kidney disease (DKD) with inflammatory bowel disease (IBD); Step 2, mining the risk genes for DKD with IBD's PPI network; Step 3, probing the pathways and biological process, gene-disease enrichment analysis related to obtained important intersection protein/gene, and then validation with a literature review.

for DKD with IBD, including matrix metalloproteinase 2 (MMP2), hepatocyte growth factor (HGF), fibroblast growth factor 2 (FGF2), interleukin (IL)-18, IL-13, and C-C motif chemokine ligand 5 (CCL5), and their detailed information in the PPI network is displayed in [Table 1](#).

GO and KEGG pathway enrichment

To elucidate the complex mechanisms of DKD complicated with IBD, we analyzed the GO biological process (BP), cell component (CC), and molecular function (MF) of 459 possible risk genes and six identified key risk genes, respectively, and the most relevant results that were chosen by *p*-value are presented in [Figures 4A, B](#), correspondingly. The specific entries of GO enrichment analysis for BP, CC, and MF of all risk genes and key risk genes are listed in [Supplementary Tables S2, S3](#), respectively. The regulation of cytokine production and the regulation of inflammatory response were among the most closely related biological processes, which was in accord with our general cognition to the disease. Moreover, the relationships between the risk genes and the obtained GO enrichment entries are depicted in [Figure 5](#).

To explore the underlying mechanisms of DKD complicated with IBD, KEGG pathway enrichment analysis was also performed on the risk genes and identified key risk genes, respectively, and the most relevant results are presented in [Figures 6A, B](#),

correspondingly. The detailed information of KEGG enrichment analysis for all risk genes and key risk genes is listed in [Supplementary Tables S4, S5](#), respectively. As shown in [Supplementary Table S4](#) and [Figure 6A](#), there were 181 major pathways involved in DKD combined with IBD, $p < 0.05$. These 181 pathways were involved in human diseases, pathophysiological mechanisms, and signaling pathways. The top 10 significantly enriched signaling pathways include the advanced glycation end product–receptor for AGE (AGE-RAGE) signaling pathway, Toll-like receptor signaling pathway, PI3K-Akt signaling pathway, hypoxia-inducible factor (HIF)-1 signaling pathway, tumor necrosis factor (TNF) signaling pathway, Janus kinase–signal transducer and activator of transcription (JAK-STAT) signaling pathway, IL-17 signaling pathway, T-cell receptor signaling pathway, mitogen-activated protein kinase (MAPK) signaling pathway, and Rap1 signaling pathway. The risk genes for DKD with IBD in the PI3K-Akt signaling pathway are depicted in [Figure 7](#). These results suggest that the pathogenesis of DKD combined with IBD is regulated through the regulation of multiple pathways, and many risk genes for DKD combined with IBD play their roles in multiple pathways simultaneously.

Discussion

Inflammatory bowel disease (IBD) is an autoimmune disease consisting of Crohn's disease (CD), ulcerative colitis (UC), and

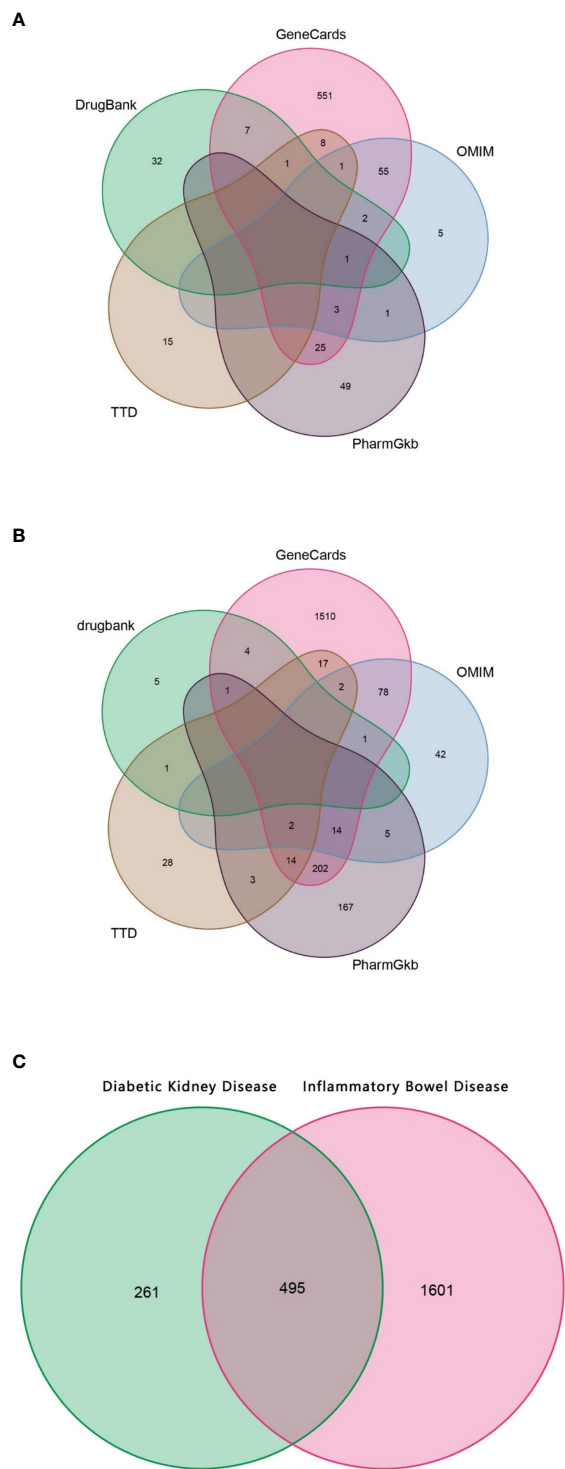


FIGURE 2
The Venn diagram. **(A)** Collection of gene targets associated with DKD from databases. **(B)** Collection of gene targets associated with IBD from databases. **(C)** Identification of the possible risk genes of DKD complicated with IBD.

indeterminate colitis. IBD is most common in Western countries, especially in North America and northern Europe; its prevalence is increasing year by year, and its cause is still unclear (20, 21). Genetic, environmental, and host-related

factors are associated with the exacerbation of gut inflammation (22). The classical presentations of IBD are malabsorption and gastrointestinal symptoms; however, CD is more likely to manifest as watery diarrhea and vague symptoms,

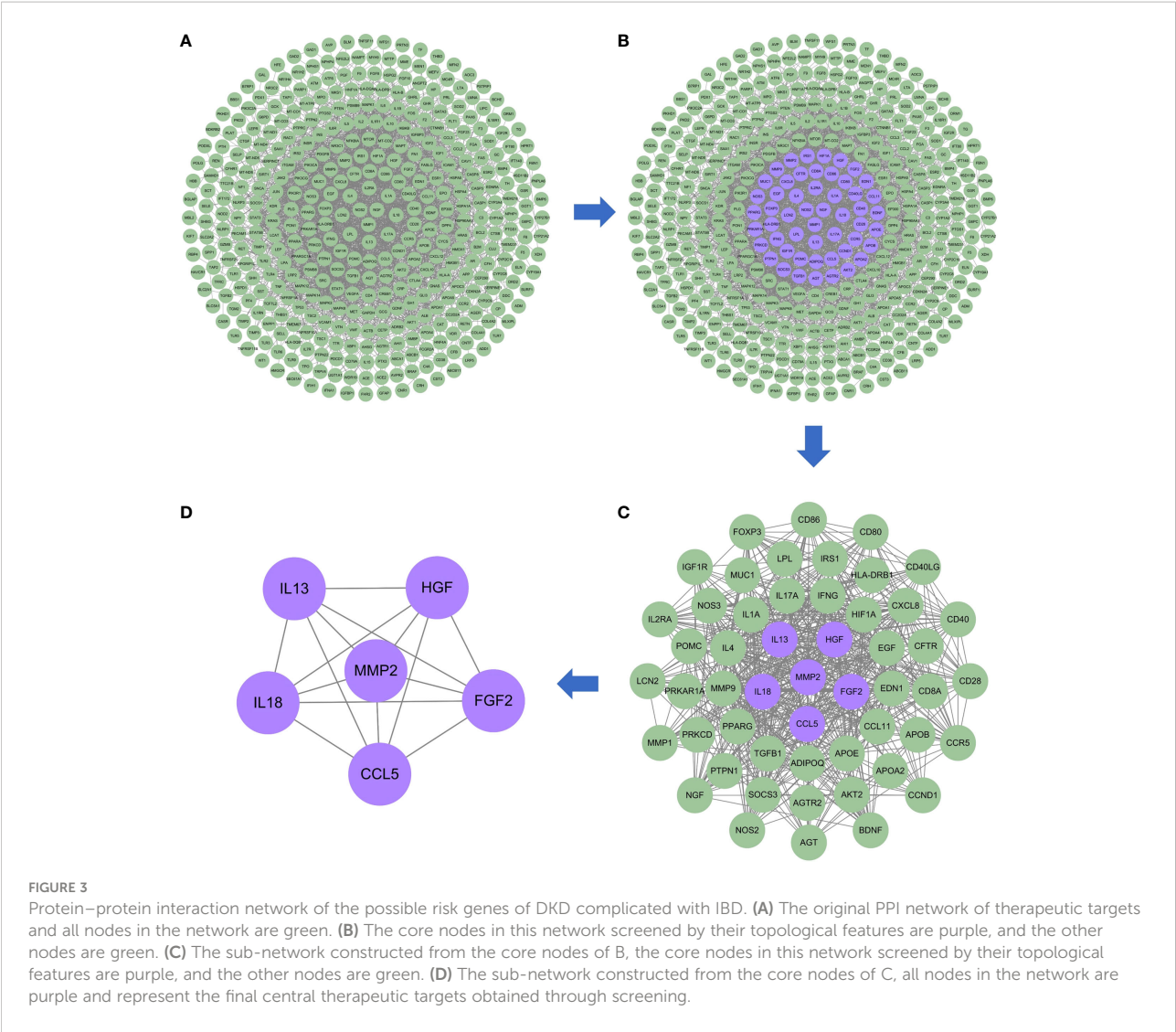


TABLE 1 Central risk genes for diabetic kidney disease with inflammatory bowel disease.

Gene symbol	Protein names	Uniprot ID	Betweenness centrality	Closeness centrality	Degree	Clustering coefficient
MMP2	Matrix metalloproteinase 2	P08253	0.006506	0.366096	24	0.391304
HGF	Hepatocyte growth factor	P14210	0.004258	0.374885	24	0.40942
FGF2	Fibroblast growth factor 2	P09038	0.01366	0.360248	26	0.375385
IL18	Interleukin-18	Q14116	0.004962	0.35961	21	0.42381
IL13	Interleukin-13	P35225	0.002312	0.338616	16	0.425
CCL5	C–C motif chemokine 5	P13501	0.001432	0.346712	15	0.657143

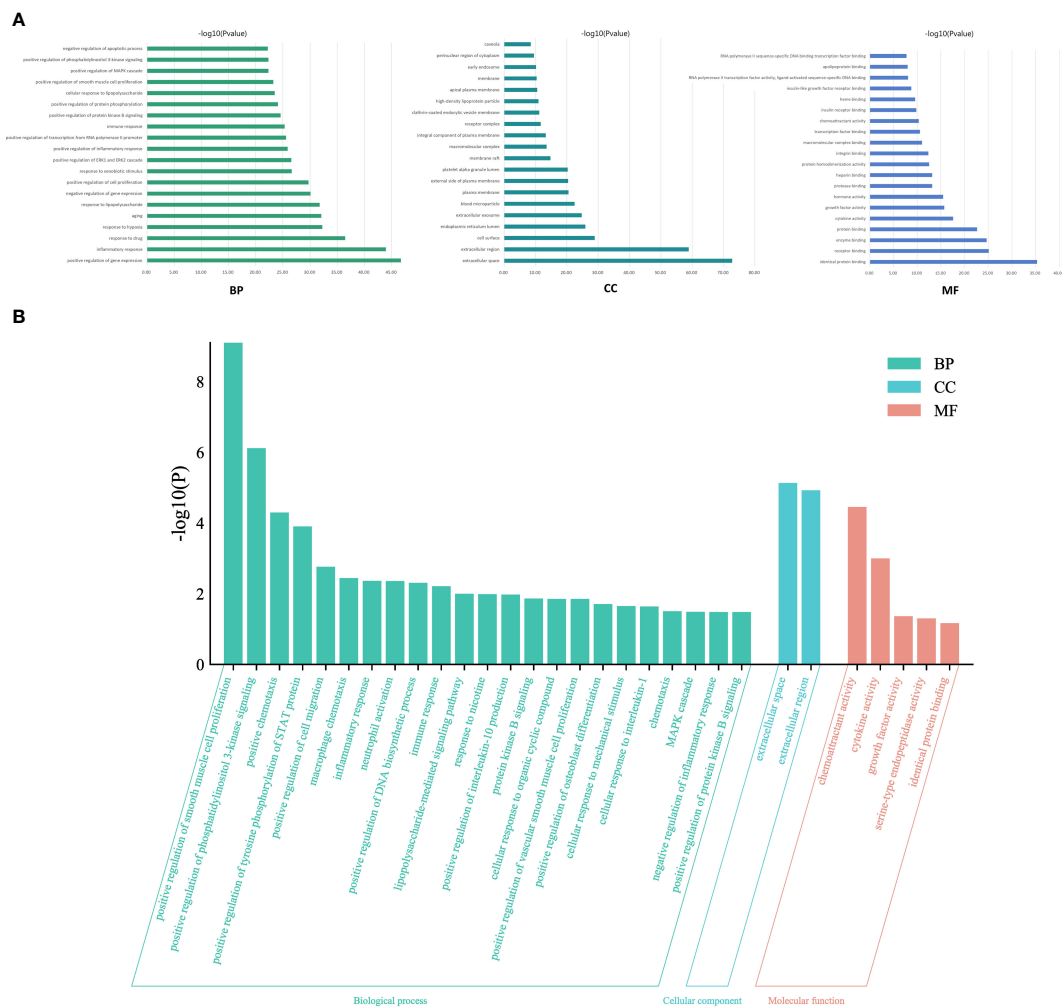


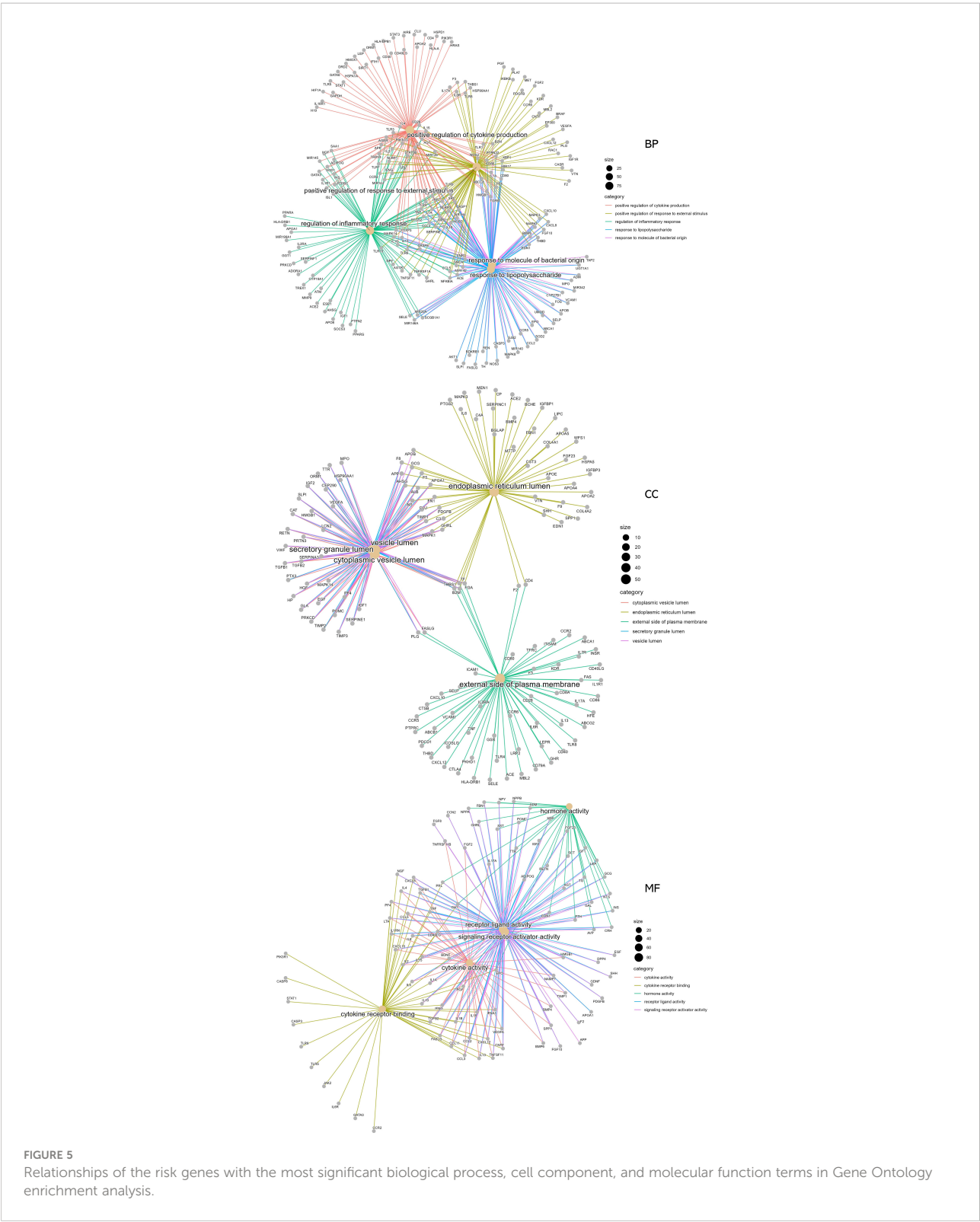
FIGURE 4

Gene Ontology enrichment analysis. **(A)** The most relevant biological process, cell component, and molecular function terms in all risk genes of DKD complicated with IBD. **(B)** The most relevant biological process, cell component, and molecular function terms in the key risk genes of DKD complicated with IBD.

whereas UC is more likely to manifest as diarrhea and bleeding (23). The extraintestinal symptoms and associated diseases of IBD have been increasingly recognized in recent years. Many of these are associated with autoimmune diseases such as type 1 diabetes, thyroid disease, and dermatitis herpetiformis (7). There are many reports of combined kidney disease in patients with IBD, especially DKD (8–10). Therefore, in this study, we applied the bioinformatics approach to investigate the possible mechanisms of IBD complicated with DKD from a genetic perspective.

Through data mining, we found that IBD and DKD have many related genes in common, and MMP2, HGF, FGF2, IL-18, IL-13, and CCL5 were identified as the core risk genes for DKD with IBD by PPI analysis. MMP2 is an enzyme with gelatinase

activity. Overexpression of MMP2 in glomerulus and tubules can lead to kidney damage and fibrosis by inflammatory processes through various pathologies (24). Meanwhile, mucosal MMP2 activity has been reported to be upregulated in humans with IBD (25). It facilitates remodeling of ECM and degradation of basal membrane type IV collagen, leading to intestinal ulceration, epithelial damage, and fistula formation (26, 27). HGF is a pleiotropic factor with the activities of antiapoptotic, cytoprotective, and modulating central inflammation and immunoreaction in many diseases (28, 29). Elevated serum HGF level is significantly associated with the incidence of type 2 diabetes (T2DM) and the development of insulin resistance (IR) (30). It has a positive effect on the survival of islet β cells and could protect against high-fat diet-induced



obesity and regulate IR (31). Many studies have also found that serum HGF levels are higher in IBD patients compared with controls, which may be a good acute phase response biomarker of IBD activity (32, 33). HGF could modulate intestinal epithelial

cell proliferation and migration, thus accelerating the repair of the intestinal mucosa (34). Recombinant human HGF and HGF gene therapy eliminates the severity in some animal models of IBD and is considered as a new treatment modality (35). IL-18

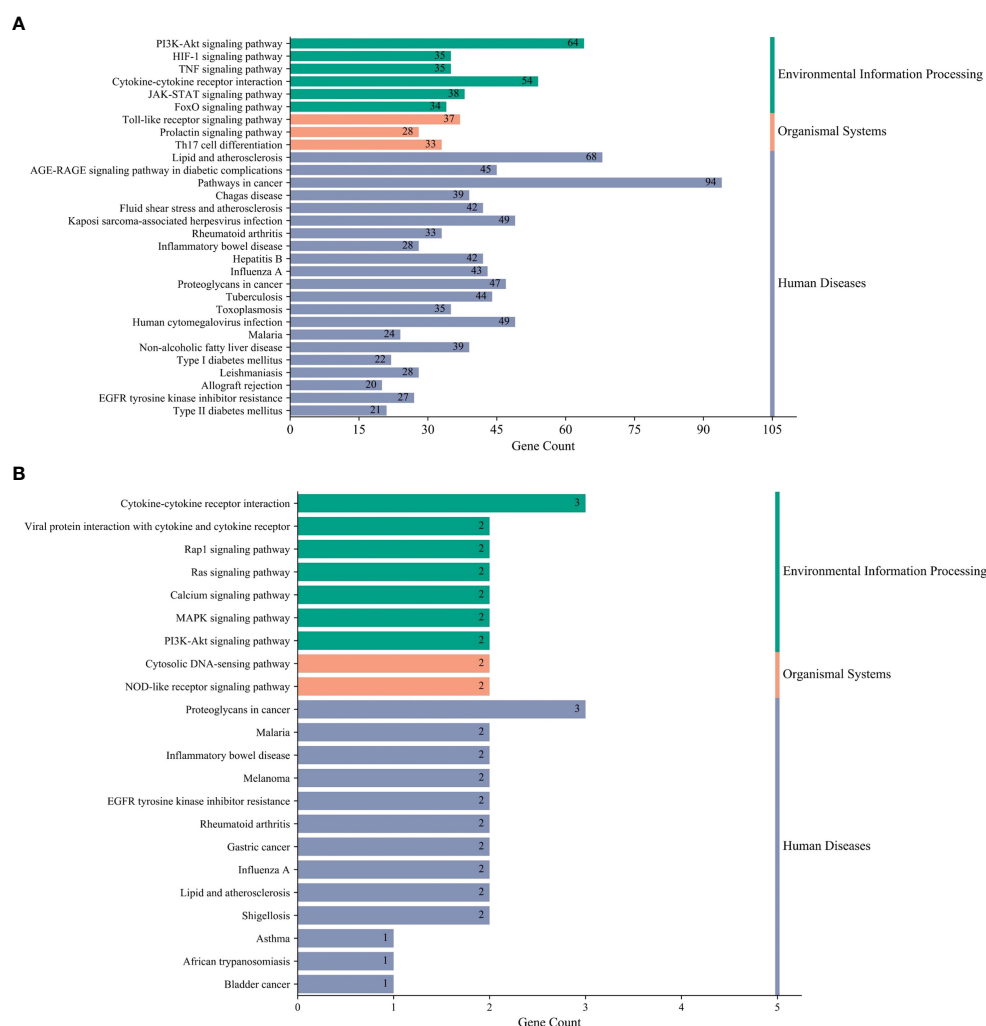
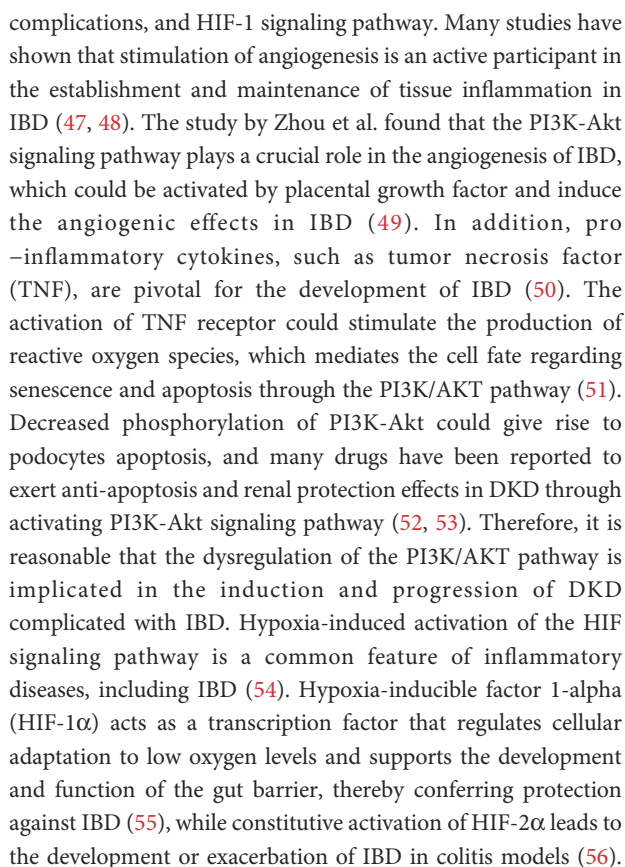


FIGURE 6
Kyoto Encyclopedia of Genes and Genomes (KEGG) terms. **(A)** The most relevant KEGG terms in all risk genes of DKD complicated with IBD. **(B)** The most relevant KEGG terms in the key risk genes of DKD complicated with IBD.

and IL-13 are both inflammatory cytokines, and CCL5 is a chemokine; inflammatory processes have been demonstrated to be associated with the development of DKD (36). It has been reported that IL-18 levels in urine and serum are increased in patients with DKD, and the serum IL-18 level is related to renal injury severity in DKD (37, 38). IL-18 could induce the release of interferon γ ; lead to the production of other inflammatory cytokines, such as IL-1 and TNF; and induce endothelial cell apoptosis (39). In fact, IL-18 is thought to be more closely related to the progression of DKD than other diabetic complications (40). CCL5 is a potent chemoattractant for macrophages, monocytes, T cells, and granulocytes. CCL5 is significantly upregulated in renal biopsy samples from patients with T2DM and overt nephropathy, and its expression in renal tubular cells has a direct correlation with the interstitial cellular infiltration

and the magnitude of proteinuria (41). The production of IL-18 was regarded as a key etiological factor for patients with IBD (42). It has been shown to disrupt the mucosal barrier, trigger inflammation, and amplify damage to the intestinal epithelium during disease (43). CCL5 also plays a crucial role in IBD; its expression is enhanced in the intestine and is closely implicated in the pathophysiology (44–46). These studies on the core risk genes for DKD with IBD validate our findings to some extent. These core risk genes may serve as the potential therapeutic targets for the development of new drugs and possible diagnostic biomarkers for the clinical identification of DKD complicated with IBD.

According to the KEGG terms, the risk genes for DKD complicated with IBD were mainly associated with the PI3K-Akt signaling pathway, AGE-RAGE signaling pathway in diabetic



Our study found that DKD and IBD share many common related genes and pathogenic mechanisms, oxidative stress, chronic inflammatory response, and immune dysfunction were possible mechanisms, and further research on these common targets for DKD complicated with IBD, especially the core targets, is important for the development of new effective drugs and the early diagnosis. Our study is based on the data mining and bioinformatics approach and has limitations due to the lack of experimental validation, mainly in the failure to validate the expression of the identified key risk genes in the blood of the patients with DKD combined with IBD and the changes in potential signaling pathways. Therefore, experiments on the key targets and related pathways of DKD combined with IBD are also needed to be conducted in the future.

The datasets presented in this study can be found in online repositories. The names of the repository/repositories and

accession number(s) can be found in the article/
Supplementary Material.

Author contributions

XZ performed the research, conducted the bioinformatics analysis, and wrote the first draft of the manuscript. HX, SF, and JY participated in data collection and analysis. YC and YJ participated in the project design and manuscript draft preparation and revision. All the authors have approved the final version of the manuscript.

Funding

This work was supported in part by grants from the National Natural Science Foundation of China (81700635 to YC), China Postdoctoral Science Foundation (2022M711298 to YC), the Natural Science Foundation of Jilin Province (20200201430JC to YJ), the Jilin Province Development and Reform Commission Project (2021C043-9 to YJ), “PRO•Run” Fund of the Nephrology Group of CEBM(KYJ202206-0003-7 to YC), and Crosswise Tasks (2020YX073 to YC).

Acknowledgments

The authors thank the contributors to the OMIM (Online Mendelian Inheritance in Man, <https://omim.org/>), GeneCards

(<https://www.genecards.org/>), PharmGkb (Pharmacogenomics Knowledge Base, <https://www.pharmgkb.org/>), TTD (Therapeutic Target Database, <http://db.idrblab.net/ttd/>), and DrugBank (<https://www.drugbank.ca/>) database for sharing data.

Conflict of interest

The authors declare that the research was conducted in the absence of any commercial or financial relationships that could be construed as a potential conflict of interest.

Publisher's note

All claims expressed in this article are solely those of the authors and do not necessarily represent those of their affiliated organizations, or those of the publisher, the editors and the reviewers. Any product that may be evaluated in this article, or claim that may be made by its manufacturer, is not guaranteed or endorsed by the publisher.

Supplementary material

The Supplementary Material for this article can be found online at: <https://www.frontiersin.org/articles/10.3389/fendo.2022.1081747/full#supplementary-material>

References

- Bonner R, Albajrami O, Hudspeth J, Upadhyay A. Diabetic kidney disease. *Prim Care* (2020) 47(4):645–59. doi: 10.1016/j.pop.2020.08.004
- Harjutsalo V, Groop PH. Epidemiology and risk factors for diabetic kidney disease. *Adv Chronic Kidney Dis* (2014) 21(3):260–6. doi: 10.1053/j.ackd.2014.03.009
- Thomas B. The global burden of diabetic kidney disease: Time trends and gender gaps. *Curr Diabetes Rep* (2019) 19(4):18. doi: 10.1007/s11892-019-1133-6
- Mak WY, Zhao M, Ng SC, Burisch J. The epidemiology of inflammatory bowel disease: East meets west. *J Gastroenterol Hepatol* (2020) 35(3):380–9. doi: 10.1111/jgh.14872
- Windsor JW, Kaplan GG. Evolving epidemiology of IBD. *Curr Gastroenterol Rep* (2019) 21(8):40. doi: 10.1007/s11894-019-0705-6
- Burisch J, Jess T, Martinato M, Lakatos PL. The burden of inflammatory bowel disease in Europe. *J Crohns Colitis* (2013) 7(4):322–37. doi: 10.1016/j.crohns.2013.01.010
- Leffler DA, Green PH, Fasano A. Extraintestinal manifestations of coeliac disease. *Nat Rev Gastroenterol Hepatol* (2015) 12(10):561–71. doi: 10.1038/ngastro.2015.131
- Cerutti F, Bruno G, Chiarelli F, Lorini R, Meschi F, Sacchetti C. Younger age at onset and sex predict celiac disease in children and adolescents with type 1 diabetes: an Italian multicenter study. *Diabetes Care* (2004) 27(6):1294–8. doi: 10.2337/diacare.27.6.1294
- Leeds JS, Hopper AD, Hadjivassiliou M, Tesfaye S, Sanders DS. High prevalence of microvascular complications in adults with type 1 diabetes and newly diagnosed celiac disease. *Diabetes Care* (2011) 34(10):2158–63. doi: 10.2337/dc11-0149
- Collin P, Syrjänen J, Partanen J, Pasternack A, Kaukinen K, Mustonen J. Celiac disease and HLA DQ in patients with IgA nephropathy. *Am J Gastroenterol* (2002) 97(10):2572–6. doi: 10.1111/j.1572-0241.2002.06025.x
- Orlov YL, Anashkina AA, Klimontov VV, Baranova AV. Medical genetics, genomics and bioinformatics aid in understanding molecular mechanisms of human diseases. *Int J Mol Sci* (2021) 22(18):9962. doi: 10.3390/ijms22189962
- Amberger JS, Bocchini CA, Schiettecatte F, Scott AF, Hamosh A. OMIM.org: Online mendelian inheritance in man (OMIM®), an online catalog of human genes and genetic disorders. *Nucleic Acids Res* (2015) 43(Database issue): D789–98. doi: 10.1093/nar/gku1205
- Stelzer G, Rosen N, Plaschkes I, Zimmerman S, Twik M, Fishilevich S, et al. The GeneCards suite: From gene data mining to disease genome sequence analyses. *Curr Protoc Bioinf* (2016) 54:1.30.1–1.3. doi: 10.1002/cpbi.5
- Gong L, Whirl-Carrillo M, Klein TE. PharmGKB, an integrated resource of pharmacogenomic knowledge. *Curr Protoc* (2021) 1(8):e226. doi: 10.1002/cpz1.226
- Wang Y, Zhang S, Li F, Zhou Y, Zhang Y, Wang Z, et al. Therapeutic target database 2020: enriched resource for facilitating research and early development of targeted therapeutics. *Nucleic Acids Res* (2020) 48(D1):D1031–d41. doi: 10.1093/nar/gkz981

16. Wishart DS, Knox C, Guo AC, Shrivastava S, Hassanali M, Stothard P, et al. DrugBank: a comprehensive resource for in silico drug discovery and exploration. *Nucleic Acids Res* (2006) 34(Database issue):D668–72. doi: 10.1093/nar/gkj067
17. Szklarczyk D, Gable AL, Nastou KC, Lyon D, Kirsch R, Pyysalo S, et al. The STRING database in 2021: customizable protein-protein networks, and functional characterization of user-uploaded gene/measurement sets. *Nucleic Acids Res* (2021) 49(D1):D605–d12. doi: 10.1093/nar/gkaa1074
18. Doncheva NT, Morris JH, Gorodkin J, Jensen LJ. Cytoscape StringApp: Network analysis and visualization of proteomics data. *J Proteome Res* (2019) 18(2):623–32. doi: 10.1021/acs.jproteome.8b00702
19. Wu T, Hu E, Xu S, Chen M, Guo P, Dai Z, et al. clusterProfiler 4.0: A universal enrichment tool for interpreting omics data. *Innovation (Camb)* (2021) 2(3):100141. doi: 10.1016/j.xinn.2021.100141
20. Greuter T, Vavricka SR. Extraintestinal manifestations in inflammatory bowel disease - epidemiology, genetics, and pathogenesis. *Expert Rev Gastroenterol Hepatol* (2019) 13(4):307–17. doi: 10.1080/17474124.2019.1574569
21. Seyedian SS, Nokhostin F, Malamir MD. A review of the diagnosis, prevention, and treatment methods of inflammatory bowel disease. *J Med Life* (2019) 12(2):113–22. doi: 10.25122/jml-2018-0075
22. Flynn S, Eisenstein S. Inflammatory bowel disease presentation and diagnosis. *Surg Clin North Am* (2019) 99(6):1051–62. doi: 10.1016/j.suc.2019.08.001
23. Mahadevan U, Silverberg MS. Inflammatory bowel disease-gastroenterology diamond jubilee review. *Gastroenterology* (2018) 154(6):1555–8. doi: 10.1053/j.gastro.2017.12.025
24. Cheng Z, Limbu MH, Wang Z, Liu J, Liu L, Zhang X, et al. MMP-2 and 9 in chronic kidney disease. *Int J Mol Sci* (2017) 18(4):776. doi: 10.3390/ijms18040776
25. Gao Q, Meijer MJ, Kubben FJ, Sier CF, Kruidenier L, van Duijn W, et al. Expression of matrix metalloproteinases-2 and -9 in intestinal tissue of patients with inflammatory bowel diseases. *Dig Liver Dis* (2005) 37(8):584–92. doi: 10.1016/j.dld.2005.02.011
26. Matsuno K, Adachi Y, Yamamoto H, Goto A, Arimura Y, Endo T, et al. The expression of matrix metalloproteinase matrilysin indicates the degree of inflammation in ulcerative colitis. *J Gastroenterol* (2003) 38(4):348–54. doi: 10.1007/s005350300062
27. McKaig BC, McWilliams D, Watson SA, Mahida YR. Expression and regulation of tissue inhibitor of metalloproteinase-1 and matrix metalloproteinases by intestinal myofibroblasts in inflammatory bowel disease. *Am J Pathol* (2003) 162(4):1355–60. doi: 10.1016/s0002-9440(10)63931-4
28. Rubin JS, Osada H, Finch PW, Taylor WG, Rudikoff S, Aaronson SA. Purification and characterization of a newly identified growth factor specific for epithelial cells. *Proc Natl Acad Sci U S A* (1989) 86(3):802–6. doi: 10.1073/pnas.86.3.802
29. Molnarfi N, Benkhoucha M, Funakoshi H, Nakamura T, Lalive PH. Hepatocyte growth factor: A regulator of inflammation and autoimmunity. *Autoimmun Rev* (2015) 14(4):293–303. doi: 10.1016/j.autrev.2014.11.013
30. Tsukagawa E, Adachi H, Hirai Y, Enomoto M, Fukami A, Ogata K, et al. Independent association of elevated serum hepatocyte growth factor levels with development of insulin resistance in a 10-year prospective study. *Clin Endocrinol (Oxf)* (2013) 79(1):43–8. doi: 10.1111/j.1365-2265.2012.04496.x
31. Oliveira AG, Araújo TG, Carvalho BM, Rocha GZ, Santos A, Saad MJA. The role of hepatocyte growth factor (HGF) in insulin resistance and diabetes. *Front Endocrinol (Lausanne)* (2018) 9:503. doi: 10.3389/fendo.2018.00503
32. Naguib R, El-Shikh WM. Clinical significance of hepatocyte growth factor and transforming growth factor-Beta-1 levels in assessing disease activity in inflammatory bowel disease. *Can J Gastroenterol Hepatol* (2020) 2020:2104314. doi: 10.1155/2020/2104314
33. Sturm A, Schulte C, Schatton R, Becker A, Cario E, Goebell H, et al. Transforming growth factor-beta and hepatocyte growth factor plasma levels in patients with inflammatory bowel disease. *Eur J Gastroenterol Hepatol* (2000) 12(4):445–50. doi: 10.1097/00042737-200012040-00013
34. Thatch KA, Mendelson KG, Haber MM, Schwartz MZ. Growth factor manipulation of intestinal angiogenesis: a possible new paradigm in the management of inflammatory bowel disease. *J Surg Res* (2009) 156(2):245–9. doi: 10.1016/j.jss.2009.01.036
35. Ido A, Numata M, Kodama M, Tsubouchi H. Mucosal repair and growth factors: recombinant human hepatocyte growth factor as an innovative therapy for inflammatory bowel disease. *J Gastroenterol* (2005) 40(10):925–31. doi: 10.1007/s00535-005-1705-x
36. Donate-Correa J, Ferri CM, Sánchez-Quintana F, Pérez-Castro A, González-Luis A, Martín-Núñez E, et al. Inflammatory cytokines in diabetic kidney disease: Pathophysiologic and therapeutic implications. *Front Med (Lausanne)* (2020) 7:628289. doi: 10.3389/fmed.2020.628289
37. Navarro-González JF, Mora-Fernández C. The role of inflammatory cytokines in diabetic nephropathy. *J Am Soc Nephrol* (2008) 19(3):433–42. doi: 10.1681/asn.2007091048
38. Sueud T, Hadi NR, Abdulameer R, Jamil DA, Al-Aubaidy HA. Assessing urinary levels of IL-18, NGAL and albumin creatinine ratio in patients with diabetic nephropathy. *Diabetes Metab Syndr* (2019) 13(1):564–8. doi: 10.1016/j.dsx.2018.11.022
39. Navarro-González JF, Mora-Fernández C, Muros de Fuentes M, García-Pérez J. Inflammatory molecules and pathways in the pathogenesis of diabetic nephropathy. *Nat Rev Nephrol* (2011) 7(6):327–40. doi: 10.1038/nrneph.2011.51
40. Fujita T, Ogihara N, Kamura Y, Satomura A, Fuke Y, Shimizu C, et al. Interleukin-18 contributes more closely to the progression of diabetic nephropathy than other diabetic complications. *Acta Diabetol* (2012) 49(2):111–7. doi: 10.1007/s00592-010-0178-4
41. Mezzano S, Aros C, Droguett A, Burgos ME, Ardiles L, Flores C, et al. NF-kappaB activation and overexpression of regulated genes in human diabetic nephropathy. *Nephrol Dial Transpl* (2004) 19(10):2505–12. doi: 10.1093/ndt/ghf207
42. Loher F, Bauer C, Landauer N, Schmall K, Siegmund B, Lehr HA, et al. The interleukin-1 beta-converting enzyme inhibitor pralnacasan reduces dextran sulfate sodium-induced murine colitis and T helper 1 T-cell activation. *J Pharmacol Exp Ther* (2004) 308(2):583–90. doi: 10.1124/jpet.103.057059
43. Williams MA, O'Callaghan A, Corr SC. IL-33 and IL-18 in inflammatory bowel disease etiology and microbial interactions. *Front Immunol* (2019) 10:1091. doi: 10.3389/fimmu.2019.01091
44. Wang Q, Zhang T, Chang X, Lim DY, Wang K, Bai R, et al. ARC is a critical protector against inflammatory bowel disease (IBD) and IBD-associated colorectal tumorigenesis. *Cancer Res* (2020) 80(19):4158–71. doi: 10.1158/0008-5472.Can-20-0469
45. Trivedi PJ, Adams DH. Chemokines and chemokine receptors as therapeutic targets in inflammatory bowel disease; pitfalls and promise. *J Crohns Colitis* (2018) 12(suppl_2):S641–s52. doi: 10.1093/ecco-jcc/jjx145
46. Masunaga Y, Noto T, Suzuki K, Takahashi K, Shimizu Y, Morokata T. Expression profiles of cytokines and chemokines in murine MDR1a-/- colitis. *Inflammation Res* (2007) 56(11):439–46. doi: 10.1007/s00011-007-6078-6
47. Gardlik R, Bartonova A, Celec P. Therapeutic DNA vaccination and RNA interference in inflammatory bowel disease. *Int J Mol Med* (2013) 32(2):492–6. doi: 10.3892/ijmm.2013.1388
48. Tolstanova G, Khomenko T, Deng X, Chen L, Tarnawski A, Ahluwalia A, et al. Neutralizing anti-vascular endothelial growth factor (VEGF) antibody reduces severity of experimental ulcerative colitis in rats: direct evidence for the pathogenic role of VEGF. *J Pharmacol Exp Ther* (2009) 328(3):749–57. doi: 10.1124/jpet.108.145128
49. Zhou Y, Tu C, Zhao Y, Liu H, Zhang S. Placental growth factor enhances angiogenesis in human intestinal microvascular endothelial cells via PI3K/Akt pathway: Potential implications of inflammation bowel disease. *Biochem Biophys Res Commun* (2016) 470(4):967–74. doi: 10.1016/j.bbrc.2016.01.073
50. Tokuhira N, Kitagishi Y, Suzuki M, Minami A, Nakanishi A, Ono Y, et al. PI3K/AKT/PTEN pathway as a target for crohn's disease therapy (Review). *Int J Mol Med* (2015) 35(1):10–6. doi: 10.3892/ijmm.2014.1981
51. Nakanishi A, Wada Y, Kitagishi Y, Matsuda S. Link between PI3K/AKT/PTEN pathway and NOX proteinin diseases. *Aging Dis* (2014) 5(3):203–11. doi: 10.14336/ad.2014.0500203
52. Takano Y, Yamauchi K, Hayakawa K, Hiramatsu N, Kasai A, Okamura M, et al. Transcriptional suppression of nephrin in podocytes by macrophages: roles of inflammatory cytokines and involvement of the PI3K/Akt pathway. *FEBS Lett* (2007) 581(3):421–6. doi: 10.1016/j.febslet.2006.12.051
53. Cheng Y, Zhang J, Guo W, Li F, Sun W, Chen J, et al. Up-regulation of Nrf2 is involved in FGF21-mediated fenofibrate protection against type 1 diabetic nephropathy. *Free Radic Biol Med* (2016) 93:94–109. doi: 10.1016/j.freeradbiomed.2016.02.002
54. Kerber EL, Padberg C, Koll N, Schuetzhold V, Fandrey J, Winning S. The importance of hypoxia-inducible factors (HIF-1 and HIF-2) for the pathophysiology of inflammatory bowel disease. *Int J Mol Sci* (2020) 21(22):8551. doi: 10.3390/ijms21228551
55. Yin J, Ren Y, Yang K, Wang W, Wang T, Xiao W, et al. The role of hypoxia-inducible factor 1-alpha in inflammatory bowel disease. *Cell Biol Int* (2022) 46(1):46–51. doi: 10.1002/cbin.11712
56. Knyazev E, Maltseva D, Raygorodskaya M, Shkurnikov M. HIF-dependent NFATC1 activation upregulates ITGA5 and PLAUR in intestinal epithelium in inflammatory bowel disease. *Front Genet* (2021) 12:791640. doi: 10.3389/fgene.2021.791640
57. Persson P, Palm F. Hypoxia-inducible factor activation in diabetic kidney disease. *Curr Opin Nephrol Hypertens* (2017) 26(5):345–50. doi: 10.1097/mnh.0000000000000341



OPEN ACCESS

EDITED BY

Guiting Lin,
University of California, San Francisco,
United States

REVIEWED BY

Ioannis Petrakis,
University of Crete, Greece
Fang Ma,
Guang'anmen Hospital, China Academy of
Chinese Medical Sciences, China

*CORRESPONDENCE

Hao Zhang

✉ zhanghaoliaoqing@163.com

[†]These authors have contributed
equally to this work and share
first authorship

SPECIALTY SECTION

This article was submitted to
Renal Endocrinology,
a section of the journal
Frontiers in Endocrinology

RECEIVED 06 September 2022

ACCEPTED 27 January 2023

PUBLISHED 10 February 2023

CITATION

Tian Z-Y, Li A-M, Chu L, Hu J, Xie X and
Zhang H (2023) Prognostic value of low-
density lipoprotein cholesterol in IgA
nephropathy and establishment of
nomogram model.

Front. Endocrinol. 14:1037773.

doi: 10.3389/fendo.2023.1037773

COPYRIGHT

© 2023 Tian, Li, Chu, Hu, Xie and Zhang.
This is an open-access article distributed
under the terms of the [Creative Commons
Attribution License \(CC BY\)](#). The use,
distribution or reproduction in other
forums is permitted, provided the original
author(s) and the copyright owner(s) are
credited and that the original publication in
this journal is cited, in accordance with
accepted academic practice. No use,
distribution or reproduction is permitted
which does not comply with these terms.

Prognostic value of low-density lipoprotein cholesterol in IgA nephropathy and establishment of nomogram model

Zhang-Yu Tian^{1†}, Ai-Mei Li^{1†}, Ling Chu², Jing Hu¹,
Xian Xie¹ and Hao Zhang^{1*}

¹Department of Nephrology, The Third Xiangya Hospital, Central South University, Changsha, Hunan, China, ²Department of Pathology, The Third Xiangya Hospital, Central South University, Changsha, Hunan, China

Background: Dyslipidemia is closely related to kidney disease. We aimed to investigate the relationship between low-density lipoprotein cholesterol (LDL-C) and prognosis of IgA nephropathy (IgAN) and build a nomogram prognostic model.

Methods: 519 IgAN patients with 61 months median follow-up were enrolled and divided into two groups based on the cut-off value of baseline LDL-C (2.60 mmol/L): the high group (n=253) and the low group (n=266). Renal survival was assessed by Kaplan-Meier (KM) survival curve. Risk factors were identified by COX regression analysis. The area under the receiver operating characteristic (ROC) curves (AUC), concordance index (C-index), and calibration curves were applied to evaluate the nomogram model.

Results: KM survival curve analysis showed that the high LDL-C group had worse renal survival than the low LDL-C group ($\chi^2 = 8.555$, $p=0.003$). After adjusting for confounding factors, Cox regression analysis showed the baseline LDL-C level was an independent risk factor of end-stage renal disease (ESRD) in IgAN (HR=3.135, 95% CI 1.240~7.926, $p=0.016$). LDL-C, segmental sclerosis, tubular atrophy/interstitial fibrosis, the prevalence of cardiovascular disease, 24-hour proteinuria were identified and entered into the nomogram models, with AUC of 0.864, 0.827, and 0.792 respectively to predict the 5-, 8-, and 10-year risk of ESRD in IgAN. The C-index of this prediction model was respectively 0.862, 0.838, and 0.800 and was well-calibrated.

Conclusion: Elevated LDL-C level is a predictive factor for the prognosis of IgAN. We developed a nomogram model that can predict the risk of ESRD in IgAN by using $\text{LDL-C} \geq 2.60 \text{ mmol/L}$.

KEYWORDS

IgA nephropathy, low-density lipoprotein cholesterol, prognosis, ESRD, nomogram prognostic model

1 Introduction

Immunoglobulin A nephropathy (IgAN) is the most common primary glomerulonephritis worldwide, and approximately 30% of IgAN patients develop ESRD within 20 years (1, 2). Recognizing risk factors of end-stage renal disease (ESRD) and establishing a nomogram prognostic model for patients with IgAN is worthwhile.

Guidelines for lipid management of chronic kidney disease (CKD), particularly in ESRD is inconsistent worldwide at present (3). The KDIGO guidelines focus on cardiovascular risk to guide treatment and do not recommend treating any patient based on “high” cholesterol levels per se. However, the 2016 European Guidelines suggest most patients with a 10-year cardiovascular risk of 5–10% would benefit from lipid-lowering therapy if their baseline LDL cholesterol was 2.6–4 mmol/l (4). KDIGO guidelines recommend that dialysis patients should not be started on statins or a combination of statins and ezetimibe (5). The 2016 Canadian Cardiovascular Society Guidelines for the Management of Dyslipidemia recommend that patients on dialysis should begin treatment if they are likely to remain on dialysis for many years or receive a transplant (6).

There is a strong, robust and graded association between LDL-C levels and cardiovascular risk, and lowering LDL-C reduces cardiovascular risk in a dose-dependent manner (7, 8). Furthermore, accumulation and lipotoxicity can lead to glomerular podocyte and proximal tubular epithelial cell dysfunction (3, 9). Study showed hypertriglyceridemia was prevalent in CKD patients, and it was independent risk factor for moderate tubular atrophy/interstitial fibrosis (10). Oxidized LDL-C (oxLDL) can promote glomerulosclerosis through infiltration of monocytes/macrophages and overexpression of adhesion molecules (11). Levels of lipids are closely related to renal function, and lipid metabolism is often disturbed in IgAN patients with predominantly nephrotic syndrome (12, 13). Hypercholesterolemia and hypertriglyceridemia are reported to be relevant to the deterioration of renal function in

adults with IgAN (14). However, the relationship between levels of LDL and prognosis of IgAN was not yet studied.

The utilization of lipid-lowering agents in early kidney disease in the 2013 KDIGO guidelines are relatively conservative (3). Assessment of lipids level in renal injury and prognosis of IgAN is currently undervalued. The aim of this study was to investigate the prognostic relevance of LDL-C levels in IgAN patients, with the expectation of informing LDL-C treatment targets in lipid management of IgAN.

2 Method

2.1 Patients selection

As shown in a flow chart (Figure 1), there were 3465 patients who underwent renal puncture biopsy between April 13, 2012 and April 29, 2022, and 657 IgAN patients were automatically screened from the electronic medical record system of the Third Xiangya Hospital of Central South University. The key inclusion criteria were primary IgA nephropathy confirmed on biopsy; estimated glomerular filtration rate (eGFR) > 15 ml·min⁻¹·(1.73 m²)⁻¹ at the time of renal biopsy; renal tissue specimens with at least 5 mm cortical and 8 glomeruli. Major exclusion criteria were combination of other types of primary glomerular disease, or secondary IgAN, or systemic disease (e.g., systemic lupus erythematosus, severe infection, etc.); immunosuppressive therapy before renal biopsy; incomplete clinical or pathological data; follow-up < 3 months. After reviewing the electronic medical records, 16 patients with secondary IgAN, 7 patients with less than 3 months follow-up before reaching endpoint, 8 patients with immunosuppressive therapy before renal biopsy, 46 patients with less than 8 glomeruli, and 61 patients with incomplete data were excluded. Finally, 519 patients were included in this study. The cut-off value of the baseline LDL-C of 519 IgAN patients were divided into two groups: the high group (LDL-C ≥ 2.60 mmol/L, n=253) and the low group (LDL-C < 2.60 mmol/L, n=266).

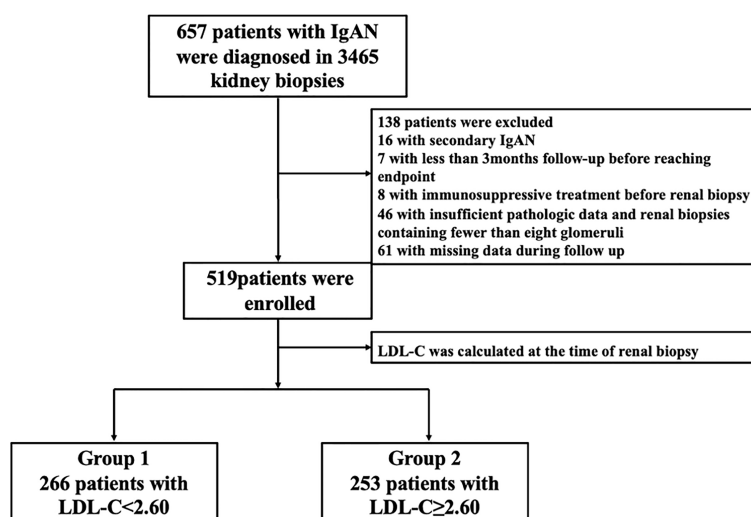


FIGURE 1

The selection process for patients in a flow chart. IgAN, IgA nephropathy; LDL-C, low-density lipoprotein cholesterol.

2.2 Ethical approval

This study was approved by the Ethics Committee of the Third Xiangya Hospital of Central South University (NO.22146)

2.3 Data collection

Age, sex, systolic blood pressure (SBP), diastolic blood pressure (DBP), cardiovascular disease (CVD), diabetes, serum albumin, serum creatinine (Scr), serum uric acid (SUA), blood urea nitrogen (BUN), estimated glomerular filtration rate (eGFR), triglyceride (TG), total cholesterol (TC), 24-hour proteinuria, pathological findings, and treatment were collected from the enrolled patients. Patients were followed up every 3 months with a follow-up deadline of July 27, 2022.

2.4 Relevant definitions

eGFR: Calculated by the MDRD formula recommended by the 2002 National Kidney Foundation - Guidelines for quality of survival in patients with kidney disease (8). $eGFR [ml \cdot min^{-1} \cdot (1.73m^2)^{-1}] = 186.3 \times [Scr (mg/dl)]^{-1.154} \times [age (years)]^{-0.203} \times 0.742$ (female).

Renal pathology: Pathological diagnosis was based on the IgAN Oxford Classification (8): (i) mesangial hypercellularity (M); (ii) endocapillary cellularity (E); (iii) segmental sclerosis (S); (iv) tubular atrophy/interstitial fibrosis (T); (v) crescents (C).

CVD: Including atherosclerosis, hypertension, myocardial infarction, and stroke.

Treatment: Treatment with glucocorticoids and/or immunosuppressants, including oral methylprednisolone or equivalent doses of prednisone for at least 3 months, and/or oral tacrolimus or mycophenolate mofetil treatment for at least 3 months.

Renal outcome: The progression to ESRD, defined by commencement of renal replacement therapy or an $eGFR < 15 ml \cdot min^{-1} \cdot (1.73 m^2)^{-1}$.

2.5 Statistics

The discriminatory power of various predictive factors for development of renal survival was tested by the area under the receiver operating characteristic curve (AUROC), and the optimal cut-off point of the LDL-C was obtained by calculating the Youden index. The Youden index is a method of evaluating the authenticity of a screening test, which represents the total ability of the screening method to detect true patients and nonpatients. A higher index is associated with a better effect and greater authenticity of the screening test. The LDL-C that corresponded to the maximum Youden index was then determined to be the optimal cut-off LDL-C in this study.

Statistical analyses were performed using SPSS 26.0 software and R statistical software. The Kolmogorov-Smirnov normality test was used to estimate the data distribution. Normally distributed data were expressed as mean \pm standard deviation ($\bar{x} \pm SD$) and one-way ANOVA was used for comparison between groups. Non-normally distributed data were expressed as median (interquartile range) and

non-parametric tests were used for comparisons between groups. The chi-square test was used to analyze the count data. $p < 0.05$ indicates statistical significance. Univariate COX regression analysis was performed to identify risk factors for IgAN. Risk factors with p values < 0.05 in the univariate analysis were included in the multivariate cox regression. Multivariate cox regression was performed to identify independent risk factors, and a nomogram prediction model was developed using a stepwise approach to identify useful combinations of factors to predict IgAN prognosis. The performance of the column line graphs was assessed using the C-index and calibration plots with bootstrap samples. The C-index is a numerical measure of discriminative ability and the calibration curve is a graphical assessment of predictive ability that compare observed probabilities with nomogram-predicted probabilities. The column line graphs are constructed using the “rms” package.

3 Results

3.1 Patients' general characteristics

519 IgAN patients were enrolled in this study, and the baseline characteristics of IgAN patients at the time of renal biopsy are shown in Table 1. The median age of IgAN patients was 32 (25, 42) years old, and 85.6% of patients were in CKD1-2 stage. Compared with patients in the low LDL-C group, patients in the high LDL-C group had lower baseline serum albumin ($p < 0.05$) and higher age, male prevalence, incidence of CVD, 24-hour proteinuria, SUN, SUA, TG, TC (all $p < 0.05$). In the IgAN Oxford Classification, the differences in M1, E1, S1, T1-2 and C1-2 prevalence were not statistically significant. But LDL-C is associated with IgA deposition ($p < 0.05$). In terms of treatment, patients in the high LDL-C group received higher glucocorticosteroid ($p < 0.001$) and immunosuppressants ($p < 0.05$) compared with the low LDL-C group, but the difference between the two groups receiving RAS inhibitors, calcium channel blocker was not statistically significant. In conclusion, patients in the high LDL-C group had worse nutritional status, more pronounced proteinuria, more incidence of CVD, higher IgA deposition, poorer renal function and other clinical indicators at compared to patients with lower LDL-C.

3.2 Relationship between LDL-C and the prognosis of IgAN

During a median follow-up time of 61 (31,89) months, 26 cases were into ESRD. There were 20 cases of ESRD events in the high LDL-C group (76.92%), including 18 cases of renal dialysis, 2 cases of $eGFR < 15 ml \cdot min^{-1} \cdot (1.73 m^2)^{-1}$. There were 6 endpoint events in the low LDL-C group (23.08%), including 5 cases of renal dialysis, 1 case of $eGFR < 15 ml \cdot min^{-1} \cdot (1.73 m^2)^{-1}$. Kaplan-Meier survival curve analysis showed that renal survival in the high LDL-C group was significantly lower than in the low LDL-C group ($\chi^2 = 8.555$, $p = 0.003$) (Figure 2). LDL-C was included in the Cox regression equation as a categorical independent variable. The univariate Cox analysis showed that high LDL-C, prevalence of CVD, SUA, BUN, Scr, 24-hour proteinuria, M1, S1, T1-2, and C1-2 were influential

TABLE 1 Demographic and clinicopathological characteristics of patients with IgAN.

Characteristic	Median (IQR) (n=519)	Low LDL-C group<2.60 (n=266)	High LDL-C group≥2.60 (n=253)	t/Z/ x ²	P value
*Age (years)	32 (25,42)	31 (24,39)	35 (26,46)	-3.094	0.002 [#]
Sex (male,%)	253 (48.7)	117 (46.2)	136 (53.8)	4.954	0.026 [#]
SBP (mmHg, $\bar{x}\pm s$)	120.63 \pm 28.12	119.86 \pm 30.453	121.43 \pm 25.480	-0.634	0.526
DBP (mmHg, $\bar{x}\pm s$)	77.29 \pm 19.03	76.74 \pm 20.259	77.88 \pm 17.674	-0.680	0.497
CVD (%)					
Prevalence of CVD	104 (20.0)	51 (49.0)	53 (51.0)	0.255	0.613
Incidence of CVD	49 (9.44)	18 (36.7)	31 (63.3)	4.565	0.033 [#]
Diabetes (%)	15 (2.9)	10 (66.7)	5 (33.3)	1.469	0.226
*eGFR[ml·min ⁻¹ ·(1.73m ²) ⁻¹]	91.70 (72.17,113.23)	95.67 (75.96, 112.06)	88.19 (68.59,116.17)	-1.583	0.113
CKD Classification (%)				12.84	0.005 [#]
CKD1	276 (53.2)	154 (55.8)	122 (44.2)		
CKD2	168 (32.4)	81 (48.2)	87 (51.8)		
CKD3	66 (12.7)	31 (47.0)	35 (53.0)		
CKD4	9 (1.7)	0 (0.00)	9 (100.00)		
* 24-hour proteinuria (mg/d)	898.0 (324.0,2326.0)	606.5 (256.0,1289.0)	1663.5 (542.5,3233.0)	-7.339	<0.001 [#]
* Scr (μ mol/L)	78 (63,98)	77 (62,94)	79 (64,102)	-1.867	0.062
SUA (μ mol/L, $\bar{x}\pm s$)	359.55 \pm 112.56	346.16 \pm 104.74	373.63 \pm 118.83	-2.797	0.005 [#]
*SUN (mmol/L)	4.87 (3.95,6.02)	4.76 (3.81,5.81)	5.00 (4.09,6.18)	-1.967	0.049 [#]
*ALB (g/L)	37.70 (32.60,41.50)	39.20 (35.90,42.20)	34.10 (24.00,39.85)	-7.853	<0.001 [#]
*TG (mmol/L)	1.36 (0.96,2.09)	1.12 (0.82,1.84)	1.67 (1.14,2.32)	-6.027	<0.001 [#]
*TC (mmol/L)	4.86 (4.09,6.05)	4.12 (3.63,4.60)	5.92 (5.21,7.52)	-17.277	<0.001 [#]
Oxford Classification (%)					
M1	161 (31.0)	75 (46.6)	86 (53.4)	2.036	0.154
E1	22 (4.2)	12 (54.5)	10 (48.9)	0.100	0.752
S1	147 (28.3)	79 (53.7)	68 (46.3)	0.509	0.476
T1-2	55 (10.6)	24 (43.6)	31 (56.4)	1.428	0.232
C1-2	59 (11.3)	29 (49.2)	30 (50.8)	0.117	0.732
IgA deposition (%)				10.488	0.033 [#]
–	4 (0.8)	1 (25.0)	3 (75.0)		
+	116 (22.4)	52 (44.8)	64 (55.2)		
++	131 (25.2)	59 (45.0)	72 (55.0)		
+++	267 (51.4)	154 (42.3)	113 (57.7)		
++++	1 (0.2)	0 (0.0)	1 (100.0)		
Treatment (%)					
ACEI or ARB agents	334 (64.4)	164 (49.1)	170 (50.9)	1.735	0.188
CCB	79 (15.2)	35 (44.3)	44 (55.7)	1.801	0.180
Glucocorticosteroid	205 (39.5)	80 (39.0)	125 (61.0)	20.279	<0.001 [#]
Immunosuppressant	145 (27.9)	59 (40.7)	86 (59.3)	8.986	0.003 [#]

*# indicates that data were not normally distributed and are expressed as median (interquartile range), M (Q). “#” indicates the difference was statistically significant (p<0.05). eGFR, estimated glomerular filtration rate; LDL-C, low-density lipoprotein cholesterol; SBP, systolic blood pressure; DBP, diastolic blood pressure; CVD, cardiovascular disease; Scr, serum creatinine; SUA, serum uric acid; BUN, blood urea nitrogen; TG, triglycerides; TC, total cholesterol; CCB, calcium channel blocker; IQR, interquartile range. –, +, ++, +++ and ++++ represent the intensity of IgA deposition in the mesangial membrane in immunohistochemistry.

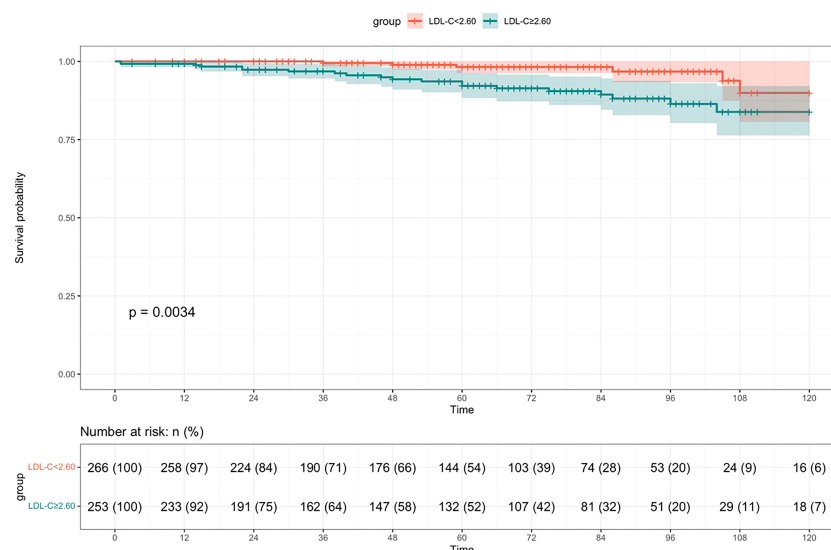


FIGURE 2
Survival rate of patients in the high LDL-C group compared to the low LDL-C group with IgAN (Kaplan-Meier survival curve).

factors of prognosis of patients with IgAN ($p < 0.05$). Multivariate Cox analysis showed that LDL-C was an independent risk factor for renal prognosis in patients with IgAN (HR=3.135, 95% CI 1.240~7.926, $p = 0.016$), suggesting that patients in the high LDL-C group had a 3.135-fold higher risk than the low group to enter ESRD. In addition to LDL-C, prevalence of CVD, S, T and 24-hour proteinuria were independent risk factors for IgAN in this COX model ($p < 0.05$) (Table 2).

3.3 Establish and validate the nomogram prognostic model

When patients with LDL-C ≥ 2.60 mmol/L, they scored higher and indicate a worse prognosis. In addition, higher prevalence of CVD, S1, T1-2, 24-hour proteinuria and higher score of renal pathology indicated worse 5-, 8-, and 10-year risk of ESRD in IgAN (Figure 3). The AUC of the nomogram model was respectively evaluated at 0.864, 0.827, and 0.792 at 5, 8, and 10 years (Figure 4) and the corresponding C indices were respectively 0.862, 0.838, and 0.800, which indicated the nomogram model was accurate in predicting risk of ESRD in IgAN. The calibration against the nomogram model was also evaluated with the calibration curve (Figure 5) and the figure shows that the predictions are close to the observed results, which further demonstrates the reliability of the nomogram model in predicting risk of ESRD in IgAN.

4 Discussion

In this study, we found that IgAN patients with higher LDL-C level had severer clinical features, interstitial renal pathology changes and higher risk of ESRD. LDL-C, prevalence of CVD, S, T, 24-hour proteinuria were independent risk factors for prognosis of IgAN.

Furthermore, we have developed a novel nomogram using these five indicators which showed valid and reliable prediction of 5-, 8-, and 10-year risk of ESRD in IgAN.

Dyslipidemia and renal function affect each. As renal function declines, a quantitative shift in lipid levels occurs which is characterized by elevated triglycerides, low HDL-C, and varying levels of ox-LDL and carbamylated LDL (c-LDL) cholesterol levels. Along with these quantitative changes, major qualitative changes in lipoprotein particles make them more atherogenic, including increased oxidation (15). Moorhead et al. suggested that dyslipidemia may be caused by loss of urinary protein and lead to compensatory reduction of lipoprotein synthesis and catabolism by the liver, which result in further renal injury (16). Tsutomu Hirano et al. proposed that renal insufficiency is linked to increased lipoprotein(a), and proteinuria is correlated with atherogenic subspecies of LDL (17). It has also been shown that hypercholesterolemia and hypertriglyceridemia are relevant to the deterioration of renal function in adults with IgAN (14). Our study found that IgAN patients with higher LDL-C level had worse renal function probably because patients in the high LDL-C group had higher oxLDL, which caused more oxidative stress resulting in glomerular and tubular damage, and thus was easier to enter ESRD.

Lipids are in close association with pathological impairment of IgAN. Hongjie Zhuang et al. showed that compared to children without dyslipidemia, children in the dyslipidemia group had severer clinical features and pathological changes, with higher proportions of S1 and C2 in the Oxford Classification of IgAN (18). Won Jung Choi et al. demonstrated that overall renal sclerosis, S, and M were higher in patients with IgAN in the high triglyceride group compared to the normal triglyceride group (19). This may be due to that dyslipidemia can cause renal tubular injury and promote renal fibrosis by inducing lipotoxicity, inflammation, oxidative stress and signaling events (20). Furthermore, the proximal tubule is rich in mitochondria, the main site of oxidative phosphorylation for energy supply, and is more susceptible to chronic inflammation and reactive

TABLE 2 Analysis of factors influencing poor renal prognosis in patients with IgAN (Cox regression equation).

Independent variables	Univariate analysis		Multivariate analysis	
	HR (95%CI)	P Value	HR (95%CI)	P Value
High LDL-C group	3.576 (1.435~8.911)	0.006 [#]	3.135 (1.240~7.926)	0.016 [#]
Female	1.481 (0.684~3.206)	0.319		
Age	1.022 (0.990~1.055)	0.175		
Prevalence of CVD	3.758 (1.735~8.140)	0.001 [#]	3.956 (1.744~8.969)	0.001 [#]
SUA	1.004 (1.001~1.007)	0.005 [#]		
Diabetes	2.371 (0.560~10.050)	0.241		
BUN	1.183 (1.113~1.256)	<0.001 [#]		
SCr	1.019 (1.014~0.103)	<0.001 [#]		
ALB	0.969 (0.930~1.010)	0.134		
24-hour proteinuria	1.000 (1.000~1.000)	<0.001 [#]	1.000 (1.000~1.000)	0.007 [#]
M1	3.581 (1.652~7.761)	0.001 [#]		
E1	3.548 (1.049~11.998)	0.080		
S1	2.900 (1.330~6.320)	0.007 [#]	2.755 (1.219~6.224)	0.015 [#]
T1-2	8.340 (3.864~18.003)	<0.001 [#]	6.033 (2.716~13.400)	<0.001 [#]
C1-2	3.988 (1.733~9.177)	0.001 [#]		
Glucocorticosteroid	0.470 (0.213~1.037)	0.061		
Immunosuppressant	0.603 (0.273~1.333)	0.211		

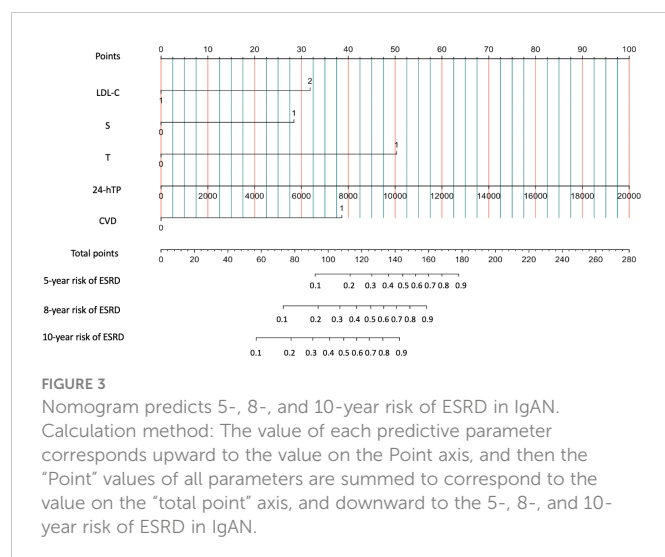
LDL-C, low-density lipoprotein cholesterol; CVD, cardiovascular disease; Scr, serum creatinine; SUA, serum uric acid; BUN, blood urea nitrogen; HR, hazard ratio; CI, confidence interval. “#” indicates the difference was statistically significant ($p < 0.05$).

oxygen species damage brought about by lipids (21). In addition, our study found that LDL-C was associated with IgA deposition, which may be related to the pathogenesis of IgAN and disease progression.

Some lipids are closely associated with the prognosis of IgAN. Studies have shown that high serum triglycerides are associated with a decrease in eGFR and a significant association with the incidence and progression of CKD (22). P Y Zuo et al. found that the ratio of NonHDLc/HDLc was an independent risk factor for the development

of CKD and was useful in identifying people at high risk of CKD (23). After adjusting for potential confounders, patients in the highest tertile of NonHDLc/HDLc had a 1.45-fold higher risk of CKD than those in the lowest tertile (23). J Syrjänen et al. showed by developing a COX regression risk model that hypertriglyceridemia and hyperuricemia at diagnosis were adverse prognostic predictors for IgAN, whereas these factors were greatly underestimated previously (24). In our study, Kaplan-Meier analysis showed that IgAN patients in the high LDL-C group were more susceptible to ESRD. Additionally, multivariate COX regression analysis showed that LDL-C was an independent risk factor for IgAN patients. Our nomogram modeling showed higher scores in the high LDL-C group and higher 5-, 8-, and 10-year risk of ESRD in IgAN patients. Further, we firstly included prevalence of CVD, S, T and 24-hour proteinuria formation into the assessment parameters in combination with LDL-C to establish a nomogram prediction model and validated the reliability of the nomogram model by C-index and calibration plots.

Studies have shown that large amounts of filtered lipoproteins could contribute to the proliferation of mesangial cells, and the deposition of apolipoproteins in the renal tubules can lead to tubulointerstitial lesions (9). This provides a theoretical basis for the idea that lipid-lowering therapy can prevent renal fibrosis. However, some studies have shown that statin therapy modestly reduces the rate of proteinuria and eGFR decline, but not the incidence of renal endpoint events (25). The 2013 KDIGO guidelines recommend that non-dialysis CKD patients ≥ 50 years of age should be treated with statins or a statin/ezetimibe combination



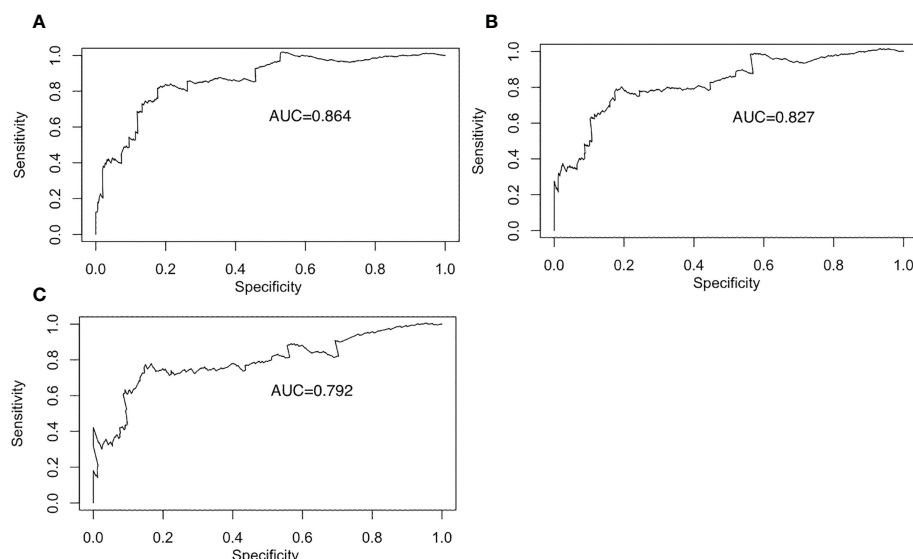


FIGURE 4

Receiver operating characteristic curve for the prediction model. Receiver operating characteristic curves for the 5-year prediction models. (A) Receiver operating characteristic curves for the 8-year prediction models. (B) Receiver operating characteristic curves for the 10-year prediction models. (C).

for lipid abnormalities, but do not specify therapeutic target values for lipids (5). In this study, we showed that the majority of IgAN patients were young adults around 33 years of age and in the early stages of CKD at the time of renal biopsy. However, LDL-C does represent an independent risk factor for the prognosis of IgAN and is more susceptible to ESRD when LDL-C ≥ 2.60 mmol/L. Therefore, the 2013 KDIGO guidelines may be too conservative in the use of lipid-lowering drugs for young IgAN patients in the early stages of CKD. Our study indicated that when LDL-C is elevated above 2.60 mmol/L, clinicians should take a serious look at it and comprehensively evaluate the use of lipid-lowering drugs.

The present study also has some limitations. First, the exact mechanism of LDL-C involvement in IgAN pathogenesis is unclear and needs to be further explored. Second, the number of patients studied in this study was small and the study was a single-center cross-sectional study. Further prospective and cross-sectional studies could be conducted, including an expanded sample size, different ethnicities, regions, etc. Furthermore, the prediction model developed in this study needs to be corroborated by further external validation, as we only used internal validation.

In conclusion, elevated LDL-C level is a predictive factor for the prognosis of IgAN. We have developed and internally validated a

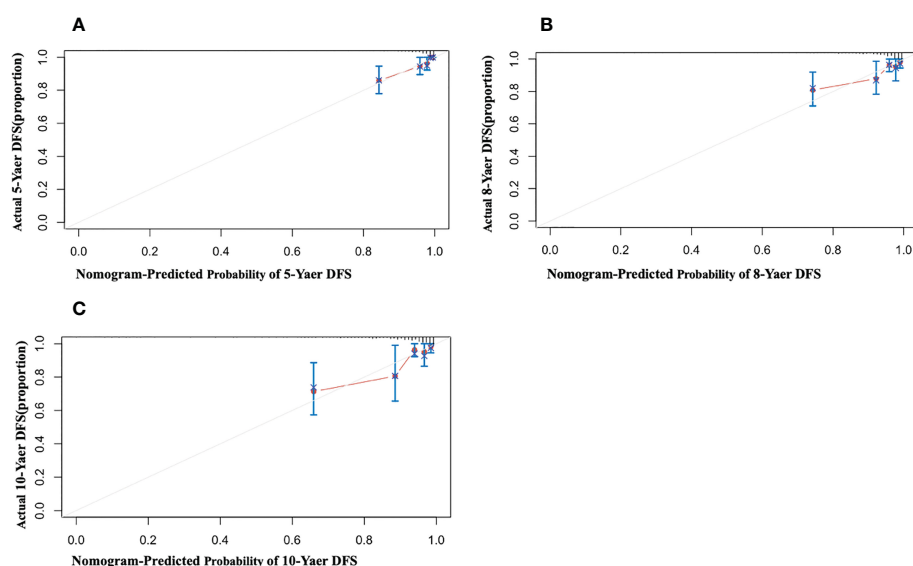


FIGURE 5

Calibration of the nomogram for Risk of ESRD in IgAN. The x-axis shows the predicted probability of risk of ESRD in IgAN, and the y-axis shows the observed probability of risk of ESRD in IgAN. (A) Nomogram of 5-year calibrated risk of ESRD in IgAN. C-index: 0.862; (B) Nomogram of 8-year calibrated risk of ESRD in IgAN. C-index: 0.838; (C) Nomogram of 10-year calibrated risk of ESRD in IgAN. C-index: 0.800.

novel nomogram which showed valid and reliable prediction of 5-, 8-, and 10-year risk of ESRD in IgAN.

Data availability statement

The raw data supporting the conclusions of this article will be made available by the authors, without undue reservation.

Ethics statement

This study was approved by the Ethics Committee of the Third Xiangya Hospital of Central South University (NO.22146). The patients/participants provided their written informed consent to participate in this study.

Author contributions

Z-YT, A-ML wrote the first draft of the manuscript. HZ, LC, JH and XX contributed to conception and design of the study. All authors contributed to manuscript revision, read, and approved the submitted version.

References

- Hassler JR. IgA nephropathy: A brief review. *Semin In Diagn Pathol* (2020) 37 (3):143–7. doi: 10.1053/j.semdp.2020.03.001
- Schena FP. A retrospective analysis of the natural history of primary IgA nephropathy worldwide. *Am J Med* (1990) 89(2):209–15. doi: 10.1016/0002-9343(90)90300-3
- Ferro CJ, Mark PB, Kanbay M, Sarafidis P, Heine GH, Rossignol P, et al. Lipid management in patients with chronic kidney disease. *Nat Rev Nephrol* (2018) 14(12):727–49. doi: 10.1038/s41581-018-0072-9
- Piepoli MF, Hoes AW, Agewall S, Albus C, Brotons C, Catapano AL, et al. 2016 European guidelines on cardiovascular disease prevention in clinical practice: The sixth joint task force of the European society of cardiology and other societies on cardiovascular disease prevention in clinical practice (constituted by representatives of 10 societies and by invited experts)/Developed with the special contribution of the European association for cardiovascular prevention & rehabilitation (EACPR). *Eur Heart J* (2016) 37(29):2315–81. doi: 10.1093/eurheartj/ehw106
- Wanner C, Tonelli M. KDIGO clinical practice guideline for lipid management in CKD: summary of recommendation statements and clinical approach to the patient. *Kidney Int* (2014) 85(6):1303–9. doi: 10.1038/ki.2014.31
- Anderson TJ, Grégoire J, Pearson GJ, Barry AR, Couture P, Dawes M, et al. 2016 Canadian cardiovascular society guidelines for the management of dyslipidemia for the prevention of cardiovascular disease in the adult. *Can J Cardiol* (2016) 32(11):1263–82. doi: 10.1016/j.cjca.2016.07.510
- Baigent C, Blackwell L, Emberson J, Holland LE, Reith C, Bhalan N, et al. Efficacy and safety of more intensive lowering of LDL cholesterol: a meta-analysis of data from 170,000 participants in 26 randomised trials. *Lancet (London England)* (2010) 376(9753):1670–81. doi: 10.1016/S0140-6736(10)61350-5
- Fulcher J, O'Connell R, Voysey M, Emberson J, Blackwell L, Mihaylova B, et al. Efficacy and safety of LDL-lowering therapy among men and women: meta-analysis of individual data from 174,000 participants in 27 randomised trials. *Lancet (London England)* (2015) 385(9976):1397–405. doi: 10.1016/S0140-6736(14)61368-4
- Gyebi L, Soltani Z, Reisin E. Lipid nephrotoxicity: new concept for an old disease. *Curr Hypertens Rep* (2012) 14(2):177–81. doi: 10.1007/s11906-012-0250-2
- Liu B-M, Zhao L-Y, Yang Q-Q, Zha D-G, Si X-Y. Hyperuricemia and hypertriglyceridemia indicate tubular atrophy/interstitial fibrosis in patients with IgA nephropathy and membranous nephropathy. *Int Urol Nephrol* (2021) 53(11):2321–32. doi: 10.1007/s11255-021-02844-4
- Nistala R, Whaley-Connell A, Sowers JR. Redox control of renal function and hypertension. *Antioxid Redox Signaling* (2008) 10(12):2047–89. doi: 10.1089/ars.2008.2034
- Zhang X-L, Wang B-Y, Yang J, Wang J-C, Yu Y-R, Jiang C-F, et al. Serum lipids and risk of rapid renal function decline in treated hypertensive adults with normal renal function. *Am J Hypertens* (2019) 32(4):393–401. doi: 10.1093/ajh/hpz001
- Kuma A, Uchino B, Ochiai Y, Kawashima M, Enta K, Tamura M, et al. Impact of low-density lipoprotein cholesterol on decline in estimated glomerular filtration rate in apparently healthy young to middle-aged working men. *Clin Exp Nephrol* (2018) 22 (1):15–27. doi: 10.1007/s10157-017-1407-8
- Le W-B, Liang S-S, Hu Y-L, Deng K-P, Bao H, Zeng C-H, et al. Long-term renal survival and related risk factors in patients with IgA nephropathy: results from a cohort of 1155 cases in a Chinese adult population. *Nephrol Dial Transplant* (2012) 27(4):1479–85. doi: 10.1093/ndt/gfr527
- Vaziri ND. Dyslipidemia of chronic renal failure: the nature, mechanisms, and potential consequences. *Am J Physiol Renal Physiol* (2006) 290(2):F262–72. doi: 10.1152/ajprenal.00099.2005
- Moorhead JF, Chan MK, El-Nahas M, Varghese Z. Lipid nephrotoxicity in chronic progressive glomerular and tubulo-interstitial disease. *Lancet (London England)* (1982) 2 (8311):1309–11. doi: 10.1016/S0140-6736(82)91513-6
- Hirano T, Satoh N, Kodera R, Hirashima T, Suzuki N, Aoki E, et al. Dyslipidemia in diabetic kidney disease classified by proteinuria and renal dysfunction: A cross-sectional study from a regional diabetes cohort. *J Diabetes Invest* (2022) 13(4):657–67. doi: 10.1111/jdi.13697
- Zhuang H-J, Lin Z-L, Zeng S-H, Jiang M-J, Chen L-Z, Jiang X-Y, et al. Dyslipidemia may be a risk factor for progression in children with IgA nephropathy. *Pediatr Nephrol (Berlin Germany)* (2022) 37(12):3147–56. doi: 10.1007/s00467-022-05480-x
- Choi WJ, Hong YA, Min JW, Koh ES, Kim HD, Ban TH, et al. Hypertriglyceridemia is associated with more severe histological glomerulosclerosis in IgA nephropathy. *J Clin Med* (2021) 10(18):4236. doi: 10.3390/jcm10184236
- Chen S-X, Chen J-X, Li S-M, Guo F-B, Li A-F, Wu H, et al. High-fat diet-induced renal proximal tubular inflammatory injury: Emerging risk factor of chronic kidney disease. *Front In Physiol* (2021) 12:786599. doi: 10.3389/fphys.2021.786599

Funding

This study was funded by the National Natural Science Foundation of China (No. 81870498, No. 82000696), Natural Science Foundation of Hunan Province (No. 2021JJ40925) and Wisdom Accumulation and Talent Cultivation Project of the Third Xiangya Hospital of Central South University (YX202207).

Conflict of interest

The authors declare that the research was conducted in the absence of any commercial or financial relationships that could be construed as a potential conflict of interest.

Publisher's note

All claims expressed in this article are solely those of the authors and do not necessarily represent those of their affiliated organizations, or those of the publisher, the editors and the reviewers. Any product that may be evaluated in this article, or claim that may be made by its manufacturer, is not guaranteed or endorsed by the publisher.

21. Du X-G, Ruan X-Z. Lipid metabolism disorder and renal fibrosis. *Adv In Exp Med Biol* (2019) 1165:525–41. doi: 10.1007/978-981-13-8871-2_26
22. Tsuruya K, Yoshida H, Nagata M, Kitazono T, Iseki K, Iseki C, et al. Association of hypertriglyceridemia with the incidence and progression of chronic kidney disease and modification of the association by daily alcohol consumption. *J Renal Nutr* (2017) 27(6):381–94. doi: 10.1053/j.jrn.2017.05.002
23. Zuo P-Y, Chen X-L, Liu Y-W, Zhang R, He X-X, Liu C-Y, et al. Non-HDL-cholesterol to HDL-cholesterol ratio as an independent risk factor for the development of chronic kidney disease. *Nutr Metab Cardiovasc Dis* (2015) 25(6):582–7. doi: 10.1016/j.numecd.2015.03.003
24. Syrjänen J, Mustonen J, Pasternack A. Hypertriglyceridaemia and hyperuricaemia are risk factors for progression of IgA nephropathy. *Nephrol Dial Transplant* (2000) 15(1):34–42. doi: 10.1093/ndt/15.1.34
25. Su X-L, Zhang L, Lv J-C, Wang J-W, Hou W-Y, Xie X-F, et al. Effect of statins on kidney disease outcomes: A systematic review and meta-analysis. *Am J Kidney Dis* (2016) 67(6):881–92. doi: 10.1053/j.ajkd.2016.01.016



OPEN ACCESS

EDITED BY

Ningning Hou,
Affiliated Hospital of Weifang Medical
University, China

REVIEWED BY

Lale Ertuglu,
Vanderbilt University Medical Center,
United States
Fernando P. Dominici,
University of Buenos Aires, Argentina

*CORRESPONDENCE

Bingzi Dong

✉ dongbingzi@hotmail.com

Lili Xu

✉ qdfyxl@qdu.edu.cn

SPECIALTY SECTION

This article was submitted to
Cellular Endocrinology,
a section of the journal
Frontiers in Endocrinology

RECEIVED 16 December 2022

ACCEPTED 26 January 2023

PUBLISHED 13 February 2023

CITATION

Lv R, Xu L, Che L, Liu S, Wang Y and
Dong B (2023) Cardiovascular-renal
protective effect and molecular
mechanism of finerenone in type 2 diabetic
mellitus.

Front. Endocrinol. 14:1125693.

doi: 10.3389/fendo.2023.1125693

COPYRIGHT

© 2023 Lv, Xu, Che, Liu, Wang and Dong.

This is an open-access article distributed
under the terms of the [Creative Commons
Attribution License \(CC BY\)](https://creativecommons.org/licenses/by/4.0/). The use,
distribution or reproduction in other
forums is permitted, provided the original
author(s) and the copyright owner(s) are
credited and that the original publication in
this journal is cited, in accordance with
accepted academic practice. No use,
distribution or reproduction is permitted
which does not comply with these terms.

Cardiovascular-renal protective effect and molecular mechanism of finerenone in type 2 diabetic mellitus

Ruolin Lv¹, Lili Xu^{1*}, Lin Che², Song Liu³, Yangang Wang¹
and Bingzi Dong^{1*}

¹Department of Endocrinology and Metabolism, The Affiliated Hospital of Qingdao University, Qingdao, China, ²Department of Nephrology, The Affiliated Hospital of Qingdao University, Qingdao, China, ³Department of Cardiology, The Affiliated Hospital of Qingdao University, Qingdao, China

Chronic kidney diseases (CKD) and cardiovascular diseases (CVD) are the main complications in type 2 diabetic mellitus (T2DM), increasing the risk of cardiovascular and all-cause mortality. Current therapeutic strategies that delay the progression of CKD and the development of CVD include angiotensin-converting enzyme inhibitors (ACEI), angiotensin II receptor blockers (ARB), sodium-glucose co-transporter 2 inhibitors (SGLT-2i) and GLP-1 receptor agonists (GLP-1RA). In the progression of CKD and CVD, mineralocorticoid receptor (MR) overactivation leads to inflammation and fibrosis in the heart, kidney and vascular system, making mineralocorticoid receptor antagonists (MRAs) as a promising therapeutic option in T2DM with CKD and CVD. Finerenone is the third generation highly selective non-steroidal MRAs. It significantly reduces the risk of cardiovascular and renal complications. Finerenone also improves the cardiovascular-renal outcomes in T2DM patients with CKD and/or chronic heart failure (CHF). It is safer and more effective than the first- and second-generation MRAs due to its higher selectivity and specificity, resulting in a lower incidence of adverse effects including hyperkalemia, renal insufficiency and androgen-like effects. Finerenone shows potent effect on improving the outcomes of CHF, refractory hypertension, and diabetic nephropathy. Recently studies have shown that finerenone may have potential therapeutic effect on diabetic retinopathy, primary aldosteronism, atrial fibrillation, pulmonary hypertension and so on. In this review, we discuss the characteristics of finerenone, the new third-generation MRA, and compared with the first- and second-generation steroidal MRAs and other nonsteroidal MRAs. We also focus on its safety and efficacy of clinical application on CKD with T2DM patients. We hope to provide new insights for the clinical application and therapeutic prospect.

KEYWORDS

T2DM, finerenone, mineralocorticoid receptor antagonists, chronic kidney disease, cardiorenal protection

1 Introduction

Type 2 diabetes mellitus (T2DM) is a metabolic disorder characterized by hyperglycemia with insulin resistance. The management of T2DM requires multifactorial behavioral and pharmacological treatments to prevent or delay complications, and improves the quality of life. CKD and CVD are the common complications of T2DM (1). Among patients with T2DM, cardiovascular complications are the leading cause of morbidity and mortality, and kidney complications are highly prevalent in patients with T2DM (2). Available therapeutic strategies that delay the progression of CKD and the development of CVD include angiotensin-converting enzyme inhibitors (ACEI), angiotensin II receptor blockers (ARB), sodium-glucose co-transporter 2 inhibitors (SGLT-2i) and GLP-1 receptor agonists (GLP-1RA).

Finerenone is a structurally novel non-steroidal mineralocorticoid receptor antagonist (MRAs), which exhibits outstanding effect on cardio-renal protection (3). The mineralocorticoid receptors (MRs) are widely distributed in the heart, kidney, brain, lung, colon, skin, liver, skeletal muscle, saliva, sweat gland, and fat (4). MRs are mainly expressed in the cardiovascular system and kidney, and play vital role in ventricular remodeling and chronic heart failure (CHF) progression (5). Aldosterone, the MR, maintains the sodium/potassium homeostasis and the electrolyte balance of the body. In addition, an increasing number of studies have shown that inflammatory and fibrotic effect is mediated by excessive activation of MRs, leading to the adverse cardiac and renal outcomes. It could be an important therapeutic target for chronic kidney disease (CKD) induced by T2DM. Finerenone, a third-generation highly selective MRA, can directly and specifically block MR hyperactivation, and promote the anti-inflammatory and anti-fibrotic effects. In this way, finerenone exhibits cardiovascular and renal double-benefits, and is used in the treatment of T2DM-related CKD (diabetic kidney disease, DKD) to reduce the risk of persistent decline in glomerular filtration rate (eGFR) and the progression of end stage renal disease (ESRD). In general, finerenone could reduce the risk of cardiovascular and renal outcomes (3, 6).

A number of large-scaled clinical trials have proved that finerenone can significantly reduce both cardiorenal endpoints and the adverse reactions such as electrolyte disorders and sex hormone-like effects (7). In this review, we discuss the pharmacological characteristic, molecular mechanism, effectiveness and safety of finerenone in the treatment of T2DM with CKD/DKD and CVD, to provide clinical evidence and deep insight for therapeutic strategies.

2 The mechanism of MR activation on kidney and cardiovascular system

2.1 The physiological action of MR and MRAs

The physiological ligands of MR are mainly aldosterone and cortisol. MR is expressed in a variety of tissues and cells, including cardiomyocytes, vascular endothelial cells, vascular smooth muscle cells, renal tubular epithelial cells and macrophages (4). Aldosterone

binds to MR in the distal renal tubular epithelial cells to form aldosterone-MR complex, which promotes the reabsorption of sodium and excretion of potassium and hydrogen ions, suggesting MR plays an important physiological role in the regulation of water and salt balance, blood pressure and circulating blood volume (8).

2.2 The pathological effect and mechanism of MR activation

MR is also involved in the inflammatory response, regulating the expression of cytokines and inflammatory mediators, the activation of the inflammatory pathways and infiltration of inflammatory cells (9). Excessive activation of MR promotes reactive oxygen species (ROS) production, mediates the inflammatory and fibrogenic processes, and ultimately leads to myocardial hypertrophy and ventricular remodeling (10), as well as the renal damage, glomerular hypertrophy, glomerulosclerosis, and vascular damage such as vascular endothelial dysfunction and vascular smooth muscle cells proliferation (5). MR overactivation act directly on vascular smooth muscle cells *via* the MR-VEGFR1 pathway, leading to cell proliferation and enhanced vascular fibrosis, thickness and stiffness. In addition, MR overactivation also promotes the differentiation of inflammatory cells such as macrophages, T lymph cells into a pro-inflammatory phenotype in mice model. It further promotes the chronic inflammation microenvironment, and damages target organs and accelerates the disease process (11). MR overactivation results in renal injury and mineralocorticoid sensitive hypertension directly through the MR-Rac1 pathway, and cause glomerular hyperfiltration. In animal study, MR gene knockdown in cardiovascular endothelial cells improves renal inflammation and fibrosis by reducing inflammatory macrophage differentiation and inhibiting the expression of inflammatory and fibrosis-related genes (12).

Therefore, blocking MR over-activation could be beneficial to improve target organ damage.

3 Cardio-renal protective mechanism of finerenone

3.1 Moderating mechanism of finerenone on cardiovascular protection

CVD is a common co-morbidity of T2DM. MR overactivation plays an important role in the cardiovascular progression of T2DM with CVD. The mechanism of MR overactivation involving in cardiovascular damage is as follows. (1) MR overactivation increases NADPH oxidase activity to induce a series of oxidative stress responses in adult rat models, leading to the inflammatory and fibrotic process, finally results in the cardiac lesions such as myocardial hypertrophy, ventricular remodeling, myocardial ischemia/infarction, and ultimately to the development and progression of cardiovascular disease and renal disease (13, 14). (2) In addition, high aldosterone levels cause water and sodium retention and sodium overload, and increase production of ROS, thus exerting inflammatory reaction, fibrotic progression and oxidative stress (15). Those factors act on the heart result in remodeling of the heart and

arteries, triggering the risk of decreased left heart function, ventricular remodeling, and arrhythmias, all can deteriorate myocardial infarction and heart failure (HF) (12). (3) Furthermore, MR activation leads to vascular smooth muscle cell proliferation, increases vascular stiffness through vascular endothelial growth factor receptor 1 (VEGFR1), worsens vascular injury by decreasing nitric oxide, disturbs vascular endothelial dysfunction and vasoconstriction in rats (16). Therefore, targeted blockade of MR overactivation can ameliorate the inflammatory and fibrotic injury mediated by this pathway (17) (Figure 1). It is a key therapeutic target for patients with T2DM-related CVD.

MRAs promote co-factor SRC-1 recruitment to an MR-dependent promoter. The third-generation MRA finerenone has highly potent and selectivity for MR. Compared to spironolactone, finerenone binds to MR in a manner of unstable receptor-ligand complex, and leads to less recruit co-regulators (18). Finerenone delays the nuclear accumulation of MR-aldosterone complex, and blocks the recruitment of critical transcription cofactors. Thus, finerenone disturbs the steps downstream of MR pathway, and

decreased expression of pro-inflammatory and pro-fibrotic factors. MRA acts on cardiomyocytes hypertrophy by affecting gene transcription (19). In animal study, knockdown of MR in T-cells attenuates cardiac hypertrophy. The administration of MRA in mice also blocks MR signaling, reduces oxidative stress in cardiomyocytes, inhibits inflammation and fibrosis, and reduces the extent of macrophage infiltration (20). MRAs attenuate proinflammatory molecule expression in the rat heart and subsequent vascular and myocardial damage. Thus, we can infer that finerenone treatment in rats with severe hypertension and the vascular inflammation phenotype in the heart is effective (21).

3.2 The mechanism of finerenone on kidney

On the kidney, MR overactivation leads to glomerular hypertrophy, sclerosis, and renal fibrosis with reduced renal blood flow, finally results in renal injury and renal dysfunction (22). Finerenone reduces the formation of damaged vascular neointima

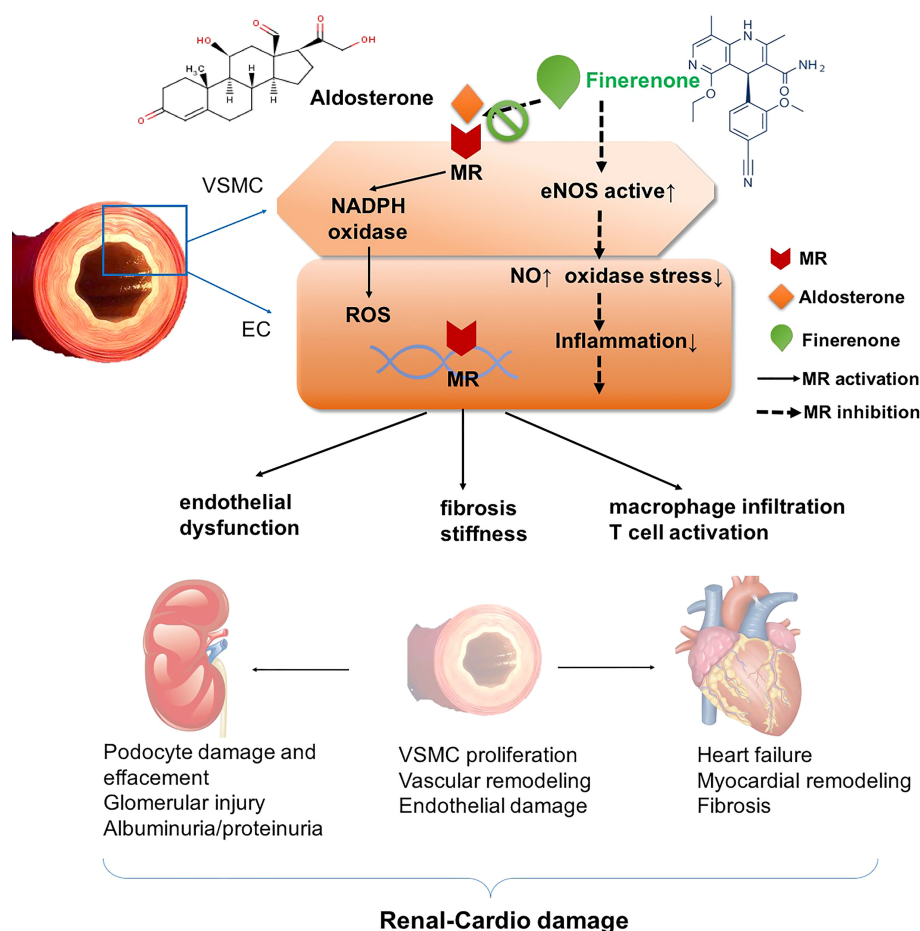


FIGURE 1

Mechanism of renal-cardio damage by mineralocorticoid receptor (MR) overactivation. MR activation plays important role in promoting NADPH oxidase, and enhancing ROS accumulation in VSMCs and ECs, and induces oxidase stress. In this way, MR agonist such as aldosterone results in endothelial dysfunction, macrophage infiltration and T cell activation, inflammatory progenitors including cytokines collection, and acts on VSMC leading to fibrosis and stiffness. MR activation affects kidney, aggravates podocyte damage and effacement, glomerular injury, and VSMC proliferation and endothelial damage, leading to vascular remodeling. On heart, MR activation exacerbates heart failure, myocardial remodeling and fibrosis. On contrast, MR antagonist finerenone blocks the binding of aldosterone and MR, then attenuates those pathophysiological progressions. In this way, finerenone shows renal-cardio protective effect. MR, mineralocorticoid receptor. EC, endothelial cells. VSMC, vascular smooth muscle cells. ROS, reactive oxygen species. NADPH, nicotinamide adenine dinucleotide phosphate.

by reducing endothelial cell apoptosis and inhibiting smooth muscle cell proliferation. Finerenone can prevent adverse vascular remodeling while restoring vascular integrity, and it can also block the damage to the kidney from MR overactivation, delaying the progression of nephropathy and bringing renal benefit (23).

Finerenone reduces endothelial cell apoptosis, attenuates smooth muscle cells proliferation, and decreases leukocyte recruitment and inflammatory response after vascular injury, thereby promoting endothelial repair and preventing adverse vascular remodeling. In a mouse model of DM induced CKD, finerenone treatment shows a significant reduction of proteinuria (24). Kolkhof et al. reported that in a rat model, the expression of genes related with renal hypertrophy, proteinuria and renal inflammatory are down-regulated in finerenone-treated group compared to isodose eplerenone group (8). In addition, finerenone prevents from functional and structural heart and kidney damage in a dose-dependent manner, without affecting blood pressure. Finerenone reduced cardiac hypertrophy, plasma pro-BNP, and proteinuria more efficiently than eplerenone. In the mice model of non-diabetic nephropathy, finerenone reduces the levels of inflammatory factors, fibrogenic markers and deposition of perinephric macrophages, reduces proteinuria and tubulointerstitial fibrosis. This anti-fibrotic process is independent of blood pressure, and exhibit a dose-dependent reduction in fibroblast accumulation and collagen deposition (25). The MRA treatment also reduces glomerular pathological injury and improves renal function in glomerulonephritis mice models. In addition, finerenone treatment may also prevent ischemia-reperfusion-induced renal tubular injury (19).

In general, MR activation promotes NADPH oxidase, and enhances ROS accumulation in VSMCs and ECs. In this way, MR agonist such as aldosterone results in endothelial dysfunction, macrophage infiltration and T cell activation, inflammatory cytokines accumulation, leading to fibrosis and stiffness. MR activation aggravates podocyte damage and effacement, glomerular injury and endothelial damage, leading to vascular remodeling. MRA finerenone blocks the binding of aldosterone and MR, then attenuates those pathophysiological progressions. In this way, finerenone shows renal-cardio protective effect (Figure 1).

4 Pharmacological characteristic and safety of finerenone

Finerenone is innovative in its molecular structure. Finerenone induces MR conformational changes mainly through its side chain, leading to the prominence of helix 12 of the c-terminal, activating functional domain of the MR receptor. It affects the recruitment of co-regulatory factors and alters MR stability, nuclear translocation and activation. Finerenone has a high selectivity and innovative molecular structure compared to the first- and second-generation of MRAs.

Finerenone binds to MR with greater affinity through a large number of van der Waals forces and hydrogen bonds, has a stronger antagonistic effect, completely blocks the transcription factor aggregation caused by aldosterone-MR receptor complex, and inhibits MR overactivation. Finerenone has a short elimination

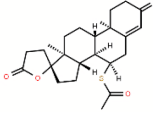
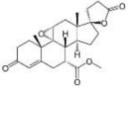
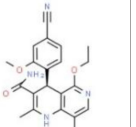
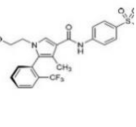
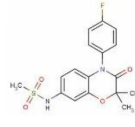
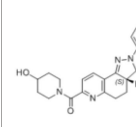
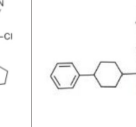
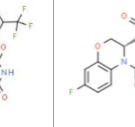
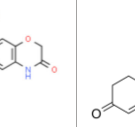
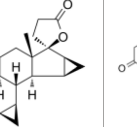
half-life of only two hours. Finerenone displays shorter Tmax of 0.5~0.75h than spironolactone and eplerenone of 1-2h. Spironolactone exhibits multiple active metabolites, such as canrenone, while eplerenone and finerenone has no active metabolites. Finerenone has a weak affinity for androgen and progesterone receptors. Spironolactone displays non-specific binding to steroid receptors, thus, it shows anti-androgenic effect. Compared to the first-generation MRA spironolactone, eplerenone is 40-fold less potent than spironolactone. However, eplerenone and those non-steroidal MRAs (including finerenone, esaxerenone, ocedurenone, balcinrenone, ect.) generally display exhibits greater selectivity for MR over other steroid hormone receptors. Therefore, finerenone shows less risk of sex hormone related adverse effects (26).

Finerenone shows similar potency to spironolactone, but high affinity to MR. Compared to the previous steroidal MRAs spironolactone or eplerenone, the new-generation MRA finerenone shows its superiority (Table 1). The side effects including sex hormone associated adverse effects, risk of hyperkalemia and renal insufficiency are lower in finerenone (26). It is safer and more favorable for T2DM patients' treatment. Finerenone also inhibits the expression of downstream pro-inflammatory and pro-fibrotic factors, providing effective anti-inflammatory and anti-fibrotic effects.

Finerenone, the new oral MRA is a kind of naphthyridine derivatives based on dihydropyridines (DHP) structure, inhibits MR activation precisely and potently, and show stronger anti-inflammatory and anti-fibrotic effects than the first- and second-generation of steroidal MRAs. Finerenone is balanced distributed in heart and kidney (8), therefore, it has cardio-renal double benefits. While spironolactone and eplerenone mainly distributes in the kidney (19). Otherwise, finerenone is not allowed to across the blood-brain barrier (BBB). Quantitative whole-body autoradiography with [14C]-labeled finerenone does not demonstrate in brain (27). Both finerenone and spironolactone act as affecting the transcriptional process. Spironolactone inhibits the binding of cortisol to the receptor while also acting as a partial agonist. However, finerenone acts as an inverse agonist after binding to the promoter, reducing the activation of a kind of transcriptional cofactors (SRC-1) and inhibiting the transcriptional process even in the absence of aldosterone (28). In phase II trials, the novel MRAs have comparable efficacy compared to the conventional MRAs, but exhibiting a significant safety profile in patients with HF and renal dysfunction (29).

In the safety analysis of FIDELITY study, the discontinuation of finerenone associated hyperkalemia is low, and is comparable to placebo (30). In the FIDELITY study, the incidence of treatment-emergent adverse events (TEAE) is similar in the finerenone and placebo groups, with no increase in sex hormone-related side effects compared to the placebo group. In addition, finerenone has no effect on glycated hemoglobin A1c (HbA1c). In terms of CKD stage, the safety profile of finerenone in T2DM patients with CKD stage 4 is consistent with that of CKD stages 1 to 3 (31). In the FIDELIO-DKD study, emergency adverse events, diarrhea, nausea, vomiting, and hypovolemia are analyzed, and those adverse events in the treatment group are similar to placebo group. The conventional steroidal MRAs have limited long-term usage due to the potential adverse effects such as hyperkalemia, but the advent of finerenone shows a promising direction for the treatment of T2DM with CKD and CVD (32).

TABLE 1 The Pharmacokinetics of MRAs.

Agent	Spironolactone	Eplerenone	Finerenone	Esaxerenone	Apararenone	Ocedurenone	Miricorilant	Balcinrenone	Drospirenone/ Esterol	Canrenone
Name	SC 9420		BAY 94-8862	CS-3150	MT-3995	KBP-5074	CORT-118335	AZD-9977		SC 9376
Dose	10mg/20mg	25mg/50mg	10mg/20mg	1.25mg/2.5mg/5mg	2.5mg/5mg/10mg	0.25mg/0.5mg	in development	in development		
Company	Pfizer	Pfizer	Bayer	Daiichi-Sankyo Company Limited, Japan	Mitsubishi Tanabe Pharma Corporation	KBP Biosciences	Corcept, Argenta Discovery	AstraZeneca	Mithra Pharmaceuticals, Estetra S.A., Libbs	
Generation of MRA	first	second	third	third	MRA	MRA	GRA; MRA	MR regulator	MRA; PR agonist; ARA; selective ER regulator	first
Steroidal/ Nonsteroidal	steroidal	steroidal	nonsteroidal	nonsteroidal	nonsteroidal	nonsteroidal	nonsteroidal	nonsteroidal		steroidal
Molecular Formular	C ₂₄ H ₃₂ O ₄ S	C ₂₄ H ₃₀ O ₆	C ₂₁ H ₂₂ N ₄ O ₃	C ₂₂ H ₂₁ F ₃ N ₂ O ₄ S	C ₁₇ H ₁₇ FN ₂ O ₄ S	C ₂₈ H ₃₀ ClN ₅ O ₂	C ₂₄ H ₂₃ F ₃ N ₂ O ₂	C ₂₀ H ₁₈ FN ₃ O ₅	C ₂₄ H ₃₀ O ₃	C ₂₂ H ₂₈ O ₃
Structure										
Characteristic	potent and unselective	less potent and more selective than spironolactone	more potent and more selective than spironolactone	more potent and more selective than eplerenone	more potent and more selective than spironolactone		more potent and more selective; moderate affinity to MR	no affinity to GR/ PR/AR		
Heart-kidney distribution ratio	1:6	1:3	1:1; cannot across the Blood-Brain Barrier	1:1						
t_{1/2}	13~24h(qd/bid); 9~16hqid	4-6h	1.7-2.8h	20-30h	275-285h for parent drug; >1000h for active metabolite			increased with dose	31h	
T_{max}	2.6-3.05h	1.5h	0.75-1h	1.5-4h	4h			0.5-0.8h	1-2h	
C_{max}	209-301ng/ml	–	160ug/L(20mg)						37ng/ml	
MR IC₅₀	24	990	17.8				moderate affinity to MR			
AR IC₅₀	77	≥21240	≥10000					almost no affinity to GR/PR/AR	almost no affinity to GR/AR	
GR IC₅₀	2410	≥21980	≥10000							

(Continued)

TABLE 1 Continued

Agent	Spironolactone	Eplerenone	Finerenone	Esaxerenone	Apararenone	Ocedurenone	Miricorilant	Balcinrenone	Drospirenone/ Esterol	Canrenone
PR IC50	740	≥31210	≥10000							
Oral bioavailability	>90%	69%	86.50%						76-85%	
Protein binding ratio	>90%	33%-60%	92%						95-97%	
Metabolism	prodrug with multiple active metabolites	no active metabolites	no active metabolites	n/a	metabolite with low activity (MR binding affinity one-fiftieth of that of apararenone)			n/a		the active metabolites of spironolactone
Hyperkalemia	high risk	high risk	low risk	low risk					no risk	
Excretion	<1% unchanged drug recovered in urine; 10-15% of dose excreted in urine form of metabolites	66% of dose excreted via urine; <3% unchanged drug recovered from urine	80% of dose excreted via urine; <1% unchanged drug excreted in urine	38.5% of dose excreted in urine; <2% unchanged drug excreted in urine	<14% of dose excreted in urine			24-37% of dose excreted in urine; 20% of dose excreted unchanged in urine		
Sex-like ADR	common	less than spironolactone	no statistics difference with placebo group							
Dose adjust based on renal function	excretion through the kidney	cannot be removed by hemodialysis	decrease dose in patients with eGFR≤60 and prohibit when eGFR<25						decrease dose in patients with eGFR 30-50	
Indication	PA; HBP; hypokalemia; edema; HF	congestive heart failure; HBP	T2DM with CKD, ESRD, CVD, congestive heart failure	HBP, DKD(clinical trial phase)	DKD	HBP, DKD, HN	obesity; prostate cancer; metabolism disorder	DKD	contraception	HBP
Contraindication	not recommended to CRF	not recommended to CRF								

The unit of IC50 is nmol/L. the unit of eGFR is ml/min/1.73m². PR, progesterone receptor. ER, estrogen receptor. AR, androgen receptor. MRA, mineralocorticoid receptor antagonist. t_{1/2}, geometric mean terminal half-life. Tmax, median time to maximum plasma concentration. Cmax, maximum plasma concentration. ADR, adverse drug reactions. eGFR, estimated glomerular filtration rate. PA, primary aldosteronism. HBP, hypertension. CKD, chronic kidney diseases. DKD, diabetic kidney diseases. HN, hypertensive nephropathy. ESRD, end-stage renal disease.

5 Effect of finerenone on cardiovascular disease outcomes in T2DM

Clinical studies show the protective effect of finerenone on cardiovascular outcomes to provide evidence (Table 2). Both the Efficacy and Safety of Finerenone in Subjects With Type 2 Diabetes Mellitus and the Clinical Diagnosis of Diabetic Kidney Disease (FIGARO-DKD) and Efficacy and Safety of Finerenone in Subjects With Type 2 Diabetes Mellitus and Diabetic Kidney Disease (FIDELIO-DKD) studies are large-scaled multicenter phase III clinical studies, focusing on the effect of finerenone on the composite cardiovascular-renal outcomes as the primary endpoints in T2DM patients with CKD (3, 6, 26). The findings of FIGARO-DKD study ultimately show 13% reduction in cardiovascular composite endpoint events (including cardiovascular death, nonfatal myocardial infarction, nonfatal stroke, or hospitalization

for HF) with finerenone in T2DM patients with CKD. In the patients with well-controlled blood pressure and glycemic levels, or using a combination of RAAS inhibitors, finerenone also shows the consistent results (6). There was no significant difference in safety from placebo. The results of the FIDELIO-DKD study shows that finerenone significantly reduce the risk of composite cardiovascular outcomes compared with placebo, with no significant difference in outcomes in patients with or without established ASCVD. Furthermore, the rate of treatment discontinuation due to hyperkalemia is low (26). The FIDELITY study is the meta-analysis study based on the FIDELIO-DKD study and the FIGARO-DKD study. The results of the study show that finerenone significantly reduce the risk of cardiovascular composite endpoint events in patients with T2DM with CKD by 14% (HR=0.86; 95% CI: 0.78-0.95; P=0.0018) compared to placebo independent of established ASCVD. The risk of HF associated hospitalization is significantly reduced by 18% (RR=0.82; 95% CI: 0.71-0.94), and the risk of all-cause mortality is reduced by 15% (RR=0.85; 95% CI: 0.74-0.99) (31, 61).

TABLE 2 The Trials Information of MRAs.

Drug	Trial	Characteristic	n	Groups	Median Follow-up	Inclusion criteria	Outcome	Conclusion
Spironolactone								
SPI	RALES (Pitt et al.) (33)	a double-blind RCT	1663	standard therapy and SPI or placebo	24 months	severe HF with LVEF≤35%	death from all causes	SPI, in addition to standard therapy, substantially reduces the risk of both morbidity and death among patients with severe HF.
SPI	Tseng et al. (Taiwan National Health Insurance Research Database) (34)	retrospective cohort study	27213	SPI usage +/-before	3-4 years	CKD stage 5	all-cause mortality, HHF and MACE (the composite of AMI and ischemic stroke)	SPI may be associated with higher risks for all-cause and infection-related mortality and HHF in pre-dialysis stage 5 CKD patients.
SPI	Yang et al. (primary data from Taiwan's National Health Insurance Research Database) (35)	retrospective cohort study	2079	SPI usage +/-before	\	CKD stage 3-4	ESRD, MACE, HHF, HKAH, all-cause mortality and CV mortality	SPI represented a promising treatment option to retard CKD progression to ESRD amongst stage 3-4 CKD patients, but strategic treatments to prevent hyperkalemia should be enforced.
SPI	TOPCAT (NCT00094302) (36)	RCT(phase III)	3445	SPI vs. placebo	6 years	HFpEF (symptomatic, HHF within the past year)	composite outcome of CV mortality, aborted cardiac arrest, or HHF	SPI does not significantly reduce the incidence of the primary composite outcome of death from CV causes, aborted heart arrest or HHF in patients with HFpEF. Greater potassium and creatinine changes and possible clinical benefits with SPI in patients with HFpEF from the Americas.
SPI	Enzan et al. (Japanese Cardiac Registry of Heart Failure in	retrospective registration study	457	SPI usage +/-before	2.2 years	HFmEF (LVEF 40%-49%)	a composite of all-cause death or HHF	Among patients with HHF for HFmEF, SPI shows better long-term outcomes.

(Continued)

TABLE 2 Continued

Drug	Trial	Characteristic	n	Groups	Median Follow-up	Inclusion criteria	Outcome	Conclusion
	Cardiology database) (37)							
SPI	Krieger et al. (NCT01643434) (38)	multicenter RCT study	1597	SPI vs. clonidine	3 months	resistant hypertension	BP control during office (<140/90 mm Hg) and 24h ambulatory (<130/80 mm Hg) BP monitoring	SPI promotes greater decrease in 24h systolic and DBP and diastolic daytime ambulatory BP than clonidine
Eplerenone								
EPL	Minakuchi et al. (UMIN000008521) (39)	a single-blinded placebo-controlled prospective observational study	48	ACEI/ARB + EPL or placebo	24-36 months	patients with CKD stage 2-3 whose plasma ALD concentration was above 15 ng/dL	change in eGFR	MRA can be an effective in preventing CKD progression, especially in patients with high plasma ALD.
EPL	ElMokadem et al. (NCT04143412) (40)	a single-blind RCT	75	ramipril or EPL or both	24 weeks	T2DM +hypertension and DKD (microalbuminuria)	BP, UACR, serum creatinine, eGFR and serum K level	Addition of EPL to ACEI shows an added anti-albuminuria effect without significant change of the serum potassium level compared with EPL or ACEI.
EPL	EPOCH(NCT01832558) (41)	a exploratory RCT study	15	ACEI + EPL or placebo	10 weeks	CKD stages 2-3 and albuminuria due to DKD	quantify plasma angiotensin levels, renin and ALD in PA for 8 weeks MRA treatment.	Combined EPL and ACEI therapy increases Ang-(1-7) levels in patients with CKD indicating a unique nephroprotective RAAS pattern with considerable therapeutic implications.
EPL	EPHESU (42)	a multicenter, international, double-blind, phase III RCT	6442	different dosage of EPL vs. placebo	16 months	AMI after 3-14 days with HFrEF (LVEF≤40%)	death from any cause and death from CV causes or HHF, AMI, stroke, or ventricular arrhythmia	The addition of EPL to optimal medical therapy reduces morbidity and mortality among patients with AMI complicated with HFrEF.
EPL	EMPHASIS-HF (NCT00232180) (43)	a double-blind phase III RCT study	2737	different dosage of EPL vs. placebo	21 months	HFrEF (NYHA II) with LVEF≤35%	a composite of death from CV causes or HHF	EPL reduces both the risk of death and the risk of hospitalization among patients with systolic HF and mild symptoms.
EPL	RAAM-PEF (NCT00108251) (44)	a double-blind, placebo-controlled RCT	44	EPL vs. placebo	6 months	HFpEF and hypertension with/without T2DM	changes in 6-minute walk distance, diastolic function, and biomarkers of collagen turnover	EPL is associated with significant reduction in markers of collagen turnover and improvement in diastolic function.
EPL	Schneider et al. (NCT00138944) (45)	a double-blind, placebo-controlled, parallel group RCT	51	regular BP medication + low dosage EPL or placebo	6 months	TRH	LVM assessed by MRI before and after treatment	MRA should be used preferentially in patients with TRH in order to achieve an effective reduction of LVM along with the improvement of BP control.
EPL	Kalizki et al. (NCT00138944) (46)	double-blinded, placebo-controlled	51	regular BP medication + low dosage EPL or placebo	6 months	TRH	vascular parameters including PWV, AIx, AP,	EPL beneficially affects markers of arterial stiffness and wave reflection in patients

(Continued)

TABLE 2 Continued

Drug	Trial	Characteristic	n	Groups	Median Follow-up	Inclusion criteria	Outcome	Conclusion
		parallel-group RCT					AP@HR75, RRI, IMT and UAER	with TRH, independently of BP lowering.
EPL	OWASE (UMIN000005956) (47)	a multicenter, prospective, open-label RCT	195	EPL vs. thiazide diuretic	48 weeks	ARB-treated hypertension and albuminuria	the change of UACR from baseline to 48 weeks	The antialbuminuric effects and safety of EPL therapy are similar to thiazide diuretics when combined with ARBs in patients with hypertension and albuminuria.
EPL	Karashima et al.(UMIN000004581) (48)	an open-label, non-controlled, prospective cohort study	54	EPL vs. SPI	12 months	PA	metabolic factors including BMI, HOMA-IR, serum creatinine, potassium and lipids, UAE and PAC and PRA	EPL and SPI decreases BP and increases serum potassium levels to similar degrees. PAC and PRA are similar between the two groups.
EPL	EPATH(NCT02136771) (49)	RCT and observational data prospective cohort study	4	different dosage EPL vs. placebo	8 weeks	PA	ARR	MRA does not significantly alter the ARR in primary hyperparathyroidism patients but significantly reduces the ARR in PA patients.
Finerenone (BAY 94-8862)								
FIN	ARTS(NCT01807221; NCT01874431) (7)	multicenter, parallel-group, phase II study, with double-blind placebo and open-label SPI comparator arms phase II RCT	458	standard therapy and different dosage (2.5mg/5mg/10mg qd) FIN or placebo	about 30 days	HFrEF (NYHA II-III, LVEF≤40%) and mild or moderate CKD (eGFR 60 to <90 and 30-60 mL/min/1.73 m ² , respectively)	serum potassium concentration, eGFR, and albuminuria	In patients with HFrEF and moderate CKD, BAY 94-8862 5–10 mg/day was at least as effective as SPI 25 or 50 mg/day in decreasing biomarkers of hemodynamic stress, but it was associated with lower incidences of hyperkalemia and WRF.
FIN	ARTS-HF (NCT01807221) (50)	a double-blind placebo and open-label SPI comparator arms phase IIb RCT study	1066	different dosage FIN vs. EPL	90 days	worsening CHF with exasperated HFrEF and CKD and/or T2DM requiring hospitalization and intravenous diuretic therapy	the percentage of participants with a relative decrease in NT-proBNP of more than 30% from baseline to day 90	FIN is well tolerated and induced a 30% or greater decrease in NT-proBNP levels in a similar proportion of patients to EPL.
FIN	ARTS-DN (NCT01874431) (51)	a multicenter, double-blind, placebo-controlled, parallel-group phase II RCT	823	ACEI/ARB + different dosage FIN or placebo	90 days	T2DM with DKD (albuminuria)	ratio of UACR at day 90 to UACR at baseline	Among patients with DN, most receiving an ACEI/ARB, the addition of FIN compared with placebo resulted in improvement in the UACR.
FIN	FIDELIO-DKD (NCT02540993) (52)	a double-blind, placebo-controlled, parallel-group, multicenter, event-driven phase III study	5734	ACEI/ARB + FIN (10mg/20mg qd) or placebo	32 months (2.6 years)	T2DM with DKD	the first occurrence of the composite endpoint of onset of kidney failure, a sustained decrease of eGFR ≥40% from baseline over at least 4 weeks, or renal death	In patients with CKD and T2DM, FIN lowers the risks of CKD progression and CV events than placebo.

(Continued)

TABLE 2 Continued

Drug	Trial	Characteristic	n	Groups	Median Follow-up	Inclusion criteria	Outcome	Conclusion
FIN	FIGARO-DKD (NCT02545049) (3)	a double-blind, placebo-controlled, parallel-group, multicenter, event-driven phase III study	7337	standard therapy + FIN or placebo	41 months (3.4 years)	T2DM with DKD	the first occurrence of the composite endpoint of CV death, non-fatal myocardial infarction, nonfatal stroke, or HHF	T2DM and stage 2 to 4 CKD with moderately elevated albuminuria or stage 1 or 2 CKD with severely elevated albuminuria, FIN therapy improved CV outcomes as compared with placebo.
FIN	FIDELITY (NCT02540993; NCT02545049) (31)	meta analysis (FIDELIO-DKD and FIGARO-DKD)	13026	standard therapy + FIN or placebo	2.3-3.8 years	T2DM with DKD	a composite of CV death, non-fatal MI, non-fatal stroke, or HHF, and a composite of kidney failure, a sustained $\geq 57\%$ decrease in eGFR from baseline over ≥ 4 weeks, or renal death	FIN reduces the risk of clinically important CV and kidney outcomes vs. placebo across the spectrum of CKD in T2DM
FIN	FINEARTS-HF (NCT04435626)	a double-blind, placebo-controlled, parallel-group, multicenter phase III Study	5500	different dosage of FIN	–	HFmEF (LVEF $\geq 40\%$) with clinical symptom	number of CV deaths and HF events	ongoing
FIN	FIND-DKD (NCT05047263)	a randomized, double-blind, placebo-controlled, parallel-group, multicenter phase III study	1500	FIN vs. placebo	–	CKD without T2DM	change of the slope of eGFR	ongoing
FIN	CONFIDENCE (NCT05254002)	a parallel-group treatment, phase II, double-blind, three-arms study	807	FIN +empagliflozin vs. FIN +placebo vs. empagliflozin +placebo	180-210 days	CKD with T2DM	relative changes from baseline in UACR at 180 days in combination therapy group versus empagliflozin/FIN alone	ongoing
FIN	Fu et al. (53)	meta-analysis	7048	standard therapy + FIN or placebo	–	DM patients with CKD (phase 2)	assessed at least one of the following outcomes: UACR, eGFR, adverse events including CV disorders and hyperkalemia	FIN confers an important antiproteinuric effect on patients with CKD and reduces the risk of CV disorders
FIN	Pei et al. (54)	meta-analysis	1520	FIN vs. SPI vs. EPL	–	CHF with HFrEF	effective number of cases with a 30% reduction in NT-proBNP	FIN reduces NT-proBNP, UACR, and other biochemical indicators in a dose-dependent manner.
Esaxerenone (CS-3150)								
ESA	ESAX-HTN (NCT02890173) (55)	double-blind, three parallel placebo comparator arms phase III trial	1001	different dosage of ESA or EPL	12 weeks	essential hypertension	changes in SBP/DBP at rest relative to baseline after 12 weeks	ESA is an effective and well-tolerated MRA in Japanese patients with essential hypertension, with BP-lowering activity

(Continued)

TABLE 2 Continued

Drug	Trial	Characteristic	n	Groups	Median Follow-up	Inclusion criteria	Outcome	Conclusion
								at least equivalent to EPL.
ESA	ESAX-DN(JapicCTI-173695) (56)	multicenter, double-blind, placebo control, two-arm, parallel group, comparison study	449	CS-3150 vs. placebo	52 weeks	T2DM with microalbuminuria taking ACEI/ARB	UACR remission rate at the end of the treatment	Adding ESA to existing RAAS inhibitors therapy in patients with T2DM and microalbuminuria increased the likelihood of albuminuria returning to normal levels, and reduced progression of albuminuria to higher levels.
Apararenone (MT-3995)								
APA	Izumi et al.(NCT02517320; NCT02676401) (57)	a double-blind, placebo-controlled study	293/241	different dosage of APA vs. placebo	24-52 weeks	stage 2 diabetic nephropathy (DN)	the 24-week percent change from baseline in UACR and 24- and 52-week UACR remission rates	The UACR-lowering effect of APA administered once daily for 24 weeks in patients with stage 2 DN was confirmed, and the 52-week administration was safe and tolerable.
Ocedurenone (KBP-5074)								
OCE	BLOCK-CKD (NCT03574363) (58)	a double-blind, placebo-controlled, global, multicenter phase IIb trial	162	different dosage of APA vs. placebo	12 weeks	moderate-to-severe (stage 3b/4; eGFR 15-44 mL/min/1.73m ²) CKD and uncontrolled hypertension	changes in trough-cuff seated SBP/DBP and UACR from baseline to day 84	KBP-5074 demonstrated a clinically meaningful trend in the reduction of UACR.
OCE	CLARION-CKD (NCT04968184)	a phase 3 double-Blind placebo-controlled multicenter study	600	OCE vs. placebo	52 weeks	uncontrolled hypertension and moderate or severe CKD (stage 3b/4)	changes in seated trough-cuff SBP from baseline to week 12/48/52	ongoing
Canrenone								
CAN	COFFEE-IT (NCT03263962) (59)	a multicenter, retrospective, observational study	532	treated +/- CAN	10 years	CHF with HFpEF (LVEF ≥ 50%)	the rate of CV mortality in CHF and the rate of death and survival.	CAN preserves systolic fraction, reduces mortality and extends life in CHF patients.
CAN	AREA-in-CHF (NCT00403910) (60)	RCT (phase 3)	500	CAN vs. placebo	12 months	compensated HFpEF with LVEF≤45%	changes in echocardiographic left ventricular diastolic volume	CAN, with optimal therapy (ACEI/ARB, β-blockers) in patients with metabolic syndrome, stabilized HF with reduced EF, protects deterioration of myocardial mechano-energetic efficiency, improves diastolic dysfunction and maximizes the decrease in BNP.

ALD, aldosterone. SPI, spironolactone. EPL, eplerenone. FIN, finerenone. ESA, esaxerenone. APA, apararenone. OCE, ocedurenone. CAN, canrenone. RCT, randomized controlled trials. MACE, major adverse cardiovascular events. ESRD, end-stage renal disease. HHF, hospitalization for heart failure. HKAH, hyperkalemia-associated hospitalization. CV, cardiovascular. CHF, chronic heart failure. HF, heart failure. HFmEF, heart failure with mild ejection fraction. HFREF, heart failure with reduced ejection fraction. HFpEF, heart failure with preserved ejection fraction. NT-proBNP, amino-terminal pro-B-type natriuretic peptide. AMI, acute myocardial infarction. LVM, left ventricular mass. BP, blood pressure. SBP, systolic blood pressure. DBP, diastolic blood pressure. TRH, treatment-resistant hypertension. CKD, chronic kidney diseases. DKD, diabetic kidney diseases. T2DM, type-2 diabetic mellitus. DN, diabetic nephropathy. eGFR, estimated glomerular filtration rate. UACR, urinary albumin-to-creatinine ratio. MRA, mineralocorticoid receptor antagonists. RAAS, renin-angiotensin-aldosterone system. ACEI, angiotensin-converting enzyme inhibitors. ARB, angiotensin II receptor blockers. PA, primary aldosteronism. ARR, aldosterone to renin ratio. PAC, plasma aldosterone concentration. DRC, direct renin concentration. PWV, pulse wave velocity. AIx, augmentation index. AP, augmentation pressure. AP@HR75, AP normalized to a heart rate of 75/min. RPI, renal resistive index. IMT, intima-media thickness. UAER, and urinary albumin excretion rate. BMI, body mass index. HOMA-IR, homeostasis model assessment-insulin resistance. UAE, urinary albumin excretion. PAC, plasma aldosterone concentration. PRA, plasma renin activity. WRF, worsening renal failure. NCT, the number of trials in ClinicalTrials.gov. UMIN, the number of trials in UMIN Clinical Trials Registry (UMIN-CTR); JapicCTI, the number of trials in JAPIC Clinical Trials Information.

6 Effects of finerenone on renal outcomes in T2DM patients with CKD

MR overactivation is one of the key pathophysiological mechanism in patients with T2DM and CKD. The inflammatory and fibrotic mediated effects occur when MR is overactivated, leading to the progression of CKD (62). Finerenone reduces the urinary albumin-to-creatinine ratio (UACR) in T2DM with CKD patients (63). Proteinuria is also an independent predictor of CVD risk. Elevated proteinuria portends pre-existing endothelial damage (64). Overactivation of MR is an important mechanism leading to endothelial damage (Figure 1). Thus inhibition of MR overactivation is essential to suppress endothelial injury, reduce CV risk, and delay progression of CKD (65).

FIGARO-DKD and FIDELIO-DKD are two large-scaled phase III clinical studies (Table 2), involving T2DM with CKD patients, and the endpoints are cardiorenal outcomes. In the FIGARO-DKD study, finerenone significantly reduces renal composite endpoint events (occurrence of renal failure, sustained decline in eGFR $\geq 57\%$ from baseline, or death from renal disease) by 23% (6). The results of the FIDELIO-DKD study show that finerenone significantly reduces the risk of renal composite endpoint events by 18% compared with placebo on the basis of standard treatment (HR=0.82; 95% CI[0.73-0.93]; $P=0.0001$) (52). Finerenone reduces albuminuria in short-term intervention involving T2DM patients with CKD. However, the long-term effects on renal and cardiovascular outcomes are unknown. Finerenone reduces the risk of major outcome events including renal failure, 40% reduction in eGFR or death due to renal diseases, while the adverse events are comparable to placebo group (52).

The results of the FIDELITY study, a pooled analysis of the FIDELIO-DKD and FIGARO-DKD studies, show that finerenone significantly reduce the risk of renal composite events by up to 23% (HR=0.77; 95% CI: 0.67-0.88; $P=0.0002$) and significantly reduced UACR by 32% compared to placebo. Further analysis reveals that finerenone decreases the incidence of all non-lethal renal outcomes, including end-stage renal disease (ESRD). Finerenone reduces cardiovascular risk in T2DM patients with CKD in all UACR and eGFR stages (51, 66). Finerenone significantly reduced the risk of renal composite events by 29% (RR=0.71; 95% CI: 0.57-0.88) in patients with established ASCVD and by 19% in patients without ASCVD history compared with placebo (RR=0.81; 95% CI: 0.68-0.97). The renal benefit of finerenone and the effect of reducing all-cause mortality are not affected by ASCVD history (67).

7 Finerenone in combination therapy with ACEI/ARB and SGLT-2i/GLP-1RA

Finerenone therapy improved cardiovascular and kidney outcomes in the FIDELITY pooled analysis (66). SGLT-2i and GLP-1RA can also improve cardio-renal endings independently, which play a significant role in inhibiting fibrillation, reducing urine protein, controlling inflammation, anti-oxidative stress and delaying atherosclerosis (68). However, the effect and mechanism on combination with ACEI/ARB and SGLT-2i/GLP-1RA, the established cardio-renal protective anti-hypertension or anti-diabetic agents, are unclear. Finerenone combines with either SGLT-2i/GLP-1 RA may enhance the effect of anti-inflammation, anti-oxidative stress, and endothelial protection. Whereas, clinical trials and deep

mechanism research are needed to provide evidence. A meta-analysis based on the combination therapy of oral glycemic-lowering agents with finerenone included FIDELIO-DKD and FIGARO-DKD, with the primary outcomes of MACE events, illustrates that finerenone does not significantly increase cardiovascular benefit in T2DM patients with “add-on” the SGLT-2i or GLP-1RA, but confirms the significant efficacy of single-agent finerenone in cardio-renal improvement (69). It provides a basis for guiding clinical use. However, the evidence may be not conclusive due to the limited number of RCTs.

In the subgroup analysis from FIDELIO-DKD trial, finerenone reduces UACR by 31% in patients with or without GLP-1RA usage at baseline. It suggests that finerenone improve the kidney and CV outcomes independent of GLP-1RA use (66). It suggests the renal-protective effect of finerenone in patients already treated with GLP-1RA and demonstrates that GLP-1RA is also a UACR-reducing treatment since previous meta-analysis has shown that GLP-1RA is marginally reduced UACR (70, 71). Animal studies clarify that the combination of finerenone and SGLT-2i provides renal protection effect in a mouse model of hypertension-induced cardiorenal disease. The combination administration significantly reduces proteinuria levels in mice compared to single agents (72). However, several clinical studies, including FIDELIO-DKD, have shown that finerenone alone reduces UACR independent of SGLT-2i, and similar in heart failure with reduced ejection fraction (HFrEF) patients, SGLT-2i alone significantly improves cardiovascular outcomes, even without finerenone (73).

The CONFIDENCE study (A Study to Learn How Well the Treatment Combination of Finerenone and Empagliflozin Works and How Safe it is Compared to Each Treatment Alone in Adult Participants With Long-term Kidney Disease and Type 2 Diabetes, NCT05254002) is an ongoing randomized controlled study of the efficacy of finerenone in combination with SGLT-2i Empagliflozin in T2DM patients with CKD. Both finerenone and empagliflozin are guideline-recommended clinical agents for the treatment of DKD. The study was designed to investigate whether the two-agents combination is superior to monotherapy, focusing on the endpoints of UACR, eGFR change and incidence of hyperkalemia. Clinical evidence of the additional benefit of finerenone in combination with empagliflozin will be available at the end of the study (74). The analysis of the CONFIDENCE study, which is scheduled to end in May 2023, include both the combination group and the monotherapy group of empagliflozin and finerenone. Thus, the analysis of this study may provide stronger evidence to show whether the combination is superior to monotherapy for clinical use.

Another clinical study investigates the effect of finerenone on proteinuria in DKD patients, with the treatment combination with renin-angiotensin-aldosterone system (RAAS) inhibitors (ACEI/ARB) for 90 days. The results show a significant and dose-dependent improvement of UACR in all dose-groups of finerenone compared to the placebo group (51). A meta-analysis of combination therapy for DKD show that the combination of MRA with ACEI/ARB further reduce the urine albumin excretion rate (UAER) compared with ACEI/ARB monotherapy. eGFR is not statistically different between the two groups, but the serum creatinine level is significantly increased in the combination group. A subgroup analysis based on different MRAs yields that the relative risk of hyperkalemia with the ACEI/ARB combination with finerenone is lower than with eplerenone or spironolactone (75).

In summary, either finerenone alone or in combination with SGLT-2i or GLP-1RA may improve DKD outcomes and risk of

cardiovascular events in T2DM patients, but the results of clinical studies for combination versus monotherapy varies. More clinical trials are needed to provide conclusive evidence. The deep-insight of molecular mechanism and the cross-talk links among finerenone and ACEI/ARB and SGLT-2i/GLP-1RA agents unclear. Thus, further basic studies are expected.

8 Prospects for finerenone treatment

In clinical observation, finerenone show potential therapeutic effects in diabetic retinopathy (DR). A phase III clinical trial ReFineDR (NCT04477707)/DeFineDR (NCT04795726) on the effect of finerenone on slowing the progression of non-proliferative diabetic retinopathy (NPDR) is currently ongoing. A total of 244 patients with DR at baseline (134 in the finerenone group and 110 in the placebo group) are enrolled from the FIDELIO-DKD or FIGARO-DKD studies to investigate, with the primary outcome of the NPDR progression. At baseline, most patients had mild-to-moderate NPDR. After two-year observation, 3.7% and 6.4% of patients in the finerenone and placebo groups, respectively, show vision-threatening events, and fewer participants in the finerenone group require ocular intervention (76). The results of this trial are pending and the data are continuously being updated.

In the FIGARO-DKD study, HF or exacerbation of HF causing death as endpoints, finerenone reduces the risk of new-onset HF and improves exacerbation of HF in T2DM patients with CKD, regardless of the prior HF history (6). In the FIDELIO-DKD study, finerenone reduces the risk of new-onset atrial flutter or atrial fibrillation (AFF) in T2DM patients with CKD and T2DM, regardless of the AFF history at baseline (77).

Both pre-clinical and clinical studies support the correlation between increase adiposity and MR activation. In an cohort analysis, obesity was correlated with elevated aldosterone levels (78). In animal study, finerenone improves metabolic parameters, including the glucose-lipid metabolism and insulin resistance in high-fat-diet mice. Finerenone stimulates the brown adipose tissue function, and increases the expression of uncoupling protein-1 (UCP-1) through AMP-activated protein kinase (AMPK)-UCP-1 pathway (79). The effect of finerenone on anti-obesity and regulation of metabolic parameters needs more clinical evidence.

Primary hyperaldosteronism (PA) is a common cause of secondary increased hypertension, which also acceleration the progression of cardiovascular complication. Unilateral adrenal hyperplasia or adenoma is first-line treated by surgery, while bilateral adrenal hyperplasia or idiopathic hyperaldosteronism is treated by MRAs (80). Spironolactone and eplerenone are commonly recommended choice at present. Finerenone as a new MRAs, may have more prominent advantages in the treatment of PA. Further clinical studies on this agent will provide supportive evidence.

Obstructive sleep apnea hypopnea syndrome (OSAHS) is considered as an independent risk factor for hypertension, and the pathophysiological mechanisms include RAAS activation, oxidative stress, endothelial cell damage, and sympathetic nerve excitation. The elevated aldosterone levels can increase nocturnal fluid transfer, and aggravate OSAHS. There is an interaction between OSAHS and aldosterone, which aggravate the occurrence of hypertension in OSAHS patients. MRA can improve the control of hypertension

and delay the development of OSAHS. Therefore, the application of aldosterone receptor antagonist can improve OSAHS related Hypertension. Finerenone as a novel MRA also may be a promising therapeutic strategy of OSAHS and OSA-related hypertension (81).

A rat experiment demonstrates that MR is overexpressed in experimental and human pulmonary arterial hypertension (PAH), with the monocrotaline and sugen/hypoxia rat models. In addition, hMR+ (human MR overexpressing) mice display increased right ventricular systolic pressure, right ventricular hypertrophy, and remodeling of pulmonary arterioles. Finerenone-feeding mice show reversed PAH in some extent and decreased inflammatory cell infiltration and vascular cell proliferation. This experiment confirmed that finerenone appears to a potential therapy for PAH (9).

9 Summary

Finerenone is marketed as the first third-generation highly selective non-steroidal MRA for improving cardiorenal prognosis in T2DM patients with CKD and CVD. Several large-scaled clinical trials show that, regardless of ASCVD history, finerenone reduces the risk of cardiovascular and renal adverse events in T2DM patients, delays the disease progression and improves cardiac and renal outcomes. Improving cardiorenal outcomes and delaying the progression of complications are the vital strategy for diabetic management. The integrated management of diabetic-cardio-renal contributes to long-term prognosis of diabetic patients, especially combined with CKD and CVD. Finerenone provides organ protection, also has a lower incidence of electrolyte disturbances such as hyperkalemia than those conventional MRAs due to its high selectivity and affinity to MR. There is potential effect on the treatment of primary aldosteronism (PA), diabetic retinopathy (DR), atrial fibrillation and pulmonary hypertension. It suggests that finerenone may be a potential therapeutic strategy for treatment of CKD and CVD.

Author contributions

RL and BD drafted the manuscript. LC, SL, and YW provided helpful suggestions. LX conceived the study. BD designed the study and take responsibility for this study. All authors contributed to the article and approved the submitted version.

Funding

This work was supported by a grant from the National Natural Science Foundation of China (no. 81600691) and a China Postdoctoral Science Foundation-funded project (no. 2018M640615). The content of the article has not been influenced by the sponsors.

Conflict of interest

The authors declare that the research was conducted in the absence of any commercial or financial relationships that could be construed as a potential conflict of interest.

Publisher's note

All claims expressed in this article are solely those of the authors and do not necessarily represent those of their affiliated

organizations, or those of the publisher, the editors and the reviewers. Any product that may be evaluated in this article, or claim that may be made by its manufacturer, is not guaranteed or endorsed by the publisher.

References

- Davies MJ, Aroda VR, Collins BS, Gabbay RA, Green J, Maruthur NM, et al. Management of hyperglycaemia in type 2 diabetes, 2022. a consensus report by the American diabetes association (ADA) and the European association for the study of diabetes (EASD). *Diabetologia* (2022) 65(12):1925–66. doi: 10.1007/s00125-022-05787-2
- Zheng Y, Ley SH, Hu FB. Global aetiology and epidemiology of type 2 diabetes mellitus and its complications. *nature reviews. Endocrinology* (2018) 14(2):88–98. doi: 10.1038/nrendo.2017.151
- Pitt B, Filippatos G, Agarwal R, Anker SD, Bakris GL, Rossing P, et al. Cardiovascular events with finerenone in kidney disease and type 2 diabetes. *New Engl J Med* (2021) 385(24):2252–63. doi: 10.1056/NEJMoa2110956
- Jaisser F, Farman N. Emerging roles of the mineralocorticoid receptor in pathology: Toward new paradigms in clinical pharmacology. *Pharmacol Rev* (2016) 68(1):49–75. doi: 10.1124/pr.115.011106
- Barrera-Chimal J, Bonnard B, Jaisser F. Roles of mineralocorticoid receptors in cardiovascular and cardiorenal diseases. *Annu Rev Physiol* (2022) 84:585–610. doi: 10.1146/annurev-physiol-060821-013950
- Filippatos G, Anker SD, Agarwal R, Ruilope LM, Rossing P, Bakris GL, et al. Finerenone reduces risk of incident heart failure in patients with chronic kidney disease and type 2 diabetes: Analyses from the FIGARO-DKD trial. *Circulation* (2022) 145(6):437–47. doi: 10.1161/CIRCULATIONAHA.121.057983
- Pitt B, Kober L, Ponikowski P, Gheorghiade M, Filippatos G, Krum H, et al. Safety and tolerability of the novel non-steroidal mineralocorticoid receptor antagonist BAY 94-8862 in patients with chronic heart failure and mild or moderate chronic kidney disease: a randomized, double-blind trial. *Eur Heart J* (2013) 34(31):2453–63. doi: 10.1093/eurheartj/ehs187
- Kolkhof P, Delbeck M, Kretschmer A, Steinke W, Hartmann E, Bärfacker L, et al. Finerenone, a novel selective nonsteroidal mineralocorticoid receptor antagonist protects from rat cardiorenal injury. *J Cardiovasc Pharmacol* (2014) 64(1):69–78. doi: 10.1097/FJC.0000000000000091
- Tu L, Thuillet R, Perrot J, Ottaviani M, Ponsardin E, Kolkhof P, et al. Mineralocorticoid receptor antagonism by finerenone attenuates established pulmonary hypertension in rats. *Hypertension (Dallas Tex 1979)* (2022) 79(10):2262–73. doi: 10.1161/HYPERTENSIONAHA.122.19207
- van den Berg TNA, Rongen GA, Fröhlich GM, Deinum J, Hausenloy DJ, Riksen NP, et al. The cardioprotective effects of mineralocorticoid receptor antagonists. *Pharmacol Ther* (2014) 142(1):72–87. doi: 10.1016/j.pharmthera.2013.11.006
- Ferreira NS, Tostes RC, Paradis P, Schiffrin EL. Aldosterone, inflammation, immune system, and hypertension. *Am J Hypertension* (2021) 34(1):15–27. doi: 10.1093/ajh/hpaa137
- Bauersachs J, López-Andrés N. Mineralocorticoid receptor in cardiovascular diseases-clinical trials and mechanistic insights. *Br J Pharmacol* (2022) 179(13):3119–34. doi: 10.1111/bph.15708
- Sinphitukkul K, Manotham K, Eiam-Ong S, Eiam-Ong S. Aldosterone nongenomically induces angiotensin II receptor dimerization in rat kidney: role of mineralocorticoid receptor and NADPH oxidase. *Arch Med Sci AMS* (2019) 15(6):1589–98. doi: 10.5114/aoms.2019.87135
- Rude MK, Duhaney T-AS, Kuster GM, Judge S, Heo J, Colucci WS, et al. Aldosterone stimulates matrix metalloproteinases and reactive oxygen species in adult rat ventricular cardiomyocytes. *Hypertension (Dallas Tex 1979)* (2005) 46(3):555–61. doi: 10.1161/01.HYP.0000176236.55322.18
- Connell JMC, Davies E. The new biology of aldosterone. *J Endocrinol* (2005) 186(1):1–20. doi: 10.1677/joe.1.06017
- Callera GE, Montezano ACI, Yogi A, Tostes RC, He Y, Schiffrin EL, et al. C-src-dependent nongenomic signaling responses to aldosterone are increased in vascular myocytes from spontaneously hypertensive rats. *Hypertension (Dallas Tex 1979)* (2005) 46(4):1032–8. doi: 10.1161/01.HYP.0000176588.51027.35
- Briet M, Schiffrin EL. Aldosterone: effects on the kidney and cardiovascular system. *nature reviews. Nephrology* (2010) 6(5):261–73. doi: 10.1038/nrneph.2010.30
- Palanisamy S, Hernandez Funes M, Chang TI, Mahaffey KW. Cardiovascular and renal outcomes with finerenone, a selective mineralocorticoid receptor antagonist. *Cardiol Ther* (2022) 11(3):337–54. doi: 10.1007/s40119-022-00269-3
- Agarwal R, Kolkhof P, Bakris G, Bauersachs J, Haller H, Wada T, et al. Steroidal and non-steroidal mineralocorticoid receptor antagonists in cardiorenal medicine. *Eur Heart J* (2021) 42(2):152–61. doi: 10.1093/eurheartj/ehaa736
- Grune J, Beyhoff N, Smeir E, Chudek R, Blumrich A, Ban Z, et al. Selective mineralocorticoid receptor cofactor modulation as molecular basis for finerenone's antifibrotic activity. *Hypertension (Dallas Tex 1979)* (2018) 71(4):599–608. doi: 10.1161/HYPERTENSIONAHA.117.10360
- Rocha R, Rudolph AE, Friedrich GE, Nachowiak DA, Kekec BK, Blomme EAG, et al. Aldosterone induces a vascular inflammatory phenotype in the rat heart. *Am J Physiol Heart Circulatory Physiol* (2002) 283(5):H1802–10. doi: 10.1152/ajpheart.01096.2001
- Barrera-Chimal J, Estrela R, Lechner SM, Giraud S, Moghrabi El S, Kaaki S, et al. The myeloid mineralocorticoid receptor controls inflammatory and fibrotic responses after renal injury via macrophage interleukin-4 receptor signaling. *Kidney Int* (2018) 93(6):1344–55. doi: 10.1016/j.kint.2017.12.016
- Dutzmann J, Musmann R-J, Haertle M, Daniel J-M, Sonnenschein K, Schäfer A, et al. The novel mineralocorticoid receptor antagonist finerenone attenuates neointima formation after vascular injury. *PloS One* (2017) 12(9):e0184888. doi: 10.1371/journal.pone.0184888
- Hirohama D, Nishimoto M, Ayuzawa N, Kawarazaki W, Fujii W, Oba S, et al. Activation of Rac1-mineralocorticoid receptor pathway contributes to renal injury in salt-loaded mice. *Hypertension (Dallas Tex 1979)* (2021) 78(1):82–93. doi: 10.1161/HYPERTENSIONAHA.121.17263
- Lattenist L, Lechner SM, Messaoudi S, Le Mercier A, El Moghrabi S, Prince S, et al. Nonsteroidal mineralocorticoid receptor antagonist finerenone protects against acute kidney injury-mediated chronic kidney disease: Role of oxidative stress. *Hypertension (Dallas Tex 1979)* (2017) 69(5):870–8. doi: 10.1161/HYPERTENSIONAHA.116.08526
- Agarwal R, Joseph A, Anker SD, Filippatos G, Rossing P, Ruilope LM, et al. Hyperkalemia risk with finerenone: Results from the FIDELIO-DKD trial. *J Am Soc Nephrol JASN* (2022) 33(1):225–37. doi: 10.1681/ASN.2021070942
- Kolkhof P, Bärfacker L. 30 YEARS OF THE MINERALOCORTICOID RECEPTOR: Mineralocorticoid receptor antagonists: 60 years of research and development. *J Endocrinol* (2017) 234(1):T125–40. doi: 10.1530/JOE-16-0600
- Amazit L, Le Billan F, Kolkhof P, Lamribet K, Viengchareun S, Fay MR, et al. Finerenone impedes aldosterone-dependent nuclear import of the mineralocorticoid receptor and prevents genomic recruitment of steroid receptor coactivator-1. *J Biol Chem* (2015) 290(36):21876–89. doi: 10.1074/jbc.M115.657957
- Barrera-Chimal J, Kolkhof P, Lima-Posada I, Joachim A, Rossignol P, Jaisser F. Differentiation between emerging non-steroidal and established steroidal mineralocorticoid receptor antagonists: head-to-head comparisons of pharmacological and clinical characteristics. *Expert Opin On Investigational Drugs* (2021) 30(11):1141–57. doi: 10.1080/13543784.2021.2002844
- Gouloze SC, Snelder N, Seelmann A, Horvat-Broecker A, Brinker M, Joseph A, et al. Finerenone dose-Exposure-Serum potassium response analysis of FIDELIO-DKD phase III: The role of dosing, titration, and inclusion criteria. *Clin Pharmacokinet* (2022) 61(3):451–62. doi: 10.1007/s40262-021-01083-1
- Agarwal R, Filippatos G, Pitt B, Anker SD, Rossing P, Joseph A, et al. Cardiovascular and kidney outcomes with finerenone in patients with type 2 diabetes and chronic kidney disease: the FIDELITY pooled analysis. *Eur Heart J* (2022) 43(6):474–84. doi: 10.1093/eurheartj/ehab777
- Lytvyn Y, Godoy LC, Scholtes RA, Raalte van DH, Cherney DZ. Mineralocorticoid antagonism and diabetic kidney disease. *Curr Diabetes Rep* (2019) 19(1):4. doi: 10.1007/s11892-019-1123-8
- Pitt B, Zannad F, Remme WJ, Cody R, Castaigne A, Perez A, et al. The effect of spironolactone on morbidity and mortality in patients with severe heart failure. randomized aldactone evaluation study investigators. *New Engl J Med* (1999) 341(10):709–17. doi: 10.1056/NEJM199909023411001
- Tseng W-C, Liu J-S, Hung S-C, Kuo K-L, Chen Y-H, Tarng D-C, et al. Effect of spironolactone on the risks of mortality and hospitalization for heart failure in pre-dialysis advanced chronic kidney disease: A nationwide population-based study. *Int J Cardiol* (2017) 238:72–8. doi: 10.1016/j.ijcard.2017.03.080
- Yang C-T, Kor C-T, Hsieh Y-P. Long-term effects of spironolactone on kidney function and hyperkalemia-associated hospitalization in patients with chronic kidney disease. *J Clin Med* (2018) 7(11):459. doi: 10.3390/jcm7110459
- Pitt B, Pfeffer MA, Assmann SF, Boineau R, Anand IS, Claggett B, et al. Spironolactone for heart failure with preserved ejection fraction. *New Engl J Med* (2014) 370(15):1383–92. doi: 10.1056/NEJMoa1313731
- Enzan N, Matsushima S, Ide T, Kaku H, Higo T, Tsuchihashi-Makaya M, et al. Spironolactone use is associated with improved outcomes in heart failure with mid-range ejection fraction. *ESC Heart Failure* (2020) 7(1):339–47. doi: 10.1002/ehf2.12571
- Krieger EM, Dräger LF, Giorgi DMA, Pereira AC, Barreto-Filho JAS, Nogueira AR, et al. Spironolactone versus clonidine as a fourth-drug therapy for resistant hypertension:

The ReHOT randomized study (Resistant hypertension optimal treatment). *Hypertension (Dallas Tex 1979)* (2018) 71(4):681–90. doi: 10.1161/HYPERTENSIONAHA.117.10662

39. Minakuchi H, Wakino S, Urai H, Kurokouchi A, Hasegawa K, Kanda T, et al. The effect of aldosterone and aldosterone blockade on the progression of chronic kidney disease: a randomized placebo-controlled clinical trial. *Sci Rep* (2020) 10(1):16626. doi: 10.1038/s41598-020-73638-4

40. El Mokadem M, Abd El Hady Y, Aziz A. A prospective single-blind randomized trial of ramipril, eplerenone and their combination in type 2 diabetic nephropathy. *Cardiorenal Med* (2020) 10(6):392–401. doi: 10.1159/000508670

41. Kovarik JJ, Kaltenecker CC, Domenig O, Antlanger M, Poglitsch M, Kopecky C, et al. Effect of mineralocorticoid receptor antagonism and ACE inhibition on angiotensin profiles in diabetic kidney disease: An exploratory study. *Diabetes Ther Research Treat Educ Diabetes Related Disord* (2021) 12(9):2485–98. doi: 10.1007/s13300-021-01118-7

42. Pitt B, Remme W, Zannad F, Neaton J, Martinez F, Roniker B, et al. Eplerenone, a selective aldosterone blocker, in patients with left ventricular dysfunction after myocardial infarction. *New Engl J Med* (2003) 348(14):1309–21. doi: 10.1056/NEJMoa030207

43. Zannad F, McMurray JJV, Krum H, van Veldhuisen DJ, Swedberg K, Shi H, et al. Eplerenone in patients with systolic heart failure and mild symptoms. *New Engl J Med* (2011) 364(1):11–21. doi: 10.1056/NEJMoa1009492

44. Deswal A, Richardson P, Bozkurt B, Mann DL. Results of the randomized aldosterone antagonism in heart failure with preserved ejection fraction trial (RAAM-PEF). *J Cardiac Failure* (2011) 17(8):634–42. doi: 10.1016/j.cardfail.2011.04.007

45. Schneider A, Schwab J, Karg MV, Kalizki T, Reinold A, Schneider MP, et al. Low-dose eplerenone decreases left ventricular mass in treatment-resistant hypertension. *J Hypertension* (2017) 35(5):1086–92. doi: 10.1097/HJH.0000000000001264

46. Kalizki T, Schmidt BMW, Raff U, Reinold A, Schwarz TK, Schneider MP, et al. Low dose-eplerenone treatment decreases aortic stiffness in patients with resistant hypertension. *J Clin Hypertension (Greenwich Conn.)* (2017) 19(7):669–76. doi: 10.1111/jch.12986

47. Sawai T, Dohi K, Fujimoto N, Okubo S, Isaka N, Ichikawa T, et al. Antialbuminuric effect of eplerenone in comparison to thiazide diuretics in patients with hypertension. *J Clin Hypertension (Greenwich Conn.)* (2017) 19(10):990–8. doi: 10.1111/jch.13054

48. Karashima S, Yoneda T, Kometani M, Ohe M, Mori S, Sawamura T, et al. Comparison of eplerenone and spironolactone for the treatment of primary aldosteronism. *Hypertension Res Off J Japanese Soc Hypertension* (2016) 39(3):133–7. doi: 10.1038/hr.2015.129

49. Pilz S, Trummer C, Verheyen N, Schwetz V, Pandis M, Aberer F, et al. Mineralocorticoid receptor blockers and aldosterone to renin ratio: A randomized controlled trial and observational data. *Hormone Metab Res = Hormon- Und Stoffwechselforschung = Hormones Et Metabolisme* (2018) 50(5):375–82. doi: 10.1055/a-0604-3249

50. Filippatos G, Anker SD, Böhm M, Gheorghide M, Køber L, Krum H, et al. A randomized controlled study of finerenone vs. eplerenone in patients with worsening chronic heart failure and diabetes mellitus and/or chronic kidney disease. *Eur Heart J* (2016) 37(27):2105–14. doi: 10.1093/eurheartj/ehw132

51. Bakris GL, Agarwal R, Chan JC, Cooper ME, Gansevoort RT, Haller H, et al. Effect of finerenone on albuminuria in patients with diabetic nephropathy: A randomized clinical trial. *JAMA* (2015) 314(9):884–94. doi: 10.1001/jama.2015.10081

52. Bakris GL, Agarwal R, Anker SD, Pitt B, Ruilope LM, Rossing P, et al. Effect of finerenone on chronic kidney disease outcomes in type 2 diabetes. *New Engl J Med* (2020) 383(23):2219–29. doi: 10.1056/NEJMoa2025845

53. Fu Z, Geng X, Chi K, Song C, Wu D, Liu C, et al. Efficacy and safety of finerenone in patients with chronic kidney disease: a systematic review with meta-analysis and trial sequential analysis. *Ann Palliative Med* (2021) 10(7):7428–39. doi: 10.21037/apm-21-763

54. Pei H, Wang W, Zhao D, Wang L, Su G-H, Zhao Z. The use of a novel non-steroidal mineralocorticoid receptor antagonist finerenone for the treatment of chronic heart failure: A systematic review and meta-analysis. *Medicine* (2018) 97(16):e0254. doi: 10.1097/MD.00000000000010254

55. Ito S, Itoh H, Rakugi H, Okuda Y, Yoshimura M, Yamakawa S. Double-blind randomized phase 3 study comparing esaxerenone (CS-3150) and eplerenone in patients with essential hypertension (ESAX-HTN study). *Hypertension (Dallas Tex 1979)* (2020) 75(1):51–8. doi: 10.1161/HYPERTENSIONAHA.119.13569

56. Ito S, Kashiwara N, Shikata K, Nangaku M, Wada T, Okuda Y, et al. Esaxerenone (CS-3150) in patients with type 2 diabetes and microalbuminuria (ESAX-DN): Phase 3 randomized controlled clinical trial. *Clin J Am Soc Nephrol CJASN* (2020) 15(12):1715–27. doi: 10.2215/CJN.06870520

57. Wada T, Inagaki M, Yoshinari T, Terata R, Totsuka N, Gotou M, et al. Apararenone in patients with diabetic nephropathy: results of a randomized, double-blind, placebo-controlled phase 2 dose-response study and open-label extension study. *Clin Exp Nephrol* (2021) 25(2):120–30. doi: 10.1007/s10157-020-01963-z

58. Bakris G, Pergola PE, Delgado B, Genov D, Doliashvili T, Vo N, et al. Effect of KBP-5074 on blood pressure in advanced chronic kidney disease: Results of the BLOCK-CKD study. *Hypertension (Dallas Tex 1979)* (2021) 78(1):74–81. doi: 10.1161/HYPERTENSIONAHA.121.17073

59. Derosa G, Maffioli P, Scelsi L, Bestetti A, Vanasia M, Cicero AFG, et al. Canrenone on cardiovascular mortality in congestive heart failure: CanrenOne eFFects on cardiovascular mortality in patiEnts with congEstive heart Failure: The COFFEE-IT study. *Pharmacol Res* (2019) 141:46–52. doi: 10.1016/j.phrs.2018.11.037

60. Boccanelli A, Mureddu GF, Cacciatore G, Clemenza F, Lenarda Di A, Gavazzi A, et al. Anti-remodelling effect of canrenone in patients with mild chronic heart failure

(AREA IN-CHF study): final results. *Eur J Heart Failure* (2009) 11(1):68–76. doi: 10.1093/eurjhf/hfn015

61. Bakris GL, Ruilope LM, Anker SD, Filippatos G, Pitt B, Rossing P, et al. A prespecified exploratory analysis from FIDELITY examined finerenone use and kidney outcomes in patients with chronic kidney disease and type 2 diabetes. *Kidney Int* (2022) 103(1):196–206. doi: 10.1016/j.kint.2022.08.040

62. Kolkhof P, Joseph A, Kintscher U. Nonsteroidal mineralocorticoid receptor antagonism for cardiovascular and renal disorders - new perspectives for combination therapy. *Pharmacol Res* (2021) 172:105859. doi: 10.1016/j.phrs.2021.105859

63. Bao W, Zhang M, Li N, Yao Z, Sun L. Efficacy and safety of finerenone in chronic kidney disease associated with type 2 diabetes: a systematic review and meta-analysis of randomized clinical trials. *Eur J Clin Pharmacol* (2022) 78(12):1877–87. doi: 10.1007/s00228-022-03408-w

64. Fukui A, Kaneko H, Okada A, Yano Y, Itoh H, Matsuoka S, et al. Semiquantitative assessed proteinuria and risk of heart failure: analysis of a nationwide epidemiological database. *Nephrol Dialysis Transplant* (2022) 37(9):1691–9. doi: 10.1093/ndt/gfab248

65. Liu LCY, Schutte E, Gansevoort RT, van der Meer P, Voors AA. Finerenone - third-generation mineralocorticoid receptor antagonist for the treatment of heart failure and diabetic kidney disease. *Expert Opin On Investigational Drugs* (2015) 24(8):1123–35. doi: 10.1517/13543784.2015.1059819

66. Rossing P, Agarwal R, Anker SD, Filippatos G, Pitt B, Ruilope LM, et al. Efficacy and safety of finerenone in patients with chronic kidney disease and type 2 diabetes by GLP-1RA treatment: A subgroup analysis from the FIDELIO-DKD trial. *Diabetes Obes Metab* (2022) 24(1):125–34. doi: 10.1111/dom.14558

67. Filippatos G, Anker SD, Pitt B, McGuire DK, Rossing P, Ruilope LM, et al. Finerenone efficacy in patients with chronic kidney disease, type 2 diabetes and atherosclerotic cardiovascular disease. *Eur Heart J Cardiovasc Pharmacol* (2022) 9(1):85–93. doi: 10.1093/ehjcvp/pvac054

68. Dong B, Lv R, Wang J, Che L, Wang Z, Hua Z, et al. The extraglycemic effect of SGLT-2is on mineral and bone metabolism and bone fracture. *Front In Endocrinol* (2022) 13:918350. doi: 10.3389/fendo.2022.918350

69. Sodium-glucose cotransporter protein-2 (SGLT-2) inhibitors and glucagon-like peptide-1 (GLP-1) receptor agonists for type 2 diabetes: systematic review and network meta-analysis of randomised controlled trials. *BMJ (Clinical Res ed.)* (2022) 376:o109. doi: 10.1136/bmj.o109

70. Kristensen SL, Rørth R, Jhund PS, Docherty KF, Sattar N, Preiss D, et al. Cardiovascular, mortality, and kidney outcomes with GLP-1 receptor agonists in patients with type 2 diabetes: a systematic review and meta-analysis of cardiovascular outcome trials. *Lancet Diabetes Endocrinol* (2019) 7(10):776–85. doi: 10.1016/S2213-8587(19)30249-9

71. Maruthur NM, Tseng E, Hutfless S, Wilson LM, Suarez-Cuervo C, Berger Z, et al. Diabetes medications as monotherapy or metformin-based combination therapy for type 2 diabetes: A systematic review and meta-analysis. *Ann Internal Med* (2016) 164(11):740–51. doi: 10.7326/M15-2650

72. Kolkhof P, Hartmann E, Freyberger A, Pavkovic M, Mathar I, Sandner P, et al. Effects of finerenone combined with empagliflozin in a model of hypertension-induced end-organ damage. *Am J Nephrol* (2021) 52(8):642–52. doi: 10.1159/000516213

73. Vaduganathan M, Docherty KF, Claggett BL, Jhund PS, Boer RA, Hernandez AF, et al. SGLT-2 inhibitors in patients with heart failure: a comprehensive meta-analysis of five randomised controlled trials. *Lancet (London England)* (2022) 400(10354):757–67. doi: 10.1016/S0140-6736(22)01429-5

74. Green JB, Mottl K, Bakris G, Heerspink HJL, Mann JFE, McGill JB, et al. Design of the Combination effect of Finerenone and Empagliflozin in participants with chronic kidney disease and type 2 diabetes using an UACR endpoint study (CONFIDENCE). *Nephrol Dialysis Transplant* (2022) 0:1–10. doi: 10.1093/ndt/gfac198

75. Zuo C, Xu G. Efficacy and safety of mineralocorticoid receptor antagonists with ACEI/ARB treatment for diabetic nephropathy: A meta-analysis. *Int J Clin Pract* (2019) 00:e13413. doi: 10.1111/ijcp.13413

76. Rossing P, Garweg G, Anker SD, Osonoi T, Pitt B, Rosas SE, et al. Effect of finerenone on occurrence of vision-threatening complications in patients with non-proliferative diabetic retinopathy: pooled analysis of two studies using routine ophthalmological examinations from clinical trial participants (ReFINErDR/DeFINErDR). *Diabetes Obes Metab* (2022) 25(3):142–52. doi: 10.1111/dom.14915

77. Filippatos G, Bakris GL, Pitt B, Agarwal R, Rossing P, Ruilope LM, et al. Finerenone reduces new-onset atrial fibrillation in patients with chronic kidney disease and type 2 diabetes. *J Am Coll Cardiol* (2021) 78(2):142–52. doi: 10.1016/j.jacc.2021.04.079

78. Kathiresan S, Larson MG, Benjamin EJ, Corey D, Murabito JM, Fox CS, et al. Clinical and genetic correlates of serum aldosterone in the community: the framingham heart study. *Am J Hypertension* (2005) 18(5 Pt 1):657–65. doi: 10.1016/j.amjhyper.2004.12.005

79. Marzolla V, Feraco A, Gorini S, Mammi C, Marrese C, Mularoni V, et al. The novel non-steroidal MR antagonist finerenone improves metabolic parameters in high-fat diet-fed mice and activates brown adipose tissue via AMPK-ATGL pathway. *FASEB J* (2020) 34(9):12450–65. doi: 10.1096/fj.202000164R

80. Reincke M, Bancos I, Mulatero P, Scholl UI, Stowasser M, Williams TA. Diagnosis and treatment of primary aldosteronism. *Lancet Diabetes Endocrinol* (2021) 9(12):876–92. doi: 10.1016/S2213-8587(21)00210-2

81. Wang Y, Li CX, Lin YN, Zhang LY, Li SQ, Zhang L, et al. The role of aldosterone in OSA and OSA-related hypertension. *Front In Endocrinol* (2021) 12:801689. doi: 10.3389/fendo.2021.801689



OPEN ACCESS

EDITED BY

Weixia Sun,
Department of Nephrology, The First
Hospital of Jilin University, China

REVIEWED BY

Mohd Murshad Ahmed,
Jamia Millia Islamia, India
Nirmal Kumar Ganguly,
Indraprastha Apollo Hospitals, India

*CORRESPONDENCE

Xuan Zhang

✉ zhangxuantj@163.com
Kaishan Tao

✉ taokaishan0686@163.com
Zhaoxu Yang

✉ 15829057616@163.com

[†]These authors have contributed equally to
this work

SPECIALTY SECTION

This article was submitted to
Cellular Endocrinology,
a section of the journal
Frontiers in Endocrinology

RECEIVED 16 December 2022

ACCEPTED 09 February 2023

PUBLISHED 27 February 2023

CITATION

Cao Y, Du Y, Jia W, Ding J, Yuan J,
Zhang H, Zhang X, Tao K and Yang Z
(2023) Identification of biomarkers for the
diagnosis of chronic kidney disease (CKD)
with non-alcoholic fatty liver disease
(NAFLD) by bioinformatics analysis and
machine learning.
Front. Endocrinol. 14:1125829.
doi: 10.3389/fendo.2023.1125829

COPYRIGHT

© 2023 Cao, Du, Jia, Ding, Yuan, Zhang,
Zhang, Tao and Yang. This is an open-access
article distributed under the terms of the
[Creative Commons Attribution License](#)
(CC BY). The use, distribution or
reproduction in other forums is permitted,
provided the original author(s) and the
copyright owner(s) are credited and that
the original publication in this journal is
cited, in accordance with accepted
academic practice. No use, distribution or
reproduction is permitted which does not
comply with these terms.

Identification of biomarkers for the diagnosis of chronic kidney disease (CKD) with non-alcoholic fatty liver disease (NAFLD) by bioinformatics analysis and machine learning

Yang Cao^{1†}, Yiwei Du^{2†}, Weili Jia^{1†}, Jian Ding¹, Juzheng Yuan³,
Hong Zhang¹, Xuan Zhang^{1*}, Kaishan Tao^{1*} and Zhaoxu Yang^{1*}

¹Department of Hepatobiliary Surgery, Xijing Hospital, The Fourth Military Medical University, Xi'an, China, ²Department of Nephrology, Tangdu Hospital, The Fourth Military Medical University, Xi'an, China, ³Department of General Surgery, Xijing Hospital, The Fourth Military Medical University, Xi'an, China

Background: Chronic kidney disease (CKD) and non-alcoholic fatty liver disease (NAFLD) are closely related to immune and inflammatory pathways. This study aimed to explore the diagnostic markers for CKD patients with NAFLD.

Methods: CKD and NAFLD microarray data sets were screened from the GEO database and analyzed the differentially expressed genes (DEGs) in GSE10495 of CKD data set. Weighted Gene Co-Expression Network Analysis (WGCNA) method was used to construct gene coexpression networks and identify functional modules of NAFLD in GSE89632 data set. Then obtaining NAFLD-related share genes by intersecting DEGs of CKD and modular genes of NAFLD. Then functional enrichment analysis of NAFLD-related share genes was performed. The NAFLD-related hub genes come from intersection of cytoscape software and machine learning. ROC curves were used to examine the diagnostic value of NAFLD related hub genes in the CKD data sets and GSE89632 data set of NAFLD. CIBERSORTx was also used to explore the immune landscape in GSE104954, and the correlation between immune infiltration and hub genes expression was investigated.

Results: A total of 45 NAFLD-related share genes were obtained, and 4 were NAFLD-related hub genes. Enrichment analysis showed that the NAFLD-related share genes were significantly enriched in immune-related pathways, programmed cell death, and inflammatory response. ROC curve confirmed 4 NAFLD-related hub genes in CKD training set GSE104954 and other validation sets. Then they were used as diagnostic markers for CKD. Interestingly, these 4 diagnostic markers of CKD also showed good diagnostic value in the NAFLD data

set GSE89632, so these genes may be important targets of NAFLD in the development of CKD. The expression levels of the 4 diagnostic markers for CKD were significantly correlated with the infiltration of immune cells.

Conclusion: 4 NAFLD-related genes (DUSP1, NR4A1, FOSB, ZFP36) were identified as diagnostic markers in CKD patients with NAFLD. Our study may provide diagnostic markers and therapeutic targets for CKD patients with NAFLD.

KEYWORDS

hub genes, chronic kidney disease, non-alcoholic fatty liver disease, immune, inflammation

1 Introduction

Chronic kidney disease (CKD) is defined as structural or functional abnormalities of the kidney caused by various causes for ≥ 3 months (1). Epidemiological studies show that there are approximately 434.3 million people with CKD in Asia, most of whom come from developing countries like China and India (2). The effective control of chronic kidney disease is a huge public health challenge worldwide (3).

Previous studies have suggested that acute kidney injury, hypertension, and diabetes are risk factors for CKD (4). Recently, accumulating evidence indicates that Non-alcoholic fatty liver disease (NAFLD) may be associated with the development of CKD (5–8).

NAFLD is a heterogeneous disease in which the vast majority are non-alcoholic fatty liver (NAFL) and less than 20% are non-alcoholic steatohepatitis (NASH). NASH has typical characteristics which include inflammation, hepatocyte ballooning, and hepatic injury with or without fibrosis (9, 10). NAFLD is often associated with a variety of metabolic diseases, including hypertension, diabetes, insulin resistance, etc, which are risk factors for CKD. However, the degree of fibrosis in NAFLD was independently associated with CKD progression even when confounding factors such as metabolic diseases were excluded (11–15). Excess fat may association with CKD progression in NAFLD patients by inducing lipotoxicity, inflammation, oxidative stress and fibrosis through pro-inflammatory adipokines and lipocalin (16, 17).

Despite growing evidence of the strong association between NAFLD and CKD, the key molecules and potential mechanisms involved remain unclear. Here, bioinformatics and machine learning were attempted to discover the diagnostic markers and related signaling pathways of CKD in the context of NAFLD, which were hoped to provide a basis for the clinical treatment of CKD patients with NAFLD.

Abbreviations: NAFLD, Non-alcoholic fatty liver disease; CKD, Chronic kidney disease; NASH, non-alcoholic steatohepatitis; WGCNA, Weighted gene co-expression network analysis.

2 Materials and methods

2.1 Data acquisition and preliminary processing

Four data sets [GSE104954, GSE104948 (18), GSE32591 (19), GSE66494 (20)] containing gene expression profiles for Chronic kidney disease (CKD) samples and one data set [GSE89632 (21)] of non-alcoholic fatty liver disease (NAFLD) were downloaded from the GEO database (<https://www.ncbi.nlm.nih.gov/geo/>). Details for the data sets were provided in Table 1. The principal search flow of the article was illustrated in Figure 1.

2.2 Weighted gene co-expression network analysis and module gene selection in NAFLD patients

The WGCNA method was used to construct gene coexpression networks and identify functional modules. First, the median absolute deviation (MAD) of each gene was determined, and genes with MAD values in the bottom 50% were removed. Second, ineligible genes and samples were removed with the goodSamplesGenes function, and a scale-free coexpression network was built. Third, an appropriate “soft” threshold power (β) was determined to calculate intergenic adjacency; then, the adjacency values were converted into a topological overlap matrix (TOM), and gene proportions and phase dissimilarities are determined. Fourth, modules were detected using hierarchical clustering and dynamic tree cutting functions. Finally, gene significance (GS) and module membership (MM) correlations were calculated, and the corresponding module gene information was extracted for further analysis.

2.3 Identification of differentially expressed genes between CKD samples and controls

The DEGs were found in GSE104954 data set using the “limma” R package with inclusion criteria of $|\log_2 \text{FC}| \geq 0.5$ and $p\text{-adjust} < 0.05$. DEGs were shown by volcano and expression levels of the 50 most significantly expressed genes were displayed by heatmaps, respectively.

2.4 Acquisition of NAFLD-related shared genes

Intersection of DEGs in GSE104954 and WGCNA module genes in GSE89632 were defined as NAFLD-related shared genes, represented by a Venn schema by the online website jvenn (<http://jvenn.toulouse.inra.fr/app/example.html>).

2.5 Enrichment analysis

For enrichment analysis of NAFLD-related shared genes, Gene Ontology (GO) annotations of genes from the R package org.Hs.eg.db based on the R package “clusterProfiler”, and the minimum number of genes per gene set was 5 and the maximum was 5000. Gene annotations for Kyoto Encyclopedia of Genes and Genomes (KEGG) pathways were operated through KOBAS-i online tool (<http://kobas.cbi.pku.edu.cn/>) (22), and a false discovery rate <0.05 was considered statistically significant.

2.6 Establishment of protein-protein interaction network and identification of NAFLD-related hub genes by cytoscape software and machine learning

The NAFLD-related shared genes were uploaded to the STRING database (<http://string-db.org/>) to construct the PPI network with a PPI score threshold (medium confidence ≥ 0.700). Hub genes were screened by the Cytoscape (Version 3.9.1) plug-in APP MCODE (Version 2.0.0). At the same time, the machine learning methods random forest (RF) were used to screen for hub genes. The MeanDecreaseGini (MDG) was used to measure the importance of genes by the RF algorithm with “randomForest” package, and hub genes were defined as MDG greater than 1.5. The final NAFLD-related hub genes were obtained by the intersection of the results of cytoscape software and machine learning.

2.7 Verification of NAFLD-related hub genes expression in the CKD data sets

Data set GSE32591 and GSE66494 were used to identify the expression level of the hub genes. GSE 32591 is composed of 29 control samples and 64 samples with lupus nephritis. GSE66494 contains 53 biopsy samples, including 8 control samples and 45 CKD samples.

2.8 Construction of receiver-operating characteristic curves to assess diagnostic efficacy

ROC curves were constructed by “pROC” package in Xiantao Academic (<https://www.xiantao.love/products>) to evaluate the diagnostic value of NAFLD-related hub genes in the CKD training set GSE104954 and other CKD validation data sets (GSE32591, GSE66494 and GSE104948). Further the diagnostic value of hub gene in the NAFLD data set GSE89632 was also evaluated.

2.9 Immune infiltration analysis and correlation analysis

The composition and abundance of 22 types immune cells can be estimated from the CKD and control samples transcriptome in GSE104954 data set by CIBERSORTx (<https://cibersortx.stanford.edu/>). The correlations of NAFLD-related hub genes expression with immune cell infiltrations were investigated in Xiantao Academic, as were their respective correlations.

2.10 Statistical analysis

All statistical analyses of bioinformatics studies in this study were conducted using R software. The differences between the groups were tested using a nonparametric Wilcoxon signed-rank test. Correlation analysis was performed using Spearman’s correlation. In comparison, $p < 0.05$ was considered statistically significant (* $p < 0.05$, ** $p < 0.01$, *** $p < 0.001$, **** $p < 0.0001$).

3 Results

3.1 Key module genes in NAFLD samples were identified by WGCNA

GSE89632 is a representative dataset for investigation of NAFLD and we used it to obtain the most relevant modular genes for NAFLD (23–25). First, WGCNA was used for the identification of the most relevant modular genes for NAFLD. $\beta = 26$ (scale-free $R^2 = 0.85$) was selected as the “soft” threshold based on the scale independence and average connectivity (Figure 2A). Then, different colors are chosen to represent 9 gene co-expression

TABLE 1 Details regarding the 5 data sets, type of samples, test platforms, numbers of samples, samples application types and source documentation.

Data sets	Platforms	Type of Samples	Control sample size	CKD or NAFLD sample size	Applications	References (PMID)
GSE104954 or GSE104948	GPL22945 GPL24120	CKD	21	169	Discovery of DEGs	29724730
GSE89632 GSE32591	GPL14951 GPL14663	NAFLD	24 29	39 64	Discovery of Modular genes Validation of hub genes	25581263 22723521
GSE66494	GPL6480	CKD	8	53	Validation of hub genes	26317775

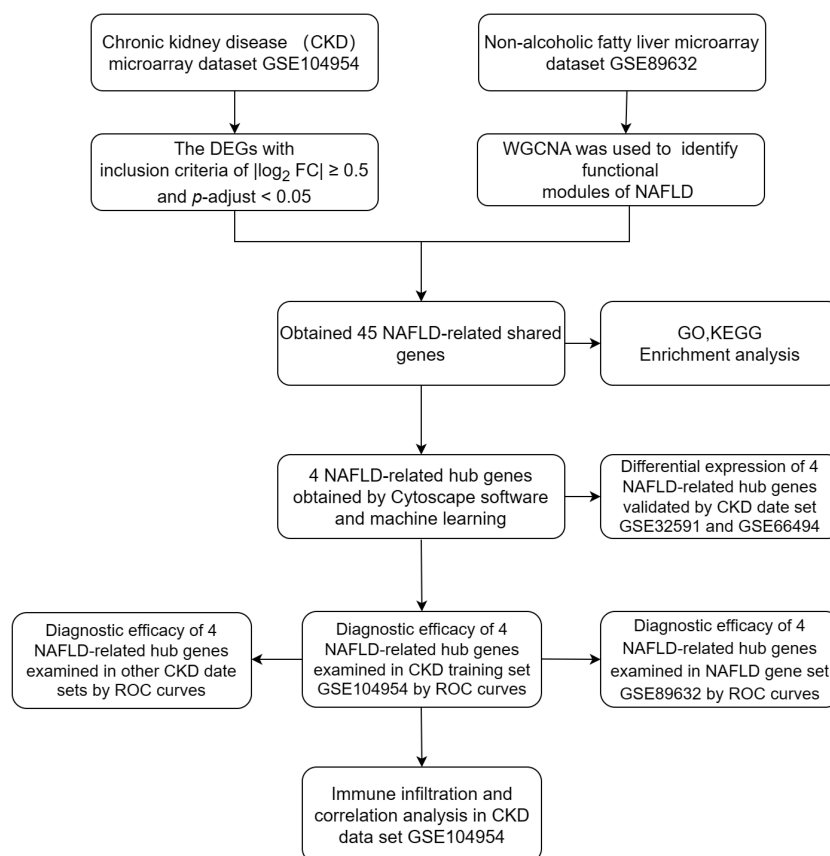


FIGURE 1
Roadmap of the main research ideas in this article.

modules (GCMs), which are presented in [Figure 2B](#). The correlation between NAFLD samples and GCMs is shown in [Figure 2C](#), and the darkturquoise module (412 genes) which was regarded as critical modules demonstrated the highest correlation with NAFLD samples (correlation coefficient = -0.85, $p = 5.3 \times 10^{-19}$). In addition, a significant positive correlation was observed between module membership and gene significance in darkturquoise modules for NAFLD samples ($r = 0.68$, $p = 4.2 \times 10^{-57}$), as shown in [Figure 2D](#).

3.2 Identification of NAFLD-related shared genes between CKD and NAFLD

Next, 386 DEGs were found in GSE104954 data set, of which 227 were up-regulated, and 159 of these genes were down-regulated. [Figure 3A](#) shows the DEGs by the volcano diagram. The heatmap of the top 50 most significant DEGs in the data set is plotted in [Figure 3B](#). Then, 386 DEGs and 412 module genes were intersected, and 45 NAFLD-related shared genes were subsequently obtained, as presented in the Venn diagram in [Figure 3C](#) (Detailed results were provided in [Supplementary Materials S1](#)).

3.3 Enrichment analyses of 45 NAFLD-related shared genes

In order to explore the biological functions and pathways of NAFLD-related shared genes in the development of CKD, GO and KEGG enrichment analyses were performed for 45 shared genes. A total of 563 significantly related biological processes and 23 KEGG signaling pathways were obtained (Detailed results were provided in [Supplementary Materials S2](#)). GO analysis of shared genes was performed to reveal their biological functions ([Figures 4A–C](#)). As we have seen, in the GO category, most of the share genes mostly involved in the “programmed cell death”, “inflammatory response”, “positive regulation of metabolic process”, and “immune system process”(BP); “Extracellular matrix”, “collagen-containing extracellular matrix” (CC); “DNA-binding transcription activator activity, RNA polymerase II-specific”, “DNA-binding transcription factor activity”, etc (MF). The results of KEGG pathway enrichment showed that the most involved pathways were the IL-17 signaling pathway, TNF signaling pathway, MAPK signaling pathway, Apoptosis, Toll-like receptor signaling pathway, and so on, which are closely related to the immune response and inflammation ([Figure 4D](#)).

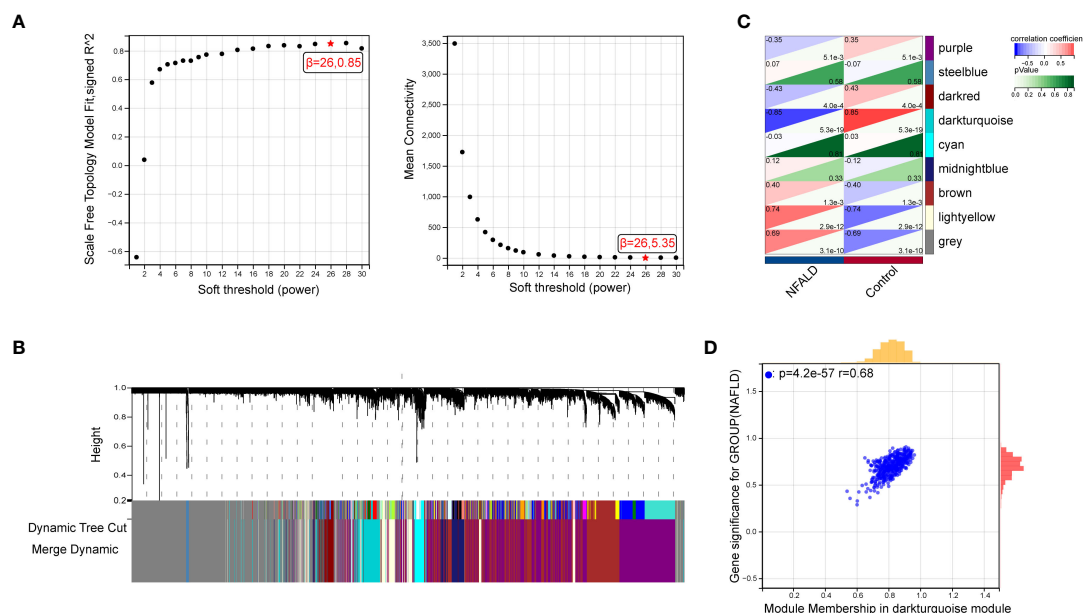


FIGURE 2

Identification of module genes *via* WGCNA in NAFLD data set GSE89632. (A) $\beta = 26$ is selected as the "soft" threshold with the combined analysis of scale independence and average connectivity. (B) Gene coexpression modules represented by different colors under the gene tree. (C) Correlation plot between module membership and gene significance of genes included in the darkturquoise module. (D) Heatmap of the association between the darkturquoise modules and NAFLD samples. NAFLD, Non-alcoholic fatty liver disease; WGCNA, weighted gene co-expression network analysis.

3.4 Identification of NAFLD-related hub genes *via* cytoscape software and machine learning and their differential expression was validated

To reveal the interaction of each protein, the PPI network of the shared genes were built according to the STRING database. There were 38 edges and 45 nodes in Figure 5A, followed by analysis using Cytoscape software. MCODE plugin was used to discover the important modules in the PPI network and the results showed that 8 hub genes in two clusters were tightly connected as the important modules in Figure 5B. On the other hand, 7 hub genes with $\text{MeanDecreaseGini} > 1.5$ were determined by the random forest algorithm in Figure 5C. A Venn diagram in Figure 5D showed the intersection of 4 hub genes (DUSP1, FOSB, NR4A1, ZFP36), which were used as NAFLD-related hub genes. Moreover, in the other two CKD datasets (GSE32591, GSE66494), the 4 NAFLD-related genes were significantly down-regulated (Figures 6A, B), which was consistent with the change in GSE104954 (Supplementary Materials S3).

3.5 The ROC curve was used to evaluate diagnostic efficacy in CKD and NAFLD

The ROC curves of 4 NAFLD-related genes (DUSP1, FOSB, NR4A1, ZFP36) with AUCs of 0.961, 0.954, 0.866, and 0.960 in the training set GSE104954, respectively (Figure 7A). Meanwhile, in the validation set GSE32591, the AUCs of these hub genes were

0.828, 0.796, 0.927 and 0.689, respectively, which did not distinguish whether the source of the sample was glomerular or tubulointerstitial (Figure 7B). At the same time, in the other validation set GSE66494, the AUCs of hub genes were 0.958, 1.000, 0.889, and 0.932, respectively (Figure 7C). Comprehensive analysis of the results of the validation and training sets showed that the 4 NAFLD-related genes can serve as effective markers for the diagnosis of CKD.

GSE104948 and GSE104954, as sister datasets, represent glomerular and tubulointerstitial transcript level information of the same cohort of samples, respectively. 4 NAFLD-associated hub genes have the same good diagnostic efficacy for CKD in GSE104948 (Supplementary Materials S4). Similarly, in the data set GSE32591, both tubulointerstitial and glomerular samples were sampled, and further exploration revealed that the 4 diagnostic markers showed good efficacy in different anatomical structures (Supplementary Materials S5). What should be noted is that these 4 CKD diagnostic markers also have good diagnostic value for NAFLD in GSE89632 data set, and the ROC curves with AUCs of 0.951, 0.968, 0.974, and 0.915, respectively (Figure 7D). This finding may suggest that four genes may play a significant role in the development of CKD patients with NAFLD.

3.6 Immune infiltration analysis and correlation analysis

According to the results of enrichment analysis, NAFLD-related shared genes may be involved in the immune-related mechanisms

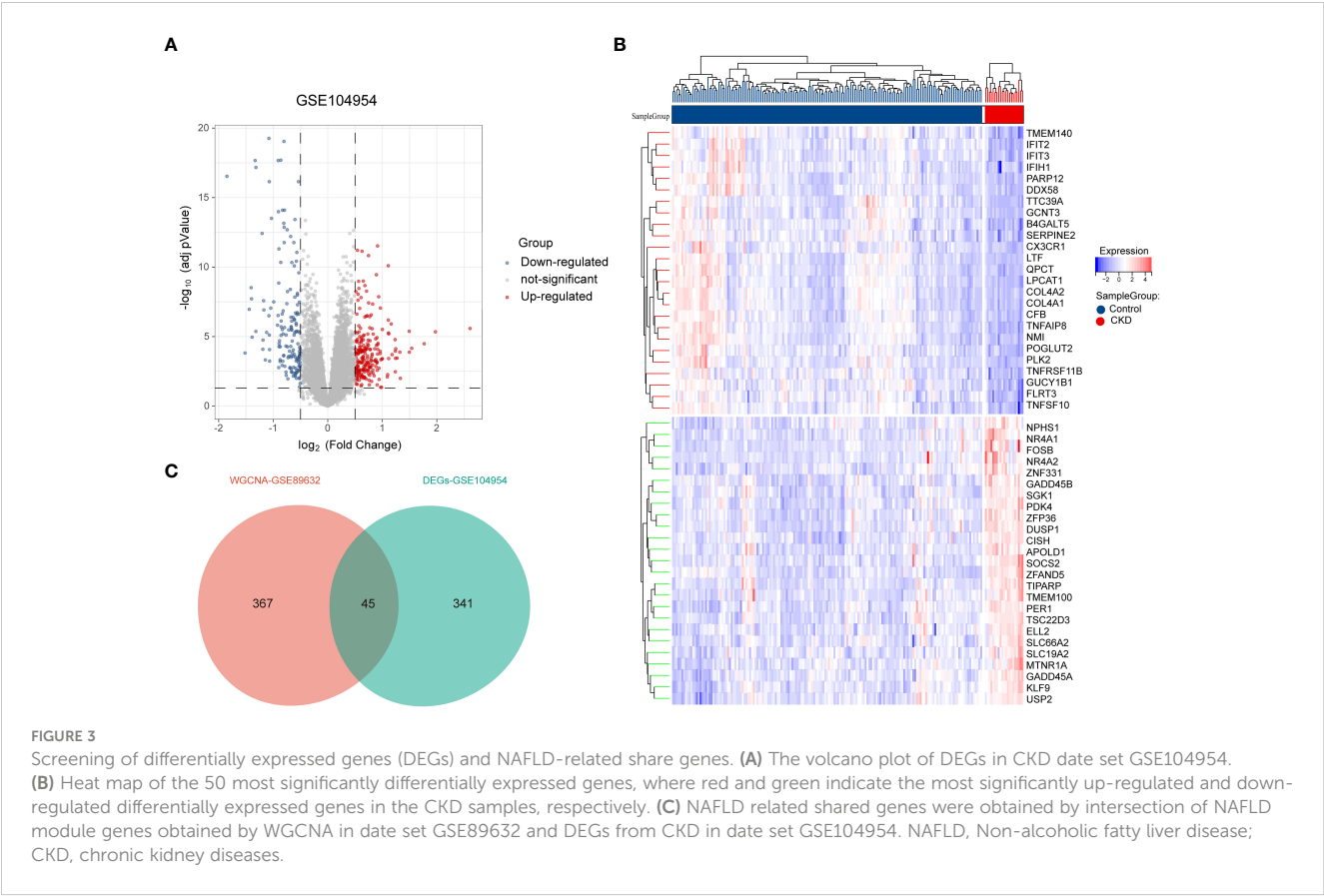


FIGURE 3 Screening of differentially expressed genes (DEGs) and NAFLD-related share genes. **(A)** The volcano plot of DEGs in CKD data set GSE104954. **(B)** Heat map of the 50 most significantly differentially expressed genes, where red and green indicate the most significantly up-regulated and down-regulated differentially expressed genes in the CKD samples, respectively. **(C)** NAFLD related shared genes were obtained by intersection of NAFLD module genes obtained by WGCNA in data set GSE89632 and DEGs from CKD in data set GSE104954. NAFLD, Non-alcoholic fatty liver disease; CKD, chronic kidney diseases.

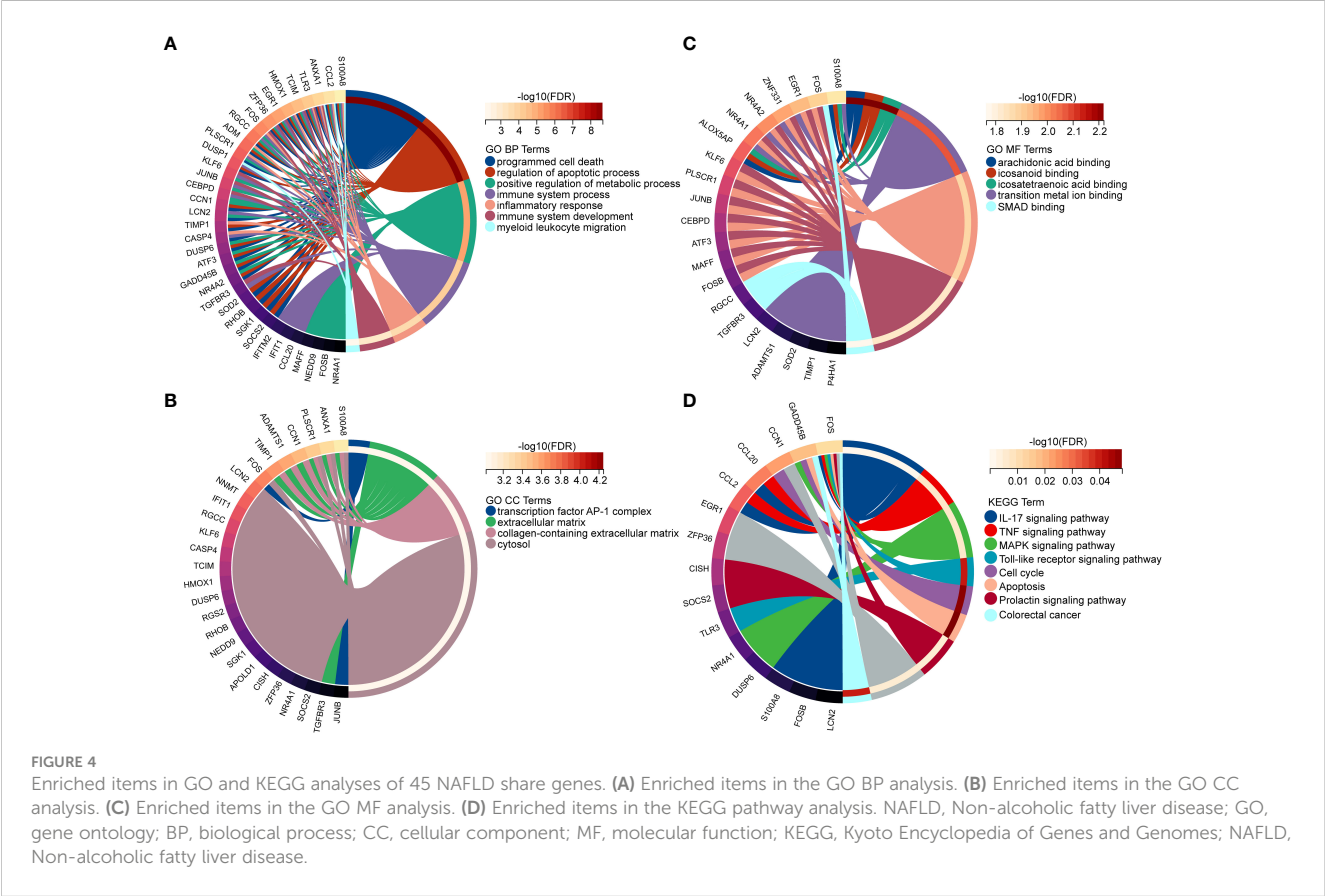


FIGURE 4 Enriched items in GO and KEGG analyses of 45 NAFLD share genes. **(A)** Enriched items in the GO BP analysis. **(B)** Enriched items in the GO CC analysis. **(C)** Enriched items in the GO MF analysis. **(D)** Enriched items in the KEGG pathway analysis. NAFLD, Non-alcoholic fatty liver disease; GO, gene ontology; BP, biological process; CC, cellular component; MF, molecular function; KEGG, Kyoto Encyclopedia of Genes and Genomes; NAFLD, Non-alcoholic fatty liver disease.

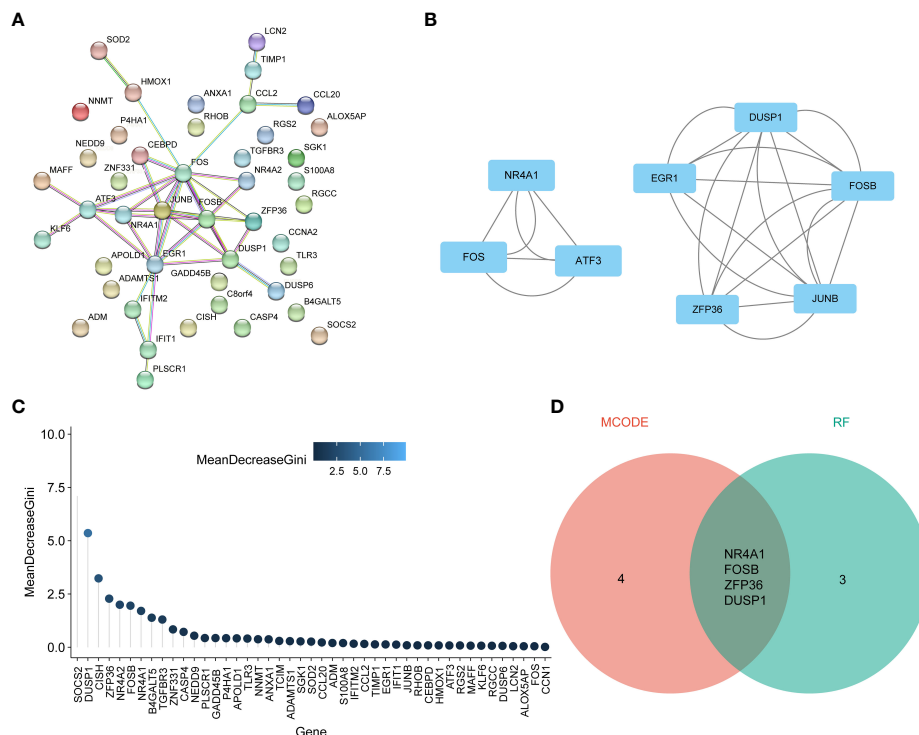


FIGURE 5

Identification of NAFLD-related hub genes by the intersection of cytoscape software and machine learning. (A) Protein-protein interaction (PPI) network of 45 NAFLD-related share genes. (B) The 8 genes in two clusters with the most significant associations were accessed using the MCODE plug-in. (C) Random Forest analysis for NAFLD-related hub DEGs. (D) Venn diagram demonstrates the final NAFLD-related hub genes obtained by the intersection of cytoscape software and machine learning. DEGs, differentially expressed genes; NAFLD, Non-alcoholic fatty liver disease; MCODE, molecular complex detection.

of CKD progression. Therefore, the correlation between the 4 diagnostic markers genes with immune cell infiltration in CKD is noteworthy for further exploration. First, CIBERSORTx was used to evaluate the proportions of 22 immune cell in GSE104954 data set (Figure 8A). B cells memory, Macrophages M1, Mast cells resting, T cells gamma delta were significantly upregulated in CKD samples; however, the levels of B cells naive, Treg cells, Mast cells activated were significantly decreased. Next, the correlation of the four diagnostic markers genes with CKD immune cells was explored (Figure 8B). The FOSB expression was positively correlated with the ratios of B cells naive, Treg cells and Mast cells activated, and negatively correlated with Mast cells resting, T cells gamma delta, M0 Macrophages and M1 Macrophages. ZFP36 and DUSP1 were negatively correlated with the ratios of Treg cells and NK cells resting. NR4A1 was positively correlated with the ratios of B cells naive, Dendritic cells resting and Mast cells activated, and negatively correlated with Mast cells resting, M1 Macrophages and B cells memory. When exploring the interrelationships between the expression of the four diagnostic markers genes, it is interesting to note that they were all positively correlated with each other (Figure 8C), suggesting that they may participate in a common mechanism to promote CKD development. Additionally, the interplay of immune cells was explored (Figure 8D). Treg cells and Mast cells activated had the strongest positive correlation with one another ($r = 0.53$). In contrast, resting

mast cells showed the strongest negative correlation with activated mast cells ($r = -0.83$).

In summary, CKD samples showed significant changes in immune cell infiltration compared with controls, and the four diagnostic markers genes expression was significantly correlated with immune cell infiltration.

4 Discussion

NAFLD and CKD are both significant global public health burden, and there is evidence that NAFLD is independently associated with a high risk of CKD despite the exclusion of other metabolic diseases, while the underlying mechanisms are not clear (26). In our study, by obtaining DEGs and important module genes by WGCNA, 45 NAFLD-related share genes were obtained, and their enrichment analysis revealed that immune, inflammatory and programmed cell death pathways were significantly enriched. Further, 4 CKD diagnostic markers genes were obtained by cytoscape software and machine learning, which demonstrated good diagnostic value in both the training and validation sets of CKD. Interestingly, 4 CKD biomarkers also had good diagnostic performance for NAFLD in dataset GSE89632, indicating that they may be important targets for the development of CKD in NAFLD patient.

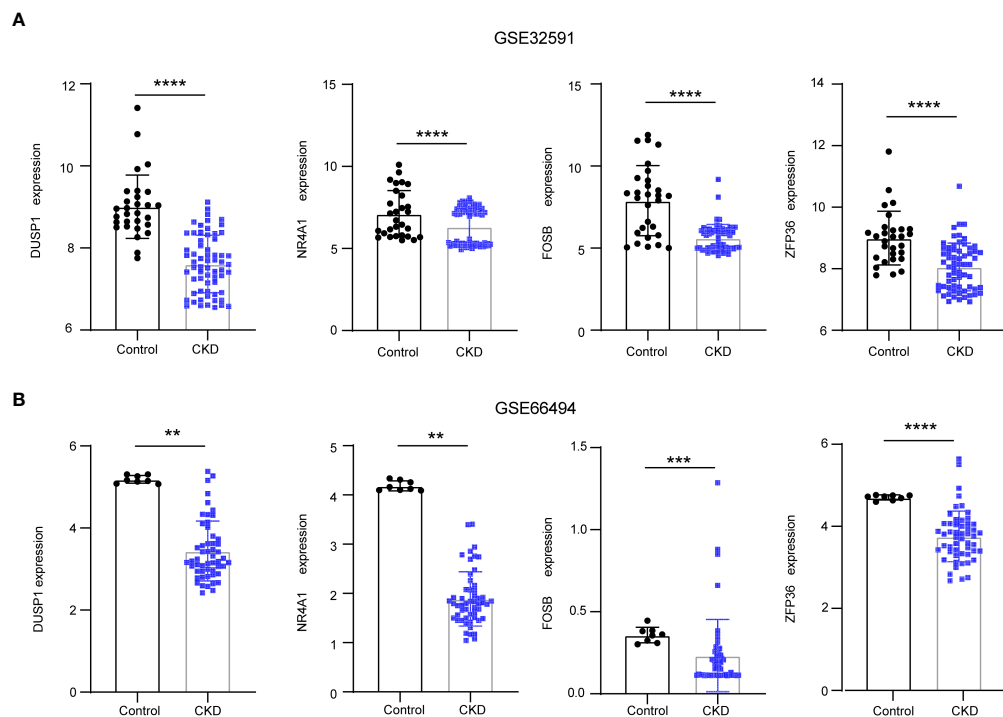


FIGURE 6

The downregulation of 4 NAFLD-related hub genes was verified by two CKD data set. **(A)** Expression of NAFLD-related hub genes in the GSE32591 date set. **(B)** Expression of NAFLD-related hub genes in the GSE66494 date set. NAFLD, Non-alcoholic fatty liver disease; CKD, chronic kidney diseases.

DUSP1, dual-specificity protein phosphatase 1, is a member of the dual-specific phosphatase (DUSPs) family. Mitogen-activated protein kinases (MAPKs) was closely related to inflammation and immune, and DUSP1 improves microvascular fibrosis and inflammation through dephosphorylation of MAPKs (27, 28). Overexpression of DUSP1 alleviates renal tubular injury by regulating mitophagy and interrupte Mff-related excessive mitochondrial fission. At the same time, lncRNA NR_038323 reduced the degree of renal fibrosis by targeting DUSP1, suggesting that DUSP1 is a potential therapeutic target for CKD with NAFLD (29–31). However, the main evidence come from

diabetic renal disease, and whether it is applicable to other types of CKD requires further study.

FOSB is a member of the FOS family, which is part of activator protein-1 (AP-1). AP-1 is associated with immune and cancer progression. Previous studies have shown that FOSB can be used as a diagnostic marker for IgA kidney disease (32). It has also been shown that MicroRNA-27a-3p targets FOSB to regulate the level of inflammation and fibrosis in IgA nephropathy (33). Zinc finger protein 36 (ZFP36) participates in posttranscriptional regulation by targeting different mRNAs, which was closely related to inflammatory diseases and autoimmune disease (34). The

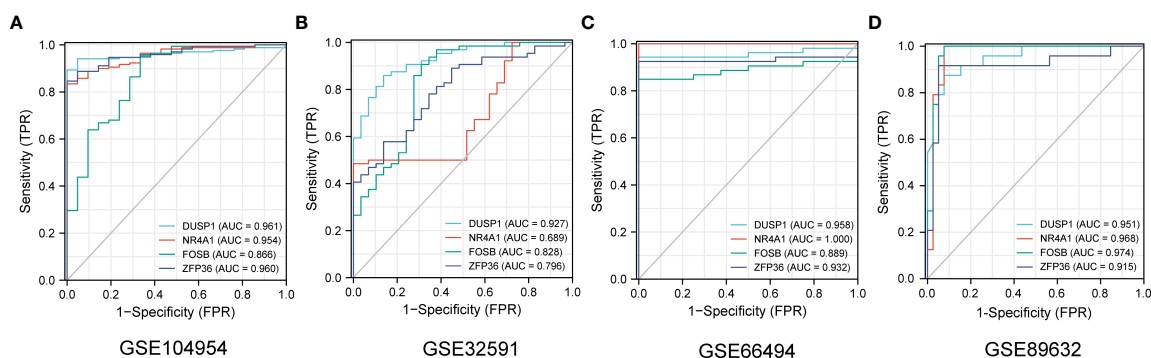


FIGURE 7

The diagnostic efficacy of 4 NAFLD-related hub genes was verified by ROC curve in CKD and NAFLD data sets. **(A–D)** The ROC curve of 4 NAFLD-related hub genes in date set GSE104954, GSE32591, GSE66494 and GSE89632.

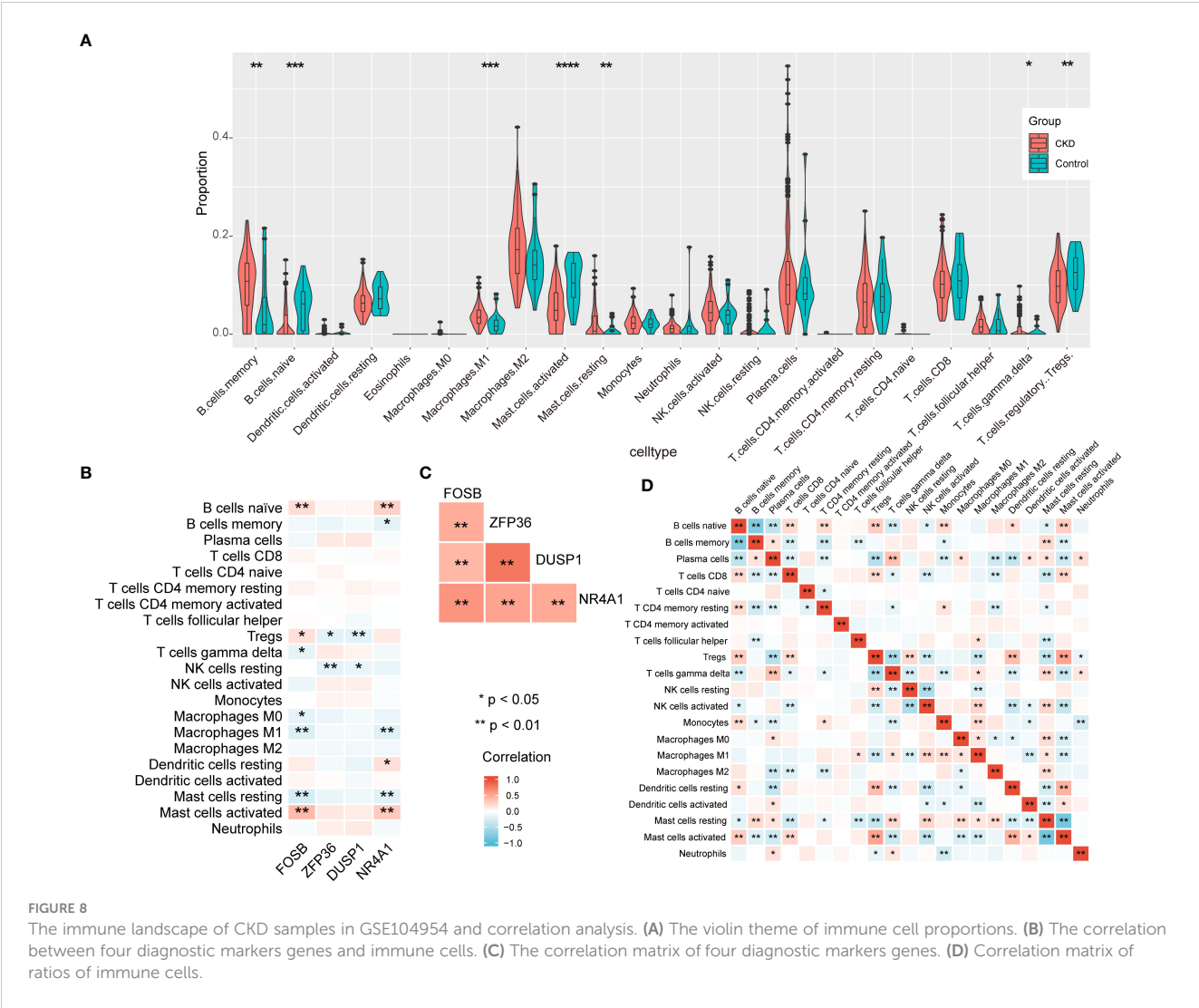


FIGURE 8
The immune landscape of CKD samples in GSE104954 and correlation analysis. **(A)** The violin theme of immune cell proportions. **(B)** The correlation between four diagnostic markers genes and immune cells. **(C)** The correlation matrix of four diagnostic markers genes. **(D)** Correlation matrix of ratios of immune cells.

dysregulated expression of ZFP36 may play an important role in the pathogenesis of inflammatory diseases including CKD. While it has been suggested that it could be used as a diagnostic marker of CKD (35, 36). Further studies are needed to identify the underlying mechanism for FOSB and ZFP36 in CKD with NAFLD.

The orphan nuclear receptor 4A1 (NR4A1), which is also known as Nur77, belongs to the nuclear receptor superfamily, and is involved in inflammation and energy metabolism pathways (37). Previous studies have shown that it can be used as a therapeutic target for chronic kidney disease, which is consistent with our study (38). There are also studies show that Yiqi Huoxue Tongluo recipe, a traditional Chinese medicine, can alleviate renal inflammation and fibrosis by increasing the expression level of NR4A1. In contrast, the loss of NA4A1 results in increased kidney injury associated with macrophage. Interestingly, in our results, NR4A1 expression was significantly negatively correlated with proinflammatory M1 macrophage infiltration. A recent study showed that the induction of anti-inflammatory macrophages expressing NR4A1/EAR2 could suppress M1 proinflammatory

responses, thereby inhibiting immune-mediated crescent glomerulonephritis (39–41). Therefore, increasing the expression level of NR4A1 may be one of the potential strategies for the treatment of CKD with NAFLD.

Dysfunction of immune cells promotes inflammation and kidney fibrosis in CKD, so the immune infiltration status of CKD samples was explored (42). Previous studies have demonstrated that macrophage polarization plays an important role in CKD development (43). In our results, M1 macrophages were significantly upregulated. However, M2 macrophages are believed to be associated with fibrosis, but not M1 macrophages. While the role of M2 macrophages in CKD is contradictory (44, 45).

Tregs cells are down-regulated in CKD, which is consistent with our results (46). There is some evidence to suggest that Tregs cells can inhibit inflammation and fibrosis in CKD (47). In turn, the CKD microenvironment changes the energetic metabolism of Tregs cells, thus inhibiting the protective effect of Tregs (48). Therefore, immune cells interact with the inflammatory microenvironment. B cells are thought to be involved in the progression of

Membranous nephropathy (MN) by releasing antibodies against podocytes, so depletion therapy targeting B cells may be a potential treatment (49). However, existing data suggest that depletion of B cells does not achieve the expected effect in IgA nephropathy (50). Because of the significant heterogeneity of CKD, the potential significance of B-cell depleting therapy requires specific analysis (51). The MC-specific protease tryptase is released by mast cells, thereby activating significant fibrosis and inflammation (52). In our results, the expression of four CKD diagnostic markers was closely related to the infiltration of multiple immune cells, which also confirmed the important role of immune mechanisms in the development of inflammatory and fibrosis in CKD patients with NAFLD.

There are limitations to our study. First, CKD is an umbrella term with significant heterogeneity, and we were not able to analyze specific types of CKD; Second, we focus on the pathogenesis and diagnostic markers of CKD in the context of NAFLD, and it is important to note that CKD has the opposite effect on NAFLD, which is beyond the scope of our discussion; Third, our findings were required to validate *in vivo* and *in vitro* to better guide clinical practice, although the decreased expression of DUSP1 and ZFP36 in CKD has been confirmed by related studies (36, 53).

5 Conclusion

In this study, 4 NAFLD-related genes (DUSP1, NR4A1, FOSB, ZFP36) were identified as diagnostic markers in CKD patients, and NAFLD may accelerate the development of CKD through immune and inflammatory pathways. The changes in immune cell infiltration in CKD and the significant correlation with diagnostic markers were also elucidated. Our study may provide diagnostic markers and therapeutic targets for CKD patients with NAFLD.

Data availability statement

The datasets presented in this study can be found in online repositories. The names of the repository/repositories and accession number(s) can be found in the article/**Supplementary Material**.

Author contributions

YC, YD, and WJ contributed equally to this work. YC and YD wrote the manuscript. WJ performed the data processing. JD, JY and HZ Participated in chart making. XZ edited the article. KT and ZY conceived and designed the scientific question. All authors contributed to the article and approved the submitted version.

References

1. Stevens PE, Levin A. Evaluation and management of chronic kidney disease: Synopsis of the kidney disease: Improving global outcomes 2012 clinical practice guideline. *Ann Intern Med* (2013) 158(11):825–30. doi: 10.7326/0003-4819-158-11-201306040-00007
2. Liyanage T, Toyama T, Hockham C, Ninomiya T, Perkovic V, Woodward M, et al. Prevalence of chronic kidney disease in Asia: A systematic review and analysis. *BMJ Glob Health* (2022) 7(1):e007525. doi: 10.1136/bmjgh-2021-007525

Funding

This study was funded by the National Natural Science Foundation of China (Grant numbers: 81870446, 82070671, 82170667, 81970566, 81900571, 82070681).

Acknowledgments

We sincerely thank the researchers who uploaded their data to the GEO database.

Conflict of interest

The authors declare that the research was conducted in the absence of any commercial or financial relationships that could be construed as a potential conflict of interest.

Publisher's note

All claims expressed in this article are solely those of the authors and do not necessarily represent those of their affiliated organizations, or those of the publisher, the editors and the reviewers. Any product that may be evaluated in this article, or claim that may be made by its manufacturer, is not guaranteed or endorsed by the publisher.

Supplementary material

The Supplementary Material for this article can be found online at: <https://www.frontiersin.org/articles/10.3389/fendo.2023.1125829/full#supplementary-material>

SUPPLEMENTARY MATERIALS S1

A list of 45 NAFLD-related shared genes.

SUPPLEMENTARY MATERIALS S2

Results of GO and KEGG enrichment analysis of 45 NAFLD-related share genes.

SUPPLEMENTARY MATERIALS S3

4 NAFLD-related hub genes were downregulated in GSE104954 dataset.

SUPPLEMENTARY FIGURE 1

Diagnostic value of 4 NAFLD-related hub genes in GSE104948 tested by ROC curves.

SUPPLEMENTARY FIGURE 2

Diagnostic value of 4 NAFLD-related hub genes in different sample sites of GSE32591 examined by ROC curves.

3. Lin MY, Fiorentino M, Wu IW. Editorial: Public health for chronic kidney disease prevention and care. *Front Public Health* (2022) 10:1021075. doi: 10.3389/fpubh.2022.1021075
4. Jonsson AJ, Lund SH, Eriksen BO, Pålsson R, Indridason OS. Incidence of and risk factors of chronic kidney disease: Results of a nationwide study in Iceland. *Clin Kidney J* (2022) 15(7):1290–9. doi: 10.1093/ckj/sfac051
5. Tao Z, Li Y, Cheng B, Zhou T, Gao Y. Influence of nonalcoholic fatty liver disease on the occurrence and severity of chronic kidney disease. *J Clin Transl Hepatol* (2022) 10(1):164–73. doi: 10.14218/JCTH.2021.00171
6. Mantovani A, Petracca G, Beatrice G, Csermely A, Lonardo A, Schattenberg JM, et al. Non-alcoholic fatty liver disease and risk of incident chronic kidney disease: An updated meta-analysis. *Gut* (2022) 71(1):156–62. doi: 10.1136/gutjnl-2020-323082
7. Yi M, Peng W, Feng X, Teng F, Tang Y, Kong Q, et al. Extrahepatic morbidities and mortality of NAFLD: An umbrella review of meta-analyses. *Aliment Pharmacol Ther* (2022) 56(7):1119–30. doi: 10.1111/apt.17165
8. Byrne CD, Targher G. NAFLD as a driver of chronic kidney disease. *J Hepatol* (2020) 72(4):785–801. doi: 10.1016/j.jhep.2020.01.013
9. Powell EE, Wong VW, Rinella M. Non-alcoholic fatty liver disease. *Lancet* (2021) 397(10290):2212–24. doi: 10.1016/S0140-6736(20)32511-3
10. Wang XJ, Malhi H. Nonalcoholic fatty liver disease. *Ann Intern Med* (2018) 169(9):ITC65–80. doi: 10.7326/AITC201811060
11. Musso G, Gambino R, Tabibian JH, Ekstedt M, Kechagias S, Hamaguchi M, et al. Association of non-alcoholic fatty liver disease with chronic kidney disease: A systematic review and meta-analysis. *PLoS Med* (2014) 11(7):e1001680. doi: 10.1371/journal.pmed.1001680
12. Targher G, Bertolini L, Rodella S, Lippi G, Zoppini G, Chonchol M. Relationship between kidney function and liver histology in subjects with nonalcoholic steatohepatitis. *Clin J Am Soc Nephrol* (2010) 5(12):2166–71. doi: 10.2215/CJN.05050610
13. Targher G, Chonchol M, Bertolini L, Rodella S, Zenari L, Lippi G, et al. Increased risk of CKD among type 2 diabetics with nonalcoholic fatty liver disease. *J Am Soc Nephrol* (2008) 19(8):1564–70. doi: 10.1681/ASN.2007101155
14. Park H, Dawwas GK, Liu X, Nguyen MH. Nonalcoholic fatty liver disease increases risk of incident advanced chronic kidney disease: A propensity-matched cohort study. *J Intern Med* (2019) 286(6):711–22. doi: 10.1111/joim.12964
15. Sinn DH, Kang D, Jang HR, Gu S, Cho SJ, Paik SW, et al. Development of chronic kidney disease in patients with non-alcoholic fatty liver disease: A cohort study. *J Hepatol* (2017) 67(6):1274–80. doi: 10.1016/j.jhep.2017.08.024
16. Nassir F. NAFLD: Mechanisms, treatments, and biomarkers. *Biomolecules* (2022) 12(6):824. doi: 10.3390/biom12060824
17. Czaja-Stolc S, Potrykus M, Stankiewicz M, Kaska Ł, Małgorzewicz S. Pro-inflammatory profile of adipokines in obesity contributes to pathogenesis, nutritional disorders, and cardiovascular risk in chronic kidney disease. *Nutrients* (2022) 14(7):1457. doi: 10.3390/nu14071457
18. Grayson PC, Eddy S, Taroni JN, Lightfoot YL, Mariani L, Parikh H, et al. Metabolic pathways and immunometabolism in rare kidney diseases. *Ann Rheum Dis* (2018) 77(8):1226–33. doi: 10.1136/annrheumdis-2017-212935
19. Berthier CC, Bethunaickan R, Gonzalez-Rivera T, Nair V, Ramanujam M, Zhang W, et al. Cross-species transcriptional network analysis defines shared inflammatory responses in murine and human lupus nephritis. *J Immunol* (2012) 189(2):988–1001. doi: 10.4049/jimmunol.1103031
20. Nakagawa S, Nishihara K, Miyata H, Shinke H, Tomita E, Kajiwaru M, et al. Molecular markers of tubulointerstitial fibrosis and tubular cell damage in patients with chronic kidney disease. *PLoS One* (2015) 10(8):e0136994. doi: 10.1371/journal.pone.0136994
21. Arendt BM, Comelli EM, Ma DW, Lou W, Teterina A, Kim T, et al. Altered hepatic gene expression in nonalcoholic fatty liver disease is associated with lower hepatic n-3 and n-6 polyunsaturated fatty acids. *Hepatology* (2015) 61(5):1565–78. doi: 10.1002/hep.27695
22. Bu D, Luo H, Huo P, Wang Z, Zhang S, He Z, et al. KOBAS-i: Intelligent prioritization and exploratory visualization of biological functions for gene enrichment analysis. *Nucleic Acids Res* (2021) 49(W1):W317–25. doi: 10.1093/nar/gkab447
23. Chai C, Cox B, Yaish D, Gross D, Rosenberg N, Amblard F, et al. Agonist of RORA attenuates nonalcoholic fatty liver progression in mice via up-regulation of MicroRNA 122. *Gastroenterology* (2020) 159(3):999–1014.e9. doi: 10.1053/j.gastro.2020.05.056
24. Chen L, Chen L, Li X, Qin L, Zhu Y, Zhang Q, et al. Transcriptomic profiling of hepatic tissues for drug metabolism genes in nonalcoholic fatty liver disease: A study of human and animals. *Front Endocrinol (Lausanne)* (2022) 13:1034494. doi: 10.3389/fendo.2022.1034494
25. Zeng T, Chen G, Qiao X, Chen H, Sun L, Ma Q, et al. NUSAP1 could be a potential target for preventing NAFLD progression to liver cancer. *Front Pharmacol* (2022) 13:823140. doi: 10.3389/fphar.2022.823140
26. Lonardo A, Mantovani A, Targher G, Baffy G. Nonalcoholic fatty liver disease and chronic kidney disease: Epidemiology, pathogenesis, and clinical and research implications. *Int J Mol Sci* (2022) 23(21):13320. doi: 10.3390/ijms232113320
27. Chen HF, Chuang HC, Tan TH. Regulation of dual-specificity phosphatase (DUSP) ubiquitination and protein stability. *Int J Mol Sci* (2019) 20(11):2668. doi: 10.3390/ijms20112668
28. Kyriakis JM, Avruch J. Mammalian MAPK signal transduction pathways activated by stress and inflammation: A 10-year update. *Physiol Rev* (2012) 92(2):689–737. doi: 10.1152/physrev.00028.2011
29. Lu C, Wu B, Liao Z, Xue M, Zou Z, Feng J, et al. DUSP1 overexpression attenuates renal tubular mitochondrial dysfunction by restoring parkin-mediated mitophagy in diabetic nephropathy. *Biochem Biophys Res Commun* (2021) 559:141–7. doi: 10.1016/j.bbrc.2021.04.032
30. Sheng J, Li H, Dai Q, Lu C, Xu M, Zhang J, et al. DUSP1 recuses diabetic nephropathy via repressing JNK-mff-mitochondrial fission pathways. *J Cell Physiol* (2019) 234(3):3043–57. doi: 10.1002/jcp.27124
31. Ge Y, Wu D, Zhou Y, Qiu S, Chen J, et al. lncRNA NR_038323 suppresses renal fibrosis in diabetic nephropathy by targeting the miR-324-3p/DUSP1 axis. *Mol Ther Nucleic Acids* (2019) 17:741–53. doi: 10.1016/j.omtn.2019.07.007
32. Al MMH, Maniruzzaman M, Shin J. Identification of key candidate genes for IgA nephropathy using machine learning and statistics-based bioinformatics models. *Sci Rep* (2022) 12(1):13963. doi: 10.1038/s41598-022-18273-x
33. Liao Y, Wang Z, Wang L, Lin Y, Ye Z, Zeng X, et al. MicroRNA-27a-3p directly targets FosB to regulate cell proliferation, apoptosis, and inflammation responses in immunoglobulin A nephropathy. *Biochem Biophys Res Commun* (2020) 529(4):1124–30. doi: 10.1016/j.bbrc.2020.06.115
34. Makita S, Takatori H, Nakajima H. Post-transcriptional regulation of immune responses and inflammatory diseases by RNA-binding ZFP36 family proteins. *Front Immunol* (2021) 12:711633. doi: 10.3389/fimmu.2021.711633
35. Ma J, Li C, Liu T, Zhang L, Wen X, Liu X, et al. Identification of markers for diagnosis and treatment of diabetic kidney disease based on the ferroptosis and immune. *Oxid Med Cell Longev* (2022) 2022:9957172. doi: 10.1155/2022/9957172
36. Zhou Y, Yu Z, Liu L, Wei L, Zhao L, Huang L, et al. Construction and evaluation of an integrated predictive model for chronic kidney disease based on the random forest and artificial neural network approaches. *Biochem Biophys Res Commun* (2022) 603:21–8. doi: 10.1016/j.bbrc.2022.02.099
37. Safe S, Jin UH, Morpurgo B, Abudayyeh A, Singh M, Tjalkens RB, et al. Nuclear receptor 4A (NR4A) family - orphans no more. *J Steroid Biochem Mol Biol* (2016) 157:48–60. doi: 10.1016/j.jsbmb.2015.04.016
38. Ma G, Chen F, Liu Y, Zheng L, Jiang X, Tian H, et al. Nur77 ameliorates age-related renal tubulointerstitial fibrosis by suppressing the TGF-β/Smads signaling pathway. *FASEB J* (2022) 36(2):e22124. doi: 10.1096/fj.202101332R
39. He Z, Zhang M, Xu H, Zhou W, Xu C, Wang Z, et al. Yiqi huoxue tongluo recipe regulates NR4A1 to improve renal mitochondrial function in unilateral ureteral obstruction (UUO) rats. *Pharm Biol* (2022) 60(1):2308–18. doi: 10.1080/13880209.2022.2148168
40. Westbrook L, Johnson AC, Regner KR, Williams JM, Mattson DL, Kyle PB, et al. Genetic susceptibility and loss of Nr4a1 enhances macrophage-mediated renal injury in CKD. *J Am Soc Nephrol* (2014) 25(11):2499–510. doi: 10.1681/ASN.2013070786
41. Chen J, Huang XR, Yang F, Yiu WH, Yu X, Tang S, et al. Single-cell RNA sequencing identified novel Nr4a1(+) Ear2(+) anti-inflammatory macrophage phenotype under myeloid-TLR4 dependent regulation in anti-glomerular basement membrane (GBM) crescentic glomerulonephritis (cGN). *Adv Sci (Weinh)* (2022) 9(18):e2200668. doi: 10.1002/advs.202200668
42. Tang PC, Chan AS, Zhang CB, García CC, Zhang YY, To KF, et al. TGF-β1 signaling: Immune dynamics of chronic kidney diseases. *Front Med (Lausanne)* (2021) 8:628519. doi: 10.3389/fmed.2021.628519
43. Lee H, Fessler MB, Qu P, Heymann J, Kopp JB. Macrophage polarization in innate immune responses contributing to pathogenesis of chronic kidney disease. *BMC Nephrol* (2020) 21(1):270. doi: 10.1186/s12882-020-01921-7
44. Han Y, Ma FY, Tesch GH, Manthey CL, Nikolic-Paterson DJ. Role of macrophages in the fibrotic phase of rat crescentic glomerulonephritis. *Am J Physiol Renal Physiol* (2013) 304(8):F1043–53. doi: 10.1152/ajprenal.00389.2012
45. Anders HJ, Ryu M. Renal microenvironments and macrophage phenotypes determine progression or resolution of renal inflammation and fibrosis. *Kidney Int* (2011) 80(9):915–25. doi: 10.1038/ki.2011.217
46. Zhu X, Li S, Zhang Q, Zhu D, Xu Y, Zhang P, et al. Correlation of increased Th17/Treg cell ratio with endoplasmic reticulum stress in chronic kidney disease. *Med (Baltimore)* (2018) 97(20):e10748. doi: 10.1097/MD.00000000000010748
47. Bendickova K, Fric J. Roles of IL-2 in bridging adaptive and innate immunity, and as a tool for cellular immunotherapy. *J Leukoc Biol* (2020) 108(1):427–37. doi: 10.1002/JLB.5MIR0420-055R
48. Han Z, Ma K, Tao H, Liu H, Zhang J, Sai X, et al. A deep insight into regulatory T cell metabolism in renal disease: Facts and perspectives. *Front Immunol* (2022) 13:826732. doi: 10.3389/fimmu.2022.826732
49. So B, Yap D, Chan TM. B cells in primary membranous nephropathy: Escape from immune tolerance and implications for patient management. *Int J Mol Sci* (2021) 22(24):13560. doi: 10.3390/ijms222413560
50. Lafayette RA, Canetta PA, Rovin BH, Appel GB, Novak J, Nath KA, et al. A randomized, controlled trial of rituximab in IgA nephropathy with proteinuria and renal dysfunction. *J Am Soc Nephrol* (2017) 28(4):1306–13. doi: 10.1681/ASN.2016060640

51. Hartinger JM, Kratky V, Hruskova Z, Slanar O, Tesar V. Implications of rituximab pharmacokinetic and pharmacodynamic alterations in various immune-mediated glomerulopathies and potential anti-CD20 therapy alternatives. *Front Immunol* (2022) 13:1024068. doi: 10.3389/fimmu.2022.1024068
52. Owens EP, Vesey DA, Kassianos AJ, Healy H, Hoy WE, Gobe GC. Biomarkers and the role of mast cells as facilitators of inflammation an fibrosis in chronic kidney disease. *Transl Androl Urol* (2019) 8(Suppl 2):S175–83. doi: 10.21037/tau.2018.11.03
53. Fu S, Cheng Y, Wang X, Huang J, Su S, Wu H, et al. Identification of diagnostic gene biomarkers and immune infiltration in patients with diabetic kidney disease using machine learning strategies and bioinformatic analysis. *Front Med (Lausanne)* (2022) 9:918657. doi: 10.3389/fmed.2022.918657



OPEN ACCESS

EDITED BY

Guiting Lin,
University of California, San Francisco,
United States

REVIEWED BY

Zhengbing Zhuge,
Karolinska Institutet (KI), Sweden
Yuanqing Feng,
University of Pennsylvania, United States
Kai Wang,
First Affiliated Hospital of Wenzhou Medical
University, China

*CORRESPONDENCE

Ling-Bo Qian
✉ bioqian@163.com
Xin-Ru Zhou
✉ yorise9098@163.com

SPECIALTY SECTION

This article was submitted to
Cellular Endocrinology,
a section of the journal
Frontiers in Endocrinology

RECEIVED 07 January 2023

ACCEPTED 07 March 2023

PUBLISHED 20 March 2023

CITATION

Han Y-P, Liu L-J, Yan J-L, Chen M-Y,
Meng X-F, Zhou X-R and Qian L-B (2023)
Autophagy and its therapeutic potential in
diabetic nephropathy.
Front. Endocrinol. 14:1139444.
doi: 10.3389/fendo.2023.1139444

COPYRIGHT

© 2023 Han, Liu, Yan, Chen, Meng, Zhou
and Qian. This is an open-access article
distributed under the terms of the [Creative
Commons Attribution License \(CC BY\)](#). The
use, distribution or reproduction in other
forums is permitted, provided the original
author(s) and the copyright owner(s) are
credited and that the original publication in
this journal is cited, in accordance with
accepted academic practice. No use,
distribution or reproduction is permitted
which does not comply with these terms.

Autophagy and its therapeutic potential in diabetic nephropathy

Yu-Peng Han, Li-Juan Liu, Jia-Lin Yan, Meng-Yuan Chen,
Xiang-Fei Meng, Xin-Ru Zhou* and Ling-Bo Qian*

School of Basic Medical Sciences & Forensic Medicine, Hangzhou Medical College, Hangzhou, China

Diabetic nephropathy (DN), the leading cause of end-stage renal disease, is the most significant microvascular complication of diabetes and poses a severe public health concern due to a lack of effective clinical treatments. Autophagy is a lysosomal process that degrades damaged proteins and organelles to preserve cellular homeostasis. Emerging studies have shown that disorder in autophagy results in the accumulation of damaged proteins and organelles in diabetic renal cells and promotes the development of DN. Autophagy is regulated by nutrient-sensing pathways including AMPK, mTOR, and Sirt1, and several intracellular stress signaling pathways such as oxidative stress and endoplasmic reticulum stress. An abnormal nutritional status and excess cellular stresses caused by diabetes-related metabolic disorders disturb the autophagic flux, leading to cellular dysfunction and DN. Here, we summarized the role of autophagy in DN focusing on signaling pathways to modulate autophagy and therapeutic interferences of autophagy in DN.

KEYWORDS

diabetic nephropathy, autophagy, nutrient-sensing pathway, cellular stress, renal cell

1 Introduction

Diabetic nephropathy (DN), a major cause contributing to end-stage renal disease (ESRD), is one of the microvascular complications of diabetes and is commonly rendered by persistent hyperglycemia and the subsequent chronic inflammatory response (1, 2). Almost 35%-40% of diabetic patients finally lead to DN (3), which poses a huge number of diabetic death and a serious threat to the quality of life in diabetes (4). International Diabetes Federation (IDF) Diabetes Atlas (the 10th edition) showed that the number of adult diabetes worldwide will increase from 537 million in 2021 to 643 million by 2030 and over 6.7 million diabetes aged 20-79 years died from diabetes-related diseases in 2021 (<http://diabetesatlas.org/atlas/tenth-edition/>). Long-term diabetes can damage many organs to cause disabling and life-threatening complications including cardiovascular diseases, neuropathy, and nephropathy. DN, with clinical manifestations including progressive proteinuria as well as decreased glomerular filtration rate (3), and pathological features such as glomerular hypertrophy, glomerular basement membrane (GBM) thickening, mesangial proliferation, and podocyte loss (5), is one of the early complications in diabetes. Though keeping blood pressure, blood glucose, and the renin-

angiotensin system (RAS) under control is a primary therapy to relieve proteinuria in diabetes, treatment-resistant proteinuria and ESRD have not been fully avoided (6). Exploring the underlying mechanism of DN and finding novel targets to effectively prevent DN have become urgent for improving the quality of life in diabetes.

The pathogenesis of DN is multifactorial (4), including oxidative stress, inflammatory cascade reaction, and other disorders of metabolic pathways under persistent hyperglycemia (7). Growing evidence reveals that along with diabetes, the accumulation of damaged organelles and proteins owing to impaired autophagy has been reported to disrupt cellular homeostasis and result in the development of DN (3, 7–10). Autophagy normally is activated to degrade impaired organelles or misfolded proteins as a recycling response to nutrition deprivation or starvation (10). The metabolic disorder manifested as persistent high blood glucose and lipids causes a state of overnutrition and suppresses autophagy in diabetic renal cells (11–13), while promoting autophagy lessens renal injury in diabetes (14, 15). All these clues suggest that activating autophagy may be a novel therapeutic target to prevent DN and shed light on treating DN based on the balance of autophagy.

Although the relationship between autophagy and DN has not been fully clarified, numerous studies have confirmed that the development of DN is linked to autophagy. Detailed exploration of autophagy in the pathogenesis of DN can provide new ideas for preventing DN. Thus, this review aims to understand the cellular and molecular bases of autophagy, the role of autophagy in the development of DN, and therapeutic strategies targeting autophagy for the prevention of DN by summarizing current evidence.

2 Profile of autophagy in DN

Autophagy is a highly conserved cellular mechanism by which cytoplasmic constituents including proteins and organelles are transported to lysosomes for degradation and preserving cellular homeostasis (9, 16). Basal cellular autophagy is necessary for keeping physiological functions, whereas autophagy in response to stress serves as an adaptive reaction to ensure cell survival (16). Autophagy is a multistep process that involves the formation of isolation membrane, extension, formation of autophagosome, and final fusion with lysosomes to degrade phagocytic materials and is regulated by multiple protein kinase complexes and autophagy-related proteins, such as autophagy-related gene 5 (Atg5), Atg7, Atg12 and so on (8, 17). Among them, activation of the unc-51-like kinase 1 (ULK1) complex is responsible for the initiation of autophagy (3, 10). The class III phosphatidylinositol 3-kinase (PI3K) complex generates phosphatidylinositol 3-phosphate at the neogenetic autophagosomal membrane to facilitate phagophore nucleation (18). Two ubiquitin-like coupling systems, Atg5-Atg12-Atg16L and Atg8/microtubule-associated protein 1A/1B-light chain 3 (LC3) are involved in autophagosome extension and autolysosome formation (19). Atg4 cleaves LC3 to form cytosolic LC3I, which is then ubiquitinated by Atg7 and Atg3 and binds to phosphatidyl ethanolamine to form autophagosome membrane-bound LC3II (17). Thus, LC3II is evidenced as a marker for

autophagosome formation in cells. This conjugated response of LC3II is positively regulated by Atg5-Atg12-Atg16L. Sequestosome 1, known as p62, interacts with LC3II to confine autophagosomes and is repeatedly digested by the autophagy-lysosome system. Significantly, malfunctioned autophagy during diabetes causes intracellular accumulation of p62 leading to further inhibition of autophagic flux, thus forming a vicious cycle to promote diabetic complications including diabetic cardiomyopathy, diabetic peripheral neuropathy and DN (20–22).

Autophagy can be triggered by various intracellular stresses, such as reactive oxygen species (ROS), endoplasmic reticulum (ER) stress, and hypoxia (23–25), all of which are involved in the development of DN. Increasing evidence indicates that the abnormal alteration of autophagy appears to be directly linked to the emergence of DN (26, 27). Autophagy is closely associated with nutrient-sensing signal pathways and stress metabolism and is essential to maintain homeostasis in the kidney (3). Although the mechanism of autophagy in DN remains to be elucidated, it has been known that the impaired autophagy is evidenced by the increased collection of p62 and the decreased expression of autophagy-related proteins in diabetic kidney tissues and cells (28–30). The shortage of autophagy results in the accumulation of misfolded or aging proteins and dysfunctional organelles to deteriorate kidney disease in diabetes (19). Activation of autophagy alleviates kidney lesions in diabetes (31, 32) while inhibition of autophagy worsens these diabetic injuries (33, 34), indicating that autophagy might be a promising therapeutic target for DN.

3 Autophagy in renal cells during diabetes

Though different types of renal cells are all damaged by the dysfunctional autophagy in the progression of DN, as shown in Figure 1, these four resident renal cells including podocytes, renal tubular epithelial cells (RTECs), glomerular mesangial cells (GMCs), and glomerular endothelial cells (GEnCs) may be particularly vulnerable to attack from the disorder of autophagy and contribute to DN. Thus, we summarized recent findings of renal cells in diabetic environments to better understand autophagy in DN (Table 1).

3.1 Podocytes

Podocytes, highly differentiated epithelial cells with a limited capacity for proliferation, tightly attach to the GBM (62) and work as an important part of the glomerular filtration barrier (GFB) (63, 64). The damage and apoptosis of podocytes can destroy the integrity of the GFB (31), leading to proteinuria, renal lesions, and finally DN (7, 8, 65).

A high level of autophagy in podocytes is necessary to keep the physiological function (8, 39), which is regulated by the adenosine 5'-monophosphate-activated protein kinase (AMPK) pathway

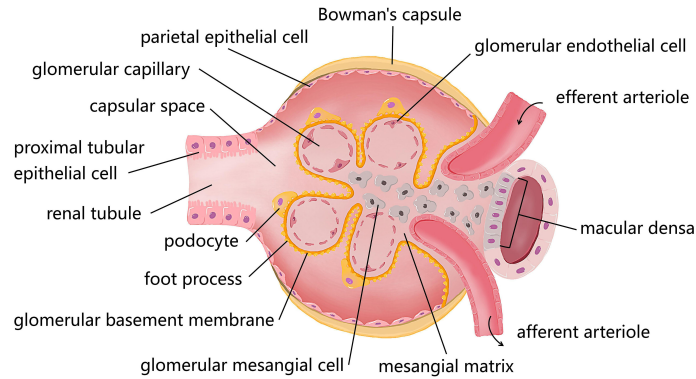


FIGURE 1
The diagram of resident cells in the glomerulus and proximal tubule. There are four kinds of major resident cells in the glomerulus, glomerular endothelial cells (GEnCs), podocytes, glomerular mesangial cells (GMCs), and parietal epithelial cells. Tubular epithelial cells form the extension of Bowman's capsule, that is, the renal tubule. Podocytes with their interdigitating foot processes are arranged on the lateral side of the glomerular basement membrane (GBM). GMCs located between glomerular capillary loops, adjacent to endothelial cells or basement membranes are irregularly shaped. GEnCs are flat cells attached to the GBM. GEnCs and podocytes form the glomerular filtration barrier.

TABLE 1 Autophagy in four types of renal cells during diabetes.

Cell types	Major findings
Podocytes	<ul style="list-style-type: none">• Silence of miR-150-5p attenuates DN by targeting Sirt1/p53/AMPK-dependent autophagy (12) and suppression of miR-383-5p alleviates high glucose-induced apoptosis via the activation of autophagy (35), while miR-25-3p attenuates high glucose-induced injury through suppressing dual specificity protein phosphatase 1 and subsequently activating autophagy in podocytes (36).• Promotion of autophagy by inhibiting Akt/mTOR pathway protects the DN serum-treated or high glucose-treated podocytes against apoptosis (34, 37, 38).• Activation of epidermal growth factor receptor in podocytes contributes to progression of DN partly caused by up-regulating rubicon and inhibiting the subsequent autophagy (39).• Regulating Bcl-2-mediated crosstalk between autophagy and apoptosis attenuates podocytes injury in diabetes (40).• Activation of AMPK and Sirt1-mediated autophagy ameliorates lipid accumulation, oxidative stress, apoptosis, and inflammation in podocytes exposed to high glucose (41–43).• Promotion of autophagy by regulating Sirt1/glycogen synthase kinase 3β and Sirt1/NF-κB pathways reduces podocytes injury in diabetes (22, 44, 45).• Promotion of autophagy by inhibiting AMPK/mTOR pathway prevents diabetic podocytes injury (46–48).• Inhibition of autophagy by activating liver X receptor aggravates podocytes injury in diabetes (49).• Progranulin facilitates mitophagy and mitochondrial homeostasis via Sirt1-PGC-1α/FoxO1 signaling to prevent podocytes injury in DN (50).
Renal tubular epithelial cells	<ul style="list-style-type: none">• High glucose-induced lipophagy deficiency in tubular cells causes ectopic lipid accumulation-associated kidney damage, which is relieved by promoting autophagy (29).• Smad family member 3 directly binds to the 3' untranslated region of transcription factor EB and suppresses lysosome biogenesis to inhibit autophagy in tubular epithelial cells in DN (30).• Inhibition of autophagy by miR-22 targeting phosphatase and tensin homolog and miR-155-5p targeting Sirt1 induces renal tubular fibrosis in DN (32).• Promotion of autophagy by up-regulating AMPK pathway improves mitochondrial health (11, 51) and reduces fibrosis (52, 53) in renal tubular epithelial cells to reduce DN.• Autophagy causes the degradation of AGEs by up-regulation of lysosomal biogenesis and function in tubular epithelial cells to reduce DN (54).• Promotion of autophagy by inhibiting mTOR pathway counteracts high glucose-induced injury in tubular epithelial cells (55).
Glomerular mesangial cells	<ul style="list-style-type: none">• Promotion of autophagy by activating AMPK/Sirt1 pathway (28, 56) or by Sirt1/NF-κB pathway (33) relieves high glucose-induced injury in glomerular mesangial cells.• Activation of Akt/mTOR pathway inhibits autophagy and accelerates inflammation and fibrosis in high glucose-treated glomerular mesangial cells (57, 58).
Glomerular endothelial cells	<ul style="list-style-type: none">• Inhibition of AGE/RAGE axis restores the disturbed autophagy to alleviate glomerular endothelial permeability in DN (59).• Autophagy deficiency accompanying oxidative stress and apoptosis in high glucose-cultured glomerular endothelial cells is associated with CaMKKβ-LKB1-AMPK pathway (60).• Promotion of autophagy by inhibiting miR-34a/Atg4b pathway in glomerular endothelial cells relieves diabetic kidney damage (61).

DN, diabetic nephropathy; Sirt1, silent information regulator of transcription 1; AMPK, adenosine 5'-monophosphate-activated protein kinase; Akt, protein kinase B; mTOR, mammalian target of rapamycin; Bcl-2, B-cell lymphoma-2; NF-κB, nuclear factor kappa-B; PGC-1α, peroxisome proliferator-activated receptor-gamma coactivator-1α; FoxO1, forkhead box O1; AGEs, advanced glycation end-products; CAMKKβ, calcium/calmodulin-dependent protein kinase kinase β; LKB1, liver kinase B1; Atg, autophagy-related gene.

rather than the mammalian target of rapamycin (mTOR) (66). The impairment of autophagy in diabetic podocytes as evidenced by the decreased expression of autophagy-related proteins (beclin1, LC3II/I, Atg12, Atg7, etc.) and the accumulation of the autophagic substrate p62 (40, 67) exacerbates the loss of podocytes with the help of the increased cellular lipid accumulation, oxidative stress, and inflammation (11, 41). Knockout of the Atg5 in podocytes has been reported to cause glomerular lesions accompanied by podocyte loss and albuminuria (68). These findings imply that the shortage of autophagy mediates podocyte damage in diabetes (22). It is interesting to note that the increased autophagosomes in high glucose-treated podocytes was not consistent with the impaired autophagy in the diabetic rat kidney characterized by glomerular hypertrophy, renal tubular expansion, and mesangial cell proliferation (44). To further clarify whether the rise in autophagosomes is caused by autophagy induction or the obstructed fusion of autophagosomes and lysosomes, the fusion inhibitor such as chloroquine can be adopted or the colocalization of LC3 and lysosomes need to be explored. In addition, this contradiction in different diabetic kidney models might be related to the different roles of autophagy in each stage of diabetes (3).

Nutrient signaling pathways are involved in the disorder of autophagy in diabetic podocytes. Increased mTOR activity and decreased expression of AMPK and silent information regulator of transcription 1 (Sirt1) in diabetes can inhibit autophagy to aggravate cellular dysfunction and the progression of DN (69, 70). The silence of AMPK or Sirt1 was reported to inhibit autophagy and promote the loss of podocyte function in a high glucose environment (12, 42, 43). Furthermore, the up-regulation AMPK/mTOR signaling pathway-mediated autophagy prevents the loss of podocyte markers (nephrin, podocin) and ameliorates diabetic kidney injury (46–48). Liver X receptor and high mobility group box 1 also induce podocyte injury by altering autophagy through the nutrient-sensing signal pathway (34, 49).

3.2 Renal tubular epithelial cells

The enhancement of autophagy in proximal tubular epithelial cells (PTECs) in response to multiple stresses such as ischemia and nephrotoxic medications has been reported to protect the kidney (71). Morphological alterations including hypertrophy, hyperplasia and epithelial-mesenchymal transition (EMT) in RTECs, especially in PTECs, primarily owing to the shortage of autophagy in diabetes, are regarded as an early sign of DN, which can easily cause renal dysfunction and even ESRD if not corrected in time (51, 72, 73).

It is noteworthy that the interaction of autophagy with EMT in RTECs is complicated, various factors and signaling pathways are associated with the effect of autophagy-related EMT on the progression of DN (33, 74). The role of rapamycin in reducing profibrotic cytokines, fibroblast proliferation, tubulointerstitial inflammation, and EMT confirms that mTOR-regulated autophagy is necessary for EMT in diabetic RTECs (69, 75). Interestingly, hyperglycemia-induced miR-22 promotes EMT by suppressing autophagy *via* targeting phosphatase and tensin homolog/protein kinase B (Akt)/mTOR signaling pathway, which

suggests that targeting miRNA may be a promising therapeutic approach in preventing DN (32). Recently, mesenchymal stem cell-derived exosomes was reported to activate autophagy to inhibit transforming growth factor- β (TGF- β)-induced EMT progression in RTECs (76). Thus, the role of exosomes on the EMT in diabetic RTECs is worth further investigation.

In the presence of diabetes, carbonyl compounds created by advanced glycation end-products (AGEs) are filtered by the glomerulus and then reabsorbed by the proximal tubule, easily resulting in tubular toxicity (77, 78). Through interaction with the receptor for AGEs (RAGE), accumulation of AGEs triggers various abnormal cellular cascades like oxidative stress, inflammation, and apoptosis and inhibits the protective effect of autophagy in the diabetic kidney (79). The impairment of the autophagy-lysosomal pathway in diabetes promotes the accumulation of AGEs and the excessive AGEs aggravates lysosomal dysfunction, thus forming positive feedback to allow tubulointerstitial inflammation and fibrosis, which might be crucial to the development of DN (17, 80). Inhibiting AGEs/RAGE signaling is reported to restore the disturbed autophagy in glomerular endothelial cells and attenuate DN (59). It is said that AGEs can enhance the expression of profibrotic molecules linked to EMT and ER stress in the human renal tubular epithelial cell line to gradually render renal fibrosis (81), which is prevented by the enhancement of autophagy in RTECs (54). Therefore, the specific role of the AGEs/RAGE axis in DN is worthy of exploring.

3.3 Glomerular mesangial cells

Proliferation and hypertrophy in GMCs and mesangial expansion manifested as excess extracellular matrix (ECM) derived from GMCs are two pathological characteristics of DN, which lead to glomerulosclerosis and tubulointerstitial fibrosis (82, 83). Hyperglycemia, AGEs, and ROS all effectively activate TGF- β to cause ECM accumulation both in Smad-dependent and -independent pathways (84–86), which can be reversed by the up-regulation of autophagy (33, 57).

Sirt1 has been revealed to inhibit ECM accumulation in high glucose-treated GMCs *via* enhancing autophagy (33) and blocking mTOR-suppressed autophagy has also been documented to effectively reduce inflammation, proliferation, and fibrosis in diabetic GMCs (15, 28, 57). All of the above indicate that autophagy is important for maintaining the structural and functional integrity of GMCs to resist DN.

3.4 Glomerular endothelial cells

GECs, the first barrier of glomerular filtration, are vulnerable to hyperglycemia. The abnormal structure manifested as endothelial glycocalyx and endothelial-mesenchymal transition usually occur in the early stage of DN (87). Severe damage to the glomerular endothelium owing to autophagy reduction has been reported in endothelial-specific autophagy-deficient mice and Atg16L-knockdown GECs (88, 89). In addition, activation of

calcium/calmodulin-dependent protein kinase kinase β (CAMKK β)/liver kinase B1 (LKB1)/AMPK signaling (60) and inhibition of miR-34a/Atg4b signaling (61) promote autophagy in GEnCs to attenuate DN. It is well established that the interplay of podocytes, GEnCs, and GMCs is key to keep the integrity of the GFB and the pathological alteration in one component evidently affects the other two (87, 90, 91). These results imply that appropriate autophagy in GEnCs can minimize DN by preserving glomerular structural integrity.

4 Autophagic pathways in DN

Autophagy in eukaryotic cells is tightly regulated to adapt or counteract cellular stresses through multiple signaling pathways (17) because both insufficient and excessive autophagy are harmful (92). Nutrient-sensing pathways including AMPK, mTOR, and Sirt1 are well-recognized to regulate autophagy in diabetic complications (10). Moreover, various cellular stresses such as ROS, ER stress, and hypoxia are involved in pathogenic

autophagy in DN (Figure 2) (93). Thus, autophagy in the development of DN is precisely regulated.

4.1 Nutrient-sensing pathways

4.1.1 mTOR pathway

Rapamycin-sensitive type of mTOR (mTORC1), a master inhibitor of autophagy, is inhibited by starvation to reduce the phosphorylation of ULK1 at Ser757, which frees ULK1 to be activated by AMPK and then initiates autophagy to provide nutrients for the cell's use by degrading the captured cytoplasmic components (94, 95). mTOR is over-mobilized in the diabetic kidney to promote the inflammatory response and exacerbate renal impairment (96, 97), which is reversed by rapamycin (98). In addition, the mTOR signaling pathway can be activated by vascular endothelial growth factor *via* PI3K/Akt cascade, which suppresses autophagy *via* phosphorylating its downstream phosphoprotein 70 ribosomal protein S6 kinase (p70S6K) and exacerbates DN (99, 100). All of these suggest that the

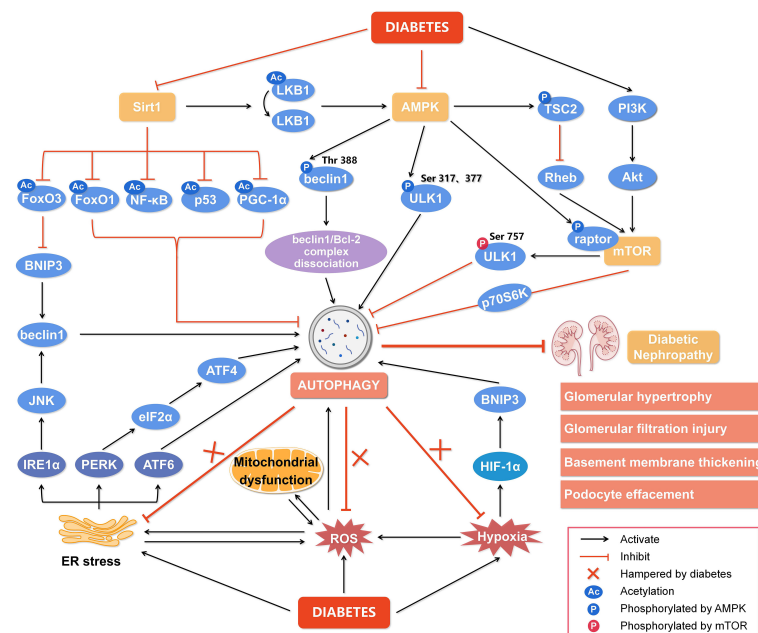


FIGURE 2

Regulation of autophagy during diabetic nephropathy. Hyperglycemia is considered a state of overnutrition, leading to over-activation of the mammalian target of rapamycin (mTOR) and inhibition of adenosine 5'-monophosphate-activated protein kinase (AMPK) and silent information regulator of transcription 1 (Sirt1). The activated mTOR inhibits autophagy by blocking unc-51-like kinase 1 (ULK1) activation by AMPK and its downstream target phosphoprotein 70 ribosomal protein S6 kinase (p70S6K). The inhibition of AMPK blocks the dissociation of the beclin1/Bcl-2 (B-cell lymphoma-2) complex and the phosphorylation of ULK1, while promotes mTOR activity to reduce autophagy. The inactivated Sirt1 reduces the deacetylation of several target genes like forkhead box O3 (FoxO3), FoxO1, nuclear factor kappa-B (NF- κ B), p53, and peroxisome proliferator-activated receptor- γ coactivator-1 α (PGC-1 α) to inhibit autophagy. In addition, other cellular events, including reactive oxygen species (ROS), endoplasmic reticulum (ER) stress, and hypoxia, can also regulate autophagy to affect the development of diabetic nephropathy. Hypoxia-inducible factor 1 α (HIF-1 α) induced by hypoxia promotes the transcription of Bcl-2/adenovirus E1V19-kDa interacting protein 3 (BNIP3) and induces autophagy. ER stress enhances the expression of ER membrane proteins like protein kinase RNA-like ER kinase (PERK), inositol-requiring enzyme 1 α (IRE1 α), and activating transcription factor 6 (ATF6), leading to autophagy. In addition, autophagy under ER stress may be associated with the signaling pathway of PERK/ α -subunit of eukaryotic initiation factor 2 (eIF2 α)/ATF4 and IRE1 α /c-Jun N-terminal kinase (JNK)/Beclin1. Significantly, the endogenous autophagy induced by ER stress, oxidative stress and hypoxia in diabetes is hampered, which aggravates the progression of diabetic nephropathy. Thus, impaired autophagy accelerates the progression of diabetic nephropathy, resulting in a series of renal pathological damages. Rheb, ras homolog enriched in brain; PI3K, class III phosphatidylinositol-3-kinase; Akt, protein kinase B.

overactivation of the mTOR pathway is extremely detrimental to the development of DN (101, 102). Numerous studies have demonstrated the critical role that long noncoding RNAs (LncRNAs) play in the pathophysiology of DN (103). LncRNAs potentially affect the pathological alteration in the diabetic kidney by inhibiting the autophagy-related Akt/mTOR pathway, which has been supported by growing evidence that LncRNA silencing sperm-associated antigen 5 antisense RNA1 promotes hyperglycemia-induced injury in podocytes targeting Akt/mTOR signaling (37), and LncRNA nuclear enriched abundant transcript 1 accelerates (58), whereas LncRNA SOX2 overlapping transcript inhibits (15), proliferation and fibrosis in diabetic GMCs *via* modulating Akt/mTOR signaling-related autophagy. Thus, the effect of LncRNAs is diversified depending on the type of LncRNAs in the development of DN though the same target of Akt/mTOR signaling-related autophagy may be involved.

4.1.2 AMPK pathway

AMPK belongs to the serine/threonine protein kinase family and is composed of the catalytic subunit α and the regulatory subunits β and γ (104). The phosphorylation of the threonine 172 (Thr172) site on the subunit α is necessary for the activation of AMPK (105). AMPK is regulated by the AMP/ATP ratio as an energy sensor (3). Under harmful conditions like hunger and hypoxia, the ratio of AMP/ATP ratio rises and renders AMP binding to the subunit γ of AMPK, which promotes Thr172 phosphorylation by LKB1 (106). In addition, AMPK is even activated by CAMKK β and TGF- β -activated kinase by the action of hormones, drugs, or proinflammatory cytokines (106, 107) to trigger autophagy for keeping cellular energy homeostasis under starvation.

It has been shown that AMPK and autophagy are deactivated in the diabetic kidney accompanied by proteinuria and renal pathological alterations (11, 45, 56, 108). As shown in Figure 2, AMPK can phosphorylate ULK1 at Ser317 and Ser377 to directly initiate autophagy (109, 110) or indirectly promote autophagy by blocking mTORC1 to release ULK1 through phosphorylating tuberous sclerosis complex 2 (TSC2) and raptor, the critical mTORC1-binding subunit (111), which benefits to hinder the progression of DN (112). In addition, AMPK activates Sirt1 by increasing cellular NAD⁺ levels (56) or phosphorylating and redistributing glyceraldehyde 3-phosphate dehydrogenase into the nucleus to free Sirt1 (111), which promotes autophagy and alleviates DN (28, 56). AMPK can promote the dissociation of the beclin1/B-cell lymphoma-2 (Bcl-2) complex *via* phosphorylating beclin1 at Thr388 to initiate autophagy (113). Thus, AMPK-regulated autophagy is key to the development of DN and AMPK may be a promising target for preventing DN.

4.1.3 Sirt1 pathway

Sirt1, the most widely studied NAD-dependent deacetylase in the Sirtuin family (114, 115), is highly expressed in renal tubular cells and podocytes (115) and has been reported to attenuate diabetic kidney disease by reducing the phosphorylation and acetylation levels of NF- κ B and signal transducer and activator of

transcription 3 (33, 44, 116). In addition, Sirt1 reduces acetylation or phosphorylation of several target genes such as AMPK, forkhead box O1 (FoxO1), p53, and peroxisome proliferator-activated receptor- γ coactivator-1 α (PGC-1 α) to enhance autophagy (Figure 2) (28, 50, 117). As a positive regulator of autophagy, Sirt1 has been revealed to up-regulate Bcl-2/adenovirus E1V19-kDa interacting protein 3 (BNIP3) by deacetylating the transcription factor FoxO3 to enhance autophagy and inhibit DN (118, 119). LKB1 deacetylated by Sirt1 activates AMPK to enhance autophagy (120, 121). In addition, deacetylation of p53 by Sirt1 potentially activates AMPK-dependent autophagy to ameliorate DN (12) and this protective effect of Sirt1 against DN is inhibited by several miRNAs including miR-135a-5p (122), miR-138 (65), miR-150-5p (12), miR-155-5p (123), and miR-217 (124) targeting the 3' untranslated region of Sirt1. The relationship between miRNAs and Sirt1 is complicated in the progression of DN and more efforts are needed to clarify the underlying mechanism by which Sirt1-regulated autophagy prevents DN.

4.2 Cellular stress signaling

4.2.1 Oxidative stress

Excessive production of ROS and/or reactive nitrogen species beyond the endogenous scavenging capacity leads to oxidative stress. Oxidative damage of cellular lipids, proteins, nucleic acids, and carbohydrates breaks the structural integrity and results in physiological dysfunction (125). Oxidative stress induced by hyperglycemia through *de novo* ROS generation and suppression of the antioxidant defense system promotes mitochondria swelling, cristae breakage, and mitochondrial disintegration in the diabetic kidney, which can be reversed by the enhancing autophagy to eliminate damaged mitochondria (126).

It should be noted that autophagy and oxidative stress are interactive. ROS are reported as an early inducer for autophagy initiation and execution, which may be a crucial adaptive response to reduce oxidative stress and obtain the nutrient for reuse through autophagy-dependent degrading oxidative damaged cellular components (127). On the contrary, oxidative modification of key upstream autophagy regulators and autophagy core proteins including AMPK, Sirt1, Atg4, and Parkin impair autophagy (128). Thus, oxidative stress affects autophagy in the development of DN as a two-edged sword and antioxidant therapy may protect the kidney against diabetes through activating autophagy. This notion has been supported by some evidence that antioxidant compounds derived from plants such as betulinic acid, ursolic acid, genistein, and luteolin effectively attenuate the kidney injury induced by diabetes or poisons by promoting autophagy (38, 129–132).

4.2.2 Endoplasmic reticulum stress

The accumulation of unfolded or misfolded proteins in the ER lumen leads to ER stress which is evident in DN (24, 133). Overproduction of ROS due to chronic hyperglycemia disrupts intracellular Ca²⁺ homeostasis and oxidation of ER-resident proteins to trigger ER stress, in turn, hyperactivates the oxidative

folding machinery to correct improper disulfide bonds, further producing ROS (134, 135). This vicious cycle leads to the disruption of cellular homeostasis (Figure 2). Emerging evidence suggests that autophagy is linked to the unfolded protein response (UPR) to relieve ER stress by clearing misfolded proteins (24, 136, 137). Under ER stress, the UPR is triggered by three protein sensors, protein kinase RNA-like ER kinase (PERK), inositol-requiring enzyme 1 α (IRE1 α), and activating transcription factor 6 (ATF6) after accumulation of misfolded proteins (24). As shown in Figure 2, all these three sensors of the UPR under ER stress can induce autophagy *via* activating signaling pathways of PERK/ α -subunit of eukaryotic initiation factor 2/activating transcription factor 4 (PERK/eIF2 α /ATF4) (138), IRE1 α /c-Jun N-terminal kinase (JNK)/beclin1 and ATF6 (24, 139). The negative regulator of autophagy mTOR in diabetic PTECs is activated accompanying the increase of ER stress (140) and activating autophagy by Jujuboside A potentially attenuates ER stress and cell death in the diabetic kidney (141). The autophagy in the kidney is usually inhibited under diabetic status (142, 143), which is reversed by the ER stress inhibitors salubrinal and tauroursodeoxycholic acid (143). Since ER stress inhibitors such as tauroursodeoxycholic acid, ursodeoxycholic acid, and 4-phenylbutyrate potentially rescue diabetic renal tubules and podocytes (144, 145), investigating in detail the interaction between ER stress and autophagy in the progression of DN is promising.

4.2.3 Hypoxia stress

Kidney hypoxia, preceding the onset of albuminuria (146) and correlating with reduced glomerular filtration rate, runs through the whole stage of DN owing to the limited capacity of enhancing renal plasma flow and oxygen delivery (147). Hypoxia-inducible factor (HIF) is key to adaptively maintain cellular homeostasis by transcriptionally activating the expression of several target genes in response to hypoxia (148, 149).

Accumulating evidence shows that hypoxia is an important pathogenic factor for DN. Deficiency of HIF-1 α has been reported to aggravate renal dysfunction (150), while up-regulation of HIF-1 α effectively enhances autophagy to mitigate DN, which may associate with the increased expression of Sirt1, FoxO3, and BNIP3 (119, 151, 152). Recent studies demonstrate that up-regulation of sestrin2 by HIF-1 α is involved in hypoxia-related diseases (153), which may modulate AMPK and mTORC1-dependent autophagy to reduce the production of ROS and attenuate DN (154, 155). Thus, the deteriorating effect of hypoxia on the diabetic kidney is not ignored and HIF-1 α -related autophagy may be a potential target for treating DN.

5 Therapeutic strategies targeting autophagy for DN

The symptomatic treatment for DN usually includes glycemic control, reducing albuminuria, and blocking RAS with the usage of angiotensin-converting enzyme inhibitors (ACEI) and angiotensin

receptor antagonists (ARB) (156, 157). New hypoglycemic agents such as sodium-glucose cotransporter 2 (SGLT2) inhibitors, glucagon-like peptide 1 receptor (GLP-1R) agonists, and dipeptidyl peptidase-4 (DPP-4) inhibitors have been shown to protect the diabetic kidney *via* modulating autophagy (Table 2).

Inhibiting SGLT2, located on the lumen surface of PTECs, potentially lowers blood glucose by reducing the reabsorption of glucose (163). SGLT2 inhibitors empagliflozin and dapagliflozin have been shown to enhance autophagy depending on AMPK/mTOR pathway to attenuate diabetic kidney injury (51, 55, 158). Additionally, the progression of renal complications in pre-diabetes is slowed by dapagliflozin through the suppression of renal inflammation, ER stress, and apoptosis (159). Although the commercially available SGLT2 inhibitors including empagliflozin, dapagliflozin, and canagliflozin have been used in clinics (147), the protective effect against DN has not been fully elucidated (164).

Liraglutide, a GLP-1R analogue to lower blood glucose, has been shown to significantly improve the prognosis for DN (165), which may be related to reducing apoptosis and oxidative stress through promoting AMPK-regulated autophagy (161, 166). DPP-4 inhibitor linagliptin not only hinders the degradation of endogenous GLP-1 to lower blood glucose, but also alleviates mesangial expansion, podocyte foot process effacement, and albuminuria excretion in the diabetic kidney by reactivating autophagy (160). Additionally, the hypoglycemic agent metformin was reported to mitigate tubulointerstitial fibrosis and oxidative stress in diabetes by enhancing autophagy through AMPK/Sirt1/FoxO1 pathway (28, 52). Rapamycin has been shown to improve the short-term pathological alterations in DN by enhancing autophagy by blocking the mTORC1/ULK1 pathway (9). However, the serious side effect of rapamycin limits its use in long-term clinical treatment (75). Animal studies showed that melatonin, resveratrol, and vitamin D analogs prevent DN by modulating AMPK-regulated autophagy (11, 35, 53, 162), which may be the candidate drug for treating DN in the clinic.

Recently, exosome is becoming a promising therapeutic target for DN treatment (167). Exosome, as a kind of extracellular vesicles, is involved in intercellular communication by carrying various biomolecules and may be a novel biomarker for evaluating the progression of DN (168, 169). MiRNAs contained in the exosome derived from different cells attenuate high glucose-induced renal cell injury by promoting autophagy (36, 170, 171). Additionally, mesenchymal stem cell-derived exosomes induce autophagy *via* inhibiting mTOR to attenuate diabetic renal fibrosis (172). It is evident that the more we understand DN, the more we can do about DN. Exosome therapy combined with autophagy regulation may be promising for treating DN.

6 Conclusion

The significant increase in the incidence of diabetes has become a serious worldwide health issue. The high mortality of diabetes is strongly correlated with DN and the subsequent ESRD. Due to the

TABLE 2 Agents targeting autophagy for diabetic nephropathy.

Agent		Experimental models	Effect for pathology of renal injuries	Reference
SGLT2 inhibitors	Dapagliflozin	Human PTECs (HK-2 cell) exposed to high glucose	Ameliorating autophagic flux and reducing inflammation by inhibiting NF- κ B pathway through AMPK activation.	(55)
		HFD-induced prediabetic rats	Reducing oxidative stress, ER stress, inflammation, and apoptosis and up-regulating autophagy.	(158, 159)
	Empagliflozin	STZ-induced diabetic mice; Human PTECs (HKC-8) exposed to high glucose	Enhancing autophagy and mitochondrial function to reverse renal morphological changes.	(51)
		db/db mice	Reactivating autophagy and improving glomerular morphology.	(160)
GLP-1R agonists	Liraglutide	Zucker diabetic fatty rats; Human PTECs (HKC-8) exposed to AGEs	Activating autophagy and reducing oxidative stress <i>via</i> AMPK/mTOR pathway.	(161)
DPP-4 inhibitors	Linagliptin	db/db mice	Reactivating glomerular autophagy and improving glomerular morphology.	(160)
Metformin		HFD/STZ-induced diabetic rats; Renal mesangial cells exposed to high glucose	Enhancing autophagy <i>via</i> AMPK/Sirt1-FoxO1 pathway and alleviating oxidative stress.	(28)
		HFD/STZ-induced diabetic rats; RTECs exposed to high glucose	Attenuating renal fibrosis <i>via</i> activating AMPK-induced autophagy and suppressing EMT.	(52)
Rapamycin		STZ-induced diabetic rats	Enhancing autophagy by inhibiting mTOR and improving renal function.	(14)
		db/db mice	Reducing fat deposition, pathological changes and renal dysfunctions <i>via</i> inhibiting mTOR.	(98)
Other candidate drugs	Melatonin	STZ-induced diabetic rats; RTECs (NRK52E) exposed to high glucose	Enhancing autophagy and mitochondrial biogenesis <i>via</i> activating the AMPK/Sirt1 axis.	(11)
	Resveratrol	db/db mice; Human podocytes exposed to high glucose	Activating autophagy and attenuating apoptosis through the suppression of miR-383-5p.	(35)
		STZ-induced diabetic rats	Normalizing lipid metabolism by inducing AMPK/mTOR-mediated autophagy.	(162)
	Vitamin D analogs	STZ-induced diabetic mice; Human PTECs (HK-2 cell) exposed to high glucose	Restoring defective autophagy through CAMKK β -AMPK pathway.	(53)

SGLT2, sodium-glucose cotransporter 2; PTECs, proximal tubular epithelial cells; NF- κ B, nuclear factor kappa-B; AMPK, adenosine 5'-monophosphate-activated protein kinase; HFD, high-fat diet; ER, endoplasmic reticulum; STZ, streptozotocin; GLP-1R, glucagon-like peptide 1 receptor; AGEs, advanced glycation end-products; mTOR, mammalian target of rapamycin; DPP-4, dipeptidyl peptidase-4; FoxO1, forkhead box O1; EMT, epithelial-mesenchymal transition; CAMKK β , calcium/calmodulin-dependent protein kinase kinase β .

complexity and diversity of the pathogenesis of DN, both rigorous control of blood glucose and cholesterol and blocking RAS with the usage of ACEI and ARB do not improve the endpoint of DN. The role of autophagy in the progression of DN sheds light on treating DN and how to keep the balance of autophagy in the diabetic kidney may be a new direction for prevention and management of DN though more efforts should be paid to exploring the precise regulation of autophagy in DN.

Author contributions

Y-PH wrote the manuscript. Y-PH, L-JL, J-LY, M-YC, X-FM, X-RZ, and L-BQ designed the figures and edited the manuscript. X-RZ and L-BQ supervised the writing. All authors contributed to the article and approved the submitted version.

Funding

This work was supported by National Natural Science Foundation of China (81772035), Scientific Research Project of Education Department of Zhejiang Province (Y202045357), Basic Research Fee for Basic Research Business of Hangzhou Medical College (KYQN202005) and Program of Cultivating Zhejiang Provincial High-level Personnel in Health (Innovative Talent in 2021).

Conflict of interest

The authors declare that the research was conducted in the absence of any commercial or financial relationships that could be construed as a potential conflict of interest.

Publisher's note

All claims expressed in this article are solely those of the authors and do not necessarily represent those of their affiliated

organizations, or those of the publisher, the editors and the reviewers. Any product that may be evaluated in this article, or claim that may be made by its manufacturer, is not guaranteed or endorsed by the publisher.

References

- Reidy K, Kang HM, Hostetter T, Susztak K. Molecular mechanisms of diabetic kidney disease. *J Clin Invest* (2014) 124:2333–40. doi: 10.1172/JCI72271
- Lassén E, Daehn IS. Molecular mechanisms in early diabetic kidney disease: glomerular endothelial cell dysfunction. *Int J Mol Sci* (2020) 21:E9456. doi: 10.3390/ijms21249456
- Yang D, Livingston MJ, Liu Z, Dong G, Zhang M, Chen J-K, et al. Autophagy in diabetic kidney disease: regulation, pathological role and therapeutic potential. *Cell Mol Life Sci* (2018) 75:669–88. doi: 10.1007/s00018-017-2639-1
- Cao Z, Cooper ME. Pathogenesis of diabetic nephropathy. *J Diabetes Investig* (2011) 2:243–7. doi: 10.1111/j.2040-1124.2011.00131.x
- Fu H, Liu S, Bastacky SI, Wang X, Tian X-J, Zhou D. Diabetic kidney diseases revisited: A new perspective for a new era. *Mol Metab* (2019) 30:250–63. doi: 10.1016/j.molmet.2019.10.005
- Yamahara K, Yasuda M, Kume S, Koya D, Maegawa H, Uzu T. The role of autophagy in the pathogenesis of diabetic nephropathy. *J Diabetes Res* (2013) 2013:193757. doi: 10.1155/2013/193757
- Wang W, Sun W, Cheng Y, Xu Z, Cai L. Role of sirtuin-1 in diabetic nephropathy. *J Mol Med Berl Ger* (2019) 97:291–309. doi: 10.1007/s00109-019-01743-7
- Lin T-A, Wu VC-C, Wang C-Y. Autophagy in chronic kidney diseases. *Cells* (2019) 8:E61. doi: 10.3390/cells8010061
- Gonzalez CD, Carro Negueruela MP, Nicora Santamarina C, Resnik R, Vaccaro MI. Autophagy dysregulation in diabetic kidney disease: From pathophysiology to pharmacological interventions. *Cells* (2021) 10:2497. doi: 10.3390/cells10092497
- Parmar UM, Jalgaonkar MP, Kulkarni YA, Oza MJ. Autophagy-nutrient sensing pathways in diabetic complications. *Pharmacol Res* (2022) 184:106408. doi: 10.1016/j.phrs.2022.106408
- Siddhi J, Sherkhane B, Kalavala AK, Arruri V, Velayutham R, Kumar A. Melatonin prevents diabetes-induced nephropathy by modulating the AMPK/Sirt1 axis: Focus on autophagy and mitochondrial dysfunction. *Cell Biol Int* (2022) 46:2142–57. doi: 10.1002/cbin.11899
- Dong W, Zhang H, Zhao C, Luo Y, Chen Y. Silencing of miR-150-5p ameliorates diabetic nephropathy by targeting Sirt1/p53/AMPK pathway. *Front Physiol* (2021) 12:624989. doi: 10.3389/fphys.2021.624989
- Ayinde KS, Olaoba OT, Ibrahim B, Lei D, Lu Q, Yin X, et al. AMPK allosteric: A therapeutic target for the management/treatment of diabetic nephropathy. *Life Sci* (2020) 261:118455. doi: 10.1016/j.lfs.2020.118455
- Liu L, Yang L, Chang B, Zhang J, Guo Y, Yang X. The protective effects of rapamycin on cell autophagy in the renal tissues of rats with diabetic nephropathy via mTOR-S6K1-LC3II signaling pathway. *Ren Fail* (2018) 40:492–7. doi: 10.1080/0886022X.2018.1489287
- Chen K, Yu B, Liao J. LncRNA SOX2OT alleviates mesangial cell proliferation and fibrosis in diabetic nephropathy via Akt/mTOR-mediated autophagy. *Mol Med Camb Mass* (2021) 27:71. doi: 10.1186/s10020-021-00310-6
- Shamekhi Amiri F. Intracellular organelles in health and kidney disease. *Nephrol Ther* (2019) 15:9–21. doi: 10.1016/j.nephro.2018.04.002
- Tang C, Livingston MJ, Liu Z, Dong Z. Autophagy in kidney homeostasis and disease. *Nat Rev Nephrol* (2023) 16:489–508. doi: 10.1038/s41581-020-0309-2
- Bhattacharya D, Mukhopadhyay M, Bhattacharyya M, Karmakar P. Is autophagy associated with diabetes mellitus and its complications? a review. *EXCLI J* (2018) 17:709–20. doi: 10.17179/excli2018-1353
- Koch EAT, Nakhoul R, Nakhoul F, Nakhoul N. Autophagy in diabetic nephropathy: a review. *Int Urol Nephrol* (2020) 52:1705–12. doi: 10.1007/s11255-020-02545-4
- Xiao C, Chen M-Y, Han Y-P, Liu L-J, Yan J-L, Qian L-B. The protection of luteolin against diabetic cardiomyopathy in rats is related to reversing JNK-suppressed autophagy. *Food Funct* (2023). doi: 10.1039/d2fo03871d
- Abdelkader NF, Elbaset MA, Moustafa PE, Ibrahim SM. Empagliflozin mitigates type 2 diabetes-associated peripheral neuropathy: a glucose-independent effect through AMPK signaling. *Arch Pharm Res* (2022) 45:475–93. doi: 10.1007/s12272-022-01391-5
- Su P-P, Liu D-W, Zhou S-J, Chen H, Wu X-M, Liu Z-S. Down-regulation of risa improves podocyte injury by enhancing autophagy in diabetic nephropathy. *Mil Med Res* (2022) 9:23. doi: 10.1186/s40779-022-00385-0
- Koya D, Hayashi K, Kitada M, Kashiwagi A, Kikkawa R, Haneda M. Effects of antioxidants in diabetes-induced oxidative stress in the glomeruli of diabetic rats. *J Am Soc Nephrol* (2003) 14:S250–3. doi: 10.1097/01.asn.0000077412.07578.44
- Cybulsky AV. Endoplasmic reticulum stress, the unfolded protein response and autophagy in kidney diseases. *Nat Rev Nephrol* (2017) 13:681–96. doi: 10.1038/nrneph.2017.129
- Liu H, Li Y, Xiong J. The role of hypoxia-inducible factor-1 alpha in renal disease. *Mol Basel Switz* (2022) 27:7318. doi: 10.3390/molecules27217318
- Takabatake Y, Kimura T, Takahashi A, Isaka Y. Autophagy and the kidney: health and disease. *Nephrol Dial Transplant* (2014) 29:1639–47. doi: 10.1093/ndt/gft535
- Gonzalez CD, Lee M-S, Marchetti P, Pietropaolo M, Towns R, Vaccaro MI, et al. The emerging role of autophagy in the pathophysiology of diabetes mellitus. *Autophagy* (2011) 7:2–11. doi: 10.4161/auto.7.1.13044
- Ren H, Shao Y, Wu C, Ma X, Lv C, Wang Q. Metformin alleviates oxidative stress and enhances autophagy in diabetic kidney disease via AMPK/Sirt1-FoxO1 pathway. *Mol Cell Endocrinol* (2020) 500:110628. doi: 10.1016/j.mce.2019.110628
- Han Y, Xiong S, Zhao H, Yang S, Yang M, Zhu X, et al. Lipophagy deficiency exacerbates ectopic lipid accumulation and tubular cells injury in diabetic nephropathy. *Cell Death Dis* (2021) 12:1031. doi: 10.1038/s41419-021-04326-y
- Yang C, Chen X-C, Li Z-H, Wu H-L, Jing K-P, Huang X-R, et al. SMAD3 promotes autophagy dysregulation by triggering lysosome depletion in tubular epithelial cells in diabetic nephropathy. *Autophagy* (2021) 17:2325–44. doi: 10.1080/15548627.2020.1824694
- Ding Y, Choi ME. Autophagy in diabetic nephropathy. *J Endocrinol* (2015) 224: R15–30. doi: 10.1530/JOE-14-0437
- Zhang Y, Zhao S, Wu D, Liu X, Shi M, Wang Y, et al. MicroRNA-22 promotes renal tubulointerstitial fibrosis by targeting PTEN and suppressing autophagy in diabetic nephropathy. *J Diabetes Res* (2018) 2018:4728645. doi: 10.1155/2018/4728645
- Wang X, Gao Y, Tian N, Zhu Z, Wang T, Xu J, et al. Astragaloside IV represses high glucose-induced mesangial cells activation by enhancing autophagy via Sirt1 deacetylation of NF- κ B p65 subunit. *Drug Des Devel Ther* (2018) 12:2971–80. doi: 10.2147/DDDT.S174058
- Jin J, Gong J, Zhao L, Zhang H, He Q, Jiang X. Inhibition of high mobility group box 1 (HMGB1) attenuates podocyte apoptosis and epithelial-mesenchymal transition by regulating autophagy flux. *J Diabetes* (2019) 11:826–36. doi: 10.1111/1753-0407.12914
- Huang S-S, Ding D-F, Chen S, Dong C-L, Ye X-L, Yuan Y-G, et al. Resveratrol protects podocytes against apoptosis via stimulation of autophagy in a mouse model of diabetic nephropathy. *Sci Rep* (2017) 7:45692. doi: 10.1038/srep45692
- Huang H, Liu H, Tang J, Xu W, Gan H, Fan Q, et al. M2 macrophage-derived exosomal miR-25-3p improves high glucose-induced podocytes injury through activation autophagy via inhibiting DUSP1 expression. *IUBMB Life* (2020) 72:2651–62. doi: 10.1002/iub.2393
- Xu J, Deng Y, Wang Y, Sun X, Chen S, Fu G. SPAG5-AS1 inhibited autophagy and aggravated apoptosis of podocytes via SPAG5/Akt/mTOR pathway. *Cell Prolif* (2020) 53:e12738. doi: 10.1111/cpr.12738
- Xu L, Fan Q, Wang X, Li L, Lu X, Yue Y, et al. Ursolic acid improves podocyte injury caused by high glucose. *Nephrol Dial Transplant* (2017) 32:1285–93. doi: 10.1093/ndt/gfv382
- Li Y, Pan Y, Cao S, Sasaki K, Wang Y, Niu A, et al. Podocyte EGFR inhibits autophagy through upregulation of Rubicon in type 2 diabetic nephropathy. *Diabetes* (2021) 70:562–76. doi: 10.2337/db20-0660
- Liu X-Q, Jiang L, Li Y-Y, Huang Y-B, Hu X-R, Zhu W, et al. Wogonin protects glomerular podocytes by targeting bcl-2-mediated autophagy and apoptosis in diabetic kidney disease. *Acta Pharmacol Sin* (2022) 43:96–110. doi: 10.1038/s41401-021-00721-5
- Zhang Y, Yao H, Li C, Sun W, Chen X, Cao Y, et al. Gandi capsule improved podocyte lipid metabolism of diabetic nephropathy mice through Sirt1/AMPK/HNF4A pathway. *Oxid Med Cell Longev* (2022) 2022:6275505. doi: 10.1155/2022/6275505
- Li F, Song L, Chen J, Chen Y, Li Y, Huang M, et al. Effect of genipin-1- β -D-gentiobioside on diabetic nephropathy in mice by activating AMP-activated protein kinase/silencing information regulator-related enzyme 1/ nuclear factor- κ B pathway. *J Pharm Pharmacol* (2021) 73:1201–11. doi: 10.1093/jpp/rgab041
- Wang S, Huang Y, Luo G, Yang X, Huang W. Cyanidin-3-O-glucoside attenuates high glucose-induced podocyte dysfunction by inhibiting apoptosis and promoting autophagy via activation of Sirt1/AMPK pathway. *Can J Physiol Pharmacol* (2021) 99:589–98. doi: 10.1139/cjpp-2020-0341

44. Liu Y, Liu W, Zhang Z, Hu Y, Zhang X, Sun Y, et al. Yishen capsule promotes podocyte autophagy through regulating Sirt1/NF- κ B signaling pathway to improve diabetic nephropathy. *Ren Fail* (2021) 43:128–40. doi: 10.1080/0886022X.2020.1869043
45. Chen J, Yang Y, Lv Z, Shu A, Du Q, Wang W, et al. Study on the inhibitive effect of catalpol on diabetic nephropathy. *Life Sci* (2020) 257:118120. doi: 10.1016/j.lfs.2020.118120
46. Zhang X, Zhang L, Chen Z, Li S, Che B, Wang N, et al. Exogenous spermine attenuates diabetic kidney injury in rats by inhibiting AMPK/mTOR signaling pathway. *Int J Mol Med* (2021) 47:27. doi: 10.3892/ijmm.2021.4860
47. Liu H, Wang Q, Shi G, Yang W, Zhang Y, Chen W, et al. Emodin ameliorates renal damage and podocyte injury in a rat model of diabetic nephropathy via regulating AMPK/mTOR-mediated autophagy signaling pathway. *Diabetes Metab Syndr Obes Targets Ther* (2021) 14:1253–66. doi: 10.2147/DMSO.S299375
48. Yang L, Liang B, Li J, Zhang X, Chen H, Sun J, et al. Dapagliflozin alleviates advanced glycation end product induced podocyte injury through AMPK/mTOR mediated autophagy pathway. *Cell Signal* (2022) 90:110206. doi: 10.1016/j.cellsig.2021.110206
49. Zhang Z, Tang S, Gui W, Lin X, Zheng F, Wu F, et al. Liver X receptor activation induces podocyte injury via inhibiting autophagic activity. *J Physiol Biochem* (2020) 76:317–28. doi: 10.1007/s13105-020-00737-1
50. Zhou D, Zhou M, Wang Z, Fu Y, Jia M, Wang X, et al. PGRN acts as a novel regulator of mitochondrial homeostasis by facilitating mitophagy and mitochondrial biogenesis to prevent podocyte injury in diabetic nephropathy. *Cell Death Dis* (2019) 10:524. doi: 10.1038/s41419-019-1754-3
51. Lee YH, Kim SH, Kang JM, Heo JH, Kim D-J, Park SH, et al. Empagliflozin attenuates diabetic tubulopathy by improving mitochondrial fragmentation and autophagy. *Am J Physiol Renal Physiol* (2019) 317:F767–80. doi: 10.1152/ajprenal.00565.2018
52. Wang F, Sun H, Zuo B, Shi K, Zhang X, Zhang C, et al. Metformin attenuates renal tubulointerstitial fibrosis via upgrading autophagy in the early stage of diabetic nephropathy. *Sci Rep* (2021) 11:16362. doi: 10.1038/s41598-021-95827-5
53. Li A, Yi B, Han H, Yang S, Hu Z, Zheng L, et al. Vitamin D-VDR (vitamin d receptor) regulates defective autophagy in renal tubular epithelial cell in streptozotocin-induced diabetic mice via the AMPK pathway. *Autophagy* (2022) 18:877–90. doi: 10.1080/15548627.2021.1962681
54. Takahashi A, Takabatake Y, Kimura T, Maejima I, Namba T, Yamamoto T, et al. Autophagy inhibits the accumulation of advanced glycation end products by promoting lysosomal biogenesis and function in the kidney proximal tubules. *Diabetes* (2017) 66:1359–72. doi: 10.2337/db16-0397
55. Xu J, Kitada M, Ogura Y, Liu H, Koya D. Dapagliflozin restores impaired autophagy and suppresses inflammation in high glucose-treated HK-2 cells. *Cells* (2021) 10:1457. doi: 10.3390/cells10061457
56. Shati AA. Salidroside ameliorates diabetic nephropathy in rats by activating renal AMPK/Sirt1 signaling pathway. *J Food Biochem* (2020) 44:e13158. doi: 10.1111/jfbc.13158
57. Gao C, Fan F, Chen J, Long Y, Tang S, Jiang C, et al. FBW7 regulates the autophagy signal in mesangial cells induced by high glucose. *BioMed Res Int* (2019) 2019:6061594. doi: 10.1155/2019/6061594
58. Huang S, Xu Y, Ge X, Xu B, Peng W, Jiang X, et al. Long noncoding RNA NEAT1 accelerates the proliferation and fibrosis in diabetic nephropathy through activating Akt/mTOR signaling pathway. *J Cell Physiol* (2019) 234:11200–7. doi: 10.1002/jcp.27770
59. Hou B, Qiang G, Zhao Y, Yang X, Chen X, Yan Y, et al. Salvianolic acid A protects against diabetic nephropathy through ameliorating glomerular endothelial dysfunction via inhibiting AGE-RAGE signaling. *Cell Physiol Biochem* (2017) 44:2378–94. doi: 10.1159/000486154
60. Lim Jih, Kim Hw, Kim My, Kim Tw, Kim En, Kim Y, et al. Cinacalcet-mediated activation of the CaMKK β -LKB1-AMPK pathway attenuates diabetic nephropathy in db/db mice by modulation of apoptosis and autophagy. *Cell Death Dis* (2018) 9:270. doi: 10.1038/s41419-018-0324-4
61. Jianbing H, Xiaotian L, Jie T, Xueying C, Hong J, Bo Z, et al. The effect of allograft inflammatory factor-1 on inflammation, oxidative stress, and autophagy via miR-34a/Atg4b pathway in diabetic kidney disease. *Oxid Med Cell Longev* (2022) 2022:1668000. doi: 10.1155/2022/1668000
62. Nagata M. Podocyte injury and its consequences. *Kidney Int* (2016) 89:1221–30. doi: 10.1016/j.kint.2016.01.012
63. Hartleben B, Gödel M, Meyer-Schwesinger C, Liu S, Ulrich T, Köbler S, et al. Autophagy influences glomerular disease susceptibility and maintains podocyte homeostasis in aging mice. *J Clin Invest* (2010) 120:1084–96. doi: 10.1172/JCI39492
64. Hong Q, Zhang L, Das B, Li Z, Liu B, Cai G, et al. Increased podocyte sirtuin-1 function attenuates diabetic kidney injury. *Kidney Int* (2018) 93:1330–43. doi: 10.1016/j.kint.2017.12.008
65. Liu F, Guo J, Qiao Y, Pan S, Duan J, Liu D, et al. MiR-138 plays an important role in diabetic nephropathy through Sirt1-p38-TTP regulatory axis. *J Cell Physiol* (2021) 236:6607–18. doi: 10.1002/jcp.30238
66. Bork T, Liang W, Yamahara K, Lee P, Tian Z, Liu S, et al. Podocytes maintain high basal levels of autophagy independent of mtor signaling. *Autophagy* (2020) 16:1932–48. doi: 10.1080/15548627.2019.1705007
67. Wang Z, Choi ME. Autophagy in kidney health and disease. *Antioxid Redox Signal* (2014) 20:519–37. doi: 10.1089/ars.2013.5363
68. Yin L, Yu L, He JC, Chen A. Controversies in podocyte loss: death or detachment? *Front Cell Dev Biol* (2021) 9:771931. doi: 10.3389/fcell.2021.771931
69. Kume S. Pathophysiological roles of nutrient-sensing mechanisms in diabetes and its complications. *Diabetol Int* (2019) 10:245–9. doi: 10.1007/s13340-019-00406-9
70. Kume S, Thomas MC, Koya D. Nutrient sensing, autophagy, and diabetic nephropathy. *Diabetes* (2012) 61:23–9. doi: 10.2337/db11-0555
71. Sugawara H, Moniwa N, Kuno A, Ohwada W, Osanami A, Shibata S, et al. Activation of the angiotensin II receptor promotes autophagy in renal proximal tubular cells and affords protection from ischemia/reperfusion injury. *J Pharmacol Sci* (2021) 145:187–97. doi: 10.1016/j.jphs.2020.12.001
72. Haraguchi R, Kohara Y, Matsubayashi K, Kitazawa R, Kitazawa S. New insights into the pathogenesis of diabetic nephropathy: Proximal renal tubules are primary target of oxidative stress in diabetic kidney. *Acta Histochem Cytochem* (2020) 53:21–31. doi: 10.1267/ahc.20008
73. Wu M, Zhang M, Zhang Y, Li Z, Li X, Liu Z, et al. Relationship between lysosomal dyshomeostasis and progression of diabetic kidney disease. *Cell Death Dis* (2021) 12:958. doi: 10.1038/s41419-021-04271-w
74. Shin JH, Kim KM, Jeong JU, Shin JM, Kang JH, Bang K, et al. Nrf2-heme oxygenase-1 attenuates high-glucose-induced epithelial-to-mesenchymal transition of renal tubule cells by inhibiting ROS-mediated PI3K/Akt/GSK-3 β signaling. *J Diabetes Res* (2019) 2019:2510105. doi: 10.1155/2019/2510105
75. Lieberthal W, Levine JS. The role of the mammalian target of rapamycin (mTOR) in renal disease. *J Am Soc Nephrol* (2009) 20:2493–502. doi: 10.1681/ASN.2008111186
76. Yin S, Zhou S, Ren D, Zhang J, Xin H, He X, et al. Mesenchymal stem cell-derived exosomes attenuate epithelial-mesenchymal transition of HK-2 cells. *Tissue Eng Part A* (2022) 28:651–9. doi: 10.1089/ten.TEA.2021.0190
77. Kuwahara S, Hosojima M, Kaneko R, Aoki H, Nakano D, Sasagawa T, et al. Megalin-mediated tubuloglomerular alterations in high-fat diet-induced kidney disease. *J Am Soc Nephrol* (2016) 27:1996–2008. doi: 10.1681/ASN.2015020190
78. Saito A, Takeda T, Sato K, Hama H, Tanuma A, Kaseda R, et al. Significance of proximal tubular metabolism of advanced glycation end products in kidney diseases. *Ann N Y Acad Sci* (2005) 1043:637–43. doi: 10.1196/annals.1333.072
79. Wu X-Q, Zhang D-D, Wang Y-N, Tan Y-Q, Yu X-Y, Zhao Y-Y. AGE/RAGE in diabetic kidney disease and ageing kidney. *Free Radic Biol Med* (2021) 171:260–71. doi: 10.1016/j.freeradbiomed.2021.05.025
80. Wendt T, Tanji N, Guo J, Hudson BI, Bierhaus A, Ramasamy R, et al. Glucose, glycation, and RAGE: implications for amplification of cellular dysfunction in diabetic nephropathy. *J Am Soc Nephrol* (2003) 14:1383–95. doi: 10.1097/01.asn.0000065100.17349.ca
81. Jeon GY, Nam M-H, Lee K-W. Inhibitory effect of caffeic acid on advanced glycation end product-induced renal fibrosis *in vitro*: A potential therapeutic target. *J Food Sci* (2021) 86:579–86. doi: 10.1111/1750-3841.15588
82. Liu H-F, Liu H, Lv L-L, Ma K-L, Wen Y, Chen L, et al. CCN3 suppresses TGF- β 1-induced extracellular matrix accumulation in human mesangial cells. *Acta Pharmacol Sin* (2018) 39:222–9. doi: 10.1038/aps.2017.87
83. Thomas HY, Ford Versypt AN. Pathophysiology of mesangial expansion in diabetic nephropathy: mesangial structure, glomerular biomechanics, and biochemical signaling and regulation. *J Biol Eng* (2022) 16:19. doi: 10.1186/s13036-022-00299-4
84. Baccora MHA, Cortes P, Hassett C, Taube DW, Yee J. Effects of long-term elevated glucose on collagen formation by mesangial cells. *Kidney Int* (2007) 72:1216–25. doi: 10.1038/sj.ki.5002517
85. Donate-Correa J, Luis-Rodríguez D, Martín-Núñez E, Tagua VG, Hernández-Carballo C, Ferri C, et al. Inflammatory targets in diabetic nephropathy. *J Clin Med* (2020) 9:458. doi: 10.3390/jcm9020458
86. Zhang Y, Jin D, Kang X, Zhou R, Sun Y, Lian F, et al. Signaling pathways involved in diabetic renal fibrosis. *Front Cell Dev Biol* (2021) 9:696542. doi: 10.3389/fcell.2021.696542
87. Sol M, Kamps JAAM, van den Born J, van den Heuvel MC, van der Vlag J, Krenning G, et al. Glomerular endothelial cells as instigators of glomerular sclerosis. *Front Pharmacol* (2020) 11:573557. doi: 10.3389/fphar.2020.573557
88. Matsuda J, Namba T, Takabatake Y, Kimura T, Takahashi A, Yamamoto T, et al. Antioxidant role of autophagy in maintaining the integrity of glomerular capillaries. *Autophagy* (2018) 14:53–65. doi: 10.1080/15548627.2017.1391428
89. Gui Z, Suo C, Wang Z, Zheng M, Fei S, Chen H, et al. Impaired Atg16L1-dependent autophagy promotes renal interstitial fibrosis in chronic renal graft dysfunction through inducing EndMT by NF- κ B signal pathway. *Front Immunol* (2021) 12:650424. doi: 10.3389/fimmu.2021.650424
90. Casalena GA, Yu L, Gil R, Rodriguez S, Sosa S, Janssen W, et al. The diabetic microenvironment causes mitochondrial oxidative stress in glomerular endothelial cells and pathological crosstalk with podocytes. *Cell Commun Signal* (2020) 18:105. doi: 10.1186/s12964-020-00605-x
91. Lenoir O, Jasiek M, Hénique C, Guyonnet L, Hartleben B, Bork T, et al. Endothelial cell and podocyte autophagy synergistically protect from diabetes-induced glomerulosclerosis. *Autophagy* (2015) 11:1130–45. doi: 10.1080/15548627.2015.1049799

92. Wang L, Wang J, Cretioiu D, Li G, Xiao J. Exercise-mediated regulation of autophagy in the cardiovascular system. *J Sport Health Sci* (2020) 9:203–10. doi: 10.1016/j.jshs.2019.10.001
93. Kroemer G, Mariño G, Levine B. Autophagy and the integrated stress response. *Mol Cell* (2010) 40:280–93. doi: 10.1016/j.molcel.2010.09.023
94. Russell RC, Yuan H-X, Guan K-L. Autophagy regulation by nutrient signaling. *Cell Res* (2014) 24:42–57. doi: 10.1038/cr.2013.166
95. Chan EYW, Kir S, Tooze SA. siRNA screening of the kinome identifies ULK1 as a multidomain modulator of autophagy. *J Biol Chem* (2007) 282:25464–74. doi: 10.1074/jbc.M703663200
96. Packer M. Interplay of adenosine monophosphate-activated protein kinase/sirtuin-1 activation and sodium influx inhibition mediates the renal benefits of sodium-glucose co-transporter-2 inhibitors in type 2 diabetes: A novel conceptual framework. *Diabetes Obes Metab* (2020) 22:734–42. doi: 10.1111/dom.13961
97. Packer M. Role of impaired nutrient and oxygen deprivation signaling and deficient autophagic flux in diabetic CKD development: Implications for understanding the effects of sodium-glucose cotransporter 2-inhibitors. *J Am Soc Nephrol* (2020) 31:907–19. doi: 10.1681/ASN.2020010010
98. Mori H, Inoki K, Masutani K, Wakabayashi Y, Komai K, Nakagawa R, et al. The mTOR pathway is highly activated in diabetic nephropathy and rapamycin has a strong therapeutic potential. *Biochem Biophys Res Commun* (2009) 384:471–5. doi: 10.1016/j.bbrc.2009.04.136
99. Zhang M-Z, Wang Y, Pauksakorn P, Harris RC. Epidermal growth factor receptor inhibition slows progression of diabetic nephropathy in association with a decrease in endoplasmic reticulum stress and an increase in autophagy. *Diabetes* (2014) 63:2063–72. doi: 10.2337/db13-1279
100. Wang Y, Lu Y-H, Tang C, Xue M, Li X-Y, Chang Y-P, et al. Calcium dobesilate restores autophagy by inhibiting the VEGF/PI3K/Akt/mTOR signaling pathway. *Front Pharmacol* (2019) 10:886. doi: 10.3389/fphar.2019.00886
101. Inoki K, Mori H, Wang J, Suzuki T, Hong S, Yoshida S, et al. mTORC1 activation in podocytes is a critical step in the development of diabetic nephropathy in mice. *J Clin Invest* (2011) 121:2181–96. doi: 10.1172/JCI44771
102. Grahammer F, Huber TB, Artunc F. Role of mTOR signaling for tubular function and disease. *Physiology* (2021) 36:350–8. doi: 10.1152/physiol.00021.2021
103. Guo J, Liu Z, Gong R. Long noncoding RNA: an emerging player in diabetes and diabetic kidney disease. *Clin Sci Lond Engl* 1979 (2019) 133:1321–39. doi: 10.1042/CS20190372
104. Steinberg GR, Kemp BE. AMPK in health and disease. *Physiol Rev* (2009) 89:1025–78. doi: 10.1152/physrev.00011.2008
105. Herzig S, Shaw RJ. AMPK: guardian of metabolism and mitochondrial homeostasis. *Nat Rev Mol Cell Biol* (2018) 19:121–35. doi: 10.1038/nrm.2017.95
106. Hardie DG. AMPK: positive and negative regulation, and its role in whole-body energy homeostasis. *Curr Opin Cell Biol* (2015) 33:1–7. doi: 10.1016/j.cceb.2014.09.004
107. Momcilovic M, Hong S-P, Carlson M. Mammalian TAK1 activates Snf1 protein kinase in yeast and phosphorylates AMP-activated protein kinase. *vitro. J Biol Chem* (2006) 281:25336–43. doi: 10.1074/jbc.M604399200
108. Wei X, Lu Z, Li L, Zhang H, Sun F, Ma H, et al. Reducing NADPH synthesis counteracts diabetic nephropathy through restoration of AMPK activity in type 1 diabetic rats. *Cell Rep* (2020) 32:108207. doi: 10.1016/j.celrep.2020.108207
109. Mack HID, Zheng B, Asara JM, Thomas SM. AMPK-dependent phosphorylation of ULK1 regulates Atg9 localization. *Autophagy* (2012) 8:1197–214. doi: 10.4161/auto.20586
110. Kim S-J, Tang T, Abbott M, Viscarra JA, Wang Y, Sul HS. AMPK phosphorylates Desnutrin/Atg1 and hormone-sensitive lipase to regulate lipolysis and fatty acid oxidation within adipose tissue. *Mol Cell Biol* (2016) 36:1961–76. doi: 10.1128/MCB.00244-16
111. Chang C, Su H, Zhang D, Wang Y, Shen Q, Liu B, et al. AMPK-dependent phosphorylation of GAPDH triggers Sirt1 activation and is necessary for autophagy upon glucose starvation. *Mol Cell* (2015) 60:930–40. doi: 10.1016/j.molcel.2015.10.037
112. Dusabimana T, Park EJ, Je J, Jeong K, Yun SP, Kim HJ, et al. Geniposide improves diabetic nephropathy by enhancing ULK1-mediated autophagy and reducing oxidative stress through AMPK activation. *Int J Mol Sci* (2021) 22:1651. doi: 10.3390/ijms22041651
113. Kim J, Kim YC, Fang C, Russell RC, Kim JH, Fan W, et al. Differential regulation of distinct Vps34 complexes by AMPK in nutrient stress and autophagy. *Cell* (2013) 152:290–303. doi: 10.1016/j.cell.2012.12.016
114. Juszczak F, Caron N, Mathew AV, Declèves A-E. Critical role for AMPK in metabolic disease-induced chronic kidney disease. *Int J Mol Sci* (2020) 21:E7994. doi: 10.3390/ijms21217994
115. Morigi M, Perico L, Benigni A. Sirtuins in renal health and disease. *J Am Soc Nephrol* (2018) 29:1799–809. doi: 10.1681/ASN.201711218
116. Liu R, Zhong Y, Li X, Chen H, Jim B, Zhou M-M, et al. Role of transcription factor acetylation in diabetic kidney disease. *Diabetes* (2014) 63:2440–53. doi: 10.2337/db13-1810
117. Zhang H, Yang X, Pang X, Zhao Z, Yu H, Zhou H. Genistein protects against ox-LDL-induced senescence through enhancing Sirt1/LKB1/AMPK-mediated autophagy flux in HUVECs. *Mol Cell Biochem* (2019) 455:127–34. doi: 10.1007/s11010-018-3476-8
118. Zhang N, Li L, Wang J, Cao M, Liu G, Xie G, et al. Study of autophagy-related protein light chain 3 (LC3)-II expression levels in thyroid diseases. *BioMed Pharmacother* (2015) 69:306–10. doi: 10.1016/j.biopha.2014.12.021
119. Ma L, Fu R, Duan Z, Lu J, Gao J, Tian L, et al. Sirt1 is essential for resveratrol enhancement of hypoxia-induced autophagy in the type 2 diabetic nephropathy rat. *Pathol Res Pract* (2016) 212:310–8. doi: 10.1016/j.prp.2016.02.001
120. Lan F, Cacicado JM, Ruderman N, Ido Y. Sirt1 modulation of the acetylation status, cytosolic localization, and activity of LKB1: possible role in AMP-activated protein kinase activation. *J Biol Chem* (2008) 283:27628–35. doi: 10.1074/jbc.M805711200
121. Ghosh HS, McBurney M, Robbins PD. Sirt1 negatively regulates the mammalian target of rapamycin. *PLoS One* (2010) 5:e9199. doi: 10.1371/journal.pone.0009199
122. Zhang J, Zhang L, Zha D, Wu X. Inhibition of miRNA-135a-5p ameliorates TGF- β 1-induced human renal fibrosis by targeting Sirt1 in diabetic nephropathy. *Int J Mol Med* (2020) 46:1063–73. doi: 10.3892/ijmm.2020.4647
123. Wang Y, Zheng Z-J, Jia Y-J, Yang Y-L, Xue Y-M. Role of p53/miR-155-5p/Sirt1 loop in renal tubular injury of diabetic kidney disease. *J Transl Med* (2018) 16:146. doi: 10.1186/s12967-018-1486-7
124. Shao Y, Lv C, Wu C, Zhou Y, Wang Q. Mir-217 promotes inflammation and fibrosis in high glucose cultured rat glomerular mesangial cells via Sirt1/HIF-1 α signaling pathway. *Diabetes Metab Res Rev* (2016) 32:534–43. doi: 10.1002/dmrr.2788
125. Sies H. Oxidative stress: a concept in redox biology and medicine. *Redox Biol* (2015) 4:180–3. doi: 10.1016/j.redox.2015.01.002
126. Kaushal GP, Chandrashekar K, Juncos LA. Molecular interactions between reactive oxygen species and autophagy in kidney disease. *Int J Mol Sci* (2019) 20:3791. doi: 10.3390/ijms20153791
127. Filomeni G, De Zio D, Cecconi F. Oxidative stress and autophagy: the clash between damage and metabolic needs. *Cell Death Differ* (2015) 22:377–88. doi: 10.1038/cdd.2014.150
128. Pajares M, Cuadrado A, Engedal N, Jirsova Z, Cahova M. The role of free radicals in autophagy regulation: Implications for ageing. *Oxid Med Cell Longev* (2018) 2018:2450748. doi: 10.1155/2018/2450748
129. Ogura Y, Kitada M, Xu J, Monno I, Koya D. CD38 inhibition by apigenin ameliorates mitochondrial oxidative stress through restoration of the intracellular NAD⁺/NADH ratio and Sirt3 activity in renal tubular cells in diabetic rats. *Aging* (2020) 12:11325–36. doi: 10.18632/aging.103410
130. Hu Q, Qu C, Xiao X, Zhang W, Jiang Y, Wu Z, et al. Flavonoids on diabetic nephropathy: advances and therapeutic opportunities. *Chin Med* (2021) 16:74. doi: 10.1186/s13020-021-00485-4
131. Xu X, Yu Z, Han B, Li S, Sun Y, Du Y, et al. Luteolin alleviates inorganic mercury-induced kidney injury via activation of the AMPK/mTOR autophagy pathway. *J Inorg Biochem* (2021) 224:111583. doi: 10.1016/j.jinorgbio.2021.111583
132. Lu X, Fan Q, Xu L, Li L, Yue Y, Xu Y, et al. Ursolic acid attenuates diabetic mesangial cell injury through the up-regulation of autophagy via miRNA-21/PTEN/Akt/mTOR suppression. *PLoS One* (2015) 10:e0117400. doi: 10.1371/journal.pone.0117400
133. Volpe CMO, Villar-Delfino PH, Dos Anjos PMF, Nogueira-Machado JA. Cellular death, reactive oxygen species (ROS) and diabetic complications. *Cell Death Dis* (2018) 9:119. doi: 10.1038/s41419-017-0135-z
134. Görlach A, Klappa P, Kietzmann T. The endoplasmic reticulum: folding, calcium homeostasis, signaling, and redox control. *Antioxid Redox Signal* (2006) 8:1391–418. doi: 10.1089/ars.2006.8.1391
135. Burgos-Morón E, Abad-Jiménez Z, de Marañón AM, Iannantuoni F, Escribano-López I, López-Domènech S, et al. Relationship between oxidative stress, ER stress, and inflammation in type 2 diabetes: The battle continues. *J Clin Med* (2019) 8:1385. doi: 10.3390/jcm8091385
136. Cybulsky AV. The intersecting roles of endoplasmic reticulum stress, ubiquitin-proteasome system, and autophagy in the pathogenesis of proteinuric kidney disease. *Kidney Int* (2013) 84:25–33. doi: 10.1038/ki.2012.390
137. Cunard R. Endoplasmic reticulum stress in the diabetic kidney, the good, the bad and the ugly. *J Clin Med* (2015) 4:715–40. doi: 10.3390/jcm4040715
138. Xu X, Chen B, Huang Q, Wu Y, Liang T. The effects of puerarin on autophagy through regulating of the PERK/eIF2 α /ATF4 signaling pathway influences renal function in diabetic nephropathy. *Diabetes Metab Syndr Obes Targets Ther* (2020) 13:2583–92. doi: 10.2147/DMSO.S256457
139. Wei Y, Sinha S, Levine B. Dual role of JNK1-mediated phosphorylation of bcl-2 in autophagy and apoptosis regulation. *Autophagy* (2008) 4:494–51. doi: 10.4161/auto.6788
140. Dorotea D, Jiang S, Pak ES, Son JB, Choi HG, Ahn S-M, et al. Pan-src kinase inhibitor treatment attenuates diabetic kidney injury via inhibition of fyn kinase-mediated endoplasmic reticulum stress. *Exp Mol Med* (2022) 54:1086–97. doi: 10.1038/s12276-022-00810-3
141. Zhong Y, Luo R, Liu Q, Zhu J, Lei M, Liang X, et al. Jujuboside a ameliorates high fat diet and streptozotocin induced diabetic nephropathy via suppressing

- oxidative stress, apoptosis, and enhancing autophagy. *Food Chem Toxicol* (2022) 159:112697. doi: 10.1016/j.fct.2021.112697
142. Ni L, Yuan C, Wu X. Endoplasmic reticulum stress in diabetic nephropathy: regulation, pathological role, and therapeutic potential. *Oxid Med Cell Longev* (2021) 2021:7277966. doi: 10.1155/2021/7277966
143. Fang L, Zhou Y, Cao H, Wen P, Jiang L, He W, et al. Autophagy attenuates diabetic glomerular damage through protection of hyperglycemia-induced podocyte injury. *PLoS One* (2013) 8:e60546. doi: 10.1371/journal.pone.0060546
144. Zhang J, Fan Y, Zeng C, He L, Wang N. Tauroursodeoxycholic acid attenuates renal tubular injury in a mouse model of type 2 diabetes. *Nutrients* (2016) 8:589. doi: 10.3390/nu8100589
145. Cao A-L, Wang L, Chen X, Wang Y-M, Guo H-J, Chu S, et al. Ursodeoxycholic acid and 4-phenylbutyrate prevent endoplasmic reticulum stress-induced podocyte apoptosis in diabetic nephropathy. *Lab Invest J Tech Methods Pathol* (2016) 96:610–22. doi: 10.1038/labinvest.2016.44
146. Franzen S, Pihl L, Khan N, Gustafsson H, Palm F. Pronounced kidney hypoxia precedes albuminuria in type 1 diabetic mice. *Am J Physiol Renal Physiol* (2016) 310: F807–809. doi: 10.1152/ajprenal.00049.2016
147. DeFronzo RA, Reeves WB, Awad AS. Pathophysiology of diabetic kidney disease: impact of SGLT2 inhibitors. *Nat Rev Nephrol* (2021) 17:319–34. doi: 10.1038/s41581-021-00393-8
148. Semenza GL. Pharmacologic targeting of hypoxia-inducible factors. *Annu Rev Pharmacol Toxicol* (2019) 59:379–403. doi: 10.1146/annurev-pharmtox-010818-021637
149. Catrina S-B, Zheng X. Hypoxia and hypoxia-inducible factors in diabetes and its complications. *Diabetologia* (2021) 64:709–16. doi: 10.1007/s00125-021-05380-z
150. Jiang N, Zhao H, Han Y, Li L, Xiong S, Zeng L, et al. HIF-1 α ameliorates tubular injury in diabetic nephropathy via HO-1-mediated control of mitochondrial dynamics. *Cell Prolif* (2020) 53:e12909. doi: 10.1111/cpr.12909
151. Li L, Kang H, Zhang Q, D'Agati VD, Al-Awqati Q, Lin F. FoxO3 activation in hypoxic tubules prevents chronic kidney disease. *J Clin Invest* (2019) 129:2374–89. doi: 10.1172/JCI122256
152. Lin Q, Li S, Jiang N, Jin H, Shao X, Zhu X, et al. Inhibiting NLRP3 inflammasome attenuates apoptosis in contrast-induced acute kidney injury through the upregulation of HIF1 α and BNIP3-mediated mitophagy. *Autophagy* (2021) 17:2975–90. doi: 10.1080/15548627.2020.1848971
153. Pan C, Chen Z, Li C, Han T, Liu H, Wang X. Sestrin2 as a gatekeeper of cellular homeostasis: Physiological effects for the regulation of hypoxia-related diseases. *J Cell Mol Med* (2021) 25:5341–50. doi: 10.1111/jcmm.16540
154. Eid AA, Lee D-Y, Roman LJ, Khazim K, Gorin Y. Sestrin 2 and AMPK connect hyperglycemia to Nox4-dependent endothelial nitric oxide synthase uncoupling and matrix protein expression. *Mol Cell Biol* (2013) 33:3439–60. doi: 10.1128/MCB.00217-13
155. Ala M, Eftekhari SP. Target sestrin2 to rescue the damaged organ: Mechanistic insight into its function. *Oxid Med Cell Longev* (2021) 2021:8790369. doi: 10.1155/2021/8790369
156. Greco EV, Russo G, Giandalia A, Viazzi F, Pontremoli R, De Cosmo S. GLP-1 receptor agonists and kidney protection. *Med Kaunas Lith* (2019) 55:233. doi: 10.3390/medicina55060233
157. Abdel-Rahman EM, Saadulla L, Reeves WB, Awad AS. Therapeutic modalities in diabetic nephropathy: standard and emerging approaches. *J Gen Intern Med* (2012) 27:458–68. doi: 10.1007/s11606-011-1912-5
158. Jaikumkao K, Promsan S, Thongnak L, Swe MT, Tapanya M, Htun KT, et al. Dapagliflozin ameliorates pancreatic injury and activates kidney autophagy by modulating the AMPK/mTOR signaling pathway in obese rats. *J Cell Physiol* (2021) 236:6424–40. doi: 10.1002/jcp.30316
159. Jaikumkao K, Pongchaidecha A, Chueakula N, Thongnak L-O, Wanchai K, Chatsudthipong V, et al. Dapagliflozin, a sodium-glucose co-transporter-2 inhibitor, slows the progression of renal complications through the suppression of renal inflammation, endoplasmic reticulum stress and apoptosis in prediabetic rats. *Diabetes Obes Metab* (2018) 20:2617–26. doi: 10.1111/dom.13441
160. Korb AI, Taskaeva IS, Bgatova NP, Muraleva NA, Orlov NB, Dashkin MV, et al. SGLT2 inhibitor empagliflozin and DPP4 inhibitor linagliptin reactivate glomerular autophagy in db/db mice, a model of type 2 diabetes. *Int J Mol Sci* (2020) 21:2987. doi: 10.3390/ijms21082987
161. Yang S, Lin C, Zhuo X, Wang J, Rao S, Xu W, et al. Glucagon-like peptide-1 alleviates diabetic kidney disease through activation of autophagy by regulating AMP-activated protein kinase-mammalian target of rapamycin pathway. *Am J Physiol Endocrinol Metab* (2020) 319:E1019–30. doi: 10.1152/ajpendo.00195.2019
162. Zhu H, Zhong S, Yan H, Wang K, Chen L, Zhou M, et al. Resveratrol reverts streptozotocin-induced diabetic nephropathy. *Front Biosci Landmark Ed* (2020) 25:699–709. doi: 10.2741/4829
163. Sarafidis P, Ferro CJ, Morales E, Ortiz A, Malyszko J, Hojs R, et al. SGLT-2 inhibitors and GLP-1 receptor agonists for nephroprotection and cardioprotection in patients with diabetes mellitus and chronic kidney disease. a consensus statement by the EURECA-m and the DIABESITY working groups of the ERA-EDTA. *Nephrol Dial Transplant* (2019) 34:208–30. doi: 10.1093/ndt/gfy407
164. Barutta F, Bernardi S, Gargiulo G, Durazzo M, Gruden G. SGLT2 inhibition to address the unmet needs in diabetic nephropathy. *Diabetes Metab Res Rev* (2019) 35: e3171. doi: 10.1002/dmrr.3171
165. Su K, Yi B, Yao B-Q, Xia T, Yang Y-F, Zhang Z-H, et al. Liraglutide attenuates renal tubular ectopic lipid deposition in rats with diabetic nephropathy by inhibiting lipid synthesis and promoting lipolysis. *Pharmacol Res* (2020) 156:104778. doi: 10.1016/j.phrs.2020.104778
166. Miao X, Gu Z, Liu Y, Jin M, Lu Y, Gong Y, et al. The glucagon-like peptide-1 analogue liraglutide promotes autophagy through the modulation of 5'-AMP-activated protein kinase in INS-1 β -cells under high glucose conditions. *Peptides* (2018) 100:127–39. doi: 10.1016/j.peptides.2017.07.006
167. Thongboonkerd V, Kanlaya R. The divergent roles of exosomes in kidney diseases: Pathogenesis, diagnostics, prognostics and therapeutics. *Int J Biochem Cell Biol* (2022) 149:106262. doi: 10.1016/j.biocel.2022.106262
168. Mohan A, Singh RS, Kumari M, Garg D, Upadhyay A, Ecelbarger CM, et al. Urinary exosomal microRNA-451-5p is a potential early biomarker of diabetic nephropathy in rats. *PLoS One* (2016) 11:e0154055. doi: 10.1371/journal.pone.0154055
169. Yamamoto CM, Murakami T, Oakes ML, Mitsuhashi M, Kelly C, Henry RR, et al. Uromodulin mRNA from urinary extracellular vesicles correlate to kidney function decline in type 2 diabetes mellitus. *Am J Nephrol* (2018) 47:283–91. doi: 10.1159/000489129
170. Jin J, Shi Y, Gong J, Zhao L, Li Y, He Q, et al. Exosome secreted from adipose-derived stem cells attenuates diabetic nephropathy by promoting autophagy flux and inhibiting apoptosis in podocyte. *Stem Cell Res Ther* (2019) 10:95. doi: 10.1186/s13287-019-1177-1
171. Zhao J, Chen J, Zhu W, Qi X-M, Wu Y-G. Exosomal miR-7002-5p derived from highglucose-induced macrophages suppresses autophagy in tubular epithelial cells by targeting Atg9b. *FASEB J* (2022) 36:e22501. doi: 10.1096/fj.202200550RR
172. Ebrahim N, Ahmed IA, Hussien NI, Dessouky AA, Farid AS, Elshazly AM, et al. Mesenchymal stem cell-derived exosomes ameliorated diabetic nephropathy by autophagy induction through the mTOR signaling pathway. *Cells* (2018) 7:226. doi: 10.3390/cells7120226

Glossary

ACEI	angiotensin-converting enzyme inhibitors
AGEs	advanced glycation end-products
Akt	protein kinase B
Atg	autophagy-related gene
AMPK	adenosine 5'-monophosphate-activated protein kinase
ARB	angiotensin receptor antagonists
ATF	activating transcription factor
Bcl-2	B-cell lymphoma-2
BNIP3	Bcl-2/adenovirus E1V19-kDa interacting protein 3
CAMKK β	calcium/calmodulin-dependent protein kinase kinase β
DN	diabetic nephropathy
DPP-4	dipeptidyl peptidase-4
ECM	extracellular matrix
EMT	epithelial-mesenchymal transition
ER	endoplasmic reticulum
ESRD	end-stage renal disease
eIF2 α	α -subunit of eukaryotic initiation factor 2
FoxO	forkhead box O
GBM	glomerular basement membrane
GENCs	glomerular endothelial cells
GFB	glomerular filtration barrier
GLP-1R	glucagon-like peptide 1 receptor
GMCs	glomerular mesangial cells
HFD	high-fat diet
HIF	hypoxia-inducible factor
IDF	International Diabetes Federation
IRE1 α	inositol-requiring enzyme 1 α
JNK	c-Jun N-terminal kinase
LC3	microtubule-associated protein 1A/1B-light chain 3
LKB1	liver kinase B1
LncRNAs	long noncoding RNAs
mTOR	mammalian target of rapamycin
NF- κ B	nuclear factor kappa-B
PERK	protein kinase RNA-like ER kinase
p70S6K	phosphoprotein 70 ribosomal protein S6 kinase
PGC-1 α	peroxisome proliferator-activated receptor-gamma coactivator-1 α
PI3K	class III phosphatidylinositol-3-kinase
PTECs	proximal tubular epithelial cells

(Continued)

Continued

RAS	renin-angiotensin system
RAGE	receptor for advanced glycation end-products
Rheb	ras homolog enriched in brain
ROS	reactive oxygen species
RTECs	renal tubular epithelial cells
SGLT2	sodium-glucose cotransporter 2
Sirt1	silent information regulator of transcription 1
STZ	streptozotocin
TGF- β	transforming growth factor- β
TSC2	tuberous sclerosis complex 2
ULK1	unc-51-like kinase 1
UPR	unfolded protein response



OPEN ACCESS

EDITED BY

Ningning Hou,
Affiliated Hospital of Weifang Medical
University, China

REVIEWED BY

David Cruz Robles,
National Cardiology Institute Ignacio
Chavez, Mexico
Jad Ahmad Degheili,
Children's Hospital of Eastern Ontario
(CHEO), Canada

*CORRESPONDENCE

Wei Wang

✉ wangweimiwai@126.com

Yunwu Hao

✉ haoyunwu2002@163.com

[†]These authors have contributed equally to
this work

RECEIVED 15 February 2023

ACCEPTED 04 May 2023

PUBLISHED 22 May 2023

CITATION

Guo Z, Li G, Chen Y, Fan S, Sun S,
Hao Y and Wang W (2023) Could
METS-VF provide a clue as to the
formation of kidney stones?
Front. Endocrinol. 14:1166922.
doi: 10.3389/fendo.2023.1166922

COPYRIGHT

© 2023 Guo, Li, Chen, Fan, Sun, Hao and
Wang. This is an open-access article
distributed under the terms of the [Creative
Commons Attribution License \(CC BY\)](#). The
use, distribution or reproduction in other
forums is permitted, provided the original
author(s) and the copyright owner(s) are
credited and that the original publication in
this journal is cited, in accordance with
accepted academic practice. No use,
distribution or reproduction is permitted
which does not comply with these terms.

Could METS-VF provide a clue as to the formation of kidney stones?

Zhenyu Guo^{1,2,3†}, Guoxiang Li^{1,2,3†}, Yan Chen^{4†}, Shuai Fan^{1,2,3},
Shuai Sun^{1,2,3}, Yunwu Hao^{5*} and Wei Wang^{1,2,3*}

¹Department of Urology, the First Affiliated Hospital of Anhui Medical University, Hefei, China,

²Institute of Urology, Anhui Medical University, Hefei, China, ³Anhui Province Key Laboratory of
Genitourinary Diseases, Anhui Medical University, Hefei, China, ⁴Department of General Practice,
Wuhu City Second People's Hospital, Wuhu, China, ⁵Department of Urology, Lu'an Hospital Affiliated
of Anhui Medical University, Lu'an, China

Objective: The lifetime occurrence rate of kidney stones is 14%, making it one of the most prevalent urological conditions. Other contributing elements, such as obesity, diabetes, diet, and heredity, are also taken into account. Our research sought to explore the potential link between high visceral fat scores (METS-VF) and the occurrence of kidney stones, as a means of understanding how to prevent them.

Methods: This research utilized data from the National Health and Nutrition Examination Survey (NHANES), mirroring the demographics of the United States. We carried out an in-depth analysis of the connection between METS-VF and kidney stones, based on data from 29,246 participants in the National Health and Nutrition Examination Survey spanning 2007 to 2018, involving logistic regression, segmentation, and dose-response curve analysis.

Results: Our study of 29,246 potential participants found that METS-VF was positively associated with the prevalence and progression of kidney stones. After subgroup analysis by gender, race, blood pressure, and blood glucose, our results showed that the ORs for METS-VF and kidney stones were (1.49, 1.44) in males and females, respectively; while in Mexicans, whites, blacks, and In other populations, the OR values were (1.33, 1.43, 1.54, 1.86); in hypertensive and normal populations, the OR values were (1.23, 1.48); in diabetic patients and normoglycemic patients were (1.36, 1.43). This proves that it works for all groups of people.

Summary: Our studies demonstrate a strong connection between METS-FV and the emergence of kidney stones. It would be beneficial to investigate METS-VF as a marker for kidney stone development and progression in light of these findings.

KEYWORDS

METS-VF, kidney stones, obesity, NHANES, clue

Abbreviations: NHANES, National Health and Nutrition Examination Survey; METS-VF, Metabolic score for Visceral Fat; OR, Odds ratio; BMI, Body mass index; IR, insulin resistance; WHtR, waist-height ratio; CKD, Chronic kidney injury; BIA, bioelectric impedance analysis; VAT, visceral adipose tissue; VIF, variance inflation factor.

Introduction

An accumulation of crystalline substances, such as uric acid, calcium oxalate, and calcium phosphate, at the point where the renal pelvis and ureter join can lead to the development of kidney stones, a common urinary disorder (1, 2). Various metabolic imbalances (e.g. hyperparathyroidism, hypercortisolism, hyperglycemia), lack of physical activity, lack of essential vitamins and minerals (3) (such as Vitamin B6 and magnesium), blockage of the urinary tract, infection, foreign objects, and drug use are all potential causes of kidney stone formation (4, 5). Though the symptoms of kidney stones may be less visible than those of urolithiasis, they can be more severe and can significantly reduce a patient's quality of life, with the possibility of developing hematuria, pain, urinary tract infection, and renal dysfunction (6). Consequently, it is essential to acquire a better comprehension of the potential causes that could lead to its emergence.

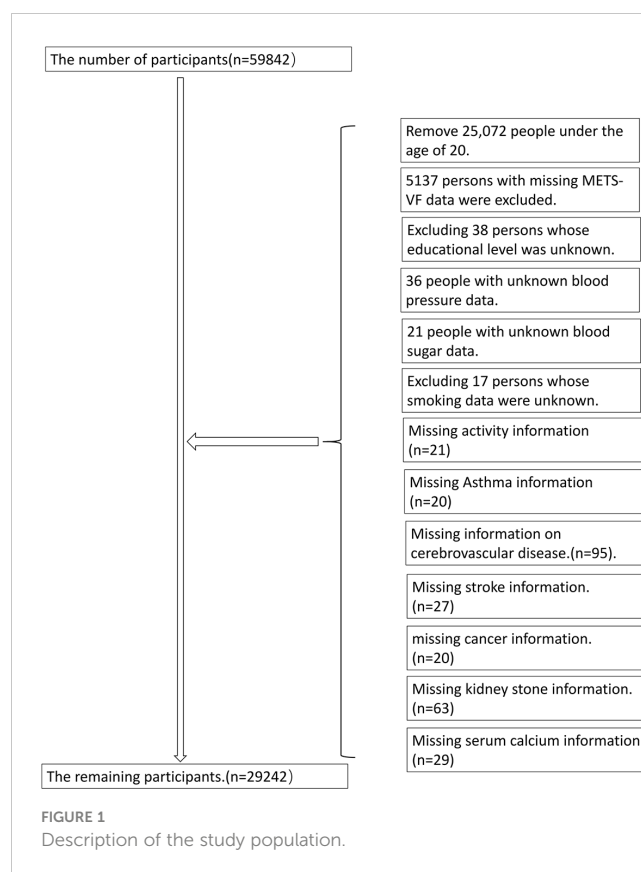
Having an elevated Body Mass Index (BMI) is the most commonly used way to gauge if one is at risk of forming kidney stones (7, 8), which can be caused by being overweight. However, BMI is not without its drawbacks (9). For example, BMI does not take into account the difference between lean and fat bodies. The METS-VF is an assessment of fat metabolism inside the body which utilizes the insulin resistance index (IR), age, waist-to-height ratio (WHtR), and gender to create a score (10). MRI and BIA have been employed to ascertain the amount of visceral adipose tissue in overseas populations, and it has been proven to be more effective than other surrogate measurements of VAT (11). It can prevent diabetes and fight high blood pressure (12).

We hypothesize that METS-VF could potentially play a role in the emergence and advancement of kidney stones. We conducted a nationwide inquiry to examine the correlation between METS-VF and kidney stones, taking into account numerous potential factors that could affect the possibility of developing kidney stones. The initial inquiry into whether METS-VF is linked to the likelihood of developing kidney stones will begin here.

Materials and methods

Study population

This project was carried out in conjunction with the CDC Institutional Review Committee, who utilized complex data analysis methods to analyze the data from the NHANES database; furthermore, all individuals involved gave their consent. Every year, the National Center for Health Statistics conducts a survey that evaluates a certain group of people at a single moment. The National Health and Nutrition Examination Survey is an investigation implemented in the United States to evaluate the wellbeing and dietary habits of a broad range of individuals, particularly those from ethnic minorities and those with low incomes. The research encompassed a total of 29,246 participants (Figure 1).



Data collection and definition

The visceral fat metabolism rating was taken into consideration as a factor in the experiment. We defined METS-VF as $4.466 + 0.011 * (\ln(\text{METS-IR}))^3 + 3.239 * (\ln(\text{WHtR}))^3 + 0.319 * (\text{Sex}) + 0.594 * (\ln(\text{Age}))$. The multivariable models indicated potential outside factors that may interfere with the connection between METS-VF and kidney stones. In this research, sex (male/female), race, educational attainment, marital status (married/single), alcohol intake (drinker/non-drinker), high blood pressure, diabetes, smoking (smoker/non-smoker) and physical activity were all taken into consideration. The exact severity is unknown.

Statistical methods

The analysis employed an appropriate sample size from NHANES, and a complicated multi-stage cluster survey design was taken into account. The R language's survey design package was employed to illustrate the intricate multi-stage hierarchical sampling technique of NHANES with the help of the weights from the dataset. To put it succinctly, study-weighted means and 95% confidence intervals are used to illustrate continuous variables, while study-weighted means and 95% confidence levels are applied to describe categorical variables. The linear regression model with study-weighted adjustments was used to determine the impact of the groups on continuous data, and the study-weighted chi-square tests were applied to investigate the effects of

the groups on categorical data. The three cohorts were studied to ascertain the relationship between METS-VF and kidney stones *via* the utilization of a multivariate Logistic regression model that was based on pre-defined protocols. Model 1 did not incorporate any changes to the covariates. Model 2 was tailored to take into account characteristics such as gender, ethnicity, educational level, marital status, hypertension, and diabetes. The parameters of Model 3 were modified to include all types of illnesses. In order to gain a more comprehensive insight into the correlation between METS-VF and kidney stones, a penalty spline technique and a generalized additive model regression were employed to fit the data. The saturation threshold effect was tested using the maximum link-like natural ratio to determine the potential threshold value when non-linear relationships exist.

Values with a likelihood lower than 0.05 were considered to be statistically significant. The analyses were conducted using both Empower[®] software (www.empowerstats.com; X&Y Solutions, Inc., Boston, MA, USA) and R 4.0.2 (<http://www.r-project.org>, The R Foundation).

Results

Increased METS-VF levels are associated with a higher chance of developing kidney stones

Table 1 outlines the demographics of the participants involved in the study and provides a visual representation of the proportion of characteristics. The results from **Table 1** showed that the stone group had significantly higher METS-VF levels compared to the standard population group. The METS-VF score may be related to a higher rate of kidney stones, and the VIF analysis of the covariates indicated that all VIF values were less than 5, suggesting that there were no issues with collinearity in the data. The logistic regression showed that there was a significant relationship between METS-VF

and the development of kidney stones, with Model 3 taking into account all other variables; for each one unit rise in the METS-VF index, there was a 43% higher risk of kidney stones (OR=1.43, 95% CI: 1.32-1.55). We split METS-VF into three sections and re-ran the logistic regression analysis, which revealed that the top section had a higher value than the bottom part in the third model.

Subgroup analysis

We also controlled for sex, race, hypertension, and diabetes using subgroup analysis. The univariate logistic regression between kidney stone prevalence and METS-VF showed a positive relationship, with an odds ratio of 1.49 (95% CI: 1.33-1.67) compared to 1.44 (95% CI: 1.29 – 1.62), (**Table 2**). The likelihood of Mexicans being affected by the outcome was 1.33 times greater than the general population (95% CI 1.11-1.60). The average odds ratios for whites, blacks and other races (non-Mexican) were respectively 1.28-1.59 (95% confidence interval), 1.25-1.89 (95% confidence interval), and 1.42-2.44 (95% confidence interval). The hypertensive group had an odds ratio of 1.23 (95% CI 1.08 to 1.41), while the nonhypertensive group had an odds ratio of 1.48 (95% CI 1.34 to 1.64) in the hypertension stratification. When segregated by diabetes, the probability ratio was 1.36 (95% CI 1.07-1.72) for those with diabetes and 1.43 (95% CI 1.32-1.56) for those without.

Dose-response and threshold effect analysis of the METS-VF index on the prevalence of kidney stones

A research project was conducted to investigate the link between the METS-VF index and the frequency of kidney stones, utilizing a generalized additive model and a smooth curve fitting approach. Our study has revealed a significant link between the METS-VF index and the occurrence of kidney stones (**Figure 2**).

TABLE 1 The characteristics of the participants selected.

Characteristic	Nonstone formers N=26492	Stone formers N=2754
Age(years)	46.56 (46.09,47.02)	53.17 (52.53,53.80)
Cholesterol(MG/DL)	194.11 (193.11,195.10)	192.39 (189.89,194.89)
Serum Calcium (MG/DL)	9.39 (9.38,9.41)	9.37 (9.34,9.40)
Serum Creatinine (MG/DL)	0.87 (0.87,0.88)	0.93 (0.91,0.94)
METS-VF	5.90 (5.88,5.92)	6.02 (5.97,6.07)
Gender(%)		
Male	47.74 (47.04,48.44)	55.46 (52.78,58.11)
Female	52.26 (51.56,52.96)	44.54 (41.89,47.22)
Race(%)		
Mexican American	14.98 (13.09,17.10)	11.30 (9.34,13.61)

(Continued)

TABLE 1 Continued

Characteristic	Nonstone formers N=26492	Stone formers N=2754
White	65.65 (62.78,68.42)	76.97 (73.84,79.83)
Black	11.15 (9.78,12.69)	5.66 (4.67,6.83)
Other Race	8.21 (7.36,9.15)	6.07 (4.87,7.54)
Education Level(%)		
Less than high school	20.39 (18.97,21.89)	19.72 (17.79,21.81)
High school	28.66 (27.48,29.87)	31.44 (28.63,34.39)
More than high school	50.95 (49.08,52.82)	48.84 (45.69,52.00)
Marital Status(%)		
Cohabitation	63.40 (62.12,64.66)	69.45 (66.85,71.93)
Solitude	36.60 (35.34,37.88)	30.55 (28.07,33.15)
Alcohol(%)		
Yes	61.15 (59.67,62.61)	60.07 (56.99,63.07)
No	18.50 (17.44,19.61)	19.27 (17.06,21.69)
Unclear	20.35 (19.25,21.50)	20.66 (17.97,23.64)
High Blood Pressure (%)		
Yes	29.65 (28.65,30.67)	46.24 (43.34,49.17)
No	70.35 (69.33,71.35)	53.76 (50.83,56.66)
Diabetes(%)		
Yes	8.49 (8.02,9.00)	17.49 (15.75,19.37)
No	91.51 (91.00,91.98)	82.51 (80.63,84.25)
Smoked(%)		
Yes	43.57 (42.36,44.79)	49.41 (46.56,52.26)
No	56.43 (55.21,57.64)	50.59 (47.74,53.44)
Physical Activity (%)		
Never	25.99 (25.01,26.99)	29.75 (27.52,32.08)
Moderate	31.97 (30.99,32.96)	31.42 (29.12,33.81)
Vigorous	42.04 (40.93,43.17)	38.83 (36.10,41.63)
Asthma (%)		
No	85.52 (84.82,86.20)	82.75 (80.77,84.57)
Yes	14.48 (13.80,15.18)	17.25 (15.43,19.23)
Coronary Heart Disease (%)		
Yes	3.07 (2.70,3.49)	6.28 (5.20,7.57)
No	96.93 (96.51,97.30)	93.72 (92.43,94.80)
Cancers(%)		
Yes	9.33 (8.85,9.84)	15.77 (14.24,17.43)
No	90.67 (90.16,91.15)	84.23 (82.57,85.76)
PIR(%)		
<1.39	20.13 (18.90,21.43)	18.02 (16.29,19.90)

(Continued)

TABLE 1 Continued

Characteristic	Nonstone formers N=26492	Stone formers N=2754
1.39-3.49	32.50 (31.25,33.77)	35.06 (32.48,37.73)
≥3.49	40.04 (38.16,41.94)	40.05 (36.78,43.42)
Unclear	7.33 (6.69,8.03)	6.86 (5.61,8.37)
Total Kcal (%)		
Tertile 1	39.11 (38.29,39.94)	40.24 (38.01,42.51)
Tertile 2	46.02 (45.04,47.01)	46.53 (43.81,49.26)
Tertile 3	14.87 (14.08,15.69)	13.23 (11.50,15.18)
Total Sugar (%)		
Tertile 1	36.46 (35.61,37.33)	36.73 (33.94,39.63)
Tertile 2	37.22 (36.2,38.19)	37.09 (34.15,40.14)
Tertile 3	26.31 (25.50,27.14)	26.17 (23.87,28.61)
Total Water (%)		
Tertile 1	38.92 (38.00,39.84)	37.39 (34.92,39.94)
Tertile 2	46.22 (45.28,47.16)	49.38 (46.60,52.15)
Tertile 3	14.87 (14.08,15.69)	13.23 (11.50,15.18)
Drxttfat.D2.New (%)		
Tertile 1	38.92 (38.00,39.84)	37.39 (34.92,39.94)
Tertile 2	46.22 (45.28,47.16)	49.38 (46.60,52.15)
Tertile 3	14.87 (14.08,15.69)	13.23 (11.5,15.18)

TABLE 2 Subgroup analysis between METS-IR index with kidney stone formation.

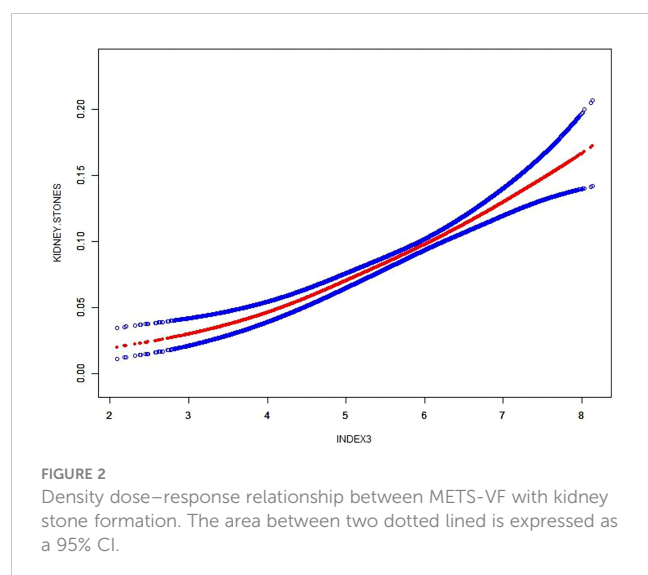
Exposure	Model1	Model2	Model3
METS-VF	1.07 (1.03,1.11)	1.81 (1.68,1.94)	1.43 (1.32,1.55)
Gender (%)			
Male	1.73 (1.58,1.91)	1.92 (1.72,2.13)	1.49 (1.33,1.67)
Female	1.76 (1.60,1.95)	1.78 (1.60,1.97)	1.44 (1.29,1.62)
Race (%)			
Mexican American	1.01 (0.94,1.08)	1.84 (1.55,2.18)	1.33 (1.11,1.60)
White	1.05 (1.00,1.11)	1.77 (1.60,1.95)	1.43 (1.28,1.59)
Black	1.23 (1.11,1.36)	1.89 (1.56,2.28)	1.54 (1.25,1.89)
Other Race	1.36 (1.16,1.58)	2.43 (1.89,3.12)	1.86 (1.42,2.44)
High Blood Pressure (%)			
Yes	0.91 (0.86,0.96)	1.38 (1.21,1.57)	1.23 (1.08,1.41)
No	1.07 (1.02,1.13)	1.67 (1.52,1.84)	1.48 (1.34,1.64)
Diabetes (%)			
Yes	0.87 (0.80,0.95)	1.46 (1.16,1.84)	1.36 (1.07,1.72)
No	1.07 (1.03,1.12)	1.67 (1.54,1.81)	1.43 (1.32,1.56)

Model 1 = no covariates were adjusted.

Model 2 = Model 1+ GENDR, RACE, EDUCATION, MARITAL.

Model 3 = adjusted for all covariates except effect modifier.

*Means only in model 3.



Discussion

Our investigation has revealed a significant association between METS-VF and the development of kidney stones. After accounting for potential confounding variables, this relationship remained significant. Our findings provide valuable insight into the etiology of nephrolithiasis and suggest the need for further research to explore the underlying mechanisms of this association. METS-VF is an accurate measure for assessing the likelihood of kidney stones and can be utilized to monitor their progression. The index measures total energy expenditure during physical activity, as well as the frequency and intensity of activity. Furthermore, this index has been found to be a useful tool for monitoring kidney stone progression in those who already have kidney stones. This is the initial assessment to ascertain if there is a relationship between METS-VF and the development of kidney stones. More in-depth study should be conducted to gain a clearer comprehension of the correlation between METS-VF and kidney stones, as well as to pinpoint other possible sources of risk. This research could pave the way for more successful approaches to averting and managing kidney stones.

Carrying excess weight around the abdomen increases the likelihood of developing kidney disease (13). Adipose tissue helps maintain the equilibrium between food intake and energy expenditure through the production of adipokines under normal physiological conditions. The adipose tissue contributes significantly to the maintenance of the nutritional balance and energy metabolism of the body by releasing a variety of molecules called adipokines, which can influence appetite, metabolism, inflammation, and other bodily functions. These adipokines are secreted in response to various cues, such as nutrient availability, hormones, and physical activity, allowing the body to effectively adjust energy and nutrient levels. The importance of adipose tissue in controlling these activities is paramount for achieving optimal health and well-being. When abnormalities occur, the overgrowth and build-up of fatty tissue can cause biological abnormalities and dysfunction, which can result in the deposition of excessive fat in

other areas and eventually lead to malfunctioning organs. Pathological conditions that lead to an overgrowth and buildup of fat cells can result in biological abnormalities and disruption of the fatty tissue. Pathological states that cause an abnormal increase in fat deposits can lead to a range of biological issues and interfere with the typical functioning of fatty tissue. This can negatively affect a person's health and well-being and can lead to further complications. It is important to monitor fatty tissue health and take steps to maintain healthy body composition, to avoid these adverse effects. Associated with this is the accumulation of ectopic fat, which can lead to impaired organ function. The accumulation of ectopic fat is a serious medical condition that can have far-reaching consequences. It occurs when fat accumulates in areas other than the body's normal fat deposits, such as the liver, heart, and muscles. This can lead to impaired organ function, including heart and liver damage, insulin resistance, and even an increased risk of certain types of cancer. Therefore, it is important to understand the potential risks associated with ectopic fat accumulation and take steps to reduce the risks. This includes maintaining a healthy diet and exercising regularly. It is also important to talk to your doctor if you are at risk for this condition. This can have serious consequences for a person's health and well-being. The repercussions of poor health and well-being can be far-reaching and long-lasting. From physical and mental health issues to financial and social difficulties, the effects can be devastating. When individuals do not prioritize their health and well-being, it can cause a ripple effect in all aspects of life. It can cause a drop in efficiency on the job, a lack of attention and focus, and an overall reduction in well-being. It is essential to prioritize and maintain health and well-being, as it can have serious implications for an individual's life. It is critical to be mindful of the potential issues that can stem from adipose tissue disorders, and to reach out to a medical professional if any warning signs occur. It is critical to be mindful of the risks of pathological adipose tissue and to take proactive steps to address any signs of dysfunction. Adipose tissue dysfunction can manifest in a variety of ways, including weight gain, excessive fat deposition, and metabolic disturbances. If any of these symptoms or signs occur, seek medical advice from a qualified healthcare practitioner so that the situation can be assessed and an appropriate treatment plan can be instituted. Early detection and treatment of adipose tissue dysfunction can help prevent further complications and may even help to reverse existing conditions. Multiple investigations have been conducted to explore the relationship between abdominal fat and kidney performance. A research paper examining the relationship between obesity, metabolic disorders, and CKD progression revealed that individuals with obesity and metabolic disorders had an elevated risk of CKD compared to those without such conditions (14). This research is comparable to our study in that they both explore the association between fat and kidney damage, however, it is a broad analysis of the relationship between obesity and kidney injury and not a more nuanced examination of the different kinds of fat, whereas our study is a more in-depth look at the link between visceral fat accumulation and kidney stones, with more convincing results. Kang and their associates used bioelectrical impedance measurements at different frequencies to determine visceral fat

levels and observed a clear association between increased amounts of visceral fat and an amplified risk of chronic kidney damage. This link persisted even when accounting for factors like age, gender, diabetes, and high blood pressure (15). Instead of using the multifrequency bioelectric impedance analysis method to assess visceral body fat, we opted for METS-VF which made our research more feasible and enabled us to include a greater number of participants. Additionally, visceral fat has been linked to the progression of kidney disease. In Japan, researchers utilized computed tomography to evaluate the proportion of visceral and subcutaneous fat in patients with preexisting chronic kidney disease. They found that individuals with a higher ratio of visceral to subcutaneous fat experienced a reduction in eGFR of at least 30% (16).

This research serves as a starting point for further study of the association between METS-FV and kidney stones, thus emphasizing the relevance of METS-VF in the creation of kidney stones. This study has shown that the collaboration between these two elements is essential for this condition. This extensive research showed that individuals who engaged in higher levels of strenuous physical activity were more likely to develop kidney stones. The significance of regular physical activity in keeping kidney health in check is underscored by this discovery. More studies must be conducted to gain an in-depth knowledge of the precise processes that connect physical activity to the development of kidney stones. This research proposes that METS-VF, a marker of visceral fat, could possibly be used to anticipate the appearance and advancement of kidney stones. The rise of visceral fat has been linked to the start of metabolic syndrome and type 2 diabetes, which both raise the odds of kidney stones forming. Moreover, elevated quantities of visceral fat can cause heightened levels of particular hormones and inflammatory substances, which can be responsible for the emergence and worsening of kidney stones. Consequently, additional investigations should be conducted to assess if METS-VF can be utilized as a reliable marker of kidney stone development and advancement. The results of this study indicated that the relationship studied had strong implications when broken down by sex, ethnicity, hypertension, and diabetes, implying that it is relevant across all populations. The researchers analyzed the association between two factors, and broke down the results by gender, ethnicity, hypertension, and diabetes. The results of our study suggested that this relationship had distinct impact levels when grouped by gender, ethnicity, hypertension, and diabetes, implying that it could be pertinent to a broad range of individuals. The possible reasons are as follows: METS-VF is an indicator of obesity (17), Obese people usually have higher fat and calorie intake and control high blood pressure and diabetes (18, 19), Thus reducing the correlation of METS-VF with kidney stones compared to the disease.

We have several hypotheses regarding the relationship between visceral fat and kidney stones, including: ① An overabundance of fat which causes triglyceride droplets to accumulate in the tubular epithelial cells, high cholesterol levels in the podocytes that disrupt the wall's stability, and high glucose levels stimulating fat gene expression and reducing β -oxidation. The abnormal glucose and

lipid metabolism contribute to a disruption of cellular structure and inflammation of the kidneys, resulting in the formation of kidney stones. ②A rise in visceral fat may be associated with an elevation in serum uric acid levels. This heightens the likelihood of uric acid stones forming in the kidneys (20). ③Excess body weight can cause an increase in the amount of sodium that is reabsorbed by the kidneys, thus activating the renin-angiotensin and sympathetic nervous systems (21), which in turn leads to an increased prevalence of nephrolithiasis (22). ④In obese patients, the fat around the kidney can compress the kidney, leading to intraarterial hypertension around the kidney and then nephrogenic hypertension (23). It is widely accepted that having elevated blood pressure can significantly increase the likelihood of developing kidney stones.

This study offers a thorough examination of the correlation between METS-VF and the potential for kidney stone formation, an area that has seen relatively little prior investigation. This research is groundbreaking in that it marks the first investigation of the association between METS-VF and kidney stone development (24). This study provides crucial information on the possible link between the two conditions, as well as the potential consequences for diagnosing and treating kidney stones. In addition, this research may pave the way for further investigation into the correlation between METS-VF and kidney stone prevalence, potentially leading to better patient care (25). Despite this, our research has four significant drawbacks. To begin with, we took into account factors such as ethnicity, gender, educational attainment, matrimonial status, exercise routine, smoking habits, alcohol intake, blood pressure, and blood glucose levels to control for any confounding effects. It is possible that other yet-unidentified or unmeasured elements could impact the accuracy of METS-VF in predicting the likelihood of kidney stones. Additionally, it is difficult to accurately measure visceral fat with MRI or CT scans due to a lack of reliable data. Finally, because the number of participants in our research was limited, it is not clear if METS-VF can be used to anticipate the occurrence of kidney stones in other groups. Fourth, a cross-sectional study found no specific causal relationship between METS-VF and kidney stone prevalence.

Conclusion

Our research, taking into account a plethora of US population-related data, revealed an incredibly strong correlation between visceral fat metabolism index and the emergence and progression of kidney stones. Our research could offer novel approaches for the avoidance and management of kidney stones. Further exploration is essential to uncover the underlying causes of this phenomenon.

Data availability statement

The original contributions presented in the study are included in the article/supplementary material. Further inquiries can be directed to the corresponding authors.

Author contributions

ZG, GL, YC: Conceptualization, Methodology, Software. SS, SF: Visualization, Investigation. WW, YH: Writing - review and editing. All authors contributed to the article and approved the submitted version.

Funding

Supported by the National Natural Science Foundation of China (No.81900616, 82270737, 81970597) and the Youth Support Program of the First Affiliated Hospital of Anhui Medical University (2017kj13, 2778).

Acknowledgments

The authors thank the other members of the Department of Urology for their valuable support and helpful discussions. We

would also like to thank all participants and the National Health and Nutrition Examination Survey research team.

Conflict of interest

The authors declare that the research was conducted in the absence of any commercial or financial relationships that could be construed as a potential conflict of interest.

Publisher's note

All claims expressed in this article are solely those of the authors and do not necessarily represent those of their affiliated organizations, or those of the publisher, the editors and the reviewers. Any product that may be evaluated in this article, or claim that may be made by its manufacturer, is not guaranteed or endorsed by the publisher.

References

- Xua J-Z, Lia C, Xia Q-D, Lu J-L, Wan Z-C, Hu L, et al. Sex disparities and the risk of urolithiasis: a large cross-sectional study. *Ann Med* (2022) 54(1):1627–35. doi: 10.1080/07853890.2022.2085882
- Sun P, Liao S-G, Yang R-Q, Lu C-L, Ji K-L, Cao D-H, et al. Aspidopterys obcordate vine inulin fructan affects urolithiasis by modifying calcium oxalate crystallization. *Carbohydr Polym* (2022) 294:119777. doi: 10.1016/j.carbpol.2022.119777
- Sorokin I, Mamoulakis C, Miyazawa K, Rodgers A, Talati J, Lotan Y, et al. Epidemiology of stone disease across the world. *World J Urol* (2017) 35(9):1301–20. doi: 10.1007/s00345-017-2008-6
- Cha'on U, Tippayawat P, Saeung N, et al. High prevalence of chronic kidney disease and its related risk factors in rural areas of northeast Thailand. *Sci Rep* (2022) 12(1):18188s. doi: 10.1038/s41598-022-22538-w
- D'Ambrosio V, Ferraro PM, Lombardi G, Pinlaor P, Sirithanaphol W, Theeranut A, et al. Unravelling the complex relationship between diet and nephrolithiasis: the role of nutrigenomics and nutrigenetics. *Nutrients* (2022) 14(23):4961. doi: 10.3390/nu14234961
- Coel FL, Worcester EM, Evan AP. Idiopathic hypercalciuria and formation of calcium renal stones. *Nat Rev Nephrol* (2016) 12(9):519–33. doi: 10.1038/nrneph.2016.101
- Siener R, Ersten C, Bitterlich N, Altheld B, Metzner C. Effect of two different dietary weight loss strategies on risk factors for urinary stone formation and cardiometabolic risk profile in overweight women. *Nutrients* (2022) 14(23):5054. doi: 10.3390/nu14235054
- Holwerda SW, Gangwisha ME, Luehrs RE, Nuckols VR, Thyfault JP, Miles JM, et al. Concomitantly higher resting arterial blood pressure and transduction of sympathetic neural activity in human obesity without hypertension. *J Hypertens* (2023) 41(2):326–35. doi: 10.1097/HJH.0000000000003335
- Dierkes J, Dahl H, Welland NL, Sandnes K, Sæle K, Sekse I, et al. High rates of central obesity and sarcopenia in CKD irrespective of renal replacement therapy – an observational cross-sectional study. *BMC Nephrol* (2018) 19(1):259. doi: 10.1186/s12882-018-1055-6
- Song W, Hu H, Ni J, Zhang H, Zhang H, Yang G, et al. The relationship between ethylene oxide levels in hemoglobin and the prevalence of kidney stones in US adults: an exposure-response analysis from NHANES 2013–2016. *Environ Sci Pollut Res Int* (2022) 30(10):26357–66. doi: 10.1007/s11356-022-24086-2
- Bello-Chavolla OY, Antonio-Villa NE, Vargas-Vázquez A, Viveros-Ruiz TL, Almeda-Valdes P, Gomez-Velasco D, et al. Metabolic score for visceral fat (METS-VF), a novel estimator of intra-abdominal fat content and cardio-metabolic health. *Clin Nutr* (2020) 39(5):1613–21. doi: 10.1016/j.clnu.2019.07.012
- Faria MdS, Pimentel VE, Helaehil JV, Bertolo MC, Horas Santos NT, da Silva-Neto PV, et al. Caloric restriction overcomes pre-diabetes and hypertension induced by a high fat diet and renal artery stenosis. *Mol Biol Rep* (2022) 49:5883–95. doi: 10.1007/s11033-022-07370-9
- Feng L, Chen T, Wang X, Xiong C, Chen J, Wu S, et al. Metabolism score for visceral fat (METS-VF): a new predictive surrogate for CKD risk. *Diabetes Metab Syndr Obes* (2022) 15:2249–58. doi: 10.2147/DMSO.S370222
- Yun H-R, Kim H, Park JT, Chang TI, Yoo T-H, Kang S-W, et al. Obesity, metabolic abnormality, and progression of CKD. *Am J Kidney Dis* (2018) 72(3):400–10. doi: 10.1053/j.ajkd.2018.02.362
- Kang SH, Cho KH, Park JW, Yoon KW, Do JY. Association of visceral fat area with chronic kidney disease and metabolic syndrome risk in the general population: analysis using multifrequency bioimpedance. *Kidney Blood Press Res* (2015) 40(3):223–30. doi: 10.1159/000368498
- Kataoka ID H, Mochizuki T, Iwadoh K, Ushio Y, Kawachi K, Watanabe S, et al. Visceral to subcutaneous fat ratio as an indicator of $\geq 30\%$ eGFR decline in chronic kidney disease. *PLoS One* (2020) 15(11):e0241626. doi: 10.1371/journal.pone.0241626
- Kapoor N, Jiwanmalla SA, Nandyal MB, Kattula D, Paravathareddy S, Paul TV, et al. Metabolic score for visceral fat (METS-VF) estimation – a novel cost-effective obesity indicator for visceral adipose tissue estimation. *Diabetes Metab Syndr Obes* (2020) 16:13:3261–3267. doi: 10.2147/dms.o.s266277
- Hassapidou M, Vlassopoulos A, Kalliostra M, Govers E, Mulrooney H, Ellis L, et al. European Association for the study of obesity position statement on medical nutrition therapy for the management of overweight and obesity in adults developed in collaboration with the European federation of the associations of dietitians. *Obes Facts* (2022) 15:1–18. doi: 10.1159/000528083
- Key TJ, Papier K, Tong TYN. Plant-based diets and long-term health: findings from the EPIC-Oxford study. *Proc Nutr Soc* (2022) 81(2):190–8. doi: 10.1017/S0029665121003748
- Siener R, Metzner C. Dietary weight loss strategies for kidney stone patients. *World J Urol* (2023).
- Hall JE. The kidney, hypertension, and obesity. *Hypertension* (2003) 41(3 Pt 2):625–33. doi: 10.1161/01.HYP.0000052314.95497.78
- Dong B, Chen Y, Liu X, Wang Y, Wang F, Zhao Y, et al. Identification of compound mutations of SLC12A3 gene in a Chinese pedigree with gitelman syndrome exhibiting bartter syndrome-like phenotypes. *BMC Nephrol* (2020) 21(1):328. doi: 10.1186/s12882-020-01996-2
- Hall JE, Carmo JM, Silva AA, Wang Z, Hall ME. Obesity, kidney dysfunction, and hypertension: mechanistic links. *Nat Rev Nephrol* (2019) 15(6):367–85. doi: 10.1038/s41581-019-0145-4
- Yu P, Meng X, Kan R, Wang Z, Yu X. Association between metabolic scores for visceral fat and chronic kidney disease: a cross-sectional study. *Front Endocrinol (Lausanne)* (2022) 13:1052736. doi: 10.3389/fendo.2022.1052736
- Takahashi S, Yamamoto T, Tsutsumi Z, Moriwaki Y, Higashino K. Close correlation between visceral fat accumulation and uric acid metabolism in healthy men. *Metabolism* (1997) 46(10):1162–5. doi: 10.1016/S0026-0495(97)90210-9



OPEN ACCESS

EDITED BY

Guiting Lin,
University of California, San Francisco,
United States

REVIEWED BY

Yuxuan Song,
Peking University People's Hospital, China
Qiangqiang He,
Tsinghua University, China
Xiao-qiang Liu,
Tianjin Medical University General
Hospital, China
Hanping Shi,
Capital Medical University, China

*CORRESPONDENCE

Huihui Bao

✉ huihui_bao77@126.com

Xiaoshu Cheng

✉ xiaoshumenfan126@163.com

RECEIVED 19 March 2023

ACCEPTED 02 June 2023

PUBLISHED 21 June 2023

CITATION

Yuan T, Ding C, Xie Y, Zhou X, Xie C,
Wang T, Yu C, Zhou W, Zhu L, Bao H and
Cheng X (2023) Association between
remnant cholesterol and chronic kidney
disease in Chinese hypertensive patients.
Front. Endocrinol. 14:1189574.
doi: 10.3389/fendo.2023.1189574

COPYRIGHT

© 2023 Yuan, Ding, Xie, Zhou, Xie, Wang, Yu,
Zhou, Zhu, Bao and Cheng. This is an open-
access article distributed under the terms of
the [Creative Commons Attribution License \(CC BY\)](https://creativecommons.org/licenses/by/4.0/). The use, distribution or
reproduction in other forums is permitted,
provided the original author(s) and the
copyright owner(s) are credited and that
the original publication in this journal is
cited, in accordance with accepted
academic practice. No use, distribution or
reproduction is permitted which does not
comply with these terms.

Association between remnant cholesterol and chronic kidney disease in Chinese hypertensive patients

Ting Yuan^{1,2,3}, Congcong Ding^{1,2,3}, Yanyou Xie^{1,2,3},
Xinlei Zhou^{1,2,3}, Chong Xie^{1,2,3}, Tao Wang^{2,3,4}, Chao Yu^{2,3,4},
Wei Zhou^{2,3,4}, Lingjuan Zhu^{2,3,4}, Huihui Bao^{1,2,3,4*}
and Xiaoshu Cheng^{1,2,3,4*}

¹Department of Cardiology, The Second Affiliated Hospital of Nanchang University, Nanchang, Jiangxi, China, ²Center for Prevention and Treatment of Cardiovascular Diseases, The Second Affiliated Hospital of Nanchang University, Nanchang, Jiangxi, China, ³Jiangxi Provincial Cardiovascular Disease Clinical Medical Research Center, Nanchang, Jiangxi, China, ⁴Jiangxi Sub-center of National Clinical Research Center for Cardiovascular Diseases, Nanchang, Jiangxi, China

Background: Remnant cholesterol (RC) and chronic kidney disease (CKD) have not been definitively linked in individuals with different characteristics. This study aims to investigate the relationship between serum RC level and CKD and examine possible effect modifiers in Chinese patients with hypertension.

Methods: Our study is based on the Chinese H-type Hypertension Project, which is an observational registry study conducted in real-world settings. The outcome was CKD, defined as an estimated glomerular filtration rate of less than 60 ml/min·1.73 m². Multivariate logistic regression and smooth curve fitting were used to analyze the association between RC and CKD. Subgroup analyses were subsequently conducted to examine the effects of other variables.

Results: The mean age of the 13,024 patients with hypertension at baseline was 63.8 ± 9.4 years, and 46.8% were male. A conspicuous linear positive association was observed between RC level and CKD (per SD increment; odds ratio [OR], 1.15; 95% confidence interval [CI], 1.08–1.23). Compared with the lowest quartile group of RC, the risk of CKD was 53% higher (OR, 1.53; 95% CI, 1.26–1.86) in the highest quartile group. Furthermore, a stronger positive association between RC level and CKD was found among participants with a higher body mass index (BMI <24 vs. ≥24 kg/m²; *P*-interaction = 0.034) or current non-smokers (smoker vs. non-smoker; *P*-interaction = 0.024).

Conclusions: Among Chinese adults with hypertension, RC level was positively associated with CKD, particularly in those with a BMI of ≥24 kg/m² and current non-smokers. These findings may help improve lipid management regimens in patients with hypertension.

KEYWORDS

remnant cholesterol, chronic kidney disease, Chinese hypertensive population, cross-sectional study, lipid metabolism

1 Introduction

Chronic kidney disease (CKD) has high morbidity and mortality, particularly among people with diabetes and hypertension (1). By 2040, CKD is predicted to become the fifth leading cause of mortality worldwide (2). Common factors promoting the occurrence and development of CKD include diabetes, hypertension, dyslipidemia, and smoking (3). Lipid metabolism disorders are common in patients with CKD. Previous studies have shown various lipid concentrations and structural changes, including higher triglyceride (TG) levels, in patients with CKD (4, 5). Nevertheless, most of the existing research is focused on traditional lipid profiles.

Remnant cholesterol (RC) is a recently described lipid indicator. It is the cholesterol component of triglyceride-rich lipoproteins, consisting of cholesterol cargo of very low-density lipoprotein (VLDL) and medium-density lipoprotein (IDL) in the fasting state and chylomicron (CM) remnants in the non-fasting state (6). Previous research has shown that recurrent atherosclerotic cardiovascular disease (ASCVD) can occur even when the low-density lipoprotein cholesterol (LDL-C) concentration is reduced to an optimal level. This residual risk is believed to be caused by remnant cholesterol (RC) (7, 8). As a new cholesterol index, in the past ten years, RC has been confirmed by extensive research to be related to the initiation and progression of atherosclerosis and ASCVD (9–11).

Previous studies have demonstrated inconsistent results regarding the association between RC levels and CKD. Some studies have shown that elevated levels of RC or its components (comprising VLDL and IDL cholesterol) are associated with an increased risk of CKD, whereas others have not found this association. However, the hypertensive population is unique and is a high-risk subgroup for CKD. A discussion of the relationship between RC and CKD in patients with hypertension may provide a new direction for lipid management in populations with hypertension in the future. Therefore, the association between RC levels and CKD risk in a Chinese population with hypertension needs to be assessed.

2 Materials and methods

2.1 Study population and design

This cross-sectional study used observational data from the Chinese hypertension Registry. The study was conducted in July 2018 in Wuyuan, Jiangxi Province, China. A total of 14,268 participants aged ≥ 18 years were included after excluding those who were unable to provide informed consent or failed to complete follow-up for various reasons. Patients with hypertension are defined as those with systolic blood pressure (SBP) ≥ 140 mmHg and/or diastolic blood pressure (DBP) ≥ 90 mmHg with a previous diagnosis of hypertension or currently taking antihypertensive medication. This study was approved by the Ethics Committee of the Biomedical Institute of Anhui Medical University, and written informed consent was obtained from all study participants.

Among the 14,268 participants, we excluded those without hypertension ($n = 34$), those with missing data for total cholesterol (TC), high-density lipoprotein cholesterol (HDL-C), LDL-C ($n = 7$), use of lipid-lowering drugs ($n = 506$), and individuals with extreme values of RC ($n = 697$). Ultimately, 13,024 participants were included in the final analysis (Figure S1).

2.2 Data collection

We collected basic information on all the participants, including sex, age, height, weight, waist circumference (WC), drinking status, and smoking status. All blood samples were collected by professionals to examine fasting TC, TG, HDL-C, LDL-C, aspartate aminotransferase (AST), alanine transaminase (ALT), plasma homocysteine (Hcy), fasting blood glucose (FBG), and serum creatinine levels. All parameters were tested using a professional instrument (Beckman Coulter) at the Biaojia Biotechnology Laboratory, Shenzhen, China.

Based on the previous description, the RC was calculated as $RC = TC - (HDL-C) - (LDL-C)$. CKD was defined as an estimated glomerular filtration rate (eGFR) of less than $60 \text{ ml/min-1.73 m}^2$. The eGFR was calculated according to the Chronic Kidney Disease Epidemiology Collaboration (12). Body mass index (BMI) was calculated by dividing the weight by the square of height.

2.3 Covariates

The selected covariates related to CKD included sex, age, WC, BMI, DBP, drinking status, smoking status, SBP, Hcy, TG, diabetes, coronary heart disease (CAD), stroke, and use of antihypertensive drugs.

2.4 Statistical analysis

For continuous variables, we used means with standard deviations (SDs) or median (interquartile range), and categorical variables included the characteristics of the study population (percentages). To demonstrate the relationship between RC levels and CKD more intuitively, we used a generalized additive model and smooth curve fitting (penalty-spline method). Multivariate logistic regression was used to evaluate the odds ratios (ORs) and 95% confidence intervals (CIs) for CKD in RC (as a continuous variable and quartiles). We established two models in which the fully adjusted model (Model II) was adjusted for sex, age, WC, BMI, drinking status, smoking status, SBP, DBP, diabetes, CAD, stroke, antihypertensive drugs, Hcy, and TG. Subgroup and interaction analyses were used to further explore the potential effect modifiers. A sensitivity analysis was performed to confirm the robustness of the relationship between RC levels and CKD. All statistical analyses were performed using the statistical package R (<http://www.R-project.org>) and EmpowerStats (<http://www.empowerstats.com>, X&Y Solutions, Inc., Boston, MA), and a two-tailed $P < 0.05$ was considered statistically significant.

3 Results

3.1 Baseline characteristics of the study population

The baseline characteristics of the 13,024 participants are described in [Table 1](#). Overall, their average age was 63.8 ± 9.4 years, and 6,099 participants were male, accounting for 46.8%. The baseline characteristics of the study participants were stratified according to RC quartiles. The RC ranges for the quartiles were ≤ 0.41 mmol/L, 0.41–0.63 mmol/L, 0.63–0.83 mmol/L, and ≥ 0.83 mmol/L. Compared with the lowest quartile of RC, the population in the highest quartile mostly comprised older female participants who did not smoke or drink at the time and were more likely to have a history of diabetes mellitus. The values of BMI, WC, TC, SBP, LDL-C, FBG, TG, and UA were also higher. HDL-C level and eGFR were lower, and a smaller proportion of people took antihypertensive drugs.

3.2 Association between RC and CKD

As shown in [Table 2](#), multiple logistic regression models were constructed to assess the association between RC levels and CKD, and a positive association was observed. In a complete adjustment model, which adjusted for sex, age, WC, SBP, BMI, DBP, smoking status, drinking status; Hcy, TG, diabetes, stroke, CAD, and antihypertensive drugs, for each SD increment in RC, the risk of CKD increased by 15% (adjusted OR, 1.15; 95% CI: 1.08–1.23). Consistently, when serum RC level was assessed as quartiles, compared with the Q1, the adjusted ORs in the Q2, Q3, and Q4 were 1.12 (95% CI: 0.95–1.53), 1.15 (95% CI: 0.95–1.39), and 1.53 (95% CI: 1.26–1.86), respectively. Our research also found that compared with RC level <0.83 mmol/L, RC level ≥ 0.83 mmol/L significantly increased the risk of CKD, (OR, 1.40; 95% CI: 1.21–1.62). In addition, we used a generalized additive model and smooth curve fitting (penalized spline method) to represent the association between RC levels and CKD. As shown in [Figure 1](#), a linear relationship ($P = 0.007$) was observed between RC levels and CKD. We also analyzed the association between RC levels and eGFR. Moreover, the RC level was negatively associated with the eGFR. Further multiple linear regression analysis showed that for every SD increment in RC, eGFR decreased by $1.97 \text{ ml/min} \cdot 1.73 \text{ m}^2$ (95% CI: -2.29 to -1.65). Compared with the lowest quartile of RC, the eGFR of participants in the highest quartile decreased significantly ($\beta = -6.35$, 95% CI: -7.20 to -5.51) ([Table S1](#)).

3.3 Subgroup analyses

To further explore the possible effect of modifiers on the relationship between RC levels and CKD, we performed a stratified analysis. In [Figure 2](#), the association between RC level and increased CKD risk is significantly stronger in the subgroup of patients with BMI $\geq 24 \text{ kg/m}^2$ than in those with BMI $<24 \text{ kg/m}^2$ and in non-smoking participants than in smoking patients

(interaction $P=0.034$, 0.024 respectively). In participants with BMI $\geq 24 \text{ kg/m}^2$, for every unit increment in RC, the risk of CKD increased by 73% (OR, 1.73; 95% CI: 1.33–2.24; $P = 0.034$). Similarly, in current non-smokers, every additional unit of RC increased the risk of CKD by 60% (OR, 1.60; 95% CI: 1.32–1.95). However, sex, age, SBP, DBP, alcohol consumption status, diabetes, and antihypertensive drug use did not significantly modify the relationship between RC levels and CKD.

3.4 Sensitivity analysis

Owing to the close association between the RC and TG levels, the concentration of RC increased with an increase in the TG level ([9](#), [13](#)). Therefore, we carried out the sensitivity analysis, which explored the relationship between RC levels and CKD in populations with hypertension and normal TG levels. In [Table S2](#), for each SD increment in RC, the risk of CKD increases by 11% (OR, 1.11; 95% CI: 1.02–1.19). Compared with Q1, the adjusted ORs in Q2, Q3, and Q4 were 1.17 (95% CI: 0.92–1.49), 1.11 (95% CI: 0.87–1.41), and 1.42 (95% CI: 1.12–1.79), respectively. In the previous analysis, given that RC was calculated from TC, LDL-C, and HDL-C, no adjustments were made in the model, but their collinearity with RC was considered to be large. In order to verify whether the relationship between RC and CKD obtained in this study is independent of traditional lipid indexes, residual analysis was conducted ([Table S3](#)). The positive association between RC and CKD risk still exists after adjusting for TC residuals, LDL-C residuals, and HDL-C residuals. This shows that the relationship between RC and CKD is independent of traditional lipid indexes.

4 Discussion

In this study, we found that the RC level was positively associated with the risk of CKD in a Chinese population with hypertension. This positive association was only significant in patients with BMI $\geq 24 \text{ kg/m}^2$ who did not smoke, not in those with BMI $<24 \text{ kg/m}^2$ who smoked. These findings suggest that BMI and smoking status are significant effect modifiers.

Previous studies have indicated that dyslipidemia is related to renal insufficiency ([14](#), [15](#)); however, most are limited to traditional lipid indices, such as TG and HDL-C ([16](#), [17](#)). Few studies have investigated the relationship between unconventional lipid profiles and kidney disease. Qi et al. ([18](#)) designed a prospective cohort study of 3,909 participants with normal eGFR and a baseline age of ≥ 40 years, and the results showed that elevated blood lipid levels during follow-up increased the risk of eGFR decline. Higher RC levels are associated with the early progression of renal injuries. A cross-sectional study conducted by Marcelino et al. ([19](#)) involving 395 non-diabetic individuals who did not receive statins showed that the RC level of patients with CKD increased and was positively associated with the CKD stage. A cross-sectional study of 146 participants with type 2 diabetes at different CKD stages showed that lower renal function was associated with increased concentrations of CM, VLDL, or both ([20](#)). Apolipoprotein (apo) B48 is a specific marker of CM. A

TABLE 1 Characteristics of study participants by RC.

Variables	Total	RC, mmol/L				P value
		Q1 (<0.41)	Q2 (0.41-0.63)	Q3 (0.63-0.83)	Q4 (≥0.83)	
N	13024	3150	3319	3205	3350	
Age, years	63.8 ± 9.4	63.9 ± 9.1	63.7 ± 9.6	64.1 ± 9.3	63.4 ± 9.6	0.037
Male, n (%)	6099 (46.8)	1628 (51.7)	1722 (51.9)	1436 (44.8)	1313 (39.2)	<0.001
BMI, kg/m2	23.6 ± 3.7	23.3 ± 4.4	23.4 ± 3.5	23.7 ± 3.5	24.0 ± 3.5	<0.001
WC, cm	83.8 ± 9.8	82.9 ± 10.0	83.4 ± 9.7	84.1 ± 9.8	84.8 ± 9.8	<0.001
SBP, mmHg	148.5 ± 17.8	149.3 ± 17.7	147.7 ± 17.8	147.8 ± 17.6	149.4 ± 18.1	<0.001
DBP, mmHg	89.1 ± 10.8	88.8 ± 10.6	88.9 ± 10.8	89.0 ± 10.7	89.5 ± 11.0	0.095
Education status, n (%)						0.014
Primary school graduate or below	8571 (80.0)	1509 (80.7)	2216 (78.6)	2376 (80.5)	2470 (80.3)	
Middle/high/special school	2088 (19.5)	356 (19.0)	579 (20.5)	568 (19.2)	585 (19.0)	
College graduate or above	58 (0.5)	6 (0.3)	24 (0.9)	7 (0.2)	21 (0.7)	
Current smoking, n (%)	3335 (25.6)	865 (27.5)	905 (27.3)	790 (24.7)	775 (23.1)	<0.001
Current alcohol drinking, n (%)	2817 (21.6)	757 (24.0)	730 (22.0)	649 (20.3)	681 (20.3)	<0.001
Laboratory results						
Total cholesterol, mmol/L	5.2 ± 1.1	4.7 ± 1.0	4.9 ± 0.9	5.3 ± 0.9	6.0 ± 1.1	<0.001
Triglycerides, mmol/L	1.8 ± 1.3	1.3 ± 0.6	1.5 ± 0.8	1.8 ± 1.0	2.6 ± 1.8	<0.001
HDL-C, mmol/L	1.6 ± 0.4	1.7 ± 0.4	1.6 ± 0.4	1.5 ± 0.4	1.5 ± 0.4	<0.001
LDL-C, mmol/L	3.0 ± 0.8	2.8 ± 0.8	2.8 ± 0.7	3.1 ± 0.7	3.3 ± 0.9	<0.001
Fasting glucose, mmol/L	6.2 ± 1.6	6.0 ± 1.3	6.0 ± 1.3	6.2 ± 1.6	6.6 ± 2.0	<0.001
Total homocysteine, μmol/L	15.0 (12.4-19.1)	15.2 (12.6-19.4)	14.8 (12.4-19.0)	14.8 (12.4-19.0)	15.0 (12.5-18.8)	0.054
Uric acid, μmol/L	420.0 ± 121.0	397.4 ± 113.4	415.6 ± 118.3	421.9 ± 122.8	443.9 ± 124.6	<0.001
eGFR, ml/min/1.73 m²	88.3 ± 20.1	91.4 ± 20.6	88.5 ± 19.8	87.4 ± 19.3	86.0 ± 20.2	<0.001
History of disease						
Diabetes mellitus, n (%)	2341 (18.0)	453 (14.4)	474 (14.3)	570 (17.8)	844 (25.2)	<0.001
Coronary heart disease, n (%)	609 (4.7)	129 (4.1)	147 (4.4)	150 (4.7)	183 (5.5)	0.058
Stroke, n (%)	788 (6.1)	197 (6.3)	211 (6.4)	180 (5.6)	200 (6.0)	0.598
Medication use, n (%)						
Antihypertensive drugs	8298 (63.7)	2107 (66.9)	2101 (63.3)	1980 (61.8)	2110 (63.0)	<0.001
Glucose-lowering drugs	635 (4.9)	147 (4.7)	137 (4.1)	155 (4.8)	196 (5.9)	0.011
Antiplatelet drugs	289 (2.2)	72 (2.3)	76 (2.3)	71 (2.2)	70 (2.1)	0.94

Data are expressed as mean ± SD or median (interquartile range) and numbers (percentage) as appropriate.
RC, remnant cholesterol; BMI, body mass index; WC, waist circumference; SBP, systolic blood pressure; DBP, diastolic blood pressure; eGFR, estimated glomerular filtration rate; HDL-C, high-density lipoprotein cholesterol; LDL-C, low-density lipoprotein cholesterol.

study of 101 participants with diabetic nephropathy of different stages showed that plasma apob48 levels increased with the progression of diabetic nephropathy (21). In contrast, a prospective cohort study by Rahman et al. showed no independent association between VLDL cholesterol levels and kidney disease progression (22). Some of these results were consistent with our conclusions, whereas others were not. The reason for this may be the different selections of race, population, and sample sizes. Yan et al. (23) conducted a cross-sectional study of

7,356 participants aged ≥40 years in China showing that a higher RC level is an independent risk factor for CKD (OR: 1.344, 95% CI: 1.097–1.648). This result is mostly consistent with the results of our study. However, as a high-risk group for CKD, patients with hypertension need to be considered as a special population to analyze the relationship between RC levels and CKD. Previous studies have confirmed that RC is a powerful lipid component that promotes atherosclerosis, and RC can act on the arterial wall through

TABLE 2 Association between RC and CKD in different models.

RC, mmol/L	Participants, n	Events, n (%)	Crude model		Model I		Model II	
			OR (95% CI)	P value	OR (95% CI)	P value	OR (95% CI)	P value
RC Z score	13024	1243 (9.5)	1.14 (1.09, 1.21)	<0.001	1.20 (1.13, 1.27)	<0.001	1.15 (1.08, 1.23)	<0.001
Quartiles								
Q1 (<0.41)	3150	257 (8.2)	Ref.		Ref.		Ref.	
Q2 (0.41-0.63)	3319	299 (9.0)	1.11 (0.94, 1.33)	0.223	1.12 (0.93, 1.34)	0.212	1.12 (0.93, 1.35)	0.245
Q3 (0.63-0.83)	3205	297 (9.3)	1.15 (0.97, 1.37)	0.118	1.17 (0.97, 1.40)	0.092	1.15 (0.95, 1.39)	0.156
Q4 (\geq 0.83)	3350	390 (11.6)	1.48 (1.26, 1.75)	<0.001	1.68 (1.41, 2.00)	<0.001	1.53 (1.26, 1.86)	<0.001
P for trend				<0.001		<0.001		<0.001
Categories								
Q1-Q3 (<0.83)	9674	853 (8.8)	Ref.		Ref.		Ref.	
Q4 (\geq 0.83)	3350	390 (11.6)	1.36 (1.20, 1.55)	<0.001	1.53 (1.34, 1.75)	<0.001	1.40 (1.21, 1.62)	<0.001

Crude model was adjusted for None; Model I was adjusted for age, sex, BMI, WC; Model II was adjusted for age, sex, BMI, WC, SBP, DBP, TG, smoking status, alcohol drinking status, Hcy, diabetes, stroke, coronary heart disease, antihypertensive drugs.

RC, remnant cholesterol; OR, odd ratio; 95% CI, 95% confidence interval, TG, triglycerides; Hcy, homocysteine.

oxidative stress and low-grade inflammation, resulting in endothelial dysfunction and atherosclerosis, which can lead to the development of ASCVD and CKD (6, 24, 25). Although previous studies have discussed the relationship between RC levels and CKD, no study has investigated this association in populations with hypertension.

As a risk factor for CKD, a high TG level is related to the occurrence and progression of CKD. Hypertriglyceridemia is the prevalent feature of lipid metabolism disorders in patients with CKD. Therefore, we investigated the relationship between RC levels and CKD under normal TG levels and concluded that even if the TG level was normal, an increase in RC level was independently and positively associated with the risk of CKD. In further subgroup analysis, the positive association was more significant for people with BMI ≥ 24 kg/m² (Figure S2).

In addition, we found that BMI and smoking status significantly modified the relationship between RC levels and CKD in a Chinese

population with hypertension. With the increase in RC levels, participants with BMI ≥ 24 kg/m² who did not smoke had a greater risk of CKD. For overweight or obese populations, the possible mechanisms are as follows. First, obesity can cause abnormal lipid metabolism in the human body, including an increase in TG concentration (26). This will increase the RC level and, thus, the risk of CKD. Second, being overweight or obese is a risk factor for developing CKD (27). Its impacts on renal function may be associated with comorbidities, such as diabetes or hypertension. However, it also leads to inflammation, oxidative stress, activation of the renal angiotensin-aldosterone system, and insulin resistance through the production of hormones, such as adiponectin, leptin, and resistin, resulting in increased glomerular hypertension and permeability, and ultimately, CKD (28–30). In previous studies, the effect of smoking on eGFR was unclear. Some studies have suggested that smoking is negatively correlated with

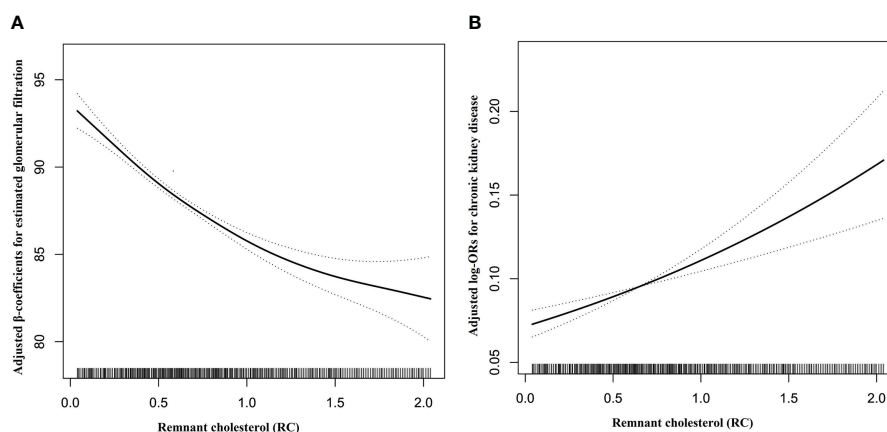


FIGURE 1

Dose-response relationships between RC and the risk of eGFR decline (A) and CKD (B). Adjustment factors included age, sex, BMI, WC, SBP, DBP, TG, smoking status, drinking status, Hcy, diabetes, stroke, coronary heart disease, and antihypertensive drugs at baseline.

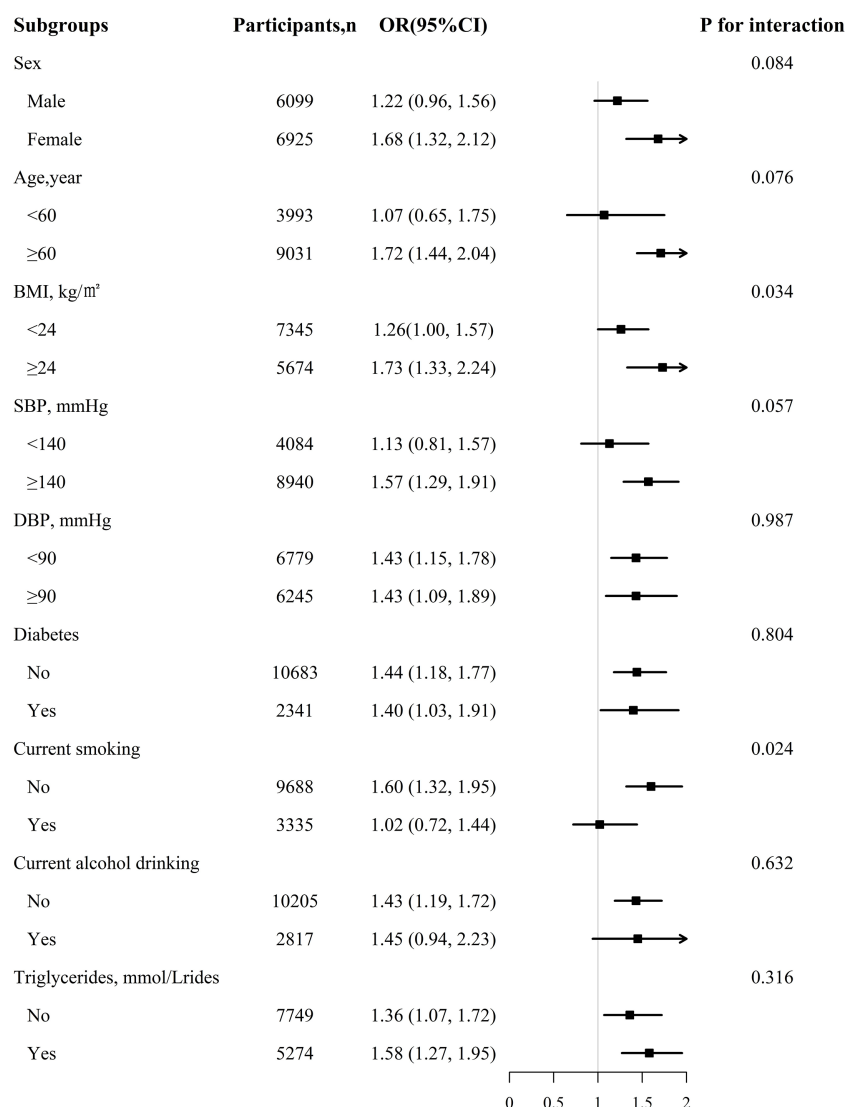


FIGURE 2

The association between RC and CKD in various subgroups. Each subgroup analysis adjusted, if not stratified, for age, sex, BMI, WC, SBP, DBP, TG, smoking status, drinking status, Hcy, diabetes, stroke, coronary heart disease, antihypertensive drugs at baseline.

eGFR, whereas others have suggested that smoking could increase eGFR (31–33). In our study, CKD was defined as eGFR less than 60 ml/min·1.73 m²; therefore, current non-smokers had a higher risk of CKD because non-smokers had lower eGFR values than smokers. This may be because of the following mechanisms. First, previous literature reviews have shown that current smokers tend to weigh less than non-smokers. It is well known that the source of creatinine in serum is muscle cells; therefore, in earlier studies, it was also found that the serum creatinine content in smokers was low (34, 35). However, the lower serum creatinine level in smokers may not simply be explained by the fact that smokers have less body fat and muscle mass, as the lower serum creatinine level remains even after adjusting for BMI (36). Consequently, smokers may have increased creatinine excretion, thereby increasing the eGFR (37). Second, smoking causes recurrent transient decreases in renal plasma flow and eGFR. This small recurrent transient renal hypoperfusion may damage some glomeruli and, thus, lead to aging of the peritubular

blood vessels and glomeruli and result in residual glomerular compensatory hypertrophy and hyperfiltration, ultimately leading to an elevated eGFR (38, 39). However, this compensatory increase in eGFR is limited, and as smoking volume and duration increase, renal function will eventually be severely impaired. In addition, previous studies have confirmed that smoking can damage kidney function. Perhaps, when smoking seriously damages kidney function (40, 41), the damage caused by increased RC on kidney function is not obvious. However, no definitive conclusions have been drawn regarding the effect of smoking on eGFR. According to existing research results, we believe that smokers have an increased compensatory eGFR in the early stages and a downward trend in eGFR in the latter stages owing to the aggravated impairment of renal function. Further research is required to explore this relationship in detail.

As a lipid index, RC has been studied more in cardiovascular diseases; however, studies on the relationship between RC levels and

CKD have not received much attention in the past, let alone in individuals with hypertension. The guideline of the European Atherosclerosis Association (42) defines a high RC level as a fasting RC level ≥ 0.8 mmol/L and/or postprandial RC level ≥ 0.9 mmol/L; however, our research found that RC level ≥ 0.83 mmol/L significantly increased the risk of CKD, (OR, 1.40; 95% CI: 1.21–1.62), which suggests that reducing RC levels below 0.8 can reduce the risk of cardiovascular disease and CKS in both the general population and the population with hypertension. In our future clinical studies, we aim to calculate the value of RC levels using a simple formula and evaluate whether further lipid-lowering treatments are required. Whether a further reduction in RC levels can reduce the incidence rate requires further prospective research.

5 Study strengths and limitations

To the best of our knowledge, this is the first study to investigate the association between RC levels and CKD in a Chinese population with hypertension. However, this study has several limitations. First, we could not establish a causal relationship between RC levels and CKD because of the cross-sectional nature of the study. Second, the study population included participants with hypertension from rural areas of southern China who were aged over 18 years. Therefore, the results of this study cannot be generalized to individuals of other ages, regions, or disease types.

6 Conclusion

In the present study, we observed an independent positive association between elevated RC levels and CKD risk in a Chinese population with hypertension. This relationship seems to be more significant in patients with BMI ≥ 24 kg/m² and current non-smokers. RC ≥ 0.83 mmol/L seems to be a rough cut-off point, which can be used to suggest that patients with hypertension need further lipid-lowering treatment. However, further studies are required to verify this. Our results are significant for clinical lipid management in patients with hypertension.

Data availability statement

The raw data supporting the conclusions of this article will be made available by the authors, without undue reservation.

Ethics statement

The studies involving human participants were reviewed and approved by the ethics committee of the Institute of biomedical research of Anhui Medical University. The patients/participants provided their written informed consent to participate in this study.

Author contributions

TY, HB, and XC conceived and designed the study. TY, CD, and YX contributed to statistical analysis. TY drafted the manuscript. All authors contributed to the data collection and reviewed/edited the manuscript's important intellectual content. All authors contributed to the article and approved the submitted version.

Funding

This work was supported by the Cultivation of backup projects for National Science and Technology Awards (20223AEI91007), Jiangxi Science and Technology Innovation Base Plan - Jiangxi Clinical Medical Research Center (20223BCG74012), Science and Technology Innovation Base Construction Project (20221ZDG02010), Jiangxi Science and Technology Innovation Platform Project (20165BCD41005), Jiangxi Provincial Natural Science Foundation (20212ACB206019, 20224BAB206090), Key R&D Projects, Jiangxi (20203BBGL73173), Jiangxi Provincial Health Commission Science and Technology Project (202130440, 202210495, 202310528), Jiangxi Provincial Drug Administration Science and Technology Project (2022JS41), Fund project of the Second Affiliated Hospital of Nanchang University (2016YNQN12034, 2019YNLZ12010, 2021efyA01, 2021YNFY2024).

Acknowledgments

Thanks to all the investigators and subjects who participated in the China Hypertension Registry Study.

Conflict of interest

The authors declare that the research was conducted in the absence of any commercial or financial relationships that could be construed as a potential conflict of interest.

Publisher's note

All claims expressed in this article are solely those of the authors and do not necessarily represent those of their affiliated organizations, or those of the publisher, the editors and the reviewers. Any product that may be evaluated in this article, or claim that may be made by its manufacturer, is not guaranteed or endorsed by the publisher.

Supplementary material

The Supplementary Material for this article can be found online at: <https://www.frontiersin.org/articles/10.3389/fendo.2023.1189574/full#supplementary-material>

SUPPLEMENTARY FIGURE 1
Flow chart of participants.

References

- Kalantar-Zadeh K, Jafar TH, Nitsch D, Neuen BL, Perkovic V. Chronic kidney disease. *Lancet* (2021) 398(10302):786–802. doi: 10.1016/S0140-6736(21)00519-5
- Foreman KJ, Marquez N, Dolgert A, Fukutaki K, Fullman N, McGaughey M, et al. Forecasting life expectancy, years of life lost, and all-cause and cause-specific mortality for 250 causes of death: reference and alternative scenarios for 2016–40 for 195 countries and territories. *Lancet* (2018) 392(10159):2052–90. doi: 10.1016/S0140-6736(18)31694-5
- Webster AC, Nagler EV, Morton RL, Masson P. Chronic kidney disease. *Lancet* (2017) 389(10075):1238–52. doi: 10.1016/S0140-6736(16)32064-5
- Bowe B, Xie Y, Xian H, Balasubramanian S, Al-Aly Z. Low levels of high-density lipoprotein cholesterol increase the risk of incident kidney disease and its progression. *Kidney Int* (2016) 89(4):886–96. doi: 10.1016/j.kint.2015.12.034
- Harper CR, Jacobson TA. Managing dyslipidemia in chronic kidney disease. *J Am Coll Cardiol* (2008) 51(25):2375–84. doi: 10.1016/j.jacc.2008.03.025
- Sandesara PB, Virani SS, Fazio S, Shapiro MD. The forgotten lipids: triglycerides, remnant cholesterol, and atherosclerotic cardiovascular disease risk. *Endocr Rev* (2019) 40(2):537–57. doi: 10.1210/er.2018-00184
- Mora S, Wenger NK, Demicco DA, Breazna A, Boekholdt SM, Arsenault BJ, et al. Determinants of residual risk in secondary prevention patients treated with high- versus low-dose statin therapy: the treating to new targets (TNT) study. *Circulation* (2012) 125(16):1979–87. doi: 10.1161/CIRCULATIONAHA.111.088591
- Furchart JC, Sacks FM, Hermans MP, Assmann G, Brown WV, Ceska R, et al. The residual risk reduction initiative: a call to action to reduce residual vascular risk in dyslipidaemic patient. *Diabetes Vasc Dis Res* (2008) 5(4):319–35. doi: 10.3132/dvdr.2008.046
- Varbo A, Benn M, Tybjaerg-Hansen A, Jørgensen AB, Frikke-Schmidt R, Nordestgaard BG, et al. Remnant cholesterol as a causal risk factor for ischemic heart disease. *J Am Coll Cardiol* (2013) 61(4):427–36. doi: 10.1016/j.jacc.2012.08.1026
- Castañer O, Pínto X, Subirana I, Amor AJ, Ros E, Hernáez Á, et al. Remnant cholesterol, not LDL cholesterol, is associated with incident cardiovascular disease. *J Am Coll Cardiol* (2020) 76(23):2712–24. doi: 10.1016/j.jacc.2020.10.008
- Burnett JR, Hooper AJ, Hegde RA. Remnant cholesterol and atherosclerotic cardiovascular disease risk. *J Am Coll Cardiol* (2020) 76(23):2736–9. doi: 10.1016/j.jacc.2020.10.029
- Zhai Q, Dou J, Wen J, Wang M, Zuo Y, Su X, et al. Association between changes in lipid indexes and early progression of kidney dysfunction in participants with normal estimated glomerular filtration rate: a prospective cohort study. *Endocrine* (2022) 76(2):312–23. doi: 10.1007/s12020-022-03012-z
- Bermudez-Lopez M, Forne C, Amigo N, Bozic M, Arroyo D, Bretones T, et al. An in-depth analysis shows a hidden atherogenic lipoprotein profile in non-diabetic chronic kidney disease patients. *Expert Opin Ther Targets* (2019) 23(7):619–30. doi: 10.1080/14728222.2019.1620206
- Sonoda M, Shoji T, Kimoto E, Okute Y, Shima H, Naganuma T, et al. Kidney function, cholesterol absorption and remnant lipoprotein accumulation in patients with diabetes mellitus. *J Atheroscl Thromb* (2014) 21(4):346–54. doi: 10.5551/jat.20594
- Hayashi T, Hirano T, Taira T, Tokuno A, Mori Y, Koba S, et al. Remarkable increase of apolipoprotein B48 level in diabetic patients with end-stage renal disease. *Atherosclerosis* (2008) 197(1):154–8. doi: 10.1016/j.atherosclerosis.2007.03.015
- Rahman M, Yang W, Akkina S, Alper A, Anderson AH, Appel LJ, et al. Relation of serum lipids and lipoproteins with progression of CKD: the CRIC study. *Clin J Am Soc Nephrol* (2014) 9(7):1190–8. doi: 10.2215/CJN.09320913
- Levey AS, Stevens LA, Schmid CH, Zhang YL, Castro AF 3rd, Feldman HI, et al. A new equation to estimate glomerular filtration rate. *Ann Intern Med* (2009) 150(9):604–12. doi: 10.7326/0003-4819-150-9-200905050-00006
- Vaziri ND. Dyslipidemia of chronic renal failure: the nature, mechanisms, and potential consequences. *Am J Physiology-Renal Physiol* (2006) 290(2):F262–72. doi: 10.1152/ajprenal.00099.2005
- Noels H, Lehrke M, Vanholder R, Jankowski J. Lipoproteins and fatty acids in chronic kidney disease: molecular and metabolic alterations. *Nat Rev Nephrol* (2021) 17(8):528–42. doi: 10.1038/s41581-021-00423-5
- Kwan BCH, Kronenberg F, Beddhu S, Cheung AK. Lipoprotein metabolism and lipid management in chronic kidney disease. *J Am Soc Nephrol* (2007) 18(4):1246–61. doi: 10.1681/ASN.2006091006
- Navaneethan SD, Schold JD, Arrigain S, Thomas G, Jolly SE, Poggio ED, et al. Serum triglycerides and risk for death in stage 3 and stage 4 chronic kidney disease. *Nephrol Dialysis Transplant* (2012) 27(8):3228–34. doi: 10.1093/ndt/gfs058
- Zewinger S, Speer T, Kleber ME, Scharnagl H, Woitas R, Lepper PM, et al. HDL cholesterol is not associated with lower mortality in patients with kidney dysfunction. *J Am Soc Nephrol* (2014) 25(5):1073–82. doi: 10.1681/ASN.2013050482
- Yan P, Xu Y, Miao Y, Bai X, Wu Y, Tang Q, et al. Association of remnant cholesterol with chronic kidney disease in middle-aged and elderly Chinese: a population-based study. *Acta Diabetologica* (2021) 58(12):1615–25. doi: 10.1007/s00592-021-01765-z
- Varbo A, Benn M, Tybjaerg-Hansen A, Nordestgaard BG. Elevated remnant cholesterol causes both low-grade inflammation and ischemic heart disease, whereas elevated low-density lipoprotein cholesterol causes ischemic heart disease without inflammation. *Circulation* (2013) 128(12):1298–309. doi: 10.1161/CIRCULATIONAHA.113.003008
- Varbo A, Nordestgaard BG. Remnant cholesterol and triglyceride-rich lipoproteins in atherosclerosis progression and cardiovascular disease. *Arteriosclerosis Thrombosis Vasc Biol* (2016) 36(11):2133–5. doi: 10.1161/ATVBAHA.116.308305
- Franssen R, Monajemi H, Stroes ES, Kastelein JJ. Obesity and dyslipidemia. *Med Clin North America* (2011) 95(5):893–902. doi: 10.1016/j.mcna.2011.06.003
- de Vries APJ, Ruggerenti P, Ruan XZ, Praga M, Cruzado JM, Bajema IM, et al. Fatty kidney: emerging role of ectopic lipid in obesity-related renal disease. *Lancet Diabetes Endocrinol* (2014) 2(5):417–26. doi: 10.1016/S2213-8587(14)70065-8
- Kovesdy CP, Furth SL, Zoccali C. Obesity and kidney disease: hidden consequences of the epidemic. *Kidney Int* (2017) 91(2):260–2. doi: 10.1016/j.kint.2016.10.019
- Wahba IM, Mak RH. Obesity and obesity-initiated metabolic syndrome: mechanistic links to chronic kidney disease. *Clin J Am Soc Nephrol* (2007) 2(3):550–62. doi: 10.2215/CJN.04071206
- Xu T, Sheng Z, Yao L. Obesity-related glomerulopathy: pathogenesis, pathologic, clinical characteristics and treatment. *Front Med* (2017) 11(3):340–8. doi: 10.1007/s11684-017-0570-3
- Ishizaka N, Ishizaka Y, Toda E, Shimomura H, Koike K, Seki G, et al. Association between cigarette smoking and chronic kidney disease in Japanese men. *Hypertens Res* (2008) 31(3):485–92. doi: 10.1291/hypres.31.485
- Yoon H, Park M, Yoon H, Son KY, Cho B, Kim S. The differential effect of cigarette smoking on glomerular filtration rate and proteinuria in an apparently healthy population. *Hypertension Res* (2009) 32(3):214. doi: 10.1038/hr.2008.37
- Garcia-Esquinas E, Loeffler LF, Weaver VM, Fadzowski JJ, Navas-Acien A. Kidney function and tobacco smoke exposure in US adolescents. *Pediatrics* (2013) 131(5):e1415–23. doi: 10.1542/peds.2012-3201
- Dales LG, Friedman GD, Siegel AB, Seltzer CC. Cigarette smoking and serum chemistry tests. *J Chronic Dis* (1974) 27(6):293–307. doi: 10.1016/0021-9681(74)90093-9
- Savdie E, Grosslight GM, Adena MA. Relation of alcohol and cigarette consumption to blood pressure and serum creatinine levels. *J Chronic Dis* (1984) 37(8):617–23. doi: 10.1016/0021-9681(84)90111-5
- Noborisaka Y, Ishizaki M, Nakata M, Yamada Y, Honda R, Yokoyama H, et al. Cigarette smoking, proteinuria, and renal function in middle-aged Japanese men from an occupational population. *Environ Health Prev Med* (2012) 17(2):147–56. doi: 10.1007/s12199-011-0234-x
- Goetz FC, Jacobs DR Jr, Chavers B, Roel J, Yelle M, Sprafka JM, et al. Risk factors for kidney damage in the adult population of wadena, Minnesota. *A prospective study Am J Epidemiol* (1997) 145(2):91–102. doi: 10.1093/oxfordjournals.aje.a009091
- Halimi JM, Giraudeau B, Vol S, Cacès E, Nivet H, Lebranchu Y, et al. Effects of current smoking and smoking discontinuation on renal function and proteinuria in the general population. *Kidney Int* (2000) 58(3):1285–92. doi: 10.1046/j.1523-1755.2000.00284.x
- Remuzzi G. Cigarette smoking and renal function impairment. *Am J Kidney Dis* (1999) 33(4):807–10. doi: 10.1016/S0272-6386(99)70241-6
- Pinto-Sietsma SJ, Mulder J, Janssen WM, Hillege HL, de Zeeuw D, de Jong PE, et al. Smoking is related to albuminuria and abnormal renal function in nondiabetic persons. *Ann Intern Med* (2000) 133(8):585–91. doi: 10.7326/0003-4819-133-8-200010170-00008
- Fu YC, Xu ZL, Zhao MY, Xu K. The association between smoking and renal function in people over 20 years old. *Front Med (Lausanne)* (2022) 9:870278. doi: 10.3389/fmed.2022.870278
- Catapano AL, Graham I, De Backer G, Wiklund O, Chapman MJ, Drexel H, et al. 2016 ESC/EAS guidelines for the management of dyslipidaemias: the task force for the management of dyslipidaemias of the European society of cardiology (ESC) and European atherosclerosis society (EAS) developed with the special contribution of the European association for cardiovascular prevention & rehabilitation (EACPR). *Atherosclerosis* (2016) 253:281–344. doi: 10.1016/j.atherosclerosis.2016.08.018



OPEN ACCESS

EDITED BY

Ningning Hou,
Affiliated Hospital of Weifang Medical
University, China

REVIEWED BY

Bojana Kistic,
University of Pristina, Serbia
Roberto Palacios-Ramirez,
University of Valladolid, Spain

*CORRESPONDENCE

Velia Cassano

✉ velia.cassano@unicz.it

[†]These authors have contributed equally to
this work

RECEIVED 15 April 2023

ACCEPTED 20 June 2023

PUBLISHED 06 July 2023

CITATION

Cassano V, Pelaia C, Armentaro G, Miceli S,
Tallarico V, Perini DD, Fiorentino VT,
Imbalzano E, Maio R, Succurro E,
Hribal ML, Andreozzi F, Sesti G and
Sciacqua A (2023) New potential
biomarkers for early chronic kidney disease
diagnosis in patients with different glucose
tolerance status.
Front. Endocrinol. 14:1206336.
doi: 10.3389/fendo.2023.1206336

COPYRIGHT

© 2023 Cassano, Pelaia, Armentaro, Miceli,
Tallarico, Perini, Fiorentino, Imbalzano, Maio,
Succurro, Hribal, Andreozzi, Sesti and
Sciacqua. This is an open-access article
distributed under the terms of the [Creative
Commons Attribution License \(CC BY\)](#). The
use, distribution or reproduction in other
forums is permitted, provided the original
author(s) and the copyright owner(s) are
credited and that the original publication in
this journal is cited, in accordance with
accepted academic practice. No use,
distribution or reproduction is permitted
which does not comply with these terms.

New potential biomarkers for early chronic kidney disease diagnosis in patients with different glucose tolerance status

Velia Cassano^{1*†}, Corrado Pelaia^{1†}, Giuseppe Armentaro¹,
Sofia Miceli¹, Valeria Tallarico¹, Daniele Dallimonti Perini²,
Vanessa T. Fiorentino¹, Egidio Imbalzano³, Raffaele Maio¹,
Elena Succurro¹, Marta L. Hribal¹, Francesco Andreozzi¹,
Giorgio Sesti⁴ and Angela Sciacqua¹

¹Department of Medical and Surgical Sciences, University Magna Græcia of Catanzaro, Catanzaro, Italy, ²Department of Experimental and Clinical Medicine, University Magna Græcia of Catanzaro, Catanzaro, Italy, ³Department of Clinical and Experimental Medicine, Polyclinic University of Messina, Messina, Italy, ⁴Department of Clinical and Molecular Medicine, Sapienza University of Rome, Rome, Italy

Background: The purpose of the present study was to investigate the role of oxidative stress, platelet activation, and endocan levels in renal dysfunction in normal glucose tolerance (NGT) patients with 1-h plasma glucose values ≥ 155 mg/dl (NGT ≥ 155), compared to NGT < 155 , impaired glucose tolerance (IGT), and type 2 diabetes mellitus (T2DM) newly diagnosed subjects. We enlisted 233 patients subjected to an oral glucose tolerance test (OGTT).

Materials and methods: The serum levels of platelet activation (glycoprotein VI and sP-selectin), oxidative stress biomarkers (8-isoprostane and Nox-2), and endocan were evaluated using an ELISA test.

Results: Among NGT < 155 patients and the T2DM group, there was a statistically significant increase in 8-isoprostane ($p < 0.0001$), Nox-2 ($p < 0.0001$), glycoprotein VI ($p < 0.0001$), and sP-selectin ($p < 0.0001$) serum levels. Higher serum endocan levels were found with the worsening of metabolic profile ($p < 0.0001$); specifically, NGT ≥ 155 patients presented higher serum endocan values when compared to NGT < 155 patients ($p < 0.0001$). From the multivariate linear regression analysis, 1-h glucose resulted in the major predictor of estimated glomerular filtration rate (e-GFR) justifying 23.6% of its variation ($p < 0.0001$); 8-isoprostane and Nox-2 added respectively another 6.0% ($p < 0.0001$) and 3.2% ($p = 0.001$).

Conclusion: Our study confirmed the link between 1-h post-load glucose ≥ 155 mg/dl during OGTT and the possible increased risk for chronic kidney disease (CKD) in newly diagnosed patients. The novelty is that we demonstrated a progressive increase in oxidative stress, platelet activation, and serum endocan levels with the worsening of metabolic profile, which becomes evident early during the progression of CKD.

KEYWORDS

oxidative stress, renal function, glucose tolerance, endocan, platelets activation

1 Introduction

The progressive decline in renal function is a public health problem with a prevalence of $>10\%$ worldwide. Chronic kidney disease (CKD) determines patients with decreased renal function, independently from underlying pathophysiological processes (1). Patients with renal dysfunction, in particular subjects with advanced CKD, present an increased risk for cardiovascular (CV) events and dysfunction in the hemostatic system, in particular bleeding disorders and thrombosis (2).

In this context, oxidative stress has a central role in the pathophysiology, development, and complications of CKD; it is characterized by a disproportion between excessive oxidant radicals and inadequate degradation of radicals by antioxidant systems. Oxidant complexes such as reactive nitrogen species (RNS) and reactive oxygen species (ROS) are produced under physiological conditions and are eliminated by the antioxidant defense mechanism (3). In case of an imbalance in the equilibrium between prooxidants and antioxidants, oxidative stress leads to oxidative injury in cells, tissues, and organs (4). A deregulated equilibrium between ROS and reduction in the antioxidant system, which in turn increases oxidase enzyme activity and phagocyte activation and causes further oxidative stress, is a characteristic feature observed in CKD (4). The link between oxidative stress, CKD, and its complications is mediated by various mechanisms, such as increased nicotinamide adenine dinucleotide phosphate-oxidase (NADPH oxidases (NOX) activity), uremic toxin-induced endothelial nitric oxide synthase (eNOS), and decreased antioxidant defenses (5–7). Moreover, many studies reported that oxidative stress may alter the beneficial antioxidant properties of albumin, the most abundant circulating protein, which exerts important antioxidant activity and whose lower levels are associated with CKD progression (8, 9).

In addition, recent studies highlighted that endothelial dysfunction plays a significant role in CKD; in particular, endocan, a soluble proteoglycan secreted by endothelial cells and considered a novel biomarker of endothelial dysfunction, has been shown to contribute to various renal diseases such as diabetic nephropathy and autosomal dominant polycystic kidney disease (10). A study directed by Gunay et al. demonstrated that serum endocan levels were associated with endothelial dysfunction and

inflammation in individuals with acute kidney injury (11); moreover, Cikrikcioglu and collaborators investigated the link existing between endocan levels and the early phase of diabetic nephropathy in patients with type 2 diabetes mellitus (T2DM), indicating that endocan may be a possible monitoring biomarker of the progression of diabetic nephropathy (12).

Subjects with 1-h plasma glucose values ≥ 155 mg/dl (normal glucose tolerance (NGT) ≥ 155), detected during oral glucose tolerance test (OGTT), are at increased risk to develop T2DM among subjects with normal glucose tolerance test (13). Moreover, recent observations highlighted that these subjects have a worse cardiometabolic risk profile and an increased risk for CKD (14–17). Recently, a study performed by our group proved that NGT ≥ 155 subjects exhibited prematurely increased levels of oxidative stress when compared to NGT < 155 subjects, indicating subclinical organ damage (18).

Based on past evidence present in the literature, the aim of the current study was to test the role of oxidative stress, platelet activation, and endocan levels in renal dysfunction in NGT < 155 , NGT ≥ 155 , impaired glucose tolerance (IGT), and T2DM individuals.

2 Materials and methods

2.1 Study population

We enlisted 233 Caucasian newly diagnosed hypertensive patients (132 men and 101 women, mean age 58.4 ± 11.0) referring to Catanzaro Metabolic Risk Factors (CATAMERI) Study (19). Exclusion criteria were causes of secondary hypertension, diagnosis of anemia, clinical evidence of heart failure, history of chronic or malignant respiratory disease, malabsorption diseases, endocrinological pathologies, alcohol, smoking, or drug abuse. No patients presented CKD. All participants underwent a review of their medical history, physical estimation, and anthropometrical evaluation with an evaluation of height, weight, and body mass index (BMI).

The ethics committee authorized the protocol, and informed written consent was acquired from all subjects (code protocol number 2012.63). All evaluations were performed in agreement with the principles of the Declaration of Helsinki.

2.2 Blood pressure measurement

Clinical blood pressure (BP) evaluations were acquired according to current guidelines. Measurements of BP were acquired in the left arm of patients in a sitting position, using a semi-automatic sphygmomanometer (OMRON, M7 Intelli IT) after 5 min of rest. BP values were the average of three measurements. This evaluation was repeated on three different occasions at least 2 weeks apart. Subjects with a clinic systolic BP (SBP) >140 mmHg and/or diastolic BP (DBP) >90 mmHg were defined as hypertensive (20). Pulse pressure (PP) values were acquired as the difference between systolic and diastolic BP measurements.

2.3 Laboratory determination

All laboratory determinations were executed after at least 12 h of fasting. A 75-g OGTT was executed with 0-, 30-, 60-, 90-, and 120-min sampling for insulin and plasma glucose. Glucose tolerance status was defined on the basis of OGTT using the World Health Organization (WHO) criteria, and T2DM was described according to the American Diabetes Association (ADA) criteria. Plasma glucose was estimated by the glucose oxidation method (Beckman Glucose Analyzer II; Beckman Instruments, Milan, Italy), and plasma insulin concentration was detected by a chemiluminescence-based assay (Roche Diagnostics, Milan, Italy).

Insulin sensitivity was estimated using the Matsuda index (insulin sensitivity index [ISI]), calculated as follows: $10,000 / \text{square root of [fasting glucose (millimoles per liter)} \times \text{fasting insulin (milliunits per liter)]} \times [\text{mean glucose/mean insulin during OGTT}]$. The Matsuda index is strongly related to the euglycemic-hyperinsulinemic clamp, which represents the gold standard test for measuring insulin sensitivity (21).

Serum creatinine was evaluated by an automated technique based on the Jaffé creatinine compensated method for plasma and serum (Roche Diagnostics) implemented in an auto-analyzer. Albumin concentration was estimated with an Alb2 kit on a Cobas C6000 analyzer (Roche Diagnostics, Milan, Italy). Triglycerides, total, high-density lipoprotein (HDL), and low-density lipoprotein (LDL) cholesterol values were determined by enzymatic methods (Roche Diagnostics, Mannheim, Germany). Values of estimated glomerular filtration rate (e-GFR) were determined by using the equation proposed in the chronic kidney disease epidemiology (CKD-EPI) collaboration (22).

2.3.1 Serum levels of oxidative stress biomarkers, platelet activation, and endocan quantification

Blood samples, acquired from fasted subjects, were taken in tubes with separator gel and centrifuged for 15 min at 4,000 rpm to acquire serum samples that were directly stored at -80°C . In order to prevent oxidation, samples were stocked at -80°C in the presence of 0.005% butylated-hydroxy-toluene (BHT) (10 μl of 5 mg/ml solution in ethanol per 1-ml sample).

Quantitative determination of the serum 8-isoprostane (ELISA kit, Cayman Chemical, Ann Arbor, MI, USA) and Nox-2 (ELISA

kit, MyBioSource, San Diego, CA, USA) was executed with commercial ELISA immunoassays in accordance with the manufacturer's instructions. The 8-isoprostane values were reported as pg/ml; the lower detection limit of the assay was 0.8 pg/ml. Levels of Nox-2 were reported as nmol/L, and the lower detection limit of the assay was 0.25 nmol/L. The coefficient of variation (CV %) was <9%. Serum levels of human sP-selectin and glycoprotein VI were quantified using commercial ELISA immunoassays according to the manufacturer's instructions (ELISA kit MyBioSource, San Diego, CA, USA). Values of glycoprotein VI were reported as pg/ml, the lowest detectable concentration was 46.88 pg/ml, and the CV (%) was <8%; values of sP-selectin were expressed in ng/ml, and the minimum detectable concentration was 15 ng/ml.

Quantitative determination of serum endocan levels was detected with a commercial ELISA immunosorbent assay kit (Abcam, Cambridge, MA < USA). Values of endocan were reported as ng/ml, the sensitivity was 0.12 ng/ml, and CV (%) was 4.2%.

2.4 Statistical methods

Normally distributed data were reported as mean \pm SD. To investigate the differences between groups, analysis of variance (ANOVA) for biological and clinical was performed, followed by the Bonferroni *post-hoc* test for multiple comparisons. A chi-squared test was considered for categorical variables. A linear correlation analysis was performed in the entire study population, with the aim to evaluate the possible correlation between e-GFR, considered as dependent variables, and different covariates. Subsequently, variables achieving statistical significance were inserted in a multiple stepwise multivariate linear regression model to detect the independent predictor of e-GFR. Data were considered significant at $p < 0.05$. All comparisons were executed using the SPSS 20.0 for Windows (SPSS Inc., Chicago, IL, USA) statistical package.

3 Results

3.1 Study population

In the present study population, 233 patients were divided into four groups: 77 were NGT < 155, 57 were NGT \geq 155, 61 were IGT, and 38 were T2DM. The mean age was 58.4 ± 11.0 . The demographic, biochemical, and clinical characteristics of the patients are reported in Table 1, in accordance with distinct different metabolic states.

Among the four study groups, no significant differences were observed regarding age and gender distribution, anthropometric indicators, DBP, PP, total, LDL, and HDL cholesterol.

By contrast, among the study groups, there was a significant increase in SBP ($p = 0.031$), triglyceride ($p < 0.0001$), fasting plasma glucose (FPG) ($p < 0.0001$), 1-h glucose ($p < 0.0001$), and 2-h

TABLE 1 Anthropometric, biochemical, and hemodynamic characteristics of the study population according to glucose tolerance status.

Variables	All (n = 233)	NGT < 155 (n = 77)	NGT ≥ 155 (n = 57)	IGT (n = 61)	T2DM (ND) (n = 38)	p ^a
Gender, M/F	132/101	37/40	30/27	40/21	25/13	0.113*
Age, years	61.4 ± 10.7	58.0 ± 12.2	65.0 ± 8.0	61.6 ± 11.2	62.2 ± 9.4	0.120
BMI, kg/m ²	31.2 ± 6.5	30.3 ± 6.5	31.6 ± 6.2	32.2 ± 7.41	31.0 ± 4.8	0.402
SBP, mmHg	133.7 ± 8.6	130.8 ± 11.1	134.6 ± 6.2	135.4 ± 6.6	135.6 ± 7.4	0.031
DBP, mmHg	79.9 ± 8.1	77.8 ± 8.2	80.9 ± 8.6	80.9 ± 7.6	81.4 ± 7.4	0.766
PP, mmHg	54.7 ± 12.2	51.1 ± 13.1	53.4 ± 13.2	56.2 ± 11.1	60.4 ± 8.8	0.061
FPG, mg/dl	96.8 ± 12.3	87.6 ± 8.2	95.9 ± 8.9	100.4 ± 10.7	111.1 ± 9.7	<0.0001
1-h glucose, mg/dl	177.0 ± 45.5	128.9 ± 19.0	174.0 ± 23.5	200.2 ± 22.6	241.6 ± 24.1	<0.0001
2-h glucose, mg/dl	150.0 ± 46.1	112.0 ± 21.1	126.6 ± 11.5	174.7 ± 14.6	227.4 ± 23.5	<0.0001
Fasting insulin, μU/ml	15.2 ± 6.2	9.9 ± 2.7	15.0 ± 4.0	18.7 ± 6.4	20.8 ± 4.9	<0.0001
1-h insulin, μU/ml	101.8 ± 48.5	79.0 ± 47.7	119.6 ± 25.0	120.0 ± 60.2	92.2 ± 32.5	0.001
2-h insulin, μU/ml	105.6 ± 55.7	66.6 ± 27.6	95.0 ± 24.5	140.3 ± 58.6	144.6 ± 67.1	<0.0001
Matsuda/ISI	54.3 ± 28.5	84.8 ± 28.2	47.1 ± 10.4	36.9 ± 10.2	31.3 ± 8.7	<0.0001
Na, mmol/L	140.2 ± 2.6	140.3 ± 2.9	140.4 ± 2.8	139.8 ± 2.4	140.4 ± 1.6	0.480
K, mmol/L	4.2 ± 0.4	4.1 ± 0.3	4.3 ± 0.4	4.2 ± 0.4	4.2 ± 0.3	0.347
P, mg/dl	3.3 ± 0.5	3.3 ± 0.5	3.4 ± 0.5	3.2 ± 0.5	3.3 ± 0.5	0.393
Ca, mmol/L	9.3 ± 0.4	9.2 ± 0.4	9.3 ± 0.5	9.3 ± 0.4	9.3 ± 0.4	0.190
Total cholesterol, mg/dl	182.3 ± 33.1	185.6 ± 32.9	185.1 ± 27.3	175.7 ± 32.6	181.8 ± 41.3	0.280
Triglyceride, mg/dl	139.8 ± 63.6	135.2 ± 63.4	133.0 ± 45.7	139.2 ± 66.4	160.2 ± 66.4	<0.0001
HDL, mg/dl	48.3 ± 11.2	51.9 ± 10.8	49.7 ± 11.9	45.5 ± 9.6	43.3 ± 11.0	0.170
LDL, mg/dl	118.5 ± 31.0	120.7 ± 29.5	119.0 ± 28.8	114.7 ± 30.8	119.2 ± 37.4	0.576
hs-CRP, mg/L	3.1 ± 2.6	1.5 ± 1.0	3.4 ± 1.5	4.2 ± 3.7	4.4 ± 2.2	<0.0001
e-GFR, ml/min/1.73 m ²	104.7 ± 18.0	119.2 ± 12.0	102.7 ± 13.8	95.1 ± 16.5	95.2 ± 17.0	<0.0001
Albumin, g/dl	4.5 ± 0.3	4.5 ± 0.3	4.5 ± 0.3	4.5 ± 0.3	4.3 ± 0.2	0.001
Albuminuria, mg/dl	16.5 ± 8.8	12.4 ± 6.5	16.3 ± 7.9	17.0 ± 8.2	24.2 ± 10.0	<0.0001
Creatinine, mg/dl	0.8 ± 0.1	0.7 ± 0.1	0.8 ± 0.1	0.8 ± 0.1	0.8 ± 0.1	<0.0001
Azotemia, mg/dl	35.3 ± 11.3	32.1 ± 10.0	34.9 ± 9.2	36.6 ± 10.3	40.4 ± 15.5	0.002
PLT, 10 ³ /μl	215.2 ± 56.0	200.8 ± 46.3	214.2 ± 62.0	223.2 ± 58.2	232.6 ± 55.5	0.017
MPV, fl	9.1 ± 1.2	7.8 ± 0.6	8.4 ± 0.5	9.9 ± 0.6	11.2 ± 1.4	<0.0001

Data are mean ± SD.

NGT, normal glucose tolerance; IGT, impaired glucose tolerance; T2DM, type 2 diabetes mellitus; BMI, body mass index; SBP, systolic blood pressure; DBP, diastolic blood pressure; PP, pulse pressure; FPG, fasting plasma glucose; Na, sodium; K, potassium; P, phosphorus; Ca, calcium; HDL, high-density lipoprotein; LDL, low-density lipoprotein; hs-CRP, high-sensitivity C-reactive protein; e-GFR, estimated glomerular filtration rate; PLT, platelets; MPV, mean platelet volume.

^aOverall difference among groups (ANOVA).

* Overall differences among groups (χ^2).

glucose ($p < 0.0001$) during OGTT, as well as fasting insulin ($p < 0.0001$), 1-h insulin ($p < 0.0001$), and 2-h insulin ($p < 0.0001$). As awaited, there was a worsening of insulin sensitivity accounting for the decrease of Matsuda/ISI ($p < 0.0001$). Moreover, we observed a worsening of the inflammatory profile with the deterioration of glucose tolerance, as attested by high-sensitivity C-reactive protein

(hs-CRP) values ($p < 0.0001$) and an increase in platelet count ($p = 0.017$) and mean platelet volume (MPV) ($p < 0.0001$).

Post-hoc analysis by Bonferroni test proved that NGT ≥ 155 patients exhibited significantly reduced insulin sensitivity as showed by lower Matsuda/ISI (47.1 ± 10.4 vs. 84.8 ± 28.2 , $p < 0.0001$) and higher values of hs-CRP (3.4 ± 1.5 vs. 1.5 ± 1.0 , $p < 0.0001$) when

compared with NGT < 155 patients and similar to the IGT group. In addition, NGT \geq 155 subjects presented higher MPV values in comparison with NGT < 155 subjects ($p < 0.0001$).

As already demonstrated, there was a decrease in renal function, as demonstrated by e-GFR values, with the deterioration of metabolic status ($p < 0.0001$); moreover, there was a statistically significant rise in creatinine ($p < 0.0001$) and azotemia values ($p = 0.002$). Comparison between groups highlighted a worsening of renal function in NGT \geq 155 subjects, as evidenced by decreased values of e-GFR (102.7 ± 13.8 vs. 119.2 ± 12.0 , $p < 0.0001$) when compared to NGT < 155 subjects.

Moreover, serum albumin levels were significantly decreased with the worsening of glucose tolerance status ($p = 0.001$).

Among NGT < 155 patients and the T2DM group, there was a statistically significant increase in oxidative stress parameters such as 8-isoprostane ($p < 0.0001$) and Nox-2 ($p < 0.0001$) serum levels, denoting a rise in oxidative stress levels, with the worsening of metabolic profile. Particularly, NGT \geq 155 subjects presented increased values of 8-isoprostane (43.6 ± 9.7 vs. 30.1 ± 5.5 , $p < 0.0001$) and Nox-2 (1.2 ± 0.2 vs. 0.9 ± 0.1 , $p < 0.0001$) when compared to NGT < 155 and comparable to IGT patients. Furthermore, among groups, a statistically significant increase

was observed in platelet activation parameters such as glycoprotein VI ($p < 0.0001$) and sP-selectin ($p < 0.0001$).

A comparison between groups demonstrated that NGT \geq 155 subjects had increased values of glycoprotein VI (60.2 ± 14.2 vs. 47.3 ± 4.6 , $p < 0.0001$) and sP-selectin (109.9 ± 37.7 vs. 84.9 ± 20.6 , $p < 0.0001$) in comparison with NGT < 155 subjects.

Of interest, higher serum endocan levels were found with the worsening of metabolic profile ($p < 0.0001$); in particular, NGT \geq 155 patients presented higher serum endocan values when compared to NGT < 155 patients (42.4 ± 7.2 vs. 26.1 ± 3.4 , $p < 0.0001$) (Figure 1).

3.2 Correlation analysis

From the linear correlation analysis, e-GFR resulted significantly and negatively correlated with 1-h glucose ($r = -0.489$, $p < 0.0001$), 8-isoprostane ($r = -0.473$, $p < 0.0001$), Nox-2 ($r = -0.479$, $p < 0.0001$), endocan ($r = -0.476$, $p < 0.0001$), glycoprotein VI ($r = -0.238$, $p < 0.0001$), sP-selectin ($r = -0.368$, $p < 0.0001$), and hs-CRP ($r = -0.171$, $p = 0.005$) and positively correlated with Matsuda/ISI ($r = 0.418$, $p < 0.0001$) (Table 2).

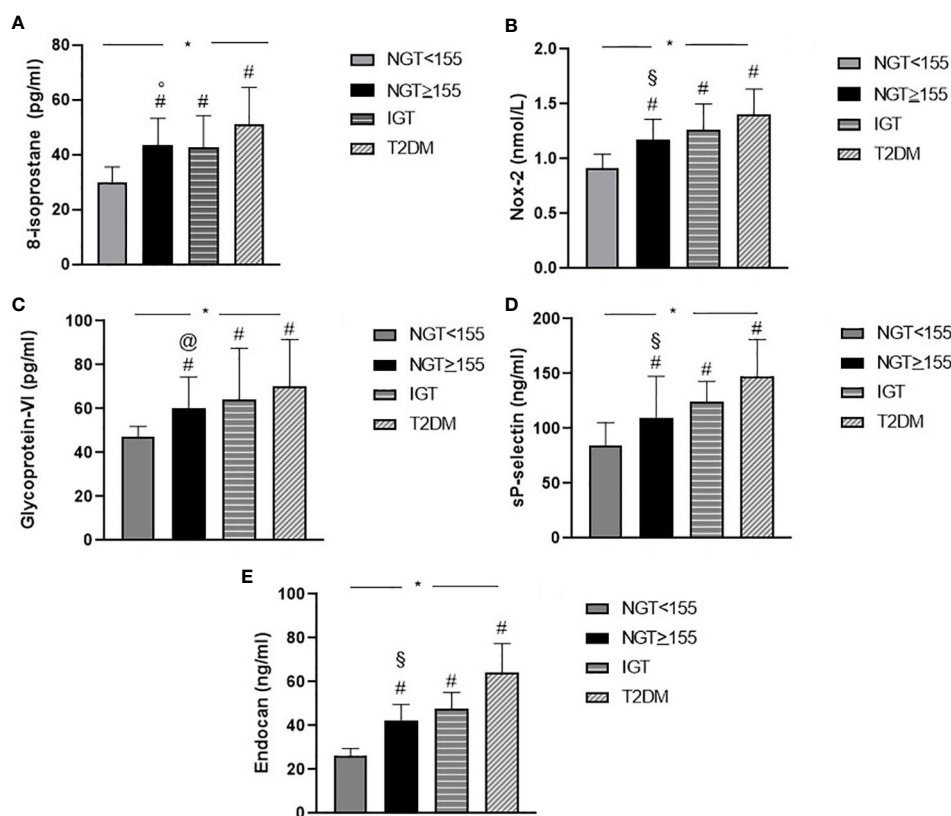


FIGURE 1

Graphical illustration of serum biomarkers levels of oxidative stress 8-isoprostane (A), Nox-2 (B), platelet activation glycoprotein VI (C), sP-selectin (D), and serum endocan (E) levels of the study population according to glucose tolerance status. * $p < 0.0001$, overall difference among groups (ANOVA). # $p < 0.0001$ other groups (NGT < 155, IGT, and T2DM) vs. NGT < 155 (Bonferroni *post-hoc* test). § $p < 0.0001$ NGT \geq 155 vs. T2DM (Bonferroni *post-hoc* test). @ $p = 0.030$ NGT \geq 155 vs. T2DM (Bonferroni *post-hoc* test). NGT, normal glucose tolerance; IGT, impaired glucose tolerance; T2DM, type 2 diabetes mellitus.

TABLE 2 Linear correlation analysis between e-GFR, as dependent variables, and different covariates in the entire study population.

	e-GFR
	r/p
Matsuda/ISI	0.418/<0.0001
1-h glucose, mg/dl	−0.489/<0.0001
8-isoprostane, pg/ml	−0.473/<0.0001
Nox-2, nmol/L	−0.479/<0.0001
Endocan, ng/ml	−0.476/<0.0001
Glycoprotein VI, pg/ml	−0.238/<0.0001
sP-selectin, ng/ml	−0.368/<0.0001
h-CRP, mg/L	−0.171/0.005

e-GFR, estimated glomerular filtration rate; hs-CRP, high-sensitivity C-reactive protein.

Variables reaching statistical significance were included in a stepwise multivariate linear regression model to detect the independent predictors of e-GFR; 1-h glucose resulted in the major predictor of e-GFR justifying 23.6% of its variation ($p < 0.0001$); 8-isoprostane and Nox-2 added respectively another 6.0% ($p < 0.0001$) and 3.2% ($p = 0.001$) (Table 3).

4 Discussion

In the current study, we investigated the association among oxidative stress biomarkers, platelet activation, endocan serum levels, and renal function in newly diagnosed hypertensive patients subjected to OGTT, highlighting also that hypertension is a risk factor for CKD disease. The patients were divided into four groups (NGT < 155, NGT ≥ 155, IGT, and T2DM) according to glucose tolerance status and considering the cutoff point of ≥155 mg/dl at 1 h during OGTT. Serum levels of endocan and biomarkers of oxidative stress and platelet activation were significantly higher in NGT ≥ 155 subjects than in NGT < 155 subjects and comparable to those in IGT subjects. Moreover, data acquired from the current study confirmed that NGT ≥ 155 patients not only are at increased risk to develop T2DM and CV disease but are also at increased risk to develop CKD. In detail, NGT ≥ 155 patients presented lower values of e-GFR, the most commonly employed marker of kidney function, than did NGT < 155 patients. It is interesting that in a linear correlation analysis, e-GFR was significantly correlated with oxidative stress, platelet activation,

serum endocan, and hs-CRP; moreover, from the stepwise multivariate linear regression model, 1-h glucose resulted as the major predictor of the worsening of e-GFR, justifying 23.6% of its variation, and 8-isoprostane and Nox-2 were responsible respectively for 6.0% and 3.2% of the e-GFR variation. In addition, there was a progressive reduction in albumin, from the first to the fourth group, although it remained in the range of reference values, attributable to the increase in oxidative stress (8). However, it is important to highlight that despite high blood pressure values and high glucose levels, none of the patients had CKD, and creatinine and e-GFR values were within the normal range values.

In spite of their well-established relationship, complex interactions between oxidative stress, endothelial dysfunction, and renal damage make it arduous to differentiate which process is principally responsible for initiating the series of events that possibly lead to kidney failure.

Mechanistically, chronic hyperglycemia increases oxidative stress, and oxidative stress, endothelial dysfunction, and inflammation are detectable even at a very early stage of CKD (23, 24). The principally pathological mechanism that correlates oxidative stress with CKD progression is defined by an early impairment in the kidney due to the activities of intra- and extracellular oxygen-derived radicals and the resultant inflammatory response. The free radical molecules ROS interact with molecular components of nephrons, resulting in decreased membrane viability and cleavage and cross-linking of renal DNA with the consequence of malignant mutations and immediate nephron damage (25). Numerous intracellular mechanisms are implicated in ROS production at the renal level, involving cytochrome P450 system, xanthine oxidase, mitochondrial respiratory chain, and NOXs. Of interest, NOXs are particularly relevant since they have been recognized to generate ROS not as by-products but as their sole biological function (26). Under physiological conditions, NOXs present very low or no constitutive activity, but their expression may be increased in pathological states such as hypertension and diabetes. In experimental *in vitro* models, NOX isoforms are upregulated in glomerular cells in response to high glucose levels (27). The Nox-2 isoform, the classic prototype of NOX isoforms expressed in mesangial cells, endothelial cells, vascular smooth muscle cells, immune cells, tubular epithelial cells, and podocytes, contributes to renal injury. Data acquired from our study demonstrated that there was a significant increase in serum Nox-2 levels, from the first to the fourth group, denoting an increase of oxidative stress with the deterioration of metabolic status, and the linear correlation analysis highlighted the link between oxidative stress, inflammation, and renal function. In addition,

TABLE 3 Stepwise multiple regression analysis on e-GFR in the entire study population.

	e-GFR		
	Partial R ²	Total R ²	p
1-h glucose, mg/dl	23.6	23.6	<0.0001
8-isoprostane, pg/ml	6.0	29.6	<0.0001
Nox-2, nmol/L	3.2	32.8	0.001

e-GFR, estimated glomerular filtration rate.

in our study, we observed higher serum 8-isoprostane levels and decreased e-GFR with the deterioration of glucose tolerance status. In fact, the 8-isoprostane, an accurate marker of endogenous lipid peroxidation and oxidative stress, increases prematurely during CKD progression (28). Moreover, low serum albumin levels may rely on several mechanisms involving inflammation, nutritional issues, and renal disease (29). Antecedent studies described that, in T2DM patients, albumin undergoes glycation, loses its antioxidant properties, and may exhibit prooxidant properties. These modifications may have an adverse influence on the coagulation system, as albumin has antiplatelet and anticoagulant characteristics through mechanisms related to its antioxidant effects; in particular, albumin impairs platelet aggregation with a mechanism connected to Nox-2 downregulation.

In this context, it is important to emphasize that renal dysfunction is associated with increasing molecule adhesion, a factor associated with platelet hyperactivity; furthermore, platelet activation in diabetic, obese, and hypertensive patients is imputed to endothelial dysfunction, oxidative stress, subclinical inflammation, and altered renin-angiotensin aldosterone system (RAAS) (2, 30). To investigate this issue, we analyzed platelet activation biomarkers in the complete study population and the four subgroups in accordance with glucose tolerance status. We observed a progressive increase of sP-selectin and glycoprotein VI serum levels, with the worsening of glucose tolerance status and the progressive decrease of e-GFR.

In detail, platelets' surface can present higher levels of p-selectin and glycoprotein VI, denoting a release of α -granules. Furthermore, p-selectin promotes the formation of platelet-erythrocyte aggregates in subjects with advanced CKD (2). Platelet erythrocyte aggregation and platelet hyperactivation are involved in the increased risk of thrombosis. These molecular mechanisms may explain why CKD patients present an increased risk of thrombotic and CV complications.

Oxidative stress has also a main role in progressive endothelial dysfunction, which has a main role in promoting atherogenesis in CKD subjects. Endocan, a marker involved in many pathological conditions such as endothelial dysfunction and inflammation, is increased in CKD patients. Results obtained from our study demonstrated a progressive increase of endocan serum levels with the worsening of metabolic status, and a strong and inverse correlation between endocan and e-GFR; however, endocan did not enter into stepwise multivariate linear regression model because of collinearity with oxidative stress biomarkers. A previous study conducted by Yilmaz et al. proved that plasma endocan was correlated with e-GFR; in fact, subjects with CKD presented higher endocan levels compared to control subjects (31).

In conclusion, our study confirmed the link between 1-h post-load glucose ≥ 155 mg/dl during OGTT and the possible increased risk for CKD in newly diagnosed patients. The novelty of the present study is that we demonstrated a progressive increase in oxidative stress and platelet activation with the worsening of metabolic profile and significantly early during the progression of CKD; in particular, NGT ≥ 155 patients exhibited higher serum levels when compared to NGT < 155 patients. Moreover, our data demonstrated a progressive increase in serum endocan levels, an emerging molecule secreted by endothelial cells, and it seems to be involved in many pathological processes such as CKD. Furthermore, more studies are needed to investigate whether

endocan is only a marker of a negative prognosis in these conditions or has an active role. In addition, biomarkers evaluated in this study could be used as potential biomarkers in early diagnosis of CKD in patients with different glucose tolerance status.

However, the present study has a study limitation; in fact, the markers analyzed in this study underlie the molecular mechanisms of interconnected diseases, in particular the high levels of oxidative stress caused by chronic hyperglycemia, which have a negative effect on the systemic level. Therefore, the values of these biomarkers should be contextualized inherently to the patient's clinical phenotype.

Data availability statement

The raw data supporting the conclusions of this article will be made available by the authors, without undue reservation.

Ethics statement

The studies involving human participants were reviewed and approved by Comitato Etico Azienda Ospedaliera "Mater Domini". The patients/participants provided their written informed consent to participate in this study. The ethics committee approved the protocol, and informed written consent was obtained from all participants (code protocol number 2012.63). All investigations were performed in accordance with the principles of the Declaration of Helsinki.

Author contributions

Conceptualization: AS and VC Methodology: VC. Formal analysis: VC and CP. Investigation: VC and SM. Writing—original draft preparation: VC and CP. Writing—review and editing: AS, MLH, and GA. Supervision: AS, MLH, RM, GA, VT, DDP, ES, FA, GS, VTF, and EI. All authors contributed to the article and approved the submitted version.

Conflict of interest

The authors declare that the research was conducted in the absence of any commercial or financial relationships that could be construed as a potential conflict of interest.

Publisher's note

All claims expressed in this article are solely those of the authors and do not necessarily represent those of their affiliated organizations, or those of the publisher, the editors and the reviewers. Any product that may be evaluated in this article, or claim that may be made by its manufacturer, is not guaranteed or endorsed by the publisher.

References

- Kassianides X. Markers of oxidative stress, inflammation and endothelial function following high-dose intravenous iron in patients with non-Dialysis-Dependent chronic kidney disease—a pooled analysis. *Int J Mol Sci* (2022) 23:16016. doi: 10.3390/ijms232416016
- Lutz PDMJ, Jurk PDRnK. Platelets in advanced chronic kidney disease: two sides of the coin. *Semin Thromb Hemost* (2020) 46:342–56. doi: 10.1055/s-0040-1708841
- Locatelli F. Oxidative stress in end-stage renal disease: an emerging threat to patient outcome. *Nephrol Dial Transpl* (2003) 18:1272–80. doi: 10.1093/ndt/gfg074
- Ling XC, Kuo KL. Oxidative stress in chronic kidney disease. *Ren Replace Ther* (2018) 4:53. doi: 10.1186/s41100-018-0195-2
- Sibal L, Agarwal CS, Home DP, Boger RH. The role of asymmetric dimethylarginine (ADMA) in endothelial dysfunction and cardiovascular disease. *Curr Cardiol Rev* (2010) 6:82–90. doi: 10.2174/157340310791162659
- Yu M, Kim YJ, Kang DH. Indoxyl sulfate-induced endothelial dysfunction in patients with chronic kidney disease via an induction of oxidative stress. *Clin J Am Soc Nephrol* (2011) 6:30–9. doi: 10.2215/CJN.05340610
- Tbahriti HF, Kaddous A, Bouchenak M, Mekki K. Effect of different stages of chronic kidney disease and renal replacement therapies on oxidant-antioxidant balance in uremic patients. *Biochem Res Int* (2013). doi: 10.1155/2013/358985
- Roche M, Rondeau P, Singh NR, Tarnus E, Bourdon E. The antioxidant properties of serum albumin. *FEBS Lett* (2008) 582:1783–7. doi: 10.1016/j.febslet.2008.04.057
- Sun J, Su H, Lou Y, Wang M. Association between serum albumin level and all-cause mortality in patients with chronic kidney disease: a retrospective cohort study. *Am J Med Sci* (2021) 361:451–60. doi: 10.1016/j.amjms.2020.07.020
- Samouilidou E, Athanasiadou V, Grapsa E. Prognostic and diagnostic value of endocan in kidney diseases. *Int J Nephrol* (2022) 2022:3861092. doi: 10.1155/2022/3861092
- Gunay M. Endocan, a new marker for inflammation and endothelial dysfunction, increases in acute kidney injury. *North Clin Istanbul* (2018) 6. doi: 10.14744/nci.2018.70446
- Cikrikcioglu MA, Erturk Z, Kilic E, Celik K, Ekinci I, Yasin Cetin AI, et al. Endocan and albuminuria in type 2 diabetes mellitus. *Ren Fail* (2016) 38:1647–53. doi: 10.1080/0886022X.2016.1229966
- Abdul-Ghani MA, Ali N, Abdul-Ghani T, Defronzo RA. One-hour plasma glucose concentration and the metabolic syndrome identify subjects at high risk for future type 2 diabetes. *Diabetes Care* (2008) 31:1650–5. doi: 10.2337/dc08-0225
- Succurro E, Arturi F, Lugarà M, Grembale A, Fiorentino TV, Caruso V, et al. One-hour postload plasma glucose levels are associated with kidney dysfunction. *Clin J Am Soc Nephrol* (2010) 5:1922–7. doi: 10.2215/CJN.03240410
- Sciacqua A, Perticone M, Miceli S, Pinto A, Cassano V, Succurro E, et al. Elevated 1-h post-load plasma glucose is associated with right ventricular morphofunctional parameters in hypertensive patients. *Endocrine* (2019) 64:525–35. doi: 10.1007/s12020-019-01873-5
- Sciacqua A, Miceli S, Carullo G, Greco L, Succurro E, Arturi F, et al. One-hour postload plasma glucose levels and left ventricular mass in hypertensive patients. *Diabetes Care* (2011) 34:1406–11. doi: 10.2337/dc11-0155
- Sciacqua A, Maio R, Miceli S, Pascale A, Carullo G, Grillo N, et al. Association between one-hour post-load plasma glucose levels and vascular stiffness in essential hypertension. *PloS One* (2012) 7(9): e44470. doi: 10.1371/journal.pone.0044470
- Cassano V, Miceli S, Armentaro G, Mannino GC, Fiorentino VT, Perticone M, et al. Oxidative stress and left ventricular performance in patients with different glycometabolic phenotypes. *Nutrients* (2022) 14(6):1299. doi: 10.3390/nu14061299
- Andreozzi F, Succurro E, Mancuso MR, Perticone M, Sciacqua A, Perticone F, et al. Metabolic and cardiovascular risk factors in subjects with impaired fasting glucose: the 100 versus 110 mg/dL threshold. *Diabetes Metab Res Rev* (2007) 23:547–50. doi: 10.1002/dmrr.724
- Williams B, Mancia G, Spiering W, Rosei EA, Azizi M, Burnier M, et al. 2018 ESC/ESH guidelines for the management of arterial hypertension. (2018). pp. 3021–104. doi: 10.1093/eurheartj/ehy339.
- Matsuda M, DeFronzo RA. Insulin sensitivity indices obtained from oral glucose tolerance testing: comparison with the euglycemic insulin clamp. *Diabetes Care* (1999) 22:1462–70. doi: 10.2337/diacare.22.9.1462
- Levey AS, Stevens LA, Schmid CH, Zhang Y, Castro AF, Feldman HI, et al. A new equation to estimate glomerular filtration rate. *Ann Intern Med* (2009) 150:604–12. doi: 10.7326/0003-4819-150-9-200905050-00006
- Aghadavod E, Khodadadi S, Baradaran A, Nasri P, Bahmani M, Rafeian-Kopaei M. Role of oxidative stress and inflammatory factors in diabetic kidney disease. *Iran J Kidney Dis* (2016) 10:337–43. doi: 10.1111/j.1755-5922.2010.00218.x
- Ravarotto V, Simioni F, Pagnin E, Davis PA, Calò LA. Oxidative stress – chronic kidney disease – cardiovascular disease: a vicious circle. *Life Sci* (2018) 210:125–31. doi: 10.1016/j.lfs.2018.08.067
- Evans MD, Dizdaroglu M, Cooke MS. Oxidative DNA damage and disease: induction, repair and significance. *Mutat Res - Rev Mutat Res* (2004) 567:1–61. doi: 10.1016/j.mrrev.2003.11.001
- Bedard K, Krause KH. The NOX family of ROS-generating NADPH oxidases: physiology and pathophysiology. *Physiol Rev* (2007) 87:245–313. doi: 10.1152/physrev.00044.2005
- Jha JC, Banal C, Chow BSM, Cooper ME, Jandeleit-Dahm K. Diabetes and kidney disease: role of oxidative stress. *Antioxid Redox Signal* (2016) 25:657–84. doi: 10.1089/ars.2016.6664
- Dounousi E, Papavasiliou E, Makedou A, Ioannou K, Katopodis KP, Tselepis A, et al. Oxidative stress is progressively enhanced with advancing stages of CKD. *Am J Kidney Dis* (2006) 48:752–60. doi: 10.1053/j.ajkd.2006.08.015
- Succurro E, Andreozzi F, Carnevale R, Sciacqua A, Cammisotto V, Cassano V, et al. Nox2 up-regulation and hypoalbuminemia in patients with type 2 diabetes mellitus. *Free Radic Biol Med* (2021) 168:1–5. doi: 10.1016/j.freeradbiomed.2021.03.026
- Cassano V. Short-term effect of sacubitril/valsartan on endothelial dysfunction and arterial stiffness in patients with chronic heart failure. *Front Pharmacol* (2022) 13:1069828. doi: 10.3389/fphar.2022.1069828
- Yilmaz MI, Siritopul D, Saglam M, Kurt YG, Unal HU, Eyileten T, et al. Plasma endocan levels associate with inflammation, vascular abnormalities, cardiovascular events, and survival in chronic kidney disease. *Kidney Int* (2014) 86:1213–20. doi: 10.1038/ki.2014.227



OPEN ACCESS

EDITED BY

Weixia Sun,
The First hospital of Jilin University, China

REVIEWED BY

Sree Bhushan Raju,
Nizam's Institute of Medical Sciences, India
Aixia Sun,
Michigan State University, United States

*CORRESPONDENCE

Ai Lian Liu
✉ liualian@dmu.edu.cn

[†]These authors have contributed
equally to this work

RECEIVED 15 March 2023

ACCEPTED 04 July 2023

PUBLISHED 21 July 2023

CITATION

Wang Y, Ju Y, An Q, Lin L and Liu AL (2023)
mDIXON-Quant for differentiation of renal
damage degree in patients with chronic
kidney disease.

Front. Endocrinol. 14:1187042.
doi: 10.3389/fendo.2023.1187042

COPYRIGHT

© 2023 Wang, Ju, An, Lin and Liu. This is an
open-access article distributed under the
terms of the [Creative Commons Attribution
License \(CC BY\)](#). The use, distribution or
reproduction in other forums is permitted,
provided the original author(s) and the
copyright owner(s) are credited and that
the original publication in this journal is
cited, in accordance with accepted
academic practice. No use, distribution or
reproduction is permitted which does not
comply with these terms.

mDIXON-Quant for differentiation of renal damage degree in patients with chronic kidney disease

Yue Wang^{1†}, Ye Ju^{1†}, Qi An¹, Liangjie Lin² and Ai Lian Liu^{1*}

¹First Affiliated Hospital, Dalian Medical University, Dalian, China, ²Clinical and Technical Support,
Philips Healthcare, Beijing, China

Background: Chronic kidney disease (CKD) is a complex syndrome with high morbidity and slow progression. Early stages of CKD are asymptomatic and lack of awareness at this stage allows CKD to progress through to advanced stages. Early detection of CKD is critical for the early intervention and prognosis improvement.

Purpose: To assess the capability of mDIXON-Quant imaging to detect early CKD and evaluate the degree of renal damage in patients with CKD.

Study type: Retrospective.

Population: 35 patients with CKD: 18 cases were classified as the mild renal damage group (group A) and 17 cases were classified as the moderate to severe renal damage group (group B). 22 healthy volunteers (group C).

Field strength/sequence: A 3.0 T/T₁WI, T₂WI and mDIXON-Quant sequences.

Assessment: Transverse relaxation rate (R2*) values and fat fraction (FF) values derived from the mDIXON-Quant were calculated and compared among the three groups.

Statistical tests: The intra-class correlation (ICC) test; Chi-square test or Fisher's exact test; Shapiro-Wilk test; Kruskal Wallis test with adjustments for multiplicity (Bonferroni test); Area under the receiver operating characteristic (ROC) curve (AUC). The significance threshold was set at $P < 0.05$.

Results: Cortex FF values and cortex R2* values were significantly different among the three groups ($P=0.028$, <0.001), while medulla R2* values and medulla FF values were not ($P=0.110$, 0.139). Cortex FF values of group B was significantly higher than that of group A (Bonferroni adjusted $P = 0.027$). Cortex R2* values of group A and group B were both significantly higher than that of group C (Bonferroni adjusted $P = 0.012$, 0.001). The AUC of cortex FF values in distinguishing group A and group B was 0.766. The diagnostic efficiency of

cortex $R2^*$ values in distinguishing group A vs. group C and group B vs. group C were 0.788 and 0.829.

Conclusion: The mDIXON-Quant imaging had a potential clinical value in early diagnosis of CKD and assessing the degree of renal damage in CKD patients.

KEYWORDS

MRI, mDIXON-Quant, $R2^*$, fat fraction, chronic kidney disease

Highlights

1. mDIXON-Quant imaging may provide a reference for the early intervention and diagnosis of CKD.
2. The $R2^*$ and FF values of mDIXON-Quant imaging can reflect the degree of tissue hypoxia and lipid deposition in CKD with different degrees of renal damage;
3. The $R2^*$ values have good sensitivity and specificity in the early diagnosis of CKD.

Introduction

Chronic kidney disease (CKD) is a complex syndrome with a high morbidity (affects approximately 10–13% of the world's population) (1). It is characterized by the irreversible changes in renal function and structure, and slow progression of the disease (2). According to the Kidney Outcomes Quality Initiative (KDIGO) CKD guideline (1, 3), CKD is defined as glomerular filtration rate (GFR) <60 mL/min/1.73 m² lasting at least 3 months, or $\text{GFR} \geq 60$ mL/min/1.73 m², but with evidence of injury of the renal structure. Early stages of CKD are asymptomatic and patients have no clinical manifestation in most cases (1, 4). Lack of awareness and intervention at this stage allows CKD to progress through to advanced stages of the disease, even may reach an endpoint of end-stage kidney disease (ESKD) or uremia (4) requiring renal replacement therapy, as well as causing a significant clinical and economic burden. Therefore, the early detection of CKD renal function is critical for the timely treatment of the disease, and is helpful for improving outcomes and decreasing mortality.

In clinical routine practice, renal function has been commonly monitored by the GFR based on blood serum creatinine level (sCr) or

by the gold standard kidney biopsy. However, those methods have some limitations and drawbacks. GFR lacks sensibility and accuracy, and cannot offer a split renal function measurement. Kidney biopsy is invasive and have a risk of bleeding and pain. Besides, the sampling limitations may lead to bias of the diagnosis (5, 6).

Functional magnetic resonance imaging (fMRI) provides comprehensive tools for noninvasive evaluation of renal function including diffusion, perfusion, oxygenation, hemodynamics and others (6, 7). In CKD, chronic hypoxia and lipid metabolism abnormality have been recognized to play a pivotal role. Peritubular capillaries injury, constant oxygen consumption and inflammation induce low renal perfusion and hypoxia damage (8). Deregulated fatty acid metabolism and renal lipid accumulation cause inflammation, oxidative stress and fibrosis, exacerbating existing kidney damage (9). Blood oxygen level-dependent (BOLD) MRI is a noninvasive imaging method to assess oxygenation changes and has been widely used in different kidney diseases (10–12). It is based on the paramagnetic deoxyhemoglobin. An increase in the $R2^*$ value indicates a decrease of local tissue oxygen content. However, it cannot assess kidney fat deposition quantitatively.

mDIXON-Quant is a non-invasive three-dimensional (3D) multi-echo gradient-echo (GRE) sequence, generating water, fat, water-fat in-phase, water-fat anti-phase as well as the transverse relaxation rate ($R2^*$) and fat fraction (FF) images (13). $R2^*$ is proportional to the deoxyhemoglobin content, which can indirectly reflect the partial pressure of oxygen in the local tissue. FF value can assess fat content quantitatively (14). mDIXON-Quant has been applied in the fat quantitative research of the liver (15, 16) and skeletal system (17, 18), etc. Only a limited number of studies concern the application of renal fat quantitative imaging in CKD (19, 20). To our knowledge, the studies of using mDIXON-Quant imaging to evaluate the degree of renal function impairment is extremely lacking.

Hence, the aim of the study was to assess the capability of mDIXON-Quant imaging to detect early CKD and evaluate the degree of renal damage in patients with CKD.

Materials and methods

Subjects

Patients with chronic kidney disease who underwent 3.0 T MR scans from August 2019 to October 2020 were retrospectively

Abbreviations: MRI, magnetic resonance imaging; CKD, chronic kidney disease; ESKD, end-stage kidney disease; GFR, glomerular filtration rate; ROC, receiver operating characteristic; FF, fat fraction; sCr, serum creatinine; fMRI, functional magnetic resonance imaging; BOLD, blood oxygen level-dependent; NKF-KDIGO, National Kidney Foundation: Kidney Disease Improving Global Outcomes; T1WI, T1 weighted imaging; T2WI, T2 weighted imaging; TR, repetition time; TE, echo time; FOV, field of view; MDRD, Modification of Diet in Renal Disease; ICC, intraclass correlation coefficient; AUC, area under the curves; CI, confidence interval; PDFF, proton-density fat fraction; FFA, free fatty acids; ROS, reactive oxygen species.

collected. Inclusion criteria were: (1) age >18 years; (2) CKD, in line with the definition of kidney disease proposed by the KDIGO (3), and the aetiology included type II diabetes, hypertension, IgA nephropathy, chronic glomerulonephritis etc.; (3) received complete MR scans, including conventional renal MR scan sequences (T_1 WI, T_2 WI) and mDIXON-Quant sequence. Exclusion criteria were: (1) kidney stones, hydronephrosis, renal tumor, polycystic kidney disease, and other renal occupational diseases; (2) taking drugs that may affect creatinine levels (such as cimetidine, trimethoprim, or cefotaxime) or receiving renal replacement therapy; (3) poor image quality: the images were not clear enough or had respiratory and motion artifacts; (4) severe metabolic syndrome, insulin resistance, etc., or receiving related treatments that cause nutritional, metabolic disorders such as parenteral nutrition, taking glucocorticoids, etc. (5) body mass index (BMI) ≥ 30 kg/m² (the people who were considered obese) (21), or use of other drugs which may affect the lipid metabolism such as statin therapy. Finally, 35 CKD patients (Asian, 18 males and 17 females) were enrolled.

At the same time, 22 healthy volunteers were included in the control group (group C: Asian, 5 males and 17 females, average age 33.74 ± 11.63 years old, range 24–60 years old). Inclusion criteria were the following: (1) healthy adults over 18 years old who had undergone regular physical examinations; (2) had no previous history of urinary system diseases, systemic metabolic or endocrine diseases, diabetes, or hypertension; (3) had no contraindications of MRI examination. Exclusion criteria were: (1) renal insufficiency caused by renal space-occupying lesions, hydronephrosis, and infectious lesions confirmed by MRI; (2) taking vascular or nephrotoxic drugs within the first three months of examination; (3) poor image quality: the images were not clear enough or had respiratory and motion artifacts.

Finally, all the participants were Asian people. The flow chart of study population in the study is shown in Figure 1.

MR scanning protocol

Kidney MR scans were performed with a 3.0 T MR scanner (Ingenia CX, Philips Healthcare, Best, the Netherlands) using a 32-channel abdominal coil. All subjects were required to fast for more than 6 hours before scanning. The mDIXON-Quant sequence acquired under multiple breath-holds, and the flip angle was 3 degree. The scan parameters of T_1 WI, T_2 WI and mDIXON-Quant sequence were shown in Table 1.

Image analysis and data measurement

All images were transferred to the ISP (Intellispace Portal 9, Philips Healthcare) workstation for analysis. The post-processing of mDixon-Quant imaging was performed on the MR console after data collection. After phase correction, accurate fat quantification was achieved with a seven-peak spectral fat model that enabled T_2^* corrections (22). The proton density fat fraction (FF) map was computed as the ratio of the fat signal over the sum of fat and water signals. We performed an mDIXON-Quant image analysis on the right kidney. The reasons are: (1) the anatomical position of the right kidney is relatively fixed and is less affected by respiratory movement and intraperitoneal intestinal gas compared to the left kidney; (2) to ensure the homogeneity of the B0 and B1 fields. The evaluation was performed independently by two radiologists with 2 and 8 years experiences in abdominal imaging diagnosis. They were both blinded to the clinical and imaging information. The first step was to record whether the kidneys had cysts or other space occupying lesion. When there was a disagreement, the result of the negotiation was decided. Second, the two individuals completed the measurement of mDixon-Quant data independently. They respectively identified the renal cortex and medulla and other anatomical structures based on T_1 WI and T_2 WI, and selected a

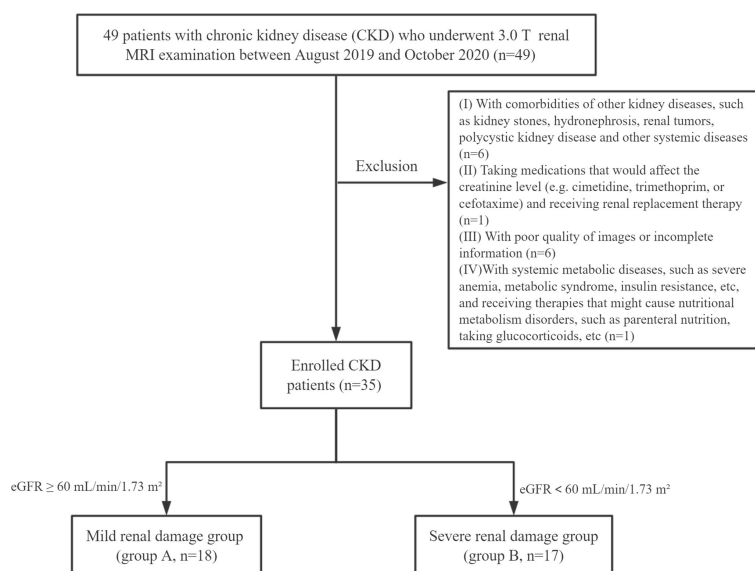


FIGURE 1
Flow chart of study population in the study.

TABLE 1 Scan parameters.

Sequences	Scan Duration (s)	Flip Angle	TR/TE (ms)	FOV(mm)	ACQ Voxel Size (mm)	Slice Thickness/ Slice gap (mm)
T ₁ WI	90	15°	10/2	392	1.40/1.95/6.00	6.0/-2.0
T ₂ WI	150	90°	1500/117	380	0.88/0.88/6.00	6.0/1.0
mDIXON-Quant	15	3°	6/1.04	375	2.29/1.85/5.00	5.0/-2.5

T₁WI, T₁ weighted imaging; T₂WI, T₂ weighted imaging; TR, time of repetition; TE, time of echo; FOV, field of view; ACQ, actual acquisition.

slice in the upper, middle, and lower poles of the right kidney. The six ROIs were carefully placed on the cortex and medulla, with an area of about 10–25 mm², avoiding renal sinus, large blood vessels, and perirenal tissue. Finally, the averaged R2* and FF values from three levels of cortex or medulla were measured and analyzed.

Assessment of GFR

Serum creatinine (Scr) values were measured on the day of the MRI examination for all subjects. GFR was calculated using the Modification of Diet in Renal Disease (MDRD) formula (23): $GFR (ml/min/1.73 m^2) = 175 \times (Scr/88.4)^{-1.154} \times (Age)^{-0.203} \times (0.742 \text{ if female})$. Patients with CKD were divided into two subgroups according to GFR (1, 3): mild renal damage group (group A, GFR ≥ 60 ml/min/1.73 m²); moderate to severe renal damage group (group B, GFR < 60 ml/min/1.73 m²).

Statistical analysis

Data were analyzed by SPSS 26.0 (IBM, Armonk, NY, USA) and MedCalc 11.4 (MedCalc, Mariakerke, Belgium). We have performed repeated measurements of mDIXON-Quant parameters for two radiology doctors (with 8 years and 2 years of experiences in abdominal imaging) to analyze the inter- and intra-observer variability, and intra-class correlation (ICC) under a two-way random model with the absolute agreement was applied for the assessment. ICC values lower than 0.40, between 0.40 and 0.75 and greater than 0.75 were considered to have low, medium, and high consistency, respectively. Categorical variables presented as counts or percentages were compared using a chi-square test or Fisher's exact test. The Shapiro-Wilk test was used to test the normality of the continuous variables. According to the distribution of the parameters, the parameters were expressed as mean \pm standard deviation (normal distribution) or median with interquartile range (non-normal distribution). The parameters among three groups were analyzed using Kruskal Wallis test. *Post-hoc* multiple pairwise comparisons were performed with the Bonferroni test. Receiver operating characteristic (ROC) curve analysis was used to analyze the diagnostic efficacy of the parameters and their combination to evaluate the renal function.

This study was approved by the Medical Ethics Committee of our hospital (approval number: PJ-KS-KY-2021-250).

Results

Demographics and CKD stages of subjects

According to the GFRs, CKD patients were divided into mild renal damage group (group A, 18 cases, 9 males and 9 females, average age 46.33 ± 15.27 years old, range 19–75 years old), and moderate to severe renal damage group (group B, 17 cases, 9 males and 8 females, mean age 45.94 ± 14.89 years old, range 27–74 years old). The GFRs of healthy volunteers were all within normal limits.

CKD is categorized into five stages according to the GFR (1). The demographics of all subjects and CKD stages of the patients were shown in Table 2.

Renal T₂WI, R2*, and FF images in healthy volunteers and CKD patients

All images have adequate quality for structure visualization and data measurements. Representative kidney T₁WI, T₂WI, R2*, and FF maps in different groups were shown in Figures 2–4.

Measurement consistency between two observers

The ICC values of each parameter between the two observers were all > 0.75 , suggesting good consistency. The data measured by observer 1 (with longer years of experience) was then used for subsequent data analysis. The Shapiro-Wilk test results showed that the data was not in normal distribution and was expressed as median (25th percentile, 75th percentile). The parameters of the three groups and ICC tests results were shown in Table 3.

Comparison of FF values and R2* values of the cortex and medulla among the three groups

The Kruskal Wallis test showed that cortex FF values and cortex R2* values were significantly different among the three groups

TABLE 2 The demographics of all subjects and CKD stages of the patients.

Class	Number	Age (range, mean± standard deviation)	GFR (ml/min/1.73 m ²)
Healthy volunteer	22	24-60, 33.73 ± 11.63	/
CKD 1	9	19-60, 44.11 ± 14.56	120.91 ± 15.84
CKD 2	9	23-75, 48.56 ± 16.50	78.86 ± 6.89
CKD 3	2	34-59, 46.50 ± 17.68	42.82 ± 14.17
CKD 4	4	34-74, 56.50 ± 16.67	22.79 ± 5.157
CKD 5	11	27-70, 42.00 ± 13.36	8.03 ± 2.78

CKD, Chronic Kidney Disease; GFR, glomerular filtration rate; CKD 1, GFR ≥ 90 ml/min/1.73 m²; CKD 2, 60 ml/min/1.73 m² < GFR ≤ 89 ml/min/1.73 m²; CKD 3, 30 ml/min/1.73 m² < GFR ≤ 59 ml/min/1.73 m²; CKD 4, 15 ml/min/1.73 m² < GFR ≤ 30 ml/min/1.73 m²; CKD 5, GFR < 15 ml/min/1.73 m².

($P=0.028$, <0.001), while medulla R2* values and medulla FF values were not ($P=0.110$, 0.139).

The cortex FF values of the moderate to severe renal damage group (group B) was significantly higher than that of the mild renal damage group (group A) (Bonferroni adjusted $P = 0.027$). The cortex R2* values of group A and group B were both significantly higher than that of group C (Bonferroni adjusted $P = 0.012$, 0.001) (Figure 5).

The diagnostic efficacy of the parameters in evaluating the renal function of CKD patients and healthy volunteers

The diagnostic efficiency of cortex FF values in distinguishing group A and group B was 0.766, with a sensitivity and specificity of 66.7% and 82.4%, respectively, which means that cortex FF values may be helpful to distinguish the degree of renal function damage in CKD patients and stage the diseases. Meanwhile, the diagnostic efficiency of cortex R2* values in distinguishing group A and group C was 0.788, with sensitivity and specificity of 88.9% and 68.2%, respectively, which reflects that cortex R2* values have the potential for early diagnosis of CKD. Besides, the diagnostic efficiency of cortex R2* values in distinguishing group B and group C was 0.829, with sensitivity and specificity of 70.6% and 81.8%, respectively, which means cortex R2* values can noninvasively distinguish patients with severe CKD from healthy volunteers.

The AUC values, 95% confidence interval (CI), cutoff values, sensitivities, and specificities of the parameters in evaluating the renal function of CKD patients and healthy volunteers were shown in Table 4. The ROC curves were shown in Figures 6–8.

Discussion

We explored the renal R2* and FF values derived from mDIXON-Quant imaging in evaluating the renal function of

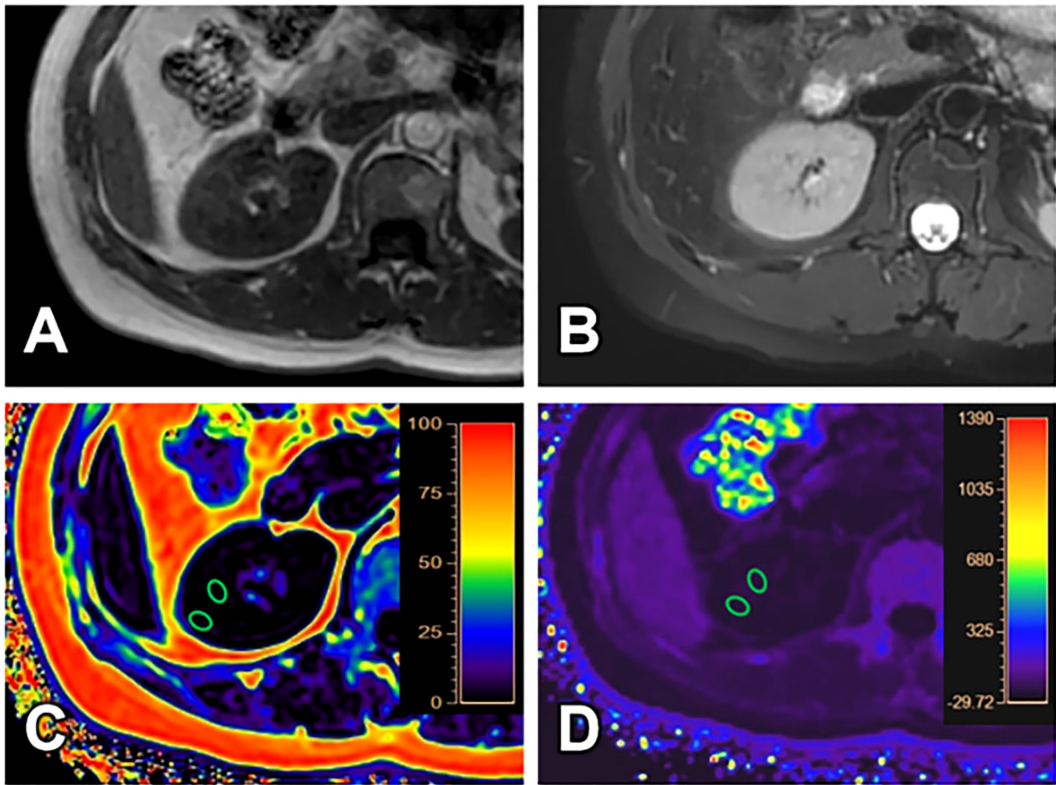


FIGURE 2 A 40-year-old female with GFR (128.11 ml/min/1.73 m²) and clinical CKD stage I (mild renal damage group). T₁WI (A), T₂WI (B), FF (C) and R2* (D) images. The cortex and medulla R2* values are 16.17/s and 21.52/s; the cortex and medulla FF values are 0.61% and 0.64%, respectively.

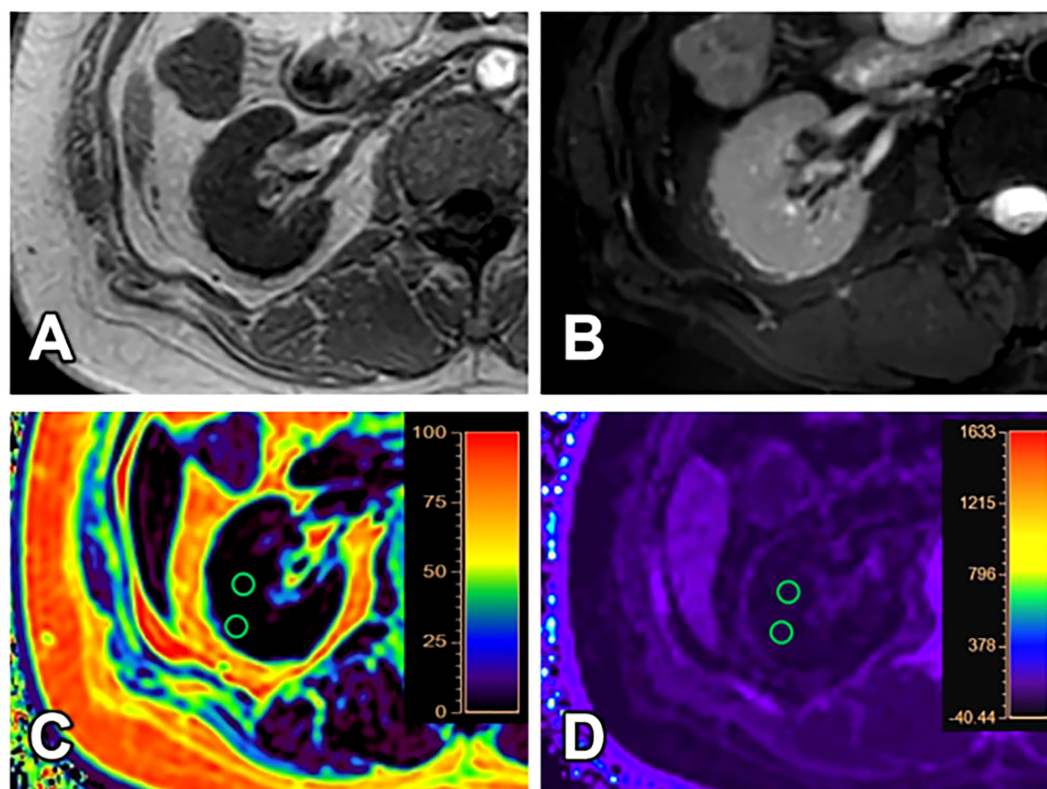


FIGURE 3

A 31-year-old female with GFR (8.16 ml/min/1.73 m²) and clinical CKD stage IV (moderate to severe renal damage group). T₁WI (A), T₂WI (B), FF (C) and R2* (D) images. The cortex and medulla R2* values are 18.87/s and 15.90/s; the cortex and medulla FF values are 1.30% and 1.79%, respectively.

CKD patients with different degrees of kidney damage and healthy volunteers. The results showed that the cortex R2* values of the mild and moderate to severe renal damage groups were both higher than that of the healthy control group; the cortex FF values in the moderate to severe renal damage group were significantly higher than in the mild renal damage group; there was no significant difference in medulla R2* values and medulla FF values among the three groups. The mDIXON-Quant imaging had a potential clinical value in assessing the degree of renal damage in CKD patients.

The cortex R2* values of the mild and moderate to severe renal damage groups were higher than that of the healthy control group

The R2* values are proportional to the concentration of deoxyhemoglobin, which can indirectly reflect the partial pressure of oxygen in local tissues. This study showed that the cortex R2* values of the mild and moderate to severe renal damage groups were higher than that of the healthy control group, which was consistent with the results of previous related studies (24–27). The possible reasons are: CKD is accompanied by different degrees of glomerular atrophy and tubular fibrosis, which may change the local hemodynamics of the kidney and cause damage to the capillary endothelium and microvessels, resulting in decreased renal perfusion

and chronic hypoxia. The renal cortex is rich in capillaries, and the renal blood flow reduction in CKD mainly occurs in the cortex (28); besides, the proximal tubular cells are the predominant cell type in the cortex. This kind of cells have a large number of mitochondria and have active transport activity which consumes a lot of energy and oxygen. So the cortex is more susceptible to the level of oxygenation and hypoxic injury, which is consistent with the cortex R2* values in the mild and moderate to severe renal damage group being higher than those in the healthy control group, but the medulla R2* values have no significant difference among the three groups. Therefore, the cortex R2* values reflect the degree of renal hypoxia and have the potential for noninvasively early diagnosis of CKD. It also can effectively distinguish CKD patients from healthy person.

Besides, the cortex R2* values in mild renal damage group and moderate to severe renal damage group have no significant difference, though had an increasing trend with the decline of renal function. We think it might be limited by the sample size and a larger sample size in future might acquire significantly difference.

Some previous studies showed no significant difference in the medulla R2* values of the BOLD-MRI between the control group and the CKD group (29, 30), which are consistent with our study. On the contrary, other BOLD-MRI studies about medulla R2* values showed that with the decline of GFR or the aggravation of renal damage in CKD patients, the medulla R2* values decreased (12, 24), which suggested that with the decline of renal function, the oxygenation level of the medulla gradually increased. These data are not

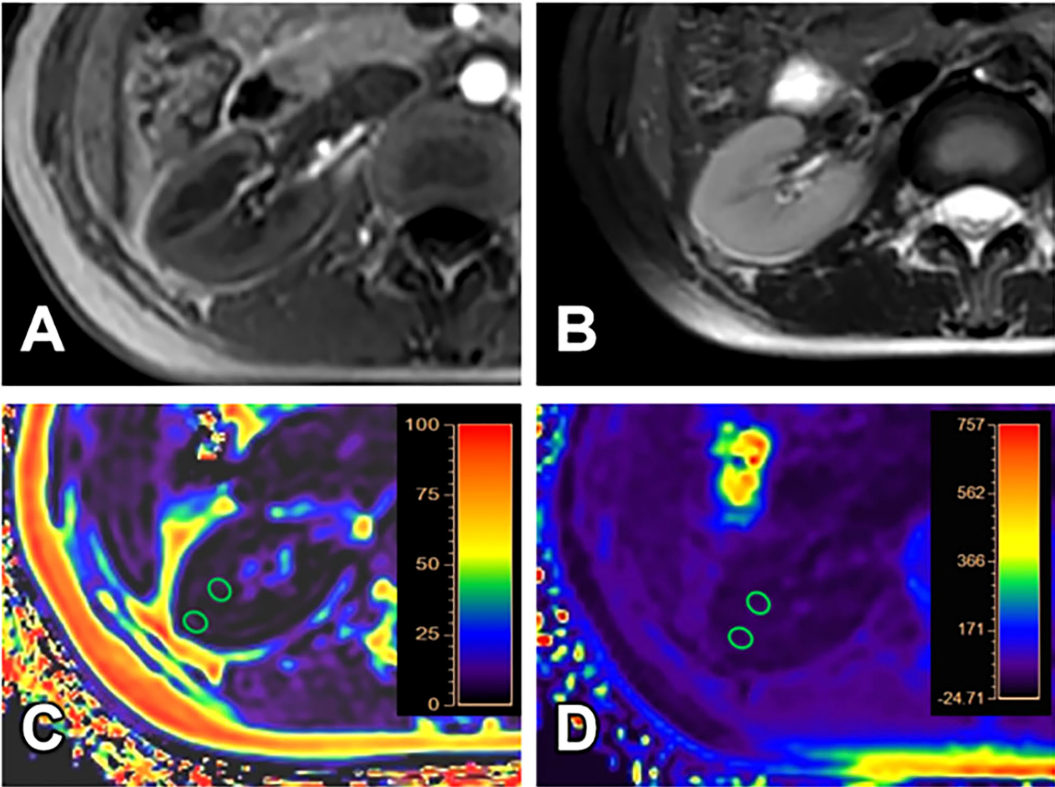


FIGURE 4
A 24-year-old female volunteer (healthy volunteer group). T₁WI (A), T₂WI (B), FF (C) and R2* (D) images. The cortex and medulla R2* values are 19.27/s and 21.67/s; the cortex and medulla FF values are 1.32% and 1.82%, respectively.

consistent with the results of our study. In our study, although the medulla R2* values had a decreasing trend across the three groups, there was no statistical difference. The possible reasons for this are: (1) most of the blood in the kidney is transported to the renal cortex, while only 10% - 15% of blood is sent to the renal medulla (28); as a result, the medulla is relatively not sensitive to hypoxia injury; (2) with the aggravation of renal function damage, the GFR decreases, the ultrafiltration function of the kidney also decreases, and the active

TABLE 3 Intra-observer agreement on the measurement of imaging parameters.

Parameters	Groups	Observer 1	Observer 2	ICC values
Cortex FF values (%)	Group A (n = 18)	1.13 (0.61, 1.58)	1.06 (0.70, 1.65)	0.915
	Group B (n = 17)	1.72 (1.31, 2.61)	1.60 (1.31, 2.49)	0.997
	Group C (n = 22)	1.19 (0.90, 2.01)	1.23 (0.79, 2.14)	0.987
medulla FF values (%)	Group A (n = 18)	0.90 (0.63, 1.73)	1.22 (0.90, 2.39)	0.854
	Group B (n = 17)	1.71 (0.87, 4.26)	2.56 (1.50, 3.78)	0.942
	Group C (n = 22)	1.28 (0.65, 2.02)	1.42 (1.07, 2.72)	0.821
cortex R2* values (/s)	Group A (n = 18)	17.23 (16.14, 19.02)	18.21 (16.37, 19.59)	0.763
	Group B (n = 17)	18.81 (16.55, 20.05)	19.31 (17.80, 20.05)	0.954
	Group C (n = 22)	15.38 (14.45, 16.92)	17.04 (14.69, 18.14)	0.857
medulla R2* values (/s)	Group A (n = 18)	21.60 (19.28, 23.53)	21.69 (17.48, 26.59)	0.860
	Group B (n = 17)	21.34 (17.60, 22.80)	21.56 (17.48, 23.62)	0.972
	Group C (n = 22)	19.82 (19.01, 20.73)	22.52 (19.46, 23.42)	0.759

Observer 1 and 2, two radiologists with 8 years and 2 years of experiences in abdominal imaging; ICC, intra-class correlation; ICC values lower than 0.40, between 0.40 and 0.75 and greater than 0.75 were considered to have low, medium, and high consistency, respectively; Group A, mild renal damage group; group B, moderate to severe renal damage group; group C, healthy control group; FF, fat fraction; R2*, transverse relaxation rate.

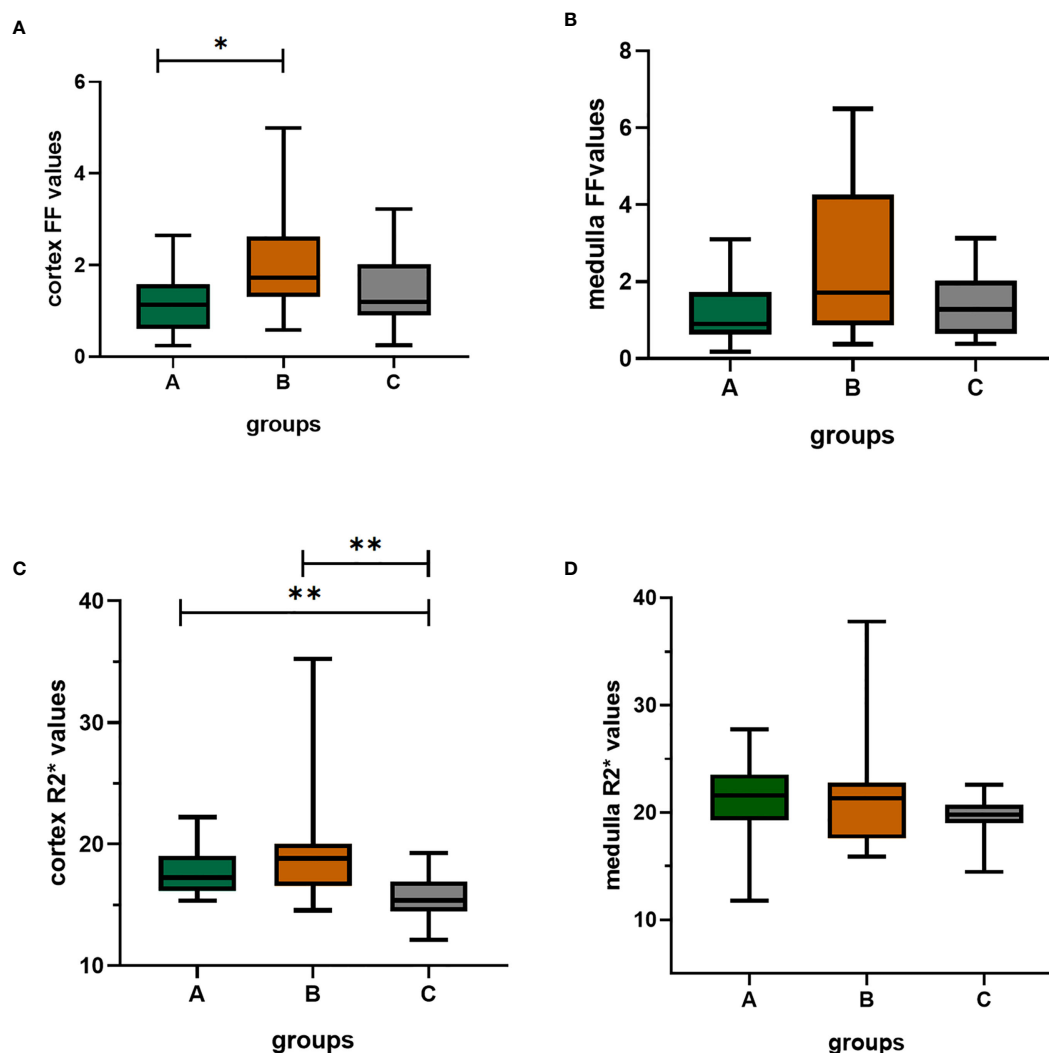


FIGURE 5

The box-plots of FF(%) values and R2*(/s) values of the cortex and medulla in the three groups. (A–D) showed the differences among three groups, respectively. There was significant difference in cortex FF values between group A and group B; the group A and group B both had significantly differences with group C; Bonferroni adjusted P values (adj. P): *, adj. P < 0.05; **, adj. P < 0.01. Group A, mild renal damage group; group B, moderate to severe renal damage group; group C, healthy control group; FF(%), fat fraction; R2*(/s), transverse relaxation rate.

TABLE 4 Sensitivities, specificities, and area under curve (AUC) values of the parameters in evaluating the degree of renal damage in CKD.

Group vs. Group	Parameter	AUC	95% CI	Cutoff value	Sensitivity (%)	Specificity (%)
Group A vs. Group B	cortex FF (%)	0.766	0.593 - 0.892	1.27	66.7	82.4
Group A vs. Group C	cortex R2* (/s)	0.788	0.630 - 0.901	15.87	88.9	68.2
Group B vs. Group C	cortex R2* (/s)	0.829	0.674 - 0.930	16.97	70.6	81.8

Group A, mild renal damage group; group B, moderate to severe renal damage group; group C, healthy control group; CI, confidence interval; AUC, area under curve; FF, fat fraction.

absorption of NaCl in the proximal tubules of the medulla weakens; tubular atrophy and reduced active transport of small molecules may lead to reduced Na⁺-K⁺-ATP pump function and reduced oxygen consumption, thereby alleviating renal medulla hypoxia (24); (3) moreover, the R2* values may not only affected by changes in oxygen

partial pressure but also by magnetic field strength, homogeneity, pulse parameters, and human physiological data (e.g., pH, temperature, hematocrit) (29) which needs further investigations. Therefore, there was no significant difference in the medulla R2* value among the three groups.

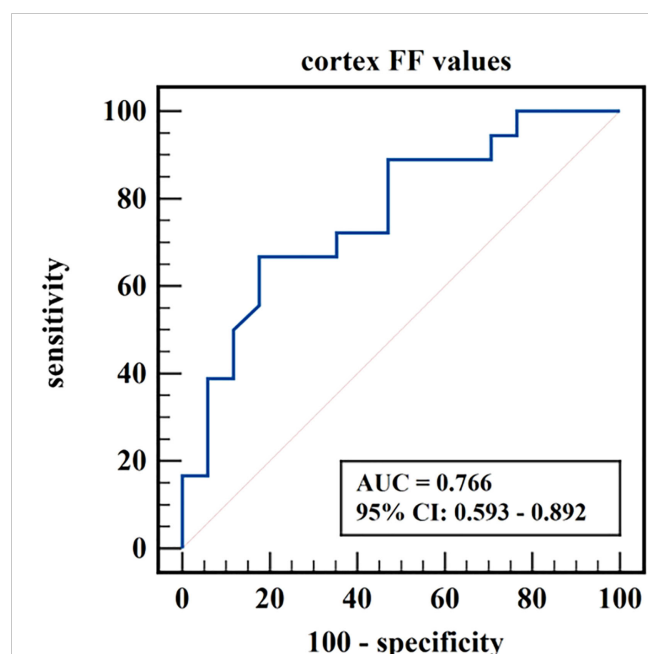


FIGURE 6

ROC curve of cortex FF values in distinguishing mild renal damage group from moderate to severe renal damage group.

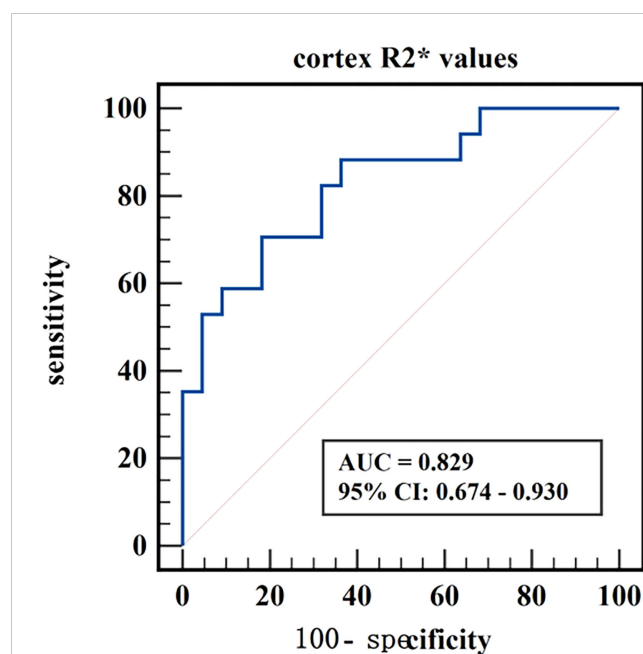


FIGURE 8

ROC curve of cortex R2* values in distinguishing moderate to severe renal damage group from healthy control group.

The cortex FF values in the moderate to severe renal damage group was significantly higher than that in the mild renal damage group

FF values can accurately quantify the lipid deposition in tissue. This study showed that the cortex FF values in the moderate to

severe renal damage group was significantly higher than in the mild renal damage group. Previous mDIXON-Quant related studies found that the renal lipid content in the type II diabetes group was significantly higher than that in the non-type II diabetes group, and the corresponding proton-density fat fraction (PDFF) was also higher (20, 31). Another study showed that the renal FF values were higher in patients with early diabetic nephropathy with microalbuminuria compared to those without microalbuminuria and the control group (19). Differently, previous studies measured the renal fat deposition based on the entire renal parenchyma, and we measured the FF values on the cortex and medulla of the kidneys respectively. Besides, previous studies mainly focused on the fat content of diabetic nephropathy, and we expanded the categories of enrolled CKD cases. We also divided the CKD patients into mild renal damage and moderate to severe renal damage group according to the GFR, to explore the feasibility of FF values in the assessment of kidney function in CKD. Similarly, our study and previous studies all indicated that CKD patients have renal fat deposition. The likely reasons may be that obesity and hyperlipidemia are the most common independent risk factors for CKD. A high-fat diet increases the intake of free fatty acids (FFA), CD36 scavenger receptors, fatty acid transporters, and other fatty acids. Overexpression of the uptake system and reduced β -oxidation rate can lead to intracellular lipid accumulation in non-adipose tissue, including kidney. Additionally, excess FFAs can damage podocytes, proximal tubular epithelial cells, and tubular interstitium through multiple mechanisms, especially by promoting the production of reactive oxygen species (ROS) and lipid peroxidation, which in turn promotes mitochondrial damage and tissue inflammation, leading to glomerular and tubular lesions (9, 32). Therefore, CKD renal damage is often accompanied by lipid

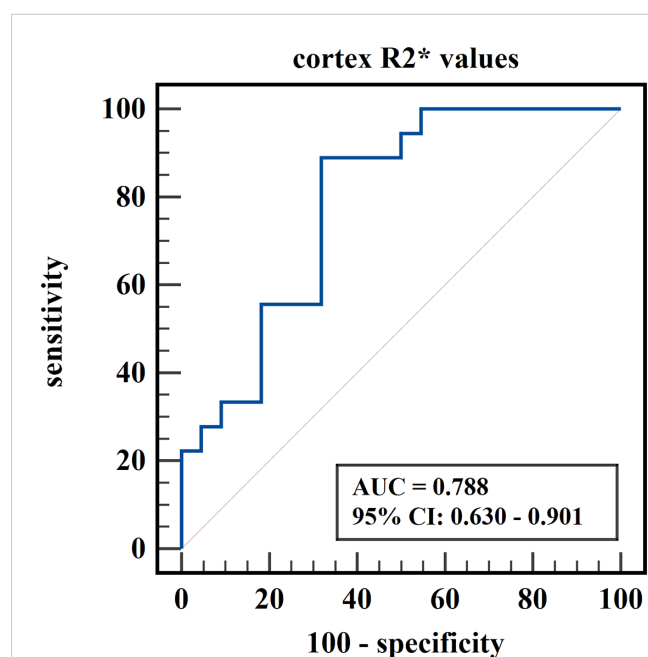


FIGURE 7

ROC curve of cortex R2* values in distinguishing mild renal damage group from healthy control group.

metabolism disorder and lipid deposition, and the lipid deposition (especially the deposition of FFA) further aggravates renal function damage. Based on those reasons, we speculated that the renal fat deposition increases with the development of the renal injury. Therefore, the cortex FF values of the moderate to severe renal damage group were significantly higher than that of mild renal damage group. Cortex FF values may be helpful to distinguish the degree of renal function damage in CKD patients and stage the diseases.

Yet, in this study, there was no significant difference in medulla FF values among the three groups. And, there was no significant difference in cortex FF values for mild renal damage group vs. healthy control group and moderate to severe renal damage group vs. healthy control group. Theoretically, lipid levels continue to increase with the progression of kidney lesions, but our results does not show this kind of tendency. On the one hand, high fat diet, obesity and body mass index (BMI) may have a certain effect on renal fat deposition, even in healthy people (33). On the other hand, when the renal function is damaged mildly, the kidney has a certain self-regulation mechanism which may help to decrease the lipid content. Besides, there could be local inhomogeneities in fat distribution across different parts of the kidney, and the ROI placements on the renal cortex and medulla may produce some deviation. More research based on this field is needful in future.

The study has a few limitations: (1) this is a retrospective study with a relatively small sample size, which may cause that the range of parameters of one group covers those of other groups. We will expand the sample size to for further study in the future. Also, the patients were not classified according to different etiologies for the high expense of MRI and the emerging technology, and further clinical research on CKD caused by different etiologies is still needed. (2) The kidney structure is heterogeneous, and with the development of renal damage, the boundary between the medulla and cortex was unclear, which may affect the accuracy of ROI placement and measurement; thus, the observer consistency test was performed to reduce measurement errors as much as possible. Besides, we used ROI placements instead of segmentations of the renal cortex and medulla, and there could be local inhomogeneities in fat distribution and deoxygenation across different parts of the kidney; (3) Finally, detailed studies of renal pathology have not been carried out, and our team will improve the research in future.

Conclusion

The R2* and FF values derived from mDIXON-Quant imaging may reflect the degree of tissue hypoxia and lipid deposition in CKD with different degrees of renal damage. The cortex R2* values have the potential for noninvasively early diagnosis of CKD and earlier intervention. It also can effectively distinguish CKD patients from healthy person and provide useful diagnostic information for

physicians. Though the cortex FF values could not be an early indicator for the early diagnosis of CKD, it can be helpful to distinguish the degree of renal function damage in CKD patients and stage the diseases. Therefore, mDIXON-Quant imaging may be an early indicator modality for the non-invasive early diagnosis of CKD, and also can provide a reference for the effective diagnosis, personalized treatment and evaluation of prognosis of CKD.

Data availability statement

The raw data supporting the conclusions of this article will be made available by the authors, without undue reservation.

Ethics statement

This study was approved by the Medical Ethics Committee of the First Affiliated Hospital of Dalian Medical University (approval number: PJ-KS-XJS-2022-66). The ethics committee waived the requirement of written informed consent for participation. Written informed consent was obtained from the individual(s) for the publication of any potentially identifiable images or data included in this article.

Author contributions

Guarantor of the article: AL. Conception and design: AL, YW, and YJ. Collection and assembly of data: YW, YJ, and QA. Data analysis and interpretation: YW and YJ. Manuscript writing: YW. Manuscript editing: YW, AL, YJ, and LL. All authors contributed to the article and approved the submitted version.

Conflict of interest

Liangjie Lin was employed by Clinical and Technical Support, Philips Healthcare, Beijing, China.

The remaining authors declare that the research was conducted in the absence of any commercial or financial relationships that could be constructed as a potential conflict of interest.

Publisher's note

All claims expressed in this article are solely those of the authors and do not necessarily represent those of their affiliated organizations, or those of the publisher, the editors and the reviewers. Any product that may be evaluated in this article, or claim that may be made by its manufacturer, is not guaranteed or endorsed by the publisher.

References

1. Ammirati AL. Chronic kidney disease. *Rev Assoc Med Bras* (1992) (2020) 66Suppl 1(Suppl 1):s03–9. doi: 10.1590/1806-9282.66.s1.3
2. Evans M, Lewis RD, Morgan AR, Whyte MB, Hanif W, Bain SC, et al. A narrative review of chronic kidney disease in clinical practice: current challenges and future perspectives. *Adv Ther* (2022) 39(1):33–43. doi: 10.1007/s12325-021-01927-z
3. Inker LA, Astor BC, Fox CH, Isakova T, Lash JP, Peralta CA, et al. KDOQI US commentary on the 2012 KDIGO clinical practice guideline for the evaluation and management of CKD. *Am J Kidney Dis* (2014) 63(5):713–35. doi: 10.1053/j.ajkd.2014.01.416
4. Chu CD, Chen MH, McCulloch CE, Powe NR, Estrella MM, Shlipak MG, et al. Patient awareness of CKD: a systematic review and meta-analysis of patient-oriented questions and study setting. *Kidney Med* (2021) 3(4):576–585 e571. doi: 10.1016/j.kme.2021.03.014
5. Ju Y, Liu A, Wang Y, Chen L, Wang N, Bu X, et al. Amide proton transfer magnetic resonance imaging to evaluate renal impairment in patients with chronic kidney disease. *Magn Reson Imaging* (2022) 87:177–82. doi: 10.1016/j.mri.2021.11.015
6. Alnazer I, Bourdon P, Urruty T, Falou O, Khalil M, Shahin A, et al. Recent advances in medical image processing for the evaluation of chronic kidney disease. *Med Image Anal* (2021) 69:101960. doi: 10.1016/j.media.2021.101960
7. Mora-Gutierrez JM, Fernandez-Seara MA, Echeverria-Chasco R, Garcia-Fernandez N. Perspectives on the role of magnetic resonance imaging (MRI) for noninvasive evaluation of diabetic kidney disease. *J Clin Med* (2021) 10(11). doi: 10.3390/jcm10112461
8. Chen F, Yan H, Yang F, Cheng L, Zhang S, Li S, et al. Evaluation of renal tissue oxygenation using blood oxygen level-dependent magnetic resonance imaging in chronic kidney disease. *Kidney Blood Press Res* (2021) 46(4):441–51. doi: 10.1159/000515709
9. Gai Z, Wang T, Visentin M, Kullak-Ublick GA, Fu X, Wang Z. Lipid accumulation and chronic kidney disease. *Nutrients* (2019) 11(4):722. doi: 10.3390/nu11040722
10. Cheng ZY, Lin QT, Chen PK, Si-Tu DK, Qian L, Feng YZ, et al. Combined application of DTI and BOLD-MRI in the assessment of renal injury with hyperuricemia. *Abdom Radiol (NY)* (2021) 46(4):1694–702. doi: 10.1007/s00261-020-02804-z
11. Li LP, Milani B, Pruijm M, Kohn O, Sprague S, Hack B, et al. Renal BOLD MRI in patients with chronic kidney disease: comparison of the semi-automated twelve layer concentric objects (TLCO) and manual ROI methods. *MAGMA* (2020) 33(1):113–20. doi: 10.1007/s10334-019-00808-5
12. Li LP, Thacker JM, Li W, Hack B, Wang C, Kohn O, et al. Medullary blood oxygen level-dependent MRI index (R2*) is associated with annual loss of kidney function in moderate CKD. *Am J Nephrol* (2020) 51(12):966–74. doi: 10.1159/000512854
13. Yu F, He B, Chen L, Wang F, Zhu H, Dong Y, et al. Intermuscular fat content in young Chinese men with newly diagnosed type 2 diabetes: based on MR mDIXON-quant quantitative technique. *Front Endocrinol (Lausanne)* (2021) 12:536018. doi: 10.3389/fendo.2021.536018
14. Chu C, Feng Q, Zhang H, Zhao S, Chen W, He J, et al. Evaluation of salivary gland fat fraction values in patients with primary sjogren's syndrome by mDIXON quant imaging: initial findings. *Eur J Radiol* (2020) 123:108776. doi: 10.1016/j.ejrad.2019.108776
15. Wagih Shaltout S, Abd El-Maksoud M, Abdel Rahman A, Yousef AM, El Sherbiny W. Clinical spectrum of nonalcoholic fatty liver disease in patients with chronic obstructive pulmonary disease. *Turkish Thorac J* (2022) 23(6):420–5. doi: 10.5152/TurkThoracJ.2022.22002
16. Rodge GA, Goenka MK, Goenka U, Afzalpurkar S, Shah BB. Quantification of liver fat by MRI-PDFF imaging in patients with suspected non-alcoholic fatty liver disease and its correlation with metabolic syndrome, liver function test and ultrasonography. *J Clin Exp Hepatol* (2021) 11(5):586–91. doi: 10.1016/j.jceh.2020.11.004
17. Zhao Y, Huang M, Ding J, Zhang X, Spuhler K, Hu S, et al. Prediction of abnormal bone density and osteoporosis from lumbar spine MR using modified Dixon quant in 257 subjects with quantitative computed tomography as reference. *J Magn Reson Imaging* (2019) 49(2):390–9. doi: 10.1002/jmri.26233
18. Zhang Y, Zhou Z, Wang C, Cheng X, Wang L, Duanmu Y, et al. Reliability of measuring the fat content of the lumbar vertebral marrow and paraspinal muscles using MRI mDIXON-quant sequence. *Diagn Interv Radiol* (2018) 24(5):302–7. doi: 10.5152/dir.2018.17323
19. Wang YC, Feng Y, Lu CQ, Ju S. Renal fat fraction and diffusion tensor imaging in patients with early-stage diabetic nephropathy. *Eur Radiol* (2018) 28(8):3326–34. doi: 10.1007/s00330-017-5298-6
20. Yokoo T, Clark HR, Pedrosa I, Yuan Q, Dimitrov I, Zhang Y, et al. Quantification of renal steatosis in type II diabetes mellitus using dixon-based MRI. *J Magn Reson Imaging* (2016) 44(5):1312–9. doi: 10.1002/jmri.25252
21. Weir CB, Jan A. *BMI classification percentile and cut off points*. Treasure Island (FL: StatPearls Publishing) (2023).
22. Lohofer FK, Kaissis GA, Muller-Leisse C, Franz D, Katemann C, Hock A, et al. Acceleration of chemical shift encoding-based water fat MRI for liver proton density fat fraction and T2* mapping using compressed sensing. *PLoS One* (2019) 14(11):e0224988. doi: 10.1371/journal.pone.0224988
23. Tang B, Tu W, Zhao J, Deng X, Tan I, Butlin M, et al. Relationship between arterial stiffness and renal function determined by chronic kidney disease epidemiology collaboration (CKD-EPI) and modification of diet in renal disease (MDRD) equations in a Chinese cohort undergoing health examination. *BioMed Res Int* (2022) 2022:8218053. doi: 10.1155/2022/8218053
24. Li C, Liu H, Li X, Zhou L, Wang R, Zhang Y. Application of BOLD-MRI in the classification of renal function in chronic kidney disease. *Abdom Radiol (NY)* (2019) 44(2):604–11. doi: 10.1007/s00261-018-1750-6
25. Milani B, Ansaloni A, Sousa-Guimaraes S, Vakizadeh N, Piskunowicz M, Vogt B, et al. Reduction of cortical oxygenation in chronic kidney disease: evidence obtained with a new analysis method of blood oxygenation level-dependent magnetic resonance imaging. *Nephrol Dial Transplant* (2017) 32(12):2097–105. doi: 10.1093/ndt/gfw362
26. Prasad PV, Li LP, Thacker JM, Li W, Hack B, Kohn O, et al. Cortical perfusion and tubular function as evaluated by magnetic resonance imaging correlates with annual loss in renal function in moderate chronic kidney disease. *Am J Nephrol* (2019) 49(2):114–24. doi: 10.1159/000496161
27. Pruijm M, Milani B, Pivin E, Podhajska A, Vogt B, Stuber M, et al. Reduced cortical oxygenation predicts a progressive decline of renal function in patients with chronic kidney disease. *Kidney Int* (2018) 93(4):932–40. doi: 10.1016/j.kint.2017.10.020
28. Wang B, Li ZL, Zhang YL, Wen Y, Gao YM, Liu BC. Hypoxia and chronic kidney disease. *EBioMedicine* (2022) 77:103942. doi: 10.1016/j.ebiom.2022.103942
29. Luo F, Liao Y, Cui K, Tao Y. Noninvasive evaluation of renal oxygenation in children with chronic kidney disease using blood-oxygen-level-dependent magnetic resonance imaging. *Pediatr Radiol* (2020) 50(6):848–54. doi: 10.1007/s00247-020-04630-3
30. Prasad PV, Thacker J, Li LP, Haque M, Li W, Koenigs H, et al. Multi-parametric evaluation of chronic kidney disease by MRI: a preliminary cross-sectional study. *PLoS One* (2015) 10(10):e0139661. doi: 10.1371/journal.pone.0139661
31. Shen Y, Xie L, Chen X, Mao L, Qin Y, Lan R, et al. Renal fat fraction is significantly associated with the risk of chronic kidney disease in patients with type 2 diabetes. *Front Endocrinol (Lausanne)* (2022) 13:995028. doi: 10.3389/fendo.2022.995028
32. Nishi H, Higashihara T, Inagi R. Lipotoxicity in kidney, heart, and skeletal muscle dysfunction. *Nutrients* (2019) 11(7):1664. doi: 10.3390/nu11071664
33. Stasi A, Cosola C, Caggiano G, Cimmarusti MT, Palieri R, Acquaviva PM, et al. Obesity-related chronic kidney disease: principal mechanisms and new approaches in nutritional management. *Front Nutr* (2022) 9:925619. doi: 10.3389/fnut.2022.925619



OPEN ACCESS

EDITED BY

Weixia Sun,
The First Hospital of Jilin University, China

REVIEWED BY

Benli Su,
Second Hospital of Dalian Medical
University, Dalian, China
Miguel Murguía-Romero,
National Autonomous University of Mexico,
Mexico

*CORRESPONDENCE

Qingnan He
✉ heqn2629@csu.edu.cn
Mingyi Zhao
✉ zhao_mingyi@csu.edu.cn

RECEIVED 05 January 2023

ACCEPTED 28 June 2023

PUBLISHED 26 July 2023

CITATION

Tian Q, He C, Wang Z, Hun M, Fu Y-C,
Zhao M and He Q (2023) Relationship
between serum uric acid and estimated
glomerular filtration rate in adolescents
aged 12–19 years with different body mass
indices: a cross-sectional study.
Front. Endocrinol. 14:1138513.
doi: 10.3389/fendo.2023.1138513

COPYRIGHT

© 2023 Tian, He, Wang, Hun, Fu, Zhao and
He. This is an open-access article distributed
under the terms of the [Creative Commons
Attribution License \(CC BY\)](#). The use,
distribution or reproduction in other
forums is permitted, provided the original
author(s) and the copyright owner(s) are
credited and that the original publication in
this journal is cited, in accordance with
accepted academic practice. No use,
distribution or reproduction is permitted
which does not comply with these terms.

Relationship between serum uric acid and estimated glomerular filtration rate in adolescents aged 12–19 years with different body mass indices: a cross-sectional study

Qiuwei Tian¹, Caixia He¹, Zisai Wang¹, Marady Hun¹,
Yi-Cheng Fu², Mingyi Zhao^{1*} and Qingnan He^{1*}

¹Department of Pediatrics, The Third Xiangya Hospital, Central South University, Changsha, China,

²Department of Pediatrics, Renmin Hospital of Wuhan University, Wuhan University, Wuhan, China

Background: Globally, chronic kidney disease (CKD) is a growing public health concern. Serum uric acid (SUA) is an easily detectable and readily available biochemical indicator that has long been recognized as an independent risk factor for CKD. In addition, studies have indicated a potential relationship between SUA and body mass index (BMI). However, studies on the effect of SUA levels on the estimated glomerular filtration rate (eGFR) in adolescents with different BMIs are very rare.

Methods: Weighted multiple regression analysis was used to estimate the independent relationship between SUA and log-transformed eGFR. Additionally, we used a weighted generalized additive model and smooth curve fitting to describe the nonlinear relationships in the subgroup analysis.

Results: First, SUA was negatively associated with log-transformed eGFR even after adjusting for all covariates ($\beta = -0.0177$, 95% CI: -0.0203 – -0.0151 , $P < 0.0001$). Second, the results of the stratified analysis found that after adjusting for all covariates, the decrease in log-transformed eGFR due to changes in per SUA levels (Per 1, mg/dL increase) was elevated in female adolescents ($\beta = -0.0177$, 95% CI: -0.0216 , -0.0138 , $P < 0.0001$), adolescents aged 12–15 years ($\beta = -0.0163$, 95% CI: -0.0200 , -0.0125 , $P < 0.0001$) and black ($\beta = -0.0199$, 95% CI: -0.0251 , -0.0148 , $P < 0.0001$) adolescents. Furthermore, we found that adolescents with a higher BMI had higher SUA levels, and the effect of SUA on eGFR was significantly higher in underweight adolescents ($\beta = -0.0386$, 95% CI: -0.0550 , -0.0223 , $P < 0.0001$).

Conclusion: SUA was negatively associated with the eGFR in adolescents aged 12–19 years. Furthermore, we found for the first time that SUA affects the eGFR differently in adolescents with different BMIs. This effect was particularly significant in underweight adolescents.

KEYWORDS

serum uric acid, estimated glomerular filtration rate, BMI, adolescents, NHANES

Introduction

Chronic kidney disease (CKD) is a growing global public health problem. Over the nearly 30 years from 1990 to 2017, the global prevalence of CKD at all ages increased by 29.3%, while the age-standardized prevalence remained stable (1). Previous studies on adults have found that both poor lifestyle habits, such as smoking, alcohol consumption and sedentary lifestyle, as well as a polluted atmosphere, such as elevated fine particulate matter (PM_{2.5}) in the air, and even low birth weight in infants can be risk factors for the development and progression of CKD (2–4). Although epidemiological studies on CKD in adolescents are very limited, it is indisputable that CKD in children and adolescents has become one of the most significant diseases affecting their lives. Therefore, it is critical to find a biomarker that facilitates early prediction and timely intervention by clinicians for the prevention of CKD in adolescents.

It is well known that uric acid is the final product of purine metabolism. As a clinically easily detectable and available biochemical indicator, SUA is closely associated with diseases such as hypertension (5–7), diabetes (7–10), and metabolic syndrome (11, 12) and has been recognized as an independent risk factor for the development of CKD (13, 14). Meanwhile, SUA levels are also correlated with body mass index (BMI). For example, some scholars have found a nonlinear relationship between BMI and SUA in adults (15). In addition, studies in obese patients have also found that elevated SUA levels are always accompanied by obesity in both adults and adolescents (16, 17). This may be related to oxidative stress and the inflammatory response induced by xanthine oxidoreductase-derived reactive oxygen species and uric acid (18, 19). Therefore, based on the findings of previous studies, we hypothesized that controlling BMI might enable the modification of SUA levels in adolescents.

Previous findings have indicated that serum uric acid can cause renal injury through both crystal-dependent and crystal-independent mechanisms (20, 21). Therefore, in this study, we used the estimated glomerular filtration rate (eGFR) as a measure of basal renal function in adolescents based on a cross-sectional survey from the National Health and Nutrition Examination Survey (NHANES) database with the aim of exploring two main questions. First, we investigated the relationship between SUA and eGFR in adolescents in a cross-sectional survey with a large sample size. Second, we investigated the effect of SUA levels on renal function in adolescents with different BMIs, with the aim of exploring whether the renal injury effect of SUA can be reduced by controlling the BMI of adolescents, thus preventing the occurrence of CKD in adolescents.

Materials and methods

Study population

The National Health and Nutrition Examination Survey (NHANES) is a large cross-sectional survey based on the U.S.

population with a two-year survey cycle. This survey collected a large amount of survey information from the general U.S. population through a complex, multistage, probability sampling design. All adult participants provided written informed consent, and participants under 18 years of age were required to submit the consent of their parents or guardians. For data researchers and users, the survey data from NHANES are publicly available at www.cdc.gov/nchs/nhanes/. NHANES has been reviewed by the National Center for Health Statistics Research Ethics Review Board.

Our study collected relevant data, including demographics, physical examinations, laboratory tests, and questionnaires, during the three survey cycles of NHANES 2011–2016 and analyzed them. The inclusion and exclusion details of the study population in this study are shown in Figure 1.

Variables

The exposure variable in this study was SUA. The DxC800 uses a timed endpoint method to measure the concentration of uric acid in serum, plasma or urine. The outcome variable was the estimated glomerular filtration rate (eGFR), calculated using the latest modified Schwartz equation: $eGFR = 0.413 \times [\text{height (cm)} / \text{serum creatinine (mg/dL)}]$ (22). The body measurement data were collected in the Mobile Examination Center (MEC) by trained health technicians. The poverty income ratio is the ratio of family income to poverty and is calculated using the Department of Health and Human Services (HHS) poverty guidelines as the poverty measure. The scale includes the following terms and corresponding values: “mild” (poverty income ratio < 1.99), “moderate” ($1.99 \leq \text{poverty income ratio} \leq 3.49$), and “severe” (poverty income ratio > 3.49). The BMI (body mass index), expressed as weight in kilograms divided by height in meters squared (kg/m²), is commonly used to classify weight status. The definitions of underweight, normal weight, overweight, and obesity in children and adolescents are not directly comparable with the definitions in adults, which were defined as “underweight” (BMI < 5th percentile), “normal weight” (BMI 5th to < 85th percentiles), “overweight” (BMI 85th to < 95th percentiles) and “obese” (BMI ≥ 95th percentile) (23). Some details of other incorporated variables are openly available at www.cdc.gov/nchs/nhanes/.

Based on previous relevant studies, clinical experience, and data collected in the NHANES database, the continuous variables among the covariates included in this study were age, weight, waist circumference, BMI, systolic blood pressure (SBP), diastolic blood pressure (DBP), albumin, globulin, total protein, alanine aminotransferase (ALT), aspartate aminotransferase (AST), gamma glutamyl transaminase (GGT), lactate dehydrogenase (LDH), blood urea nitrogen (BUN), serum glucose, total cholesterol, triglycerides, low-density lipoprotein (LDL), high-density lipoprotein (HDL), and urinary albumin creatinine ratio (ACR). The categorical variables among the covariates were sex, race, education level, poverty income ratio, and BMI category. In addition, height and serum creatinine were not included as covariates because of their involvement in the calculation of the eGFR.

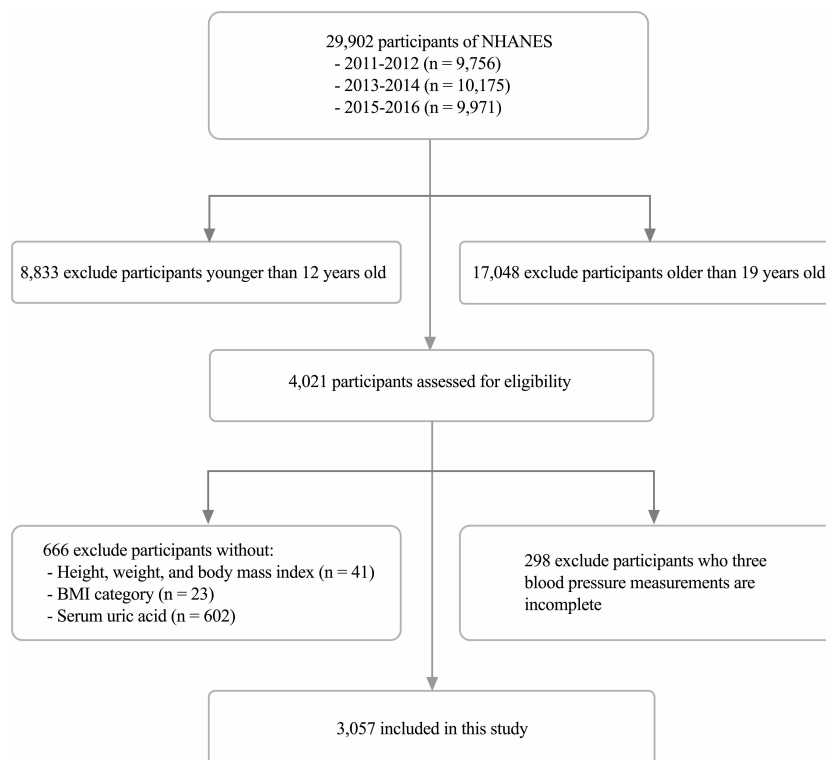


FIGURE 1
Flow of participants through the study.

Data analysis

Data analysis for this study was completed under the guidance of the CDC guidelines. Furthermore, given the complexity and nonresponse of the NHANES survey design, we used sample weights to analyze the data. Because of the skewed distribution of the eGFR, we used the log-transformed eGFR (LgeGFR) for the analysis of the eGFR. First, the sample weights were used in the analysis of weighted means (continuous variables), percentages (categorical variables), and standard errors of baseline characteristics. Second, after adjustment for potential confounders, weighted multiple regression analysis was used to estimate the independent relationship between SUA and LgeGFR. Third, weighted generalized additive models and smooth curve fitting were used to describe the nonlinear relationships in the subgroup analysis. Three models were used in the regression analysis: Model 1 was the crude model and did not include any covariates for adjustment; Model 2 was adjusted for age, sex, race, and BMI; Model 3 was adjusted for age, sex, race, education attainment, poverty income ratio, weight, waist circumference, BMI, BMI category, SBP, DBP, albumin, globulin, total protein, ALT, AST, GGT, LDH, BUN, serum glucose, total cholesterol, triglycerides, LDL, HDL, and the ACR.

Categorical variables are expressed as frequencies or percentages, and continuous variables are expressed as the means \pm standard deviations. All data analyses were performed using the R package data software (<http://www.R-project.org>) and

Empower (<http://www.empowerstats.com>). $P < 0.05$ was considered statistically significant.

Results

Description of baseline characteristics

The weighted demographic and medical characteristics are described in Table 1. A total of 3057 adolescents aged 12–19 years were included in our study, of whom 51.88% were male, 48.12% were female, 55.17% were white, 13.84% were black, 14.40% were Mexican American, and 16.60% were of other races. Significant differences were found in each of the baseline characteristics of the groups according to the four subgroups of SUA, except for poverty income ratio, globulin and total cholesterol. In addition, participants with SUA in the lower range (Q1: <4.00 mg/dL, Q2: 4.10–4.80 mg/dL) were more likely to be female (79.67%, 69.51%), while those in the higher range (Q3: 4.90–5.70 mg/dL, Q4: ≥ 5.80 mg/dL) were more likely to be male (64.32%, 81.21%). Compared to other subgroups, participants in the top quartile of SUA levels had a higher weight, height, waist circumference, BMI, SBP, DBP, albumin, ALT, AST, LDH, BUN, serum creatinine, serum glucose, total cholesterol, triglycerides, and LDL and lower levels of HDL and eGFR. Additionally, we observed that participants in the lowest quartile of SUA levels had much higher urinary albumin creatinine ratios than those in the other groups.

TABLE 1 Description of 3,057 participants included in the present study.

Characteristics	Serum uric acid, mg/dL					
	Total	Q1 (<4.00)	Q2 (4.10-4.80)	Q3 (4.90-5.70)	Q4 (≥5.80)	P value
n	3057	735	759	769	794	
Age, years	15.35 ± 2.23	15.08 ± 2.22	15.09 ± 2.22	15.28 ± 2.22	15.89 ± 2.15	<0.0001
Sex (%)						<0.0001
Male	51.88	20.33	34.49	64.32	81.21	
Female	48.12	79.67	65.51	35.68	18.79	
Race (%)						0.0015
White	55.17	48.11	55.68	58	57.64	
Black	13.84	18.39	14.22	12.25	11.35	
Mexican American	14.4	16.22	14.5	13.05	14.15	
Other	16.6	17.28	15.6	16.69	16.86	
Education attainment (%)						0.001
Less than high school	85.31	87.95	87.97	85.24	80.81	
High school	8.51	7.69	7.86	7.96	10.3	
Higher than high school	6.15	4.36	4.17	6.8	8.79	
Other	0.03				0.1	
Poverty income ratio (%)						0.4619
Low	29.51	31.16	29.24	28.6	29.29	
Middle	36.67	34.91	38.07	39.13	34.41	
High	27.9	27.78	26.11	26.98	30.55	
Not recorded	5.92	6.15	6.58	5.28	5.75	
Weight (Kg)	66.47 ± 19.83	56.92 ± 14.73	60.65 ± 14.66	66.03 ± 16.62	80.00 ± 22.94	<0.0001
Height (cm)	165.62 ± 9.88	160.46 ± 8.26	162.66 ± 8.47	166.91 ± 9.67	171.26 ± 9.28	<0.0001
Waist circumference (cm)	82.25 ± 14.92	76.64 ± 11.33	79.00 ± 12.20	81.59 ± 13.64	90.43 ± 17.33	<0.0001
BMI (kg/m ²)	24.05 ± 6.19	21.98 ± 5.01	22.86 ± 5.04	23.66 ± 5.54	27.21 ± 7.30	<0.0001
BMI category (%)						<0.0001
Underweight	3.71	4.65	4.41	3.63	2.38	
Healthy weight	58.5	73	63.73	60.04	40.4	
Overweight	17.61	13.75	17.8	18.49	19.71	
Obese	20.18	8.61	14.05	17.84	37.51	
SBP (mmHg)	109.17 ± 9.53	106.39 ± 8.59	107.14 ± 8.78	109.70 ± 9.67	112.77 ± 9.53	<0.0001
DBP (mmHg)	59.17 ± 11.93	58.69 ± 11.13	59.05 ± 11.75	58.68 ± 12.50	60.16 ± 12.10	0.042
Albumin (g/dL)	4.50 ± 0.30	4.44 ± 0.29	4.46 ± 0.32	4.54 ± 0.30	4.56 ± 0.30	<0.0001
Globulin (g/dL)	2.72 ± 0.38	2.75 ± 0.37	2.70 ± 0.41	2.71 ± 0.37	2.72 ± 0.37	0.0953
Total protein (g/dL)	7.22 ± 0.41	7.19 ± 0.40	7.16 ± 0.40	7.25 ± 0.42	7.28 ± 0.41	<0.0001
ALT (U/L)	19.32 ± 12.34	15.49 ± 5.41	17.78 ± 13.04	18.93 ± 9.99	24.22 ± 15.79	<0.0001
AST (U/L)	23.80 ± 11.14	21.92 ± 5.53	22.55 ± 6.26	24.09 ± 12.22	26.20 ± 15.58	<0.0001
GGT (U/L)	14.33 ± 9.62	11.81 ± 4.27	13.31 ± 12.29	13.84 ± 5.61	17.78 ± 11.89	<0.0001
LDH (U/L)	129.98 ± 29.06	128.12 ± 25.72	128.37 ± 26.34	129.54 ± 27.86	133.40 ± 34.38	0.0008

(Continued)

TABLE 1 Continued

Characteristics	Serum uric acid, mg/dL					
	Total	Q1 (<4.00)	Q2 (4.10-4.80)	Q3 (4.90-5.70)	Q4 (≥5.80)	P value
BUN (mg/dL)	11.07 ± 3.43	10.51 ± 3.15	10.68 ± 3.21	11.21 ± 3.41	11.74 ± 3.73	<0.0001
Creatinine (mg/dL)	0.72 ± 0.17	0.64 ± 0.12	0.68 ± 0.14	0.75 ± 0.17	0.81 ± 0.18	<0.0001
Serum glucose (mg/dL)	88.85 ± 14.57	89.05 ± 13.87	88.81 ± 19.56	87.60 ± 9.88	89.94 ± 13.51	0.0134
Cholesterol (mg/dL)	157.51 ± 29.52	158.25 ± 27.12	156.81 ± 29.10	156.10 ± 29.23	158.93 ± 31.89	0.2027
Triglycerides (mg/dL)	99.27 ± 71.88	83.51 ± 54.80	93.45 ± 57.45	99.10 ± 70.24	117.58 ± 91.07	<0.0001
LDL (mg/dL)	86.93 ± 17.50	85.07 ± 15.24	86.63 ± 16.85	87.44 ± 17.97	88.21 ± 19.12	0.0049
HDL (mg/dL)	51.56 ± 12.12	56.62 ± 13.08	52.99 ± 11.19	51.10 ± 11.35	46.57 ± 10.80	<0.0001
ACR (mg/g)	26.97 ± 110.82	41.16 ± 153.41	26.42 ± 83.06	20.20 ± 94.88	22.61 ± 105.08	0.0016
eGFR (ml/min/1.73m ²)	98.73 ± 20.27	107.60 ± 19.63	102.24 ± 18.83	96.11 ± 20.32	90.89 ± 18.40	<0.0001
LgeGFR (ml/min/1.73m ²)	1.99 ± 0.09	2.02 ± 0.08	2.00 ± 0.08	1.97 ± 0.09	1.95 ± 0.09	<0.0001

BMI, body mass index; SBP, systolic blood pressure; DBP, diastolic blood pressure; ALT, alanine aminotransferase; AST, Aspartate Aminotransferase; GGT, Gamma glutamyl Transaminase; LDH, Lactate Dehydrogenase; BUN, Blood Urea Nitrogen; LDL, low-density lipoprotein; HDL, high-density lipoprotein; SUA, serum uric acid; ACR, albumin creatinine ratio; eGFR, estimated glomerular filtration rate. Mean ± s.d. for continuous variables: P value was calculated using a weighted linear regression model. % for Categorical variables: P value was calculated by weighted chi-square test.

Relationship between SUA and log-transformed eGFR

The results of the multivariate regression analysis are shown in **Table 2**, and the smoothed curve fits and scatter plots are shown in **Figure 2**. When not adjusted for any covariates (Model 1), SUA was negatively associated with log-transformed eGFR ($\beta = -0.0232$, 95% CI: -0.0256-0.0207, $P < 0.0001$). After adjusting for age, sex, race, and BMI category only (Model 2) ($\beta = -0.0177$, 95% CI: -0.0204- -0.0151, $P < 0.0001$) and after adjusting for all covariates (Model 3) ($\beta = -0.0177$, 95% CI: -0.0203-0.0151, $P < 0.0001$), this negative correlation remained. In addition, we found that compared to baseline levels in the lowest quartile of SUA, the log-transformed eGFR of the group in the highest quartile was 0.0508 lg (ml/min/1.73 m²) lower than that of the lowest quartile. Meanwhile, P for trend test all had $P < 0.001$, suggesting that the trend of decreased LgeGFR was significant for each increase in SUA level.

Subgroup analysis based on potential effects

Subgroup analysis according to sex, age, race, and BMI category is shown in **Table 3**. After subgroup analysis by sex, age, and race, male adolescents (SUA 5.60 ± 1.15 mg/dL), adolescents aged 16-19 years (SUA 5.19 ± 1.27 mg/dL), and white adolescents (SUA 5.12 ± 1.20 mg/dL) had higher SUA levels. After adjustment for all covariates (Model 3), the decrease in log-transformed eGFR due to changes in SUA levels (Per 1, mg/dL increase) was higher in female adolescents ($\beta = -0.0177$, 95% CI: -0.0216, -0.0138, $P < 0.0001$), adolescents aged 12-15 years ($\beta = -0.0163$, 95% CI: -0.0200, -0.0125, $P < 0.0001$) and black ($\beta = -0.0199$, 95% CI: -0.0251, -0.0148, $P < 0.0001$) adolescents. Furthermore, we found that adolescents with higher BMI had higher SUA levels, and the effect of SUA on eGFR was highest in underweight adolescents compared to other body types ($\beta = -0.0386$, 95% CI: (-0.0550, -0.0223), $P < 0.0001$). As

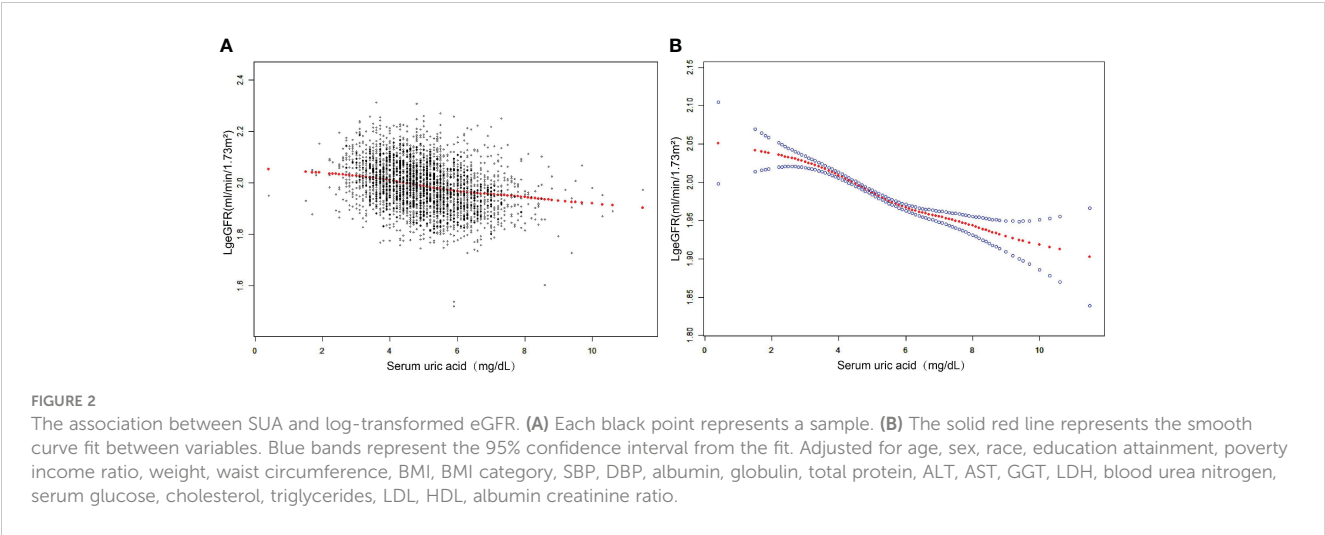
TABLE 2 Association of SUA with LgeGFR among 3,057 12–19 year-old adolescents, NHANES 2011–2016.

	Model1 β (95%CI) P value	Model2 β (95%CI) P value	Model3 β (95%CI) P value
Serum uric acid	-0.0232 (-0.0256, -0.0207) <0.0001	-0.0177 (-0.0204, -0.0151) <0.0001	-0.0177 (-0.0203, -0.0151) <0.0001
SUA categories			
Q1(0.40-4.00 mg/dL)	Reference	Reference	Reference
Q2(4.10-4.80 mg/dL)	-0.0223(-0.0310, -0.0136) <0.0001	-0.0205 (-0.0281, -0.0129) <0.0001	-0.0173 (-0.0244, -0.0101) <0.0001
Q3(4.90-5.70 mg/dL)	-0.0514(-0.0600, -0.0428) <0.0001	-0.0403 (-0.0483, -0.0323) <0.0001	-0.0372 (-0.0448, -0.0296) <0.0001
Q4(5.80-11.50 mg/dL)	-0.0748(-0.0833, -0.0662) <0.0001	-0.0544 (-0.0633, -0.0456) <0.0001	-0.0508 (-0.0593, -0.0422) <0.0001
P for trend	<0.001	<0.001	<0.001

Model 1, no covariates were adjusted.

Model 2, adjust for age, sex, race and BMI category.

Model 3, adjust for age, sex, race, education attainment, poverty income ratio, weight (Smooth), waist circumference, BMI, BMI category, SBP, DBP, albumin, globulin, total protein, ALT, AST, GGT, LDH, blood urea nitrogen, serum glucose, cholesterol, triglycerides, LDL, HDL, albumin creatinine ratio. Generalized additive models were applied.



shown in [Figure 3](#), after stratifying by age, sex, race and BMI category, we also attempted to use smoothed curve fitting to find a linear and nonlinear relationship between SUA and log-transformed eGFR in different subgroups. Finally, interaction tests showed that the relationship between SUA and log-transformed eGFR was significantly different (P for interaction < 0.05) between adolescents of different races (P for interaction = 0.015) and different BMI categories (P for interaction = 0.003), while this negative relationship was concordant across subgroups of sex and age.

Log-transformed eGFR by quartiles of SUA, stratified by age and BMI category

As shown in [Table 4](#), we stratified adolescents aged 12–19 years by age. The results showed a significant association between SUA levels and lower log-transformed eGFR (P for trend < 0.001) among all normal weight adolescents, underweight adolescents aged 16–19 years, overweight adolescents aged 12–15 years, and obese adolescents among the 3057 participants included after adjustment for age, sex, race, and BMI category. Additionally, the strongest

TABLE 3 Subgroup analyses of the effect of SUA on LgeGFR.

Subgroups	n	Mean ± SD	β (95%CI) P value	P for interaction
stratified by Sex				
Male	1567	5.60 ± 1.15	-0.0148 (-0.0183, -0.0113) <0.0001	0.587
Female	1470	4.46 ± 1.00	-0.0177 (-0.0216, -0.0138) <0.0001	
stratified by Age				
12-15 years	1591	4.93 ± 1.16	-0.0163 (-0.0200, -0.0125) <0.0001	0.961
16-19 years	1466	5.19 ± 1.27	-0.0149 (-0.0185, -0.0114) <0.0001	
stratified by Race				
White	792	5.12 ± 1.20	-0.0171 (-0.0219, -0.0123) <0.0001	0.015
Black	773	4.82 ± 1.23	-0.0199 (-0.0251, -0.0148) <0.0001	
Mexican American	642	4.99 ± 1.24	-0.0154 (-0.0210, -0.0097) <0.0001	
Other race	850	5.06 ± 1.23	-0.0140 (-0.0194, -0.0087) <0.0001	
stratified by BMI category				
Underweight	105	4.70 ± 0.98	-0.0386 (-0.0550, -0.0223) <0.0001	0.003
Normal weight	1760	4.79 ± 1.09	-0.0177 (-0.0213, -0.0141) <0.0001	
Overweight	553	5.17 ± 1.14	-0.0190 (-0.0248, -0.0132) <0.0001	
Obese	639	5.77 ± 1.36	-0.0146 (-0.0201, -0.0091) <0.0001	

Adjust for age, sex, race, education attainment, poverty income ratio, weight, waist circumference, BMI, BMI category, SBP, DBP, albumin, globulin, total protein, ALT, AST, GGT, LDH, blood urea nitrogen, serum glucose, cholesterol, triglycerides, LDL, HDL, albumin creatinine ratio. Mean ± SD for SUA.

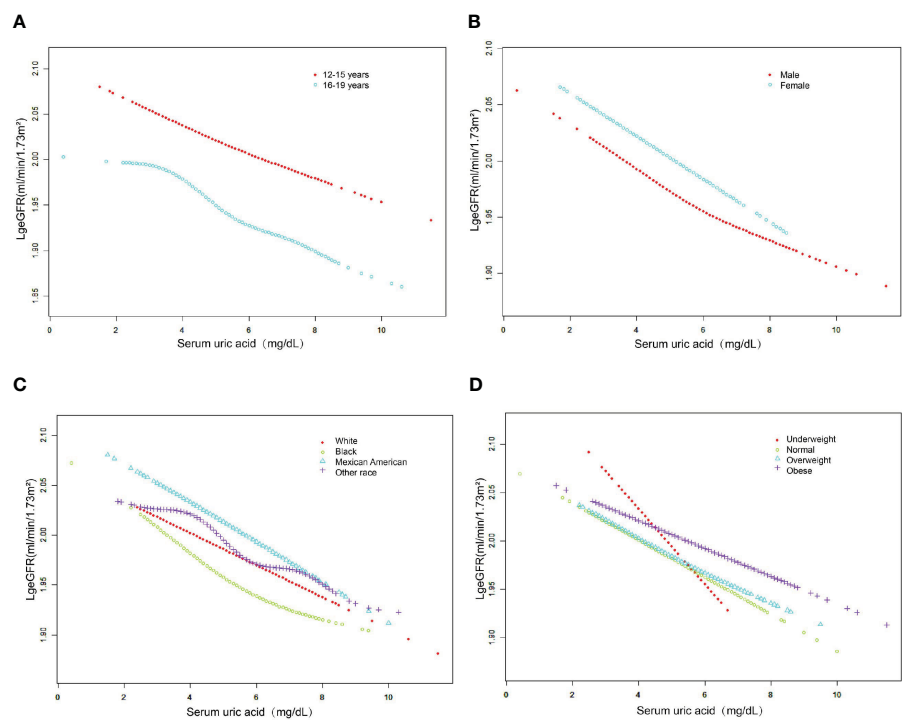


FIGURE 3
The association between serum uric acid and log-transformed eGFR stratified by age (A), sex (B), race (C) and BMI category (D). Adjusted for education attainment, poverty income ratio, weight, waist circumference, BMI, SBP, DBP, albumin, globulin, total protein, ALT, AST, GGT, LDH, blood urea nitrogen, serum glucose, cholesterol, triglycerides, LDL, HDL, albumin creatinine ratio.

TABLE 4 log-transformed eGFR by quartiles of serum uric acid, stratified by age and BMI category.

Quartiles of serum uric acid	LgeGFR (ml/min/1.73m ²) (95%CI)			
	Underweight	Normal weight	Overweight	Obese
12–15 years				
Q1 (0.40–4.00)	2.0632 (2.0126, 2.1138)	2.0421 (2.0333, 2.0508)	2.0596 (2.0351, 2.0841)	2.0723 (2.0433, 2.1012)
Q2 (4.10–4.80)	2.0725 (2.0243, 2.1207)	2.0253 (2.0168, 2.0337)	2.0347 (2.0151, 2.0543)	2.0291 (2.0085, 2.0497)
Q3 (4.90–5.70)	2.0299 (1.9675, 2.0922)	2.0112 (2.0022, 2.0203)	2.0136 (1.9947, 2.0325)	2.0303 (2.0138, 2.0469)
Q4 (5.80–11.50)	2.0156 (1.9364, 2.0948)	2.0040 (1.9903, 2.0176)	1.9641 (1.9438, 1.9845)	2.0077 (1.9931, 2.0223)
P for trend	0.192	<0.001	<0.001	<0.001
16–19 years				
Q1 (0.40–4.00)	2.0054 (1.9630, 2.0477)	1.9720 (1.9620, 1.9821)	1.9582 (1.9392, 1.9772)	1.9856 (1.9566, 2.0145)
Q2 (4.10–4.80)	2.0110 (1.9736, 2.0485)	1.9495 (1.9397, 1.9593)	1.9607 (1.9437, 1.9777)	1.9604 (1.9359, 1.9849)
Q3 (4.90–5.70)	1.9327 (1.8940, 1.9714)	1.9329 (1.9232, 1.9425)	1.9365 (1.9212, 1.9518)	1.9686 (1.9485, 1.9887)
Q4 (5.80–11.50)	1.9148 (1.8740, 1.9556)	1.9260 (1.9156, 1.9364)	1.9468 (1.9315, 1.9621)	1.9526 (1.9392, 1.9660)
P for trend	<0.001	<0.001	0.233	0.069

Adjust for age, sex, race and BMI category.

associations were observed in all normal weight adolescents combined, 16- to 19-year-old underweight adolescents, and 12- to 15-year-old overweight adolescents, all of whom had reduced log-transformed eGFR for each SUA quartile. Finally, the results of the trend test were significant (P for trend < 0.001) for all subgroups except for underweight adolescents aged 12–15 years and overweight and obese adolescents aged 16–19 years.

Discussion

In this large population-based and representative cross-sectional study, we found an inverse relationship between SUA and log-transformed eGFR, and the relationship was significantly different among adolescents of different ethnicities and BMI. Notably, compared with adolescents with other BMI categories, we found for the first time that the effect of SUA on log-transformed eGFR was greatest in underweight adolescents. Finally, this study also investigated the conclusions of a previous study that higher SUA levels are associated with higher BMI and that there are sex differences in SUA levels.

Recently, many intensive studies on SUA have found that SUA is an associated risk factor for many diseases (10, 13, 24–26). Previous studies on the effect of SUA on kidney injury have mainly focused on the prognosis of CKD. However, this field is still fraught with controversy. Sampson A.L. et al. performed a systematic review including 12 studies with 1,187 participants. The results indicated that the protective effect of uric acid-lowering therapy on renal function has obvious time-dependent effects. A decrease in serum creatinine and an increase in eGFR were observed after one year of uric acid-lowering therapy, but it showed little or no effect on eGFR after two years (27). However, another study showed different results about an inverse relationship between SUA levels and protection from CKD incidence and progression. Lower UA levels were protective for the risk of CKD incidence (RR 0.65 [95% CI 0.56–0.75]) and progression (RR 0.55 [95% CI 0.44–0.68]) (28). The results that we obtained also support this conclusion. That is, an apparent aggravated kidney injury characterized by a decrease in the eGFR is accompanied by elevated levels of serum uric acid. The reason for this result may be related to crystal-dependent or crystal-independent mechanisms of renal injury associated with SUA (20, 21). Nevertheless, further longitudinal studies are needed to verify these contradictory findings, which can be attributed to the differences in study design, study populations, and adjustment of confounding factors.

The study of uric acid has yielded a wealth of research results over the past few decades, both in the basic and clinical fields. The most discussed mechanisms of uric acid-induced kidney injury include oxidative stress, endothelial cell dysfunction, renal fibrosis, and renal inflammatory response (29). Past studies on the physiological functions of uric acid have found that it can counteract oxidative stress by avoiding oxidative inactivation of endothelial enzymes and by maintaining vascular endothelium-mediated vasodilatation (30). However, uric acid can also exacerbate cell and tissue damage due to oxidative stress by increasing the production of reactive oxygen species. For example, as precursors of uric acid, purines can

increase reactive oxygen levels by inducing IFN- γ upregulation of xanthine oxidoreductase expression (31). Excessive production of reactive oxygen species causes cellular damage, including vascular endothelial cells. Meanwhile, high-dose uric acid-mediated reduction in nitric oxide synthase activity and nitric oxide production is also involved in endothelial cell dysfunction, which ultimately increases the incidence of numerous adverse outcome events represented by cardiovascular events (32). More evidence from basic research is needed to confirm the details of this mechanism.

In the current study, we used a combination of subgroup analysis and an interaction test to find different effects of SUA on eGFR in adolescents with different BMIs. In addition, we focused for the first time on underweight adolescents as a potential at-risk population. As mentioned earlier, the effect of SUA levels on kidney function in the population can be influenced by many metabolic diseases and even by poor lifestyle habits such as smoking and alcohol consumption (33–35). Thus, the selection of adolescents can avoid the interference of these potential confounders and make them the ideal population to study.

Baseline data on renal function in underweight adolescents are limited. A study of malnutrition-inflammation-cachexia syndrome (MICS) in older individuals concluded that MICS could influence the relationship between high eGFR and mortality, particularly in people with low body mass index (36). This suggests, to some extent, that underweight adolescents may have an impairment of the glomerular filtration rate itself. Furthermore, although low SUA levels in the underweight adolescents in this study cannot be defined as hypouricemia compared to other adolescents, previous studies have found that renal hypouricemia can lead to the development of kidney stones as well as exercise-induced acute kidney injury (37, 38).

In addition, low weight is often associated with a reduced incidence of hyperuricaemia (39). A recent cohort study based on a large sample size found that SUA < 5.7 mg/dL was a key inflection point for predicting mortality risk in the population. The study showed for the first time that muscle loss and weight loss were more common in people with low SUA and were associated with higher mortality (40). A point worth noting for us is that the eGFR, which measured glomerular filtration levels in adolescents in this study, is an imperfect estimate of the true glomerular filtration rate based on creatinine measurements. Among the factors affecting creatinine concentrations are, on the one hand, residual functional clearance from the glomerulus and, on the other hand, indirect conversion of creatine from muscle metabolism. Therefore, muscle mass is a key factor influencing the magnitude of eGFR based on creatinine measurements (41). In the present study, the greatest effect of SUA on glomerular filtration rate was observed in adolescents with a lean BMI, probably due to the influence of low SUA levels in the lean adolescents themselves, and on the other hand, because eGFR based on creatinine measurements cannot avoid the interference of muscle mass due to differences in body mass. Therefore, obtaining measures of true glomerular filtration levels that are not confounded by muscle metabolic factors, such as inulin clearance and eGFR from radioactive elements, is particularly important in future studies (42, 43). Thus, this evidence may partially explain our results.

Meanwhile, case-control studies revealed that lower birth weight may be associated with the onset and progression of CKD in adulthood, possibly due to damage to the nephrons (44–47). The causes of impaired renal function may be related to the severity of perinatal complications, lower birth weight and shorter gestational age (48). However, due to the lack of the adolescents' relevant medical history dating back to birth in the NHANES database, it is not known whether there is a low glomerular filtration rate secondary to birth in the underweight adolescents in the present study. Therefore, an in-depth study based on a larger sample size is urgently needed to validate the findings of this study.

There are several limitations to our study. First, the present study is a cross-sectional study based on the NHANES database, which has the inherent weakness of being unable to reveal causal relationships between exposures and outcomes. Second, although we adjusted for numerous covariates that may influence the relationship between SUA and eGFR, the lack of prior medical history of adolescents in the database may have some impact on the effect values of the final study findings. Finally, we used the latest revision of the Schwartz formula to calculate the estimated glomerular filtration rate (22), but this is not a completely accurate proxy for the true glomerular filtration rate in adolescents of all ages. Therefore, more in-depth and well-designed longitudinal study designs are needed to elucidate the relationship between the two.

Conclusion

SUA was negatively associated with eGFR in adolescents aged 12–19 years. Furthermore, we found for the first time that SUA affects eGFR differently in adolescents with different BMIs. This effect was particularly significant in underweight adolescents. Therefore, we suggest that society and families should pay attention to the monitoring and management of BMI in adolescents, thus providing guidance for the prevention of CKD in adolescents. However, this study conclusion needs to be confirmed in further prospective studies and in a larger representative sample of underweight adolescents.

Data availability statement

The datasets presented in this study can be found in online repositories. The names of the repository/repositories and accession number(s) can be found in the article/supplementary material.

Ethics statement

The studies involving human participants were reviewed and approved by The ethics review board of the National Center for Health Statistics. Written informed consent to participate in this study was provided by the participants' legal guardian/next of kin. Written informed consent was obtained from the individual(s), and

minor(s)' legal guardian/next of kin, for the publication of any potentially identifiable images or data included in this article.

Author contributions

QT and CH had the idea for the study. QT and CH selected studies for inclusion and abstracted data. ZW, MH, YF and QT did the statistical analyses. CH and QT interpreted the data. QT wrote the first draft. MZ and QH critically revised the paper for important intellectual content. All authors contributed to the article and approved the submitted version.

Funding

This research was funded by Hunan innovative province construction project (Grant No. 2019SK2211), Key research and development project of Hunan Province (Grant No.2020SK2089), The Natural Science Foundation of Hunan province (Grant Nos 2020JJ4833, 2019SK2211, and XY040019), Hunan Province Key Field R&D Program (Grant No. 2020SK2097), and Horizontal Project (Grant Nos KY080269, KY080262, XY080323, and XY080324).

Acknowledgments

The authors appreciate the time and effort given by participants during the data collection phase of the NHANES project.

Conflict of interest

The authors declare that the research was conducted in the absence of any commercial or financial relationships that could be construed as a potential conflict of interest.

Publisher's note

All claims expressed in this article are solely those of the authors and do not necessarily represent those of their affiliated organizations, or those of the publisher, the editors and the reviewers. Any product that may be evaluated in this article, or claim that may be made by its manufacturer, is not guaranteed or endorsed by the publisher.

Supplementary material

The Supplementary Material for this article can be found online at: <https://www.frontiersin.org/articles/10.3389/fendo.2023.1138513/full#supplementary-material>

References

- Bikbov B, Purcell CA, Levey AS, Smith M, Abdoli A, Abebe M, et al. Global, regional, and national burden of chronic kidney disease, 1990–2017: a systematic analysis for the global burden of disease study 2017. *Lancet (London England)*. (2020) 395(10225):709–33.
- Kelly JT, Su G, Zhang L, Qin X, Marshall S, González-Ortiz A, et al. Modifiable lifestyle factors for primary prevention of CKD: a systematic review and meta-analysis. *J Am Soc Nephrol JASN* (2021) 32(1):239–53. doi: 10.1681/ASN.2020030384
- Duan JW, Li YL, Li SX, Yang YP, Li F, Li Y, et al. Association of long-term ambient fine particulate matter (PM_{2.5}) and incident CKD: a prospective cohort study in China. *Am J Kidney Dis* (2022) 80(5):638–47.e1. doi: 10.1053/j.ajkd.2022.03.009
- Gjerde A, Skrunes R, Reisaeter AV, Marti HP, Vikse BE. Familial contributions to the association between low birth weight and risk of CKD in adult life. *Kidney Int Rep* (2021) 6(8):2151–8. doi: 10.1016/j.ekir.2021.05.032
- Fang J, Alderman MH. Serum uric acid and cardiovascular mortality the NHANES I epidemiologic follow-up study, 1971–1992. national health and nutrition examination survey. *Jama* (2000) 283(18):2404–10. doi: 10.1001/jama.283.18.2404
- Messerli FH, Frohlich ED, Dreslinski GR, Suarez DH, Aristimuno GG. Serum uric acid in essential hypertension: an indicator of renal vascular involvement. *Ann Internal Med* (1980) 93(6):817–21. doi: 10.7326/0003-4819-93-6-817
- Viazzi F, Leoncini G, Vercelli M, Deferrari G, Pontremoli R. Serum uric acid levels predict new-onset type 2 diabetes in hospitalized patients with primary hypertension: the MAGIC study. *Diabetes Care* (2011) 34(1):126–8. doi: 10.2337/dc10-0918
- Doria A, Krolewski AS. Diabetes: lowering serum uric acid levels to prevent kidney failure. *Nat Rev Nephrol* (2011) 7(9):495–6. doi: 10.1038/nrneph.2011.107
- Allison SJ. Diabetes: serum uric acid level is associated with early GFR loss in type 1 diabetes. *Nat Rev Nephrol* (2010) 6(8):446. doi: 10.1038/nrneph.2010.92
- Ismail L, Materwala H, Al Kaabi J. Association of risk factors with type 2 diabetes: a systematic review. *Comput Struct Biotechnol J* (2021) 19:1759–85. doi: 10.1016/j.csbj.2021.03.003
- Pugliese NR, Mengozzi A, Virdis A, Casiglia E, Tikhonoff V, Cicero AFG, et al. The importance of including uric acid in the definition of metabolic syndrome when assessing the mortality risk. *Clin Res Cardiol Off J German Cardiac Soc* (2021) 110(7):1073–82. doi: 10.1007/s00392-021-01815-0
- Lee AM, Gurka MJ, DeBoer MD. Correlation of metabolic syndrome severity with cardiovascular health markers in adolescents. *Metab: Clin experiment* (2017) 69:87–95. doi: 10.1016/j.metabol.2017.01.008
- Srivastava A, Kaze AD, McMullan CJ, Isakova T, Waikar SS. Uric acid and the risks of kidney failure and death in individuals with CKD. *Am J Kidney Dis* (2018) 71(3):362–70. doi: 10.1053/j.ajkd.2017.08.017
- Carrero JJ, Stenvinkel P. Predialysis chronic kidney disease in 2010: novel targets for slowing CKD progression. *Nat Rev Nephrol* (2011) 7(2):65–6. doi: 10.1038/nrneph.2010.177
- Zhou H, Liu Z, Chao Z, Chao Y, Ma L, Cheng X, et al. Nonlinear relationship between serum uric acid and body mass index: a cross-sectional study of a general population in coastal China. *J Trans Med* (2019) 17(1):389. doi: 10.1186/s12967-019-02142-9
- Jorgensen RM, Bottger B, Vestergaard ET, Kremke B, Bahnsen RF, Nielsen BW, et al. Uric acid is elevated in children with obesity and decreases after weight loss. *Front pedia* (2021) 9:814166. doi: 10.3389/fped.2021.814166
- Zeng J, Lawrence WR, Yang J, Tian J, Li C, Lian W, et al. Association between serum uric acid and obesity in Chinese adults: a 9-year longitudinal data analysis. *BMJ Open* (2021) 11(2):e041919. doi: 10.1136/bmjopen-2020-041919
- Battelli MG, Bortolotti M, Polito L, Bolognesi A. The role of xanthine oxidoreductase and uric acid in metabolic syndrome. *Biochim Biophys Acta Mol Basis Dis* (2018) 1864(8):2557–65. doi: 10.1016/j.bbadis.2018.05.003
- Furuhashi M. New insights into purine metabolism in metabolic diseases: role of xanthine oxidoreductase activity. *Am J Physiol Endocrinol Metab* (2020) 319(5):E827–e34. doi: 10.1152/ajpendo.00378.2020
- Ejaz AA, Johnson RJ, Shimada M, Mohandas R, Alquadan KF, Beaver TM, et al. The role of uric acid in acute kidney injury. *Nephron* (2019) 142(4):275–83. doi: 10.1159/000499939
- Sharaf El Din UAA, Salem MM, Abdulazim DO. Uric acid in the pathogenesis of metabolic, renal, and cardiovascular diseases: a review. *J Adv Res* (2017) 8(5):537–48. doi: 10.1016/j.jare.2016.11.004
- Schwartz GJ, Munoz A, Schneider MF, Mak RH, Kaskel F, Warady BA, et al. New equations to estimate GFR in children with CKD. *J Am Soc Nephrol JASN* (2009) 20(3):629–37. doi: 10.1681/ASN.2008030287
- Kuczmarski RJ, Ogden CL, Guo SS, Grummer-Strawn LM, Flegal KM, Mei Z, et al. 2000 CDC growth charts for the united states: methods and development. *Vital Health Stat Ser 11 Data Natl Health Survey* (2002) 246(1):1–190.
- Ali N, Mahmood S, Islam F, Rahman S, Haque T, Islam S, et al. Relationship between serum uric acid and hypertension: a cross-sectional study in Bangladeshi adults. *Sci Rep* (2019) 9(1):9061. doi: 10.1038/s41598-019-45680-4
- Ali N, Miah R, Hasan M, Barman Z, Mou AD, Hafsa JM, et al. Association between serum uric acid and metabolic syndrome: a cross-sectional study in Bangladeshi adults. *Sci Rep* (2020) 10(1):7841. doi: 10.1038/s41598-020-64884-7
- Rocha E, Vogel M, Stanik J, Pietzner D, Willenberg A, Körner A, et al. Serum uric acid levels as an indicator for metabolically unhealthy obesity in children and adolescents. *Hormone Res paedia* (2018) 90(1):19–27. doi: 10.1159/000490113
- Sampson AL, Singer RF, Walters GD. Uric acid lowering therapies for preventing or delaying the progression of chronic kidney disease. *Cochrane Database system Rev* (2017) 10(10):Cd009460. doi: 10.1002/14651858.CD009460.pub2
- Gonçalves DLN, Moreira TR, da Silva LS. A systematic review and meta-analysis of the association between uric acid levels and chronic kidney disease. *Sci Rep* (2022) 12(1):6251. doi: 10.1038/s41598-022-10118-x
- Su HY, Yang C, Liang D, Liu HF. Research advances in the mechanisms of hyperuricemia-induced renal injury. *BioMed Res Int* (2020) 2020:5817348. doi: 10.1155/2020/5817348
- Becker BF. Towards the physiological function of uric acid. *Free Radical Biol Med* (1993) 14(6):615–31. doi: 10.1016/0891-5849(93)90143-1
- Wang H, Xie L, Song X, Wang J, Li X, Lin Z, et al. Purine-induced IFN- γ promotes uric acid production by upregulating xanthine oxidoreductase expression. *Front Immunol* (2022) 13:773001. doi: 10.3389/fimmu.2022.773001
- Park JH, Jin YM, Hwang S, Cho DH, Kang DH, Jo I. Uric acid attenuates nitric oxide production by decreasing the interaction between endothelial nitric oxide synthase and calmodulin in human umbilical vein endothelial cells: a mechanism for uric acid-induced cardiovascular disease development. *Nitric Oxide Biol Chem* (2013) 32:36–42. doi: 10.1016/j.niox.2013.04.003
- Major TJ, Topley RK, Dalbeth N, Merriman TR. Evaluation of the diet wide contribution to serum urate levels: meta-analysis of population based cohorts. *BMJ (Clinical Res ed)*. (2018) 363:k3951. doi: 10.1136/bmj.k3951
- Kim Y, Kang J. Association of urinary cotinine-verified smoking status with hyperuricemia: analysis of population-based nationally representative data. *Tobacco induced dis* (2020) 18:84. doi: 10.18332/tid/127269
- Nakagawa N, Hasebe N. Impact of mild-to-moderate alcohol consumption and smoking on kidney function. *Hypertension Res* (2017) 40(9):809–10. doi: 10.1038/hr.2017.51
- Ou SM, Chen YT, Hung SC, Shih CJ, Lin CH, Chiang CK, et al. Association of estimated glomerular filtration rate with all-cause and cardiovascular mortality: the role of malnutrition-inflammation-cachexia syndrome. *J cachexia sarcopenia muscle* (2016) 7(2):144–51. doi: 10.1002/jcsm.12053
- Ichida K, Hosoyamada M, Hisatome I, Enomoto A, Hikita M, Endou H, et al. Clinical and molecular analysis of patients with renal hypouricemia in Japan-influence of URAT1 gene on urinary urate excretion. *J Am Soc Nephrol JASN* (2004) 15(1):164–73. doi: 10.1097/01.ASN.0000105320.04395.D0
- Hosoyamada M. Hypothetical mechanism of exercise-induced acute kidney injury associated with renal hypouricemia. *Biomedicine* (2021) 9(12):1847. doi: 10.3390/biomedicine9121847
- Liu DM, Jiang LD, Gan L, Su Y, Li F. ASSOCIATION BETWEEN SERUM URIC ACID LEVEL AND BODY MASS INDEX IN SEX- AND AGE-SPECIFIC GROUPS IN SOUTHWESTERN CHINA. *Endocr Pract* (2019) 25(5):438–45. doi: 10.4158/EP-2018-0426
- Baker JF, Weber DR, Neogi T, George MD, Long J, Helget LN, et al. Associations between low serum urate, body composition, and mortality. *Arthritis Rheumatol (Hoboken NJ)* (2023) 75(1):133–40. doi: 10.1002/art.42301
- Nankivell BJ, Nankivell LFJ, Elder GJ, Gruenewald SM. How unmeasured muscle mass affects estimated GFR and diagnostic inaccuracy. *EClinicalMedicine* (2020) 29–30:100662. doi: 10.1016/j.eclinm.2020.100662
- Inker LA, Titan S. Measurement and estimation of GFR for use in clinical practice: core curriculum 2021. *Am J Kidney Dis* (2021) 78(5):736–49. doi: 10.1053/j.ajkd.2021.04.016
- Levey AS, Coresh J, Tighiouart H, Greene T, Inker LA. Measured and estimated glomerular filtration rate: current status and future directions. *Nat Rev Nephrol* (2020) 16(1):51–64. doi: 10.1038/s41581-019-0191-y
- Al Salmi I, Hoy WE, Kondalsamy-Chennakes S, Wang Z, Healy H, Shaw JE. Birth weight and stages of CKD: a case-control study in an Australian population. *Am J Kidney Dis* (2008) 52(6):1070–8. doi: 10.1053/j.ajkd.2008.04.028
- White SL, Perkovic V, Cass A, Chang CL, Poulter NR, Spector T, et al. Is low birth weight an antecedent of CKD in later life? a systematic review of observational studies. *Am J Kidney Dis* (2009) 54(2):248–61. doi: 10.1053/j.ajkd.2008.12.042
- Brathwaite KE, Levy RV, Sarathy H, Agalliu I, Johns TS, Reidy KJ, et al. Reduced kidney function and hypertension in adolescents with low birth weight, NHANES 1999–2016. *Pediatr Nephrol* (2023) 2144. doi: 10.1007/s00467-023-05958-2
- Gilarska M, Raaijmakers A, Zhang ZY, Staessen JA, Levchenko E, Klimek M, et al. Extremely low birth weight predisposes to impaired renal health: a pooled analysis. *Kidney Blood Pressure Res* (2019) 44(5):897–906. doi: 10.1159/000502715
- Goetschalckx E, Mekahli D, Levchenko E, Allegaert K. Glomerular filtration rate in former extreme low birth weight infants over the full pediatric age range: a pooled analysis. *Int J Environ Res Public Health* (2020) 17(6). doi: 10.3390/ijerph17062144



OPEN ACCESS

EDITED BY

Weixia Sun,
The First hospital of Jilin University, China

REVIEWED BY

Yifan Bu,
Harvard Medical School, United States
Giovanni Tarantino,
University of Naples Federico II, Italy
Jayanta Gupta,
Florida Gulf Coast University, United States

*CORRESPONDENCE

Qichao Yang

✉ yangqichao723@hotmail.com

[†]These authors have contributed equally to this work

RECEIVED 01 May 2023

ACCEPTED 07 August 2023

PUBLISHED 23 August 2023

CITATION

Wang Z, Qian H, Zhong S, Gu T, Xu M and Yang Q (2023) The relationship between triglyceride-glucose index and albuminuria in United States adults. *Front. Endocrinol.* 14:1215055. doi: 10.3389/fendo.2023.1215055

COPYRIGHT

© 2023 Wang, Qian, Zhong, Gu, Xu and Yang. This is an open-access article distributed under the terms of the [Creative Commons Attribution License \(CC BY\)](#). The use, distribution or reproduction in other forums is permitted, provided the original author(s) and the copyright owner(s) are credited and that the original publication in this journal is cited, in accordance with accepted academic practice. No use, distribution or reproduction is permitted which does not comply with these terms.

The relationship between triglyceride-glucose index and albuminuria in United States adults

Zhaoxiang Wang^{1†}, Han Qian^{2†}, Shao Zhong^{1†}, Tian Gu³, Mengjiao Xu³ and Qichao Yang^{3*}

¹Department of Endocrinology, Affiliated Kunshan Hospital of Jiangsu University, Kunshan, Jiangsu, China, ²Department of Cardiology, Affiliated Taicang Hospital of Soochow University, Suzhou, Jiangsu, China, ³Department of Endocrinology, Affiliated Wujin Hospital of Jiangsu University, Changzhou, Jiangsu, China

Purpose: Triglyceride-glucose (TyG) index is a simple and reliable indicator of metabolic dysfunction. We aimed to investigate a possible relationship between TyG index and albuminuria in the United States adult population.

Methods: This cross-sectional study was conducted among adults with complete TyG index and urinary albumin/urinary creatinine (UACR) from 2011-2018 National Health and Nutrition Examination Survey (NHANES). The independent relationship between TyG index and albuminuria (UACR>30mg/g) was evaluated. TyG index was compared with insulin resistance represented by homeostatic model assessment of insulin resistance (HOMA-IR), and metabolic syndrome. Subgroup analysis was also performed.

Results: A total of 9872 participants were included in this study, and the average TyG index was 8.53 ± 0.01 . The proportion of albuminuria gradually increased with the increase of TyG index quartile interval. Elevated TyG index was independently associated with albuminuria, and this association persisted after additional adjustments for HOMA-IR or dichotomous metabolic syndrome. The area under the ROC curve (AUC) of TyG index was larger than that of log (HOMA-IR). Subgroup analysis suggested that the relationship between TyG index and albuminuria is of greater concern in age<60, overweight/obese, diabetic, and metabolic syndrome patients.

Conclusion: The TyG index may be a potential epidemiological tool to quantify the role of metabolic dysfunction, rather than just insulin resistance, in albuminuria in the United States adult population. Further large-scale prospective studies are needed to confirm our findings.

KEYWORDS

triglyceride-glucose index, insulin resistance, metabolic syndrome, albuminuria, NHANES

1 Introduction

As a progressive disease, chronic kidney disease (CKD) has become one of the leading causes of death and suffering in the 21st century, affecting more than 10% of the general population worldwide (1). Patients with CKD also present with an increased risk of cardiovascular disease (2). In normal conditions, albumin is excreted in minimal amounts in the urine, making its detection challenging. However, when the glomerular filtration membrane is disrupted, the proteins in the glomerular filtration fluid are increased. In the early stages of glomerulopathy, when a routine urine protein test is negative, urinary microalbumin levels may vary and increase as the disease progresses (3). It is the most sensitive and reliable diagnostic index for early diabetic nephropathy and early hypertensive nephropathy (4, 5). Elevated albuminuria levels are an independent predictor of cardiovascular risk and have shown a strong association with non-alcoholic fatty liver disease (NAFLD) (6–10). Albuminuria is present in up to 40% of diabetic patients and has become an essential screening program for diabetic kidney disease (DKD) and diabetic cardiovascular events (11, 12).

Insulin resistance and metabolic syndrome are strongly associated with albuminuria (13–15). The HOMA-IR index was obtained using the homeostatic model assessment of insulin resistance (16). It is widely utilized in research on the development and progression of metabolic diseases, acting as a commonly employed indicator to evaluate the severity of insulin resistance (17, 18). Metabolic syndrome, defined by a combination of several laboratory and physical examination measures, is a dichotomous approach and thus does not allow for an assessment of the degree of risk (19). TyG index is a measure of metabolic dysfunction calculated from fasting triglyceride (TG, mg/dL) and fasting plasma glucose (FPG, mg/dL) measurements. It was considered a reliable surrogate marker of insulin resistance (20, 21). Multiple studies have indicated that TyG and HOMA-IR exhibit comparable accuracy in measuring insulin resistance when compared to the gold standard hyperinsulinemic-euglycemic clamp (19, 22, 23). Moreover, TyG index performed better than HOMA-IR in the diagnosis of metabolic syndrome (19, 24). NAFLD is a further expression of the metabolic syndrome (25). TyG index also serves as an effective surrogate marker for NAFLD and is associated with the underlying mechanisms of the disease, as well as NAFLD-related pathology, including extrahepatic tumors (26). Previous studies have demonstrated elevated TyG index can predict the progression of coronary artery calcification and the occurrence of adverse cardiovascular events (20, 27).

While several studies have investigated the association between TyG index and albuminuria, most of these studies have been limited to a single population and few have involved the United States population. More importantly, none of these studies considered the effects of insulin resistance and metabolic syndrome (28–31). The purpose of this study was to investigate the association between TyG index and albuminuria in the population of the National Health and Nutrition Examination Survey (NHANES) based on larger sample size. TyG index was compared vs. insulin resistance represented by HOMA-IR, and vs. metabolic syndrome.

2 Materials and methods

2.1 Data source

All the data in this study came from NHANES, which is a research program designed to assess the health and nutrition status of adults and children in the United States administered by the National Center for Health Statistics (NCHS) (32). NHANES has a complex, multistage, probability sampling design that allows it to be generalized to the US population (32). The protocol for the NHANES study was approved by the NCHS Research Ethics Review Board, and its detailed design and data are publicly available at <https://www.cdc.gov/nchs/nhanes/>. The current study included all participants older than 20 years with complete TyG index, albuminuria, and glomerular filtration rates from NHANES 2011 to 2018 who were in the fasting subsample.

2.2 Outcome definitions

Urinary albumin and creatinine were measured by solid-phase fluorescent immunoassay and modified Jaffe kinetic method, respectively. UACR was calculated by dividing the urinary albumin (mg/dL) concentration by the urinary creatinine concentration (mg/L). UACR was categorized as <30, 30–300, and ≥ 300 mg/g in subgroup analysis. Albuminuria, defined as an UACR > 30 mg/g, was considered as an outcome variable in our analysis (33). UACR 30–300 and ≥ 300 mg/g correspond to moderately increased albuminuria and severely increased albuminuria, respectively.

2.3 Exposure definitions

TyG index was calculated as $\ln(\text{fasting triglyceride}[\text{mg/dL}] \times \text{fasting plasma glucose}[\text{mg/dL}]/2)$. HOMA-IR was calculated using the following formula: $(\text{fasting insulin}[\mu\text{IU/mL}] \times \text{fasting plasma glucose}[\text{mmol/L}])/22.5$. HOMA-IR was log-transformed for modeling in this study. Metabolic syndrome is defined based on criteria developed jointly by international organizations such as the International Diabetes Federation, the National Heart, Lung and Blood Institute and the American Heart Association (34). Metabolic syndrome includes at least three of the five: elevated waist circumference (WC, cm), hypertension, hyperglycemia, elevated TG and decreased high density lipoprotein cholesterol (HDL-c, mg/dL).

2.4 Covariate definitions

Demographic data (age, gender, and race) was obtained. Some potential covariates were also included in this study, such as smoking status (never/former/current), physical activity (vigorous/moderate/less than moderate), hypertension (yes/no), diabetes (yes/no), cardiovascular disease (yes/no), body mass index (BMI, kg/m^2), WC, total cholesterol (TC, mg/dL), HDL-c, low density lipoprotein

cholesterol (LDL-c, mg/dl), serum creatinine (Scr, mg/dl), and estimated glomerular filtration rate (eGFR, ml/min/1.73 m²). BMI was categorized as <25, 25–29.9 and ≥30 kg/m², which corresponded to normal weight, overweight, and obese population for participants. The presence of cardiovascular disease was determined based on self-reported history of heart attack, stroke, congestive heart failure, coronary artery disease, or angina. eGFR was calculated according to the CKD Epidemiology Collaboration (CKD-EPI) creatinine equation consisting of age, gender, race, and Scr (35). Detailed measurement procedures for all variables in this study were publicly available in the NHANES database.

2.5 Statistical analysis

All statistical analyses were performed in accordance with Centers for Disease Control and Prevention (CDC) guidelines. A complex multistage cluster survey design was considered, and fasting subsample weights combined with four cycles were applied. Continuous variables were expressed as weighted mean with standard error (SE), and categorical parameters were presented as proportions. Weighted one-way ANOVA and weighted chi-squared tests were used for multiple-group comparisons of continuous and categorical variables respectively. Logistic and linear models were used to test the association between TyG index (continuous/quartile) and albuminuria and UACR in different models. The variance inflation factor (VIF) was employed to assess the level of collinearity among independent variables (36). The VIF is computed using a multivariate linear regression model. The VIF of each independent variable is equal to 1 divided by (1 – R²), where R² represents the coefficient of determination obtained by regressing the independent variables on the remaining independent variables. Independent variables with VIF greater than 5 were excluded. In model 1, no covariates were adjusted. In model 2, age, gender, and race were adjusted. Model 3 was adjusted for age, gender, race, smoking status, physical activity, hypertension, diabetes, cardiovascular disease, BMI, Scr, and eGFR. Weighted Pearson correlation analysis was used to evaluate the correlation between TyG index and other parameters. ROC was used to compare TyG index and TyG-derived indices with log (HOMA-IR). Age (<60/≥60 years), gender (female/male), BMI (normal weight/overweight/obese), diabetes (yes/no), hypertension (yes/no), metabolic syndrome (yes/no), cardiovascular disease (yes/no), and eGFR (<60/60–90/≥90 ml/min/1.73 m²) were stratified for subgroup analysis. Empower software (<http://www.empowerstats.com>) and R version 4.1.0 (<http://www.R-project.org>) were employed for all analyses. *P* value <0.05 was considered statistically significant.

3 Results

3.1 Baseline characteristics of study population

According to the inclusion criteria, a total of 9872 subjects were included in the study, with an average age of 46.81 ± 0.35 years,

including 48.94% male. We compared general information and clinical indicators for subjects in the non-albuminuria, moderately increased albuminuria and severely increased albuminuria groups (Table 1). Compared with non-albuminuria group, age, male, smoking proportion, less than moderate physical activity, hypertension prevalence, diabetes prevalence, cardiovascular disease prevalence, metabolic syndrome prevalence, BMI, WC, FPG, FIns, TG, Scr, urinary albumin, and HOMA-IR were significantly increased in moderately increased albuminuria and severely increased albuminuria groups (*P*<0.001), and LDL-c, HDL-c, urinary creatinine, and eGFR were decreased (*P*<0.05). There were also differences in race distribution among groups (*P*<0.001). Note that TyG levels were higher in the moderately increased albuminuria and severely increased albuminuria groups than in the non-albuminuria group (*P*<0.001).

3.2 Clinical features of the participants according to the quartiles of TyG index

According to the TyG level of all subjects, they were divided into four groups from low to high: quartile I (TyG<8.07), quartile II (8.07<TyG ≤ 8.50), quartile III (8.50<TyG ≤ 8.96), and quartile IV (TyG>8.96) (Table 2). Compared with quartile I-TyG group, age, male, smoking proportion, hypertension prevalence, diabetes prevalence, cardiovascular disease prevalence, metabolic syndrome prevalence, BMI, WC, FPG, FIns, TG, TC, Scr, urinary albumin, and HOMA-IR were significantly increased in quartile II-TyG, quartile III-TyG, and quartile IV-TyG groups increased significantly (*P*<0.001), and LDL-c, HDL-c, and eGFR decreased significantly (*P*<0.001). Most importantly, with the gradual increase of TyG level, the UACR level (19.34 ± 2.44 vs. 21.88 ± 2.94 vs. 25.75 ± 2.59 vs. 72.46 ± 10.90, *P*<0.001) and the number of people with albuminuria (7.13% vs. 7.66% vs. 8.27% vs. 16.58%, *P* <0.001) gradually increased.

3.3 Association of TyG index with albuminuria independent of HOMA-IR or metabolic syndrome

Our results showed that higher TyG index was associated with increased likelihood of increased albuminuria. This association was significant in model 1 [OR (95%CI): 1.871 (1.725–2.030), *P*<0.001], model 2 [OR (95%CI): 1.772 (1.622–1.936), *P*<0.001], model 3 [OR (95%CI): 1.391 (1.258–1.539), *P*<0.001], and the model with additional adjustment for log (HOMA-IR) [OR (95%CI): 1.346 (1.204–1.506), *P*<0.001] or metabolic syndrome [OR (95%CI): 1.316 (1.178–1.470), *P*<0.001]. We transformed TyG index from a continuous variable to a categorical variable. Compared to the lowest TyG index quartile, the highest TyG index quartile had 32.0% and 27.3% increased risk of albuminuria in the model with additional adjusted for log (HOMA-IR) or metabolic syndrome, respectively (Table 3). Using the UACR as a dependent variable for

the linear regression analysis, we can also find that TyG index is closely related to UACR (Table 4).

3.4 Correlation of TyG index with clinical parameters

Weighted Pearson correlation analysis suggested that the TyG index was consistently positively correlated with age, gender, race, smoking status, hypertension, diabetes, cardiovascular disease, WC, FPG, TG, TC, LDL-c, Scr, urinary albumin, UACR, albuminuria, and negatively correlated with HDL-c, urinary creatinine, and eGFR, whether unadjusted, or adjusted for log (HOMA-IR), metabolic syndrome ($P < 0.001$) (Table 5).

3.5 Multivariate logistic regression models of albuminuria

After removing covariates with VIF greater than 5, we performed a multivariate logistic regression analysis (Table 6). The independent variables included the TyG index, log (HOMA-IR), metabolic syndrome, age, gender, race, smoking status, physical activity, hypertension, diabetes, cardiovascular disease, BMI, Scr, and eGFR. The dependent variable was albuminuria. The results showed that TyG index [OR (95%CI): 1.283 (1.138-1.446), $P < 0.001$] was more strongly associated with albuminuria than log (HOMA-IR) [OR (95%CI): 1.138 (0.908-1.426), $P = 0.263$] and metabolic syndrome [OR (95%CI): 1.213 (1.024-1.438), $P < 0.05$].

TABLE 1 Baseline characteristics of study population according to UACR, weighted.

	Overall	Non-albuminuria	Moderately increased albuminuria	Severely increased albuminuria	P value
Age (year)	46.81 \pm 0.35	45.93 \pm 0.36	54.21 \pm 0.96	58.30 \pm 1.34	<0.001
Male gender, % (SE)	48.94 (0.57)	49.49 (0.63)	42.12 (2.06)	53.11 (4.25)	<0.001
Race, % (SE)					<0.001
Mexican American	8.99 (0.95)	8.72 (0.94)	11.17 (1.45)	13.05 (2.99)	
Other Hispanic	11.31 (0.98)	10.93 (0.95)	13.93 (1.64)	19.36 (2.96)	
Non-Hispanic White	64.40 (1.75)	65.01 (1.72)	61.07 (2.76)	47.37 (4.81)	
Non-Hispanic Black	6.39 (0.65)	6.42 (0.66)	5.59 (0.93)	9.22 (2.51)	
Other Races	8.90 (0.58)	8.92 (0.59)	8.23 (0.89)	11.00 (2.15)	
Smoking status, % (SE)					<0.001
Never	57.31 (0.97)	58.04 (0.97)	51.33 (2.32)	46.67 (3.98)	
Former	24.49 (0.78)	23.92 (0.78)	29.82 (2.29)	29.33 (3.40)	
Current	18.20 (0.82)	18.04 (0.86)	18.85 (2.19)	24.00 (4.43)	
Physical activity, % (SE)					<0.001
Vigorous	22.85 (0.72)	23.30 (0.76)	18.85 (1.97)	17.71 (3.74)	
Moderate	23.79 (0.66)	24.19 (0.75)	21.19 (1.56)	14.52 (2.80)	
Less than moderate	53.36 (0.88)	52.51 (0.97)	59.95 (2.29)	67.77 (3.96)	
Hypertension, % (SE)	32.55 (0.87)	29.98 (0.85)	52.84 (2.35)	73.71 (4.09)	<0.001
Diabetes, % (SE)	9.88 (0.46)	7.73 (0.41)	25.23 (1.98)	52.78 (4.43)	<0.001
Cardiovascular disease, % (SE)	8.90 (0.43)	7.45 (0.42)	19.16 (1.47)	37.98 (3.79)	<0.001
Metabolic syndrome, % (SE)	34.60 (0.81)	32.34 (0.85)	53.29 (2.19)	66.23 (3.70)	<0.001
BMI (kg/m ²)	29.16 \pm 0.14	29.02 \pm 0.15	30.38 \pm 0.37	31.16 \pm 0.93	<0.001
WC (cm ²)	99.47 \pm 0.36	99.01 \pm 0.36	103.08 \pm 0.84	106.65 \pm 2.31	<0.001
FPG (mg/dL)	107.22 \pm 0.47	104.88 \pm 0.40	123.93 \pm 1.96	153.55 \pm 6.08	<0.001
FIns (μ U/ml)	12.87 \pm 0.23	12.26 \pm 0.20	17.40 \pm 1.10	24.56 \pm 4.45	<0.001

(Continued)

TABLE 1 Continued

	Overall	Non-albuminuria	Moderately increased albuminuria	Severely increased albuminuria	P value
TG (mg/dL)	117.44 ± 1.71	115.03 ± 1.79	133.36 ± 4.50	172.31 ± 16.20	<0.001
TC (mg/dL)	189.27 ± 0.76	189.25 ± 0.81	189.69 ± 1.75	188.45 ± 3.65	0.930
LDL-c (mg/dL)	111.93 ± 0.58	112.24 ± 0.61	109.19 ± 1.61	108.34 ± 3.43	0.030
HDL-c (mg/dL)	54.24 ± 0.32	54.29 ± 0.31	54.48 ± 1.03	49.81 ± 1.51	0.004
Scr (mg/dl)	0.87 ± 0.00	0.86 ± 0.00	0.90 ± 0.03	1.52 ± 0.12	<0.001
eGFR (ml/min/1.73 m ²)	90.67 ± 0.51	91.11 ± 0.53	89.80 ± 1.51	70.16 ± 3.65	<0.001
Urinary albumin (mg/L)	37.13 ± 2.66	9.96 ± 0.14	86.51 ± 3.65	1334.68 ± 114.73	<0.001
Urinary creatinine (mg/dl)	127.94 ± 1.41	129.31 ± 1.55	116.96 ± 2.98	107.25 ± 5.02	<0.001
HOMA-IR	3.72 ± 0.08	3.39 ± 0.06	5.93 ± 0.45	10.74 ± 2.15	<0.001
TyG index	8.53 ± 0.01	8.50 ± 0.01	8.76 ± 0.04	9.10 ± 0.08	<0.001

BMI, body mass index; WC, Waist circumference; FPG, fasting plasma glucose; FIns, fasting plasma insulin; TG, triglyceride; TC, total cholesterol; LDL-c, low-density lipoprotein cholesterol; HDL-c, high-density lipoprotein cholesterol; SCr, serum creatinine; eGFR, estimated glomerular filtration rate; HOMA-IR, homeostatic model assessment of insulin resistance; TyG index, Triglyceride-glucose (TyG) index.

TABLE 2 Clinical and laboratory characteristics based on TyG index quartiles, weighted.

	Quartile I	Quartile II	Quartile III	Quartile IV	P value
Age (year)	40.19 ± 0.57	46.12 ± 0.50	49.33 ± 0.49	51.93 ± 0.45	<0.001
Male gender, % (SE)	39.59 (1.32)	46.99 (1.26)	51.80 (1.28)	57.95 (1.42)	<0.001
Race, % (SE)					<0.001
Mexican American	6.90 (0.95)	8.13 (0.98)	10.05 (1.06)	11.02 (1.16)	
Other Hispanic	18.50 (1.63)	12.32 (1.09)	8.05 (0.78)	6.00 (0.68)	
Non-Hispanic White	59.65 (2.19)	64.53 (1.97)	65.90 (1.96)	67.77 (1.76)	
Non-Hispanic Black	6.06 (0.86)	6.30 (0.69)	6.90 (0.70)	6.32 (0.85)	
Other Races	8.89 (0.87)	8.73 (0.71)	9.10 (0.76)	8.88 (0.76)	
Smoking status, % (SE)					<0.001
Never	65.40 (1.56)	60.26 (1.85)	54.11 (1.39)	48.95 (1.44)	
Former	20.39 (1.32)	21.91 (1.35)	26.58 (1.30)	29.35 (1.28)	
Current	14.20 (1.00)	17.84 (1.40)	19.31 (1.23)	21.70 (1.15)	
Physical activity, % (SE)					0.683
Vigorous	23.68 (1.45)	22.65 (1.40)	22.01 (1.14)	23.05 (1.20)	
Moderate	24.13 (1.24)	23.60 (1.24)	23.28 (1.15)	24.17 (1.29)	
Less than moderate	52.19 (1.51)	53.75 (1.69)	54.72 (1.36)	52.78 (1.46)	
Hypertension, % (SE)	18.90 (1.08)	27.48 (1.37)	37.24 (1.36)	47.49 (1.81)	<0.001
Diabetes, % (SE)	1.96 (0.35)	4.52 (0.50)	8.13 (0.69)	25.83 (1.43)	<0.001
Cardiovascular disease, % (SE)	4.69 (0.52)	7.71 (0.68)	10.09 (0.77)	13.40 (0.94)	<0.001
Metabolic syndrome, % (SE)	7.10 (0.76)	17.57 (1.00)	33.60 (1.24)	82.87 (1.31)	<0.001

(Continued)

TABLE 2 Continued

	Quartile I	Quartile II	Quartile III	Quartile IV	P value
BMI (kg/m ²)	26.33 ± 0.21	28.25 ± 0.20	30.17 ± 0.22	32.08 ± 0.21	<0.001
WC (cm ²)	90.76 ± 0.52	96.95 ± 0.51	102.54 ± 0.48	108.18 ± 0.52	<0.001
FPG (mg/dL)	94.82 ± 0.32	100.23 ± 0.33	105.18 ± 0.46	129.93 ± 1.34	<0.001
FIns (μIU/ml)	7.66 ± 0.22	10.49 ± 0.28	13.74 ± 0.35	20.03 ± 0.57	<0.001
TG (mg/dL)	49.94 ± 0.39	81.01 ± 0.38	118.78 ± 0.70	226.33 ± 4.23	<0.001
TC (mg/dL)	171.65 ± 1.00	185.28 ± 1.05	195.27 ± 0.97	205.95 ± 1.20	<0.001
LDL-c (mg/dL)	97.90 ± 0.90	111.53 ± 0.87	119.85 ± 0.81	118.99 ± 0.92	<0.001
HDL-c (mg/dL)	63.79 ± 0.55	57.54 ± 0.50	51.66 ± 0.32	43.28 ± 0.31	<0.001
Scr (mg/dl)	0.83 ± 0.01	0.88 ± 0.01	0.88 ± 0.01	0.90 ± 0.01	<0.001
eGFR (ml/min/1.73 m ²)	96.04 ± 0.78	89.96 ± 0.71	88.79 ± 0.66	87.65 ± 0.73	<0.001
Urinary albumin (mg/L)	22.97 ± 3.69	23.89 ± 2.70	28.57 ± 3.29	75.17 ± 11.03	<0.001
Urinary creatinine (mg/dl)	128.70 ± 2.65	125.85 ± 2.56	128.33 ± 2.32	128.89 ± 2.18	0.5275
UACR (mg/g)	19.34 ± 2.44	21.88 ± 2.94	25.75 ± 2.59	72.46 ± 10.90	<0.001
Albuminuria, % (SE)	7.13 (0.64)	7.66 (0.64)	8.27 (0.71)	16.58 (1.08)	<0.001
HOMA-IR	1.83 ± 0.06	2.69 ± 0.11	3.67 ± 0.11	6.86 ± 0.25	<0.001

3.6 Evaluation of the Impact of TyG index on albuminuria

As Figure 1 shows the performance for evaluating the endpoint among TyG index, TyG-derived indices, and log (HOMA-IR) for albuminuria risk, the AUC of the marker is as follows: BMI 0.557, WC 0.589, log (HOMA-IR) 0.597, TyG-BMI (TyG × BMI) 0.587, TyG-WC (TyG ×WC) 0.616, and TyG 0.616.

3.7 Subgroup analysis

Our subgroup analysis showed that the degree of association between TyG index levels and albuminuria was inconsistent across populations. The interaction test suggested that the relationship between TyG index and albuminuria was influenced by age (<60/≥60), BMI (normal weight/overweight/obese), diabetes (yes/no), and metabolic syndrome (yes/no) stratification (*P*<0.05). Age < 60,

TABLE 3 The association between TyG index and albuminuria.

Albuminuria	OR (95%CI) P value				
Continuous	Model 1	Model 2	Model 3	additionally adjusted for log (HOMA-IR)	additionally adjusted for metabolic syndrome
TyG index	1.871 (1.725, 2.030) <0.001	1.772 (1.622, 1.936) <0.001	1.391 (1.258, 1.539) <0.001	1.346 (1.204, 1.506) <0.001	1.316 (1.178, 1.470) <0.001
Categories					
Quartile I	1.00	1.00	1.00	1.00	1.00
Quartile II	1.317 (1.087, 1.597) 0.005	1.101 (0.902, 1.344) 0.342	1.024 (0.832, 1.260) 0.823	0.993 (0.806, 1.224) 0.950	1.005 (0.816, 1.237) 0.966
Quartile III	1.451 (1.201, 1.753) <0.001	1.139 (0.934, 1.390) 0.197	0.953 (0.772, 1.175) 0.650	0.902 (0.728, 1.118) 0.348	0.902 (0.728, 1.117) 0.344
Quartile IV	2.856 (2.401, 3.397) <0.001	2.246 (1.866, 2.705) <0.001	1.463 (1.189, 1.800) <0.001	1.320 (1.056, 1.650) 0.015	1.273 (1.014, 1.597) 0.038

OR, odds ratio.
95% CI: 95% confidence interval.
Model 1: no covariates were adjusted.
Model 2: age, gender, and race were adjusted.
Model 3: adjusted for age, gender, race, smoking status, physical activity, diabetes, hypertension, cardiovascular disease, BMI, Scr, and eGFR.

TABLE 4 The association between TyG index and UACR.

UACR	OR (95%CI) P value				
Continuous	Model 1	Model 2	Model 3	additionally adjusted for log (HOMA-IR)	additionally adjusted for metabolic syndrome
TyG index	48.614 (39.784, 57.443) <0.001	44.854 (35.497, 54.211) <0.001	28.455 (19.064, 37.846) <0.001	27.699 (17.352, 38.046) <0.001	30.348 (19.940, 40.755) <0.001
Categories					
Quartile I	1.00	1.00	1.00	1.00	1.00
Quartile II	9.474 (-7.944, 26.891) 0.286	2.632 (-15.018, 20.281) 0.770	-2.563 (-18.896, 13.769) 0.758	-4.470 (-20.961, 12.020) 0.595	-2.554 (-18.905, 13.796) 0.759
Quartile III	18.908 (1.513, 36.303) 0.033	9.161 (-8.852, 27.173) 0.318	3.249 (-13.707, 20.204) 0.707	-0.057 (-17.469, 17.354) 0.995	3.281 (-13.880, 20.441) 0.708
Quartile IV	73.236 (55.831, 90.642) <0.001	61.826 (43.435, 80.217) <0.001	28.239 (10.111, 46.367) 0.002	22.075 (2.499, 41.651) 0.027	28.346 (8.178, 48.514) 0.006

OR, odds ratio.

95% CI: 95% confidence interval.

Model 1: no covariates were adjusted.

Model 2: age, gender, and race were adjusted.

Model 3: adjusted for age, gender, race, smoking status, physical activity, diabetes, hypertension, cardiovascular disease, BMI, Scr, and eGFR.

overweight/obesity, diabetes, and metabolic syndrome may be effector modifiers (Figure 2).

4 Discussion

In this cross-sectional study of 9872 participants, we found that TyG index is a valid biomarker of metabolic dysfunction with relevancy to albuminuria in the United States population. Its

association with albuminuria appears to be largely independent of insulin resistance.

Insulin resistance is consistently associated with increased urinary albumin excretion (37, 38). Podocytes are thought to be the initial step in the development of albuminuria, and insulin signaling in podocytes appears to be important for maintaining the integrity of the glomerular filtration barrier (39, 40). Insulin resistance can also induce adipose tissue inflammation to activate and release proinflammatory cytokines such as IL-6 and TNF- α ,

TABLE 5 Correlation of TyG index with other parameters in the whole study population.

	Non-adjusted	adjusted for log (HOMA-IR)	adjusted for metabolic syndrome
log (HOMA-IR)	0.523**	–	0.349**
Metabolic syndrome	0.552**	0.399**	–
Age	0.240**	0.217**	0.118**
Gender	0.138**	0.150**	0.188**
Race	0.025*	0.083**	0.071**
Smoking status	0.110**	0.140**	0.092**
Physical activity	0.032**	0.017	0.023*
Hypertension	0.205**	0.114**	0.027**
Diabetes	0.329**	0.203**	0.177**
Cardiovascular disease	0.121**	0.073**	0.047**
BMI (kg/m ²)	0.264**	-0.028**	0.042**
WC (cm ²)	0.353**	0.079**	0.115**
FPG (mg/dL)	0.547**	0.393**	0.451**
FIns (μ U/ml)	0.266**	-0.138**	0.147**
TG (mg/dL)	0.750**	0.737**	0.701**

(Continued)

TABLE 5 Continued

	Non-adjusted	adjusted for log (HOMA-IR)	adjusted for metabolic syndrome
TC (mg/dL)	0.324**	0.374**	0.339**
LDL-c (mg/dL)	0.196**	0.211**	0.199**
HDL-c (mg/dL)	-0.464**	-0.335**	-0.331**
Scr (mg/dl)	0.066**	0.068**	0.044**
eGFR (ml/min/1.73 m2)	-0.130**	-0.136**	-0.063**
Urinary albumin (mg/L)	0.097**	0.064**	0.064**
Urinary creatinine (mg/dl)	-0.033**	-0.087**	-0.036**
UACR (mg/g)	0.108**	0.082**	0.073**
Albuminuria	0.155**	0.105**	0.074**

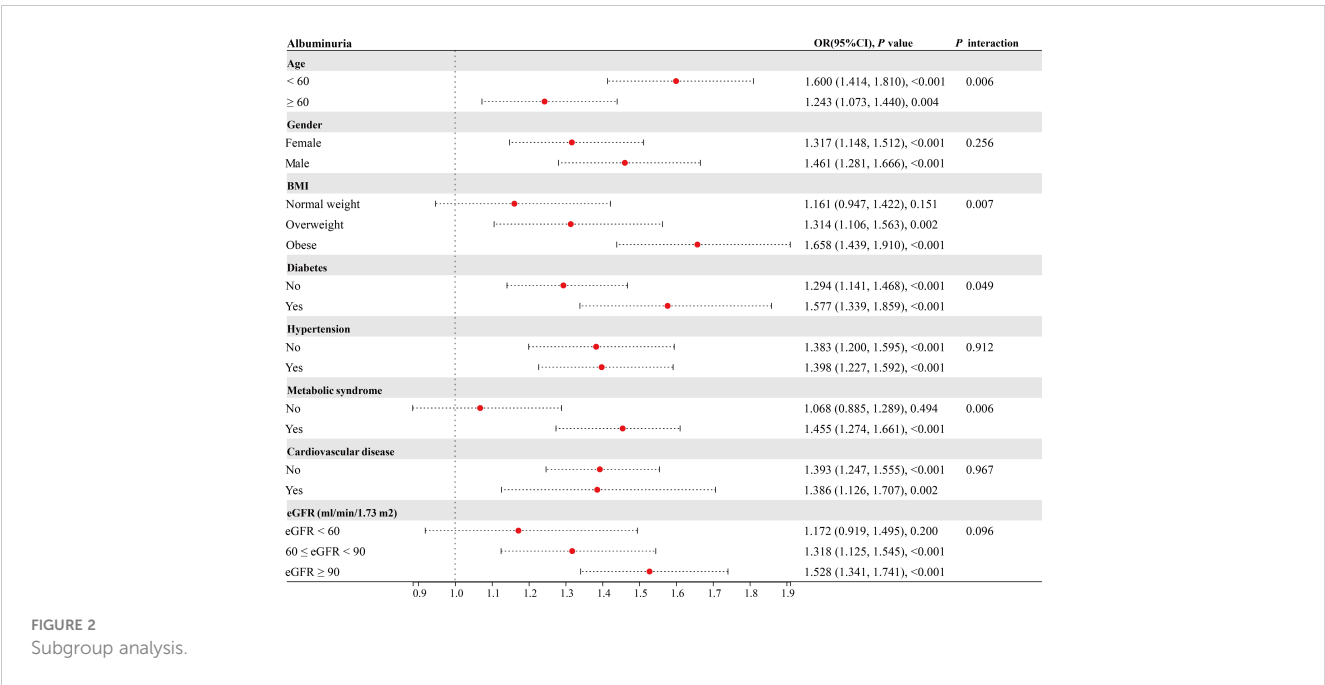
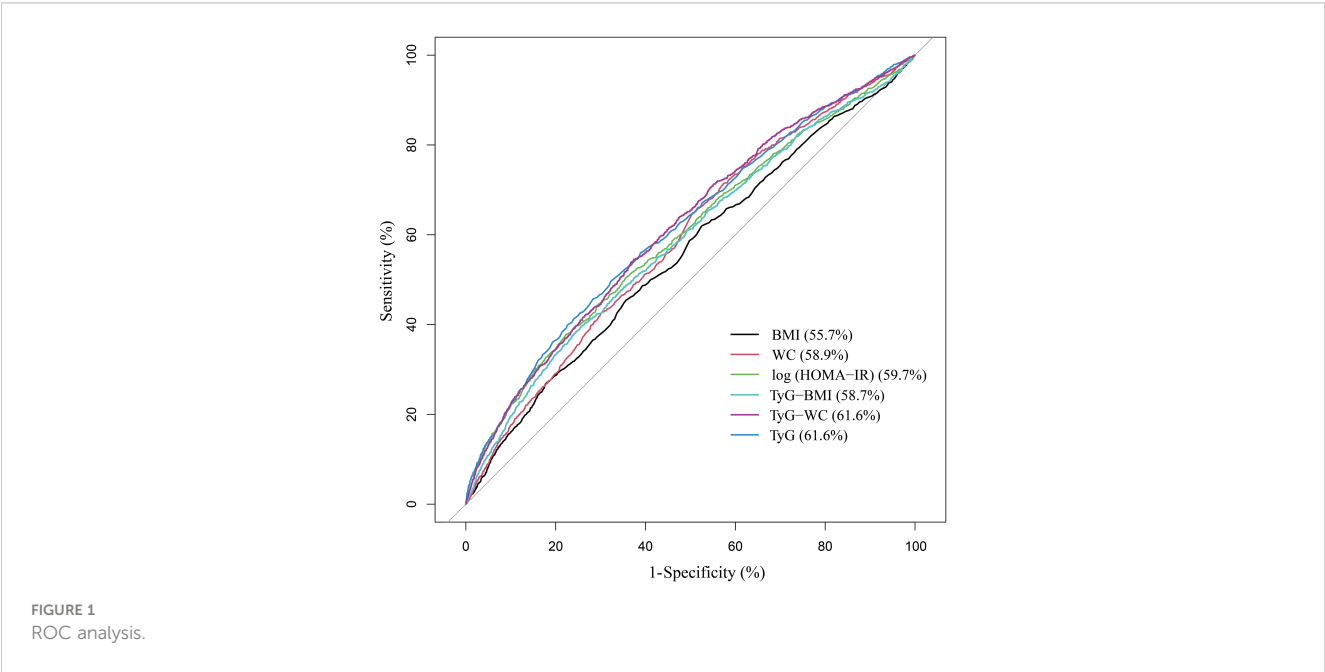
*P < 0.05; **P < 0.01.

TABLE 6 Multivariate logistic regression models of albuminuria.

	OR	95%CI lower	95%CI upper	P value
TyG index	1.283	1.138	1.446	<0.001
Log (HOMA-IR)	1.138	0.908	1.426	0.263
Metabolic syndrome (vs. no)	1.213	1.024	1.438	0.026
Age	1.028	1.023	1.034	<0.001
Gender (vs. male)	0.474	0.400	0.562	<0.001
Race (vs. Mexican American)				
Other Hispanic	0.658	0.524	0.826	0.000
Non-Hispanic White	0.728	0.593	0.895	0.003
Non-Hispanic Black	0.721	0.554	0.939	0.015
Other Races	0.904	0.712	1.147	0.407
Smoking status (vs. never)				
Former	1.072	0.913	1.257	0.396
Current	1.307	1.097	1.558	0.003
Physical activity (vs. vigorous)				
Moderate	1.061	0.857	1.314	0.587
Less than moderate	1.056	0.880	1.268	0.557
Hypertension (vs. no)	1.673	1.441	1.942	<0.001
Diabetes (vs. no)	1.954	1.656	2.305	<0.001
Cardiovascular disease (vs. no)	1.607	1.350	1.912	<0.001
BMI (kg/m ²)	0.998	0.987	1.009	0.702
Scr (mg/dl)	2.184	1.699	2.806	<0.001
eGFR (ml/min/1.73 m2)	1.025	1.019	1.030	<0.001

which induce endothelial dysfunction, leading to albuminuria and impaired renal function (41, 42). Several previous studies have also described the association between TyG and albuminuria from this perspective (28, 30, 43). However, TyG index continued to be associated with albuminuria after mutual adjustment of HOMA-

IR, suggesting that the mechanism of albuminuria induced by insulin resistance could not fully explain the effect of TyG index. This finding was also hinted at a previous longitudinal study of the Chinese population. Participants in the high TyG index, low HOMA-IR group had a higher risk of new-onset albuminuria



than participants in the low TyG index, low HOMA-IR group (44). Additionally, the ROC curves showed that the evaluation value of the TyG index for albuminuria was significantly higher than log (HOMA-IR), while the TyG-derived indices did not greatly improve. The TyG index has been extensively studied and validated as a marker of insulin resistance and metabolic abnormalities, unlike other TyG-derived indices. However, the TyG-WC index may also be valuable since it considers waist circumference, an essential measure of central obesity.

Our study further discovered that TyG's link to albuminuria persisted even after taking metabolic syndrome into account. This highlights the additive value of the TyG index in the investigation of metabolic risk factors for albuminuria. It may be more beneficial to use continuous rather than dichotomous measures of metabolic syndrome. At the same time, the results of mutual correction based on multivariate logistic regression can also be seen that the correlation between TyG index and albuminuria was stronger than that between HOMA-IR, metabolic syndrome, and albuminuria.

Further stratified subgroup analyses and interaction test suggested that the relationship between TyG index and albuminuria is of greater concern in age<60, overweight/obese, diabetic, and metabolic syndrome patients, at least in the United States population. Hypertension can worsen kidney injury and cause albuminuria, an important marker for cardiovascular events. Previous studies have also suggested a bidirectional association between hypertension and metabolic dysfunction, such as NAFLD (45). However, we did not find that hypertension or cardiovascular disease influenced the magnitude of the association between TyG index and albuminuria. This may suggest that the TyG index is more directly reflect the effects of metabolic dysfunction on albuminuria and is more valuable in people with metabolic dysfunction.

What is clear is that TyG index was associated with albuminuria, a relationship that was largely independent of insulin resistance represented by HOMA-IR. Future studies are needed to determine its performance as a predictive biomarker. In addition, special attention should be paid to differences in subgroups based on age, BMI, diabetes, and metabolic syndrome. There are some limitations in this study. First, due to the cross-sectional design of this study, a prospective study with large sample size is needed to clarify the causal relationship. Second, although we adjusted for some potential covariates, we could not completely exclude the influence of other possible confounders. Finally, the stratification of other subgroups was not considered, such as different types of diabetes, NAFLD, etc.

5 Conclusion

In a nationally representative study of adults aged ≥ 20 , the TyG index was associated with albuminuria. These findings cannot be fully explained by the insulin resistance or the dichotomous definition of metabolic syndrome. This metric shows promise as an epidemiological tool for quantifying the role of metabolic dysfunction in albuminuria and possibly for predictive value.

Data availability statement

Publicly available datasets were analyzed in this study. This data can be found here: <https://www.cdc.gov/nchs/nhanes/>.

References

1. Kovesdy CP. Epidemiology of chronic kidney disease: an update 2022. *Kidney Int Suppl* (2011) (2022) 12(1):7–11. doi: 10.1016/j.kisu.2021.11.003
2. Mathew RO, Bangalore S, Lavelle MP, Pellikka PA, Sidhu MS, Boden WE, et al. Diagnosis and management of atherosclerotic cardiovascular disease in chronic kidney disease: a review. *Kidney Int* (2017) 91(4):797–807. doi: 10.1016/j.kint.2016.09.049
3. Levey AS, Becker C, Inker LA. Glomerular filtration rate and albuminuria for detection and staging of acute and chronic kidney disease in adults: a systematic review. *Jama* (2015) 313(8):837–46. doi: 10.1001/jama.2015.0602
4. Wang XL, Lu JM, Pan CY, Tian H, Li CL. A comparison of urinary albumin excretion rate and microalbuminuria in various glucose tolerance subjects. *Diabetes Med* (2005) 22(3):332–5. doi: 10.1111/j.1464-5491.2004.01408.x
5. Griffin KA. Hypertensive kidney injury and the progression of chronic kidney disease. *Hypertension* (2017) 70(4):687–94. doi: 10.1161/HYPERTENSIONAHA.117.08314
6. Lambers Heerspink HJ, Gansevoort RT. Albuminuria is an appropriate therapeutic target in patients with CKD: the pro view. *Clin J Am Soc Nephrol* (2015) 10(6):1079–88. doi: 10.2215/CJN.11511114

Ethics statement

The studies involving human participants were reviewed and approved by National Center for Health Statistics (NCHS) Research Ethics Review Board. The patients/participants provided their written informed consent to participate in this study.

Author contributions

All authors listed have made a substantial, direct, and intellectual contribution to the work and approved it for publication.

Funding

This study was funded by the Suzhou Science and Technology Planning Project (STL2021006) and the Science and Technology Project of Changzhou Health Commission (WZ202226).

Acknowledgments

We want to acknowledge all participants of this study and the support provided by the Jiangsu University.

Conflict of interest

The authors declare that the research was conducted in the absence of any commercial or financial relationships that could be construed as a potential conflict of interest.

Publisher's note

All claims expressed in this article are solely those of the authors and do not necessarily represent those of their affiliated organizations, or those of the publisher, the editors and the reviewers. Any product that may be evaluated in this article, or claim that may be made by its manufacturer, is not guaranteed or endorsed by the publisher.

7. Perkovic V, Verdon C, Ninomiya T, Barzi F, Cass A, Patel A, et al. The relationship between proteinuria and coronary risk: a systematic review and meta-analysis. *PLoS Med* (2008) 5(10):e207. doi: 10.1371/journal.pmed.0050207
8. Jardine M, Zhou Z, Lambers Heerspink HJ, Hockham C, Li Q, Agarwal R, et al. Kidney, cardiovascular, and safety outcomes of canagliflozin according to baseline albuminuria: A CREDENCE secondary analysis. *Clin J Am Soc Nephrol* (2021) 16(3):384–95. doi: 10.2215/CJN.15260920
9. Qin Z, Li H, Wang L, Geng J, Yang Q, Su B, et al. Systemic immune-inflammation index is associated with increased urinary albumin excretion: A population-based study. *Front Immunol* (2022) 13:863640. doi: 10.3389/fimmu.2022.863640
10. Wijarnpreecha K, Thongprayoon C, Boonpheng B, Panjawanatana P, Sharma K, Ungprasert P, et al. Nonalcoholic fatty liver disease and albuminuria: a systematic review and meta-analysis. *Eur J Gastroenterol Hepatol* (2018) 30(9):986–94. doi: 10.1097/MEG.0000000000001169
11. Thoenes M, Bramlage P, Khan BV, Schieffer B, Kirch W, Weir MR. Albuminuria: pathophysiology, epidemiology and clinical relevance of an emerging marker for cardiovascular disease. *Future Cardiol* (2007) 3(5):519–24. doi: 10.2217/14796678.3.5.519
12. Lin YC, Chang YH, Yang SY, Wu KD, Chu TS. Update of pathophysiology and management of diabetic kidney disease. *J Formos Med Assoc* (2018) 117(8):662–75. doi: 10.1016/j.jfma.2018.02.007
13. Gu S, Wang A, Ning G, Zhang L, Mu Y. Insulin resistance is associated with urinary albumin-creatinine ratio in normal weight individuals with hypertension and diabetes: The REACTION study. *J Diabetes* (2020) 12(5):406–16. doi: 10.1111/1753-0407.13010
14. Park SK, Chun H, Ryoo JH, et al. A cohort study of incident microalbuminuria in relation to HOMA-IR in Korean men. *Clin Chim Acta* (2015) 446:111–6. doi: 10.1016/j.cca.2015.03.043
15. Rowley K, O'Dea K, Best JD. Association of albuminuria and the metabolic syndrome. *Curr Diabetes Rep* (2003) 3(1):80–6. doi: 10.1007/s11892-003-0058-1
16. Matthews DR, Hosker JP, Rudenski AS, Naylor BA, Treacher DF, Turner RC. Homeostasis model assessment: insulin resistance and beta-cell function from fasting plasma glucose and insulin concentrations in man. *Diabetologia* (1985) 28(7):412–9. doi: 10.1007/BF00280883
17. Wang T, Lu J, Shi L, et al. Association of insulin resistance and β -cell dysfunction with incident diabetes among adults in China: a nationwide, population-based, prospective cohort study. *Lancet Diabetes Endocrinol* (2020) 8(2):115–24. doi: 10.1016/S2213-8587(19)30425-5
18. González-González JG, Violante-Cumpa JR, Zambrano-Lucio M, et al. HOMA-IR as a predictor of health outcomes in patients with metabolic risk factors: A systematic review and meta-analysis. *High Blood Press Cardiovasc Prev* (2022) 29(6):547–64. doi: 10.1007/s40292-022-00542-5
19. Wu TD, Fawzy A, Brigham E, et al. Association of triglyceride-glucose index and lung health: A population-based study. *Chest* (2021) 160(3):1026–34. doi: 10.1016/j.chest.2021.03.056
20. Park K, Ahn CW, Lee SB, et al. Elevated tyG index predicts progression of coronary artery calcification. *Diabetes Care* (2019) 42(8):1569–73. doi: 10.2337/dc18-1920
21. Simental-Mendia LE, Rodríguez-Morán M, Guerrero-Romero F. The product of fasting glucose and triglycerides as surrogate for identifying insulin resistance in apparently healthy subjects. *Metab Syndr Relat Disord* (2008) 6(4):299–304. doi: 10.1089/met.2008.0034
22. Vasques AC, Novaes FS, de Oliveira Mda S, et al. TyG index performs better than HOMA in a Brazilian population: a hyperglycemic clamp validated study. *Diabetes Res Clin Pract* (2011) 93(3):e98–e100. doi: 10.1016/j.diabetes.2011.05.030
23. Guerrero-Romero F, Simental-Mendia LE, González-Ortiz M, et al. The product of triglycerides and glucose, a simple measure of insulin sensitivity. Comparison with the euglycemic-hyperinsulinemic clamp. *J Clin Endocrinol Metab* (2010) 95(7):3347–51. doi: 10.1210/jc.2010-0288
24. Son DH, Lee HS, Lee YJ, Lee JH, Han JH. Comparison of triglyceride-glucose index and HOMA-IR for predicting prevalence and incidence of metabolic syndrome. *Nutr Metab Cardiovasc Dis* (2022) 32(3):596–604. doi: 10.1016/j.numecd.2021.11.017
25. Tarantino G, Saldalamacchia G, Conca P, Arena A. Non-alcoholic fatty liver disease: further expression of the metabolic syndrome. *J Gastroenterol Hepatol* (2007) 22(3):293–303. doi: 10.1111/j.1440-1746.2007.04824.x
26. Tarantino G, Crocetto F, Di Vito C, Creta M, Martino R, Pandolfo SD, et al. Association of NAFLD and insulin resistance with non metastatic bladder cancer patients: A cross-sectional retrospective study. *J Clin Med* (2021) 10(2):346. doi: 10.3390/jcm10020346
27. Wang A, Tian X, Zuo Y, Chen S, Meng X, Wu S, et al. Change in triglyceride-glucose index predicts the risk of cardiovascular disease in the general population: a prospective cohort study. *Cardiovasc Diabetol* (2021) 20(1):113. doi: 10.1186/s12933-021-01305-7
28. Tian Y, Sun J, Qiu M, Lu Y, Qian X, Sun W, et al. Association between the triglyceride-glucose index and albuminuria in hypertensive individuals. *Clin Exp Hypertens* (2023) 45(1):2150204. doi: 10.1080/10641963.2022.2150204
29. Oh D, Park SH, Lee S, Yang E, Choi HY, Park HC, et al. High triglyceride-glucose index with renal hyperfiltration and albuminuria in young adults: the Korea National Health and Nutrition Examination Survey (KNHANES V, VI, and VIII). *J Clin Med* (2022) 11(21). doi: 10.3390/jcm11216419
30. Pan Y, Zhong S, Zhou K, et al. Association between diabetes complications and the triglyceride-glucose index in hospitalized patients with type 2 diabetes. *J Diabetes Res* (2021) 2021:8757996. doi: 10.1155/2021/8757996
31. Zhao S, Yu S, Chi C, et al. Association between macro- and microvascular damage and the triglyceride glucose index in community-dwelling elderly individuals: the Northern Shanghai Study. *Cardiovasc Diabetol* (2019) 18(1):95. doi: 10.1186/s12933-019-0898-x
32. Fain JA. NHANES. *Diabetes Educ* (2017) 43(2):151. doi: 10.1177/0145721716686792
33. Cho YT, Chen CW, Chen MP, et al. Diagnosis of albuminuria by tryptic digestion and matrix-assisted laser desorption/ionization/time-of-flight mass spectrometry. *Clin Chim Acta* (2013) 420:76–81. doi: 10.1016/j.cca.2012.12.016
34. Alberti KG, Eckel RH, Grundy SM, et al. Harmonizing the metabolic syndrome: a joint interim statement of the International Diabetes Federation Task Force on Epidemiology and Prevention; National Heart, Lung, and Blood Institute; American Heart Association; World Heart Federation; International Atherosclerosis Society; and International Association for the Study of Obesity. *Circulation* (2009) 120(16):1640–5. doi: 10.1161/CIRCULATIONAHA.109.192644
35. Levey AS, Stevens LA, Schmid CH, et al. A new equation to estimate glomerular filtration rate. *Ann Intern Med* (2009) 150(9):604–12. doi: 10.7326/0003-4819-150-9-200905050-00006
36. Cheng J, Sun J, Yao K, Xu M, Cao Y. A variable selection method based on mutual information and variance inflation factor. *Spectrochim Acta A Mol Biomol Spectrosc* (2022) 268:120652. doi: 10.1016/j.saa.2021.120652
37. Pilz S, Rutter F, Nijpels G, et al. Insulin sensitivity and albuminuria: the RISC study. *Diabetes Care* (2014) 37(6):1597–603. doi: 10.2337/dc13-2573
38. Fliser D, Pacini G, Engelleiter R, et al. Insulin resistance and hyperinsulinemia are already present in patients with incipient renal disease. *Kidney Int* (1998) 53(5):1343–7. doi: 10.1046/j.1523-1755.1998.00898.x
39. Welsh GI, Coward RJ. Podocytes, glucose and insulin. *Curr Opin Nephrol Hypertens* (2010) 19(4):379–84. doi: 10.1097/MNH.0b013e32833ad5e4
40. Jauregui A, Mintz DH, Mundel P, Fornoni A. Role of altered insulin signaling pathways in the pathogenesis of podocyte malfunction and microalbuminuria. *Curr Opin Nephrol Hypertens* (2009) 18(6):539–45. doi: 10.1097/MNH.0b013e32832f7002
41. De Cosmo S, Menzaghi C, Prudente S, Trischitta V. Role of insulin resistance in kidney dysfunction: insights into the mechanism and epidemiological evidence. *Nephrol Dial Transplant* (2013) 28(1):29–36. doi: 10.1093/ndt/gfs290
42. Shimobayashi M, Albert V, Woelnerhanssen B, et al. Insulin resistance causes inflammation in adipose tissue. *J Clin Invest* (2018) 128(4):1538–50. doi: 10.1172/JCI96139
43. Liu N, Liu C, Qu Z, Tan J. Association between the triglyceride-glucose index and chronic kidney disease in adults. *Int Urol Nephrol* (2023) 55(5):1279–89.
44. Gao W, Wang J, Chen Y, et al. Discordance between the triglyceride glucose index and HOMA-IR in incident albuminuria: a cohort study from China. *Lipids Health Dis* (2021) 20(1):176. doi: 10.1186/s12944-021-01602-w
45. Nakagami H. Mechanisms underlying the bidirectional association between nonalcoholic fatty liver disease and hypertension. *Hypertens Res* (2023) 46(2):539–41. doi: 10.1038/s41440-022-01117-6



OPEN ACCESS

EDITED BY

Weixia Sun,
The First Hospital of Jilin University, China

REVIEWED BY

Aydin Ece,
Dicle University, Türkiye
Jia Li,
Jilin University, China

*CORRESPONDENCE

Svetlana Lebedeva
✉ lebedeva502@yandex.ru
Kerim Mutig
✉ kerim.mutig@charite.de

RECEIVED 28 February 2023

ACCEPTED 23 August 2023

PUBLISHED 18 September 2023

CITATION

Lebedeva S, Margaryan A, Smolyarchuk E,
Nedorubov A, Materenchuk M,
Tonevitsky A and Mutig K (2023) Metabolic
effects of vasopressin in pathophysiology
of diabetic kidney disease.
Front. Endocrinol. 14:1176199.
doi: 10.3389/fendo.2023.1176199

COPYRIGHT

© 2023 Lebedeva, Margaryan, Smolyarchuk,
Nedorubov, Materenchuk, Tonevitsky and
Mutig. This is an open-access article
distributed under the terms of the [Creative
Commons Attribution License \(CC BY\)](#). The
use, distribution or reproduction in other
forums is permitted, provided the original
author(s) and the copyright owner(s) are
credited and that the original publication in
this journal is cited, in accordance with
accepted academic practice. No use,
distribution or reproduction is permitted
which does not comply with these terms.

Metabolic effects of vasopressin in pathophysiology of diabetic kidney disease

Svetlana Lebedeva^{1*}, Arus Margaryan¹, Elena Smolyarchuk¹,
Andrey Nedorubov¹, Maria Materenchuk¹,
Alexander Tonevitsky² and Kerim Mutig^{1,3*}

¹Department of Pharmacology, Institute of Pharmacy, I.M. Sechenov First Moscow State Medical University, Moscow, Russia, ²Faculty of Biology and Biotechnology, HSE University, Moscow, Russia,

³Department of Translational Physiology, Charité-Universitätsmedizin, Berlin, Germany

The diabetic kidney disease (DKD) is the major cause of the chronic kidney disease (CKD). Enhanced plasma vasopressin (VP) levels have been associated with the pathophysiology of DKD and CKD. Stimulation of VP release in DKD is caused by glucose-dependent reset of the osmostat leading to secondary pathophysiologic effects mediated by distinct VP receptor types. VP is a stress hormone exhibiting the antidiuretic action in the kidney along with broad adaptive effects in other organs. Excessive activation of the vasopressin type 2 (V2) receptor in the kidney leads to glomerular hyperfiltration and nephron loss, whereas stimulation of vasopressin V1a or V1b receptors in the liver, pancreas, and adrenal glands promotes catabolic metabolism for energy mobilization, enhancing glucose production and aggravating DKD. Increasing availability of selective VP receptor antagonists opens new therapeutic windows separating the renal and extra-renal VP effects for the concrete applications. Improved understanding of these paradigms is mandatory for further drug design and translational implementation. The present concise review focuses on metabolic effects of VP affecting DKD pathophysiology.

KEYWORDS

diabetic kidney disease, glucose metabolism, vasopressin, vasopressin V1a receptor (V1aR), vasopressin V1b receptor (V1bR)

Metabolic syndrome and diabetic kidney disease

Metabolic syndrome is a combination of homeostatic deviations associated with a high risk of cardiovascular complications, such as dysregulation of lipid metabolism, high blood glucose levels, and increased blood pressure. Development of the metabolic syndrome is frequently accompanied by insulin resistance, which is the main pathogenetic mechanism of the type 2 diabetes mellitus (DM2) (1, 2). Therefore, a large proportion of people with DM2 displays a complex picture of metabolic pathophysiology encompassing glycemic and non-glycemic components (1, 2). The etiology and pathogenesis of DM2 comprise genetic predisposition, obesity, sleep time deficit or excess, as well as other factors associated with development of insulin resistance and impaired insulin response to glucose or non-glucose

stimuli (1, 2). Because of the insulin resistance, DM2 is also referred as insulin-independent DM type. Etiology of the type 1 diabetes mellitus (DM1) includes genetic risk factors triggering pancreatic islet autoimmunity followed by insufficient insulin production and release. Apart from the genetic background, DM1 may be provoked by environmental influences such as intoxications, pancreatic infections, or cancer (1). Independently on the etiology, both DM1 and DM2 lead to progressive reduction of β -cell mass or impaired β -cell function with hyperglycemia as a clinical manifestation. People with hyperglycemia are at risk of major diabetes mellitus complications independently on the diabetes type (1, 2).

Diabetic Kidney Disease (DKD) belongs to frequent and severe complications of both insulin-dependent DM1 and insulin-independent DM2. Clinical features of DKD are largely similar in the two diabetes mellitus types, typically manifesting as enhanced urinary albumin excretion, general proteinuria, reduction of the glomerular filtration rate, disorders of electrolyte and acid-base homeostasis, or hypertension, depending on the disease progression (3). The functional renal deteriorations are strongly related to pathomorphological alterations of kidney tissue encompassing thickening of glomerular and tubular basement membrane, mesangial expansion, glomerulosclerosis, sterile inflammation, arteriolar hyalinosis, and tubulointerstitial fibrosis (4). Even though the initial pathohistological kidney damage patterns differ in patients with DM1 vs. DM2, the resulting glomerular dysfunction and morphological injury due to chronic hyperglycemia appear to play the decisive role in progression of DKD to Chronic Kidney Disease (CKD) with ensuing end stage renal failure (1, 3, 4). Along with hypertension, DKD is the most common etiologic factor of CKD (NIH) (3, 5).

CKD is caused by a heterogeneous group of disorders and characterized by the presence of morphological kidney damage or decline of renal function during three months or longer, irrespective of the cause (6). The severity of CKD is typically assessed by the grade of Glomerular Filtration Rate (GFR) reduction, albuminuria, abnormalities in urinary sediment, as well as morphological kidney damage detected by imaging techniques or histopathological biopsy analysis (6).

Despite diversity of the etiologic factors, the pathogenetic mechanisms of CKD leading to its progress to the end-stage renal failure are intersecting and include Renin-Angiotensin System (RAS) hyperactivity, glomerular hyperfiltration with ensuing glomerulosclerosis, renal vasculopathy, as well as cytokine dysregulation and activation of pro-fibrotic pathways (7–9).

In this context, epidemiologic studies revealed an association between increased vasopressin (VP) plasma levels and CKD suggesting a role of excessive VP signaling in pathophysiology of chronic kidney disorders (10). Elevated plasma VP concentrations are typically observed in DM1 and DM2 patients (11–13). Animal models of DM exhibit increased VP levels as well (10, 12). There are several lines of evidence suggesting that exaggerated VP signaling aggravates the course of DKD via renal and systemic effects including dysregulation of glucose and lipid metabolism. VP antagonists have been increasingly recognized as emerging

pharmacological strategies for prevention or retardation of CKD of diabetic and non-diabetic origin (10, 14).

While renal physiological functions of VP has been well characterized (15–18), available information on its metabolic effects in other organs and tissues is in part controversial (14). The global trend, however, is suggestive of a pathophysiological impact of VP effects on glucose metabolism in DM2 (12, 14, 19, 20). These pathophysiological effects are mediated by distinct VP receptor types providing a translational perspective of their selective targeting towards corrections of certain metabolic deviations such as hyperglycemia (14).

Apart from DM, experiments in animal suggested that enhanced VP signaling aggravates the fructose-induced metabolic syndrome (21). Improved understanding of metabolic effects and signaling mechanisms involved in the pathogenesis of DM and DKD is mandatory for clinical implementation of selective VP receptor antagonists or agonists. This concise review summarizes recent progress in this direction, with particular focus on the glucose metabolism in DM and DKD.

Vasopressin and its receptors

The neurohypophysial hormone VP, also referred to as antidiuretic hormone (ADH), fulfils multiple physiological tasks comprising preservation of water homeostasis, regulation of cardiovascular function, stimulation of hormone secretion from anterior pituitary, adjustment of glucose metabolism, and modulation of social behavior (14, 17).

VP is synthesized in the hypothalamus in form of a pre-hormone containing VP, neurophysin, and copeptin (17). After the ensuing cleavage of the pre-hormone in the neurohypophysis, all three components are released into the blood in equimolar amounts. Moreover, plasma copeptin and VP levels closely correlate over the wide range of plasma osmolalities (22). Since detection of VP in plasma is by far less reliable and more complicated than measurement of copeptin, the latter has been established as a surrogate for VP plasma levels in the clinical routine (17, 22, 23).

In addition to the peripheral VP secretion, vasopressinergic neurons of hypothalamus project to other brain regions, where they modulate diverse Central Nervous System (CNS) functions (24). The blood-brain barrier prevents infiltration of VP from the blood into the brain tissue, thus dissociating between its central vs. peripheral actions. The present review work focuses on the peripheral VP effects in the context of DKD and CKD.

VP is a nonapeptide hormone acting via three receptor types: vasopressin V1a (V1aR), V1b (V1bR), and V2 receptors (V2R) (17). The tissue distribution of these receptor types determines the local mode of VP action. V1aR and V1bR show broad expression patterns across the organs and tissues, whereas expression of V2R is limited to the kidney (14).

Despite substantial previous efforts, cell type-specific distribution of distinct VP receptor types is still subject of debates for many organs. The underlying reasons are partially related with a limited availability of selective and robust antibodies to the

individual VP receptor types due to a high homology between the VP receptor types and their low expression levels typical for the most G protein-coupled receptor (25).

Therefore, available localization data substantially rely on mRNA techniques and functional studies. Immunolabeling using commercial and non-commercial antibodies produced controversial results (15, 26). Nevertheless, recent development of selective antibodies to V1aR and V2R has enabled their cell type-specific localization in the rodent and human kidneys by knockout tissue-controlled studies (15, 16). Taken together, reliably detectable levels of V1aR expression and significant functional effects of V1aR activation have been reported in the brain, kidney, liver, heart, adrenal glands, and peripheral arteries. V1bR is less broadly distributed among organ and tissues compared to V1aR but is present at least in the pancreas and adrenal gland. Finally, significant V2R expression was detected only in the kidney tissue. The data on organ and tissue distribution of VP receptor types in rodent and human species relevant for the present review are summarized in the Table 1.

V1aR distribution

Early studies of V1aR expression in rat liver and kidney using radioactive *in situ* hybridization revealed presence of V1aR mRNA in hepatocytes, as well as in distal tubular segments of the kidney and renal vasculature (27, 32). The renal finding were largely reproduced in a later autoradiographic V1aR localization using a specific ligand (48). Evaluation of microdissected rat nephron segments and vessels using RT-PCR suggested that V1aR is expressed in renal arteries, along the cortical and medullary CD, as well as in glomeruli (31).

Application of different anti-V1aR antibodies in rodent or human kidney tissues produced controversial results with respect to its segmental and intracellular localization in mammalian kidney (16, 26, 49). Presence of V1aR at the protein level has been convincingly demonstrated in renal vasculature and intercalated cells (IC) of CNT/CD throughout the rodent and human species (16, 35). Mouse but not rat or human kidney exhibited V1aR protein in macula densa (MD) cells as well (16, 34).

TABLE 1 Distribution of distinct VP receptor types in mammalian organs and tissues.

Organ/tissue/cell type; (references)	V1a	V1b	V2
<i>Brain</i>			
Hippocampus (27, 28)	+	+	-
Arcuate nucleus (27)	+	+	-
Solitary tract (27)	+	-	-
Inferior olive (27)	+	-	-
Brainstem (27)	+	-	-
Hypothalamus (27, 28)	+	+	-
Amygdala (28)	-	+	-
Cerebellum (28)	-	+	-
Pituitary gland (14, 27–30)	+	+	-
<i>Kidney</i>			
Gl (31)	+	-	-
PT	-	-	-
TAL (15, 27, 32, 33)	-	-	+
MD (15, 16, 34)	+ (mouse only)	-	-
DCT (15, 27, 32, 33)	-	-	+
CNT/CD, PC (15, 27, 32, 33)	-	-	+
CNT/CD, IC-A (14, 16, 26, 32, 35)	+	-	-
CNT/CD, IC-B (14, 16, 26, 32, 35)	+	-	-
<i>Liver</i>			
Hepatocytes (27, 32)	+	-	-
Cholangiocytes	-	-	-
<i>Pancreatic islets</i>			
alpha-cells (36, 37)	-	+	-
beta-cells (19, 36)	+	+	-
delta-cells (36)	-	+	-
PP-cells (36)	-	-	-
<i>Adrenal gland</i>			
Zona glomerulosa (38–40)	+	-	-
Zona fasciculata (38–40)	+	-	-
Zona reticularis (38–40)	+	-	-
Medulla (38–40)	-	+	-
<i>Arteries</i> (14, 16, 27, 31, 32)	+	-	-

The Table 1 summarized evidence on expression of distinct vasopressin (VP) receptor types across mammalian organs and tissues with focus on their implications in nephrotoxic effects depicted in the Figure 1. The data rely on original localization and functional studies, as well as on comprehensive review papers. The presence of the distinct VP receptor types is indicated by (+), whereas the absence of the VP receptors or debatable data are labeled by (-). The respective organ/tissue-specific references are provided in brackets. Gl – glomerulus, PT – proximal tubule, TAL – thick ascending limb, DCT – distal convoluted tubule, CNI – connecting tubule, CD – collecting duct, PC – principal cells, IC – intercalated cells (type A or B).

Apart from the liver and kidney, expression and functional significance of V1aR have been well established in the cardiovascular system (14, 50, 51). Furthermore, functional studies suggested that V1aR is expressed in the adenohypophysis and adrenal glands with modulating functions in the endocrine homeostasis (29, 38). The V1aR expression in the adrenal gland has been verified in human tissue (39, 40). Therefore, V1aR-mediated stress response may aggravate renal damage in DKD or CKD.

V1bR distribution

V1bR expression has been mainly localized to various regions of the brain including the anterior pituitary with effects on the adrenocorticotrophic hormone (ACTH) release (14, 30). The other reported sites of V1bR expression include pancreas and adrenal glands (28, 36, 40). Overall, long-term V1bR hyperactivity may boost the Renin-Angiotensin-Aldosterone System (RAAS) and cause adverse metabolic effects in DKD patients.

V2R distribution

V2R receptor is generally considered as the kidney-specific VP receptor type (27, 32, 52). In the kidney, V2R mRNA has been detected along the entire distal nephron, comprising the thick ascending limb (TAL), the distal convoluted tubule (DCT), and the connecting tubule (CNT), as well as in collecting duct (CD) (26, 27, 32, 33). CNT and CD contain two cell types: the principal (PC) and the intercalated cells (IC). Expression of V2R is limited to PCs in these segments (33). In line with the mRNA data, V2R protein has been localized to the basolateral membranes of TAL, DCT, and PCs of CNT/CD (15). The only V2R-negative cell types within the distal nephron and CD system were the MD cells in the cortical TAL and ICs in CNT/CD (15). The kidney-specific V2R distribution pattern is compatible with the critical role of the VP-V2R signaling in the urinary concentration (53).

Vasopressin system in diabetic kidney disease

DKD belongs to frequent complications of either type 1 (insulin-dependent) or type 2 (non-insulin-dependent) diabetes mellitus. Along with hypertension, DKD is the most common cause of CKD (3). Diabetic patients usually have elevated plasma VP levels, which may be associated with a resetting of the osmostat or increased fluid turnover (11–13, 54). Chronically enhanced VP secretion may provoke the development or aggravate DKD via renal and extra-renal adverse effects.

Renal effects of vasopressin in diabetic kidney disease

Experiments in rodent DKD models showed that excessive VP signaling is associated with kidney hypertrophy, glomerular

hyperfiltration, and increased albumin excretion (10, 12, 18). Similar symptoms typically occur in diabetic patients prior to the development of DKD (3, 12). Results of chronic infusion of a selective V2R agonist dDAVP (1-deamino-D-arginine⁸ vasopressin) in normal and VP-deficient Brattleboro rats suggested that the aforementioned deleterious effects of VP are, at least partially, mediated by V2R (18, 55–57). The underlying pathophysiological mechanisms may be related to sustained stimulation of the urinary concentration promoting the NaCl reabsorption along the medullary thick ascending limb (mTAL) followed by inhibition of the tubuloglomerular feedback (TGF) mechanism and compensatory increase in the GFR (18, 57). Chronic increase of GFR is a reasonable mechanism of glomerular hyperfiltration and albuminuria in DKD (12, 57). Nephroprotective effects of V2R antagonists such as tolvaptan has been increasingly recognized, which led to their clinical approval as a part of therapy in patients with Autosomal Dominant Polycystic Kidney Disease (ADPKD) (58). Little evidence is currently available on effects of V2R antagonism in patients with DKD. Retrospective studies point to beneficial effects, as judged by milder histopathological renal damage in kidney biopsies from patients with heart failure and concomitant DKD treated with tolvaptan compared to equivalent patients without tolvaptan administration (59). Apart from that, tolvaptan appears to be instrumental for alleviation of nephrotic syndrome in DKD patients (60). Taken together, V2R antagonists bear therapeutic potential as a part of DKD treatment strategy but their pronounced diuretic action and certain hepatotoxicity may limit patient compliance and complicate the long-term application in chronic kidney disorders such as DKD or CKD (61).

While V2R-activation appears to induce glomerular hyperfiltration via the TGF mechanism, stimulation of V1aR may cause renal vasoconstriction via direct vascular effects (62). In the physiologic situation, the vasoconstrictive effects of VP are buffered by NO and prostaglandin systems (62). Diabetes mellitus impairs the autoregulation of renal blood flow and regulation of GFR via complex pathophysiologic mechanisms affecting K⁺ and Ca²⁺ channel activities in smooth muscle cells and paracrine modulation of the vascular tone (63). The net effect of these changes is pre-glomerular vasodilation and glomerular hyperfiltration with ensuing glomerular damage leading to glomerulosclerosis (3, 63). Apart from vascular effects, V1aR mediates stimulation of H⁺ secretion by type A ICs (IC-A) in response to VP, thereby promoting urinary acidification (16). This effect may be related to potentiation of aldosterone action upon concomitant V1aR activation in ICs (35). Whether V1aR-dependent modulation of urinary acidification plays a role in pathophysiology of DKD remains to be clarified. Finally, VP binding to V1aR in MD cells has been shown to increase renin secretion with resulting systemic RAS activation (16, 34). Presence of V1aR in MD cells was demonstrated in the mouse species only, whereas localization of the receptor in rat and human kidney failed to confirm this result (16). Despite potential interspecies differences in V1aR-dependent regulation of renin release, extra-renal stimulating effects of VP on RAAS activity such as enhanced ACTH or adrenal hormone secretion were extensively documented in rodent and human species (28, 29, 38, 40, 41, 64).

Effects of vasopressin on renin-angiotensin-aldosterone system in diabetic kidney disease

Several clinical studies reported increased RAAS activity in patients with type 2 diabetes, especially in the presence of DKD (65–68). RAAS hyperactivity has been well recognized as a critical pathogenetic factor contributing to progression of DKD and CKD towards advanced renal fibrosis and end-stage kidney disease (3). There is growing clinical and scientific evidence suggesting that effects of VP in different organs synergistically stimulate RAAS. VP modulates the neurohypophyseal-adrenal axis by promoting the ACTH release in the neurohypophysis, increasing the sensitivity of adrenal glands to ACTH, and enhancing the adrenal synthesis and secretion of steroid hormones including aldosterone (28, 38, 40, 69, 70). These effects are mediated by V1aR or V1bR. VP-deficient Brattleboro rats showed a dissociation between high plasma renin and low plasma aldosterone levels along with decreased amount of angiotensin II (AngII) binding sites in the adrenal glands reflecting the idea that VP may potentiate effects of AngII via regulation of the AngII receptor type 1 (AT1R) (71). Moreover, VP and AngII have been shown to strengthen effects of each other in the kidney, which may be related to the shared downstream cAMP-dependent signaling pathways (71, 72).

In contrast to hyperreninemia observed in Brattleboro rats with global suppression of VP signaling, selective deletion of V1aR in mice was associated with reduced renin expression and plasma activity (34). This discrepancy may be explained by interspecies differences in renal V1aR expression in MD cells and VP-dependent paracrine stimulation of renin-producing juxtaglomerular cells (34). Unlike mouse species, MD cells in rat and human kidney are devoid of V1aR (16). VP has been shown to suppress renin expression and plasma activity in rat and human species via the V2R-mediated signaling (44, 71, 73).

Taken together, elevated VP levels in DKD may increase the RAAS activity at different levels including stimulation of ACTH and aldosterone release, modulation of adrenal sensitivity to AngII, and direct synergism with AngII via intracellular cAMP generation. These effects are mediated by V1aR or V1bR. In contrast, activation of V2R may counterbalance the RAAS hyperactivity via suppression of renal renin expression and release. The net effect of all three VP receptor types on distinct RAAS components may be variable but clinical reports are suggestive of RAAS activation in DM patients (65, 68). In particular, enhanced aldosterone plasma levels have been closely associated with insulin resistance and DKD (68, 74). In the classic paradigm, aldosterone is considered as a Na⁺-sparing and K⁺-secreting hormone predominantly acting via modulating the relevant gene expression in the aldosterone-sensitive distal nephron (ASDN) of the kidney, which comprises the late distal convoluted tubule (DCT2), connecting tubule (CNT), and cortical collecting duct (cCD) (75). However, recent progress in understanding of genomic and non-genomic effects of aldosterone mediated by the mineralocorticoid receptors (MR) or alternative vascular aldosterone-sensitive pathways has broadened the interpretation of its role in induction and aggravation of CKD

and renal fibrosis (76). According to the accumulated clinical and scientific data, effects of aldosterone on the kidney function and morphology are wider than just regulation of electrolyte handling in CNT and CD. Aggravating effects of elevated plasma aldosterone levels in DKD may be direct or indirect including the well-known renal axis and recently identified alternative pathways. In this context, suppression of aldosterone release using V1aR or V1bR antagonists may contribute to the renoprotection in patients with DM.

Metabolic effects of vasopressin in diabetic kidney disease

Effects of vasopressin on glucose metabolism

As a stress hormone, VP exerts numerous direct and indirect metabolic effects towards energy mobilization. Glucose is a principal energy source for the brain and an important secondary energy substrate for many other organs and tissues. Importantly, the process of urine concentration requires glucose as the energy source since the medullary portions of the distal nephron and collecting duct system function upon the physiologic hypoxia and utilize glucose. Moreover, adaptations of glucose metabolism in renal epithelial cells has been implicated in pathophysiology of acute and chronic renal injuries (77). VP regulates the glucose metabolism via central and peripheral effects resulting in elevation of blood glucose levels (78). Direct effects of VP on glucose availability in the blood are mediated by V1aR in the liver and V1bR in the pancreas (27, 32, 36). Binding of VP to V1aR in the liver induces glycogen degradation thereby augmenting the blood glucose levels (32). At the same time, activation of V1bR in alpha cells of pancreatic islets stimulates glucagon release, which further promotes glycogenolysis in the liver (36). VP has been shown to increase plasma insulin levels as well, although to a lesser extent compared to glucagon (78). Since V1bR expression was predominantly reported in the glucagon-producing alpha cells of pancreatic islets, effects of VP on the insulin release are likely indirect and may be mediated by enhanced glucose concentrations in the blood (79). Stimulation of cortisol release in response to VP may further contribute to rise in blood glucose levels by promoting gluconeogenesis in the liver (41, 42). Apart from direct and indirect stimulation of the glucose production, VP has been shown to modulate insulin sensitivity and lipolytic activity in the adipose tissue, which may secondarily affect the blood glucose concentration as well (80). The net effect of the complex physiological action of VP on the glucose metabolism is an increase of the blood glucose concentration likely serving to promote the global adaptation of the energy metabolism to stress.

Enhanced VP signaling has been increasingly recognized as a critical factor aggravating the metabolic syndrome in DM2 and promoting the kidney damage in DKD and CKD (18, 57). Effects of VP on the glucose production are distinctly mediated by V1aR or V1bR, enabling their selective targeting using receptor-specific

agonists or antagonists. Development of such strategies requires improved molecular understanding of VP signaling downstream of V1aR vs. V1bR. In this context, characterization of transgenic mice with selective deletion of V1aR (V1aR^{-/-}) or V1bR (V1bR^{-/-}) produced a complex picture with respect to their individual roles in the glucose metabolism (20). Notably, effects of pharmacologic vs. genetic suppression of V1aR and V1bR types produced in part conflicting results demanding for mechanistic explanations (14).

Effects of pharmacologic vs. genetic V1a receptor inactivation on glucose homeostasis

Studies using acute and chronic administration of V1aR agonists and antagonists in rodents suggested that V1aR activation increases the blood glucose levels but reduces the glucose tolerance (37). These effects are likely mediated by increased production of glucose in the liver and modulation of insulin sensitivity in peripheral tissues. Analysis of V1aR^{-/-} mice showed impaired glucose tolerance as well, but hepatic production of glucose was increased (20, 81). Based on pharmacologic effects of V1aR antagonists, V1aR deletion was expected to suppress glycogenolysis and lower the blood glucose levels. Surprisingly, glycogen content was decreased in the liver tissue of V1aR^{-/-} mice (81). Pharmacologic stimulation of V1aR produced pro-diabetic effects, whereas V1aR antagonism revealed antidiabetic potential in rats (37). In contrast, challenging of V1aR^{-/-} mice with high-fat diet produced more pronounced obesity, hyperleptinemia, and impaired glucose tolerance compared to control mice suggesting that V1aR deletion induces a pre-diabetic condition and aggravates the metabolic syndrome in this model (20, 81). The reasons for discrepant effects of pharmacologic vs. genetic suppression of the V1aR signaling on the glucose homeostasis are still poorly understood but may be related with induction of compensatory mechanisms during embryonal and postnatal development of V1aR^{-/-} mice. Such mechanisms may include enhanced hepatic response to other stimuli for glucose production or *de novo* expression of V1bR in the liver of V1aR^{-/-} mice (21). While V1aR-deficient mice represent a valuable model for improved understanding of VP biology, detailed characterization of effects elicited by selective V1aR agonists and antagonists in rodent models of DM2 and DKD is of immediate clinical relevance (37).

Effects of pharmacologic vs. genetic V1b receptor inactivation on glucose homeostasis

V1bR is expressed in alpha cells of pancreatic islet and mediates VP-induced stimulation of glucagon release via the Ca²⁺/inositol 1,4,5-triphosphate signaling pathway (19, 36, 78). Glucagon, in turn, increases systemic glucose availability via activation of glycogenolysis in the liver and increasing gluconeogenesis in the liver and kidney. Systemic availability of glucose may be further increased by lipolysis (43). Parallel V1bR-mediated stimulation of

catecholamine release may further contribute to hyperglycemic effects of VP (82). The resulting rise in blood glucose concentration may cause a modest increase in insulin plasma concentration, which has been documented in response to VP in several *in vivo* and *ex vivo* studies (79). The idea that effects of VP on the insulin release are indirect is supported by the absence of convincing reports documenting expression of VP receptors in the beta cells of pancreatic islet, as well as by the blunted VP effects on the insulin release in the absence of concomitant increase in the blood glucose concentration. In line with this, effects of VP on the insulin plasma levels were completely abolished in V1bR^{-/-} mice (79). Studies using AVP together with selective antagonists for V1aR, V1bR or a combined V1aR and V1bR antagonist in isolated rodent pancreatic tissue also confirmed that the direct effect of AVP on the glucagon release is mediated by V1bR, whereas the effect on insulin release is indirect (79). Analysis of the glucose homeostasis in V1bR^{-/-} mice revealed decreased fasting glucagon, insulin, and glucose levels in the blood along with increased insulin sensitivity in peripheral tissues (83). Therefore, the data accumulated so far suggests that V1bR mediates effects of AVP on the blood glucose levels and may significantly contribute to the progression of DM2 and DKD.

Effects of double V1aR and V1bR inactivation and global AVP deficiency on glucose homeostasis

Since both V1aR and V1bR are implicated in the glucose homeostasis, effects of their concomitant deletion were evaluated. The phenotype of the double-knockout mice was largely reflecting the phenotype of V1aR^{-/-} mice and showed higher blood glucose and insulin levels along with impaired glucose tolerance (14, 20). Based on these results it is tempting to speculate that stimulation of V1aR may lower the blood glucose concentration. However, pharmacologic V1aR activation induced hyperglycemia, whereas administration of a V1aR antagonist blunted the AVP-induced hyperglycemia in normal rats (37). In addition, evaluation of the glucose homeostasis in VP-deficient Brattleboro rats revealed lower plasma glucose and insulin levels along with enhanced glucose tolerance (84). The in part conflicting results obtained in different models of pharmacologic or genetic inhibition of VP signaling require improved understanding and cautious interpretation with respect to potential clinical application of V1aR- or V1bR-antagonists in diabetic patients. Figure 1 provides a concept of VP-induced kidney damage combining renal and metabolic effects.

Effects of vasopressin on lipid metabolism

VP enables water conservation and at the same time functions as a stress hormone. Fat is a source of metabolic water and an energy source as well. VP exerts central and peripheral modulating effects on lipid metabolism. Indeed, the net effect of VP on the lipid homeostasis depends on the global metabolic status and combines distinct actions in different tissues (14). As a stress hormone, AVP

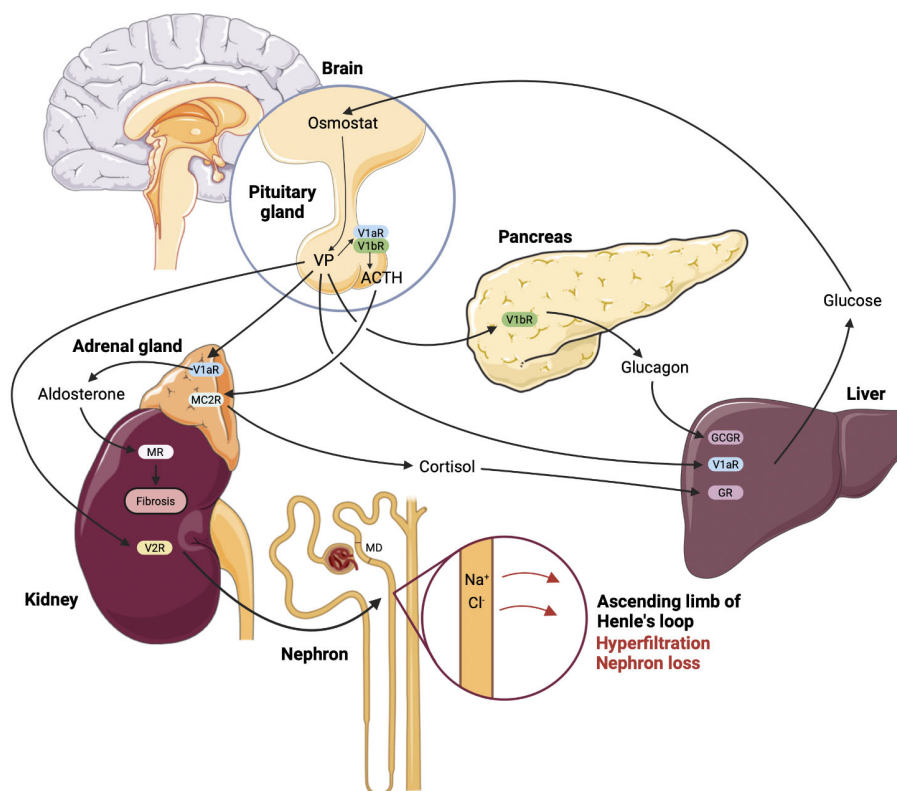


FIGURE 1

Renal and metabolic nephrotoxic effects of vasopressin mediated by the individual receptor subtypes in diabetic kidney disease. According to the current state of understanding, enhanced plasma glucose levels promote vasopressin (VP) synthesis and release due to reset of the osmostat in hypothalamus. Enhanced circulating VP causes glomerular hyperfiltration with ensuing glomerular damage via sustained stimulation of NaCl reabsorption in the thick ascending limb, decreased NaCl concentration at the macula densa (MD) site and resulting increase of glomerular filtration rate (GFR). This effect is aggravated by renin-angiotensin-aldosterone system hyperactivity caused by VP-induced increase of adrenocorticotropic hormone (ACTH) and aldosterone release, the latter is stimulated directly in the adrenal gland, as well as via the MC2R receptor to ACTH. Parallel release of cortisol potentiates effects of VP on the glucose production in the liver, whereas VP-dependent glucagon release further aggravates the hyperglycemia. Finally, enhanced blood glucose levels maintain high VP plasma levels promoting the renal damage in DKD. The effects of VP are indicated by arrows and the respective receptor type are specified using abbreviations.

enhances the sympathetic tone thereby promoting lipolysis in the adipose tissue (44–46). Concomitant VP-induced stimulation of adrenal hormone release may have multiple effects on lipid metabolism depending on the current nutrition status (85). In fact, both lipolytic and antilipolytic actions have been reported in rats depending on the experimental conditions (86). In addition to the indirect effects mediated by changes in the vegetative and endocrine status, VP affects the lipid metabolism directly by targeting several organs and tissues. Acting via V1 receptor types, VP has been reported to promote triacylglycerol mobilization in the heart, which may serve to support cardiac energy metabolism (87). However, chronically exaggerated VP signaling has been associated with cardiovascular disorders and combined V1aR/V2R antagonism demonstrated beneficial effects in patients with acute heart failure (50, 51, 88). Activation of V1aR or V1bR in the pancreas and the associated glucagon release may promote hepatic lipolysis via Ca²⁺/inositol triphosphate-dependent signaling in order to enhance the glucose production (43, 47). Peripheral effects of VP in the fat tissue are debatable since both lipolytic and anti-lipolytic actions were reported and distinct underlying mechanisms including direct and hemodynamic

effects discussed (80, 86, 89). Analysis of V1aR^{-/-} and V1bR^{-/-} mouse strains suggested that many effects of VP on lipid metabolism may be mediated by changes in insulin sensitivity (90, 91). Taken together, VP exerts complex effects on lipid homeostasis requiring further characterization. The physiological sense of these effects appears to be related to catabolic metabolism and energy substrate supply at short term (14). Chronic increases of circulating VP levels in DM2 may promote the metabolic syndrome and aggravate DKD (Table 2).

Conclusions and perspectives

Apart from the antidiuretic function, VP has been increasingly recognized as a global player in the glucose, lipid, and protein homeostasis. Unlike the V2R-dependent antidiuretic functions, metabolic effects of VP are predominantly mediated by V1aR and V1bR. Excessive V2R-mediated signaling substantially aggravates kidney damage in DKD and CKD. Selective V2R antagonists are available and even approved for treatment of hyponatremia and polycystic kidney disease (92, 93). Despite encouraging perspective

TABLE 2 Metabolic effects of vasopressin (VP) in diabetic kidney disease.

Direct and indirect metabolic effects	Involved VP receptor type/organ or tissue	Pathophysiologic effects in DKD	References
Glucose metabolism			
Glycogenolysis	V1a/liver	Hyperglycemia	(27, 32)
Glucagon release -> glycogenolysis	V1b/pancreas -> liver	Hyperglycemia	(36)
Cortisol release -> gluconeogenesis	V1a/adrenal glands -> liver	Hyperglycemia	(41–43)
Fat metabolism			
↑ sympathetic tone	V1b or V1a/hypothalamus, pituitary gland, adrenal gland -> fat tissue	Lipolysis -> insulin resistance	(44–46)
Insulin resistance	V1a or V1b/pancreas	Lipolysis -> hyperglycemia	(43, 47)

The Table 2 summarizes potential adverse metabolic effects of vasopressin (VP) in Diabetic Kidney Disease (DKD). (->) indicates sequence of events, (↑) means an increase.

of their use in DKD and CKD patients, a relatively high hepatotoxicity and poor patient compliance due to the pronounced diuretic action limit practical implementation of this strategy (61). Pharmacological targeting of V1aR or V1bR may provide metabolic benefits on glucose homeostasis indirectly protecting the kidney. Dysregulation of glucose homeostasis is a part of metabolic syndrome and may be particular relevant in pathophysiology of DM and DKD. Numerous transgenic and pharmacological models provide perspectives for selective V1aR or V1bR modulation. However, these models produced in part conflicting results complicating the clear conclusions. Nevertheless, integrative analysis of the available data suggests that selective antagonists of V1aR or V1bR bear blood glucose lowering potential. Moreover, such antagonists may produce further renoprotective benefits by suppressing RAAS and adrenal stress hormone levels. Clinical experience with V1aR or V1bR antagonists are largely limited to dual V1aR/V2R antagonism in patients with acute heart failure (94, 95). Experiments in rats suggest renoprotective effects of dual V1aR/V2R suppression due to RAAS inhibition (96). Further characterization of V1aR- vs. V1bR antagonists with respect to their metabolic effects may unravel their therapeutic potential in DKD and CKD.

Author contributions

SL – statement and development of concept, key goals and objectives. Text preparation and editing – critical revision of the manuscript draft with the valuable intellectual investment. AM, AN, ES – text preparation and editing. MM – figure and table preparation, text preparation and editing. KM – statement and development of concept, key goals and objectives, text preparation and editing, approval of the final manuscript – acceptance of

responsibility for all types of the work, integrity of all parts of the paper and its final version. AT – discussion of glucose metabolism and critical revision of the manuscript draft with the valuable intellectual investment. All authors contributed to the article and approved the submitted version.

Funding

Funded by the Sechenov First Moscow State Medical University of the Ministry of Health of the Russian Federation (Sechenov University) - grant SYSE PI/E Medical Hackathon of Scientists and Entrepreneurs (Festival of Innovative Projects), Creation of Experimental Laboratories in the Natural Sciences Program and Basic Research Program at HSE University.

Conflict of interest

The authors declare that the research was conducted in the absence of any commercial or financial relationships that could be construed as a potential conflict of interest.

Publisher's note

All claims expressed in this article are solely those of the authors and do not necessarily represent those of their affiliated organizations, or those of the publisher, the editors and the reviewers. Any product that may be evaluated in this article, or claim that may be made by its manufacturer, is not guaranteed or endorsed by the publisher.

References

1. Skyler JS, Bakris GL, Bonifacio E, Darso T, Eckel RH, Groop L, et al. Differentiation of diabetes by pathophysiology, natural history, and prognosis. *Diabetes* (2017) 66(2):241–55. doi: 10.2337/db16-0806
2. Sanches JM, Zhao LN, Salehi A, Wollheim CB, Kaldis P. Pathophysiology of type 2 diabetes and the impact of altered metabolic interorgan crosstalk. *FEBS J* (2023) 290(3):620–48. doi: 10.1111/febs.16306

3. Thomas MC, Brownlee M, Susztak K, Sharma K, Jandeleit-Dahm KAM, Zoungas S, et al. Diabetic kidney disease. *Nat Rev Dis Primers* (2015) 1(1):15018. doi: 10.1038/nrdp.2015.18
4. Fioretto P, Mauer M. Histopathology of diabetic nephropathy. *Semin Nephrol* (2007) 27(2):195–207. doi: 10.1016/j.semnephrol.2007.01.012
5. Townsend RR, Taler SJ. Management of hypertension in chronic kidney disease. *Nat Rev Nephrol* (2015) 11(9):555–63. doi: 10.1038/nrneph.2015.114
6. Chapter 1: definition and classification of CKD. *Kidney Int Suppl* (2011) (2013) 3(1):19–62. doi: 10.1038/kisup.2012.64
7. Hostetter HH. Hyperfiltration and glomerulosclerosis. *Semin Nephrol* (2003) 23(2):194–9. doi: 10.1053/snep.2003.50017
8. Hsu SI-H, Couser WG. Chronic progression of tubulointerstitial damage in proteinuric renal disease is mediated by complement activation: A therapeutic role for complement inhibitors? *JASN* (2003) 14(suppl 2):S186–91. doi: 10.1097/01.ASN.0000070032.58017.20
9. Kanwar YS, Sun L, Xie P, Liu F-Y, Chen S. A glimpse of various pathogenetic mechanisms of diabetic nephropathy. *Annu Rev Pathol* (2011) 6:395–423. doi: 10.1146/annurev.pathol.4.110807.092150
10. Bankir L, Bouby N, Ritz E. Vasopressin: a novel target for the prevention and retardation of kidney disease? *Nat Rev Nephrol* (2013) 9(4):223–39. doi: 10.1038/nrneph.2013.22
11. Kamoi K, Ishibashi M, Yamaji T. Thirst and plasma levels of vasopressin, angiotensin II and atrial natriuretic peptide in patients with non-insulin-dependent diabetes mellitus. *Diabetes Res Clin Practice* (1991) 11(3):195–202. doi: 10.1016/S0168-8227(05)80033-6
12. Bankir L, Bardoux P, Ahloul M. Vasopressin and diabetes mellitus. *Nephron* (2001) 87(1):8–18. doi: 10.1159/000045879
13. Zerbe RL, Vinicor F, Robertson GL. Plasma vasopressin in uncontrolled diabetes mellitus. *Diabetes* (1979) 28(5):503–8. doi: 10.2337/diab.28.5.503
14. Koshimizu T, Nakamura K, Egashira N, Hiroyama M, Nonoguchi H, Tanoue A. Vasopressin V1a and V1b receptors: from molecules to physiological systems. *Physiol Rev* (2012) 92(4):1813–64. doi: 10.1152/physrev.00035.2011
15. Mutig K, Borowski T, Boldt C, Borschewski A, Paliege A, Popova E, et al. Demonstration of the functional impact of vasopressin signaling in the thick ascending limb by a targeted transgenic rat approach. *Am J Physiol Renal Physiol* (2016) 311(2):F411–423. doi: 10.1152/ajprenal.00126.2016
16. Giesecke T, Himmerkus N, Leipziger J, Bleich M, Koshimizu T-A, Fähring M, et al. Vasopressin increases urinary acidification via V1a receptors in collecting duct intercalated cells. *J Am Soc Nephrol* (2019) 30(6):946–61. doi: 10.1681/ASN.2018080816
17. Bankir L, Bichet DG, Morgenthaler NG. Vasopressin: physiology, assessment and osmosensation. *J Intern Med* (2017) 282(4):284–97. doi: 10.1111/joim.12645
18. Bouby N, Ahloul M, Nsegebe E, Déchaux M, Schmitt F, Bankir L. Vasopressin increases glomerular filtration rate in conscious rats through its antidiuretic action. *J Am Soc Nephrol* (1996) 7(6):842–51. doi: 10.1681/ASN.V76842
19. Mohan S, Moffett RC, Thomas KG, Irwin N, Flatt PR. Vasopressin receptors in islets enhance glucose tolerance, pancreatic beta-cell secretory function, proliferation and survival. *Biochimie* (2019) 158:191–8. doi: 10.1016/j.biochi.2019.01.008
20. Nakamura K, Aoyagi T, Hiroyama M, Kusakawa S, Mizutani R, Sanbe A, et al. Both V1A and V1B vasopressin receptors deficiency result in impaired glucose tolerance. *Eur J Pharmacol* (2009) 613(1–3):182–8. doi: 10.1016/j.ejphar.2009.04.008
21. Andres-Hernando A, Jensen TJ, Kuwabara M, Orlicky DJ, Cicerchi C, Li N, et al. Vasopressin mediates fructose-induced metabolic syndrome by activating the V1b receptor. *JCI Insight* (2021) 6(1):e140848. doi: 10.1172/jci.insight.140848
22. Balanescu S, Kopp P, Gaskill MB, Morgenthaler NG, Schindler C, Rutishauser J. Correlation of plasma copeptin and vasopressin concentrations in hypo-, iso-, and hyperosmolar states. *J Clin Endocrinol Metab* (2011) 96(4):1046–52. doi: 10.1210/jc.2010-2499
23. Refardt J, Winzler B, Christ-Crain M. Copeptin and its role in the diagnosis of diabetes insipidus and the syndrome of inappropriate antidiuresis. *Clin Endocrinol* (2019) 91(1):22–32. doi: 10.1111/cen.13991
24. Meyer-Lindenberg A, Domes G, Kirsch P, Heinrichs M. Oxytocin and vasopressin in the human brain: social neuropeptides for translational medicine. *Nat Rev Neurosci* (2011) 12(9):524–38. doi: 10.1038/nrn3044
25. Sriram K, Wiley SZ, Moyung K, Gorr MW, Salmerón C, Marucut J, et al. Detection and quantification of GPCR mRNA: an assessment and implications of data from high-content methods. *ACS Omega* (2019) 4(16):17048–59. doi: 10.1021/acsomega.9b02811
26. Carosino M, Brooks HL, Cai Q, Davis LS, Opalenik S, Hao C, et al. Axial heterogeneity of vasopressin-receptor subtypes along the human and mouse collecting duct. *Am J Physiology-Renal Physiol* (2007) 292(1):F351–60. doi: 10.1152/ajprenal.00049.2006
27. Ostrowski NL, Lolait SJ, Bradley DJ, O'Carroll AM, Brownstein MJ, Young WS. Distribution of V1a and V2 vasopressin receptor messenger ribonucleic acids in rat liver, kidney, pituitary and brain. *Endocrinology* (1992) 131(1):533–5. doi: 10.1210/endo.131.1.1535312
28. Tanoue A, Ito S, Honda K, Oshikawa S, Kitagawa Y, Koshimizu TA, et al. The vasopressin V1b receptor critically regulates hypothalamic-pituitary-adrenal axis activity under both stress and resting conditions. *J Clin Invest* (2004) 113(2):302–9. doi: 10.1172/JCI200419656
29. Buckingham JC. Vasopressin receptors influencing the secretion of ACTH by the rat adenohypophysis. *J Endocrinol* (1987) 113(3):389–96. doi: 10.1677/joe.0.1130389
30. Sugimoto T, Saito M, Mochizuki S, Watanabe Y, Hashimoto S, Kawashima H. Molecular cloning and functional expression of a cDNA encoding the human V1b vasopressin receptor. *J Biol Chem* (1994) 269(43):27088–92. doi: 10.1016/S0021-9258(18)47129-3
31. Terada Y, Tomita K, Nonoguchi H, Yang T, Marumo F. Different localization and regulation of two types of vasopressin receptor messenger RNA in microdissected rat nephron segments using reverse transcription polymerase chain reaction. *J Clin Invest* (1993) 92(5):2339–45. doi: 10.1172/JCI116838
32. Ostrowski NL, Young WS, Knepper MA, Lolait SJ. Expression of vasopressin V1a and V2 receptor messenger ribonucleic acid in the liver and kidney of embryonic, developing, and adult rats. *Endocrinology* (1993) 133(4):1849–59. doi: 10.1210/endo.133.4.8404628
33. Mutig K, Paliege A, Kahl T, Jöns T, Müller-Esterl W, Bachmann S. Vasopressin V2 receptor expression along rat, mouse, and human renal epithelia with focus on TAL. *Am J Physiol Renal Physiol* (2007) 293(4):F1166–1177. doi: 10.1152/ajprenal.00196.2007
34. Aoyagi T, Izumi Y, Hiroyama M, Matsuzaki T, Yasuoka Y, Sanbe A, et al. Vasopressin regulates the renin-angiotensin-aldosterone system via V1a receptors in macula densa cells. *Am J Physiology-Renal Physiol* (2008) 295(1):F100–7. doi: 10.1152/ajprenal.00088.2008
35. Izumi Y, Hori K, Nakayama Y, Kimura M, Hasuike Y, Nanami M, et al. Aldosterone requires vasopressin V1a receptors on intercalated cells to mediate acid-base homeostasis. *J Am Soc Nephrol* (2011) 22(4):673–80. doi: 10.1681/ASN.2010050468
36. Folny V, Raufaste D, Lukovic L, Pouzet B, Rochard P, Pascal M, et al. Pancreatic vasopressin V_{1b} receptors: characterization in In-R1-G9 cells and localization in human pancreas. *Am J Physiology-Endocrinol Metab* (2003) 285(3):E566–76. doi: 10.1152/ajpendo.00148.2003
37. Taveau C, Chollet C, Bichet DG, Velho G, Guillon G, Corbani M, et al. Acute and chronic hyperglycemic effects of vasopressin in normal rats: involvement of V_{1A} receptors. *Am J Physiology-Endocrinol Metab* (2017) 312(3):E127–35. doi: 10.1152/ajpendo.00269.2016
38. Schneider EG. Effect of vasopressin on adrenal steroidogenesis. *Am J Physiology-Regulatory Integr Comp Physiol* (1988) 255(5):R806–11. doi: 10.1152/ajpregu.1988.255.5.R806
39. Arnaldi G, Gasc JM, de Keyser Y, Raffin-Sanson ML, Perraudin V, Kuhn JM, et al. Variable expression of the V1 vasopressin receptor modulates the phenotypic response of steroid-secreting adrenocortical tumors¹. *J Clin Endocrinol Metab* (1998) 83(6):2029–35. doi: 10.1210/jcem.83.6.4873
40. Grazzini E, Breton C, Derick S, Andres M, Raufaste D, Rickwaert F, et al. Vasopressin receptors in human adrenal medulla and pheochromocytoma¹. *J Clin Endocrinol Metab* (1999) 84(6):2195–203. doi: 10.1210/jcem.84.6.5775
41. Salata RA, Jarrett DB, Verbalis JG, Robinson AG. Vasopressin stimulation of adrenocorticotropin hormone (ACTH) in humans. *In vivo* bioassay of corticotropin-releasing factor (CRF) which provides evidence for CRF mediation of the diurnal rhythm of ACTH. *J Clin Invest* (1988) 81(3):766–74. doi: 10.1172/JCI113382
42. Perraudin V, Delarue C, Lefebvre H, Contesse V, Kuhn JM, Vaudry H. Vasopressin stimulates cortisol secretion from human adrenocortical tissue through activation of V1 receptors. *J Clin Endocrinol Metab* (1993) 76(6):1522–8. doi: 10.1210/jcem.76.6.7684742
43. Perry RJ, Zhang D, Guerra MT, Brill AL, Goedeke L, Nasiri AR, et al. Glucagon stimulates gluconeogenesis by INSP3R1-mediated hepatic lipolysis. *Nature* (2020) 579(7798):279–83. doi: 10.1038/s41586-020-2074-6
44. Reid IA, Schwartz J, Ben L, Maselli J, Keil LC. Interactions Between Vasopressin and the Renin-Angiotensin System. In: *Progress in Brain Research*. Bethesda, MD, United States: American Journal of Physiology-Renal Physiology (1983). p. 475–91.
45. Weiss B, Maickel RP. Sympathetic nervous control of adipose tissue lipolysis. *Int J Neuropharmacol* (1968) 7(4):395–403. doi: 10.1016/0028-3908(68)90023-3
46. O'Carroll A-M, Howell GM, Roberts EM, Lolait SJ. Vasopressin potentiates corticotropin-releasing hormone-induced insulin release from mouse pancreatic beta-cells. *J Endocrinol* (2008) 197(2):231–9. doi: 10.1677/JOE-07-0645
47. Hayashi Y. Glucagon regulates lipolysis and fatty acid oxidation through inositol triphosphate receptor 1 in the liver. *J Diabetes Investig* (2021) 12(1):32–4. doi: 10.1111/jdi.13315
48. Gal CS-L, Raufaste D, Marty E, Garcia C, Maffrand J-P, Le Fur G. Autoradiographic localization of vasopressin V1a receptors in the rat kidney using [3H]-SR 49059. *Kidney Int* (1996) 50(2):499–505. doi: 10.1038/ki.1996.341
49. Gonzalez CB, Figueroa CD, Reyes CE, Caorsi CE, Troncoso S, Menzel D. Immunolocalization of V1 vasopressin receptors in the rat kidney using anti-receptor antibodies. *Kidney Int* (1997) 52(5):1206–15. doi: 10.1038/ki.1997.445

50. Szczepanska-Sadowska E. The heart as a target of vasopressin and other cardiovascular peptides in health and cardiovascular diseases. *IJMS* (2022) 23(22):14414. doi: 10.3390/ijms232214414
51. Hiroyama M, Wang S, Aoyagi T, Oikawa R, Sanbe A, Takeo S, et al. Vasopressin promotes cardiomyocyte hypertrophy via the vasopressin V1A receptor in neonatal mice. *Eur J Pharmacol* (2007) 559(2–3):89–97. doi: 10.1016/j.ejphar.2006.12.010
52. Lolait SJ, O'Carroll A-M, McBride OW, Konig M, Morel A, Brownstein MJ. Cloning and characterization of a vasopressin V2 receptor and possible link to nephrogenic diabetes insipidus. *Nature* (1992) 357(6376):336–9. doi: 10.1038/357336a0
53. Yun J, Schöneberg T, Liu J, Schulz A, Ecelbarger CA, Promeneur D, et al. Generation and phenotype of mice harboring a nonsense mutation in the V2 vasopressin receptor gene. *J Clin Invest* (2000) 106(11):1361–71. doi: 10.1172/JCI9154
54. Walsh CH, Baylis PH, Malins JM. Plasma Arginine Vasopressin in diabetic ketoacidosis. *Diabetologia* (1979) 16(2):93–6. doi: 10.1007/BF01225456
55. Gellai M, Silverstein JH, Hwang JC, LaRochelle FT, Valtin H. Influence of vasopressin on renal hemodynamics in conscious Brattleboro rats. *Am J Physiology-Renal Physiol* (1984) 246(6):F819–27. doi: 10.1152/ajprenal.1984.246.6.F819
56. Bankir L, Kriz W. Adaptation of the kidney to protein intake and to urine concentrating activity: Similar consequences in health and CRF. *Kidney Int* (1995) 47(1):7–24. doi: 10.1038/ki.1995.2
57. Bardoux P, Martin H, Ahloulouy M, Schmitt F, Bouby N, Trinh-Trang-Tan MM, et al. Vasopressin contributes to hyperfiltration, albuminuria, and renal hypertrophy in diabetes mellitus: study in vasopressin-deficient Brattleboro rats. *Proc Natl Acad Sci USA* (1999) 96(18):10397–402. doi: 10.1073/pnas.96.18.10397
58. Müller RU, Messchendorp AL, Birn H, Capasso G, Cornec-Le Gall E, Devuyst O, et al. An update on the use of tolvaptan for autosomal dominant polycystic kidney disease: consensus statement on behalf of the ERA Working Group on Inherited Kidney Disorders, the European Rare Kidney Disease Reference Network and Polycystic Kidney Disease International. *Nephrol Dialysis Transplant* (2022) 37(5):825–39. doi: 10.1093/ndt/gfab312
59. Sato E, Nakamura T, Amaha M, Nomura M, Matsumura D, Yamagishi H, et al. Effect of tolvaptan in patients with chronic kidney disease due to diabetic nephropathy with heart failure. *Int Heart J* (2014) 55(6):533–8. doi: 10.1536/ihj.14-190
60. Takada T, Masaki T, Hoshiyama A, Toki T, Kamata Y, Shichiri M. Tolvaptan alleviates excessive fluid retention of nephrotic diabetic renal failure unresponsive to furosemide: Effects of tolvaptan on diabetic renal insufficiency. *Nephrology* (2018) 23(9):883–6. doi: 10.1111/nep.13390
61. Berl T, Schrier RW. Vasopressin Antagonists in Physiology and Disease. In: *Textbook of Nephro-Endocrinology*. (New York, United States: Springer-Verlag) (2018). p. 117–31.
62. Moss NG, Kopple TE, Arendshorst WJ. Renal vasoconstriction by vasopressin V1a receptors is modulated by nitric oxide, prostanooids, and superoxide but not the ADP ribosyl cyclase CD38. *Am J Physiol Renal Physiol* (2014) 306(10):F1143–1154. doi: 10.1152/ajprenal.00664.2013
63. Carmines PK. The renal vascular response to diabetes. *Curr Opin Nephrol Hypertension* (2010) 19(1):85–90. doi: 10.1097/MNH.0b013e32833240fc
64. Török B, Csikota P, Fodor A, Balázsfi D, Ferenczi S, Demeter K, et al. Rescue of vasopressin synthesis in magnocellular neurons of the supraoptic nucleus norMalises acute stress-induced adrenocorticotropin secretion and unmasks an effect on social behaviour in male vasopressin-deficient brattleboro rats. *Int J Mol Sci* (2022) 23(3):1357. doi: 10.3390/ijms23031357
65. Nicola W, Sidhom G, Khyat ZE, Ibrahim S, Salah A, Sayed AE. Plasma angiotensin II, renin activity and serum angiotensin-converting enzyme activity in non-insulin dependent diabetes mellitus patients with diabetic nephropathy. *Endocr J* (2001) 48(1):25–31. doi: 10.1507/endocrj.48.25
66. Sama IE, Voors AA. Circulating plasma angiotensin-converting enzyme 2 concentration is elevated in patients with kidney disease and diabetes. *Eur Heart J* (2020) 41(32):3099–9. doi: 10.1093/eurheartj/ehaa527
67. Huang K, Liang Y, Wang K, Ma Y, Wu J, Luo H, et al. Elevated ACE levels indicate diabetic nephropathy progression or companion retina impaired. *Front Clin Diabetes Healthc* (2022) 3:831128. doi: 10.3389/fcdhc.2022.831128
68. Hollenberg NK, Stevanovic R, Agarwal A, Lansang MC, Price DA, Laffel LM, et al. Plasma aldosterone concentration in the patient with diabetes mellitus Rapid Communication. *Kidney Int* (2004) 65(4):1435–9. doi: 10.1111/j.1523-1755.2004.00524.x
69. Wiley MK, Pearlmuter AF, Miller RE. Decreased adrenal sensitivity to ACTH in the vasopressin-deficient (Brattleboro) rat. *Neuroendocrinology* (1974) 14(5):257–70. doi: 10.1159/000122269
70. Scott LV, Dinan TG. Vasopressin and the regulation of hypothalamic-pituitary-adrenal axis function: Implications for the pathophysiology of depression. *Life Sci* (1998) 62(22):1985–98. doi: 10.1016/S0024-3205(98)00027-7
71. Somova L, Sirakova I, Sirakov L, Dashev G, Kirilov G, Vassileva M. Discrepancy between aldosterone production and renin-angiotensin system activity in Brattleboro rats. *Acta Physiol Pharmacol Bulg* (1987) 13(4):43–50.
72. Wang W, Li C, Summer S, Falk S, Schrier RW. Interaction between vasopressin and angiotensin II in vivo and in vitro: effect on aquaporins and urine concentration. *Am J Physiol Renal Physiol* (2010) 299(3):F577–584. doi: 10.1152/ajprenal.00168.2010
73. Knepel W, Reimann W, Nutto D. On the mechanism of the vasopressin-induced inhibition of renin release. *Horm Metab Res* (1982) 14(03):157–60. doi: 10.1055/s-2007-1018953
74. Kumagai E, Adachi H, Jacobs DR Jr, Hirai Y, Enomoto M, Fukami A, et al. Plasma aldosterone levels and development of insulin resistance: prospective study in a general population. *Hypertension* (2011) 58(6):1043–8. doi: 10.1161/HYPERTENSIONAHA.111.180521
75. Meneton P, Loffing J, Warnock DG. Sodium and potassium handling by the aldosterone-sensitive distal nephron: the pivotal role of the distal and connecting tubule. *Am J Physiol Renal Physiol* (2004) 287(4):F593–601. doi: 10.1152/ajprenal.00454.2003
76. Briet M, Schiffrin EL. Vascular actions of aldosterone. *J Vasc Res* (2013) 50(2):89–99. doi: 10.1159/000345243
77. Faivre A, Verissimo T, Auwerx H, Legouis D, de Seigneux S. Tubular cell glucose metabolism shift during acute and chronic injuries. *Front Med* (2021) 8:742072. doi: 10.3389/fmed.2021.742072
78. Spruce BA, McCulloch AJ, Burd J, Orskov H, Heaton A, Baylis PH, et al. The effect of vasopressin infusion on glucose metabolism in man. *Clin Endocrinol* (1985) 22(4):463–8. doi: 10.1111/j.1365-2265.1985.tb00145.x
79. Oshikawa S, Tanoue A, Koshimizu T, Kitagawa Y, Tsujimoto G. Vasopressin stimulates insulin release from islet cells through V1b receptors: a combined pharmacological/knockout approach. *Mol Pharmacol* (2004) 65(3):623–9. doi: 10.1124/mol.65.3.623
80. Rofe AM, Williamson DH. Mechanism for the A'nti-lipolytic' action of vasopressin in the starved rat. *Biochem J* (1983) 212(3):899–902. doi: 10.1042/bj2120899
81. Aoyagi T, Birumachi J, Hiroyama M, Fujiwara Y, Sanbe A, Yamauchi J, et al. Alteration of glucose homeostasis in V1a vasopressin receptor-deficient mice. *Endocrinology* (2007) 148(5):2075–84. doi: 10.1210/en.2006.1315
82. Kurokawa K, Massry SG. Evidence for stimulation of renal gluconeogenesis by catecholamines. *J Clin Invest*. (1973) 52(4):961–4. doi: 10.1172/JCI107261
83. Fujiwara Y, Hiroyama M, Sanbe A, Aoyagi T, Birumachi J, Yamauchi J, et al. Insulin hypersensitivity in mice lacking the V1b vasopressin receptor: Insulin hypersensitivity in *V1bR*^{-/-} mice. *J Physiol* (2007) 584(1):235–44. doi: 10.1113/jphysiol.2007.136481
84. Nakamura K, Yamashita T, Fujiki H, Aoyagi T, Yamauchi J, Mori T, et al. Enhanced glucose tolerance in the Brattleboro rat. *Biochem Biophys Res Commun* (2011) 405(1):64–7. doi: 10.1016/j.bbrc.2010.12.126
85. Tanoue A. New topics in vasopressin receptors and approach to novel drugs: effects of vasopressin receptor on regulations of hormone secretion and metabolisms of glucose, fat, and protein. *J Pharmacol Sci* (2009) 109(1):50–2. doi: 10.1254/jphs.08R15FM
86. Rofe AM, Williamson DH. Metabolic effects of vasopressin infusion in the starved rat. Reversal of ketonaemia. *Biochem J* (1983) 212(1):231–9. doi: 10.1042/bj2120231
87. Palazzo AJ, Malik KU, Weis MT. Vasopressin stimulates the mobilization and metabolism of triacylglycerol in perfused rabbit hearts. *Am J Physiology-Heart Circulatory Physiol* (1991) 260(2):H604–12. doi: 10.1152/ajpheart.1991.260.2.H604
88. Goldsmith SR, Elkayam U, Haught WH, Barve A, He W. Efficacy and safety of the vasopressin V1A/V2-receptor antagonist conivaptan in acute decompensated heart failure: a dose-ranging pilot study. *J Card Fail* (2008) 14(8):641–7. doi: 10.1016/j.cardfail.2008.06.003
89. Tran TDN, Yao S, Hsu WH, Gimble JM, Bunnell BA, Cheng H. Arginine vasopressin inhibits adipogenesis in human adipose-derived stem cells. *Mol Cell Endocrinol* (2015) 406:1–9. doi: 10.1016/j.mce.2015.02.009
90. Hiroyama M, Fujiwara Y, Nakamura K, Aoyagi T, Mizutani R, Sanbe A, et al. Altered lipid metabolism in vasopressin V1B receptor-deficient mice. *Eur J Pharmacol* (2009) 602(2–3):455–61. doi: 10.1016/j.ejphar.2008.11.043
91. Hiroyama M, Aoyagi T, Fujiwara Y, Birumachi J, Shigematsu Y, Kiwaki K, et al. Hypermetabolism of fat in V1a vasopressin receptor knockout mice. *Mol Endocrinol* (2007) 21(1):247–58. doi: 10.1210/me.2006-0069
92. Torres VE. Vasopressin antagonists in polycystic kidney disease. *Semin Nephrol* (2008) 28(3):306–17. doi: 10.1016/j.semnephrol.2008.03.003
93. Palmer BF. Vasopressin receptor antagonists. *Curr Hypertens Rep* (2015) 17(1):1. doi: 10.1007/s11906-014-0510-4
94. Goldsmith SR, Burkhoff D, Gustafsson F, Voors A, Zannad F, Kolkhof P, et al. Dual vasopressin receptor antagonism to improve congestion in patients with acute heart failure: design of the AVANTI trial. *J Cardiac Failure* (2021) 27(2):233–41. doi: 10.1016/j.cardfail.2020.10.007
95. Orlandi C, Zimmer CA, Gheorghiadu M. Role of vasopressin antagonists in the management of acute decompensated heart failure. *Curr Heart Fail Rep* (2005) 2(3):131–9. doi: 10.1007/s11897-005-0021-3
96. Perico N, Zoja C, Corna D, Rottoli D, Gaspari F, Haskell L, et al. V1/V2 Vasopressin receptor antagonism potentiates the renoprotection of renin-angiotensin system inhibition in rats with renal mass reduction. *Kidney Int* (2009) 76(9):960–7. doi: 10.1038/ki.2009.267



OPEN ACCESS

EDITED BY

Ningning Hou,
Affiliated Hospital of Weifang Medical
University, China

REVIEWED BY

Angela Schulz,
Leipzig University, Germany
Marta Tapparo,
University of Turin, Italy
Stanislaw Stepkowski,
University of Toledo, United States

*CORRESPONDENCE

Xiang Chen
✉ chenxiangxt@csu.edu.cn

RECEIVED 17 April 2023

ACCEPTED 25 October 2023

PUBLISHED 08 November 2023

CITATION

Dong Z, Chen F, Peng S, Liu X, Liu X,
Guo L, Wang E and Chen X (2023)
Identification of the key immune-related
genes and immune cell infiltration changes
in renal interstitial fibrosis.
Front. Endocrinol. 14:1207444.
doi: 10.3389/fendo.2023.1207444

COPYRIGHT

© 2023 Dong, Chen, Peng, Liu, Liu, Guo,
Wang and Chen. This is an open-access
article distributed under the terms of the
[Creative Commons Attribution License](#)
(CC BY). The use, distribution or
reproduction in other forums is permitted,
provided the original author(s) and the
copyright owner(s) are credited and that
the original publication in this journal is
cited, in accordance with accepted
academic practice. No use, distribution or
reproduction is permitted which does not
comply with these terms.

Identification of the key immune-related genes and immune cell infiltration changes in renal interstitial fibrosis

Zhitao Dong¹, Fangzhi Chen¹, Shuang Peng¹, Xiongfei Liu¹,
Xinyang Liu², Lizhe Guo², E. Wang^{2,3} and Xiang Chen^{2,3*}

¹Department of Urology, The Second Xiangya Hospital, Central South University, Changsha, Hunan, China, ²Department of Anesthesiology, Xiangya Hospital, Central South University, Changsha, Hunan, China, ³National Clinical Research Center for Geriatric Disorders (Xiangya Hospital), Central South University, Changsha, Hunan, China

Background: Chronic kidney disease (CKD) is the third-leading cause of premature mortality worldwide. It is characterized by rapid deterioration due to renal interstitial fibrosis (RIF) via excessive inflammatory infiltration. The aim of this study was to discover key immune-related genes (IRGs) to provide valuable insights and therapeutic targets for RIF in CKD.

Materials and methods: We screened differentially expressed genes (DEGs) between RIF samples from CKD patients and healthy controls from a public database. Least absolute shrinkage and selection operator regression analysis and receiver operating characteristic curve analysis were applied to identify significant key biomarkers. The single-sample Gene Set Enrichment Analysis (ssGSEA) algorithm was used to analyze the infiltration of immune cells between the RIF and control samples. The correlation between biomarkers and immune cell composition was assessed.

Results: A total of 928 DEGs between CKD and control samples from six microarray datasets were found, 17 overlapping immune-correlated DEGs were identified by integration with the ImmPort database, and six IRGs were finally identified in the model: apolipoprotein H (APOH), epidermal growth factor (EGF), lactotransferrin (LTF), lysozyme (LYZ), phospholipid transfer protein (PLTP), and secretory leukocyte peptidase inhibitor (SLPI). Two additional datasets and *in vivo* experiments indicated that the expression levels of APOH and EGF in the fibrosis group were significantly lower than those in the control group, while the expression levels of LTF, LYZ, PLTP, and SLPI were higher (all $P < 0.05$). These IRGs also showed a significant correlation with renal function impairment. Moreover, four upregulated IRGs were positively associated with various T cell populations, which were enriched in RIF tissues, whereas two downregulated IRGs had opposite results. Several signaling pathways, such as the “T cell receptor signaling pathway” and “positive regulation of NF- κ B signaling pathway”, were discovered to be associated not only with immune cell infiltration, but also with the expression levels of six IRGs.

Conclusion: In summary, six IRGs were identified as key biomarkers for RIF, and exhibited a strong correlation with various T cells and with the NF- κ B signaling pathway. All these IRGs and their signaling pathways may evolve as valuable therapeutic targets for RIF in CKD.

KEYWORDS

chronic kidney disease, renal interstitial fibrosis, immune cells, biomarker, NF- κ B signaling pathway

Introduction

Chronic kidney disease (CKD) is increasingly recognized as a serious public health epidemic worldwide, with a high incidence rate, high medical costs, and poor outcomes (1, 2). According to the GBD 2017 estimates, approximately 697.5 million cases were diagnosed in 2017, which was estimated to be 9.1% of the global population (3). Importantly, CKD directly causes 1.2 million deaths and an additional 1.4 million deaths from cardiovascular disease resulting from impaired kidney function, making CKD the 12th leading cause of death worldwide (3). CKD is usually caused by many conditions that put a strain on the kidneys, including glomerulonephritis, diabetes, high blood pressure, hereditary nephropathy, and renal tubulointerstitial disease (4, 5). However, renal fibrosis, particularly renal interstitial fibrosis (RIF), is the final common pathological outcome of almost all advanced kidney diseases, whatever the original etiology (6). Despite many promising clinical studies and experimental data, currently available treatment strategies can only ameliorate or delay the progression of CKD rather than reverse the renal fibrosis (5, 6). Therefore, there is an urgent need to conduct mechanistic research on renal fibrosis in CKD to understand the underlying pathogenesis of the process and to optimize treatment strategies, letting us improve the prognosis of patients with fibrotic kidney disorders.

RIF mainly manifests as sclerosis, tubular atrophy, and inflammatory infiltration, resulting in a dynamic, multifactorial process, including fibroblast activation, tubular epithelial-to-mesenchymal transition (EMT), and T-cell and monocyte/macrophage infiltration (7). The initial step of renal fibrosis is

uncontrolled or excessive inflammatory infiltration, which is a key factor that cross-talks with the progression of subsequent series of fibrosis (8). Recently, antifibrotic agents that target inflammation have been recommended as potential alternative therapies for renal fibrosis. As a general immunosuppressive cytokine, IL-10 delivered by hydrogels can reduce macrophage infiltration and apoptosis to treat renal fibrosis and chronic kidney disease (9). Similarly, I κ B (an inhibitor of NF- κ B) treatment and β 2 adrenergic receptor agonists both inhibit NF- κ B signaling and result in the inactivation of macrophages, thereby inhibiting further kidney damage (10, 11). However, these ongoing and completed clinical trials still lack sufficient evidence for successful targeted fibrosis in CKD (12). Now one opinion considers that the intracellular signaling pathways associated with fibrosis interact with other signaling transductions that affect critical cellular activation and functions. Given that inflammation is self-sustaining and multifactorial, identifying the key genes associated with inflammation and describing the interaction with the enrichment of immune cells will be significant in elaborating the potential mechanisms of RIF in CKD.

Several evidences indicating that chronic or unresolved inflammation plays a pivotal role in the onset and progression of renal fibrosis (7, 8). Inflammatory cells, such as macrophages and T lymphocytes, infiltrate the renal interstitium and continually secrete pro-inflammatory cytokines. These substances activate fibroblasts and contribute to maladaptive repair processes and progressive renal fibrosis. It has been observed that T cells polarized towards a Th2 phenotype can induce fibroblast activation and promote alternative activation of macrophages, potentially fostering renal fibrosis (13). Moreover, infiltrating immune cells locally produce TGF- β , which further amplifies renal fibrosis and inflammation by activating various signaling molecules (AKT/mTOR, Smad2/3, NF- κ B, KLF6, and Sp1) (12). Recently discovered inflammation-related biomarkers and distinct patterns of immune infiltration in RIF can offer additional insights into the risk associated with fibrosis in CKD (14). However, since renal fibrosis represents a common pathological manifestation of chronic kidney diseases with diverse causes, studies based on isolated causal samples or limited analytical dimensions may introduce biases.

Therefore, we downloaded six microarray datasets from renal interstitial tissues of CKD patients with different causes to screen coexpressed differentially expressed genes (co-DEGs) and identified key immune-related genes (IRGs) for RIF using the least absolute

Abbreviations: CKD, chronic kidney disease; RIF, renal interstitial fibrosis; IRGs, immune-related genes; DEGs, differentially expressed genes; LASSO, least absolute shrinkage and selection operator regression; ROC, receiver operating characteristic curve; GSEA, gene set enrichment analysis; ssGSEA, Single sample GSEA, EMT, epithelial to mesenchymal transition; GO, Gene Ontology; KEGG, Kyoto Encyclopedia of Genes and Genomes; GEO, Gene Expression Omnibus; TMD, thin membrane disease, MCD, minimal change disease; FSGS, focal and segmental glomerulosclerosis; MGN, membranous glomerulonephritis; RPGN, rapidly progressive glomerulonephritis; SLE, systemic lupus erythematosus; DC, dendritic cell; Treg, regulatory T cell; GFR, glomerular filtration rate; BUN, blood urea nitrogen; SCR, serum creatinine level; APOH, apolipoprotein H; EGF, epidermal growth factor; LTF, lactotransferrin; LYZ, lysozyme; PLTP, phospholipid transfer protein; SLPI, secretory leukocyte peptidase inhibitor.

shrinkage and selection operator (LASSO) regression analysis between RIF and healthy control samples, which verified with *in vivo* experiments. Next, correlation analysis was conducted between the expression level of IRGs and the infiltration of immune cells which obtained by the single-sample gene set enrichment analysis (ssGSEA) method. Kyoto Encyclopedia of Genes and Genomes (KEGG) analysis and GSEA were also performed to discover the biological function and significant signaling pathways correlated with RIF. Through a multidimensional analysis of the interrelationship between IRGs and immune cells, as well as potential pathway correlation analyses, our study aims to uncover key immune-related biomarkers and provide novel insights into the potential immune mechanisms associated with the progression of RIF.

Materials and methods

Patient cohort and data preparation

The discovery cohorts of the study, including GSE30529, GSE35487, GSE37455, GSE133288, GSE121211, and GSE32591 datasets, were downloaded from the Gene Expression Omnibus (GEO) website (<https://www.ncbi.nlm.nih.gov/geo>) for DEG analysis. All available datasets included renal interstitial samples from healthy controls and patients with CKD. Those CKD patients were mostly diagnosed with diabetic nephropathy (DN), hypertensive nephropathy, IgA nephropathy, membranous nephropathy (MN), minimal change disease (MCD), focal and segmental glomerulosclerosis (FSGS), or systemic lupus erythematosus (SLE).

The GSE12682 dataset was downloaded and analyzed to identify the key markers associated with RIF. A total of 36 renal tubulointerstitial samples, including 23 CKD samples with evidence of tubulointerstitial fibrosis and 13 healthy control samples, were enrolled in the GSE12682 dataset. In addition, the GSE76882 dataset was analyzed for external validation to examine its key gene signature. It included 99 healthy controls, 42 interstitial fibrosis and tubular atrophy (IFTA) samples, 11 IFTA with inflammation (IFTA-i) samples, and 29 IFTA with acute rejection (IFTA-AR) samples. Given that we aimed to investigate the mechanisms underlying fibrosis rather than the posttransplant immune response, we selected healthy controls and IFTA samples for further analysis. In addition, the GSE38117 dataset, which studied renal fibrosis using experimental model of ureteral unilateral obstruction (UUO) in three mice, was also used to validate the key markers associated with RIF. Surgery was performed by complete ligation of the left ureter, which the control lateral right kidney served as internal control. The basic information for the included datasets is shown in [Supplementary Table 1](#).

All the gene expression profiling data were first subjected to background correction and quartile normalization of the raw data using the “Limma” package of R, followed by batch effect elimination using the “sva” package, to obtain normally

distributed expression values. The DEGs between CKD samples and healthy control samples were those that had absolute value of log2 fold change ($|\log_2FC|$) > 1 and adjusted *P* value < 0.05. Then, the robust rank aggregation (RRA) method was used to integrate and identify overlapping DEGs (*P* value < 0.05) from the discovery cohorts.

Identification of immune-related DEGs

To identify the immune-related DEGs (IRGs), we downloaded a total of 1793 immune-related genes from the Immunology Database and Analysis Portal (ImmPort) website (<https://www.immport.org>). These immune-related genes originated from 17 immune-related categories, including antigen processing and presentation, antimicrobials, and the BCR signaling pathway. Then, we integrated the co-DEGs from the discovery cohorts and immune-related gene sets and identified the overlapping IRGs for further analysis.

Exploration of key IRGs

To explore the key genes in IRGs associated with RIF, LASSO algorithm was applied for all renal tubulointerstitial samples from the GSE12682 dataset using the “glmnet” package in R. LASSO regression is a type of linear regression that uses shrinkage to regularize regression algorithms. Regularization can solve the overfitting problem by adding more parameters, leaving fewer parameters in the model, and limiting its complexity. L1 regularization was executed by adding a penalty equal to the absolute value of the magnitude of each coefficient in the LASSO regression model. This type of regularization contributes to constructing sparse models with relatively few coefficients. Those variables whose coefficients are zero are removed from the model. Therefore, we calculated the sum of the candidate gene values multiplied by the corresponding coefficient obtained from LASSO regression analysis, and named it as risk score.

Validation of the risk score model

To evaluate the value of the risk score model, the GSE12682 dataset (training set) and the GSE76882 dataset (validation set) were used to validate the accuracy and diagnostic ability of the risk score model in CKD patients with RIF via the “pROC” package in R. We visualized the area under the curve (AUC) of the ROC curve by calculating the sensitivity and specificity values with the “pROC” package. Then calibration curve was also used to visualize the performance of the risk score model with the Hosmer-Lemeshow test using the “ResourceSelection” package in R. The Hosmer-Lemeshow test is used frequently to calculate the goodness of fit of risk prediction models, in which a *P* value > 0.05 indicates that the data fit by the risk prediction model are at an acceptable level and that the scoring model works well.

Gene set enrichment analysis

Through the DAVID tools (<http://david.ncicrf.gov/>), Gene Ontology (GO) and KEGG analyses were used to discover the biological function and significant signaling pathways correlated with RIF. The results were visualized via the “clusterProfiler” R package. We applied strict cutoff values of false discovery rate (FDR) < 0.05 and adjusted *P* value < 0.05 to detect statistically significant GO terms and KEGG pathways. GSEA was used to discover the functional terms associated with RIF with the thresholds of an NOM *P* value < 0.05 and |NES| > 1. Each analysis was performed with 1000 times of arrangements of the gene set.

Discovery of immune cell subtypes and correlation with key biomarkers

To quantify the relative infiltration of immune cells for each sample, the ssGSEA algorithm was performed to calculate the normalized enrichment scores of 28 types of immune cells in the RIF samples and control samples using the Gene Set Variation Analysis (GSVA) R package (15). In detail, expression data of renal interstitial samples between the RIF and healthy control groups were used to calculate immune cell abundances according to the GSVA algorithm and specific cell markers (Supplementary Table 2) (16). The 28 immune cells were gamma/delta T cells, activated CD4 T cells, activated CD8 T cells, activated dendritic cells (DCs), central memory CD8 T cells, central memory CD4 T cells, effector memory CD4 T cells, effector memory CD8 T cells, monocytes, macrophages, immature DCs, immature B cells, activated B cells, memory B cells, mast cells, eosinophils, myeloid-derived suppressor cells (MDSCs), CD56dim natural killer cells, CD56bright natural killer cells, natural killer cells, natural killer T cells, neutrophils, plasmacytoid DCs, regulatory T (Treg) cells, T follicular helper cells, type 1 T helper cells, type 17 T helper cells, and type 2 T helper cells. Violin plot was used to visualize the differences in the composition of 28 immune cell subtypes between the RIF samples and healthy control samples with the two-sided Wilcoxon test. We also conducted Pearson correlation analysis between key IRGs and immune cell markers in the human kidney, which were obtained from the CellMarker database (<http://biocc.hrbmu.edu.cn/CellMarker/>), as well as gene sets of specific signaling pathways from the KEGG database (<https://www.genome.jp/kegg/>).

Clinical correlation analysis

In addition, we also used the Nephroseq V5 tool (<http://v5.nephroseq.org/>) to identify the difference in risk score calculated by the expression level of key IRGs between CKD and control samples and explored the correlation between the risk score and clinical indices of renal function, including glomerular filtration rate (GFR), proteinuria, blood urea nitrogen (BUN), and serum creatinine level (SCR), in CKD patients using Pearson correlation

analysis. In the Nephroseq tool, we downloaded the clinical data of CKD patients in the GSE104954 dataset and GSE30529 dataset.

Renal interstitial fibrosis model establishment *in vivo*

To verify the key value of 6 IRGs *in vivo*, renal stone model was established by adding 1% ethylene glycol (EG) (324558, Sigma-Aldrich, USA) in drinking water for 4 weeks, as described in our previous study (17). The animal experiment was approved by the Ethics Committee for Animal Research of the Xiangya hospital of Central South University (202301003).

A total of 10 male Sprague-Dawley (SD) rats (age: 6-8 weeks, weight: 250-300 g) were purchased from the Laboratory Animal Center of Central South University (Changsha, China), and were housed in the controlled condition (12 h light/dark cycle, humidity (40-60%) and steady temperature of 22 ± 0.5°C) with free access to water and food. The rats were randomly divided into the control group and stone model group (*n* = 5 per group). In the stone model group, the rats received drinking water containing ethylene glycol (1%) for 4 weeks, while the rats in the control group had access to normal drinking water without ethylene glycol for 4 weeks. All rats were sacrificed by cervical dislocation under anesthesia [pentobarbital sodium (40 mg/kg)] after 4 weeks intervention. Kidney tissues were collected at -80°C or fixed in paraformaldehyde or formalin solution for histological study. Hematoxylin and eosin (HE) and Sirius Red staining were used to visualize the RIF in the rat with renal stone model. Finally, the stained area was observed and photographed with a bright-field microscope. Two experienced pathologists examined the extent of kidney injury. Kidney injury scores were evaluated using a scale ranging from 0 to 4 (0 indicating normal; 1 representing less than 25%; 2 indicating 25-50%; 3 representing 50-75%; and 4 indicating greater than or equal to 75%). Sirius Red positive area was quantified using Image J software (NIH Image, Bethesda, MD).

Quantitative real-time PCR

Total RNA was extracted from renal tissue using a Total RNA Kit II (R6934-01; Omega Bio-tek, Norcross, GA, USA) following the manufacturer's instructions. Then, cDNA was synthesized using an RT Reagent Kit with gDNA Eraser (No. RR047A; Takara, Tokyo, Japan). The mRNA levels of 6 IRGs were detected using All-in-One™ qPCR Mix (No: QP001; GeneCopoeia, Germantown, MD, USA). The primer sequences are listed in Supplementary Table 3. Each sample was repeated three times.

Statistical analysis

The present study performed all statistical analyses using R software (Version 4.1.1; R Foundation for Statistical Computing,

Vienna, Austria). The Wilcoxon test was run on expression data, with visualization by two groups of boxplots. Correlations among the expression levels of different genes were evaluated by Pearson correlation coefficients and were visualized using the “corrplot” package. A two-sided P value < 0.05 was accepted as statistically significant.

Results

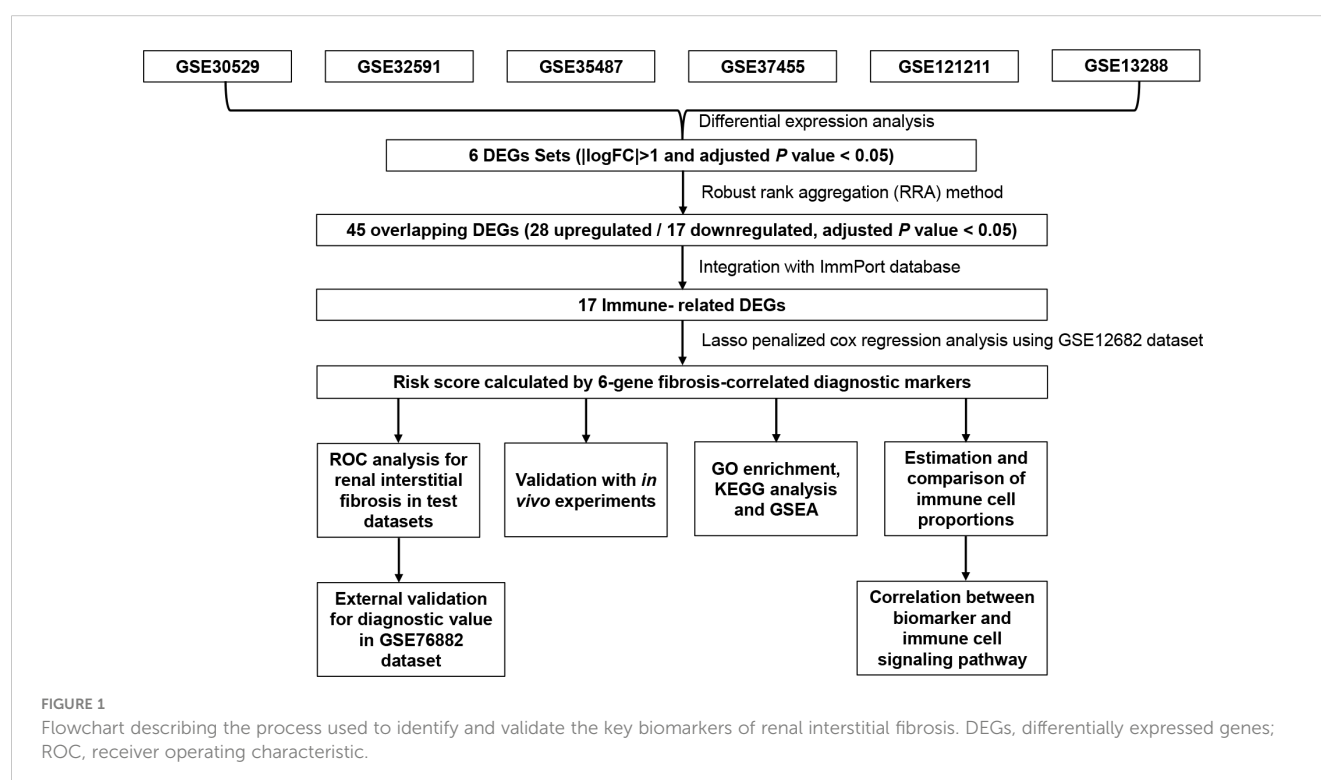
Screening of differentially expressed genes

The overall flow chart of the study design is presented in Figure 1. Given that RIF mostly results from the progression of CKD, we downloaded and analyzed six microarray expression datasets from individuals with CKD and healthy controls, including the GSE30529, GSE32591, GSE35487, GSE37455, GSE121211, and GSE133288 datasets. Of the DEGs between the CKD and control samples, 416 DEGs were identified from the GSE30529 dataset, including 298 upregulated and 118 downregulated genes (Supplementary Figure 1A). A total of 125 DEGs (including 97 upregulated and 28 downregulated genes) were screened from the GSE32591 dataset (Supplementary Figure 1B), 36 DEGs (including 0 upregulated and 36 downregulated genes) from the GSE35487 dataset (Supplementary Figure 1C), 27 DEGs (including 10 upregulated and 17 downregulated genes) from the GSE37455 dataset (Supplementary Figure 1D), 78 DEGs (including 49 upregulated and 29 downregulated genes) from the GSE121211 dataset (Supplementary Figure 1E), and 246 DEGs (including 48 upregulated and 198 downregulated genes) from the GSE133288 dataset (Supplementary Figure 1F).

Identification of immune-correlated key markers

After screening the DEGs from the six datasets, we integrated those DEG sets using the RRA method, and 45 overlapping DEGs (including 28 upregulated and 17 downregulated genes) were identified. The top 15 overlapping upregulated and downregulated DEGs in the six datasets are shown in Figure 2A. Then, we matched these 45 DEGs with immune-related gene sets from the ImmPort database and found 17 overlapping IRGs (Figure 2B). To identify the key markers associated with RIF, we performed LASSO regression analysis with those 17 IRGs for the GSE12682 dataset, which contained 23 CKD samples with evidence of tubulointerstitial fibrosis and 13 healthy control samples, and finally identified six IRGs in the model: apolipoprotein H (APOH), epidermal growth factor (EGF), lactotransferrin (LTF), lysozyme (LYZ), phospholipid transfer protein (PLTP), and secretory leukocyte peptidase inhibitor (SLPI) (Figures 2C, D).

Next, we analyzed the different expression levels of the six key IRGs between the RIF and control samples in the GSE12682 dataset and GSE76882 dataset (Figure 2E). The results from both indicated that the expression levels of APOH and EGF in the fibrosis group were significantly lower than those in the control group, while the expression levels of LTF, LYZ, PLTP, and SLPI were higher (all $P < 0.05$), which was consistent with the six sets of DEGs in CKD samples of six microarray datasets and the renal fibrosis samples in the GSE38117 dataset of UUO mice model (Supplementary Figure 2). Importantly, we collected the renal samples from the stones model group *in vivo*, which verified kidney injury and RIF in the stones model group by HE staining and Sirius Red staining (Figures 3A, B), and found same pattern of six gene expression



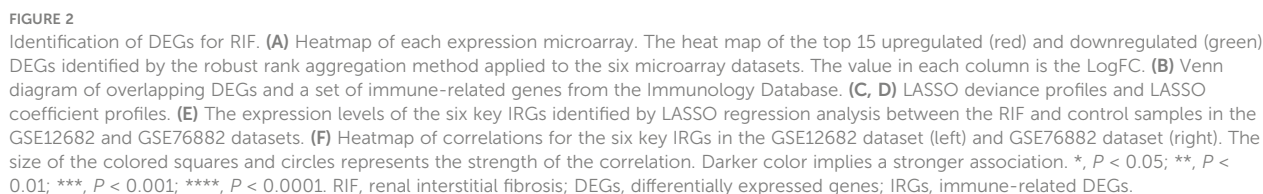


FIGURE 2
Identification of DEGs for RIF. **(A)** Heatmap of each expression microarray. The heat map of the top 15 upregulated (red) and downregulated (green) DEGs identified by the robust rank aggregation method applied to the six microarray datasets. The value in each column is the LogFC. **(B)** Venn diagram of overlapping DEGs and a set of immune-related genes from the Immunology Database. **(C, D)** LASSO deviance profiles and LASSO coefficient profiles. **(E)** The expression levels of the six key IRGs identified by LASSO regression analysis between the RIF and control samples in the GSE12682 and GSE76882 datasets. **(F)** Heatmap of correlations for the six key IRGs in the GSE12682 dataset (left) and GSE76882 dataset (right). The size of the colored squares and circles represents the strength of the correlation. Darker color implies a stronger association. *, $P < 0.05$; **, $P < 0.01$; ***, $P < 0.001$; ****, $P < 0.0001$. RIF, renal interstitial fibrosis; DEGs, differentially expressed genes; IRGs, immune-related DEGs.

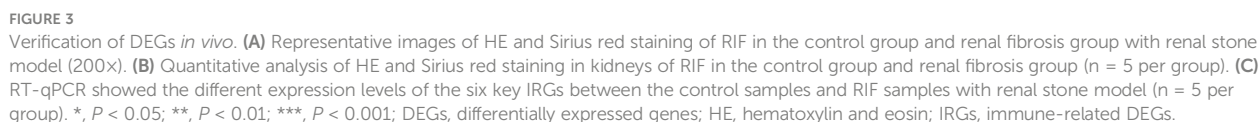


FIGURE 3
Verification of DEGs *in vivo*. **(A)** Representative images of HE and Sirius red staining of RIF in the control group and renal fibrosis group with renal stone model (200x). **(B)** Quantitative analysis of HE and Sirius red staining in kidneys of RIF in the control group and renal fibrosis group (n = 5 per group). **(C)** RT-qPCR showed the different expression levels of the six key IRGs between the control samples and RIF samples with renal stone model (n = 5 per group). * $P < 0.05$; ** $P < 0.01$; *** $P < 0.001$; DEGs, differentially expressed genes; HE, hematoxylin and eosin; IRGs, immune-related DEGs.

changes using RT-qPCR (Figure 3C). In addition, the correlation analysis suggested a significantly strong or moderate correlation among the six key markers (all $P < 0.05$) (Figure 2F, Supplementary Table 4).

Validation of immune-correlated key biomarkers

Based on the LASSO regression model, the risk score was calculated for each sample with the expression value of genes and corresponding coefficients: Risk score = $[(-0.05627) \times \text{Expression value of APOH}] + [(-0.00264 \times \text{Expression value of EGF}) + [(0.03986) \times \text{Expression value of LTF}] + [(0.02047) \times \text{Expression value of LYZ}] + [(0.02807) \times \text{Expression value of PLTP}] + [(-0.06040) \times \text{Expression value of SLPI}]$. Subsequently, ROC analysis and C-index analysis were applied to evaluate the diagnostic value of the six-gene risk scores. A favorable diagnostic efficacy of the six-gene risk scores in discriminating RIF from control samples, with an AUC of 0.926, was found in the GSE12682 dataset, and the C-index of the risk score was 0.933 (Figures 4A, B). Moreover, the risk score showed a powerful diagnostic ability in the GSE76882 dataset, with an AUC of 0.776 and C-index of 0.776 (Figures 4D, E). The fibrosis samples obtained significantly higher risk scores than the control samples in both the GSE12682 and GSE76882 datasets (all $P < 0.0001$) (Figures 4C, F).

Given that RIF is often accompanied by renal dysfunction, we explored the correlation between the risk score and clinical characteristics in the GSE104954 dataset and GSE30529 dataset, which included CKD samples with different etiologies that caused RIF, such as DN, MCD, HT, IgA nephropathy, TMD, FSGS, MGN, RPGN, and SLE (Supplementary Table 5) (6, 12). Similar to the results in the GSE12682 dataset, the risk scores in the CKD samples were significantly higher than those in the control samples (all $P < 0.0001$) (Figures 5A, I). Moreover, the risk score was strongly negatively correlated with GFR (GSE104954: $r = -0.59$, $P < 0.0001$; GSE30529: $r = -0.84$, $P < 0.0001$) (Figures 5B, J) and positively correlated with serum creatine level ($r = 0.51$, $P < 0.0001$) (Figure 5C), BUN level ($r = 0.29$, $P < 0.0001$) (Figure 5D), and proteinuria ($r = 0.47$, $P < 0.001$) (Figure 5E). No significant correlation was found with age (Figure 5F), body mass index (Figure 5G), or mean blood pressure (Figure 5H) (all $P > 0.05$).

Functional enrichment analysis of the fibrosis samples

To better understand the biological information associated with RIF, we obtained the DEGs between the RIF and control samples in the GSE12682 dataset. A total of 43 upregulated DEGs and 21

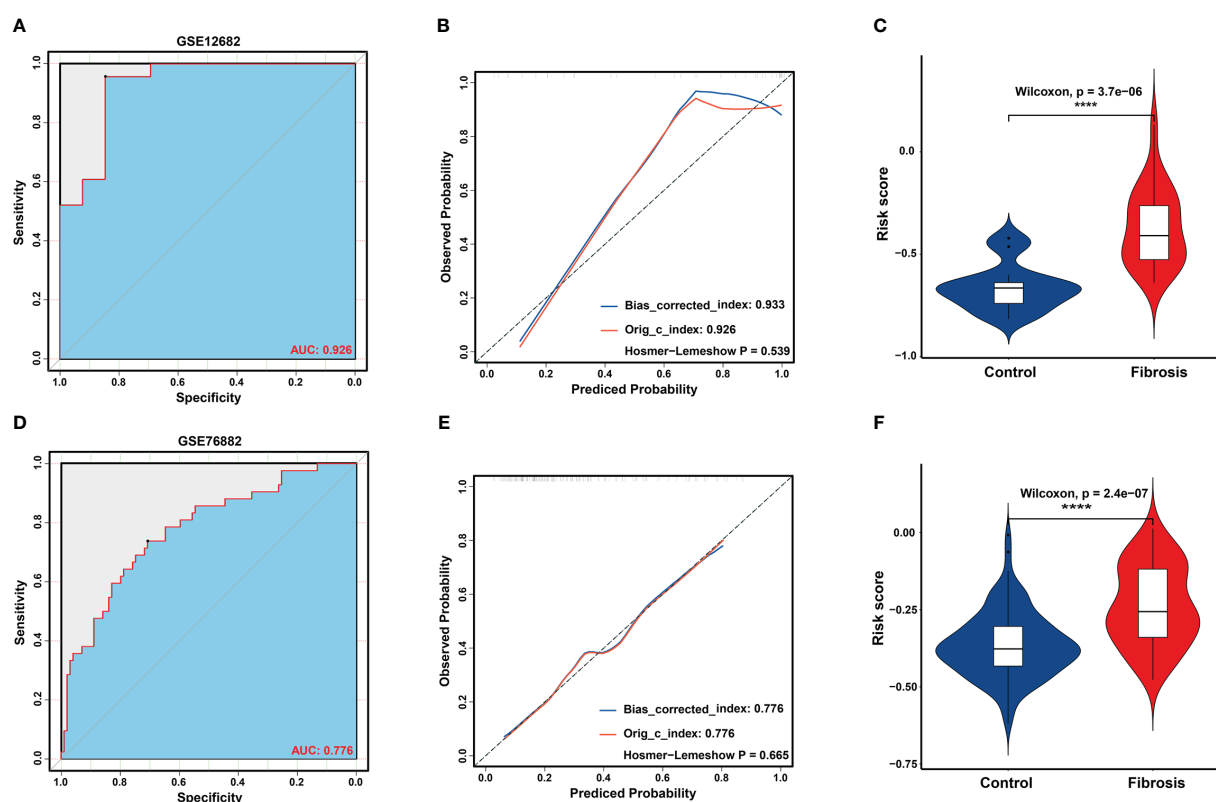


FIGURE 4

Validation of key biomarkers for RIF. (A, D) ROC analysis revealed good diagnostic performance of the risk score for RIF among the GSE12682 datasets and GSE76882 dataset. (B, E) Calibration plot of the risk score for predicting the probability of RIF among the GSE12682 datasets and GSE76882 dataset. (C, F) Violin plots of risk scores between the RIF and control groups among the GSE12682 datasets and GSE76882 dataset. ****, $P < 0.0001$.

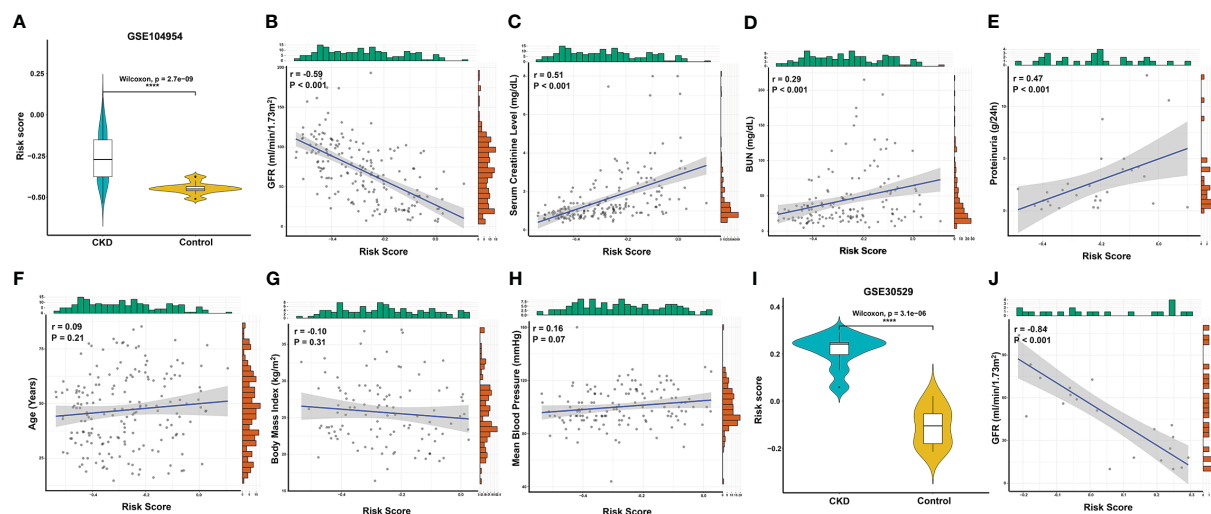


FIGURE 5

Correlation analysis between the risk score and clinical features in CKD patients. (A) Violin plots of risk scores between the CKD and control groups from the GSE104954 dataset. (B–E) Significant correlation between the risk score and GFR (B), serum creatinine level (C), BUN (D), and proteinuria (E) in CKD patients from the GSE104954 dataset. (F–H) The correlation between risk score and age (F), body mass index (G), and mean blood pressure (H) in CKD patients from the GSE104954 dataset. (I) Violin plots of the risk score between the CKD and control groups from the GSE30529 dataset. (J) Significant negative correlation between the risk score and GFR in CKD patients from the GSE30529 dataset. ****, $P < 0.0001$. GFR, glomerular filtration rate; BUN, blood urea nitrogen; CKD, chronic kidney disease.

downregulated DEGs were identified, and their different expression patterns were visualized using volcano plots and heatmaps (Figures 6A, B). Then, GO enrichment analysis and KEGG analysis were performed using the online DAVID tool. The results indicated a strong association with the adaptive innate immune response, innate immune response,

and positive regulation of NF- κ B transcription factor activity (Figure 6C, Supplementary Table 6). Moreover, GSEA was performed between the fibrosis and control samples in the GSE12682 dataset. Several immune pathways involved in fibrosis, such as the “T cell receptor signaling pathway” (NES, 1.688, NOM

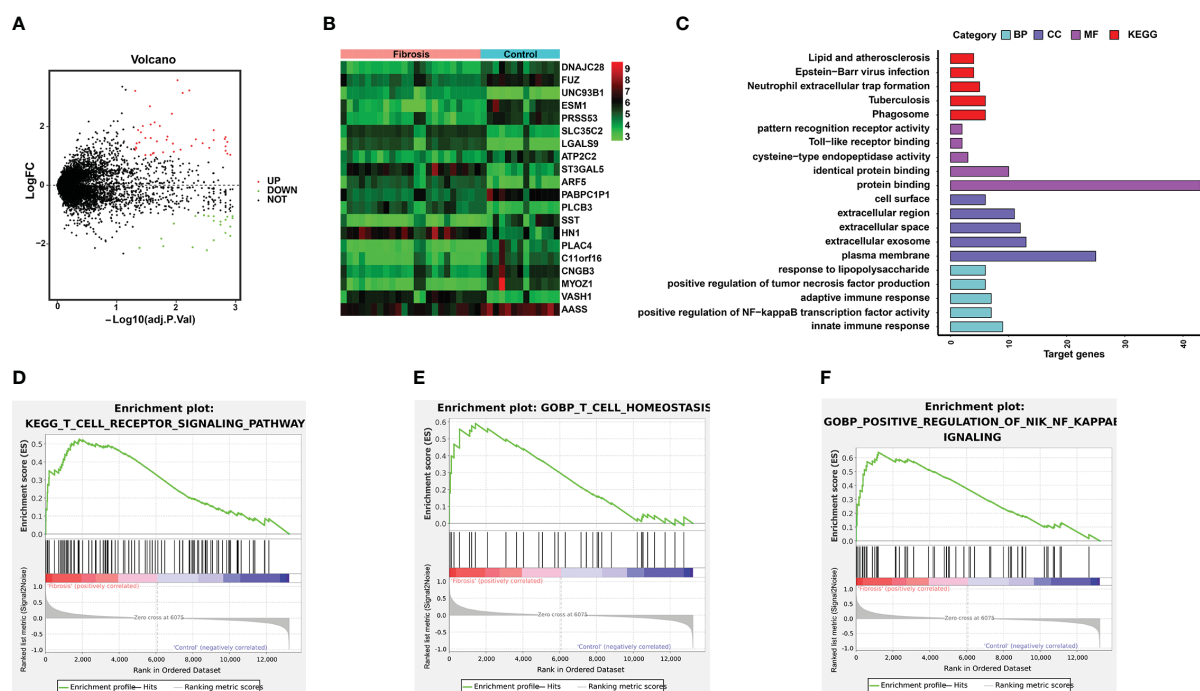


FIGURE 6

Significant pathways associated with the DEGs between the RIF and control samples in the GSE12682 dataset. (A) Volcano plot of the GSE12682 dataset. A total of 43 upregulated DEGs and 21 downregulated DEGs were identified between the RIF and control samples. (B) Heatmap of DEGs between the RIF and control samples in the GSE12682 dataset. (C) DEGs with their top 5 enriched GO terms and KEGG terms. (D–F) GSEA for the GSE12682 dataset.

p-value < 0.001), “T cell homeostasis” (NES, 1.624, NOM *p*-value = 0.008), and “positive regulation of NF-κB signaling pathway” (NES, 1.756, NOM *p*-value < 0.001) were identified (Figures 6D–F, Supplementary Table 7).

Enrichment of immune cells in the fibrosis and control samples

To explore the difference in the abundances of immune cell subtypes between the fibrosis and control groups, 28 available immune cell subtypes were assessed in the GSE12682 dataset using the ssGSVA method. The results indicated that 8 types of immune cells (including T follicular helper cells, Treg cells, MDSCs, gamma delta T cells, CD56bright natural killer cells, activated CD4 T cells, activated CD8 T cells, and activated dendritic cells) were significantly enriched in a higher proportion as in the control group

(all *P* < 0.05) (Figure 7A). Moreover, the GSE76882 dataset showed similar phenotypes of change (all *P* < 0.05) (Figure 7B). The interrelation among the various immune cell subtypes in the GSE12682 dataset varied from weak to moderate (Figure 7C). Next, we conducted correlation analyses to explore the relationship between the six key IRGs and different immune cell types (Supplementary Figure 3). As shown in Figure 7D, all six key markers showed a significantly strong correlation with six types of immune cells (all *P* < 0.05), except for gamma delta T cells and CD56bright natural killer cells. Because the NF-κB signaling pathway was associated with the progression of fibrosis, we also performed correlation analyses between eight immune cells and the genes in the NF-κB signaling pathway from the KEGG database. As shown in Figure 7E and Supplementary Figure 4, most immune cells were significantly associated with genes in the NF-κB signaling pathway, especially genes that activate the T-cell signaling pathway and noncanonical pathway (Supplementary Table 8).

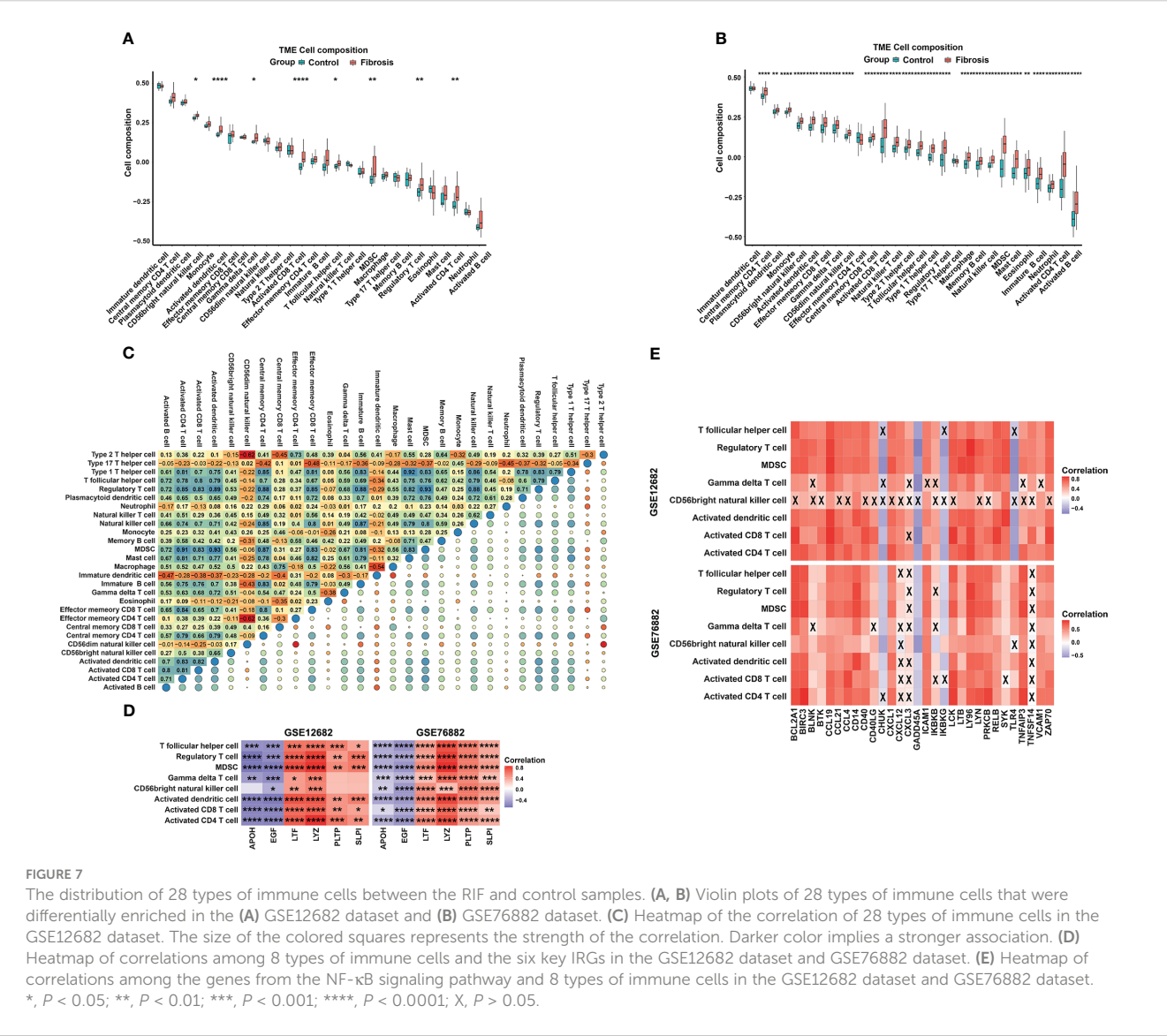
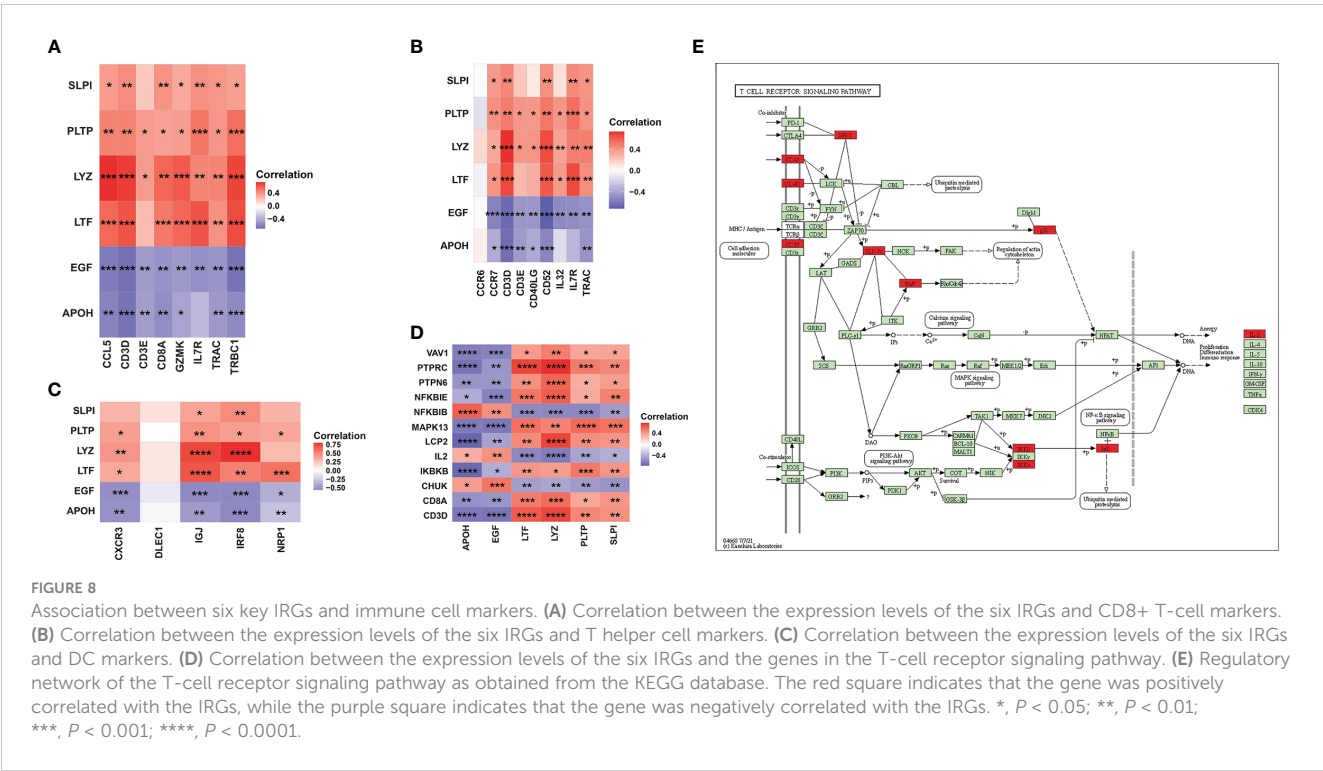


FIGURE 7
The distribution of 28 types of immune cells between the RIF and control samples. (A, B) Violin plots of 28 types of immune cells that were differentially enriched in the (A) GSE12682 dataset and (B) GSE76882 dataset. (C) Heatmap of the correlation of 28 types of immune cells in the GSE12682 dataset. The size of the colored squares represents the strength of the correlation. Darker color implies a stronger association. (D) Heatmap of correlations among 8 types of immune cells and the six key IRGs in the GSE12682 dataset and GSE76882 dataset. (E) Heatmap of correlations among the genes from the NF-κB signaling pathway and 8 types of immune cells in the GSE12682 dataset and GSE76882 dataset. *, *P* < 0.05; **, *P* < 0.01; ***, *P* < 0.001; ****, *P* < 0.0001; X, *P* > 0.05.



Involvement of key markers in DC cells and T cells

To further analyze the correlation between key markers and DC cells or T cells, we obtained gene sets related to CD8+ T-cell markers, T helper cell, and DC cell markers in human kidney from CellMarker and applied Pearson correlation analysis among the six IRGs and three gene sets in the GSE12682 dataset (Figures 8A–C, Supplementary Table 9). The results suggested that six IRGs were strongly correlated with most genes related to three immune cell markers (all $P < 0.05$), except for DLEC1 as a DC cell marker and CCR6 as a T helper cell marker (all $P > 0.05$). We also explored the correlation of six IRGs with the genes in the T-cell receptor signaling pathway (Supplementary Table 9). As shown in Figures 8D, E, all key markers were highly associated with the genes in the cell adhesion molecules (PTPRC, CD8A, CD3D, all $P < 0.05$), PI3K-Akt signaling pathway (IKBKB and CHUK, all $P < 0.05$), and NF- κ B signaling pathway (NFKBIE and NFKBIB, all $P < 0.05$). These results indicate that T cells and DCs play an important role in regulating the process of RIF.

Discussion

As the third-leading cause of premature mortality, CKD has been a major worldwide public disease burden (18). At the histological level, renal fibrosis, particularly renal interstitial fibrosis (RIF), is the ultimate common pathway of progressive kidney disease, no matter what the initial injury is (12). Importantly, immune-related genes play critical roles in the initiation and progression of renal fibrosis (19). Therefore, it is of

great clinical significance to identify immune-related biomarkers and potential immune cell infiltration changes for the intervention against RIF to ultimately improve the prognosis of CKD.

In the present study, we screened a total of 928 DEGs between CKD and control renal interstitial samples from the six microarray datasets and identified 17 overlapping immune-correlated DEGs after integration with the ImmPort database. Then, 6 IRGs, including 2 downregulated genes (APOH and EGF) and 4 upregulated genes (LTF, LYZ, PLTP, and SLPI) in CKD, were selected by LASSO regression analysis, validated as key biomarkers of RIF through ROC analysis in the GSE12682 dataset and GSE76882 dataset, and found to be significantly associated with renal function damage. GO enrichment analysis and GSEA indicated a strong association with the inflammatory response and T-cell receptor signaling pathway, as well as positive regulation of the NF- κ B signaling pathway, for the DEGs between RIF and control samples in the GSE12682 dataset. Next, we found that various immune cells, especially T cells (including activated CD4 T cells, activated CD8 T cells, Treg cells, and T follicular helper cells), were significantly enriched in the RIF samples, which is similar to the change noted for the four upregulated IRGs and contrary to that noted for the two downregulated IRGs. Importantly, the 6 IRGs were not only strongly correlated with those immune cell markers but also might interact with genes in the T-cell signaling pathway, including the NF- κ B signaling pathway and PI3K-Akt signaling pathway. Furthermore, the enriched immune cells were correlated with genes in the NF- κ B signaling pathway. All of the above evidence indicated that the biological function of the 6 IRGs might involve the immune response mediated by the NF- κ B signaling pathway and promote the progression of RIF.

RIF is considered to be a failed wound healing process that develops after chronic kidney damage from various insults (20). Initially, peritubular infiltration of numerous types of immune cells, particularly macrophages and T cells, is an early microenvironmental change that induces an inflammatory response and establishes a fibrogenic stage (21). Subsequently, myofibroblast activation and expansion, followed by EMT and cell apoptosis, result in tubular atrophy, impairment of renal function, and finally end-stage renal disease. Therefore, inflammation has an important role in the initiation and progression of renal fibrogenesis after injury (18, 22). Considerable evidence has shown that CD4⁺ T cells, Th17 cells and gamma delta T cells exert a profibrotic effect on damaged kidneys, whereas Tregs prevent kidney injury and fibrosis (23–25). Our results indicated that the infiltration of many immune cells, especially T cells with various functions (including activated CD4 T cells, activated CD8 T cells, T helper cells, and regulatory T cells) and activated DCs, was significantly increased in the RIF samples, probably contributing to RIF occurrence and progression. Although Treg cells function as anti-fibrotic immune cells, a previous study indicated that Treg cells are an important population that preferentially accumulates in fibrotic mouse kidneys (24), which is consistent with our results. Moreover, prophylactic Treg expansion confers protection against kidney injury and fibrosis development (24). Notably, CD8⁺ T cells have opposite roles in renal inflammation and fibrosis. A previous study found that CD8⁺ T cells accumulated early in the renal interstitium, reaching a peak at Day 5 in a unilateral ureter obstruction (UO) model of renal fibrosis (26). CD8⁺ T cells induce M1/M2 macrophage polarization to promote a stronger inflammatory response and facilitate the proliferation and activation of resident myofibroblasts (27, 28). However, recent studies indicated that increased infiltration of CD8⁺ T cells restrains renal fibrosis, and CD8⁺ T-cell deficiency aggravates renal fibrosis in UO-treated mice (26, 29). Therefore, immune cells play an important role in the process of renal fibrosis, but how the various immune cells induce inflammatory responses and the specific mechanisms involved in the progression of fibrosis remain to be verified.

As the initial stage of renal fibrosis, uncontrolled or excessive inflammation is bound to cause progressive renal injury in the context of CKD. We screened 6 sets of DEGs from multiple CDK renal interstitial tissues, selected immune-related DEGs, and identified 6 IRGs related to RIF. Our results demonstrated that several signaling pathways, such as the “T cell receptor signaling pathway” and “positive regulation of NF- κ B signaling pathway”, were involved in the process of RIF, and the 6 IRG expression levels were significantly correlated with the genes in these signaling pathways. Activation of the NF- κ B pathway stimulates a proinflammatory response and promotes renal fibrosis, and treatment with an NF- κ B inhibitor attenuates renal injury and inflammation in CKD tissues (30–32). In a UO model of progressive kidney disease for mice that express the human CRP gene (CRPtg), severe renal inflammation and fibrosis with a significant increase in tubulointerstitial T cells and macrophages have been found, accompanied by increased activation of both the NF- κ B/p65 and TGF- β /Smad2/3 signaling pathways (33). In

addition, a previous study found that CXCL16 plays a role in angiotensin II-induced renal inflammation and RIF in tubular epithelial cells in an NF- κ B-dependent manner, while CXCL16 deficiency inhibited the infiltration of F4/80⁺ macrophages and CD3⁺ T cells in the kidney (34). These data indicate that activation of NF- κ B signaling and infiltration of T cells might co-occur during fibrosis. However, it has not been determined how this coexpression phenotype is induced. We provide correlation analysis evidence that the 6 IRGs were strongly correlated with the genes in the NF- κ B signaling pathway, which positively regulates the T-cell signaling pathway. Moreover, the four upregulated IRGs (LTF, LYZ, PLTP, SLPI) were positively associated with various T cell populations, which were enriched in RIF tissues, whereas the two downregulated IRGs (APOH and EGF) had opposite results. Therefore, one reasonable hypothesis is that these IRGs induce inflammatory responses and promote RIF by mediating the NF- κ B signaling pathway in T cells, ultimately impairing renal function.

Six key IRGs, including APOH, EGF, LTF, LYZ, PLTP, and SLPI, were identified to be associated with RIF. APOH, also known as β_2 -glycoprotein 1 (β_2 GPI), is the most common protein for antiphospholipid antibodies in chronic disorders related to endothelial cell dysfunction (35). APOH was identified as a complement regulator and mediates innate immune regulation (36). Oxidized APOH causes DCs to mature and primes naive T lymphocytes, thus inducing T helper 1 (Th1) polarization, which involves NF- κ B activation and interleukin-1 receptor associated kinase (IRAK) phosphorylation (35, 37). In a model of STZ-DN mice, exogenously administered purified β_2 GPI decreased the expression levels of TGF- β 1 and collagen IV, with concomitant inhibition of p38 MAPK, and thus exerted renoprotective and antifibrotic effects (38). EGF, as a protein that stimulates cell growth and differentiation, was found to be expressed at low levels in the urine of end-stage kidney disease cases and strongly correlated with eGFR and urine albumin-to-creatinine ratio (39). A previous study indicated that diminished EGF levels lead to the development of kidney fibrosis associated with renal β -catenin/mTOR hyperactivation and predispose kidneys to progressive renal disease (40). Considerable evidence has shown that LTF and LYZ have important antioxidant, anti-inflammatory and nephroprotective activities (41–43). LTF inhibits TGF- β 1-induced renal fibrosis by restraining the expression of the profibrogenic genes CTGF, PAI-1 and collagen I (44). PLTP not only influences lipid transfer and lipoprotein metabolism, which is associated with cardio-metabolic diseases (45), but also plays a key role in the modulation of adaptive immune functions through alternation of T cell helper polarization (46). Similarly, the urinary levels of PLTP and SLPI are both increased in CKD patients with renal fibrosis (47, 48). SLPI is a critical mediator that controls anabolic parathyroid hormone-induced bone formation (49). As an inhibiting proteolytic enzyme, SLPI involves in immune functions of MSC to control T-cell proliferation and the regulation of damaged tissue healing, and was also identified as an ideal biomarker for kidney injury (50, 51).

Unfortunately, several limitations in the present study cannot be ignored. First, our results indicated that 6 IRGs were significantly correlated with renal function damage in CKD populations, but clinical information was not available for the RIF samples in the

GSE12682 and GSE76882 datasets. Importantly, the multiple datasets included in the analysis did not provide detailed data on the extent of fibrosis in the RIF samples. Therefore, whether the 6 IRGs play an initiating or continuing role in the fibrosis process remains unclear. Second, due to the limited research conditions, this retrospective study was performed based on microarray datasets and *in vivo* experiments. Therefore, direct evidence, such as clinical information and human RIF patient samples, is needed to uncover the potential pathophysiological mechanisms of these IRGs in the progression of RIF. Third, the immune cell infiltration in RIF samples was inferred by the ssGSEA method. These findings may deviate from the heterotypic interactions of cells, disease-induced disorders, or phenotypic plasticity, a shortcoming that needs to be addressed by further studies. A recent study demonstrated an increase in the number of infiltrating CD45⁺ cells and CD45⁺/CD3⁺ T cells in renal specimens from UUO mice with RIF. These research findings support our bioinformatics analyses regarding changes in immune cell infiltration (52). Undoubtedly, we will spare no effort to further explore the mechanisms of RIF in CKD populations.

Conclusion

In summary, six IRGs (APOH, EGF, LTF, LYZ, PLTP, and SLPI) were identified as key biomarkers for RIF. These IRGs exhibited a strong correlation with various T cells, activated DCs, and with the NF- κ B signaling pathway. All these IRGs and their signaling pathways may evolve as valuable therapeutic targets for RIF in CKD.

Data availability statement

The original contributions presented in the study are included in the article/**Supplementary Materials**, further inquiries can be directed to the corresponding author/s.

Ethics statement

The animal study was approved by the Ethics Committee for Animal Research of the Xiangya hospital of Central South University (202301003). The study was conducted in accordance with the local legislation and institutional requirements.

Author contributions

ZTD and XC supervised the project, designed the study, and interpreted the data. FZC and XC performed data management and analyzed the data. SP, XFL, XYL, and LZG took part in analyzing the data. XC wrote the first draft of the manuscript. ZTD and EW wrote and reviewed the manuscript. All of the authors approved the final version of the manuscript.

Funding

This study was funded by the National Key Research and Development Program of China (No. 2020YFC2005300) and Nature Science Foundation of Hunan Province (No. 2020JJ4783).

Conflict of interest

The authors declare that the research was conducted in the absence of any commercial or financial relationships that could be construed as a potential conflict of interest.

Publisher's note

All claims expressed in this article are solely those of the authors and do not necessarily represent those of their affiliated organizations, or those of the publisher, the editors and the reviewers. Any product that may be evaluated in this article, or claim that may be made by its manufacturer, is not guaranteed or endorsed by the publisher.

Supplementary material

The Supplementary Material for this article can be found online at: <https://www.frontiersin.org/articles/10.3389/fendo.2023.1207444/full#supplementary-material>

SUPPLEMENTARY FIGURE 1

Identification of DEGs associated with CKD. (A) Volcano plot (left) and heatmap (right) of the GSE30529 dataset. In total, 416 DEGs were identified from the GSE30529 dataset in the CKD samples vs. the control, including 298 upregulated and 118 downregulated genes. (B) Volcano plot (left) and heatmap (right) of the GSE32591 dataset. In total, 125 DEGs were identified from the GSE32591 dataset, including 97 upregulated and 28 downregulated genes. (C) Volcano plot (left) and heatmap (right) of the GSE35487 dataset. In total, 36 DEGs were identified from the GSE35487 dataset, including 36 downregulated and 0 upregulated genes. (D) Volcano plot (left) and heatmap (right) of the GSE37455 dataset. In total, 27 DEGs were identified from the GSE37455 dataset, including 10 upregulated and 17 downregulated genes. (E) Volcano plot (left) and heatmap (right) of the GSE121211 dataset. In total, 78 DEGs were identified from the GSE121211 dataset, including 49 upregulated and 29 downregulated genes. (F) Volcano plot (left) and heatmap (right) of the GSE133288 dataset. In total, 246 DEGs were identified from the GSE133288 dataset, including 198 downregulated and 48 upregulated genes. DEGs, differentially expressed genes; CKD, chronic kidney disease.

SUPPLEMENTARY FIGURE 2

The expression levels of the six key IRGs in the GSE38117 dataset. Violin plot illustrating the gene expression profile of three fibrotic kidneys with three undamaged contralateral kidneys in mice using the UUO model. *, $P < 0.05$, the paired Student's *t*-test.

SUPPLEMENTARY FIGURE 3

Correlation between the expression levels of six key IRGs and immune cell enrichment. (A-F) Correlation between the expression levels of APOH (A), EGF (B), LTF (C), LYZ (D), PLTP (E), and SLPI (F) and 28 enriched types of immune cells in the GSE12682 dataset. The size of each dot represents the strength of the correlation between the IRG and the immune cell. The color of the dot represents the *P* value; the greener the color, the higher the *P* value, and the redder the color, the lower the *P* value. $P < 0.05$ was considered statistically significant.

SUPPLEMENTARY FIGURE 4

Correlation between the infiltration of immune cells and genes in the NK- κ B signaling pathway.

References

- Jager KJ, Fraser S. The ascending rank of chronic kidney disease in the global burden of disease study. *Nephrol Dial Transpl* (2017) 32:i121–8. doi: 10.1093/ndt/gfw330
- Mills KT, Xu Y, Zhang W, Bundy JD, Chen CS, Kelly TN, et al. A systematic analysis of worldwide population-based data on the global burden of chronic kidney disease in 2010. *Kidney Int* (2015) 88:950–7. doi: 10.1038/ki.2015.230
- GBD Chronic Kidney Disease Collaboration. Global, regional, and national burden of chronic kidney disease, 1990–2017: a systematic analysis for the global burden of disease study 2017. *Lancet* (2020) 395:709–33. doi: 10.1016/S0140-6736(20)30045-3
- Barutta F, Bruno G, Mastrocola R, Bellini S, Gruden G. The role of cannabinoid signaling in acute and chronic kidney diseases. *Kidney Int* (2018) 94:252–8. doi: 10.1016/j.kint.2018.01.024
- Webster AC, Nagler EV, Morton RL, Masson P. Chronic kidney disease. *Lancet* (2017) 389:1238–52. doi: 10.1016/S0140-6736(16)32064-5
- Nastase MV, Zeng-Brouwers J, Wygrecka M, Schaefer L. Targeting renal fibrosis: mechanisms and drug delivery systems. *Adv Drug Delivery Rev* (2018) 129:295–307. doi: 10.1016/j.addr.2017.12.019
- Liu Y. Renal fibrosis: new insights into the pathogenesis and therapeutics. *Kidney Int* (2006) 69:213–7. doi: 10.1038/sj.ki.5000054
- Yan H, Xu J, Xu Z, Yang B, Luo P, He Q. Defining therapeutic targets for renal fibrosis: exploiting the biology of pathogenesis. *BioMed Pharmacother* (2021) 143:112115. doi: 10.1016/j.biopha.2021.112115
- Soranno DE, Lu HD, Weber HM, Rai R, Burdick JA. Immunotherapy with injectable hydrogels to treat obstructive nephropathy. *J BioMed Mater Res* (2014) 102:2173–80. doi: 10.1002/jbma.34902
- Noh H, Yu MR, Kim HJ, Lee JH, Park BW, Wu IH, et al. Beta 2-adrenergic receptor agonists are novel regulators of macrophage activation in diabetic renal and cardiovascular complications. *Kidney Int* (2017) 92:101–13. doi: 10.1016/j.kint.2017.02.013
- Wilson HM, Chettibi S, Jobin C, Walbaum D, Rees AJ, Kluth DC. Inhibition of macrophage nuclear factor-kappa b leads to a dominant anti-inflammatory phenotype that attenuates glomerular inflammation *in vivo*. *Am J Pathol* (2005) 167:27–37. doi: 10.1016/s0002-9440(10)62950-1
- Lv W, Booz GW, Wang Y, Fan F, Roman RJ. Inflammation and renal fibrosis: recent developments on key signaling molecules as potential therapeutic targets. *Eur J Pharmacol* (2018) 820:65–76. doi: 10.1016/j.ejphar.2017.12.016
- Tang PM, Nikolic-Paterson DJ, Lan HY. Macrophages: versatile players in renal inflammation and fibrosis. *Nat Rev Nephrol* (2019) 15:144–58. doi: 10.1038/s41581-019-0110-2
- Hu Z, Liu Y, Zhu Y, Cui H, Pan J. Identification of key biomarkers and immune infiltration in renal interstitial fibrosis. *Ann Transl Med* (2022) 10:190. doi: 10.21037/atm-22-366
- Hanzelmann S, Castelo R, Guinney J. Gsva: gene set variation analysis for microarray and rna-seq data. *BMC Bioinf* (2013) 14:7. doi: 10.1186/1471-2105-14-7
- Charoentong P, Finotello F, Angelova M, Mayer C, Efremova M, Rieder D, et al. Pan-cancer immunogenomic analyses reveal genotype-immunophenotype relationships and predictors of response to checkpoint blockade. *Cell Rep* (2017) 18:248–62. doi: 10.1016/j.celrep.2016.12.019
- Cao Y, Duan B, Gao X, Wang E, Dong Z. Itraq-based comparative proteomics analysis of urolithiasis rats induced by ethylene glycol. *BioMed Res Int* (2020) 2020:6137947. doi: 10.1155/2020/6137947
- Decleves AE, Sharma K. Novel targets of antifibrotic and anti-inflammatory treatment in ckd. *Nat Rev Nephrol* (2014) 10:257–67. doi: 10.1038/nrneph.2014.31
- Black LM, Lever JM, Agarwal A. Renal inflammation and fibrosis: a double-edged sword. *J Histochem Cytochem* (2019) 67:663–81. doi: 10.1369/0022155419852932
- Liu Y. Cellular and molecular mechanisms of renal fibrosis. *Nat Rev Nephrol* (2011) 7:684–96. doi: 10.1038/nrneph.2011.149
- Zeisberg M, Neilson EG. Mechanisms of tubulointerstitial fibrosis. *J Am Soc Nephrol* (2010) 21:1819–34. doi: 10.1681/ASN.2010080793
- Wang Y, Harris DC. Macrophages in renal disease. *J Am Soc Nephrol* (2011) 22:21–7. doi: 10.1681/ASN.2010030269
- Liu L, Kou P, Zeng Q, Pei G, Li Y, Liang H, et al. Cd4+ t lymphocytes, especially th2 cells, contribute to the progress of renal fibrosis. *Am J Nephrol* (2012) 36:386–96. doi: 10.1159/000343283
- Do VDF, Lafont A, Beibel M, Martin K, Darribat K, Cuttat R, et al. Immune cell landscaping reveals a protective role for regulatory t cells during kidney injury and fibrosis. *JCI Insight* (2020) 5(3):e130651. doi: 10.1172/jci.insight.130651
- Gao M, Wang J, Zang J, An Y, Dong Y. The mechanism of cd8(+) t cells for reducing myofibroblasts accumulation during renal fibrosis. *Biomolecules* (2021) 11(7):990. doi: 10.3390/biom11070990
- Wang H, Wang J, Bai Y, Li J, Li L, Dong Y. Cd11c(+) cd8(+) t cells reduce renal fibrosis following ureteric obstruction by inducing fibroblast apoptosis. *Int J Mol Sci* (2016) 18(1):1. doi: 10.3390/ijms18010001
- Ricardo SD, van Goor H, Eddy AA. Macrophage diversity in renal injury and repair. *J Clin Invest* (2008) 118:3522–30. doi: 10.1172/JCI36150
- Floege J, Eitner F, Alpers CE. A new look at platelet-derived growth factor in renal disease. *J Am Soc Nephrol* (2008) 19:12–23. doi: 10.1681/ASN.2007050532
- Dong Y, Yang M, Zhang J, Peng X, Cheng J, Cui T, et al. Depletion of cd8+ t cells exacerbates cd4+ t cell-induced monocyte-to-fibroblast transition in renal fibrosis. *J Immunol* (2016) 196:1874–81. doi: 10.4049/jimmunol.1501232
- Grande MT, Perez-Barriocanal F, Lopez-Novoa JM. Role of inflammation in tubulo-interstitial damage associated to obstructive nephropathy. *J Inflammation (Lond)* (2010) 7:19. doi: 10.1186/1476-9255-7-19
- Li R, Guo Y, Zhang Y, Zhang X, Zhu L, Yan T. Salidroside ameliorates renal interstitial fibrosis by inhibiting the tlr4/nf-kappab and mapk signaling pathways. *Int J Mol Sci* (2019) 20(5):1103. doi: 10.3390/ijms20051103
- Li Q, Liu BC, Lv LL, Ma KL, Zhang XL, Phillips AO. Monocytes induce proximal tubular epithelial-mesenchymal transition through nf-kappa b dependent upregulation of icam-1. *J Cell Biochem* (2011) 112:1585–92. doi: 10.1002/jcb.23074
- Li ZI, Chung AC, Zhou L, Huang XR, Liu F, Fu P, et al. C-reactive protein promotes acute renal inflammation and fibrosis in unilateral ureteral obstructive nephropathy in mice. *Lab Invest* (2011) 91:837–51. doi: 10.1038/labinvest.2011.42
- Xia Y, Entman ML, Wang Y. Critical role of cxcl16 in hypertensive kidney injury and fibrosis. *Hypertension* (2013) 62:1129–37. doi: 10.1161/HYPERTENSIONAHA.113.01837
- Buttari B, Profumo E, Mattei V, Siracusano A, Ortona E, Margutti P, et al. Oxidized beta2-glycoprotein i induces human dendritic cell maturation and promotes a t helper type 1 response. *Blood* (2005) 106:3880–7. doi: 10.1182/blood-2005-03-1201
- Gropp K, Weber N, Reuter M, Micklisch S, Kopka I, Hallstrom T, et al. Beta(2)-glycoprotein i, the major target in antiphospholipid syndrome, is a special human complement regulator. *Blood* (2011) 118:2774–83. doi: 10.1182/blood-2011-02-339564
- Zandman-Goddard G, Pierangeli SS, Gertel S, Blank M. Tolerogenic dendritic cells specific for beta2-glycoprotein-i domain-i, attenuate experimental antiphospholipid syndrome. *J Autoimmun* (2014) 54:72–80. doi: 10.1016/j.jaut.2014.06.001
- Wang T, Chen SS, Chen R, Yu DM, Yu P. Reduced beta 2 glycoprotein i improves diabetic nephropathy via inhibiting tgfbeta1-p38 mapk pathway. *Int J Clin Exp Pathol* (2015) 8:2321–33.
- Amatruda JG, Katz R, Sarnak MJ, Gutierrez OM, Greenberg JH, Cushman M, et al. Biomarkers of kidney tubule disease and risk of end-stage kidney disease in persons with diabetes and ckd. *Kidney Int Rep* (2022) 7:1514–23. doi: 10.1016/j.ekir.2022.03.033
- Zeid AM, Lamontagne JO, Zhang H, Marneros AG. Epidermal growth factor deficiency predisposes to progressive renal disease. *FASEB J* (2022) 36:e22286. doi: 10.1096/fj.202101837R
- Aslam SM, Hirawat R, Godugu C. Lactoferrin-decorated cerium oxide nanoparticles prevent renal injury and fibrosis. *Biol Trace Elem Res* (2022) 201(4):1837–45. doi: 10.1007/s12011-022-03284-6
- Hegazy R, Salama A, Mansour D, Hassan A. Renoprotective effect of lactoferrin against chromium-induced acute kidney injury in rats: involvement of il-18 and igf-1 inhibition. *PLoS One* (2016) 11:e151486. doi: 10.1371/journal.pone.0151486
- Gallo D, Cocchiello M, Masat E, Agostinis C, Harei E, Veronesi P, et al. Human recombinant lysozyme downregulates advanced glycation endproduct-induced interleukin-6 production and release in an *in-vitro* model of human proximal tubular epithelial cells. *Exp Biol Med* (Maywood) (2014) 239:337–46. doi: 10.1177/1535370213518281
- Hsu YH, Chiu IJ, Lin YF, Chen YJ, Lee YH, Chiu HW. Lactoferrin contributes a renoprotective effect in acute kidney injury and early renal fibrosis. *Pharmaceutics* (2020) 12(5):434. doi: 10.3390/pharmaceutics12050434
- Jiang XC, Yu Y. The role of phospholipid transfer protein in the development of atherosclerosis. *Curr Atheroscler Rep* (2021) 23:9. doi: 10.1007/s11883-021-00907-6
- Desrumaux C, Lemaire-Ewing S, Ogier N, Yessoufou A, Hammann A, Sequeira-Le GA, et al. Plasma phospholipid transfer protein (pltp) modulates adaptive immune functions through alternation of t helper cell polarization. *Cell Mol Immunol* (2016) 13:795–804. doi: 10.1038/cmi.2015.75
- Bergensfeldt M, Bjork P, Ohlsson K. The elimination of secretory leukocyte protease inhibitor (slpi) after intravenous injection in dog and man. *Scand J Clin Lab Invest* (1990) 50:729–37. doi: 10.1080/00365519009091066
- Yang B, Sylvius N, Luo J, Yang C, Da Z, Crotty C, et al. Identifying biomarkers from transcriptomic signatures in renal allograft biopsies using deceased and living donors. *Front Immunol* (2021) 12:657860. doi: 10.3389/fimmu.2021.657860
- Morimoto A, Kikuta J, Nishikawa K, Sudo T, Uenaka M, Furuya M, et al. Slpi is a critical mediator that controls pth-induced bone formation. *Nat Commun* (2021) 12:2136. doi: 10.1038/s41467-021-22402-x
- Vigo T, La Rocca C, Faicchia D, Procaccini C, Ruggieri M, Salvetti M, et al. Ifnbeta enhances mesenchymal stromal (stem) cells immunomodulatory function through stat1-3 activation and mtor-associated promotion of glucose metabolism. *Cell Death Dis* (2019) 10:85. doi: 10.1038/s41419-019-1336-4
- Ohlsson S, Ljungkrantz I, Ohlsson K, Segelmark M, Wieslander J. Novel distribution of the secretory leukocyte proteinase inhibitor in kidney. *Mediators Inflamm* (2001) 10:347–50. doi: 10.1080/09629350120102389
- Lindquist JA, Bernhardt A, Reichardt C, Sauter E, Brandt S, Rana R, et al. Cold shock domain protein dbpa orchestrates tubular cell damage and interstitial fibrosis in inflammatory kidney disease. *Cells-Basel* (2023) 12(10):1426. doi: 10.3390/cells12101426

Frontiers in Endocrinology

Explores the endocrine system to find new therapies for key health issues

The second most-cited endocrinology and metabolism journal, which advances our understanding of the endocrine system. It uncovers new therapies for prevalent health issues such as obesity, diabetes, reproduction, and aging.

Discover the latest Research Topics

[See more →](#)

Frontiers

Avenue du Tribunal-Fédéral 34
1005 Lausanne, Switzerland
frontiersin.org

Contact us

+41 (0)21 510 17 00
frontiersin.org/about/contact

